Electric Technology U.S.S.R.

961

ЭЛЕКТРИЧЕСТВО

1961

Published by

PERGAMON PRESS NEW YORK LONDON OXFORD PARIS

for Pergamon Institute, Washington and Oxford

Published May 1962

ELECTRIC TECHNOLOGY U.S.S.R.

VOLUMES 1—4, 1961

Selected papers from Elektrichestvo, Nos. 1—12, 1961

EDITORIAL BOARD

H. M. BARLOW (London)
F. W. BOWDEN (San Luis Obispo)
F. BRAILSFORD (London)
G. S. BROWN (Cambridge, Mass.)
F. M. BRUCE (Glasgow)
C. C. CARR (Brooklyn)
G. W. CARTER (Leeds)
A. G. CONRAD (New Haven, Conn.)
G. F. CORCORAN (College Park, Md.)
J. D. CRAGGS (Liverpool)
A. L. CULLEN (Sheffield)
G. E. DREIFKE (St. Louis)
V. EASTON (Birmingham)
A. R. ECKELS (Vermont)
W. FISHWICK (Swansea)
C. FROEHLICH (New York)
C. G. GARTON (Leatherhead)
R. S. GENS (Portland)
J. GREIG (London)
L. D. HARRIS (Salt Lake City)
J. D. HORGAN (Milwaukee)
E. C. JONES (Morgantown)
E. C. JORDAN (Urbana)
I. H. LOVETT *Rolla*, (Missouri)
J. M. MEEK (Liverpool)
J. H. MULLIGAN JNR. (N.Y.)
W. A. MURRAY (Blacksburg, Virginia)
J. E. PARTON (Nottingham)
H. A. PETERSON (Madison)
A. PORTER (London)
J. C. READ (Rugby)
W. G. SHEPHERD (Minneapolis)
W. P. SMITH (Lawrence, Kansas)
PHILIP SPORN (Chairman) (New York)
J. A. STRELZOFF (East Lansing)
F. W. TATUM (Dallas, Texas)
C. V. O. TERWILLIGER (Monterey)
D. H. TOMPSETT (Stafford)
A. TUSTIN (London)
S. REID WARREN JNR. (Philadelphia)
A. R. VAN C. WARRINGTON (Stafford)
A. H. WAYNICK (Pa.)
E. M. WILLIAMS (Pittsburg)
F. C. WILLIAMS (Manchester)
H. I. WOOD (Manchester)
C. M. ZIEMIAN (Ohio)

PERGAMON PRESS LTD.

OXFORD . LONDON . NEW YORK . PARIS

PERGAMON PRESS LTD.
Headington Hill Hall, Oxford.
4 and 5 Fitzroy Square, London, W.1.

PERGAMON PRESS INC.
122 East 55th Street, New York 22, N.Y.

GAUTHIER-VILLARS
55, Quai des Grands-Augustin, Paris VIe.

PERGAMON PRESS G.m.b.H.
Kaiserstrasse 75, Frankfurt-am-Main.

PERGAMON INSTITUTE

A DIVISION OF PERGAMON INTERNATIONAL CORPORATION, OPERATED IN THE PUBLIC SERVICE FOR THE FURTHERANCE AND DISSEMINATION OF SCIENTIFIC KNOWLEDGE.

961

President of the Scientific Advisory Council
Sir Robert Robinson, O.M., F.R.S.

Executive Director : Robert Maxwell, M.C.

Elektrichestvo

Editor-in-Chief : N. G. DROZDOV

EDITORIAL BOARD

L. A. BESSONOV, N. I. BORISENKO, G. V. BUTKEVICH, T. P. GUBENKO, A. M. FEDOSEEV, A. D. DROZDOV, L. A. DUBINSKII, L. A. ZHEKULIN, A. M. ZALESKII, M. P. KOSTENKO, V. S. KULEBAKIN, B. YU. LOMONOSOV, L. G. MAMIKONYANTS, L. R. NEIMAN, I. I. PETROV, I. M. POSTNIKOV, S. I. RABINOVICH, B. S. SOTSKOV, I. A. SYROMYATNIKOV, YU. G. TOLSTOV
M. G. CHILIKIN

AUTHOR INDEX, VOLUMES 1-4, 1961

PAGE

Al'tgauzen, O. N., Semenova, N. A. and Stepanova, A. N.: The effect of demagnetization on the permeability of materials used for magnetic circuits 7

Ankhimuk, V. L. and Il'in, O. P.: The optimum output of induction motors in reactor-controlled drives 166

Arkhangel'skii, V. I.: A continuous control system for the main drive of a reversible rolling mill 46

Azar'ev D. I.: Long distance power transmission with d.c. magnetized reactor-transformers and forced capacitor banks 333

Bashuk, I. B. and Khomenko, A. I.: Contactless control of electric coaches 495

Bauman, V. G., Ivanov, O. V. and Komarov, B. I.: The self-excitation of induction motors with series capacitors 213

Bogoroditskii, N. P., Volokobinskii, Yu. N. and Fridberg, I. D.: Graphical analysis of the thermal breakdown voltage of h.f. insulators 649

Boldov, N. A.: A method of determining the main criteria of traction machines for minimum weight per unit of output 426

Borzova, P. I. and Nefedov, A. A.: Cold-rolled non-oriented electrical steel 79

Chen'shi-Nyan' and Rozanov, M. N.: An investigation of the steady state stability limits of long distance transmission lines with controlled synchronous condensers 476

Chesnokov, A. E.: The theory and design of electromagnetic vibration equipment 619

Chesnov, M. P.: The re-synchronization of the generator by the turbine speed-governor . 36

Demirchian, K. S. and Pruss-Zhukovskii, V. V.: A study of the e.m.f. induced in electrical machines using an electrolytic tank 411

Doskin, L. I., Gershtein, A. R., Izrailevich, L. Yu., Krikunchik, A. B., Levitskii, K. K. and Ross, B. V.: The new Russian power stations 89

Ermolin, N. P.: The problems of developing new small and f.h.p. motors 377

Fleishman, L. S.: The new nine-valve six-phase rectifier units 242

Fridberg, I. D., Bogoroditskii, N. P. and Volokobinskii, Yu. N.: Graphical analysis of the thermal breakdown voltage of h.f. insulators 649

Gel'fand, Ya. S.: An analogue computer study of current transformer transients 630

Gershtein, A. R., Dvoskin, L. I., Izrailevich, L. Yu., Krikunchik, A. B., Levitskii, K. K. and Ross, B. V.: The new Russian power stations 89

Grinshtein, V. I.: A zero sequence power relay with current polarization 28

Gurevich, Yu. E., Sokolov, N. I. and Khvoshchinskaya, Z. G.: A new method of studying large complex power systems on analogue computers 193

Gutkin, B. M.: The mercury-arc rectifier drive 546

Il'in, O. P. and Ankhimiuk, V. L.: The optimum output of induction motors in reactor-controlled drives 166

Isaev, I. P. and Sonin, V. S.: A statistical method of estimating the reliability of electric locomotives 113

Ivanov, O. V., Bauman, V. G. and Komarov, B. I.: The self-excitation of induction motors with series capacitors 213

Izrailevich, L. Yu., Gershtein, A. R., Dvoskin, L. I., Krikunchik, A. B., Levitskii, K. K. and Ross, B. V.: The new Russian power stations 89

Khasayev, O. I.: Operation of an induction motor from a transistor frequency convertor . . 441

Khomenko, A. I. and Bashuk, I. B.: Contactless control of electric coaches 495

Khvoshchinskaya, Z. G., Sokolov, N. I. and Gurevich, Yu. E.: A new method of studying large complex power systems on analogue computers 193

Komarov, B. I., Bauman, V. G. and Ivanov, O. V.: The self-excitation of induction motors with series capacitors 213

Komarov, Yu. G.: A high-speed electro-dynamic circuit breaker 288

Kovalev, F. I. and Mostkova, G. P.: The design of reactor-controlled semi-conductor rectifiers 507

196

Krasnoshapka, M. M.: A new system of generating direct and stable frequency a.c. from motors which run at different speeds 273

Kravchenko, V. S. and Sun Iui-Chi: The elimination of arcing in h.f. a.c. circuits 19

Krikunchik, A. B., Gershtein, A. R., Dvoskin, L. I., Izrailevich, L. Yu., Levitskii, K. K. and Ross, B. V.: The new Russian power stations 89

Kulikov, S. V.: Temperature compensation of transistorized relay stages 585

Levitskii, K. K., Gershtein, A. R., Dvoskin, L. I., Izrailevich, L. Yu., Krikunchik, A. B. and Ross, B. V.: The new Russian power stations 89

Liashenko, V. D.: The measurement of large transient currents for switchgear 383

Lizunov, S. D.: Capacitive transmission of surge voltages in transformers having a bushing at the mid-point of the high voltage winding 63

Mel'gunov, N. M.: Inverter substations for outlying regions without local power station counter-e.m.f.'s 566

Menskii, B. M.: A method of reducing transient phenomena in circuits with inductance coils and semiconductor rectifiers 177

Mikulinskii, A. S.: Criteria of electric ore-smelting furnaces 256

Mostkova, G. P. and Kovalev, F. I.: The design of reactor-controlled semiconductor rectifiers 507

Nefedov, A. A. and Borzova, P. I.: Cold-rolled non-oriented electrical steel 79

Olson, A. B.: Design of deep grounding rods for transmission line towers 640

Palastin, L. M.: A new brushless synchronous alternator for use in aircraft 133

Parts, R. R.: A method of determining the leakage inductance of stator windings in large a.c. machines without the rotor "out" 294

Popov, D. A.: Joint selection of the motor criteria and the gear ratio 349

Pruss-Zhukovskii, V. V. and Demirchian, K. S.: A study of the e.m.f. induced in electrical machines using an electrolytic tank 411

Pruzhinina-Granovskaya, V. I., Savel'ev, V. P., Shmatovich, V. V. and Pugachev, V. K.: A magnetic rotating-arc arrester for combined protection from internal surges and lightning strikes on 500 kV transmission lines 149

Pruzinina-Granovskaya, V. I. and Vol'kenau, V. A.: How the post-breakdown voltage on an arrester depends on the length of the current wave-front 529

Pugachev, V. K., Savel'ev, V. P., Shmatovich, V. V. and Pruzhinina-Granovskaya, V. K.: A magnetic rotating-arc arrester for combined protection from internal surges and lightning strikes on 500 kV transmission lines 149

Ross, B. V., Gershtein, A. R., Dvoskin, L. I., Izrailevich, L. Yu., Krikunchik, A. B. and Levitskii, K. K.: The new Russian power stations 89

Rozanov, M. N. and Chen'shi-Nyan: An investigation of the steady state stability limits of long distance transmission lines with controlled synchronous condensers 476

Rusin, Yu. S.: The permeance of magnetic circuits with teeth 349

Savel'ev, V. P., Shmatovich, V. V., Pruzhinina-Granovskaya, V. I. and Pugachev, V. K.: A magnetic rotating-arc arrester for combined protection from internal surges and lightning strikes on 500 kV transmission lines 149

Semenova, N. A., Al'tgauzen, O. N. and Stepanova, A. N.: The effect of demagnetization on the permeability of materials used for magnetic circuits 7

Sharov, V. I.: The theory of transformer operation with a magnetized shunt 580

Sherman, Ya. N.: Direct testing of circuit breakers by the joint use of surge generators and Gorev oscillatory circuits 228

Shmatovich, V. V., Savel'ev, V. P., Pruzhinina-Granovskaya, V. I. and Pugachev, V. K.: A magnetic rotating-arc arrester for combined protection from internal surges and lightinng strikes on 500 kV transmission lines 149

Shut', V. V.: Discriminative earth-fault indication 534

Sisoyan, G. A.: The current distribution in the baths of ore-smelting furnaces 460

Sokolov, N. I., Gurevich, Yu. E. and Khvoshchinskaya, Z. G.: A new method of studying large complex power systems on analogue computers 193

Sonin, V. S. and Isaev, I. P.: A statistical method of estimating the reliability of electric locomotives 113

Stepanova, A. N., Al'tgauzen, O. N. and Semenova, N. A.: The effect of demagnetization on the permeability of materials used for magnetic circuits 7

Sukazov, E. K.: Reducing the losses in the magnetic circuit of a large ferroresonant voltage stabilizer 1

Sun Iui-Chi and Kravchenko, V. S.: The elimination of arcing in h.f. a.c. circuits 19

Syromiatnikov, I. A.: The relationship between the internal loss and reactive output of synchronous machines 123
Syromiatnikov, I. A.: Automatic equipment for improving power system continuity . . 317
Syromiatnikov, I. A.: The technical and price advantages of synchronous motors . . 599
Trushkov, A. M.: A new method of testing the brushes of electrical machines 186
Vol'kenau, V. A. and **Pruzhinina-Granovskaya, V. I.:** How the post-breakdown voltage on an arrester depends on the length of the current wave-front 529
Volokobinskii, Yu. N., Bogoroditskii, N. P. and **Fridberg, I. D.:** Graphical analysis of the thermal breakdown voltage of h.f. insulators 649

196

REDUCING THE LOSSES IN THE MAGNETIC CIRCUIT OF A LARGE FERRORESONANT VOLTAGE STABILIZER*

E. K. SUKAZOV

(Leningrad)

(Received 6 July 1960)

961

Ferroresonant voltage stabilizers have a comparatively low efficiency. The efficiency of 1 to 10 kVA stabilizers designed as in Fig. 1 is between 0.78 and 0.85 [1]. Not only are the losses themselves considerable, but they also irregularly distributed between the saturated (1) and unsaturated (2) parts of the magnetic circuit. A large part of the losses is concentrated in the core (2) which gives rise to additional difficulties in heat dissipation and also complicates the design of stabilizers over kVA.

Fig. 2 shows a typical magnetic circuit of high power ferroresonant stabilizers. The windings are in the form of cylindrical coils of identical inside diameter for technological reasons.

The core (2) must be saturated over the range of variation in the primary voltage U_1 if their performance of the stabilizers is to be satisfactory. For large ferroresonant stabilizers effective induction B_s in core 2 is usually 1.35 Vb/m^2 "in the state of the second reference point" (i.e. resonance of the currents on no load) [2]. Since B_s is linked with maximum

$$B_m = \frac{\pi}{2k_{sh}} B_s$$

and since an equal-sided trapezium with a shape factor of $k_{sh} = 1.06$ can

* *Elektrichestvo*, No. 1, 39-41, 1961.

be substituted with sufficient accuracy for the output voltage curve, maximum induction is therefore 2.0 Vb/m^2. Core 1 is 1.7 to 2 times larger in cross section than core 2.

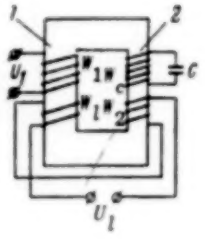

Fig. 1.

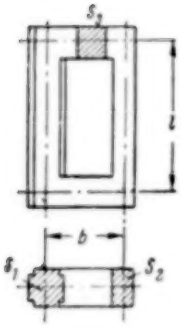

Fig. 2.

Under conditions of current resonance on no load the ratio of the losses in the saturated part to total losses in the magnetic circuit is

$$\beta_1 = \frac{S_2 l d p_1 (B_{m(2)})^2 \cdot 100\%}{S_2 l d p_1 (B_{m(2)})^2 + S_1 (l + 2b) d p_1 \left(B_{m(2)} \frac{S_2}{S_1}\right)^2} = \frac{100\%}{1 + \frac{S_2}{S_1}\left(1 + 2\frac{b}{l}\right)}, \quad (1)$$

where d is the specific gravity of transformer steel,

p_1 the specific losses in the transformer steel at maximum induction;

$B_{m(2)}$ the maximum induction in the saturated core.

But the ratio of the weight of the saturated core to the gross weight of the magnetic circuit provided $S_3 = S_1$ is

$$\beta_2 = \frac{S_2 ld \cdot 100\%}{S_2 ld + S_1 (l + 2b)\, d} = \\ = \frac{100\%}{1 + \frac{S_1}{S_2}\left(1 + 2\frac{b}{l}\right)}. \qquad (2)$$

Suppose we substitute in equations 1 and 2 the above ratio of S_1 to S_2 and the recommended ratio of b to l for the magnetic circuit [l = = (1.5 to 2.0) b] [1, 3, 4]. We then find that 45 per cent of the total loss in the magnetic circuit is concentrated in the saturated core which is only about 20 per cent by weight of the magnetic circuit.

If we can vary the operating induction in the unsaturated part of the magnetic circuit within definite limits without adversely affecting stability, the losses can then be reduced in the saturated part by reducing the specific losses of the metal.

Another way of reducing losses in the saturated core of large ferroresonant stabilizers is to increase the cross-section of the saturated core without altering the rest of the stabilizer elements. To keep the same standard of stabilization as before, the material used for the saturated core must have different properties from that used for the unsaturated part of the magnetic circuit. In his book on ferroresonant stabilizers Lur'e [2] has produced a curve showing the relationship between the magnetism of the saturated core and the stabilization and basic dimensions of the stabilizer. This characteristic represents the effective intensity H_s of the magnetic field as a function of the effective induction B_s:

$$H_s = aB_s^{m+1}. \qquad (3)$$

An increase in the cross section of the saturated core by a factor k ($k \leqslant \frac{S_1}{S_2}$) leads to a proportional decrease in core induction (for current resonance conditions on no load). To maintain the same general regularing characteristic [2] of the stabilizer, the value of the coefficient in equation (3) for the material of the saturated core should be

$$a' = ak^8, \qquad (4)$$

where a is the corresponding coefficient of the material used for the

unsaturated part of the magnetic circuit.

To define the magnetic properties of the metals by means of Lur'e's primary magnetic characteristics, the induction of the material used for the saturated core should be k-times lower than that of the material used for the unsaturated part of the magnetic circuit. If the specific losses corresponding to the maximum hysteresis cycle can be reduced to a greater extent than the saturation induction, total losses in the saturated core can then also be reduced.

The material used for the saturated core should therefore satisfy the following requirements:

$$\left.\begin{aligned} B_{\text{sat}} > B'_{\text{sat}};\quad B'_{\text{sat}} \geqslant \frac{B_{\text{sat}}}{k}; \\ \frac{p'}{p} < \frac{B'_{\text{sat}}}{B_{\text{sat}}}, \end{aligned}\right\} \tag{5}$$

where B'_{sat} and p' are respectively the saturation induction and specific losses corresponding to the maximum hysteresis cycle for the magnetic material of the saturated core; and

B_{sat} and p are the same quantities, but for the material used for unsaturated part of the magnetic circuit (transformer steel).

The losses due to hysteresis are about 85 per cent of the total losses in 0.5 to 0.35 mm gauge transformer steel on a.c. at 50 c/s with a form factor close to that of a sinusoid [5]. The specific losses can therefore only be reduced appreciably if the hysteresis losses are reduced. The hysteresis losses during one cycle can be estimated by Anderson, Lanse and Gumlikh's emphirical formula [6]:

$$p_h = \alpha B_m H_c, \tag{6}$$

where p_h represents the hysteresis losses during one cycle per unit volume of the material;

H_c the coercive force corresponding to the hysteresis cycle with the desired maximum induction, and

$$\alpha = 4\pi(0{,}225 + 0{,}89\times10^{-2}B_m + 0{,}86\times10^{-1}B_m^2).$$

The coercive force remains unchanged if the saturation induction of

ferromagnetic metal is reduced by alloying it with an element with which it forms a solid solution [5]. But in some cases H_c can be increased or decreased by extraneous phenomena. Using formula to estimate the loss due to hysteresis in the maximum cycles for certain materials with successively diminishing saturation induction we see that losses are reduced to a greater extent, the more the saturation induction is decreased. The reduction in losses is a maximum at the lower limit of saturation induction (k = 1.7 to 2).

A study has been made of various elements which form solid solutions with iron and can reduce saturation induction as required. Nickel and aluminium are of particular interest. Permalloy satisfies condition (5), but nickel is in such short supply that permalloy cannot be used for the magnetic circuits of large ferroresonant stabilizers.

In Fe-Al alloys there is a uniform reduction in saturation induction with increasing Al - content up to approximately 14.5 per cent Al.

At this point saturation induction is at a minimum.

Tests on two magnetic circuits have shown that losses then decrease in the saturated core. The dimensions of the magnetic circuits were as follows:

Magnetic circuits	l, mm	b, mm	S_1, cm^2	S_3, cm^2	S_2, cm^2
1	150	100	16.23	12.8	9.6
2	150	100	16.23	12.8	16.23

The saturated section of magnetic circuit 2 was made of sheet Fe-Al alloy 0.35 mm thick. Magnetic circuit 1 and the unsaturated part of 2 was made of E 42 grade transformer steel of the same gauge. Both magnetic circuits were tested in the ferroresonant stabilizer circuit on no load. Tests conditions were such that the induction was the same in the sections S_1 and S_3 over the entire range of variation in the primary voltage of both magnetic circuits.

The tests results showed that with the same stabilization factor the losses in the saturated section of magnetic circuit 2 over the entire range of stabilization were almost a quarter of the losses in the saturated section of magnetic circuit 1. The losses were also more uniformly distributed in magnetic circuit 2 than in 1. Winding losses were the same for both stabilizers.

In conclusion the author wishes to thank V.S. Mes'kin and M.I. Voichinskii for their assistance in this work.

Translated by O.M. Blunn

REFERENCES

1. D.G. Vlasov; *Vest. Elektroprom.*, No. 7, (1953).
2. A.G. Lur'e; *The theory of ferroresonant voltage stabilizers, (Teoriia ferrorezonansnykh stabilizatorov napriazheniia).* Gosenergoizdat, (1958).
3. V.B. Gurvich; *Vest. sviazi*, No. 10, (1951).
4. D.I. Bogdanov and G.K. Evdokimov; *Ferroresonant stabilizers, (Ferrorezonansnye stabilizatory).* Gosenergoizdat, (1958).
5. V.S. Mes'kin; *Ferromagnetic alloys, (Ferromagnitnye splavy).* ONTI, (1937).
6. I.I. Kifer and V.S. Pantiushin; *The testing of ferromagnetic materials, (Ispytanie ferromagnitnykh materialov).* Gosenergoizdat, (1955).

THE EFFECT OF DEMAGNETIZATION ON THE PERMEABILITY OF MATERIALS USED FOR MAGNETIC CIRCUITS*

O.N. AL' TGAUZEN, N.A. SEMENOVA and A.N. STEPANOVA

(Received 2 October 1959)

961

The initial and maximum magnetic permeability and the permeability in a given field are the fundamental characteristics of materials used for the magnetic circuits of transformers, apparatus and instruments etc. These characteristics are usually defined by the ballistic method. On magnetization, there are certain properties of soft magnetic materials which lead to irreproducible results in the measurement of magnetic permeability.

A study has been made of the effect of demagnetization on magnetic permeability and the variation of magnetic permeability with time for certain soft magnetic materials.

The following Fe-Ni alloys were investigated: 50N, 50NP and 65NP grades with a 50 and 65% Ni - content; 79NM with a 79% Ni-content alloyed with molybdenum; and 80NKhS grade with an 80% Ni-content alloyed with chromium and silicon [1-3]. We also investigated E42 and E43 grade hot-rolled electrical steel with a 4% Si-content and E330 grade grain-oriented cold-rolled 3% silicon steel (GOST 802-58) and an IU.16 grade Fe-Al alloy with a 16% Al-content. The testpieces were stacks of stamped rings 6 to 10 mm high with inside and outside diameters of 20 and 30, or 40 and 50 mm.

For grain-oriented alloys, the rings were formed from 10 mm strip in such a way that the direction of rolling was along the strip. The average diameter of these rings was 5 to 20 mm.

---

* *Elektrichestvo*, No. 1, 51-55, 1961.

To obtain the necessary magnetic properties and remove the cold hardening due to the rolling and stamping of the rings of bending of the strip, the testpieces were heat-treated in vacuo at 1100° for 2 to 4 hr. The residual pressure in annealing was up to 1 to 2 x 10^{-2} mm Hg.

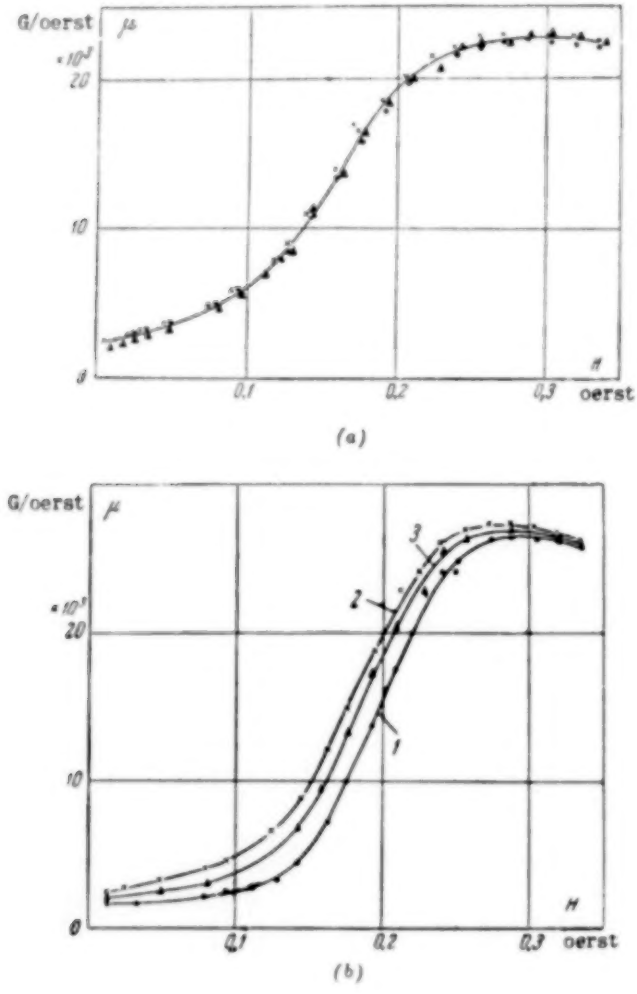

Fig. 1. Magnetic permeability as a function of field intensity for 50N grade Fe-Ni alloy:
a – thickness 1 mm; *b* – thickness 0.1 mm; *1* – after heat treatment; *2* – immediately after demagnetization; *3* – after 168 hr.

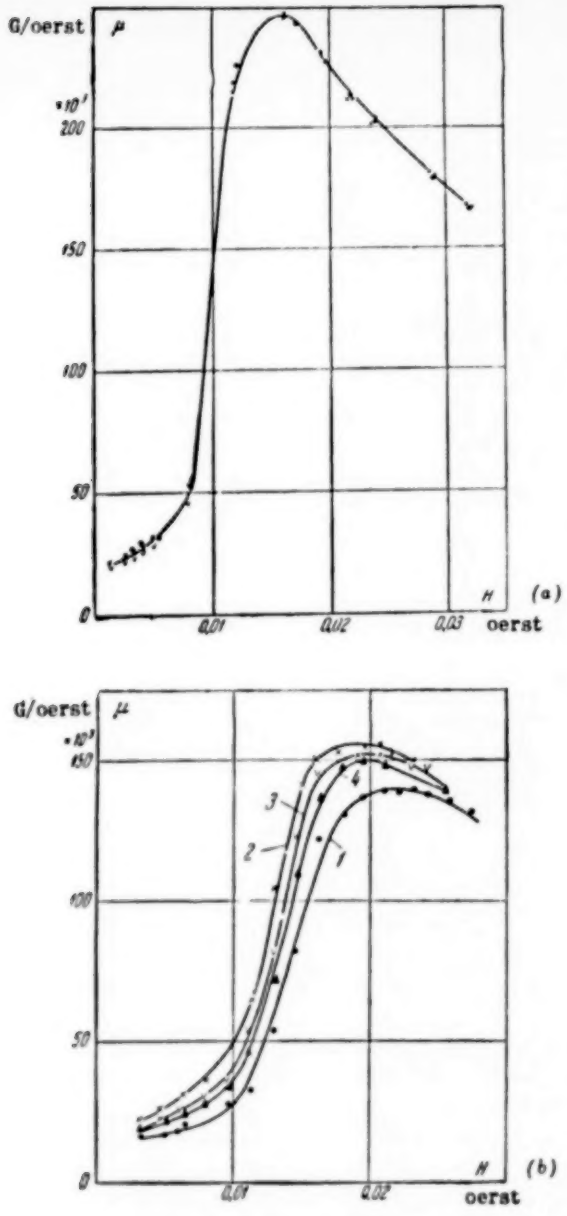

Fig. 2. Magnetic permeability as a function of field intensity for 79NM grade Fe-Ni-Mo alloy:
a – thickness 1 mm; b – thickness 0.2 mm; 1 – after heat treatment; 2 – immediately after demagnetization; 3 – after 24 hr; 4 – after 168 hr.

For hot-rolled steel delivered ex-works after high temperature annealing, the ring stampings were tempered at 750° to eliminate cold hardening. For 65 NP grade Fe-Ni alloy thermo-magnetic treatment was applied at 700° in a field of 15 oersted to obtain optimum properties after high temperature annealing [1-4].

To obtain reproducible results, the magnetic properties were measured after demagnetization of the specimens by alternating current of 50 c/s which diminished to zero.

In order to discover the effect of demagnetization on the magnetic properties, the latter were measured immediately after heat treatment of the specimens which had never before been under the influence of a magnetic field and again after demagnetization of the same specimens by an alternating field. The measurements were taken on d.c. by the ballistic method [5].

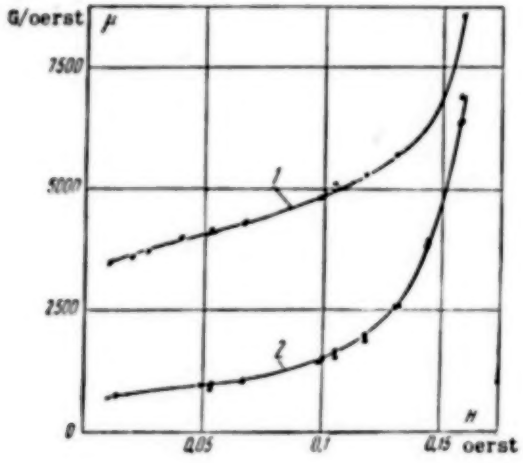

Fig. 3. Magnetic permeability as a function of field intensity for 50NP grade Fe-Ni alloy (thickness 0.05 mm):
1 - after heat treatment; 2 - immediately after demagnetization.

The variation in magnetic properties with time was also measured on these specimens. Different periods of time were allowed to elapse after demagnetization. These measurements were also taken by the ballistic method.

Demagnetization by an a.c. field was repeated after each measurement. The period of time was counted from the moment the demagnetization ceased.

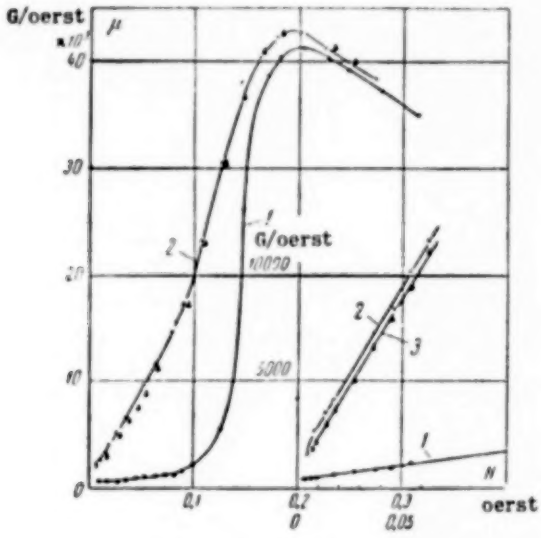

Fig. 4. Magnetic permeability as a function of field intensity for 3% silicon steel (gauge 0.2 mm): *1* – after heat treatment; *2* – immediately after demagnetization; *3* – 24 hr after demagnetization.

Figs. 1 and 2 show the as-measured magnetic permeability of various thicknesses of 50N and 79NM grade Ni-Fe and Ni-Mo-Fe alloys (similar curves were obtained for the 80NKhS grade Fe-Ni-Ch-Si alloy). Fig. 3 illustrates the 50NP grade Fe-Ni alloy and Fig. 4 the electrical steel. The magnetic properties of these alloys are given in Table 1.

The effect of demagnetization

As can be seen from Figs. 1, 2 and 4, the curve for permeability after heat treatment is below that obtained after demagnetization. Demagnetization usually gives rise to the most marked increase in magnetic permeability in the intermediate regions of permeability. Initial and maximum permeability is practically constant. For 50N (Fe-Ni), 80NKhS (Fe-Ni-Ch-Si), 79NM (Fe-Ni-Mo) and 65NP (Fe-Ni) alloys there is a more marked change in permeability with increasing thickness of the material. There is practically no change in permeability at a thickness of 1.0 mm.

TABLE 1

The magnetic properties of test alloys after heat treatment and demagnetization

Grade of alloy	Thickness, mm	Magnetic permeability G/oerst		B_s^*, G	B_r^{**}, G	H_c^{***}, oerst	Magnetic permeability after demagnetization by a.c. field of 50 c/s (magnetic permeability after heat treatment without demagnetization taken as 100%)		
		Initial μ_0	Maximum μ_{max}	Magnetization in a field of 8 oerst			$0'$, %	μ_{max}', %	Maximum change along curve, %
E42	0.5	500	7 800	—	—	—	110—120	—	—
E43	0.35	600	13 800	—	—	—	—	—	—
E330	0.5	450	—	15 500 (H=24oerst)	—	0.5	—	—	—
E330	0.35	800	45 000	14 000 (H=0.6oerst)	—	0.10	200	—	340
E330	0,2	780	42 000	17 000	13 500	0,14	220	105	1 200
50N	1	2 500	23 000	14 100	9 100	0.16	100	100	100
	0.5	2 900	32 300	14 100	10 900	0.17	110	100	110
	0.35	2 600	35 500	14 250	11 100	0,16	110	100	120
	0.2	2 000	33 500	14 500	11 700	0.21	100	100	115
	0,10	2 300	27 500	14 200	11 200	0.22	130	105	240
80NKhS	1	40 000	154 000	6 650	—	0.0135	105	105	115
	0.5	33 000	140 000	7 100	—	0.0147	110	110	130
	0.35	28 000	113 000	6 650	—	0.016	105	105	140
	0.20	30 000	80 000	7 050	—	0.02	125	110	125
	0.1	16 000	55 000	6 500	—	0.036	110	105	140

196

79NM	1	21 500	248 500	8 000	6 700	0.013	100	100	100
	0.5	21 500	274 000	8 100	5 800	0.013	120	100	165
	0.35	24 000	275 000	8 050	5 750	0.0133	120	105	250
	0.2	—	155 000	8 050	4 500	0.017	125	110	200
	0.1	28 000	135 500	8 050	5 100	0.025	120	110	165
IU16	0.35	—	67 000	5 650	3 500	0.022	130 (H=0.005oerst)	100	130
	0.10	2 400	50 000	5 250	2 600	0.03	120	110	140
65NP	0.35	1 300	412 000	13 300	B_r/B_8=0,98	0.036	200	160	—
50NP	0.05	700	62 000	14 800	B_r/B_8=0,915	0.185	15	100	Lowest value 15

* B_8 – induction in field of 8 oerst.

** B_r – residual induction.

*** H_c – coercive force.

Unlike the other Fe-Ni alloys, the curve for permeability after heat treatment is the higher in the case of 50NP grade Fe-Ni alloy (Fig. 3), and a considerable reduction in magnetic permeability occurs in the region of weak fields on demagnetization.

There was no change in the other magnetic characteristics of any of the alloys ("saturation induction", residual induction, coercive force in the maximum hysteresis cycle).

Table 1 shows the magnetic properties of these alloys, the changes in their initial and maximum permeability on demagnetization and the maximum change in their permeability for the whole curve. Table 1 also shows the changes in permeability in respect of 65NP grade Fe-Ni alloy (here the last technological operation was heat treatment with the superimposition of a magnetic field). Unlike the other alloys, there was a considerable increase in permeability on demagnetization, due chiefly to the fact that the alloy was magnetized after thermo-magnetic treatment and the measurement of permeability began from the point of residual induction.

We suppose that the effect of demagnetization on the magnetic permeability of alloys is a magnetic re-orientation ("texturing") in the material in the direction of the demagnetizing field during the process of demagnetization. High magnetic properties are produced in the 50NP grade Fe-Ni alloy during the process of heat treatment by grain orientation ("crystalographic texture") in the direction in which the strip was rolled. It is also possible that a magnetic re-orientation takes place here in the direction of rolling, whereas demagnetization by alternating current changes it and leads to a reduction in permeabili'

The decrease in permeability with time

The decrease in permeability with time has been the object of many investigations [6-12], but the majority have mainly studied the decrease which takes place in short periods of time between the end of magnetization and the beginning of the measurement. We will now give the results we obtained after periods of time lasting from 15 min to dozens of hours. Figs. 1, 2 and 5 refer to 50N grade Fe-Ni alloy and 79NM grade Fe-Ni-Mo alloy and Figs. 4, 6 and 7 to electrical steel.

It can be seen from the curves for Fe-Ni alloys that magnetic permeability usually decreases with increasing periods of time between the end of demagnetization and the start of the measurement. An increase sometimes occurs during periods of 15 to 30 min. The decrease in mag-

netic permeability is most marked at the beginning of the curve (Fig. 5). It can last dozens of hours. Every curve measured after a long period of time tends to approximate to the curve as measured after heat treatment without demagnetization. The effect of demagnetization and the drop in magnetic permeability are more pronounced, the thicker the material under investigation. No decrease with time was observed in specimens in which no demagnetization effect was observed.

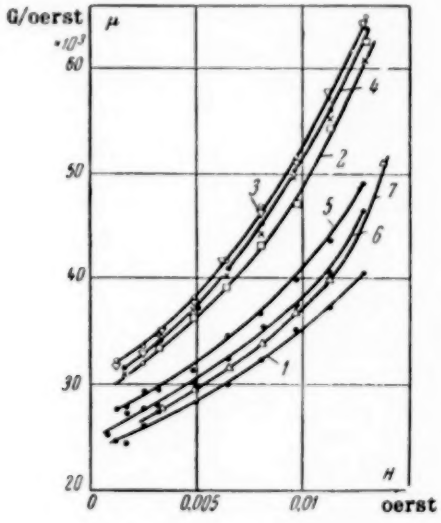

Fig. 5. The magnetic permeability of 79NM grade Fe-Ni-Mo alloy in weak fields (0.01 mm thick):
1 - after heat treatment; *2* - immediately after demagnetization; *3* - after 15 and 30 min; *4* - after 2 hr; *5* - after 24 hr; *6* - after 168 hr; *7* - after 336 hr.

In the case of electrical steel no series of tests was made on specimens of the same heat (melt) but of different gauge. No conclusions can therefore be drawn about the relationship between properties and thickness. Specimens of E-42 and E-43 grade hot-rolled steel of 0.5 mm and 0.35 mm gauge respectively were tested and a decrease with time was observed. The longer the period of time, the greater the decrease (Fig. 6).

Fig. 4 shows curves for cold-rolled 3% silicon steel of 0.2 mm gauge. Despite the considerable increase in permeability on demagnetization, the decrease with time was extremely small even after 48 hr. For E330 grade 0.5 mm gauge steel there was a notable decrease even after 15 min

(Fig. 7); the decrease in permeability continued as the waiting period was increased*. On some steel testpieces the noticeable drop in permeability which began 10 to 15 min after the end of demagnetization and continued for several hrs, can fluctuate during long periods of time. "Delays" also occurred in the start of the decrease with time (during short periods of time the magnetic permeability increased compared with that measured immediately after demagnetization), and the drop in permeability only occurred 2 hr later. At a later date it is necessary to investigate the conditions favouring the various manifestations of the decrease in permeability with time in cold-rolled electrical steel and, above all, the composition of the alloy, the production procedure and the heat treatment.

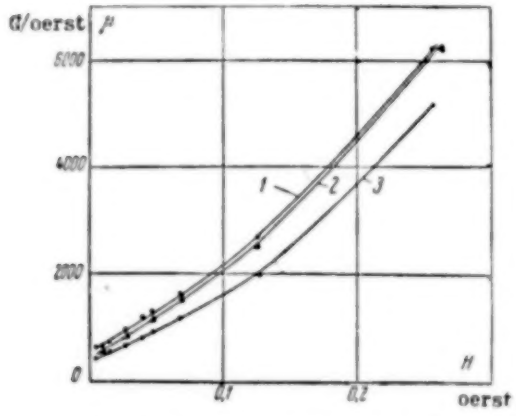

Fig. 6. The magnetic permeability of E43 grade hot-rolled electrical steel (0.35 mm gauge):
1 - immediately after demagnetization; *2* - after 2 hr; *3* - after 24 hr.

Our research into the effect on magnetic permeability of demagnetization and the decrease in permeability with time suggests that the increase in the permeability of 50N, 79NM and 80NKhS grade soft magnetic alloys (Fe-Ni, Fe-Ni-Mo and Fe-Ni-Ch-Si alloys) and the E42 and E43 grade hot-rolled steels on demagnetization is apparently due to the magnetic re-orientation, and that the decrease in permeability with time is due to its reversal. The physics of this phenomenon is not clear and a special investigation is required [6-12]. In grain-oriented material such as 50NP grade Fe-Ni alloy and cold-rolled 3% silicon steel, the cause of changes in magnetic permeability is apparently more complicated. It may be supposed that the grain orientation during heat treatment is accompanied by magnetic orientation and that demagnetization changes it

back and this may lead to an increase or a decrease in permeability. Such changes in permeability may only be partially reversible.

The observable variation in permeability as a function of the first demagnetization after heat treatment and the period of time between the end of demagnetization and the start of the test requires a standard method of determining the magnetic properties of soft magnetic alloys.

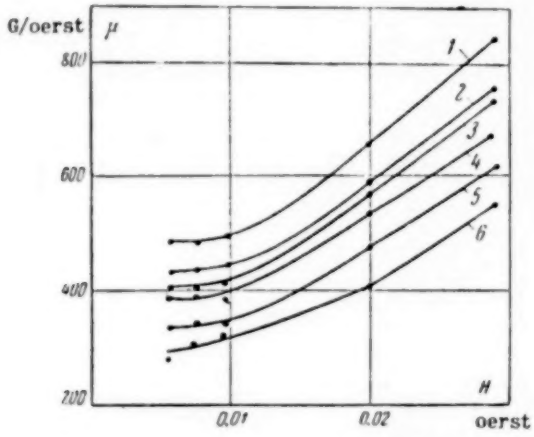

Fig. 7. The magnetic permeability of E330 grade cold-rolled electrical steel (0.5 mm gauge):
1 – immediately after demagnetization; *2* – after 15 min; *3* – after 30 min; *4* – after 1 hr; *5* – after 2 hr; *6* – after 24 hr.

Attention should be paid to the variation in permeability with the period after demagnetization when using these alloys as it can be a source of instability in the operation of electrical gear and a source of additional noise.

Translated by O.M. Blunn

REFERENCES

1. N.P. Gromov, A.I. Il'ichev and N.M. Kasatkin; *Precision alloys, (Pretsizionnye splavy).* Sborn. trud. TsNIIChM.
2. V.Ia. Skotnikov and K.D. Mart'ianova; *Precision alloys, (Pretsizionnye splavy).* Sborn. trud., TsNIIChM, Metallurgizdat, No.15, (1956).
3. V.Ia. Skotnikov and K.D. Mart'ianova; *Precision alloys (Pretsizionnye*

splavy). Sborn. trud., TsNIIChM, Metallurgizdat, No. 23, (1960).
4. O.N. Al'tgauzen, Sh.I. Zusman and A.N. Stepanova; *Metalloved. i term. obrabotka*, No. 11, (1958).
5. I.I. Kifer and V.S. Pantiushin; *The testing of ferromagnetic materials, (Ispytanie ferromagnitnykh materialov)*. Gosenergoizdat, (1955).
6. S.V. Vonsovskii and Ia.S. Shur; *Ferromagnetism, (Ferromagnetizm)*. Gostekhizdat, (1948).
7. R. Bozort; *Ferromagnetism, (Ferromagnetizm)*. *Iz. inost. lit.*, (1956).
8. Iu.S. Vail'; *Iz. Akad. Nauk SSSR, ser. fiz.*, 21, No.9, 1281, (1957).
9. V.V. Druzhinin; *Biull. tekh. inf.*, VIZ, 42, (1957).
10. R.V. Telesnin; *Scientific records of the MGU, (Uchenye zapiski MGU)*. Fiz. 6, No. 162, (1952).
11. F. Schreiber; *Z. ang. Phys.*, 9, No.4, 203, (1957).
12. E.S. Annalik and J. Singer; *J. Appl. Phys.*, 29, No. 3, 412, (1958).

THE ELIMINATION OF ARCING IN HIGH FREQUENCY A.C. CIRCUITS*

V.S. KRAVCHENKO and SUN IUI-CHI

(Mining Institute of the Academy of Sciences USSR)

(Received 20 June 1960)

The research which has so far been undertaken into the phenomena of electrical discharges in high frequency a.c. circuits [1-5] has still to provide a satisfactory answer to the problem of making such circuits free from arcing. It has been shown that arcing is more pronounced when opening capacitive-inductive circuits or circuits with a very low inductance on high frequency a.c. than on d.c. The reason is the shortened length of the discharges when quenched during the passage of current through zero.

Gavril'chenko has now discovered that the ignition currents will only increase up to a definite frequency [2]. A further increase in frequency leads to a decrease in ignition current. Thus, for example, in one series of experiments an increase in frequency up to 20 kc/s led to a fourfold increase in the value of the arcing current on a.c. as compared with d.c. In another series of experiments Gavril'chenko found that a further increase in supply frequency up to 150 kc/s reduced this current by a factor of three.

It is well known that a considerable increase in frequency leads to the failure of the electrodes to cool on the passage of current through zero and the conditions in the sparkgap continue favourable for a discharge. Thus conditions again arise at still higher frequencies which are instrumental in maintaining the electrical arc and increasing the energy developed there. This paper is a continuation of the research

* *Elektrichestvo*, No.1, 77-80, 1961.

referred to above in which a study was made of the conditions under which inductive and inductive-capactive a.c. circuits can be made proof against arcing at frequencies of 5 to 20 kc/s in hydrogen-air atmospheres of the most explosive composition (hydrogen content 20% of air by volume).

It is now considered that the arcing capacity of the discharges which occur when low-power electrical circuits are opened mainly depends on the magnitude of the energy A which enters into the discharge. For inductive-capacitive and inductive d.c. circuits (Fig. 1) the value of A is approximately [6, 7]:

$$A \approx \frac{LI^2}{2} + \frac{UI}{6}\tau_m, \tag{1}$$

where L is the inductance of the circuit;

I the current;

U the voltage of the current source; and

τ_m the maximum duration of the discharge.

Explosion of the medium takes place if $A \geq A_{min}$, where A_{min} is the minimum value of the energy sufficient to initiate an arc (limit of ignition).

Equation 1 shows that the arcing capacity of the discharges which occur when the specified circuits are opened is fully defined by the inductance, current and voltage. It is therefore customary to estimate the degree of freedom from arcing by plotting the discharge current as a function of the circuit inductance and applied voltage using the results of tests in explosion chambers with the same probability of explosion (e.g. $P = 10^{-3}$ or $P = 10^{-5}$).

For inductive-capacitive circuits (Fig. 2) in which the discharge of the capacitance takes place on the breakdown of the sparkgap, the explosion is determined by the amount of energy in the arc on the discharge of the capacitance [6]:

$$A = \frac{CU_{Cm}^2}{2}. \tag{2}$$

where U_{Cm} is the maximum possible voltage on the discharged capacitance which determines the amount of energy stored there.

The level of ignition to a large extent depends on the arc quenching

properties of the electrodes. It has been established that the arc-extinguishing effect of the electrodes diminishes the further they are apart. Therefore, the level of ignition is lowered abruptly if the gap is increased [9]. They cease to have any quenching effect when 2 mm apart and the level of ignition is then a minimum (this is also its "absolute limit", equal to 0.019 mJ for hydrogen-air and 0.28 mJ for methane-air).

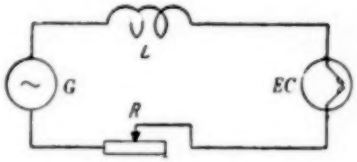

Fig. 1. Inductive circuit.
G – h.f. generator; *EC* – explosion chamber with a conventional spark-producing device.

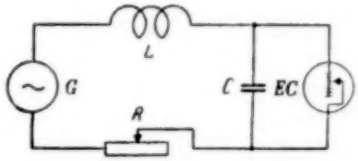

Fig. 2. Inductive-capacitive circuit.
G – h.f. generator; *EC* – explosion chamber with a "make-break"-type spark-producing device.

In accordance with equation (2) we have plotted experimental curves which take the actual conditions of arc formation into account and define the freedom from arcing of capacitive circuits. They represent the variation in maximum capacitor voltage with the magnitude of the capacitance. They are based on the results of tests in explosion chambers with the same probability of explosion [8].

These were the principles we followed in order to estimate the arcing capacity of discharges when opening a.c. circuits.

Fig. 3 shows experimentally-determined curves for estimating the extent to which d.c. and a.c. inductive circuits are proof against arcing as a function of inductance (a) and frequency (b). The effect of generator self-inductance was eliminated by shunting the inductance of

the input transformer by a "non-reactive resistance" (capacitive reactance) the magnitude of which we fixed by trial and error. The discharges were produced by parting a steel wire 0.2 mm in diameter from a steel bar 0.8 mm in diameter. The probability of explosion was $P = 10^{-3}$. The d.c. supply voltage from an accumulator was 170 V. The maximum voltage of the a.c. source was 177 V.

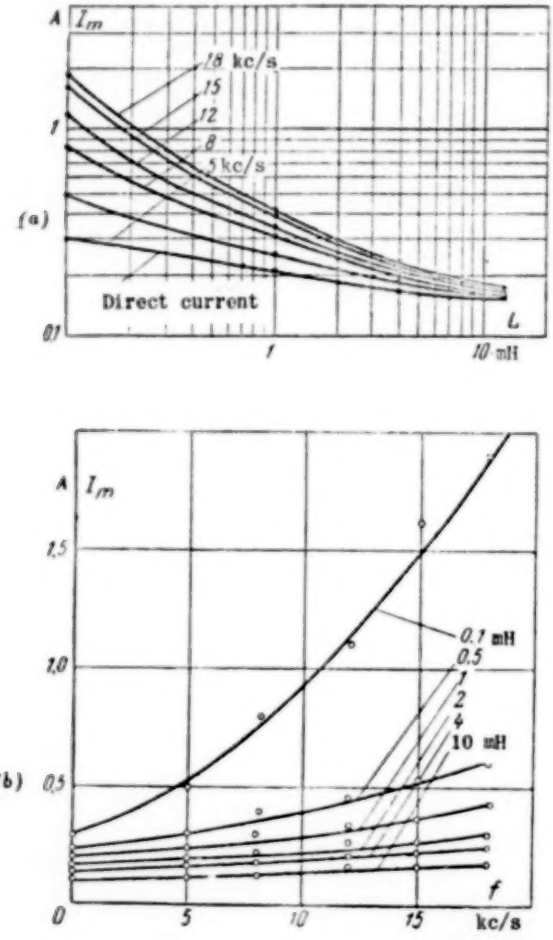

Fig. 3. Minimum ignition currents ($P = 10^{-3}$) in an inductive circuit.

The test results show that arcing currents increase in inductive circuits with increases in supply frequency up to 20 kc/s. Compared

with direct current, this increase is four times greater in a.c. circuits with a small inductance (< 0.5 mH) than in d.c. circuits, but it is barely noticeable in a.c. circuits if the inductance is greater than 1 mH. In all cases under investigation (inductances from 0.1 to 10 mH) discharges were always more dangerous (i.e. explosions occurred at lower currents) when opening d.c. circuits than when opening high frequency a.c. circuits. The difference between d.c. and a.c. arcing currents become less and less as the inductance was increased from 0.5 to 10 mH.

Fig. 4 shows the curves obtained to estimate the freedom from arcing of d.c. and a.c. inductive-capacitive circuits. The discharges were produced in a similar hydrogen-air medium by a sparking device which provided intermittent arcing (which is more dangerous in capacitive circuits) by the movement of a sharp steel wire 0.2 mm in diameter over the surface of a notched steel plate. The probability of explosion was $P = 5 \times 10^{-2}$.

We used the following formula to determine the amplitude of the capacitance alternating voltage after opening (or before making) the circuit:

$$U_{Cm} = \frac{I\sqrt{2}}{\omega C}, \tag{3}$$

where I is the effective current with open contacts, and $\omega = 2\pi f$ the angular frequency.

The maximum calculated surges on the capacitance were between 1.2 and 1.5 U_{C_m} (1.35 U_{C_m} on average) at different moments of time during the opening of the circuit.

The tests showed that the degree of proof against arcing in inductive-capacitive circuits under the given arcing conditions depends entirely on the "steady state" voltage on the capacitance at the ignition limit for the various values of capacitance and it is this characteristic which we found at frequencies of 5 to 15 kc/s and inductance of 1 to 20 mH under resonant and non-resonant conditions. The minimum ignition energy was roughly constant and equal to 0.24 ± 0.03 mJ (i.e. the average deviation was only $\pm$ 12 per cent) for circuit capacitance between 0.01 and 1 F, inductance between 1 and 20 mH, maximum voltage on the capacitance between 22 and 253 V, trip current between 0.07 and 0.42 A and at frequencies between 5 and 15 kc/s.

The minimum ignition energy was greater than the level of ignition. The explanation is the considerably flame-quenching effect of the con-

tacts, typical of ordinary conditions of interruption. Thus, in high frequency inductive-capacitive circuits the arcing capacity of the discharges in the range under investigation mainly depended on their energy. The arcing capacity was independent of frequency changes and circuit factors.

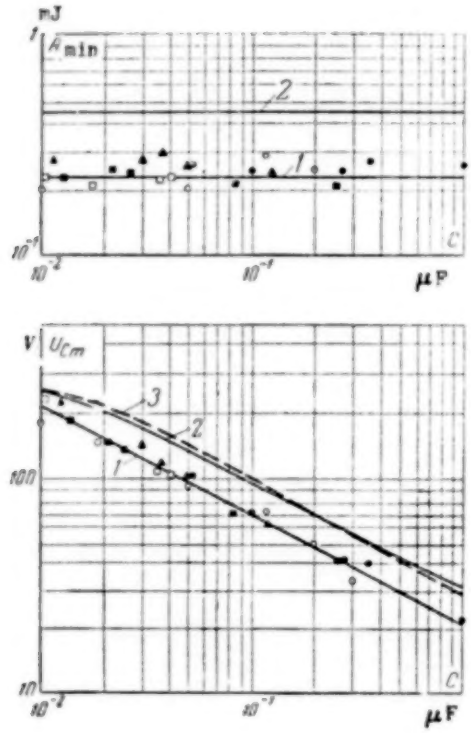

Fig. 4. Minimum ignition energy and maximum capacitor voltages ($P = 5 \times 10^{-2}$) as a function of capacitance at various frequencies and different values of circuit inductance:
1 – amplitudinal values of the steady state voltages on the capacitance and the corresponding energies; 2 – maximum values of the overvoltages on the capacitance and the corresponding energies; 3 – ignition voltages on discharge of the capacitor [8]. ▲ 15 kc/s, ■ 10 kc/s, ● 5 kc/s with resonance; □ 10 kc/s, ○ 5 kc/s without resonance.

We will now consider the effect of frequency changes on the ignition

currents for various values of circuit capacitance and inductance. It follows from equations 2 and 3 that the minimum ignition current ($A = A_{min}$) in an inductive-capacitive circuit is:

$$I_{min} = \omega \sqrt{CL_{min}} \tag{4}$$

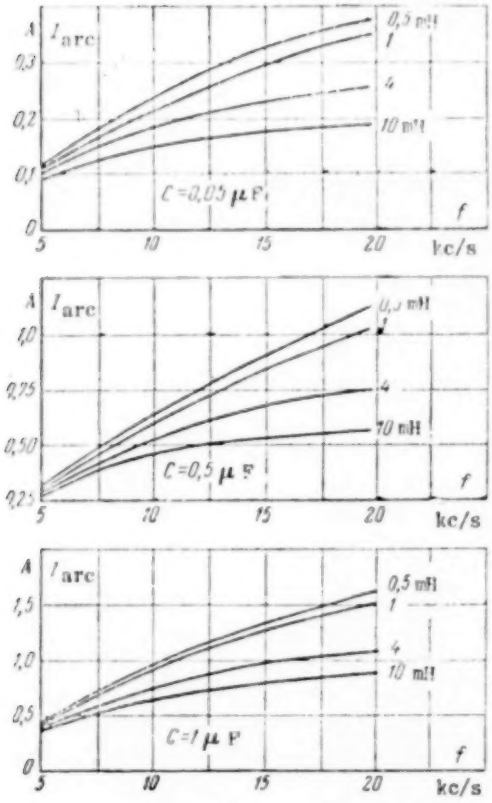

Fig. 5. The effective minimum ignition currents as measured in inductive-capacitive circuits before "opening" of the capacitance as a function of the current frequency at various values of the inductance and capacitance.

The minimum ignition current is therefore greater, the higher the frequency and capacitance and it is independent of other circuit factors.

These circuit factors can be determined from the condition of the equality of the current in an inductive-capacitive circuit to the maximum ignition current. Thus, for example, given the inductance, the explosion of the medium takes place if the resistance of the circuit does not exceed:

$$R = \sqrt{\frac{U^2}{\omega^2 C A_{\min}} - \left(\omega L - \frac{1}{\omega C}\right)^2}, \tag{5}$$

where U is the effective voltage of the h.f. current source.

The minimum ignition current in a circuit with a closed capacitance is:

$$I_{arc} = \frac{U}{\sqrt{R + \omega^2 L^2}} = \frac{U}{\sqrt{\frac{1}{\omega^2 C}\left(\frac{U^2}{A_{\min}} - \frac{1}{C}\right) + 2\frac{L}{C}}}. \tag{6}$$

Fig. 5 shows the ignition current as a function of frequency for various values of circuit inductance and capacitance. It can be seen that an increase in frequency up to 20 kc/s always entails an increase in I_{ig} within the given limits of inductance and capacitance. Large currents correspond to large capacitances and small inductances.

In connexion with the constancy of the minimum ignition energy at different voltages, capacitances, inductances and frequencies, it is of interest to mention that a considerable part of the energy entering into the discharge when an inductive circuit is opened is energy which has been stored in the inductance. With increasing inductance this component of the energy approximates to the stated limit 0.24 mJ equalling 0.22 mJ for $L = 10$ mH at frequencies between 5 and 18 kc/s ($P = 10^{-3}$). However, with decreasing inductance, the stated energy component drops abruptly and only amounts to about one tenth of the minimum ignition energy for an inductance of 0.5 mH under the same conditions. In this latter case the rest of the energy comes from the current source. As previously pointed out [5], the energy component in question is greatly dependent on frequency. Hence the effect of frequency on the ignition current is most marked in circuits with small inductance.

Conclusions

1. This analysis of the phenomena of the discharges which occur when opening high frequency circuits has confirmed that the minimum ignition energy of these discharges is constant within the investigated limits.

A mathematical expression has been derived for the arcing conditions in inductive-capacitive circuits.

2. The calculations and test results show the effect of frequency on minimum ignition currents in inductive and inductive-capacitive circuits for various values of circuit inductance and capacitance.

3. Our new experimental data concerning minimum ignition currents and voltages in inductive and inductive-capacitive high frequency circuits with and without resonance at various values of circuit inductance and capacitance can be used in the development to make a qualitative estimate of the extent to which electrical circuits are proof against arcing at frequencies up to 20 kc/s.

Translated by O.M. Blunn

961

REFERENCES

1. N.I. Brozknik and K.A. Skrynikov; *Zhur. tekh. fiz.*, 4, (1934).
2. L.I. Gavril'chenko; *The freedom of explosive mixtures from arcing in the use of h.f. currents, (Iskrobezopasnost' vzryvnykh semesei pri primenenii tokov vysokoi chastoty).*
3. A.V. Itin; *Izvest, Dnepro. gorn. inst.*, XXIII, (1958).
4. P.F. Kovalev; *Principles underlying sparkproof electrical mining equipment, (Printsipy vzryvobezopasnosti rudnichnogo elektrooboru dovaniia).* Ugletekhizdat, (1951).
5. V.S. Kravchenko; *Fundamentals of the safe use of electricity in underground workings, (Osnovy bezopasnogo primeneniia elektrichestva v podzemnykh vyrobotkakh).* Sborn. "Sov. gorn. nauk", Ugletekhizdat, (1957).
6. B.A. Petrenko; *Scientific research on the winning of coal and ore deposits, (Nauchnye issledovaniia po razrabotke ugol'nykh i rudnykh mestorozhdenii).* Gosgortekhizdat, (1959).
7. B.A. Petrenko; *The elimination of arcing in electrical equipment, (Vzryvobezopasnoe elektrooborudovanie).* TsBTI Elektroprom., (1959).
8. M.B. Blanc, P.G. Guest, G. Elbe and B. Lewis; *J. chem. phys.*, 15, No. 11, (1947).

A ZERO SEQUENCE POWER RELAY WITH CURRENT POLARIZATION*

V.I. GRINSHTEIN

(Cheboksary)

(Received 17 March 1960)

This new relay is a two-way power relay. It is for use in systems of earth fault protection and also in those cases when there is no corresponding voltage transformer. The relay has two windings. One winding carries the zero sequence current of the equipment to be protected and the other winding the polarizing current which can be obtained from current transformers. The relay can also be used for transverse differential protection.

Use is made of P7-type polarized relays as the "executive" devices in the relay in question.

The circuit of the new relay is shown in Fig. 1. It operates on the following principle.

The primary windings of the input transformers *Tr* 1 and *Tr* 2 are divided into two sections. The series and parallel connexion of these sections is used to change the sensitivity of the relay.

The secondary windings of the transformer are also sectionalized and connected in pairs so that the geometric sum of the two transformers is obtained at the output of one pair of secondary windings:

$$\dot{E}_1 + \dot{E}_2 = \dot{U}_2, \qquad (1)$$

* *Elektrichestvo*, 1, 81-82, 1960.

and their geometric difference at the output of the other pair:

$$\dot{E}_1 - \dot{E}_2 = \dot{U}_1. \tag{2}$$

The sum and difference of the voltages in question are fed to the windings of two interposing relay via rectifier bridges composed of junction-type germanium diodes.

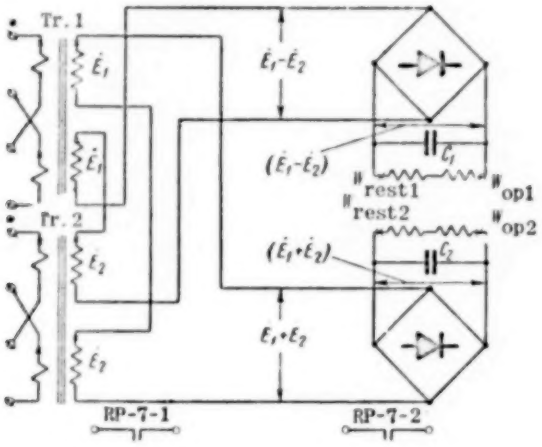

Fig. 1. Relay circuit.

The windings of the interposing relays are in two parts (the one part operating and the other restraining). The windings contain the same number of turns. The restraint winding of the first relay and the operating winding of the second relay are connected to voltage U_1, and the operating winding of the first relay and the restraint winding of the second to the voltage U_2.

The angle of maximum sensitivity $\phi_{s.s}$ is 0 and 180° for the same primary currents in the transformers. When $\phi_{s.s} = 0$

$$\dot{E}_1 - \dot{E}_2 = 0; \tag{3}$$

$$\dot{E}_1 + \dot{E}_2 = \dot{U}_2 = 2E_1. \tag{4}$$

Under these conditions maximum current flows in the operating winding of the first relay and in the restraint winding of the second relay, which leads to the operation of the first interposing relay and the restraint of the second.

The reverse takes place if $\phi_{m.s} = 180^0$.

If $\phi = \pm 90^0$, then $\dot{U}_1 = \dot{U}_2$ and the operating and restraining moments of the relays are different and the interposing relays do not function.

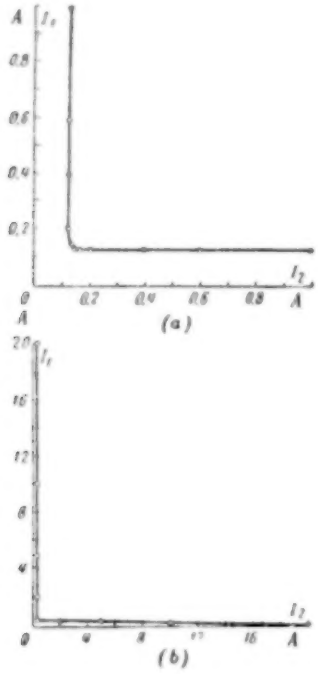

Fig. 2. I_1 as a function of I_2 at an angle $\phi_{m.s}$ of maximum sensitivity equal to 0^0 (a) and 180^0 (b).

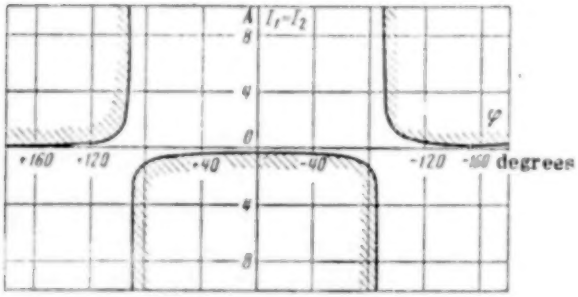

Fig. 3. Angular characteristics of the relay.

This method can therefore be used to make two-way power relays.

The operating current of the relay in question is 0182 A and the power consumption 4.5 volt-amps on each winding. The angle of maximum sensitivity is sufficiently stable over a wide range of current variation.

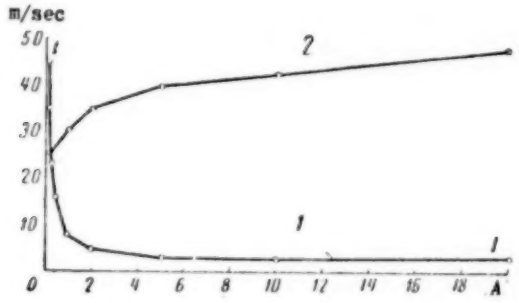

Fig. 4. Time characteristics of the relay: 1 – the time to close the normally open contact on an instantaneous increase in current; 2 – the time to open the normally open contacts on an instantaneous decrease in current from a given value to zero.

Compared with existing induction-type power relays, this new relay has smaller dimensions, lower power consumption, greater sensitivity, faster operating speed and there are no rotating parts.

Translated by O.M. Blunn

ABSTRACTS FROM PAPERS PUBLISHED IN ELEKTRICHESTVO No. 1, 1961

Design Formulae

Calculations in circuits with elements of non-linear inertia. O.M. Bogatyrev, (pp. 69-76).

A study is made of circuits with one, two and three different non-linear inert elements under steady state sinusoidal conditions. An analytical method is developed in place of the graphical method previously used. An example is given.

Magnetism

An appraisal of methods of calculating magnetic circuits with air gaps for instruments and apparatus. Z.T. Tikhomirova, (pp. 42-48).

A comparative critical analysis is made of four Soviet methods of designing the magnetic circuits of electrical apparatus on the basis of experimentally-determined data. The Sotskov graphical-analytical method is the simplest but it is only suitable for preliminary calculations. Numerical integration, graphical integration and the "isocline" method are considered. (An isocline is defined as the locus of points at which the tangents to the integral curves have the same slope).

Measuring losses in ferro-magnetic materials magnetized simultaneously by fields of different frequencies. N.M. Rudnyi, et al., (pp. 48-51).

An original method is proposed for measuring losses for the most general case of combined magnetization when the frequencies of the

individual field components are "non-multiple" and none are zero. The wattmeter measuring device is described with particular reference to a special phase-shifting voltmeter. The error is ± 5 per cent.

Power systems

The efficiency of inter-system transmission lines for supplying a local distributed load. Lo Bai-chan, (pp. 1-8).

Power systems have been developed in the U.S.S.R. and China on a regional basis owing to the vastness of these countries. The author considers the optimum conditions for inter-system links with or without uniform load distribution throughout the various regions.

The design of reinforced-aluminium conductors for transmission lines. O.G. Veksel'man, (pp. 9-15).

After reviewing Western experience with reinforced aluminium conductors, the author states the case for reducing the unnecessarily high safety factor on similar Russian constructions. The value of dampers is stressed.

Relays and Protection

Special features of relay protection on lines supplying traction substations. D.I. Veprik et al., (pp. 15-22).

The proposal to electrify about 20 thousand km of railway lines on single phase a.c. at 50 c/s under the current 7-year plan requires that the supply conditions of the substations should be arranged to meet the needs of relay protection and automatic equipment. Transverse differential directional protection, three-stage directional zero sequence current protection, automatic reclosure and 'reserve disconnexion' systems are considered.

Rotating Machines

The parameters, steady state characteristics and stability of synchronous generators with electronic self-excitation.

V.F. Chesachenko, (pp. 22-29).

A study is made of the static and dynamic stability of an unsaturated synchronous non-salient pole generator supplying infinite bus-bars through a reactance. The author studies the adjustment of the anode-grid regulation, the nominal firing angle and the transformation ratio of the anode transformer.

The motor drive of the winches for the fore cables of a dredge. B.Sh. Burgin, (pp. 30-34).

An analysis is made of cable forces and speeds in a new d.c. motor-generator system for which definite advantages are claimed over a.c. variable speed motors.

The design of current regulators for the electronic excitation systems of rolling mill motors. N.P. Kunitskii, (pp. 34-39).

A method is proposed for calculating the current winding unit in a system of ionic excitation for reversible rolling mill motors developed in the U.S.S.R. The current winding is connected via a rectifier to a voltage proportional to the difference between the voltage drop in the compensation and compole windings and a reference voltage.

Automation of the motor drive for a continuous reduction tube-rolling mill. S.S. Roizen et al., (pp. 82-85).

Excessive heating of the motors occurred on a Russian 20-stand tube rolling mill. Some of the motors were overloaded and other passed into generator conditions. It was decided to provide all the motors with regulators to maintain their speed constant to within 0.5 per cent. An account is given of how this problem was tackled by using the frequency of an a.c. tacho-generator as the speed reference together with a special converter.

Switchgear

Determining the power factor of a test circuit by means of a wattmeter vibrator. I.B. Bolotin, (pp. 66-69).

A new improved device called a "wattmeter vibrator" has been developed to measure the power factor of circuits for testing the

rupturing capacity of switchgear.

Transformers

Current transformers with an air gap in their steel core. I.M. Sirota, (pp. 56-61).

Large m.m.f. arise in current transformers used in relay protection under certain conditions. Residual magnetization has been eliminated by making the magnetic circuits of the transformers with a small gap. A study is made of the relationships governing the size of this gap. A gap equal to $\frac{1}{500}$th of the centre magnetic limb is recommended for one type of steel.

Transients in current transformers. E.M. Pevzner, (pp. 61-66).

Since relay protection operates while the current transformer is still under transient conditions, the author proposes a new practical method of calculating the transient performance of the transformer. This can be estimated to within 15 to 20 per cent. Residual induction and a number of other factors is taken into account. The peak magnetization current can be fixed in time.

THE RE-SYNCHRONIZATION OF THE GENERATOR BY THE TURBINE SPEED-GOVERNOR*

M. P. CHESNOV

Power Institute of the Academy of Sciences U.S.S.R.

(Received 12 November 1960)

1961

When the dynamic stability of a generator in a large power system is disturbed, it is possible for it to brought back into step without the interference of the service personnel [1]. Research at the Moscow Power Institute** on a dynamic simulator has shown that the motion of the generator rotor under transient out-of-step conditions is mainly determined by the speed-governor of the turbine. It is therefore of interest to study how the turbine speed-governor affects re-synchronization.

It is well known that the passage of the instantaneous slip through zero is a necessary condition for the re-synchronization of a generator. This condition can be represented in the form [2]:

$$[s_{av}(t)]_{min} \leq \sqrt{\frac{2M_{12}}{J}}. \tag{1}$$

The variation in average slip with time $s_{av}(t)$ under asynchronous conditions can be defined by the joint solution of the linear equations of the individual parts of the speed governor [3] and the linearized equation of motion of the rotor. The periodic components of the electromagnetic moment of the generator can be ignored since they have

---

*Elektrichestvo, 2, 24-28, 1961.

**The research was undertaken by the author jointly with Iu.M. Gorskii.

practically no effect on turbine torque owing to the inertia of the speed control system (this is particularly the case with hydro-electric turbines) [2, 5]. The equation of motion of the rotor can be linearized by representing the asynchronous torque curve as a series of short straight lines. Ignoring the impedance of the supply, the equation of rotor motion simplifies to

$$J\frac{ds_{av}}{dt}+(a_n+k_n s_{av})=M_t, \tag{2}$$

where $a_n + k_n s_{av}$ is the equation of the n-th section of the piecewise-linear asynchronous torque curve of the generator.

Omitting the intermediate calculations, the differential equations with respect to s_{av} in their final form are:

(a) Throttle partly open ($|\sigma|<1$)

$$\begin{aligned}&JT_iT_s\frac{d^3s_{av}}{dt^3}+[T_iT_sk_n+J(T_s+\beta T_i)]\frac{d^2s_{av}}{dt^2}+\\&+\left[(T_s+\beta T_i)k_n+iJ+\frac{T_iM_{t.nom}}{\mu_{x.x}\delta_{nu}}\right]\frac{ds_{av}}{dt}+\\&+\left[ik_n+\frac{M_{t.nom}}{\mu_{x.x}\delta_{nu}}\right]s_{av}=i(M_{t0}-a_n).\end{aligned} \tag{3}$$

(b) Throttle completely open ($|\sigma|=1$)

$$J\frac{ds_{av}}{dt}+k_ns_{av}=M_{t.c.o}-a_n\pm M_{t.nom}\frac{t}{\mu_{x.x}T_s}. \tag{4}$$

(c) For control gear of turbine completely "off":

$$J\frac{ds_{av}}{dt}+k_ns_{av}=M_{t.r}-a_n. \tag{5}$$

Unlike the previous case [2]*, the flexible feedback of the speed regulator now has to be included in forming these equations. However, equations (4) and (5) are independent of the type of speed regulator. They are identical to the corresponding equations used in the previous paper [2].

* The article referred to has already been translated and appears in Electric Technology U.S.S.R. vol. 6, 1960. The speed regulator then had rigid feedback.

We can find the average slip as a function of time by differentiating equations (3) to (5). On passing from the $(n-1)$-th straight section of the asynchronous torque curve to the n-th section, the tangent of the angle of inclination k_n of this section to the X-axis can differ from k_{n-1} both in magnitude and in sign. The coefficients which depend on k_n in the foregoing differential equations and the roots of the characteristic equations can also vary in magnitude and sign. Consequently, the solutions of equations (3) to (5) can change on moving from one linear section of the asynchronous torque curve to another.

We will now consider the most typical case when all the coefficients in (3) are positive and the general solution of (3) is:

$$s_{av}(t) = Ae^{-\alpha_1 t} + e^{-\alpha t}(B\sin\gamma t + C\cos\gamma t) + s_{av.st}, \tag{6}$$

where $s_{av.st}$ is the particular solution of equation (3), numerically equal to the slip at the point where the static characteristic of the speed regulator intersects that of the asynchronous generator torque;

$$B = \frac{(\alpha^2 - \alpha_1^2 - \gamma^2)[d + \alpha_1(s_{av0} - s_{av.st})] - (\alpha_1 - \alpha)[f - \alpha_1^2(s_{av0} - s_{av.st})]}{\gamma(\alpha^2 - \alpha_1^2 - \gamma^2) + 2\alpha(\alpha_1 - \alpha)};$$

$$d = \frac{M_{t0} - a_n - k_n s_{av0}}{J};$$

$$f = \frac{\sigma_0 M_{t.nom}}{JT_a \mu_{n.1}} - \frac{k_n}{J^2}(M_{t0} - a_n - k_n s_{av0});$$

$$C = -\frac{[d + \alpha_1(s_{av0} - s_{av.st})]2\alpha + f - \alpha_1^2(s_{av0} - s_{av.st})}{(\alpha_1 - \alpha)^2 + \gamma^2};$$

$$A = s_{av0} - s_{av.st} - C.$$

The variation in turbine torque with time can be found by equations (2) and (6):

$$M_t(t) = J[e^{-\alpha t}(C_1\cos\gamma t - B_1\sin\gamma t) - \alpha_1 Ae^{-\alpha_1 t}] + a_n + k_n s_{av}, \tag{7}$$

where

$$B_1 = \alpha B + \gamma C;$$

$$C_1 = \gamma B - \alpha C.$$

It follows from (6) and (7) that the free components of the slip $s_{av}(t)$ are damped during the passage of time and, consequently, the turbine torque $M_t(t)$ is in this case also damped. But it should be borne in mind that even if only one of the roots of the characteristic equation is positive on certain of the linear sections of the asynchronous torque curve, then these components have a tendency to increase indefinitely with time. Physically, this implies that the excess torque affecting the rotor is still further increased when the slip changes through the transient torque section in question.

Under transient asynchronous conditions, especially when the slip is considerable, part of the speed control process takes place when the governor valves are completely open and it is then represented by equation 4. The general solution of this equation is:

$$s_{av}(t) = De^{p_1 t} \pm Nt + L, \tag{8}$$

where p_1 is the root of the characteristic equation;

$$L = \frac{\mu_{x.x} k_n T_s (Ai_{t.c.o.v} - a_n) \mp JM_{t.nom}}{\mu_{x.x} T_s k_n^2};$$

$$N = \frac{M_{t.nom}}{T_s k_n \mu_{n.1}};$$

$$D = s_{av.c.o.v} - L.$$

In this case the change in the turbine torque can be found from equations (2) and (8):

$$M_t(t) = J(p_1 De^{p_1 t} \pm N) + a_n + k_n s_{av}. \tag{9}$$

If the turbine control gear is completely "off" for a certain period of time under transient conditions, the motion of the rotor is then determined by equation (5) of this section. Its general solution can be written in the form:

$$s_{av}(t) = Ge^{p_2 t} + E, \tag{10}$$

where p_2 is the root of the characteristic equation;

$$E = \frac{M_{t.r} - a_n}{k_n};$$

$$G = s_{\text{av.t.g.c}} E.$$

In analysing the transient process, the extent to which the throttle is open σ can be found from the equations of the various components of the speed regulator [3,4].

The effect of the speed regulator on the process of re-synchronization can be traced by analysing the dynamic characteristics of the speed regulator $M_t = f(s_{av})$. These give a complete picture of the generating set under transient conditions. Such curves are easy to plot if the functions $s_{av}(t)$ and $M_t(t)$ are known.

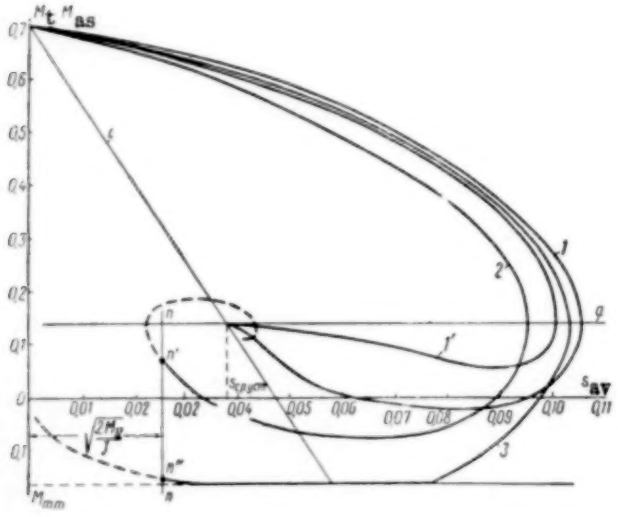

Fig. 1.

1 – $\beta = 5$ and $T_i = 8$ sec; 2 – $\beta = 5$ and $T_i = 3$ sec; 3 – $\beta = 0$ and $T_i = 8$ sec; $i = 2.35$; $\mu_{a.l} = 0.85$; $J = 15.1$ sec; 1' – experimental curve; 1 – corresponding calculated curve.

Figs. 1 and 2 show M_t as a function of s_{av} as well as the static characteristics (c, c' and c") of the speed regulator and the asynchronous torque curves (a, a' and a") of the generator. These are assumed to be linear for the sake of simplicity. This is a justi-

assumption since the asynchronous torque curve is usually a maximum when the slip is very small and the section of the curve lying to the left of this maximum can be ignored.

Out-of-step operation thus takes place on the section of the asynchronous torque curve lying to the right of the maximum. This section can usually be linearized over a considerable range of slip values for turbo and hydro-electric generators having damper windings. However, this is not a necessary simplification, and it is only made so as to reduce the amount of calculation.

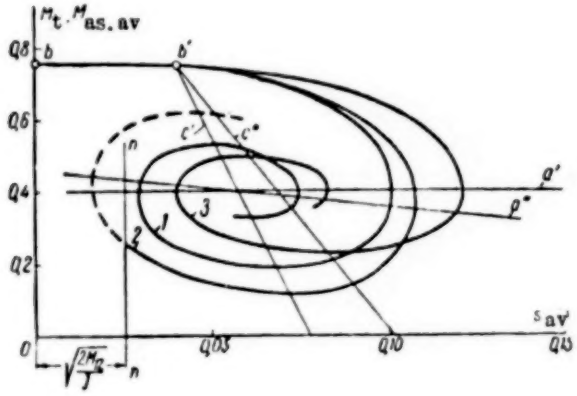

Fig. 2.

$1 - M_{as.av} = 0.5$ and $\delta_{st} = 0.05$; $2 - M_{as.av} = 0.46 - s_{av}$ and $\delta_{st} = 0.05$; $3 - M_{as.av}$ and $\delta_{st} = 0.08$; $T_s = 7$ sec; $T_i =$; $\beta = 1$; $\mu_{n.1} = 0.75$ and $J = 12.5$ sec.

It will be seen from Figs. 1 and 2 that the rotor shaft is affected under out-of-step conditions by an excess torque $M_{ex} = M_t - M_{as.av}$ which accelerates the rotor. Owing to its inherent inertia, the speed regulator cannot react to the increased slip instantaneously and therefore the turbine torque M_t will not vary along the static characteristic of the speed regulator, but along its dynamic characteristic $M_t = f(s_{av})$. The acceleration of the rotor will persist so long as $M_{ex} < 0$.

The average slip is a maximum when the torques on the rotor shaft are in equilibrium ($M_{ex} = 0$) and then deceleration of the rotor commences since the excess torque has become negative. The rotor will be retarded as long as $M_{ex} < 0$. The average slip is a minimum during this deceleration when the torques on the rotor shaft are in equilibrium

again and if there is a corresponding adjustment of the speed regulator, a positive excess moment can re-appear which re-accelerates the rotor again and so forth (see curve 3 in Fig. 1).

The maximum and minimum average values of the slip always correspond under transient asynchronous conditions to the points at which the $M_t = f(s_{av})$ curve intersects the asynchronous torque curve where the excess moment affecting the rotor changes sign.

It will be seen from Figs. 1 and 2 that in the course of time the $M_t = f(s_{av})$ curves approach the point where the static characteristics of the speed regulator intersect the asynchronous torque curves. This point corresponds to the steady asynchronous state of the generator. The shape of the $M_t = f(s_{av})$ curves as they approach this point mainly depends on the characteristics of the turbine speed regulator.

Re-synchronization of the generator under asynchronous conditions is only possible if condition 1 is satisfied. Otherwise the generator will remain out-of-step unless external conditions alter.

Fig. 1 illustrates the effect of the value of the time constant T_i of the isodrome* and the value of the feedback coefficient β on the operation of the generator during asynchronous conditions. The experimental curve 1' corresponding to the calculated curve 1 was obtained from an oscillogram taken on a dynamic simulator at the Moscow Power Institute**. Comparison of these two curves shows that there is satisfactory agreement with the dynamic characteristic of the turbine speed regulator.

An analysis of the $M_t = f(s_{av})$ curves in Fig. 1 shows that their shape on approaching the point where the static characteristics of the speed regulator and the asynchronous torque curves intersect is very much dependent on the value of T_i and β. Thus, curves 2 and 3 make a considerable detour to the left before approaching this point, whereas curve 1 approaches it more or less smoothly from the right. If T_i and β are increased, the maximum and minimum mean slip values during out-of step conditions also increase and consequently condition 1 is not necessarily fulfilled at certain of these values, i.e. re-synchronization of the generator is impossible (see curve 1 for example).

Lines n-n have been drawn parallel to the Y-axis in Figs. 1 and 2 at a point $s_{av} = \sqrt{\frac{2M_{12}}{j}}$ along the X-axis (see condition 1). If, in

* Isodrome – a hyperbolical position – determining system or curve, (Translator).

** A hydro-electric generator with a damper winding was simulated.

calculating the mean slip, the $M_t = f(s_{av})$ curve is tangential to this line or intersects it at a certain instant (Fig. 1 curves 2 and 3 point n' and n''), then condition 1 is fulfilled and from this moment on, overswings of the rotor set in after successful re-synchronization which gradually face away under the influence of damping factors so that the set returns to its original state provided the electrical system is still the same. After the overswings of the rotor have started, the mean slip is zero and therefore part of the $M_t = f(s_{av})$ curve lying beyond the point where it intersects the n-n line (marked by a dotted line in the diagrams) can only be found mathematically on the assumption that condition 1 is not fulfilled.

It will be seen from Fig. 1 that condition 1 is not fulfilled if $T_i = 8$ sec and $\beta = 5$, (curve 1) and consequently re-synchronization of the generator is impossible. If $T_i = 3$ sec or $\beta = 0$ (curves 2 and 3), condition 1 is then fulfilled and re-synchronization is therefore possible.

961

Fig. 2 shows curves 1 and 3 for various degrees of statism δ_{st} of the speed regulator ("statism" is defined as the percentage deviation of the controlled quantity at rated load from its value on open circuit, Translator). It can be seen from these curves that an increase in statism leads to a deterioration in the conditions for re-synchronization since the maximum mean slip is increased during transient asynchronous conditions and this can generally result in condition 1 not being fulfilled, Therefore, the less the statism, the more favourable the conditions for re-synchronization. Curves 1 and 3 in Fig. 2 do not intersect the n-n line and consequently condition 1 is not fulfilled, i.e. re-synchronization is impossible.

However, this diagram also illustrates the effect of asynchronous generator torque on the course of asynchronous operation. For simplicity, we confine ourselves to two straight line characteristics a' and a'' at different angles to the X-axis but having a common point of intersection with the static characteristic of the speed regulator. We can therefore trace the effect of the slope (steepness) of the asynchronous torque curve on the dynamic characteristic of the speed regulator. We can always approximate the real asynchronous torque characteristic by several linear sections if it is not a straight line and include its effect on the motion of the rotor in this way.

It can be seen from curves 1 and 2 in Fig. 2 that the conditions for re-synchronization of the generator are improved by steeper asynchronous torque curves since the minimum mean slip is then reduced. Thus, for example, curve 2 which corresponds to a steeper asynchronous torque

characteristic than curve 1, intersects the n-n line, whereas curve 1 does not even touch it. Re-synchronization is therefore possible in the first case, but impossible in the second, since condition 1 is only fulfilled in the former.

It is necessary to consider the effect of the valve limiter on the possibility of re-synchronization. The valve limiter determines the maximum load on the turbine for any position of the static characteristic of the speed regulator.

The speed regulator does not alter the turbine torque within the zone b-b' (Fig. 2) where the valve limiter is effective, and the slip remains less than the value at point b'. This shifts the dynamic characteristic of the speed regulator to the right, in which case conditions are naturally less favourable for re-synchronization since the minimum mean slip value increases by an amount approximately defined by the zone within which the valve-limiter is effective and condition 1 may not be fulfilled as a result.

Finally, without graphically illustrating the point, it can be shown that an increase in the time constant T_s of the servo motor, or a decrease in the mechanical time constant J of the machine, can reduce the maximum mean slip under asynchronous transient conditions, and that this favours conditions for re-synchronization of the generator.

If operating conditions are such that re-synchronization cannot be ensured by appropriate design of the speed regulator, special measures have to be taken [3, 5].

Symbols*

M_{12} – amplitude of the synchronous generator torque;

$M_{as,av}$ – average asynchronous torque of the generator;

$M_{t.nom}$ and M_{t0} – rated and initial turbine torque;

M_t – turbine torque;

$M_{t.r}$ – braking (restraint) torque of turbine with fully closed turbine control gear;

$M_{t.c.o.v.}$ – turbine torque at the moment when the throttle is completely open;

* Angles and time are expressed in electrical radians and other quantities in relative units.

s_{av} – average slip (positive if the speed of the rotor is above its synchronous speed);

$s_{av.\ c.o.v.}$ – average slip at the moment when the throttle is completely open;

$s_{av.\ c.g.c.}$ – average slip at the moment when the turbine control gear is fully closed;

δ – the angle between the generalized vector of the stator voltage and the transverse axis of the rotor;

$\mu_{n.l}$ – opening of the turbine control gear on no load;

σ – extent to which the throttle is open;

β – feedback coefficient;

i – the ratio of the extent of the non-uniformity of the pendulum which is left, to that still to be used;

δ_{st} – "statism" of the turbine speed regulator ("statism" is defined as the percentage deviation of the controlled quantity at rated load from its value on no load, Translator);

δ_{nu} – the non-uniformity of the pendulum to be used;

T_s – time constant of the servo motor;

T_i – time constant of the "isodrome" (hyperbolical position – determining system or curve, Translator);

J – mechanical time constant of the machine;

t – time.

Translated by V. Alford

REFERENCES

1. I.M. Markovich and S.A. Sovalov; *Elektrichestvo*, 4, (1955).
2. M.P. Chesnov; *Elektrichestvo*, No. 6, (1960); Translation printed in Electric Technology U.S.S.R., vol, 6, (1960).
3. V.A. Venikov; *Elektromechanical transients in electrical systems, (Elektromekhanicheskie perekhodnye protsessy v elektricheskikh sistemakh)*, Gosenergoizdat, (1958).
4. Iu. E. Garkavi and M.S. Smirnov; *The control of hydro-electric turbines, (Regulirovanie gidroturbin)*. Mashgiz, (1954).
5. L.G. Mamikoniants, M.G. Portnoi and A.A. Khachwturov; *Asynchronous automatic reclosure of transmission lines with two-way supply, (Nesinkhronnoe APV linii elektroperedachi s dvustoronnym pitaniem)*. Inf. mat. VNIIE', No. 37, (1959).

A CONTINUOUS CONTROL SYSTEM FOR THE MAIN DRIVE OF A REVERSIBLE ROLLING MILL*

V.I. ARKHANGEL'SKII

TsPKB Glavproektmontazhavtomatika

(Received 1 August 1960)

Contactless control systems have had to be designed in order to create optimum transient conditions in the main drives of reversible rolling mills and to improve their reliability.

Several types of contactless control system have been developed at the TsKPB for M.A.R. and amplidyne-type generator-motor drives [1,2].

In this paper a study is made of a new control system for the main drive of a reversible blooming mill (Figs. 1 and 4) which is now in use at a Soviet iron and steel works**.

Control of the armature current of the motor under regenerative braking conditions

When controlling the roll motor up to fundamental speed, i.e. no weakening of the excitation field, the armature current is low during braking and reversing and no special measures are therefore necessary to limit it. Automatic devices are only needed for limiting the armature current when reversing and braking the motor at higher speeds when the field has been weakened.

---

* *Elektrichestvo*, 2, 33-39, 1961.

** A.A. Pivovarov, T.Ia. Vashchenko, G.M. Maliutin and V.A. Lebedev took part in the development and tests of the system proposed by the author.

The explanation is that two processes take place when the command to slow down is received, namely, strengthening of the motor field and reduction in the generator voltage. These two processes acting simultaneously cause an abrupt change in the transient current in the armature of the motor. The regeneration current is usually limited by delaying the reduction in the generator voltage until the motor field has been strengthened.

These two processes are kept separate in relay-contactor control systems by degenerative (negative) feedback of the armature current at the input to the dynamoelectric amplifier (amplidyne) used for the excitation of the generators [3,4]. This was the principle used in the continuous systems described in previous works [1,2].

The disadvantage of using a current regulator to separate these two processes is the notable delay in its operation owing to the considerable magnetic inertia of the voltage control system of the generators. The command-signal to slow down cannot be blocked at the input to the amplidyne of the generators and the first change in the regeneration current is relatively large.

The second real disadvantage of regenerative current regulators is as a rule the oscillations which occur in the motor armature current.

In the circuit in Fig. 1, a saturable reactor (choke) *SR* is connected in the a.c. circuit feeding the push-pull magnetic amplifier *MA* for the excitation of the generators. If the field of the roll motor is weak, the reactor (choke) reduces the possible forcing of the generator amplidyne several times over so that during regenerative braking the reduction in motor speed from maximum to fundamental speed is almost exclusively due to field strengthening. The generator voltage remains practically constant. In this way the armature current can be strictly controlled.

When the field has been strengthened, the reactor restores a high degree of forcing which controls the voltage of the generators and ensures the required reversing speed at speeds up to the fundamental speed.

The steady state voltage of the generator is unaffected by the magnetization of the reactor (whether saturated or not).

Use is made of the following windings to control the reactor *SR* (Fig. 1b):

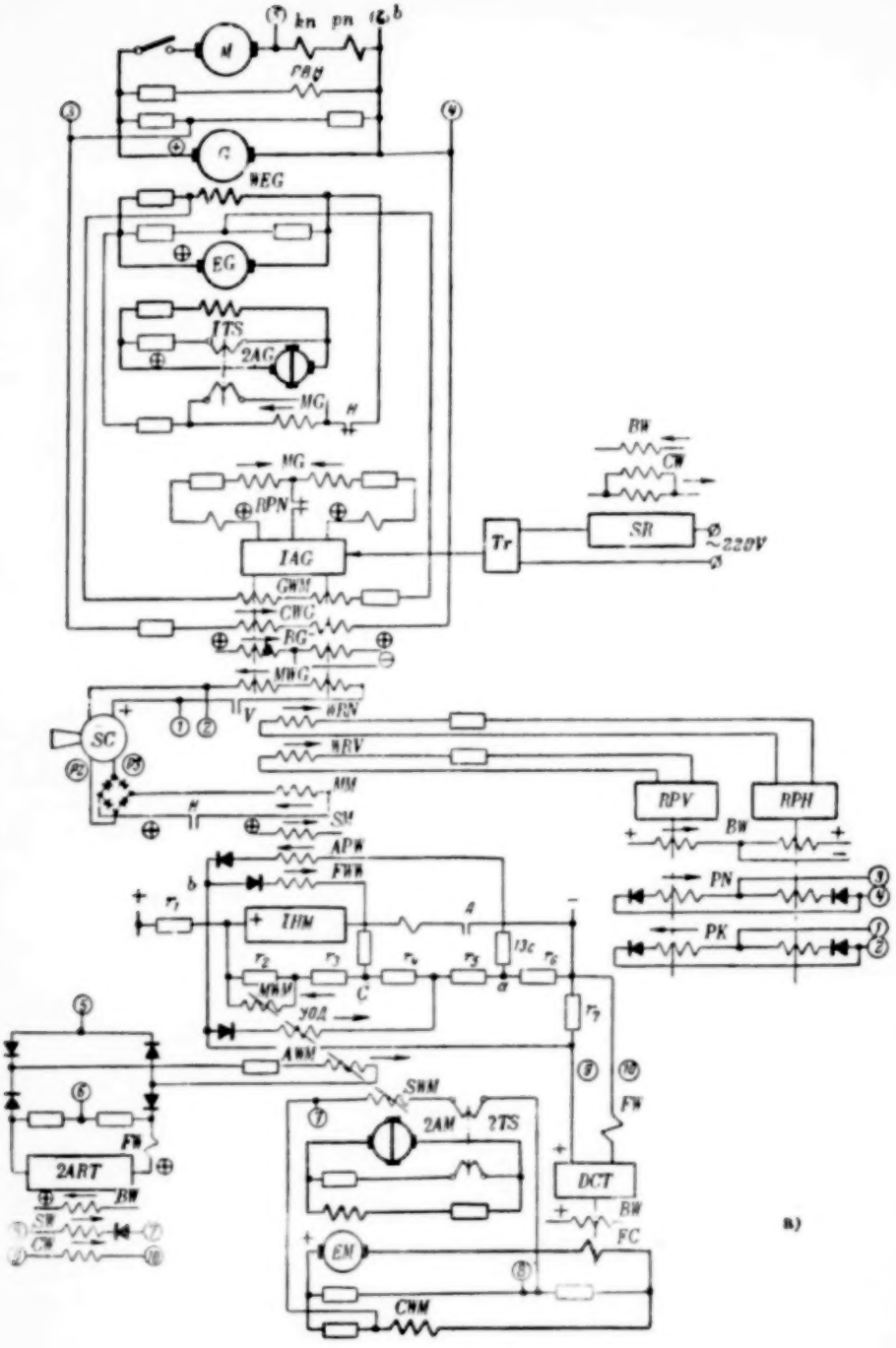
M
kn pn
PBG
G
WEG
EG
ITS
2AG
MG
RPN
IAG
Tr
SR
~220V
BW
CW
GWM
CWG
BG
MBG
SC
WBV
MM
SM
APW
FWW
IHM
RPV
RPH
PN
PK
MWW
YOA
AWM
SWM
2AM
2TS
2ART
FW
DCT
FC
EM
CWM

a)

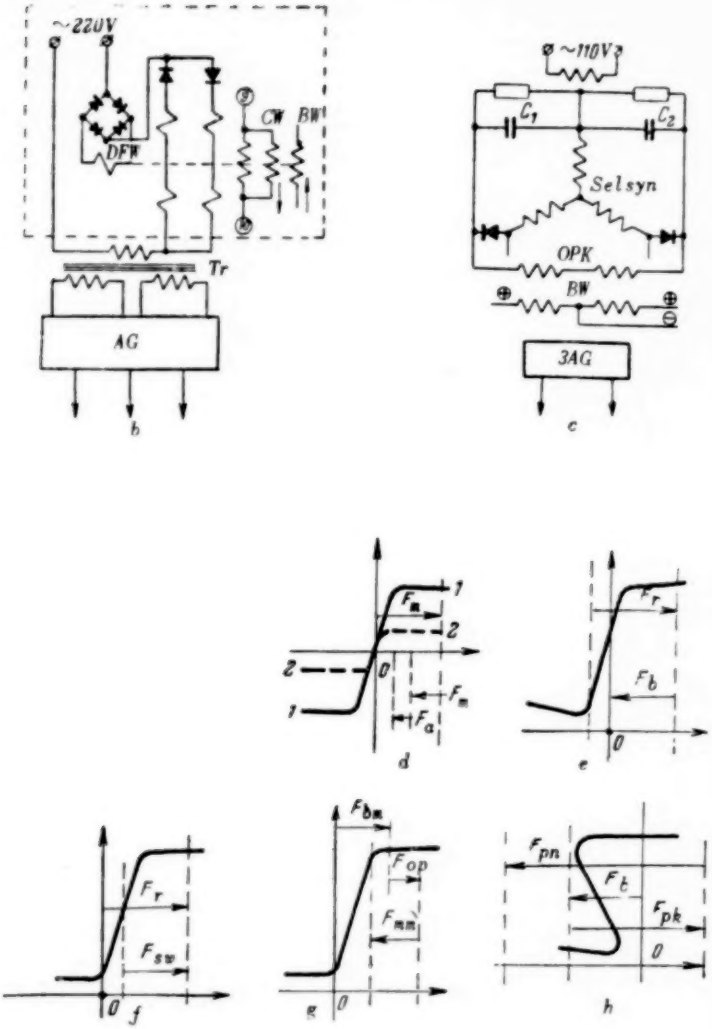

Fig. 1. *a* - continuous control system for the main drive of a reversible rolling mill; *b* - arrangement of the reactor windings; *c* - circuit of the continuous controller; *d* - characteristic of the amplifier *AG*; *e* - reactor characteristic; *f* - characteristic of the amplifier 2 *ART*; *g* - characteristic of the amplifier 1*AM*; *h* - characteristics of the contactless relays *RPV* and *RPN*.

1. A series degenerative (negative) feedback winding *DF#* for the load current of the reactor. This winding is connected via a full-wave rectifier;

2. bias winding *B#*;

3. control winding *C#* which is connected to the excitation current transformer *DCT*. Its m.m.f. is proportional to the motor excitation current.

The characteristic of the reactor is shown in Fig. 2.

The reactor is fully saturated at the rated excitation current of the motor so that the magnetic amplifier *AG* receives the maximum alternating voltage. Conversely, the rezctor is not saturated when the field of the motor has been fully weakened and the alternating voltage supplied to the amplifier *AG* is much lower.

Curve 1 for the amplifier *AG* in Fig. 3 refers to the total motor flux and curve 2 to the weakened flux.

196

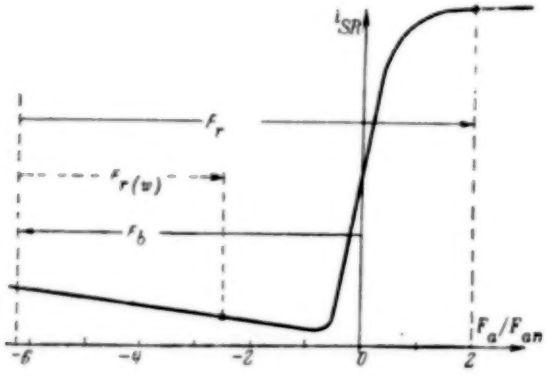

Fig. 2. Characteristic of the reactor *SR*.
$F_{r(n)}$ and $F_{r(w)}$ - m.m.f.'s of the reactor proportional to the excitation current of the roll motor for nominal and weakened motor fields;
F_b - bias m.m.f.

On acceleration of the motor to a higher speed than the fundamental speed, there is no restriction on the excitation by the reactor *SR* during the increase in generator voltage up to 80 to 85 per cent of rated forcing. When the field of the motor begins to weaken, there is

a gradual de-saturation of the reactor and the forcing of the excitation of the generator is restricted. However, this is a normal transient condition. The degree of saturation of the reactor has no effect on any further acceleration owing to the weakening of the motor field.

The command-controller *CC* ("sequence" control) issues two simultaneous commands when the motor begins to slow down from maximum speed. One is to strengthen the motor field and the other to reduce the voltage of the generators. The strengthening of the field takes place at once, but the reduction in the voltage of the generators is a gradual process since the amplifier *AG* is operating on curve 2 in Fig. 3 which excludes forced excitation of the generator. There is therefore only a slight change in the armature current. After the field of the motor has increased to 70-80 per cent of its rated value, the amplifier *AG* begins to operate on curve 1 in Fig. 3 and forcing of the generator excitation is restored.

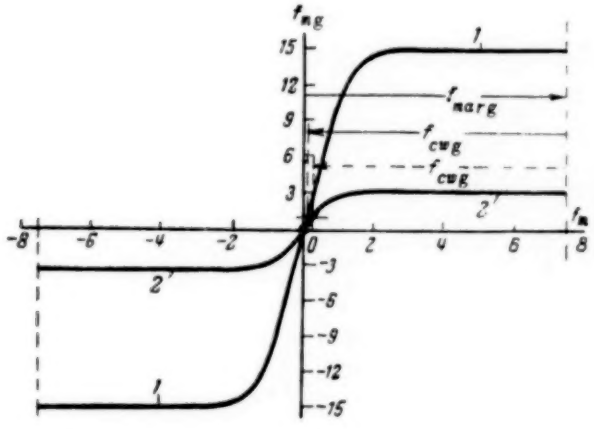

Fig. 3. Test curve for reactor-amplifier (1*AG*) unit.
1 – reactor saturated; 2 – reactor not saturated.

We will now consider the relationship between the degree of reduction in the rate of variation of the generator voltage and the magnitude of the master m.m.f. of the amplifier 2*AG*.

As an approximation, suppose that the magnetization curves of the exciter *EG*, generator *G* and amplidyne *DEA* are linear and that the electromagnetic time constant of the amplidyne is constant. We then get (Fig. 4):

$$U_{ag} = k_{ag}F_{dg}; \tag{1}$$

$$U_{eg} = k_{eg}i_{eg}; \tag{2}$$

$$U_g = k_g i_g; \tag{3}$$

$$U_{ag} = r_{eg}i_{eg}\,(1 + T_{eg}p); \tag{4}$$

$$U_{eg} = r_g i_g\,(1 + T_g p); \tag{5}$$

$$F_{dg} = F_{max.g} - F_{mg}, \tag{6}$$

where U_{ag}, U_{eg} and U_g are the voltages of the amplidyne *DEA*, the exciter *EG* and the generator *G*;

k_{ag}, k_{eg} and k_g coefficients defined from the linear sections of the magnetization characteristics;

F_{dg} - the resultant m.m.f. of the generator amplidyne;

i_{eg} and i_g - excitation current of the exciter *EG* and the generator *G*;

r_{eg} and r_g - the resistance of the excitation circuits of the exciter *EG* and generator *G* including the "additional" resistances;

T_{eg} and T_g - electromagnetic time constants of the excitation circuits of the exciter and generator;

F_{mg} - the m.m.f. of the flexible negative (degenerative) feedback created by the winding *MG* of the amplidyne.

The joint solutions of equations (1) to (6) gives:

$$U_g = \frac{k_{ag}k_{eg}k_g}{r_{eg}r_g}\,\frac{F_{dg}}{(1 + T_{eg}p)(1 + T_g p)}. \tag{7}$$

The current in the circuit of the winding *MG* is approximately proportional to the derivative of the voltage of the exciter *EG*. We can put:

$$F_{mg} = k_{mg}pU_{eg}, \tag{8}$$

where k_{mg} is the feedback coefficient of the winding *MG* which is connected to the statically-balanced dynamic bridge.

By virtue of 8, the resulting m.m.f. of the amplidyne is

$$F_{dg} = F_{max.g} - \frac{k_{mg}}{k_g} r_g p\ (1 + T_g p)\ U_g. \tag{6a}$$

The joint solution of equations 6(a) and (7) gives:

$$U_g\ (1 + T_{eg.eg}p)\ (1 + T_g p) = k_{g.eg} F_m, \tag{9}$$

where

$$\left.\begin{aligned} k_{g.eg} &= \frac{k_{ag} k_{eg} k_g}{r_{eg} r_g}; \\ T_{eg.eg} &= T_{eg} + \frac{k_{ag} k_{eg} k_{mg}}{r_{eg} r_g} = T_{eg} + T_{mg}, \end{aligned}\right\} \tag{10}$$

and $T_{eg.eq}$ is the equivalent time constant of the generator exciter consisting of the natural time constant T_{eg} and the component T_{mg}. (The subscript mg presumably refers to the *MG* winding. Translator).

The solution of equation (9) is

$$U_g = A_1 e^{\alpha_1 t} + A_2 e^{\alpha_2 t} + k_{g.eq} F_m, \tag{11}$$

where

$$\alpha_{1,2} = -\frac{1}{2}\ \frac{T_{eg.eq} - T_g}{T_{eg.eq} T_g} \pm \sqrt{\frac{1}{4}\left(\frac{T_{eg.eq} - T_g}{T_{eg.eq} T_g}\right)^2 - \frac{1}{T_{eg.eq} T_g}}; \tag{12}$$

and A_1 and A_2 are integration constants.

At the start of reversing $t = 0$, we have:

$$\left.\begin{aligned} F_m &= -F_{mw}; \\ U_g &= U_{gs}; \\ \frac{dU_g}{dt} &= 0, \end{aligned}\right\} \tag{13}$$

where F_{mw} is the reduced value of the m.m.f. of the master windings of the amplidyne on account of the reactor *SR* (Fig. 3);

U_{gs} – the steady state voltage of the generator *G*.

We can define the integration constants in equation (11) from (13). We get:

$$U_g = \frac{U_{gs} + k_{g.eq} F_{mw}}{\alpha_2 - \alpha_1} (\alpha_2 e^{\alpha_1 t} - \alpha_1 e^{\alpha_2 t}) - k_{g.eq} F_{mw}. \qquad (14)$$

Suppose we put

$$u_g = \frac{U_g}{U_{gr}}, \quad f_{mw} = \frac{F_{mw}}{F_{mr}} \text{ and } U_{gr} = k_{g.eg} F_{mr},$$

We can then re-write equation (14) in relative units

$$u_g = \frac{1}{\alpha_2 - \alpha_1} (\alpha_2 e^{\alpha_1 t} - \alpha_1 e^{\alpha_2 t}) - f_{mw} \left[1 - \frac{1}{\alpha_2 - \alpha_1} (\alpha_2 e^{\alpha_1 t} - \alpha_1 e^{\alpha_2 t}) \right], \qquad (14a)$$

where f_m is the degree of forcing of the generator excitation reduced as a result of the reactor *SR*;

F_{mr} – the m.m.f. of the amplidyne under rated excitation of the generator;

U_{gr} – the rated voltage of the generator (it is presupposed that the steady state voltage of the generator U_{gs} is equal to the rated value prior to reversing).

The radicand in (12) is often negative for large drives. In this case we can write:

$$\alpha_{1,2} = -\alpha \pm j\gamma, \qquad (15)$$

where

$$\alpha = \frac{T_{eg.eq} + T_g}{T_{eg.eq} T_g};$$

$$\gamma = \sqrt{-\frac{1}{4} \left(\frac{T_{eg.eq} + T_g}{T_{eg.eq} T_g} \right)^2 + \frac{1}{T_{eg.eq} T_g}},$$

and the solution of equation (11) is

$$u_g = e^{-\alpha t}\left(\cos\gamma t + \frac{\alpha}{\gamma}\sin\gamma t\right) - \\ - f_{mv}\left[1 - e^{-\alpha t}\left(\cos\gamma t + \frac{\alpha}{\gamma}\sin\gamma t\right)\right]. \quad (16)$$

Both equations (16) and (14a) consist of two terms. The first is solely defined by the characteristics of the excitation control system of the generator. The second describes the rate of change in the generator voltage due to the reduced m.m.f. f_{mv} of the amplidyne. The value of the second term is directly proportional to f_{mv}, the forcing of the excitation.

Since the rate of change in the generator voltage is defined by the first derivative of this quantity, we can write for equations (14a) and (16):

(a) non-periodic transient processes

$$\frac{du_g}{dt} = (1 + f_{mv})\frac{\alpha_2\alpha_1}{\alpha_2 - \alpha_1}(e^{\alpha_1 t} - e^{\alpha_2 t}); \quad (17)$$

(b) periodic processes:

$$\frac{du_g}{dt} = (1 + f_{mv})\left(1 + \frac{\alpha^2}{\gamma^2}\right)\gamma e^{-\alpha t}\sin\gamma t. \quad (18)$$

The circuit in Fig. 4, in respect of which the relations have between considered which define the rate of change in the generator boltage as a function of the degree of amplidyne forcing of the excitation f_{mv}, differs from the voltage regulator as in Fig. 1 in that the winding *MG* of the amplifier *2AG* is connected to the stabilizing transformer *ITS*. On test both regulators (given the right flexible feedback coefficient F_{mg}) produced practically identical results. The two types are therefore equally good.

For the regulator with the stabilizing transformer, oscillations occur in the system if the circuit is opened, whilst positive (regenerative) feedback may arise at the input to the amplidyne if the circuit with the dynamic bridge is opened. The latter can give rise to an excessive increase in the generator voltage.

For a 500 h.p. reversing motor (750 V 50/100 rev/min) for a rail and structural mill with a continuous control system, we have: (a) amplification factor $k_{ag} = 6.0$; $k_{eg} = 45$; $k_g = 8$; $k_{mg} = 0.3$; $k_{g.eq} = 87$;

(b) time constants T_{eg} = 0.5 sec; T_g = 1.1 sec; $T_{eg.eq}$ = 3.1 sec;
(c) resistances r_{eg} = 31 ohm; r_g = 0.8 ohm.

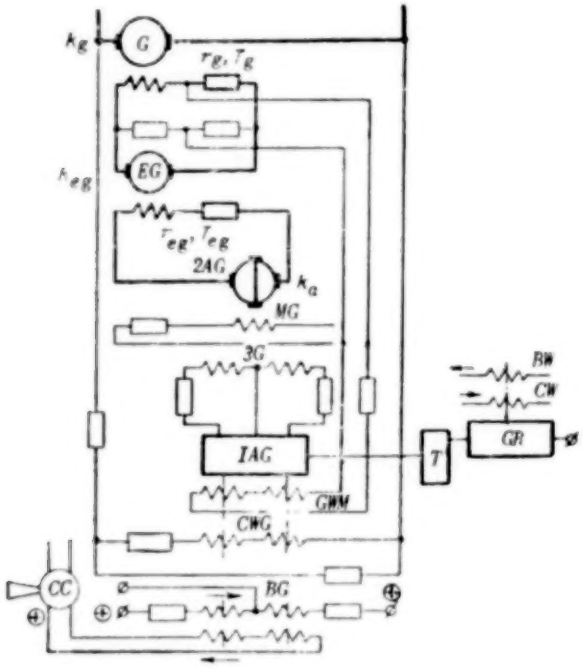

Fig. 4. Control system for the generator voltage.

The transient variation in the generator voltage on reversing is described by equation (16). Substituting numerical values for the coefficients, we get:

$$u_g = e^{-0,51t}(\cos 0,17t + 3\sin 0,17t) - \\ - f_{mw}[1 - e^{-0,51t}(\cos 0,17t + 3\sin 0,17t)]. \tag{16a}$$

Equation (18) for the first derivative of the generator voltage takes the form:

$$\frac{du_g}{dt} = 1,7\,(1 + f_{mw})\,e^{-0,51t}\sin 0,17t. \tag{18a}$$

The master m.m.f. of the amplidyne during full excitation forcing when the reactor is saturated equals $f_{m.max}$ = 15; when the reactor is

unsaturated, it is reduced to $f_{au} = 3$.

The magnetizing force (control power) of the amplidyne at the steady rated generator voltage equals $F_{a.nom} = 9.0$ VA.

Substituting these figures in (18a), we can determine the extent of the decrease in the rate of change of the generator voltage at high motor speeds at the start of reversing due to the reactor *SR*. The degree k_f of the decrease in forcing is

$$k_f = \frac{f_{an}}{f_{au}} = \frac{15}{3} = 5;$$

and the degree k_d of the reduction in the value of the derivative according to (18a) equals

$$k_d = \frac{1 + f_{an}}{1 + f_{au}} = \frac{16}{4} = 4.$$

Fig. 5 shows the magnetization curve of the amplidyne. This illustrates the effect of reducing the forcing of the generator excitations when the master m.m.f. of the amplidyne falls. It will also be seen from Fig. 5 that our conclusions cannot be significantly affected by ignoring the saturation of the magnetic circuits.

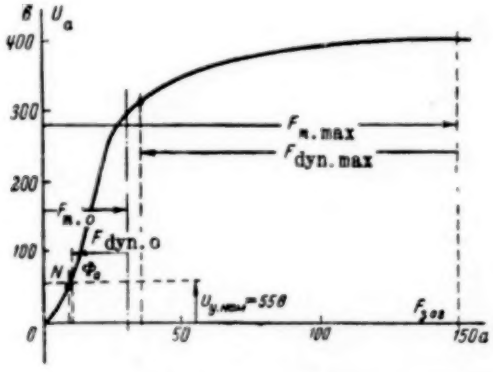

Fig. 5. The resulting characteristic 1*AG*-2*AG*. $F_{a.max}$ and $F_{dyn.max}$ – m.m.f.'s of the master and dynamic windings of the amplifier 2*AG* with the reactor saturated; $F_{a.o}$ and $F_{dyn.o}$ – the same, but with the reactor unsaturated.

Two m.m.f.'s are active at the input to the amplidyne, namely, the master m.m.f. F_m and the "dynamic" m.m.f. F_{dyn} which is subtracted from F_m. Since the difference between these two m.m.f. is much less than either component, it follows that the degree of reduction in F_{dyn} cannot be very much different from the degree of reduction in F_m. The magnitude of F_{dyn}, which is proportional to the rate of increase in the voltage of the exciter EG, defines the forcing of the generator excitation.

Incidentally, the equivalent time constant $T_{eg.eq}$ of the excitation of the generator exciter is six times greater than the electromagnetic time constant of the exciter excitation circuit (T_{eg} = 0.5 sec and $T_{eg.eq}$ = 3.1 sec).

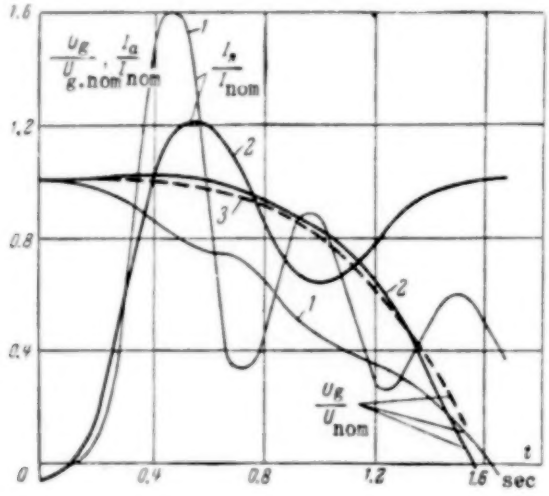

Fig. 6. Curves for the transient phenomena which take place on reversing a 5000 h.p. motor of 750V, 5400A, 50/100 rev/min and i_{en} = 340 A.

1 – contact control system; 2 – continuous control system; 3 – calculated curve for the voltage in the continuous control system; U_g – generator voltage; I_a armature current of motor.

According to expression (10), the magnitude of $T_{eg.eq}$ increases with increasing flexible feedback of the amplidyne. Its m.m.f. F_{dyn} is defined by the coefficient $k_{m.g}$. Consequently, it is not always wise to try and reduce the electromagnetic time constant T_{eg} of the exciter to a very small quantity. The second term T_{mg} in expression (10) can easily be adjusted, whereas this is not the case with T_{eg}. The system

can thus be adjusted to the desired dynamic conditions.

Fig. 6 illustrates the advantage of a regulator for the regenerative current of the motor in which the parametric principle is used without direct control over the armature current. For purposes of comparison, curves are given for the armature current and generator voltage when the motor is slowed down whilst reversing under contactor and contactless control. All the curves have been plotted from oscillograms of the transient phenomena taking place in a 5000 h.p. motor on no load. Considerable changes occur with a regenerative current regulator which lead to sparking on the motor and generator commutators, mechanical shocks in the rolling mill, a reduction in the mean torque of the motor and so on.

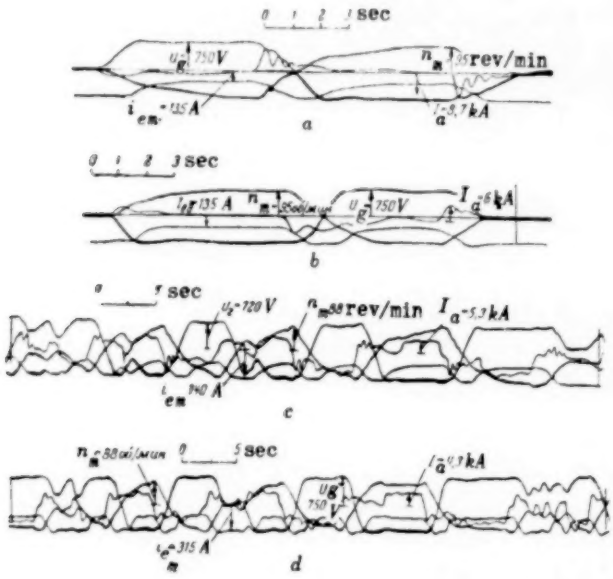

Fig. 7. Oscillograms of the transient phenomena on accelerating, reversing and braking an unloaded motor *(a, b)* and oscillograms of the rolling cycles *(c, d)*. *a* and *c* – contact control systems; *b* and *d* – continuous control systems.

The oscillograms in Fig. 7(a) and (b) show the transient conditions during acceleration, reversing and braking of the motor (when the shaft is unloaded). The changeover to contactless control considerably shortens transient conditions. The rolling cycle of one billet was accordingly reduced by 10 to 12 per cent on average.

Control of the motor excitation current

Optimum conditions for dynamic control of the motor field can be created by a special arrangement of the control windings in the magnetic amplifier 1*AM* and the amplidyne 2*AM*. The amplidyne 2*AM* uses a master winding *MWM*, a control winding *CWM*, a current winding *AWM* and a stabilization winding *SWM* (Fig. 1a).

The master winding *MWD* is connected to the d.c. 220V network via a resistor r_1 and part of the load current of the amplifier 1*AM* also flows through it. A reference voltage is produced across the resistors r_5 and r_6. These are a part of the load of the amplifier 1*AM*. The reference voltage is produced at the input to the amplifier 1*AM* by the command-controller. The master m.m.f. created by the *MWM* winding depends on the extent to which the field is weakened; it is smaller when the field is weak than when excitation is complete.

The branches *ab* and *bc* are intended to create optimum dynamic conditions for the drive. Under steady state conditions no current is carried in them since $u_a < u_b$ and $u_b < u_c$. The current in the circuit of the control winding *CWM* depends solely on the difference between the voltage drops across the resistors r_7 and r_5-r_6. The diode 1*D* only allows current to flow in the *CWM* winding if $U_{r7} > U_{r5,\ r6}$. The voltage drop U_{r7} is proportional to the excitation current of the motor. The d.c. transformer *DCT* is connected in the excitation circuit of the motor.

The reference voltage produced by the amplifier 1*AM* determines the magnitude of the excitation current of the motor. The master winding of this amplifier is supplied via a rectifier from the selsyn command-controller. The m.m.f. of this winding is proportional to the angle of deflection of the selsyn.

The control windings of the amplifier 1*AM* are connected in the branches *ab* and *bc* in order to create dynamic conditions, i.e. the winding *FWM* restricts the forcing when the field is weakened and the winding *APW* limits the initial forcing when the field of the motor is strengthened.

At the start of the field weakening the voltage drop across the resistors r_4-r_6 is sharply reduced and the potential at point *c* becomes less than that at point *b*; a current is then produced in the *FWM* winding and the positive m.m.f. of this winding slightly increases the output voltage of 1*AM*. This reduces the change in m.m.f. of the differential winding *CWM* and limits the reduction in the m.m.f. of the *MWM*

winding of the amplifier 2*AM*. The voltage drop across the resistor r_7 becomes less with decreasing motor excitation current and the current in the *FWW* winding disappears.

Under strong field conditions there is first a sudden increase in the voltage drop across the resistor r_6 and a current arises in the *APW* winding of the amplifier 1*AM*. The negative m.m.f. of this winding limits the increase in the output voltage of the amplifier 1*AM* and this in its turn limits the increase in the master m.m.f. (*MWM* winding) of the amplifier 2*AM*. Then the effect of the bc circuit is weakened and the field forcing increases with increasing motor excitation current.

In order to separate the states of control over the voltage of the generators and the field of the motor, the amplifier 1*AM* is provided with windings *WRV* and *WRN* which are supplied by the field relays *RPV* and *RPN*. The m.m.f.'s of these windings prevent the weakening of the field until the voltage of the generators reaches about 85 per cent of its rated value during acceleration. Fig. 1(g) illustrates the relationship between the m.m.f.'s of the control windings in the amplifier 1*AM*. If there are no m.m.f.'s F_{mm} and F_{op}, the amplifier 1*AM* is completely opened by the m.m.f. F_{bm} of the bias winding and the reference voltage (the output of the amplifier) is at a maximum corresponding to the rated excitation current of the motor [1].

Unlike previous systems [1,2], the proposed system of control for the motor field (Fig. 1a) provides a wider range of control over the excitation current of the motor and makes it easier to adjust for the desired conditions of dynamic control.

Conclusions

1. The continuous control system in Fig. 1(a) has real advantages over relay-contactor systems. They are:

(a) more rational conditions are created for controlling the drive which improves the efficiency of the electrical equipment and increases the productivity of the rolling mill;

(b) the control system is more reliable and easier to maintain;

(c) favourable conditions are created for applying automation to the rolling process.

2. The use of this control system on a reversible rolling mill

reduced the rolling cycle by 10 to 12 per cent.

Translated by V. Alford

REFERENCES

1. V.I. Arkhangel'skii; *Elektroprom. i priborstr.*, No.11, TsINTI Elektroprom., (1960).
2. V.I. Arkhangel'skii; *Contactless control systems for the drives of reversiable rolling mills, (Beskontaknye skhemy upravleniia elektroprivodami reversivnykh prokatnykh stanov).* Gosenergoizdat, (1960).
3. A.B. Cheliustkin and E.A. Rozenman; *Automatic control of rolling mills, (Avtomaticheskoe upravlenie prokatnymi stranami).* Metallurgizdat, (1955).

196

CAPACITIVE TRANSMISSION OF SURGE VOLTAGES IN TRANSFORMERS HAVING A BUSHING AT THE MID-POINT OF THE HIGH VOLTAGE WINDING*

S.D. LIZUNOV

Moscow Electrical Works

(Received 4 May 1960)

961

Introduction

In high voltage transformers having the line terminal at the mid-point of the high voltage winding, the induced potentials in the low-voltage winding due to surges reach considerable magnitude and in some cases (in 400-500 kV transformers) special measures must be taken to eliminate this undesirable phenomenon.

Not only may large potentials on the low voltage winding be dangerous to the earth insulation of this winding, but variations in this potential also affect the insulation between the low and high voltage windings and considerably increase the gradients** in the high tension (HT) winding. These conditions particularly affect three-winding transformers and auto-transformers when the LT winding is arranged between the high- and mid-voltage windings.

Thus, in conventional 220 kV transformers with the low tension (LT) winding in the centre, the potential induced in the middle of this

---

* *Elektrichestvo*, 2, 62-67, 1961.

** By gradients is meant the voltages on small sections of the longitudinal (centre turn) insulation.

winding by an impulse of 1.5/40 μ sec is about 30 sec per cent of that at the line end of the HT winding. This voltage has a considerable effect on the gradients and "lineals" (voltages about the line end) of the HT winding. It increases the gradients by a factor of 1.3 to 1.4 and the lineals still more owing to the oscillatory component at the natural frequency of the LT winding (Fig. 1).

The impulse method [1, 3] of determining the gradients ignores the effect of the LT winding. The potentials on the LT windings can be much larger with chopped waves. But their effect on the gradients of the HT winding is somewhat weaker owing to the short duration of the main peak in the HT gradient.

There are usually no dangerous voltages on the LT windings when the line potential is introduced at the end of the HT winding since it is earthed at both ends by the large capacitance of the network.

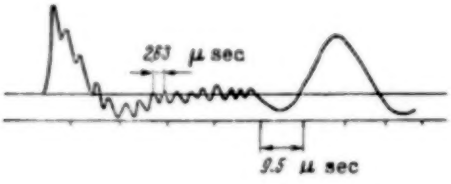

Fig. 1. Oscillogram of voltage transfer No.6 relative to the line in the HT winding of a 220 kV transformer of 40,000 kVA. The LT winding is placed between the high- and mid-voltage windings. The ends of the LT winding are earthed.

We assume throughout that the two ends of the LT winding are earthed as in impulse tests.

Capacitive transmission of the potential from the HT winding to the LT winding.

The initial induction of voltage on the LT winding by a surge with a vertical wavefront. In calculating the capacitive induction in transformers having a line terminal at the mid-point of the HT winding, we can confine ourselves to one branch and the corresponding half of the LT winding of each core; the fictitious discontinuity of the middle of the LT winding is assumed to be insulated.

We will now consider a method of estimating the capacitively-induced

voltages on the low and mid-voltage windings (i.e. the secondary windings) given a non-uniform HT winding.

The interturn capacitance of a secondary winding can greatly affect the magnitude and distribution of the voltage induced in this winding. But the effect of this capacitance on the distribution of the voltage on the primary winding is usually very small and can be neglected. There is then no difficulty in estimating the capacitive distribution of the voltage on the primary winding regardless of the interturn capacitance of the low- and mid-voltage windings for any degree of non-uniformity in this winding. The secondary windings are usually made uniform.

Given the approximate distribution of the voltage on the primary winding, even though it is non-uniform (only non-uniform interturn capacitances are in mind), by expressing it analytically we can then find an expression for the distribution of the capacitively-induced voltage on uniform secondary winding. This can be done by solving an inhomogeneous differential equation of a lower order than the homogeneous equation for the case when the primary winding is uniform but the distribution of the voltage over it unknown [3, 4].

The original distribution of the potential on the primary winding $U_{1\ \mathrm{init}}(x)$ is assumed to be given (Fig. 2). (Here x is the relative axial distance from the line end of the HT winding or from the middle of the LT winding; half the height of the winding is taken as unity).

To form the differential equation 1, we have to assume that the voltage $U_{1\ \mathrm{unit}}(x)$ is produced by an infinite power source all over the winding and that it remains unchanged on connexion of the capacitive circuit:

$$\frac{d^2 U_{2\mathrm{init}}(x)}{dx^2} - \frac{c_{12} + c_{02}}{c_{12}} U_{2\mathrm{init}}(x) = -\frac{c_{12}}{c_{12}} U_{1\mathrm{init}}(x). \tag{1}$$

where all the capacitances are referred to a unit of axial length. The subscript 1 refers to the primary winding, 2 – to the secondary (LT) winding, 1 to the interturn capacitances and 0 to the earth capacitances. The point $x = 0$ corresponds to the line end of the HT winding and the mid-point of the LT winding arranged opposite to it.

It is presupposed that the voltage in the primary winding can be defined as follows:

$$U_{1\mathrm{init}}(x) = Ae^{-\nu x} + Be^{-\nu x} \tag{2}$$

and that the windings can be regarded as infinite. Then the voltage for the potential on the secondary winding, if the boundary conditions are satisfied, is

$$U_{2\text{init}}(x) = \frac{c_{12}}{c_{12}+c_{02}}\left[A\frac{\lambda^2}{\lambda^2-\nu^2}\left(e^{-\nu x}-\frac{\nu}{\lambda}e^{-\lambda x}\right)+\right.$$
$$\left.+B\frac{\lambda^2}{\lambda^2-\eta_i^2}\left(e^{-\eta_i x}-\frac{\eta_i}{\lambda}e^{-\lambda x}\right)\right], \qquad (3)$$

where

$$\lambda = \sqrt{\frac{c_{12}+c_{02}}{c_{n2}}}.$$

The voltage at the mid-point of the LT winding (if $x = 0$) is

$$U_{B\text{init}} = U_{2\text{init}}(0) = \frac{c_{12}}{c_{12}+c_{02}}\left(A\frac{\lambda}{\lambda+\nu}+B\frac{\lambda}{\lambda+\eta_i}\right). \qquad (4)$$

If $U_{1\ \text{init}}(x) = e^{-\nu x}$, formulae (3) and (4) are simplified.

Formulae can also be obtained similarly for a three-winding transformer. To estimate the voltage induced on an LT winding placed between the high- and mid-voltage windings we can use the formulae for a two-winding transformer since in this case the interturn capacitance of the mid-voltage winding will have very little effect on the distribution of the voltage on the LT winding. The earth capacitances of the LT winding can only be estimated if the earth capacitances of the mid-voltage winding are considered.

Impulses with a finite wavefront or chopped waves. For standard impulses (1.5/40 μ sec and chopped waves) it is necessary to include the inductance if the voltage in the LT winding is to be calculated correctly.

The voltage at the mid-point of the LT winding can be calculated by a simple equivalent network which need only be valid for the point in question (point B in Fig. 3). The period of fundamental oscillations of the LT winding is found from the formula

$$T = 2\pi\sqrt{L(c_1+c_2)} = 2\pi\sqrt{\frac{1}{4}L_2(c_{12}+c_{20})h}, \qquad (5)$$

where h is the total height of the winding.

The inductance L_2 can be estimated as follows. Suppose that the LT

winding occupies a mid-way position between the high voltage and mid-voltage windings. We can then find L_2 as the leakage inductance between half of the LT winding and the adjacent windings on the assumption that the whole leakage flux travels in channels between the windings and that there is none at all in the copper.

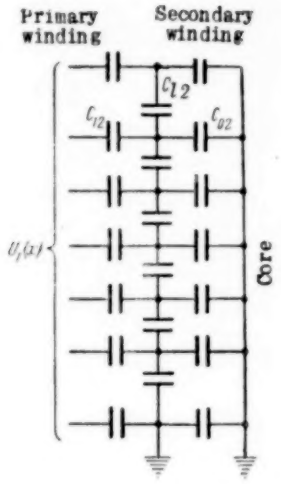

Fig. 2. Equivalent capacitive network of a two-winding transformer with a given distribution of the voltage on the primary winding.

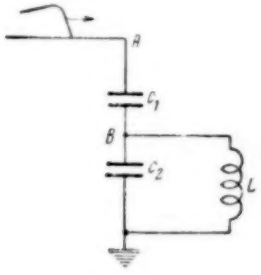

Fig. 3. Equivalent network for determining the shape of the voltage oscillations in the middle of the LT winding.

If the LT winding is at the core, L_2 is still found in the same way, but the surface of the core is regarded as a conducting screen since the

flux is excluded from the steel by the eddy currents. The residual effect of the core can be included by multiplying the value of L_2 by a factor of about 2.5. The period T is usually 3 to 6 μ sec for LT windings.

If an infintely long surge with a vertical wavefront (a "square" wave) is incident at point A, the unit amplitude of the potential at point B can be expressed by the formula*

$$U_{Bl}(t) = U_{B(\text{init})} \cos\left(2\pi \frac{t}{T}\right). \tag{6}$$

We assume that an impulse with a finite wavefront is of infinite length (this assumption has practically no effect on the magnitude of the voltage induced in the LT winding):

$$U_A(t) = 1 - e^{-mt}. \tag{7}$$

An expression can be found for the voltage induced by such a surge at the mid-point of the LT winding from formulae (6) and (7) by means of the Duhamel integral [3]. After simplifications we get:

$$U_B(t) = U_{B(\text{init})} \sin\varphi \left[\sin(\omega t + \varphi) - \sin\varphi e^{-mt}\right], \tag{8}$$

where

$$\sin\varphi = \frac{1}{\sqrt{1 + \left(\frac{\omega}{m}\right)^2}} = \frac{1}{\sqrt{1 + 5{,}2\left(\frac{s}{T}\right)^2}};$$

$U_{B(\text{init})}$ is defined by formula (4);

$\omega = \frac{2\pi}{T}$ - the "circular" (angular) frequency of the natural oscillations of the LT winding;

$s = \frac{2{,}75}{m}$ - a conventional wavefront expressed by equation (7) [2].

The incidence of the non-periodic component of formula (8) is defined by the wavefront of the effective surge. It is quite accurate to assume that expression (8) is at a maximum at the same moment as the sinusoidal term in square brackets. Hence the formula for the maximum voltage at the mid-point of the LT winding is

---

* Formulae (6), (8), (9) and (11) were derived by E.S. Frid.

$$U_{Bm} = U_{B(\text{init})} \sin\varphi (1 + \delta), \tag{9}$$

where

$$\delta = \sin\varphi e^{-\tan\varphi\left(\frac{3}{2}\pi + \varphi\right)}.$$

It follows from formula (9) that the voltage in the LT winding is smaller, the larger the ratio $\frac{S}{T}$.

With a chopped wave the induced potentials are much larger, since the inverse wave (component 2 in Fig. 4), which chiefly determines the induction with a chopped wave, is much steeper and is $1 + k_0$ times greater in amplitude than at the "chop" which is taken as 100 per cent (k_0 is the relative transition of the voltages through zero at chopping).

In addition, the potentials induced from the two components (Fig. 4) may be identical in sign at the moment the total potential is a maximum and they can be added (Fig. 5). The potential induced with the chopped wave increases as the coefficient of transition through zero increases.

Component 2 of the chopped wave (Fig. 4) can be expressed by the following formula if damping of the oscillations is excluded:

$$U_A(t) = -\frac{1 + k_0}{2}\{1 - \cos[\omega_{cp}(t - \tau_{cp})]\}, \tag{10}$$

where $\omega_{av} = \frac{2\pi}{T_{av}}$ is the angular frequency of the oscillations of the potential at point A after the "chop";

τ_{av} – the pre-discharge time (Fig. 4).

Using formulae (7), (8) and (10) and the Duhamel integral, the absolute maximum potential at point B is defined after simplification by the expression

$$U_{Bm} = U_{B(\text{init})}\left[\frac{1 + k_0}{2(1 - \beta^2)}(1 + \cos\beta\pi) - \right.$$
$$\left. - \sin\varphi \cdot \sin(\omega\tau_{cp} + \beta\pi + \varphi)\right], \tag{11}$$

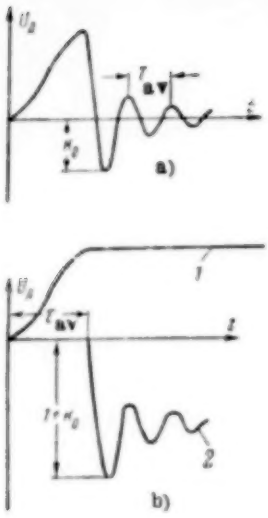

Fig. 4. The chopped waveform and its components;
a - chopped waveform;
b - expansion into its two components.
1 - un-chopped component;
2 - inverse component;

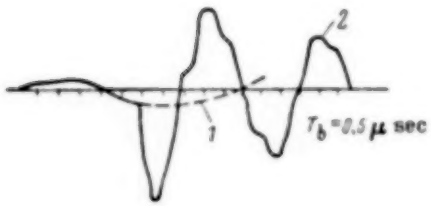

Fig. 5. Oscillogram of the potential induced in the middle of the LT winding of a 220 kV 40,000 kVA transformer due to a chopped surge. The dotted line shows the potential induced by an unchopped surge.

where

$$\beta = \frac{\omega}{\omega_{av}} = \frac{T_{av}}{T},$$

$$\sin\varphi = \frac{1}{\sqrt{1 + 5{,}2(\tau_{av}/T)^2}}.$$

Typical voltages induced in the middle of the winding of various transformers are given in the Table.

Transformer	Voltage class of mid-voltage winding, kV	Position of LT winding	Potential at the mid-point of the LT winding as a percentage			
			Total wave 1.5/40 sec		Chopped wave	
			Test	Call	Test	Call
40,000 kVA, 220kV (3-w (3-winding)	110		24	29	69	73
60,000 kVA, 400 kV (2-winding model) ..	–	–	11	15.6	33	39.6

N.B. The calculated values are angular because damping was ignored.

The capacitive effect of voltage oscillations in the LT winding on the gradients in the HT winding

Nature of the effect. The LT winding usually has a mainly capacitive effect on the gradients in the HT winding. We ignore those cases where the effect is inductive.

Corresponding to the capacitive distribution of the voltage on the HT winding (Fig. 6) the first moment after the incidence of a surge with a vertical wavefront, there is a capacitively-induced voltage distribution of the same sign on the LT winding, i.e. $U_{2\ init}(x)$. After a period of time equal to a half-wave of the natural frequency of the LT winding, this voltage changes sign on passing through zero and capacitively induces an additional voltage in the HT winding which is

opposite in sign to that of the surge.

Since the natural frequencies of the winding are widely different, it follows that we can more or less regard these oscillations as independent of each other. The change in the voltage of the LT winding relative to that at the first moment (assuming synchronous change at all points), can be expressed in the form:

$$\Delta U_2(x, t) = U_2(x, t) - U_{2\text{init}}(x)(1 - \cos \omega t), \tag{12}$$

where $\Delta U_2(x, t)$ is the change in the voltage of the LT winding affecting the HT winding;

$U_{2\ \text{init}}(x)$ the initial value of the voltage induced in the LT winding;

$U_2(x, t)$ - the voltage of the LT winding.

When studying the gradients in the HT winding it is therefore necessary to consider two actions, namely, the actual surge at the line end of the HT winding (the waveform is assumed to be square), and the wave via the capacitance on the LT winding side in the form of (12).

The criterion for estimating the gradients is the curve for the initial voltage distribution [1, 2]. For an actual surge, this initial distribution can be obtained in the usual way. It can be roughly calculated analytically for the second component given uniform windings (for a square waveform via the capacitance on the LT winding side). The line end of the HT winding must be regarded as earthed owing to the great capacitance of the line.

The voltage distribution is illustrated in Fig. 6(a) for both components.

The expression for the initial voltage distribution for calculating the induced gradients. The induction in the HT winding is calculated in a similar way to that illustrated in Fig. 2, except that the voltage $U_{2\ \text{init}}$ is now regarded as given. The differential equation is exactly the same as equation (1), it being only necessary to substitute the subscript 2 for 1.

For the sake of simplicity it is assumed that the initial voltage distribution along the LT winding is linear:

$$U_{2\text{init}}(x) = U_{B(\text{init})}(1 - x), \tag{13}$$

Operating experience with 220kV transformers has shown that expression (13) is very near the actual voltage distribution along the LT winding; the initial voltage induced in the HT winding is then

$$U_{1\text{init}}(x) = \frac{c_{12}}{c_{12} + c_{01}} U_{B(\text{init})}(1 - x - e^{-\alpha x}), \tag{14}$$

where

$$\alpha = \sqrt{\frac{c_{12} + c_{01}}{c_{11}}}. \tag{15}$$

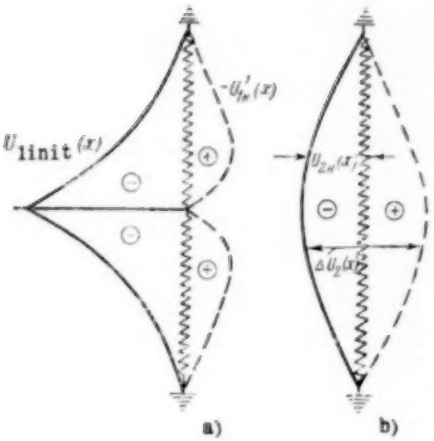

Fig. 6. The capacitive effect on the LT winding; a – initial distribution along the HT winding – two components; b – distribution along the LT winding.

Only the exponential term $-e^{-\alpha x}$ in the expression in brackets has any real importance in inducing gradients. Hence, from the point of view of calculating these gradients, the sudden application to the LT winding of a voltage which is defined at each point by expression (13), is equivalent to the square waveform of opposite polarity to that of the voltage in the LT winding at the line end of the HT winding and having an amplitude $\frac{c_{12}}{c_{12} + c_{01}} U_{B(\text{init})}$.

To calculate the induced gradients (given a synchronous change in the voltage all over the LT winding) we can replace the voltage $U_B(t)$ in the LT winding by the surge at the line end of the HT winding with the waveform

$$U'_A(t) = -\frac{c_{12}}{c_{12}+c_{02}} U_B(t). \tag{16}$$

The induced gradients with a surge having a finite wavefront. From the point of view of the effect of the oscillations in the LT winding on the gradients in the HT winding, the change in the voltage of the LT winding due to the presence of these oscillations (by analogy with formula (12) for a surge of square waveform and in accordance with (7) and (8) must be

$$\begin{aligned}\Delta U_2(x,\ t) &= U_2(x,\ t)_k - U_2(x,\ t)_a = \\ &= -U_{2\text{init}}(x)\{(1-e^{-nt}) - \\ &- [\sin\varphi\cdot\sin(\omega t+\varphi) - \sin^2\varphi\cdot e^{-nt}]\},\end{aligned} \tag{17}$$

where $\Delta U_2(x,t)$ is the change in the LT voltage affecting the HT winding;

$U_2(x,t)_a$ – the capacitively-induced voltage in the LT winding in the absence of oscillations;

$U_2(x,t)_k$ – the actual voltage in the LT winding.

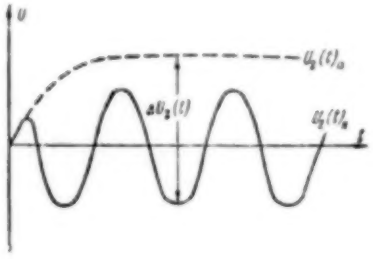

Fig. 7. The voltage of the LT winding due to a surge with a finite wavefront.

Fig. 7 shows the voltages $U_2(x,t)_k$ and $U_2(x,t)_a$ as a function of time at any point of the secondary winding.

In accordance with formula (16), the equivalent effect of a surge of

square waveform at the line end of the HT winding corresponding to the change in the voltage in the LT winding from formula (17), is found by the expression

$$U'_A(t) = \frac{c_{12}}{c_{12}+c_{01}} U_{B(\text{init})} (1 - e^{-mt}) - \\ - [\sin\varphi \cdot \sin(\omega t + \varphi) - \sin^2\varphi \cdot e^{-mt}]\}. \tag{18}$$

Formula (18) changes into formula (19) for surges of square waveform as $m \to \infty$:

$$U'_A(t) = \frac{c_{12}}{c_{12}+c_{01}} U_{B(\text{init})} [1 - \cos\omega t]. \tag{19}$$

If the frequency drops to zero, the conditional equivalent effects (18) and (19) also tend to zero and, consequently, so do the induced gradients.

Suppose we consider the components of the gradient induced in the HT winding by each term in expression (18).

The gradient of induction g'_1 from the term $\frac{c_{12}}{c_{12}+c_{01}} \times U_{B(\text{init})}$ $(1 - e^{-mt})$ in expression (18) can be estimated by the formulae for surges having a finite wavefront as proposed previously by Frid [2].

An expression for the gradient from the term $N \sin(\omega t + \phi)$ can easily be found from the formula for the gradient of a surge with a square waveform by the Duhamel integral. For example, for the second interval, i.e. if $X < Vt < (X+D)$:

$$g'_2(X, t) = -N \left\{ \frac{1}{1+\nu^2} \cos\varphi [\nu + \tan\varphi] e^{-A(X+D)} \times \right. \\ \times \sinh AVt - \frac{1}{1+\nu^2} \cos\varphi [\nu \sinh AX + \tan\varphi \cdot \cosh AX] \times \\ \times e^{-AVt} + \frac{\nu^2}{1+\nu^2} [e^{-AX}(1 - e^{-AD})] \times \\ \left. \times \sin(\omega t + \varphi) + \frac{1}{1+\nu^2} \sin\left[\omega\left(t - \frac{X}{V}\right) + \varphi\right]\right\}. \tag{20}$$

where in reference to the HT winding:

V is the velocity of propagation along the conductor (about 150 m/μsec for windings in oil and 210 m/μsec for windings in air);

D - the length of the conductor section in question;

$X = xL_w$ - the distance along the conductor from the beginning of the winding;

L_w - the total length of the winding conductor;

x - the distance from the beginning of the winding;

n - the number of turns per unit of axial length;

l_w - the average length of a turn;

$A = \alpha / l_w n$ - the capacitive parameter;

$\nu = \omega AV$ - the relative frequency of the LT winding;

$N = \frac{c_{12}}{c_{12} + c_{01}} U_B \text{ (init)} \sin \phi$ - the conventional amplitude.

It is easy to show that all the terms with the exception of that with the coefficient $\frac{\nu}{1+\nu^2}$ can be safely ignored for the usual 3-6 μ sec periods of natural oscillation in the LT winding. Expression (20) then takes the form:

$$g_2'(X, t) = -N \frac{\nu^2}{1+\nu^2} [e^{-AX}(1 - e^{-AD})] \times \sin(\omega t + \varphi). \qquad (21)$$

We would still arrive at the same expression if we were to consider the third interval, i.e. the case $Vt > (X + D)$.

The less steep the wavefront of the surge, the smaller the conventional amplitude of the gradient N, since the multiplier $\sin \phi$ is less.

In view of the short period of oscillations we can always assume that the positive half-wave of a sine curve is disposed near the maximum of the main gradient. It is therefore advisable to put $\sin(\omega t + \phi) = 1$ in formula 21.

The component of the gradient g''_2 from the term $N \sin^2 \phi \, e^{-\alpha t}$ is also easy to find. The gradient g''_2 is close in magnitude but opposite in sign to the sum of the non-periodic components of the gradient from formula (20) which we ignored; by subtracting g''_2 from that sum we get a negligible quantity which can be ignored completely (it is just the same for the third interval). Thus, the component of the gradient g''_2 can be excluded.

Formula (14) for the initial voltage distribution contains the linear component (1-x) which up to now has been ignored in deriving gradient

formulae. It can easily be shown that this component varies synchronously with the effective voltage during the course of time. It is a relatively small quantity in any section of the winding, but it is easy to calculate and no difficulties arise by including it. This gradient component is opposite in sign to the main gradient of the HT winding:

$$g_2'''(X,t) = N\frac{D}{l_w}\sin(\omega t + \varphi). \tag{22}$$

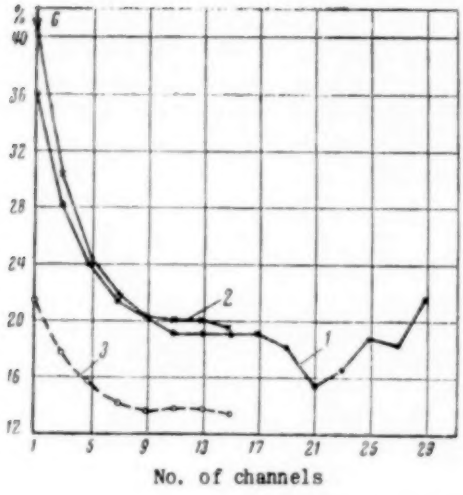

Fig. 8. Gradients of impulses of 1.5/40 μsec in a 220 kV 20,000 kVA test transformer:
1 – test data; 2 – calculated with LT effect included; 3 – calculated without LT effect included [2].

The general formula for calculating the second part of the induced gradient (corresponding to the terms in square brackets in (18)) simplifies to

$$g_2(X,t_M) = g_2'(X,t_M) + g_2'''(X,t_M) =$$

$$= \frac{c_{12}}{c_{12}+c_{01}}U_{B(\text{init})}\sin\varphi \times$$

$$\times\left\{\frac{\nu^2}{1+\nu^2}\left[e^{-AX}(1-e^{-AD})\right] - \frac{D}{L_w}\right\}. \tag{23}$$

The first component of the induced gradient due to the term $(1 - e^{-\alpha t})$ in formula (18) could have been included when calculating the main peak of the gradient. It is necessary to start from the curve for the initial voltage distribution over the HT winding calculated on the assumption of a continuous conducting and earthed screen instead of the LT winding (the capacitive parameter α is defined by formula (15)).

Fig. 8 shows typical curves for the maximum gradients of an impulse in winding of an experimental 220 kV transformer with the LT winding between the 220 kV and 110 kV windings and short insulation distances (increased effect of the LT winding). The maximum voltage at the mid-point of the LT winding as calculated by formula 9 was 33.5 per cent.

It will be seen from Fig. 8 that the maximum gradients from Frid's formulae are slightly below actual, whereas those calculated by the proposed method with the effect of the LT winding included agree satisfactorily.

Conclusions

1. Considerable potentials are capacitively-induced in the LT windings of transformers having the line voltage terminal at the mid-point of the HT winding when surges occur on the HT side.

2. The resulting oscillations of the potential in the LT winding increase the gradients in the HT winding by reverse capacitive induction.

3. The proposed method of estimating the stated effects is simple and sufficiently accurate for practical purposes.

Translated by O.M. Blunn

REFERENCES

1. E.S. Frid; *Surge gradients in transformer windings, (Impul'snye gradienty v obmotkakh transformatorov).* Diss. MEI, (1949).
2. E.S. Frid; *Elektrichestvo,* No. 9, (1959).
3. L.V. B'iulei; *Surges in transmission lines and transformers, (Volnovye protsessy v liniiakh peredachi i transformatorov).* ONTI, (1938).
4. P.A. Abetti; Trans. AIEE, III, vol. 73, 1407, (1954).

COLD-ROLLED NON-ORIENTED ELECTRICAL STEEL*

A.A. NEFEDOV and P.I. BORZOVA

Central Ferrous Metals Research Institute

(Received 4 July 1960)

961

The cold-rolled electrical steel at present produced in the U.S.S.R. is somewhat inferior in quality to that produced abroad. The explanation is that Soviet iron and steel works do not have the necessary equipment. This deficiency is shortly to be overcome by the opening of new electrical steel plants at the Novo-Lipetsk Iron and Steel Works. This works will produce top grade steel in roll and sheet form and in different gauges, widths and lengths with an insulation coating giving high space-factor. The delivery of steel in roll form will enable electrical engineering works to save steel by rationalizing the arrangement of stampings.

The Novo-Lipetsk Iron and Steel Works is also to produce a new kind of cold-rolled transformer steel developed by the Central Ferrous Metals Research Institute with a relatively non-oriented grain structure. There will be two grades, namely, a low-alloy steel with a 1.3 to 1.7% Si-content and a high-alloy steel with a 2.9 to 3.3% Si-content. Unlike conventional grain-oriented steel, these particular grades have fewer ferrite grains with the cube faces oriented along the direction of rolling. The result is that the electrical and magnetic properties of these steels are practically the same along the direction of cold-rolling as they are across it, i.e. the steel approximates to hot-rolled steel.

Trial batches of this steel have already been produced by the same process that will be used in Lipetsk. The properties of the steel have

---

* *Elektrichestvo*, 2, 85-87, 1961.

been investigated in weak, medium and strong fields. The properties of cold-rolled non-oriented 1.34% silicon steel and 3.29% silicon steel (gauge 0.5 mm) are given in the Table.

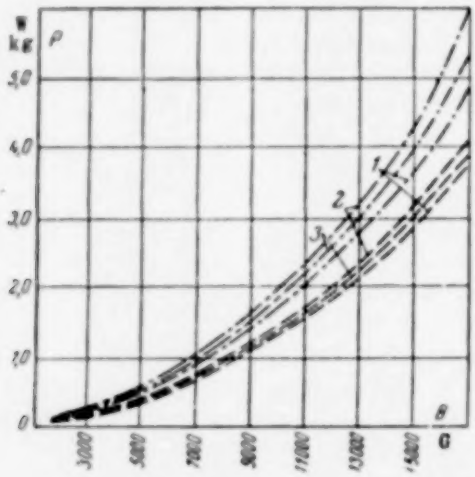

Fig. 1. Specific losses in cold-rolled non-oriented steel (gauge 0.5 mm):
– . – . – . – . low-alloy steel; -------- high-alloy steel;
Direction of specimens: 1 – lengthwise; 2 – transverse; 3 – middle (45°?).

The specific losses P_2-P_{17} and magnetic induction B_{25}-B_{100} of the steel were determined on a one-kilogram Epstein test apparatus by the absolute method. Coercive force was measured at a strength of 125 oersted. The testpieces were plates 0.5 x 30 x 250 mm in size with no special annealing to remove work hardening after cutting; when testing, the plates were "overlapped" end to end.

Magnetic induction $B_{0.002}$-B_{10} was measured on the same apparatus by the same testpieces but double overlapped. The testpieces were heat-treated at 750° before the tests to remove work hardening after cutting. More detailed information is given in Figs. 1 to 6.

From tests the magnetic induction $B_{0.002}$-$B_{0.01}$ is greatest in the high-alloy steel. It is the other way round in strong fields. As was to be expected, specific losses P_2-P_{17} were lowest in the high-alloy steel.

Properties of cold-rolled non-oriented silicon steel (gauge 0.5 mm)

Grade	Direction of specimens	Specific losses, w/kg			Magnetic permeability, G/oerst		Magnetic induction, G					Coercive free,	
		$p_{10/50}$	$p_{15/50}$	$p_{17/50}$	0.002	max	$B_{0.1}$	$B_{1.0}$	B_{10}	B_{25}	B_{50}	B_{100}	
Low-alloy (1.34% Si)	Lengthwise	1.70	3.61	4.84	450	12,030	320	10,970	16,120	16,680	17,800	19,290	0.35
	Cross	1.96	4.28	5.83	380	9,290	225	9,880	14,990	15,410	16,750	18,400	0.42
	45°	1.83	3.94	4.34	–	–	–	–	–	16,040	17,270	18,840	–
High-alloy (3.29% Si)	Lengthwise	1.30	2.80	3.67	510	10,575	310	9,970	15,280	15,930	17,150	18,540	0.30
	Cross	1.41	3.18	3.42	427	9,010	220	9,110	14,360	14,850	16,200	17,850	0.34
	45°	1.36	2.99	3.80	–	–	–	–	–	15,390	16,670	18,190	–

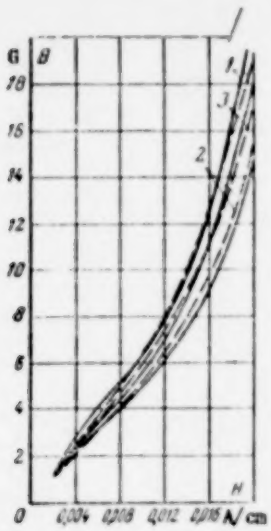

Fig. 2. Magnetic induction of cold-rolled non-oriented steel in weak field (gauge 0.5 mm). ——— low-alloy steel; - - - - high-alloy steel. Direction of specimens: 1 – lengthwise; 2 – transverse; 3 – middle (45°).

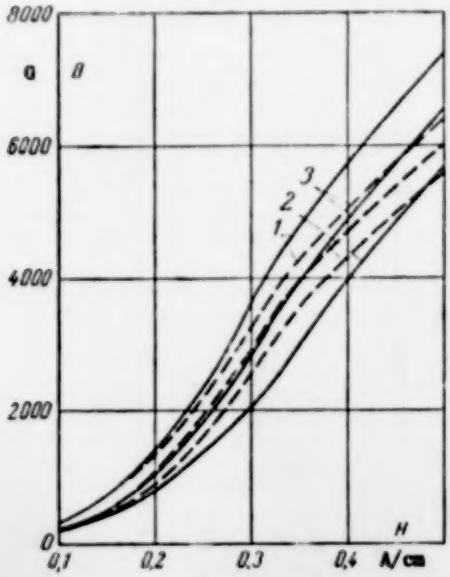

Fig. 3. Magnetic induction of cold-rolled non-oriented steel in medium fields (gauge 0.5 mm). ——— low-alloy steel; - - - - high-alloy steel. Direction of specimens: 1 – lengthwise; 2 – transverse; 3 – middle (45°).

Comparison of the properties of cold-rolled non-oriented steel with those of hot-rolled steel of the same chemical composition shows that the non-oriented cold-rolled steel is superior. It has lower specific losses and higher magnetic induction.

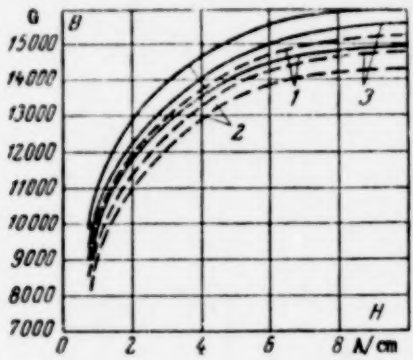

Fig. 4. Magnetic induction of cold-rolled non-oriented steel in medium fields (gauge 0.5 mm).
——— low-alloy steel; - - - - high-alloy steel.
Direction of specimens: 1 – lengthwise;
2 – transverse; 3 – middle (45°).

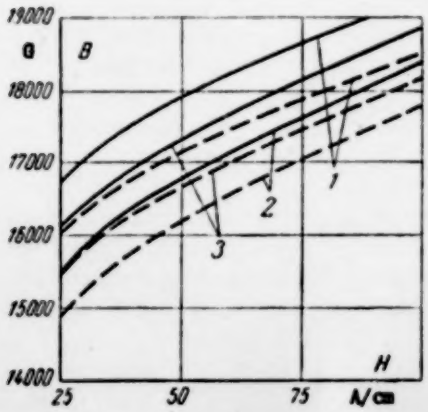

Fig. 5. Magnetic induction of cold-rolled non-oriented steel in strong fields (gauge 0.5 mm).
——— low-alloy steel; - - - - high-alloy steel.
Direction of specimens: 1 – lengthwise;
2 – transverse; 3 – middle (45°).

Satisfactory results were obtained in tests on cold-rolled non-oriented steel in electrical machines.

Samples of the steel have been produced in the Novosibirsk Iron and Steel Works under much worse conditions than at Lipetsk. This steel was tested at the "Dynamo" works. Losses were reduced 10 per cent by replacing grade E11 and E12 hot-rolled steel by cold-rolled low-alloy steel.

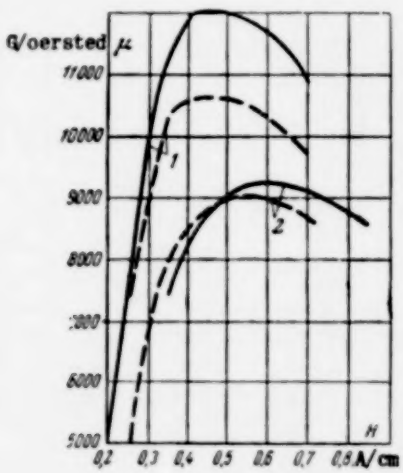

Fig. 6. Magnetic permeability of cold-rolled non-oriented steel (0.5 mm gauge).
——— low-alloy steel; - - - - high-alloy steel.
Direction of specimens: 1 - lengthwise; 2 - transverse.

Better results were obtained at the "Uralelektroapparat" works where cold-rolled high-alloy steel was substituted for grade E11 and E12 hot-rolled steel. Losses were reduced by a factor of 1.4 to 1.7 on prototype machines. Still better results are expected from the steel to be produced at Novo-Lipetsk.

Translated by O.M. Blunn

ABSTRACTS FROM PAPERS PUBLISHED IN ELEKTRICHESTVO No. 2 1961

YEAR 1961

Bushings

The Design of Oil-filled Bushings. L.I. Fedorov, (pp. 68-73).

Methods are proposed for designing bushings used for high voltage conductors, particularly from the point of view of heat dissipation and insulation.

Control Engineering

A Reversible Electronic Drive with Polarity Switch in the Power Circuit. B.R. Gendel'man, (pp. 17-24).

In 1959 the author patented a control system for the "ionic" drive of the rollgangs on a blooming mill. The system comprised one or two sets of mercury arc rectifiers and a polarity switch in the main circuit. Provision was then made for controlled starting, reversing and braking, but the author has now elaborated the system further and in this article he gives a description of a new but similar system which provides for all conditions of stepped control of the motor.

The Parameters of Non-linear Elements (with a parabolic voltampere Characteristic) connected in Pulsed-Current Circuits. B.M. Shliaposhnikov, (pp. 79-81).

Equations are produced to define the operating conditions of non-linear elements as used in modern remote control, measuring and computing devices.

Discharges across Contacts

Electrical Breakdown of Micro-Gaps in Gaseous Media. A.I. Frolov, (pp. 73-76).

A study is made of the electrical breakdown of small gaps measured in microns and tens of microns in particular reference to phenomena on Ni, Ag, Fe, Al, Cu and Pt-Ir contacts. A novel test is used.

Domestic Appliances

Concerning Domestic Power Consumption. B.L. Shifrinson, (pp. 76-78).

An account is given of the plans to increase the production of electric cookers for domestic use.

Electric Furnaces

The Calculation of Operational Short Circuit Currents in Three-phase Arc Furnaces. N.A. Markov et al., (pp. 28-33).

A practical method is proposed for calculating the asymmetrical short circuits which occur during the operation of electric arc furnaces in order to avoid the false operation of the relay protection and automatic regulators of the furnace.

Electrical and Magnetic Fields

Application of a Corollary of Green's Formula for calculating Electrical and Magnetic Fields. V.S. Khvostov et al., (pp. 14-17).

Owing to the difficulties involved in drawing the original equipotential lines in the Richter method, the author proposes a simple method of determining the potential at certain points within a region if the values of the potential are known at the boundary. An example is given.

Power systems

Consolidation of the U.S.S.R. Power pool System in Europe and Siberia.

It is recognized that industrial output will still largely be concentrated in the European part of the U.S.S.R. in the forseeable future. A detailed account is given of the planned Ural-Siberia power system which is designed to transmit electricity produced on the basis of Siberian fuel resources to the western regions.

The use of distribution coefficients in calculations with equivalent circuits. N.A. Mel'nikov, (pp. 9-13).

A description is given of a simple and accurate method of calculating complex equivalent networks on a network analyser by means of measurements of the distribution coefficients of the master currents. This method is particularly applicable to the operating conditions of electrical systems with non-linear loads if iteration is used.

YEAR
1961

Statistical Methods of calculating Electrical Loads in Industrial Networks. B.V. Gnedenko et al., (pp. 81-85).

A statistical method is proposed for estimating the future power consumption of factories and groups of factories.

Rotating Machines

The Design of Synchronous Motor Compounding Devices. V.V. Iukhov, (pp. 40-45).

A design method is proposed for current transformers in compounding schemes operating via a rectifier on the excitation winding of the exciter of a synchronous motor.

A small synchronous Motor with a Semiconductor Rectifier in its Field Circuit. Iu.I. Chkhikvadze et al., (pp. 45-48).

A description is given of a compact simplified system of excitation for small synchronous motors using a semiconductor rectifier. Many advantages are claimed for it. The special features are the connexion of the rectifier in the "open neutral" of the motor and the use of a two-winding correcting transformer. A 70 per cent reduction in cost is claimed.

Speed Control of a d.c. Motor with a Semiconductor Switch in its Armature Circuit. T.A. Glazenko et al., (pp. 49-55).

A description is given of a more compact, reliable and efficient system of controlling the speed of a reversible d.c. drive using a semi-conductor triode (transistor) as a switch in the armature circuit. Equations are also produced to determine the mechanical characteristics, the total amplitude of the pulsed current, the speed and the power losses.

Transformers

The Performance of Series-connected Transformers having different Transformation Ratios. P.F. Rybchenko, (pp. 55-61).

A study is made of the performance of series-connected transformers with different transformation ratios. A method of calculation is proposed to assist in the selection of other elements in automatic control systems without resort to time-wasting tests.

YEA
196

THE NEW RUSSIAN POWER STATIONS*

A. R. GERSHTEIN, L. I. DVOSKIN, L. UI. IZRAILEVICH
A. B. KRIKUNCHIK, K. K. LEVITSKII and B. V. ROSS

(Teploelektroproekt)

(Received 13 September 1960)

YEAR
1961

It is now planned to build 22 new coal-burning power stations in the U. S. S. R. by 1965. These stations, each of 2400 MW output, are to be equipped with 200 and 300 MW units. Each turbine will be connected to a boiler-unit producing steam at a rate of 950 t/hr (pressure 255 atm, steam temperature 585°C with reheat to 570°C).

The generators are to have hydrogen cooling (hydrogen pressure up to 3 atm). The generator voltage is 20 kV. Those produced by the Elektrosila works will have direct hydrogen cooling only for the rotor windings. Those produced by Elektrotiazhmash will have direct hydrogen cooling for both rotor and stator windings.

The Elektrosila generators will be excited direct from high frequency exciters with the current rectified by germanium rectifiers. Provision is made for standby excitation from a motor-generator set incorporating a flywheel.

The plan envisages five types of main building which differ in the position of the coal hoppers and the system of coal pulverization.

Alternative arrangements are also made for totally-enclosed and semi-enclosed turbo-generators, but there is a general specification dispensing with crane-assistance in the erection of the stator, the opening up of the regenerative air heating equipment, and the operation of the ash separators, exhaust fans and blowers in the boiler unit.

Different plans have been proposed for the system of coal pulveriza-

---

* *Elektrichestvo*, No. 3, 1-13, 1961.

tion. A central shop is provided in the fifth scheme [3]. The main building is shown in Fig. 1.

The specific capital cost is 590 to 650 roubles per kW; the specific space factor is 0.49 m^3/kW including the coal pulverization shop and auxiliary building; the specific consumption of conventional fuel is 304 g/kW. hr; the specific consumption of power for auxiliaries is nr; the specific consumption of power for auxiliaries is 3.2 to 3.7% (the feed pumps are steam-driven); the specific employment figure is 0.17 to 0.23 min per 1000 kW; 90% of the building is composed of sectional reinforced concrete components; there are 79 types of such units in the main building.

Output from the first set will commence 26 months after the start of construction. Thereafter new sets will come into operation at intervals of 3.2 months.

The electrical connexions

Provision is made for the electrical connexions to be adjusted to meet local needs and only general plans have therefore been made to supply the 110, 220 and 500 kV networks.

Use is to be made of three-phase 360 MVA booster transformers, 20/110, 20/220 and 20/330 kV and similar auto-transformers 20/110/220 and 20/110/330 kV. Single phase transformers 20/500 kV will also be used (120 and 240 MVA in one phase).

Fig. 2 illustrates the connexion of the generators to the 110 and 220 kV distribution gear. Extra reliability is provided by the use of two auto-transformers between the distributing devices. In version 1(a) the standby supply for auxiliaries is provided by step-down transformers connected to the compensation windings of the auto-transformers. With 6 kV compensation windings the standby supply is provided by line regulator transformers and reactors connected to the windings of the auto-transformers. In version 1(b) the standby transformers for auxiliaries are connected to the 110 kV feeder bus-bars, but this increases the capital cost and loss of energy. The difference in version 2 is that one of the generators is connected to the L.T. windings of the auto-transformers.

The second version entails no higher capital or running costs, but it is technically more difficult and special requirements have to be met as regards dynamic stability in the use of circuit breakers.

YEAR
1961

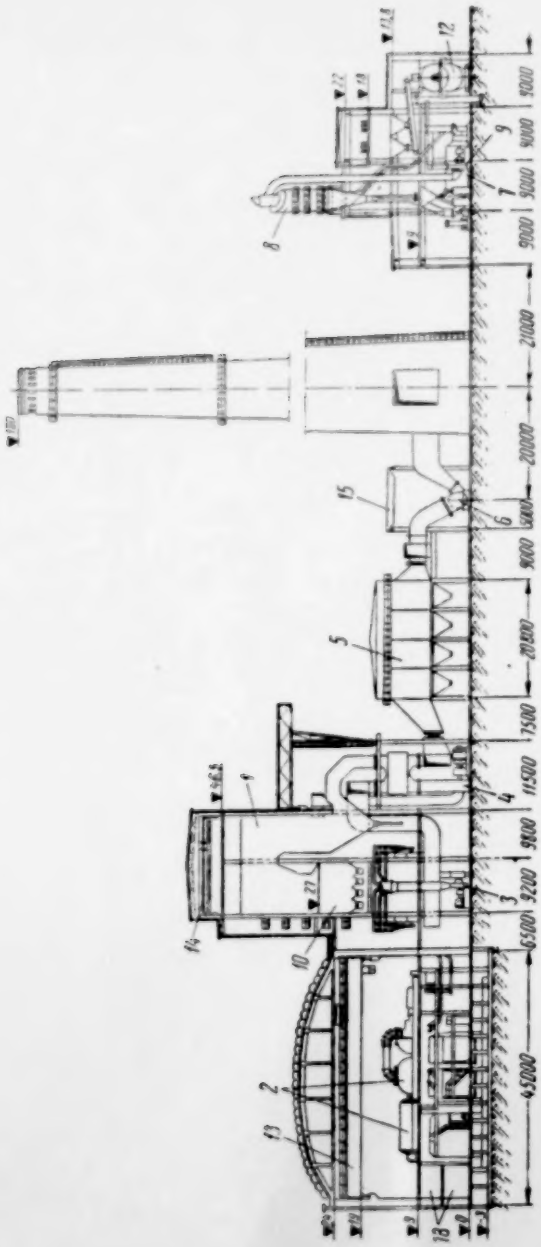
1
2
3
4
5
6
7
8
9
10
11
12
13
14
15
18
3200
9800
11500
7500
20500
9000
20000
21000
9000
9000
9000
9000
45000

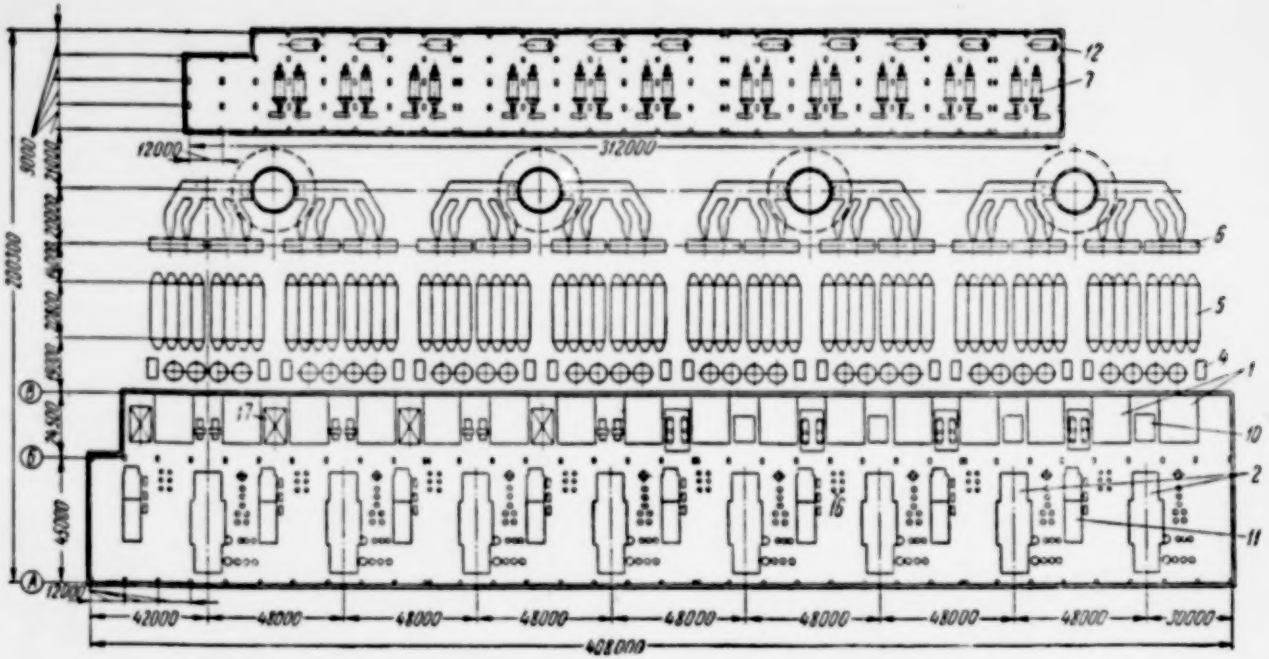

Fig. 1. Section and plan view of the main building of the 2400 MW station (variant No. 5).

1 - boiler 950 t/hr; *2* - 300 MW turbo-unit; *3* - hot blast ventilators; *4* - fans; *5* - electrostatic precipitates; *6* - exhaust fans; *7* - ball mills; *8* - coal-dust cyclones; *9* - mill fans; *10* - coal-dust hoppers; *11* - feed pumps; *12* - steam drier; *13* - 75/20 ton bridge crane; *14* - 10 ton bridge crane; *15* - 30 ton bridge crane; *16* - high pressure steam mains; *17* - control panel for two blocks; *18* - 6 kV distribution gear for internal needs.

YEA
196

The Ministry of Power Stations has recommended version 1(a) with the installation of a circuit breaker at each transformer. Three types of connexion between the generators and transformers have been considered for 500 kV (Fig. 3).

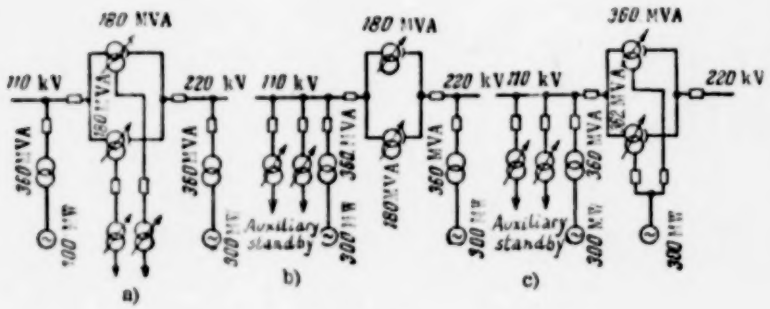

Fig. 2. Alternative systems for connecting the generators to the 110 and 220 kV distribution gear:
a – version 1(a); *b* – version 1(b); *c* – version 2

Version 1 provides two generators to one group of single phase booster transformers of 3 x 240 MVA with two low voltage windings. The 220 and 500 kV distribution gear is linked by a set of single phase 3 x 135 MVA auto-transformers. The compensation windings of the 220/500 kV auto-transformers can be used as a standby supply for the auxiliaries.

Version 2 provides for the connexion of the generators to the L. T. windings of 220/500 kV auto-transformers. One generator is connected to each set of auto-transformers. Two generators cannot be connected to the same set of auto-transformers owing to the limited power of the available auto-transformers.

In version 3 the number of large 500 kV units is reduced by connecting one generator to a 220/500 kV 3X 240 MVA auto-transformer and the other to a 20/220 kV booster transformer.

Versions 1 and 2 are the cheapest but version 2 incurs the least loss of energy, whilst version 1 is the simplest from the technical point of view.

YEAR
1961

The main system can only be selected in the light of local conditions, but a typical arrangement has been prepared (Fig. 4). Here two generators are connected to the 110 kV distribution bus, two to the 220 kV bus-bars, and four to the 500 kV bus-bars. Larger units are connected to the 500 kV bus-bars, i.e. two generators per transformer unit, to reduce the amount of expensive 500 kV switchgear. Large modern power systems have an adequate margin for the disconnexion of such units.

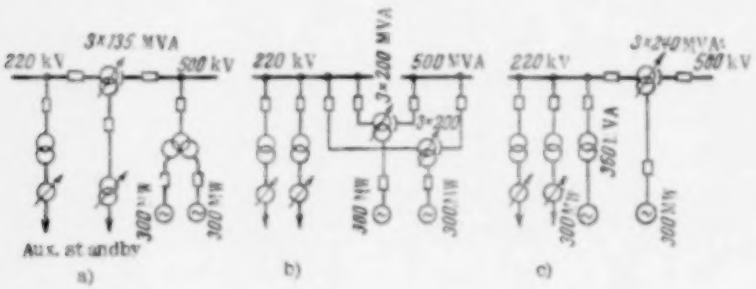

Fig. 3. Alternative systems for connecting the generators to the 220 and 500 kV distribution gear:
a – version 1; *b* – version 2; *c* – version 3.

The number of transmission lines from each station also depends on local conditions. To determine the scale of the distribution gear it was assumed that there would be about ten 110 kV lines, six 220 kV lines and three 500 kV lines.

The distribution gear is supplied by two separate bus-bar systems with a transfer bus. All the line and transformer circuits may be connected to the transfer system. If the number of outgoing lines should be less, simpler arrangements may be used (e.g. generator-transformer-line units, "bridges", "squares" etc).

Works supply

Three phase squirrel cage induction motors are used for most of the internal drives, but synchronous motors are used for the ball mills and compressors. The feed pumps are turbo-driven, except the standby pump which is driven by an induction motor.

A voltage of 6 kV has been adopted for the majority of motors at these large stations.

YEAR
1961

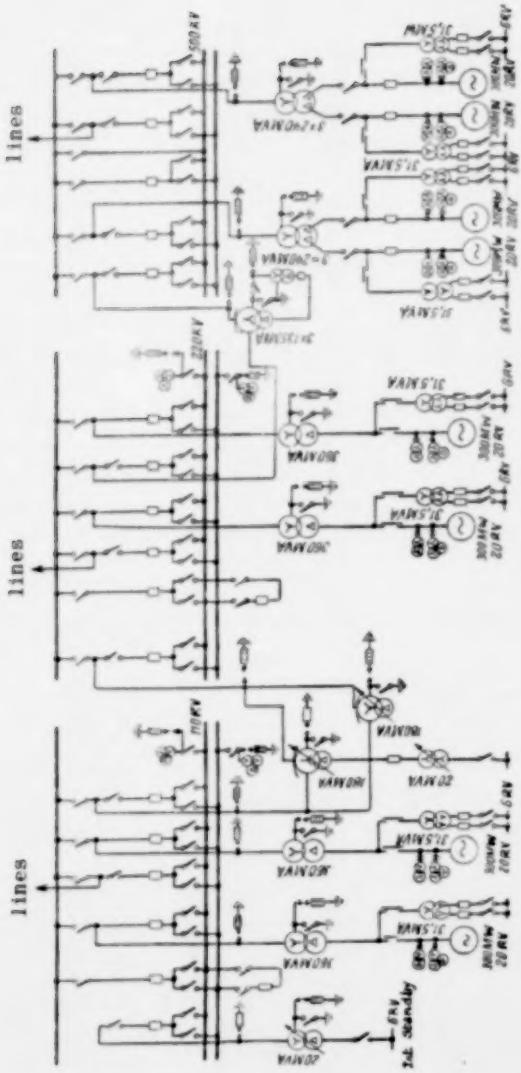

Fig. 4. The main system of electrical connexions.

The ball mills require a 2400 kW motor of 100 rev/min A synchronous motor is better suited to such speeds.

An induction motor was regarded as adequate for the standby feed pump as it is normally shut down and the advantages of a synchronous motor could not be fully used. A synchronous motor would also have led to a more complicated installation and would have increased the short circuit currents in the internal system.

The output and pressure of the standby feed pumps is regulated by hydraulic clutches. The exhaust fans are driven by two motors each of a different speed. The blowers are driven by two-speed motors. These fans and blowers are also regulated by the rotating blades of the turbine control gear.

A voltage of 380 V has been adopted for motors up to 200 kW.

The fuel supply equipment is driven by 220 V d.c. motors to achieve a wide range of speed control. They are fed from a three phase 380 V a.c. network via rectifiers. The standby oil pumps of the turbines and the equipment for the hydrogen cooling of the generators have 220 V d.c. motors so that they can be supplied from batteries in the event of the a.c. supply failing.

A voltage of 380/220 V with earthed neutral is used for the lighting.

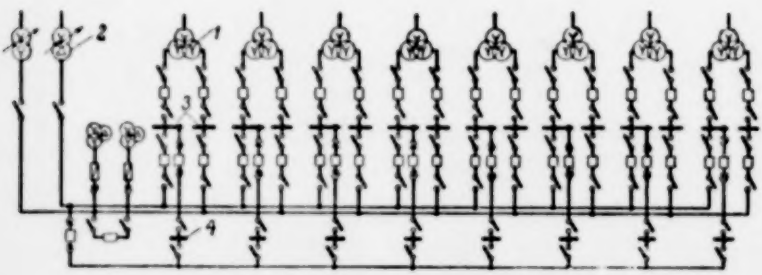

Fig. 5. The main circuit for 6 kV auxiliary power. *1* - Works transformers; 2 - standby works transformers; 3 - 6 kV busbars of the works distribution gear; 4 - the feeders of the coal pulverization shop.

The unit or "block" supply system is used for the works supply (see Figs. 5 and 6).

Each motor unit is supplied via a three phase 31.5 MVA 20/6 kV transformer with a split 6 kV winding. This transformer is connected to a tapping from the generator circuit. Such transformers make it possible to limit the short circuit currents on the 6 kV sections of the bus-bars to suit the VMG - 133 circuit oreakers and to simplify the system as a whole.

The 6 kV bus-bars of each unit are in two sections so as to separate each pair of auxiliaries. In the event of faults, at least half the turbine and boiler auxiliary drives will remain in operation.

The 6 kV motors for the general station plant are supplied from special works transformers. The motors of the standby plant are supplied from different sections in different blocks.

The 380 V works system is built on the same unit principle as the 6 kV system. Each unit has three 6/0.38 kV transformers; each supplies a particular section of the auxiliary feeders. These three sections supply all the general station plant in the main building as well as the plant in the particular blocks. The motors of general station plant outside the main building are supplied from separate transformers.

YEAR
1961

The type of internal equipment also depends on the type of coal pulverization. In one scheme the works supply is met by one central set of distribution gear and in the other schemes by a central unit with "group feeders" disposed near the motors. The second arrangement is more economical in non-ferrous metals and cable. If the separate coal pulverization shop is adopted, the 6 kV motors in this shop and some of the general station plant are supplied from the 6 kV feeders in the pulverization shop itself. It is considered desirable to have eight such feeders, the same number as there are blocks. Each feeder is supplied by cable from the main 6 kV section.

The standby works supply has two 20 MVA transformers which are either connected to the feeder busbars of the 110 kV distribution gear or to the compensation windings of the auto-transformers. These two transformers can start or stop any two blocks at the same time. A spare un-used 31.5 MVA transformer was suggested but the Ministry preferred a system in which the main works transformer would be replaced automatically and any two blocks started or stopped at the same time.

One battery is provided for each two blocks for emergency supply of the 220 V d.c. motor oil pumps, lighting and the control circuits. A reverse battery is also provided for the central control desk. The batteries are charged from dry rectifiers.

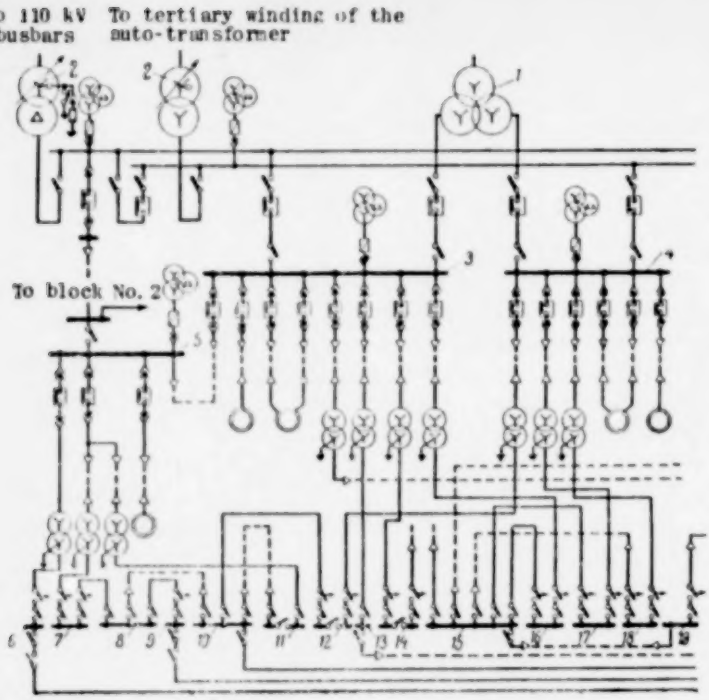

Fig. 6. The internal circuit for the first unit:
1 – No. 1 35.5 MVA works transformer 20 ± 2 x x 2.5%/6.3/6.3 kV; *2* – primary 20 MVA transformers; section 1A of the 6 kV works distribution gear;

4 – section 1B of the 6 kV works distribution gear; *5* – the 6 kV feeder of the coal pulverizing shop; *6* – the 380/220 V feeder of the coal pulverizing shop; *7* – the fuel supply feeder (section No. 1); *8* – standby fuel supply feeder of the auxiliary buildings; *11* – compressor house; *12* – feeder of auxiliary premises; *13* – the lighting in block No. 1; *14* – outdoor distribution gear; *15* – standby feeder of No. 1 block; *16* – engine room (section 1A); *17* – engine room (section 1B); *18* – boiler house (section 1C); *19* – standby feed of No. 3 block.

The electrical installation

The turbo-generators are transverse to the axis of the engine room.

The generators are connected to the booster transformers and supply the works transformers through single phase conductors in aluminium housings to eliminate interphase short circuits (Fig. 7). The conductors between the generators and transformers consist of two box-shape aluminium bus-bars 225 x 105 x 17.5 mm in section. These particular dimensions were chosen from the point of view of heating and current density.

The enclosed conductors are cooled by a closed system ventilation with a water air-cooler. The cooled air is first passed into the middle compartment. It then passes to the extreme compartments and then back to the fan. De-ionizers are fitted at the junctions between the middle compartments. The voltage transformers are connected direct on the conductors by plug (pin) contacts without voltage dividers or fuses. They are single phase with their winding connected between phase and earth.

YEAR
1961

The Electrosila works has placed the neutral leads of the 300 MW turbo-generator in the upper part of the face section in a special box which contains all the other leads and neutral leads "from two parallel branches of the generator and transformer for transverse (shunt) differential protection". This arrangement simplifies the erection and exploitation of the main leads as well as the neutral leads.

The phase and neutral leads of the 300 MW generators produced by the Electrosila works are provided with built-in TUL-20 type current transformers.

Any circuit breakers in the generator circuits are mounted under the generator.

A 75 ton bridge-crane is provided in the engine room for the erection and repair of the generator and removal of the rotor. The stator, which weighs 225 tons, is erected by a special appliance fixed to the side wall of the engine room (Fig. 8). The stator is delivered on a special transporter by rail straight into the engine room. An electric winch on a mobile "carriage" is used to lift it from the rail transporter. It is rotated 90° and drawn into the "carriage". The "carriage" is then moved through an opening in the outside wall of the engine room to its

foundations.

The best position for the internal distribution gear is on the outside wall of the engine room, but this involves taking a large number of cables through the engine room since must of the plant is near the boiler. Consequently some of the 6 kV motors are fed from the central distribution gear and others from group feeders near the motors.

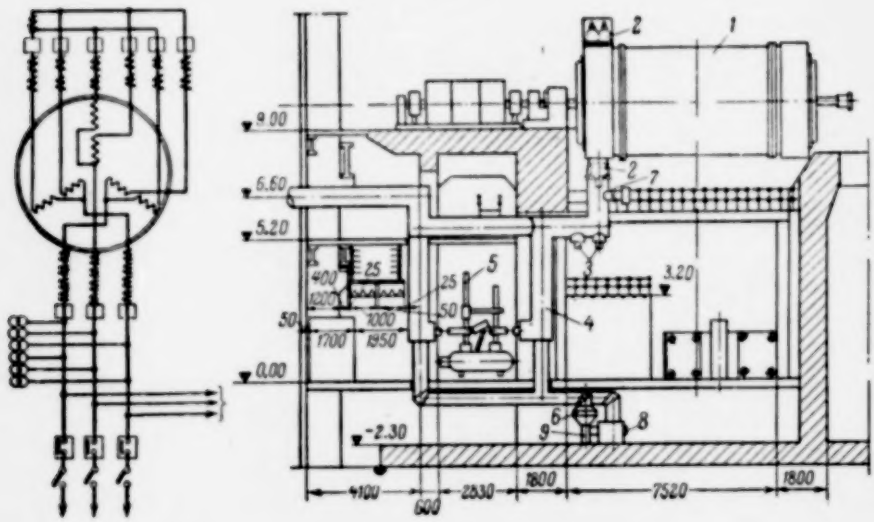

Fig. 7. The stator winding connexion of the generator and the layout of the generator in the engine room (version with a circuit breaker in the main circuit):
1 - generator; *2* - current transformers; *3* - voltage transformers; *4* - enclosed busbar feeder; *5* - air blast circuit breaker; *6* - air cooler; *7* - de-ionizer; *8* - viscous (vision) filter; *9* - centrifugal fan.

Thus the bulk of the internal electrical plant is in two tiers along the wall of the machine building (Fig. 9). This includes the central 6 kV distribution gear for all the blocks (first tier), the 380 V block control panels of the engine room, the 220 V d.c. gear for the whole station and the generator excitation equipment (second tier). There is an intermediate cable run between these two tiers.

The 380 and 220 V distribution gear and 6 kV feeders for the boiler house are either in the boiler house or in the coal store. The arrange-

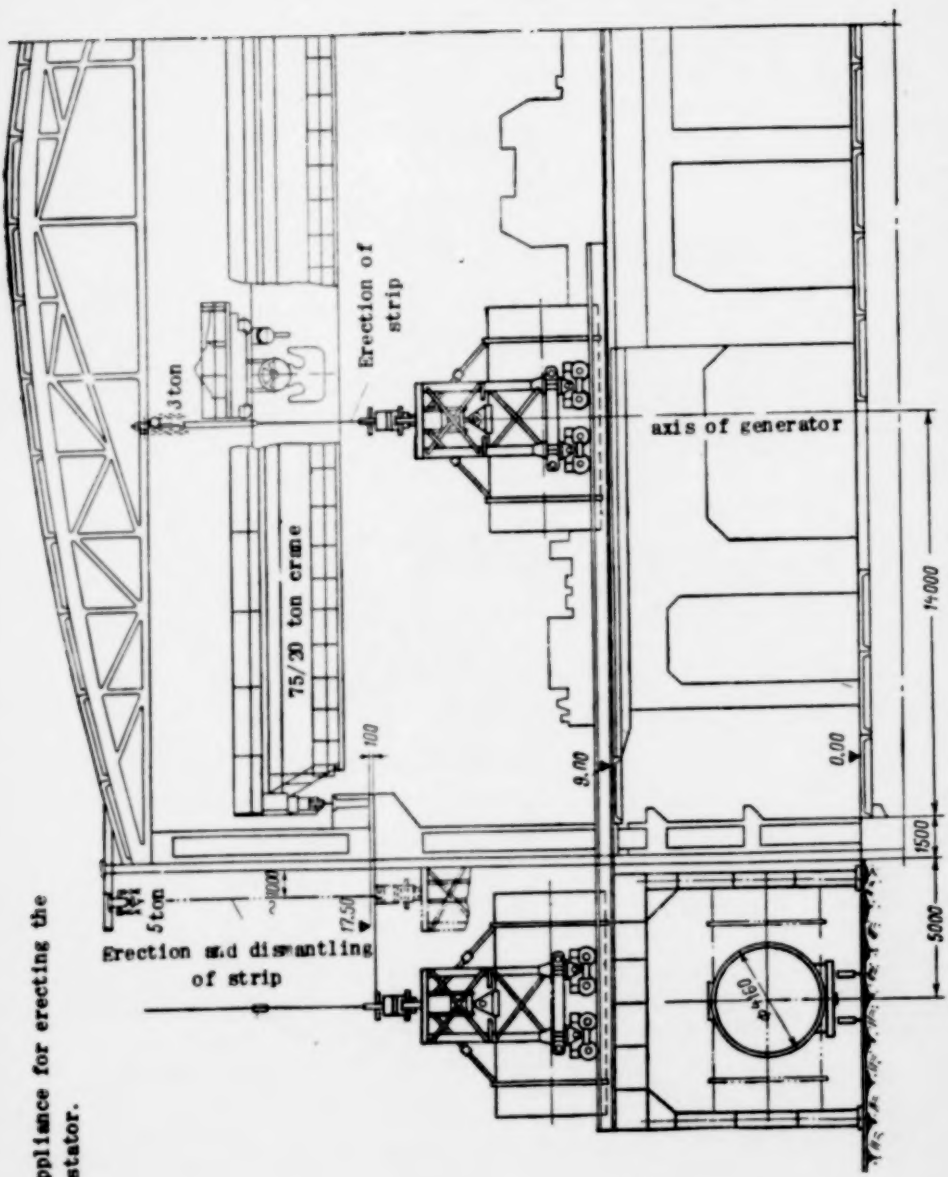

Fig. 8. Appliance for erecting the generator stator.

ment of the other equipment can be seen in Figs. 9 and 10.

The booster transformers are arranged along the railway track outside the machine house. The auto-transformers are mounted near the 110 220 and 500 kV distribution gear.

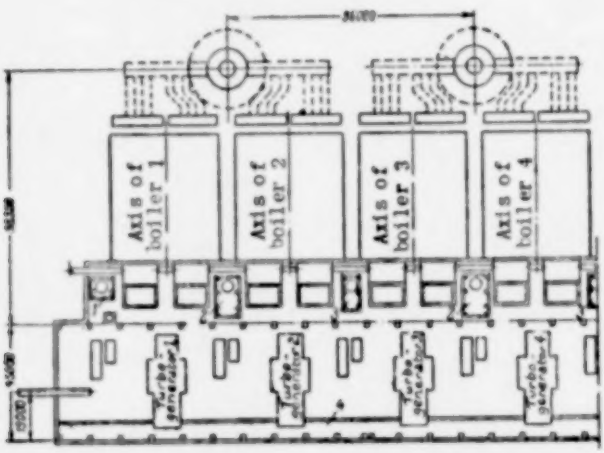

Fig. 9. Part plan of the main building.
1 – central control desk; *2* – unit control panels; *3* – 0.38 kV distribution gear; *4* – 6 kV distribution gear for works supply.

Generator-transformer units are very heavy and there is no special area available in the engine room. It is presupposed that the transformers can be repaired and inspected in situ.

The transformers are made smaller and more accessible by forced oil cooling and radiator-type air-coolers.

The weight of that part of the transformer which is raised during repairs is reduced by making the tank sides and tap detachable from the bottom so that the transformer can be stripped without lifting the core and windings. The part of the tank to be lifted weighs about 55 to 60 tons, whereas the core is about 200 to 250 tons.

On erection the transformers are taken from the transporters and mounted on their foundations by winches and jacks etc. They are delivered ready for inspection and use, only slight adjustments being required.

Fig. 11 illustrates the method of inspecting and repairing the trans-

formers. The π-shaped tower is placed over the transformer in the same plane as the main axis of the transformer. Its width depends on the length of the tank without radiators (9.5 to 10 m). It is fixed at 12 m. The tower must be high enough to lift the tank by longitudinal and transverse braces which greatly reduces the distance between the hooks of the hoist and the ground. This distance is about 15 to 16 m. The tower is dismantled by an ordinary lorry-mounted crane as no part weighs more than 5 tons.

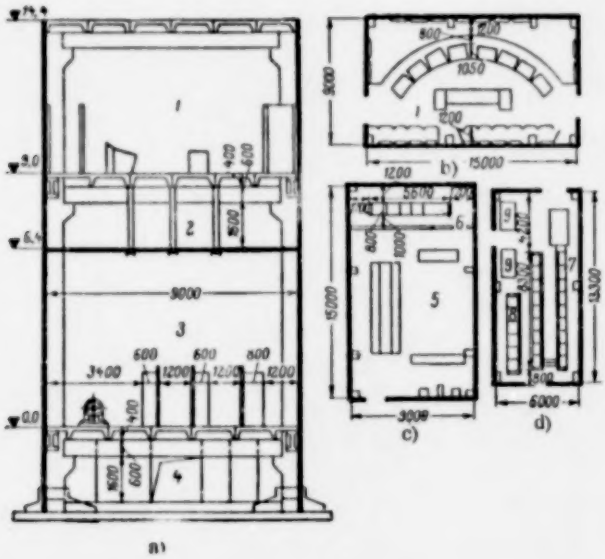

Fig. 10. Layout of the electrical equipment at the unit control panels (*a*, *b*), the central control panel (*c*) and the 0.38 kV distribution gear (*d*):
1 – unit control panel; *2* – intermediate cable run; *3* – the 0.38 kV distribution gear; *4* – cable basement; *5* – central control panel; *6* – d.c. panel; *7* – the 0.38 kV distribution gear; *8* – the d.c. boiler control panel; *9* – converters.

For the outdoor distribution gear of all voltages, use is made of a "centre arrangement" with all line and transformer circuit breakers in one row. The busbar isolators are stepped as in Fig. 12. The "cross-pieces" joining the isolators of the two sets of busbars are now underneath the busbars. This reduces the height of the pylons, simplifies

their construction and allows the use of reinforced concrete sections. The same hollow reinforced concrete pillars are used for the outdoor distribution gear as for the transmission lines. Sectional reinforced concrete structures are also used to support the distribution apparatus.

Owing to corona conditions, the leads of the 500 kV outdoor distribution gear are to be aluminium conductors with steel cores. Each phase at present consists of three such conductors but the new hollow AP-500 type aluminium conductors will make it possible for each phase to consist of two such conductors.

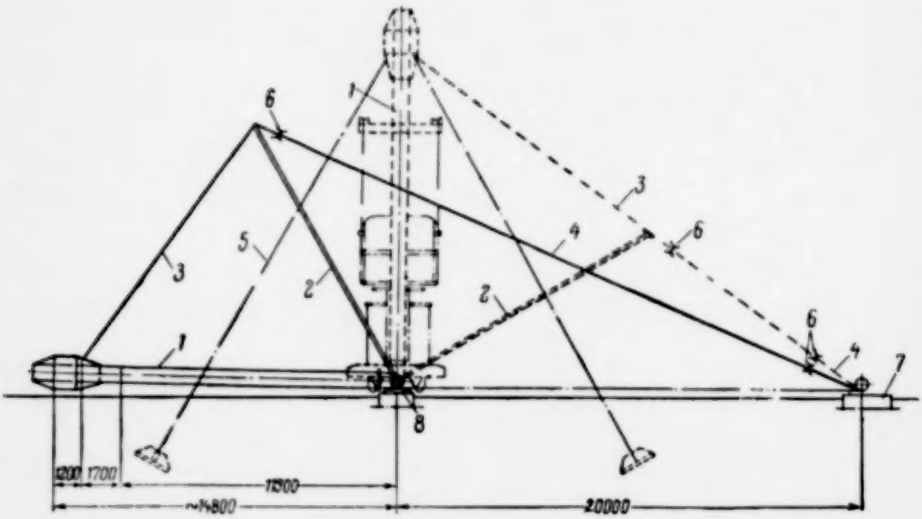

Fig. 11. Appliance for inspecting and repairing the transformers at the outdoor distribution gear: *1* - tower; *2* - A-shaped boom; *3* - rope from support to boom; *4* - rope from boom to winch; *5* - brake cable; *6* - pulley block; *7* - the 5 ton winch for lifting the tower; *8* - tower shoe.

The groups of 110/220 and 220/500 kV auto-transformers are arranged adjacent to the common points of the appropriate distribution gear.

The outdoor distribution gear may be sited in front of the engine room to the side of the engine room which is clear, or behind the coal store (Fig. 13).

In the latter arrangement each 110-330 kV booster transformer and group of single phase 500 kV transformers has a single-circuit steel

YEAR
1961

1	2	3	4	5	6	7	8
Auto-transformer	Transfer breaker	Booster tfmr 1	Outgoing line 1	Booster tfmr 2	Outgoing line 2	Gross pieces	Outgoing line 3

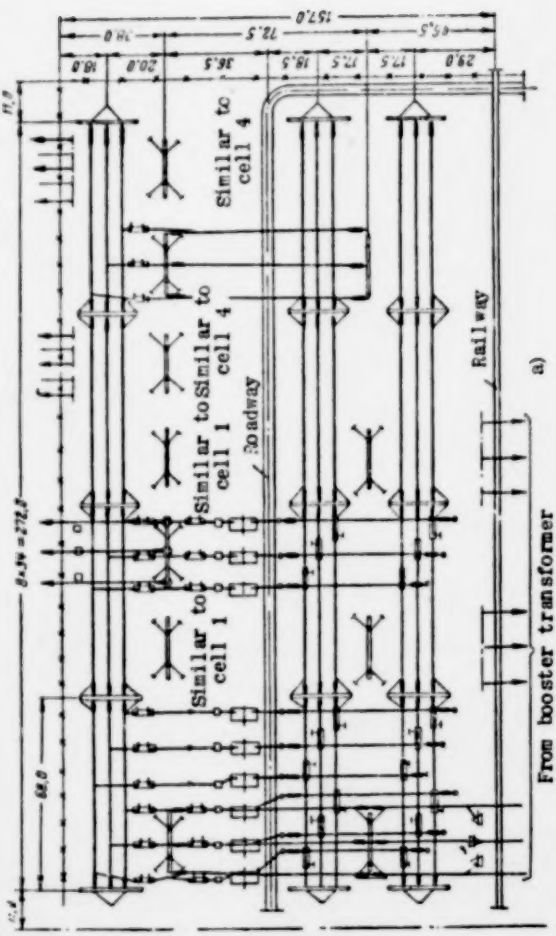

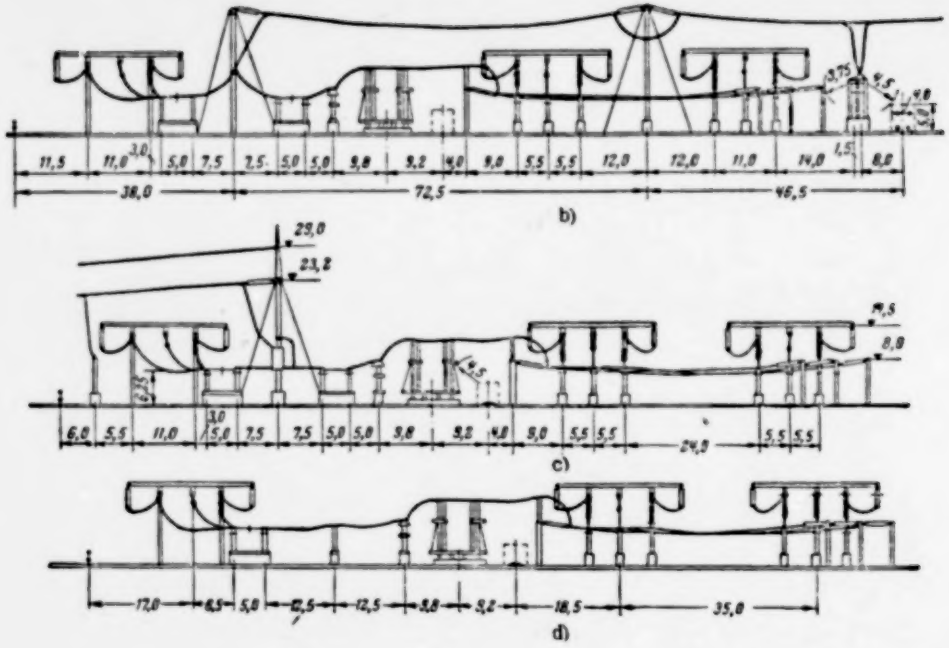

Fig. 12. The 500 kV outdoor distribution gear with sectional reinforced concrete components:

a – plan view; *b* – section across transformer cubicle; *c* – section across transmission line; *d* – section across transfer circuit breaker cubicle.

YEAR
1962

anchoring support 67 m high with the conductors in the horizontal position.

The height of the support depends on the distance between the conductors and the highest point of the main building (Fig. 15). The chimney stack acts as the next support for two 110-330 kV circuits or one 500 kV circuit. The conductors are secured on the stack at a point along ground level depending on the height of the anchor column and the permissible sag of the conductors (stress of 1.5 kg/mm^2).

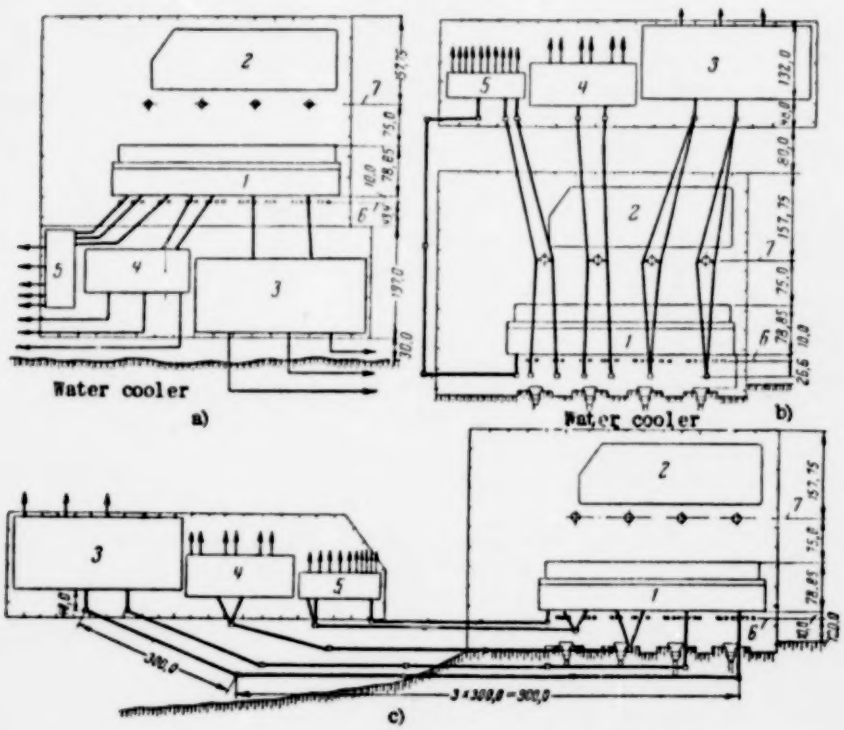

Fig. 13. Layout of the outdoor distribution gear in relation to the main building:
a - version 1, *b* - version 2; *c* - version 3.
1 - main building; *2* - coal store; *3* - the 500 kV outdoor distribution gear; *4* - the same, 220 kV; *5* - the same, 110 kV; *6* - axis of the booster transformers; *7* - axis of the chimney stacks.

No supports are fixed on the roof of the main building as this is constructed of sectional reinforced concrete units. A very large saving in cable has been made.

Control

The various control devices are operated from the various unit control panels. A control panel is installed between each pair of adjacent units.

The unit control panels are coordinated with the 110, 220 and 500 kV general station control devices on a central control desk in the main building. Manual control and visual inspection has been replaced by automatic controls to the maximum possible extent and maximum decentralization has been the aim.

Remote control and inspection devices have only been retained for work which cannot as yet be made fully automatic, for the standby controls of essential automatic devices and for inaccessible or very remote control objects.

To reduce the size of the unit and central control panels, all the relay protection and automatic devices are placed near the apparatus or objects which they protect or control.

Fig. 15 shows the central control panel.

A small despatcher-type panel is used to supervise (watch) and coordinate the station equipment and control panels.

Provision is made for automatic optimization of the distribution of the "active" and "reactive" loads between the units.

A d.c. voltage of 48 to 60 V is used to facilitate the use of soldered connexions and lightweight cheap cables.

It is planned to apply automation to all the boiler operations (combustion, water supply, coal pulverization, draught and air blast etc). and to the protection of the main and auxiliary equipment. Technological "blocking" and automatic connexion of standby equipment is employed. Boiler cleaning will also be done automatically.

The turbine unit is automatically controlled and regulated under normal operating conditions and automatic protection is provided.

YEAR
1961

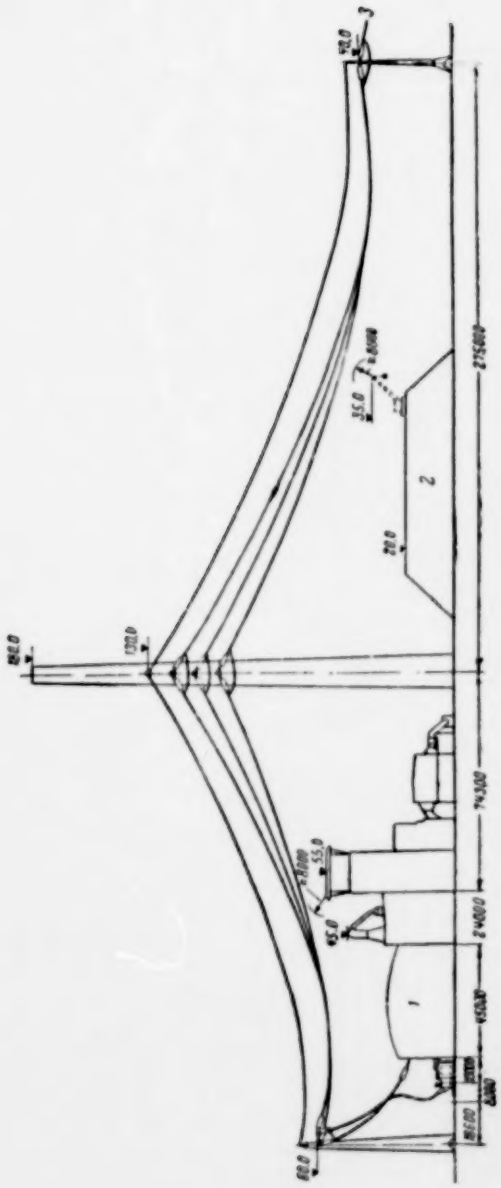

Fig. 14. The overhead transmission from the booster transformers to the outdoor distribution gear:
1 - engine room; *2* - coal store; *3* - to tower of the outdoor distribution gear.

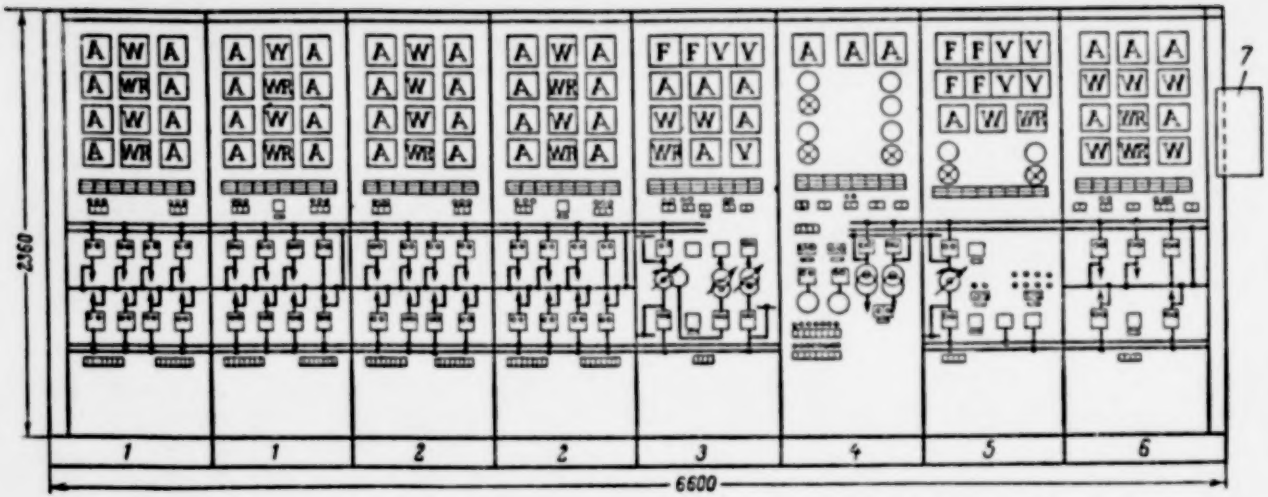

Fig. 15. Front view of central control panel:
1 - 110 kV lines; *2* - 220 kV lines; *3* - 110/220 kV auto-transformer and works transformer, bus-bars of 110 kV equipment; *4* - central indication, circuit breakers of 500 kV blocks, standby exciters, selsyns; *5* - 220-500 kV transformer and bus-bar equipment 220 kV; *6* - 500 kV lines; *7* - synchronizing column.

YEA
196

The fuel supply, water supply, and chemical water purification will be mainly automatic and technological "blocking", automatic protection and automatic connexion of the standby equipment will be provided.

If the equipment or automatic devices cease to function properly there is an alarm system to call the appropriate personnel.

A central communication system is used for inspection purposes to provide printed information, statistical control and inducation of maladjustments.

Multiple – camera television equipment is provided to review the decentralized control panels and observe the combustion process and state of the equipment.

Further automatic devices are to be installed as they become available with the ultimate aim of applying complete automation to each entire station.

YEAR
1961

Conclusion

Such big power stations were not a practical proposition until the large 330 and 500 kV transmission systems had been developed.

Work has been proceeding since 1957 on the production of steam turbines up to 300 MW, turbo-generators up to 300 MW with forced hydrogen cooling and water cooling of the stator windings, 110, 150 and 220 kV three-phase transformers, 220/110 kV auto-transformers of 120, 180 and 240 MVA rating, 330 and 500 kV transformers and auto-transformers, 110 kV and 150 kV air blast circuit breakers with rupturing capacities of 6 GVA, 220 kV breakers with rupturing capacities of 10 GVA, 330 kV breakers with a rupturing capacity of 10 GVA and of 500 kV for 12 GVA, totally enclosed single- and two- speed outdoor motors for the auxiliary equipment of the boilers, hydraulic clutches for controlling the speed of the feed pumps and compact totally enclosed conductors for generators currents of 6, 7.5 and 9 kA.

It cannot however be said that the U.S.S.R. occupies a leading world position in these matters as it does in hydro-electric power and long distance transmission. The rate of production of the large units required for fuel-fired power stations is not keeping pace with demand. About 6000 MW of new power is now being produced annually. This figure is to be increased to 12,000 MW by 1965, 18,000 MW by 1970 and 25,000 MW by 1975. The electrical industry will have to produce still larger

units if this programme is to be fulfilled.

It takes four to five years to design and actually produce a new large set. A start must therefore be made at once on still larger equipment if the requirements are to be satisfied in the period after 1965.

Turbine and generator factories are already engaged on the development of single-shaft 500 MW units and twin-shaft units of 800 and 1000 MW. But long term planning requires that boiler, transformer and switchgear works should be following suit. Research and development should commence on three-phase a.c. transmission of 750 kV and d.c. transmission of ± 700 kV together from fuel-fired power stations with units of 500, 800 and 1000 MW.

Translated by O.M. Blunn

YEA
196

REFERENCES

1. L.I Dvoskii and A.B. Krikunchuk; *Elektrichestvo*, No.11, (1957).
2. V.G. Zhilin; *Elektr. stants.*, No.8,(1959).
3. V.G. Zhilin and A.M. Nekrasov; *Elektr. stants.*, No.6, (1960).

A STATISTICAL METHOD OF ESTIMATING THE RELIABILITY OF ELECTRIC LOCOMOTIVES*

I.P. ISAEV (Moscow Institute of Railway Engineers) and
V.S. SONIN (Urals department of the TsNII MPS)

(Received 6 April 1960)

YEAR
1961

Estimates of the reliability of the individual units in the power circuit of electrical locomotive and of the system as a whole are required before better control systems can be devised.

The electrical equipment of an electric locomotive can fail suddenly because of latent defects or gradually wear out in use. Here the important factors are the standards of production and erection and the operating conditions.

On the one hand the utilization of the locomotive can be complicated by faults in design or erection, and on the other, the electrical, mechanical and thermal strength of the locomotive can be upset by incorrect use.

These various factors may be of a regular nature (e.g. non-uniform loading of the motors, amount of cooling air etc) or else random (breakdown of the insulation, rupture of the leads, incorrect operation of the relays etc).

The reliability of an electric locomotive can be reduced by all these factors.

Up to the present time the reliability of an electric locomotive has only been conceived in a purely qualitative sense. But it has been shown by an analysis of operating experience with electrified railways that a quantitative definition is also possible.

The power and control circuits of all electric locomotives consist of

* *Elektrichestvo*, 3, 18-22, 1961.

a large number of separate units, each of which can be regarded as a set of component items. Although certain units may be connected in parallel in operation, the reliability of a locomotive depends nevertheless on the reliability of each component item. Since the operating conditions vary even for the same type of item, it follows that a statistical approach must be followed [1-3].

We will define the *operational reliability of an electrical locomotive* (scheme) as the probability of faultless operation over a given distance for defined tolerances in the production and installation of the units under given operating conditions. Every random fault a_i in a unit is then defined as a function of the distribution density of the probabilities $\lambda_i(L)$ or as the probability of a fault over the given distance (0, L):

$$p(a_i) = \int_0^L \lambda_i(L)\, dL. \tag{1}$$

Conversely, the probability of faultless operation of this unit is:

$$1 - p(a_i).$$

The reliability of the locomotive circuits can therefore be established by the relation between the probability of the individual items being reliable and the probability of the whole circuit being reliable, i.e. by forming the reliability function of the system.

Since the whole system is out of order if any of the n items fail in the locomotive circuits, the general reliability function of the whole system therefore takes the form:

$$P = \prod_1^n [1 - p(a_i)]. \tag{2}$$

An analysis of this expression provides certain relationships which can be verified by operational data and these relationships can be used to solve certain new problems.

Operational faults in the electrical equipment and power circuits. The power circuit of an electric locomotive is composed of k independent units all of which may fail independently of another failure. Consequently, the reliability function on the basis of expression (2) can take the form

$$R = 1 - \prod_1^k [1 - p(a_i)]. \tag{3}$$

Since the system must possess a high degree of reliability, its unreliability can be approximated in the form:

$$R = p(\alpha_1) + p(\alpha_2) + \ldots + p(\alpha_k),$$

where $p(\alpha_i)$ is the probability of the individual units failing.

When considered with (1), we get:

$$R = \int_0^L \lambda_1(L)\,dL + \int_0^L \lambda_2(L)\,dL + \int_0^L \lambda_k(L)\,dL.$$

Suppose we put Λ for the function of the density distribution of the probability of failure in the power circuit as a single whole, then

$$R = \int_0^L \Lambda(L)\,dL, \tag{4}$$

YEAR
1961

where

$$\Lambda(L) = \sum_1^k \lambda_i(L).$$

Thus, the distribution density of faults in the power circuit equals the sum of the distribution densities of faults in the units. Having the statistical distribution of the faults in the units of the locomotive system as a function of its distance travelled, we can either define the reliability of the system for a given distance, or with the adopted probability of faultless travel, for a given degree of reliability of the locomotive system.

As an example we will consider the available data for faults in the units in the power circuits of d. c. locomotive equipped with DPE-400 type traction motors. An analysis of these data has shown that 36% of electric locomotive breakdowns are attributable to the units in the traction motors, 31% to the electrical apparatus and 3% to the auxiliary machines.

Table 1 lists the particular faults causing the failure of the least unreliable unit in locomotives (the motors) as a percentage of the total number of faults.

Table 1 shows that the most unreliable unit in the traction motor is the armature.

TABLE 1

Motor unit	Faults, %
Armature	53.7
Brush holders and brackets ..	17.3
Cable leads and cross pieces ..	14.3
Bearings	6.2
Main poles and compoles	3.7
Other	4.9

These data have been statistically treated and a bar diagram produced for the distribution of the faults over the units of the DPE-400 type traction motor as a function of distance (Fig. 1). We have also analytically established the functions for the distribution density of the probability of the individual units failing with distance (Table 2).

TABLE 2

Motor unit	Probability density of faults λ_i
Armature	$0.179L^{0.835}e^{-0.407L}$
Brush holders and brackets ..	$0.055L^{-0.755}e^{-0.037L}$
Cable leads and cross pieces ..	$0.038L^{-0.232}e^{-0.129}$
Bearings	$0.0185L^{-1.456}e^{-0.188L}$
Main poles and compoles	$0.022L^{-0.0979}e^{-0.219L}$

Using these analytical expressions it can be shown, for example, that the reliability of the armature is 0.69, that of the brush holders and brackets 0.968, the cable leads and crosspieces 0.935 and main poles and compoles 0.932 for an average distance travelled before repair (400,000 km).

Consequently, using (2), the reliability function of the locomotive power system is

$$P = \prod_{1}^{4} [1 - p(\lambda_i)] = 0.69 \cdot 0.968 \cdot 0.935 \cdot 0.932 = 0.53.$$

This means that about 53 of every hundred traction motors are free of faults up to the mean repair.

An analysis of armature faults shows that they are mainly due to the breakdown of the winding insulation.

It is therefore of practical value to obtain an estimate of the probability of a failure of the armature winding insulation for the various production standards.

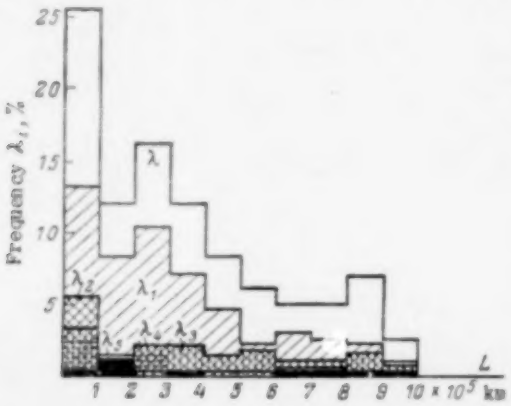

Fig. 1. Histogram of the distribution of faults in the components of DPE-400 type traction motors.

Each conductor and each section of the armature winding is insulated and fitted separately and there is no relationship between variations in binding tension, insulation thickness, or other such technological factor. We can assume that the law governing the distribution of mileage covered prior to breakdown due to the insulation of the armature winding is normally distributed about the mean mileage of the locomotive.

Suppose we put λ_S for the probability of a breakdown in the insulation of an individual section of a winding and $\lambda_b = n\ \lambda_S$ the probability of a breakdown in the insulation of an armature winding with n slots.

We then get:

$$\lambda_b = n\lambda_s = \frac{n}{\sqrt{2\pi}} \int_x^\infty e^{-\frac{x^2}{2}} dx,$$

where $$x = \frac{\overline{L} - L}{\sigma_L}.$$

Consequently,

$$\frac{\lambda_b}{n} = \frac{1}{2} - \Phi(x),$$

where $\Phi(x)$ is a Laplace function.

Since for DPE-400 type traction motors

$$\lambda_b = 0{,}64 \text{ and } n = 57,$$

it follows that

$$\Phi(x) = \frac{1}{2} - \frac{\lambda_b}{n} = 0.489,$$

which corresponds to $x = 2.3$ and, consequently, to $\overline{L} - L = 2.3\sigma_{L1}$.

Now, if we assume for purposes of comparison that the probability of the armature winding remaining intact must be at least 0.9, we then get $x = 3.6$ and $\overline{L} - L = 3{,}6\sigma_{L2}$ in a similar way.

This implies that given the type of insulation material and similar operating conditions, a 90% probability of the winding remaining intact requires an alteration in the method of production which will ensure that the mean square deviation in mileage of the locomotive σ_{L2} does not exceed 0.64 σ_{L1}.

Incidentally, in integrating the analytical relationships in Table 2 for the distribution density of faults in traction motor units with respect to mileage, we can define the faultless mileage for a given degree of reliability as the value of L corresponding to the integral in question.

The effect of tolerances. Definite tolerances are allowed in production and repair for the current I, voltage U and speed n etc.

These allowances cause a change in the function of the density of unreliability of the locomotive system equal to

$$d\Lambda = \sum_{i}^{m} \frac{\partial \Lambda}{\partial \lambda_i} d\lambda_i,$$

where $$d\lambda_i = \sum_1^k \sum_1^p \frac{\partial \lambda_i}{\partial L} \cdot \frac{dL}{dq}\, dq;$$

n – the number of nodes in the system;

k – the number of items in the i-th unit;

p – the number of standardized parameters of the i-th unit, and

q – a particular standardized parameter of the unit

In its general form the distribution density of faults in the i-th unit of the system can be represented in the form (see Table 2):

$$\lambda_i = aL^{\alpha_i} e^{-\beta_i L}.$$

Therefore,

$$d\lambda_i = \sum_1^k \sum_1^p \lambda_i \left[\frac{\alpha_i}{L} - \beta_i\right] \frac{dL}{dq}\, dq. \tag{5}$$

Thus, the estimation of tolerances merely involves determining the increment in the functions of unreliability of the system from the given parameters.

As an example, the effect of divergence in the characteristics of DPE-400 type traction motors or the unreliability of their armatures can be estimated from (5) by the increment

$$d\lambda_1 = \frac{\partial}{\partial L}\left(0.179 \cdot L^{0,835} \cdot e^{-0,407L}\right) \frac{dL}{dI}\, dI, \tag{6}$$

in which the function of the unreliability density λ_1 is taken from the first line in Table 2 and the load divergence dI is defined in terms of the standardized divergence dn of the speed characteristics of traction motors in the form:

$$\Delta I = \left| \frac{1}{\frac{\partial n}{dI}} \right| \Delta n.$$

For example, given the mean repair, the maximum divergence of the speed characteristics of DPE-400 type traction motors is + 9.5% (for the appropriate air gap tolerances) corresponds to a maximum load divergence of ± 20%[4].

The term in (6) for the rate of variation in the mileage covered as a function of the load is conventionally defined as the ratio of the mileage between repairs ΔL to the difference in loads ΔI on the traction motors between two consecutive repairs as measured by the divergence in the speed characteristics of traction motors during period overhauls (Fig. 2). This definition is used since no statistics are as yet available about variations in the characteristics of traction motors with operating time or mileage.

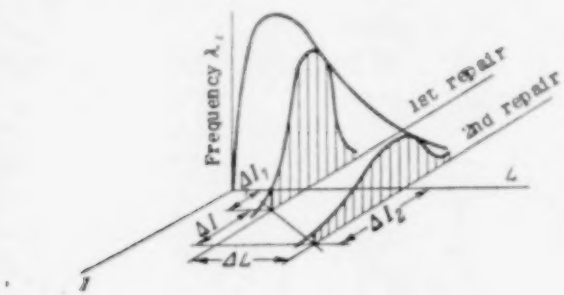

Fig. 2. The effect of tolerances on the reliability function of a locomotive unit.

As an example, for running repairs and periodic overhauls of traction motors

$$\frac{\Delta L}{\Delta I} = 6.7 \times 10^3 \text{ km/A}$$

Using (6) we can find the change in the function of the density of unreliability of the armatures of DPE-400 type traction motors (after an average overhaul):

$$\Delta\lambda_i = 0.69\left[\frac{0.835}{2\cdot 10^5} - 0.407\right]6.7\times 10^3 = \\ = -1.87\times 10^{-5}\Delta I.$$

It follows from this example that deviations in the parameters of a locomotive scheme may have a substantial effect on operational reliability.

For a fuller estimate of this influence it must be borne in mind that the statistical distribution of the deviations in the parameters between the limits of the field of tolerances is usually governed by a

normal Gaussian law [4]. Therefore, supposing $\frac{\lambda_i - \bar{\lambda}_i}{\sigma_{\lambda i}} = t$, we can establish that the distribution density of the probability of defects in the items of a scheme due to allowances for parameters is governed by a Gaussian law with a mean value $\bar{\lambda}_i$ of the probability of defects and a standard deviation

$$\sigma^2_{\lambda i} = \sum_1^k \sum_1^p \left[\bar{\lambda}_i \left(\frac{\bar{\alpha}_i}{\bar{L}} - \bar{\beta}_i \right) \frac{dL}{d\bar{q}} \right]^2 \sigma^2_q,$$

where σ^2_q is the deviation in the distribution of the parameter q of the i-th item of the system.

Similarly, from (4) we can estimate the effect of allowances on the reliability of the whole locomotive system by the parameters of the Gaussian distribution in the form $\bar{\Lambda}$ and

$$\sigma^2_\Lambda = \sum_1^m \left(\frac{\partial \Lambda}{\partial \bar{\lambda}_i} \right)^2 \sigma^2_{\lambda i},$$

Using these we can determine the reliable travel of an electric locomotive with accepted probability of defects by a Laplace function in the form:

$$L = \bar{L} - t\sigma_\Lambda.$$

The technical specifications (TU) and State Standards (GOST) which lay down the allowances for deviations in the parameters of the items and units in the electrical circuits of electric locomotives thus define the probability of reliable operation over a given mileage as well as the operational characteristics and power utilization of the locomotives.

The relationships which are obtained in this way can be used in the development of power and control circuits for new types of locomotive as well as for operational purposes in order to reduce the probability of defects in the individual units.

In addition, this method can be used to estimate the number of standby parts and arrange repair schedules etc.

The solution of such problems must be based on the cost analysis of alternative arrangements.

Translated by O.M. Blunn

REFERENCES

1. V.I. Siforov; *Methods of calculating the reliability of systems containing many items, (O metodakh rascheta nadezhnosti sistem soderzhashchikh bol'shoe kolichestvo elementov).* Akad. Nauk SSSR, OTN, No.6, (1954).
2. Sh.K. Bebiashvili; *Contribution to the theory of the reliability of systems containing many items, (K teorii nadezhnosti raboty sistem soderzhashchikh bol'shoe kolichestvo elementov).* Akad. Nauk SSSR, OTN, No.10, (1955).
3. G.V. Druzhinin; *Avtomet. i telemekh.*, No.12, (1957).
4. I.P. Isaev; *The tolerances on the characteristics of electric locomotives, (Dopuski na kharakteristiki elektricheskikh lokomotivov).* Transzheldorizdat, (1958).
5. A.S. Zingerman; *Zh. tekh. fiz.*, XVIII, No.8, (1948).

THE RELATIONSHIP BETWEEN THE INTERNAL LOSS AND REACTIVE OUTPUT OF SYNCHRONOUS MACHINES*

Professor I. A. SYROMIATNIKOV

(Received 21 October 1960)

YEAR
1961

To solve the problems connected with the choice of the rated power factor of synchronous machines and the efficient allocation of reactive output between individual sources, we need to know the marginal loss and how the losses in synchronous machines vary with their reactive output.

In synchronous generators and motors where the losses caused by the active output are constant, the internal losses caused by the reactive output depend on the losses in the stator and rotor windings. Here the variable internal losses in the stator vary in proportion to the square of the reactive power. But the losses in the rotor winding are governed by a much more complicated law [1, 2].

We will use the following notation:

$\Delta P_{s.r}$ – stator winding loss, including the additional losses, under rated conditions;

$\Delta P_{e.r}$ – excitation winding loss under rated conditions;

$I_{e.r}$ – the rated excitation current;

I_{el} – the excitation current for an active load $P_1 = \beta P_{11}$ and $\cos \phi = 1$;

β – damping coefficient;

$P_1 = \beta P_{1r}$ – the consumption of active power from the network for a motor or that supplied to the network for a generator;

P_{1r} – the same but on rated load;

---

* *Elektrichestvo*, No. 3, 44-48, 1961.

Q – the reactive power of the machine load;

Q_r – the rated reactive power;

S – total output;

I_e – the excitation for the active load $P_1 = \beta P_{1r}$ or the reactive load Q;

$Q_1 = \alpha Q_r$ – the reactive power for operation on the active load $P_1 = \beta P_{1r}$ with rated excitation current;

I_{ac} and I_{reac} – the active and reactive components of the stator current.

The losses in the stator due to the reactive power are

$$\Delta P_{s.\,reac} = \Delta P_{s.\,r} \frac{Q^2}{Q_r^2} \sin^2 \varphi_r \tag{1}$$

The losses in the rotor in synchronous generators and motors depend on the reactive power of these machines:

$$\Delta P_{e.\,reac} = \Delta P_{e.\,r} \left(\frac{I_e^2}{I_{e1}^2} - \frac{I_{e.\,r}^2}{I_{e.\,r}^2} \right). \tag{2}$$

The rotor current can safely be found from the following formula as a function of the reactive power

$$I_e = I_{e1} + (I_{e.\,r} - I_{e1}) \frac{Q}{Q_1}$$

Substituting the ratio

$$\frac{I_e}{I_{e.\,r}} = \frac{I_{e1}}{I_{e.\,r}} + \left(1 - \frac{I_{e1}}{I_{e.\,r}}\right) \frac{Q}{Q_1} = k_1 + (1 - k_1) \frac{Q}{Q_1}$$

in formula (2), we get:

$$\Delta P_{e.\,reac} = \Delta P_{e.\,r} \left[(1 - k_1)^2 \frac{Q^2}{Q_1^2} + 2k_1 (1 - k_1) \frac{Q}{Q_1} \right],$$

or

$$\Delta P_{e.\,reac} = \Delta P_{e.\,r} \left[(1 - k_1)^2 \frac{Q^2}{\alpha^2 Q_r^2} + 2k_1 (1 - k_1) \frac{Q}{\alpha Q_r} \right], \tag{3}$$

where

$$k_1 = \frac{I_{e1}}{I_{e.\,r}}.$$

The total losses depend on the reactive power

$$\Delta P_{\text{reac}} = \Delta P_{\text{s.r}} \sin^2 \varphi_{\text{r}} \frac{Q^2}{Q_{\text{r}}^2} + \Delta P_{\text{e.r}} \times \left[(1-k_1)^2 \frac{Q^2}{a^2 Q_{\text{r}}^2} + 2k_1 (1-k_1) \frac{Q}{aQ_{\text{r}}} \right]. \quad (4)$$

Suppose we put

$$A = \Delta P_{\text{s.r}} \sin^2 \varphi_{\text{r}} + \frac{\Delta P_{\text{e.r}} (1-k_1)^2}{a^2} \quad (5)$$

and

$$B = \frac{2\Delta P_{\text{e.r}} k_1 (1-k_1)}{a}, \quad (6)$$

We then get:

$$\Delta P_{\text{reac}} = A \frac{Q^2}{Q_{\text{r}}^2} + B \frac{Q}{Q_{\text{r}}}. \quad (7)$$

YEAR 1961

In synchronous compensators and variable losses in the stator vary in proportion to the square of the reactive power:

$$\Delta P_{\text{s}} = \Delta P_{\text{s.r}} \frac{Q^2}{Q_{\text{r}}^2}.$$

The total losses in the rotor are found by the formula

$$\Delta P_{\text{e}} = \frac{\Delta P_{\text{e.r}}}{I_{\text{e.r}}^2} \left[I_{\text{e.nl}} + (I_{\text{e.r}} - I_{\text{e.nl}}) \frac{Q}{Q_{\text{r}}} \right]^2,$$

where $I_{\text{e.nl}}$ is the excitation current on no load.

Putting $k_{\text{nl}} = \dfrac{I_{\text{e.nl}}}{I_{\text{e.r}}}$, we get:

$$\Delta P_{\text{e}} = \Delta P_{\text{e.r}} \left[k_{\text{nl}}^2 + (1-k_{\text{nl}})^2 \frac{Q^2}{Q_{\text{r}}^2} + 2k_{\text{nl}} (1-k_{\text{nl}}) \frac{Q}{Q_{\text{r}}} \right].$$

The total losses are

$$\Delta P = \Delta P_{\text{c}} + \Delta P_{\text{e.r}} k_{\text{nl}}^2 + [\Delta P_{\text{s.r}} + \Delta P_{\text{e.r}} (1-k_{\text{nl}})^2] \frac{Q^2}{Q_{\text{r}}^2} + \quad (8)$$

$$+ 2\Delta P_{\text{e.r}} k_{\text{nl}} (1-k_{\text{nl}}) \frac{Q}{Q_{\text{r}}},$$

or

$$\Delta P = C + A\frac{Q^2}{Q_r^2} + B\frac{Q}{Q_r}, \tag{9}$$

where

$$C = \Delta P_c + \Delta P_{e.r}\, k_{nl}^2; \tag{10}$$

$$A = \Delta P_{s.r} + \Delta P_{e.r}(1 - k_{nl})^2; \tag{11}$$

$$B = 2\Delta P_{e.r}\, k_{nl}(1 - k_{nl}); \tag{12}$$

and ΔP_c represents the constant losses.

The excitation currents I_{el}, and $I_{e.nl}$ and the reactive power Q_l have been found by a graphical-analytical method using a vector diagram of the machine. The coefficients k_l and α are defined by the formulae:

$$k_l = \sqrt{\frac{1 + \beta^2 x_d^2 \cos^2 \varphi_r}{1 + x_d^2 + 2x_d \sin \varphi_r}}; \tag{13}$$

$$\alpha = \frac{\sqrt{1 + x_d^2(1 - \beta^2 \cos^2 \varphi_r) + 2x_d \sin \varphi_r} - 1}{x_d \sin \varphi_r}. \tag{14}$$

Fig. 1 shows $(1-k_l)^2$ and $2_l(1-k_l)$ as a function of x_d for $\beta = 1$, 0.75 and 0.5 and $\cos \varphi_r = 0.8$, 0.9 and 1.

Fig. 2 shows the coefficients α and

$$\alpha_l = \frac{Q_l}{S_r} = \frac{\sqrt{1 + x_d(1 - \beta^2)} - 1}{x_d} \tag{15}$$

as a function of β for $\cos \varphi_r = 0.8$, 0.9 and 1.

Tests show that this graphical-analytical method gives much better results than Potier diagrams. Corresponding curves obtained by Potier diagrams are plotted in Fig. 1 for $\beta = 1$ by way of comparison.

The reactive power should be distributed between its various sources on an equal marginal loss basis. The marginal loss is defined as the first derivative of the internal (active), which depends on the reac-

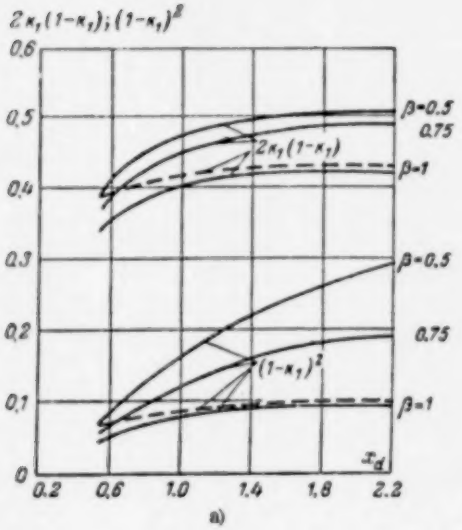

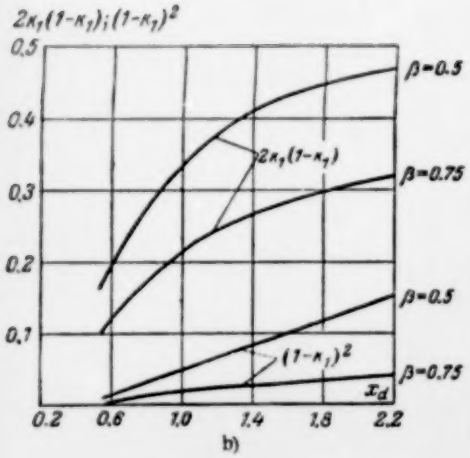

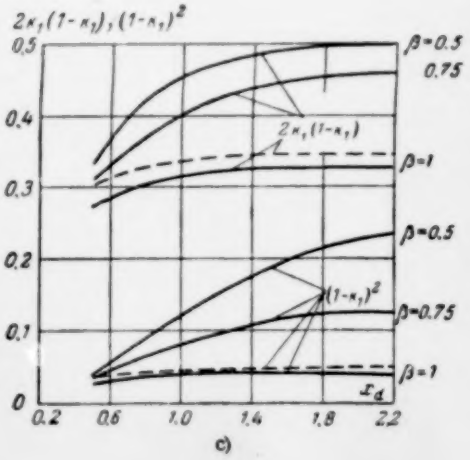

Fig. 1. The variation in $2k_1(1-k)$ and $(1-k_1)^2$ with x_d. a – when $\cos\phi_r = 0.8$; b – $\cos\phi_r = 0.9$; c – $\cos\phi_r = 1$; ---- calculated by a Potier diagram.

tive power, with respect to the reactive power

$$g = \frac{d(\Delta P_{reac})}{dQ} = \frac{2AQ}{Q_r^2} + \frac{B}{Q_r}. \qquad (16)$$

This proposition only refers to the condition when the sources of reactive power are connected in the same electrical circuit. The inclusion of a source of reactive power in a circuit can only be decided if the fixed loss component is considered; if this is neglected, wrong conclusions may be reached. Thus, for example, it was found that a synchronous compensator (or generator used as a compensator) ought to be run with a very small load. But the actual reduction in the internal loss in the synchronous compensator itself (mainly fixed losses in this case). It was therefore only permissible to include the synchronous compensator in the network (or to leave it there) if the other sources of reactive power were fully loaded up to the limit, it therefore being impossible to distribute all the reactive load between them.

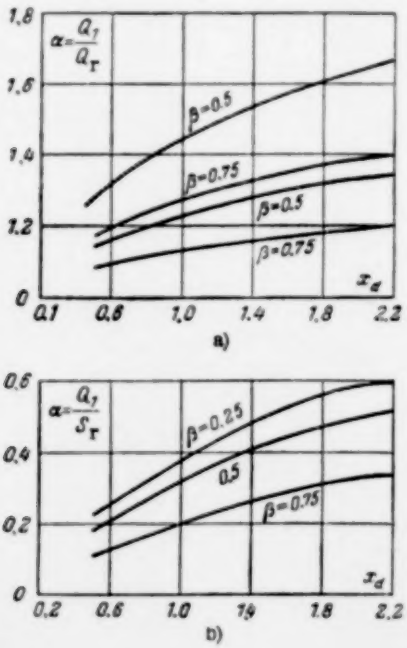

Fig. 2. The coefficient as a function of x_d for $\cos \alpha_r = 0.9$ (two upper curves) and $\cos \phi_r = 0.8$ (two lower curves) (a) and the coefficient α_1 as a function of x_d for $\cos \phi_r = 1$ (b).

The following Table shows the fixed loss components of synchronous generators (the mechanical and stator iron losses including the additional loss) and compensators.

Type		T-2-6-2	T-2-12-2	T-2-25-2	T-2-50-2	TBC-30	TB-50-2	TB-2-100-2
Generator	Fixed loss component, kW	139	205	391	918	214	368	810
Compensator	Power, MVA	7.5	10	15	30	37.5	75	–
	C, kW	104	105	196	379	188	325	–

YEAR 1961

It follows from expressions (5) and (6) that the value of A and B as well as the marginal loss all remain practically constant if the active power load varies.

Consider the following example. It is required to find the active losses ΔP_{reac} which depend on the reactive power, marginal loss or the real load for $\beta = 1$, 0.75 and 0.5 in respect of a DSP-type synchronous motor of 1300 kW, 1520 kVA, 1500 rev/min, $\cos \phi_r = 0.9$, $Q_r = 660$ kVar, $\Delta P_{s.r} = 28.6$ kW, $\Delta P_{e.r} = 8.55$ kW, $\Sigma P = 64.7$ kW and $\eta_r = 0.953$.

Assuming that $x_d = 1.6$ and from Fig. 2 that $2k_1 \cdot (1-k_1) = 0.35$, we then get for $\beta = 1$:

$$A_r = 0.436^2 \cdot 28.6 + 0.05 \cdot 8.55 = 5.86 \text{ kW}$$

$$B_r = 0.35 \cdot 8.55 = 3 \text{ kW}$$

$$\Delta P_{\text{reac. r}} = 5{,}86 \frac{Q^2}{Q_r^2} + 3 \frac{Q}{Q_r}$$

and

$$g_r' = \frac{2 \cdot 5.86 Q}{660 Q_r} + \frac{3}{660} = 0.0178 \frac{Q}{Q_r} + 0.00455.$$

For $\beta = 0.75$ and $\beta = 0.5$, we respectively get:

$$\Delta P_{\text{reac}(0.75)} = 6.1 \frac{Q^2}{Q_r^2} + 2.86 \frac{Q}{Q_r},$$

$$g_{(0.75)} = 0{,}0185\,\frac{Q}{Q_r} + 0{,}0043;$$

$$a_{(0.75)} = 1.35;$$

$$\frac{\Delta P}{\text{reac}(0.5)} = 6{,}2\,\frac{Q^2}{Q_r^2} + 2{,}7\,\frac{Q}{Q_r};$$

$$g_{(0.5)} = 0{,}0188\,\frac{Q}{Q_r} + 0{,}0041;$$

$$a_{(0.5)} = 1.57.$$

The variation in losses and the marginal increase as a function of the reactive power are practically identical for loads of 1, 0.75 and 0.5 rated load. The difference is that the motor can be loaded with a reactive load above the rated load at loads less than the rated load. Thus $a_{(0.75)} = 1.35$ for $\beta = 0.75$ and $a_{(0.5)} = 1.57$ for $\beta = 0.5$.

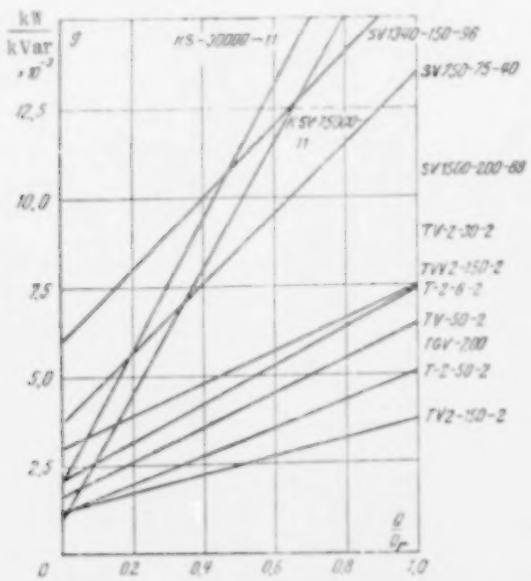

Fig. 3. Marginal loss g as a function of $\frac{Q}{Q_r}$ in synchronous compensators.

Figs. 3 and 4 show the straight line marginal loss curves of various types of synchronous machine.

The tangent of the angle of the marginal loss curve is defined by

YEAR 1961

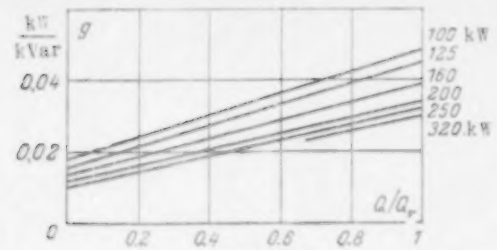

a)

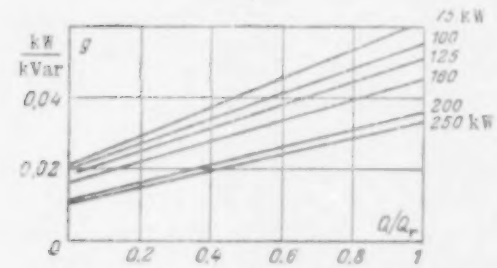

b)

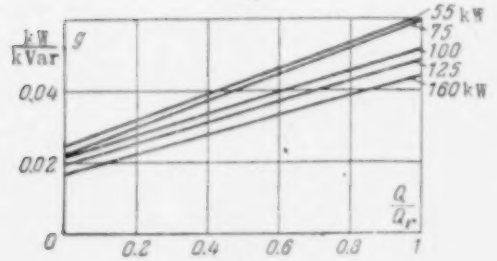

c)

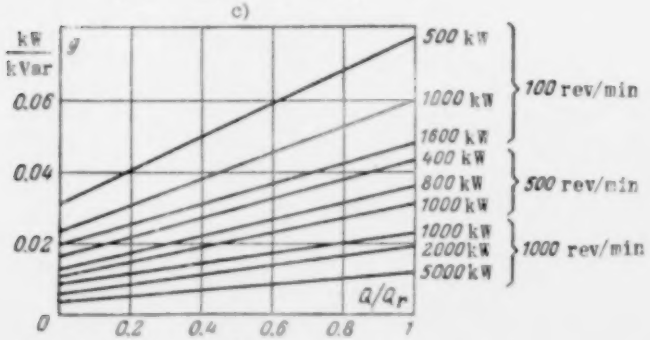

d)

Fig. 4. The marginal loss g as a function of $\frac{Q}{Q_r}$ in synchronous motors:
a – DS type motor of 380 V and 1500 rev/min for cos $\phi_r = 0.9$; c – DS type motor of 380 V and 750 rev/min for cos $\phi_r = 0.9$; d – SM type motor of 6 kV for cos $\phi_r = 0.9$.

the expression

$$\tan\psi = \frac{2A}{B}.$$

The value of tan ψ is a minimum for synchronous motors and a maximum for synchronous compensators. Thus, for example, tan ψ = 7.4 to 17 for synchronous compensators, whereas tan ψ = 1.2 to 2.2 for DS-type synchronous motors.

Translated by O.M. Blunn

REFERENCES

1. L.V. Litvak; *Prom. energet.*, No.10, (1956).
2. I.A. Syromiatnikov; *The technical and economic advantages of synchronous motors, Synchronous motors, (Teknikoekonomicheskie preimushchestva sinkhronnykh dvigatelei, Sinkhronnye dvigateli).* Gosenergoizdat, (1959).

YEA
196

A NEW BRUSHLESS SYNCHRONOUS ALTERNATOR FOR USE IN AIRCRAFT*

L. M. PALASTIN

(VNIIEM)

(Received 26 November 1961)

YEAR
1961

The electrical supply in aircraft has until recently been mainly d. c. However, high altitude flying has considerably increased the brush wear of the electrical machines due to the low humidity of the air at high altitudes and commutation has been adversely effected. The brush assemblies have to be inspected and serviced much more frequently than the other units, whilst the dismantling and replacement of the machine because of brush wear is a time-consuming and costly operation. It has therefore become an urgent matter to eliminate the brush contact from the electrical machine in civil aviation and a number of other cases. In this connexion, there has been a comparatively rapid development of synchronous brushless alternators in the U. S. A. and U. K. for the a. c. supply of aircraft.

Use is currently made of synchronous alternators of 40 to 130 kVA for aircraft purposes [1]. Alternators of such powers are usually provided with separate exciters. The alternator rotor and exciter armature are usually mounted on the same shaft. Unlike general-purpose synchronous machines, use is made of a. c. exciters with a rotating a. c. armature winding which supplies the excitation winding of the alternator via a rotating rectifier.

The following observations can be made about the brushless a. c. alternators which have been used in aircraft [1, 2].

It is inexpedient to use comparatively large asynchronous alternators in aircraft owing to the considerable weight of the capacitors and the

---

* *Elektrichestvo*, No. 3, 51-56, 1961.

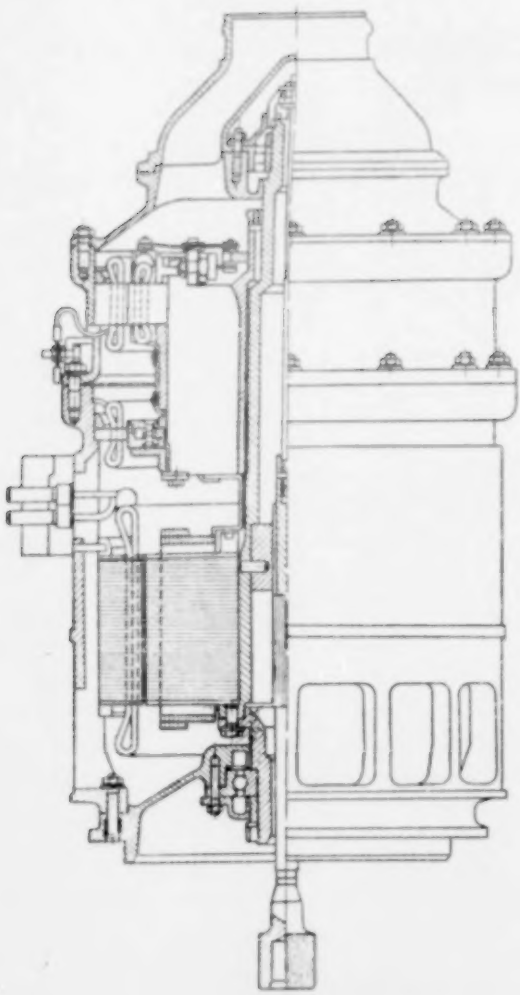

Fig. 1. A British brushless synchronous alternator of 40 kVA.

YEAR
196

devices for controlling the capacitance.

Inductor alternators have been widely used in foreign and Russian aircraft for single phase high frequency loads of relatively low power. The normal requirement is now for three phase alternators of 400 c/s with a small number of poles and it is inexpedient to use inductor alternators for this frequency. However, there is justification for using inductor alternators where an a.c. supply of 2000 c/s is required for electronic equipment.

"Cascade" alternators are heavy and bulky and there are difficulties in ventilation so that they are only used to a limited extent.

Alternators with excitation from permanent magnets have also been used abroad and in the U.S.S.R. for the supply of single and three-phase low-ohmic loads at low frequencies. But such machines have not until recently been used for outputs of the order of several dozen AVA owing to the difficulties involved in the production of relatively large rotating permanent magnets with the requisite magnetic properties and mechanical strength. Neither is there any simple and economical means of regulating the output voltage of alternators with permanent magnets.

Homopolar alternators have been produced both abroad and in the U.S.S.R. In these machines constructional parts of the machine, i.e. the frame and shields are used in the magnetic circuit. The flux is produced by one or two fixed annular excitation windings; it passes through the stator, which is external to the yoke (or frame) and shields, and then through two additional air gaps into the rotor shaft and from the shaft into the air gap stamping of the machine and the stator. These machines have not been widely used owing to their large weight and size and the difficulties involved in providing adequate excitation and ventilation.

Alternators with a fixed excitation winding have been produced by a number of American firms under the name "Seskin". Their weight has been reduced compared with machines of the foregoing type by arranging the magnetic flux in the constructional parts which enter into the rotating inductor of the alternator. The magnetic circuit has four air gaps so that a comparatively large excitation is required. The design and production of such alternators is quite a complicated matter however and they have not been extensively used owing to the difficulties involved in ventilation. Such machines may be useful for low outputs.

Synchronous brushless alternators are synchronous machines with a rotating field system, the winding of which is supplied by direct current

via rectifiers from the armature of the a.c. exciter. The rotor, excitation armature and rectifiers are all mounted on the same shaft.

Until recently, the production of brushless machines has been limited by the absence of semiconductor rectifiers with the requisite reliability, small dimensions, heat resistance and mechanical strength. Such alternators are free of the cited disadvantages. They are lighter in weight and more compact than the normal synchronous alternators with d.c. exciters.

Brushless synchronous alternators with an a.c. exciter and permanent magnet "sub-exciter" were proposed in 1955 by Bertinov [2]. A similar type of brushless synchronous alternator was produced in Great Britain in 1958.

Fig. 1 illustrates the British 40 kVA alternator on show at Farnborough in September 1958. The silicon rectifiers are mounted in a ring with their axes transverse to the axis of the shaft. The self-excitation of the alternator is provided by an auxiliary exciter in addition to the a.c. exciter. This auxiliary exciter is a synchronous alternator with excitation from permanent magnets.

The main and auxiliary exciters are machines with relatively large diameter armatures and short "active" length. The rotors of the exciters are disposed on a ribbed bush which can be slipped over the shaft. The space between the ribs of the bush allows for ventilation since there is very little aerodynamic resistance to the air entering the whole machine.

Short exciters with a relatively large diameter have a large number of poles and generate voltages of a higher frequency than that in the main alternator. Such exciters have the advantage of a short time constant which leads to a rapid recovery of the alternator voltage in the event of sudden load fluctuations.

The British company followed up with an improved version in which the auxiliary exciter was repositioned at the end of the armature of the main alternator on the drive side. This reduced the total length of the machine without adversely affecting the ventilation.

Brushless synchronous alternators have also been produced by other British and American firms for outputs up to 150 kVA.

Their main disadvantages are as follows:

1. Special measures must be taken to provide self-excitation and

these adversely affect the characteristics of the alternators. The use of a third machine with a similar outside diameter to that of the main generator and exciter considerably increases the weight, size and cost of the unit.

2. The large excitation power of an exciter with electromagnetic excitation is due to the large number of poles.

3. Multi-pole exciters with electromagnetic excitation are very complicated to make.

4. The power of the electromagnetic excitation winding of the main alternator is disproportionately large compared with other generators.

5. The time constants of the electromagnetic excitation windings of the main alternator and exciter are relatively large.

YEAR
1961

Brushless synchronous alternators with mixed excitation

The weight and size of brushless synchronous alternators can be greatly reduced if the auxiliary exciter is eliminated and self-excitation provided by the main exciter. This also improves the characteristics and reliability of the alternator.

The author has patented [3] a brushless synchronous alternator with mixed excitation (Fig. 2). The main alternator is of conventional construction having a fixed external armature 1 and a rotor with an excitation winding 2. The a.c. exciter has a fixed external controllable field circuit with excitation from permanent magnets and with a rotating armature 4 which supplies the excitation winding of the main alternator via rotating rectifiers 5. The exciter therefore combines two types of excitation, i.e. that from the permanent magnets and electromagnetic excitation. Each pole of the field circuit consists of one or two permanent magnet bars 7 and the magnetic shunt 6 made from soft magnetic steel. The inductor accommodates the coils of the regulator winding 3 which is supplied with direct current.

Under normal operating conditions the excitation of the alternator is produced by the joint effect of the permanent magnets and the control winding of the exciter field. Self-excitation of the alternator is provided by the permanent magnets of the exciter. The flux of the permanent magnets passes through the air gap and the exciter armature and is partially shunted by the magnetic shunts which increase the

leakage fluxes of the permanent magnets. The current in the control winding is in such a direction that the magnetic flux which it produces in the poles of the exciter is in the same direction as the flux produced by the permanent magnets. Hence the flux in the shunt due to the control winding is in the opposite direction to the leakage flux of the permanent magnets which is shunted through this same shunt. If it is necessary to increase the flux in the air gap of the exciter, the magnetic flux of the control winding draws the leakage flux of the magnets from the shunt into the gap.

The main alternator voltage is controlled by varying the flux in the exciter gap. This leads to a change in the flux in the gap of the main alternator.

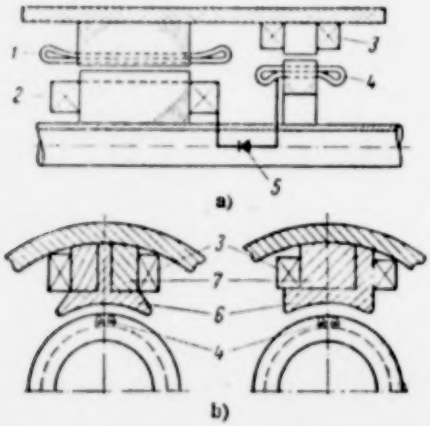

Fig. 2. Longtudinal (*a*) and cross (*b*) sections of a brushless synchronous alternator with mixed electromagnetic and permanent magnet excitation. *1* - armature winding of main alternator; *2* - excitation winding of main alternator; *3* - control winding of exciter; *4* - rotating armature winding of exciter; *5* - rotating rectifiers; *6* - magnetic shunt of soft magnetic steel; *7* - permanent magnets.

To control the alternator voltage, the control winding of the exciter must produce an m.m.f. which compensates the effect of the voltage reactions and drops in the armature circuits of the alternator and exciter. Here the control winding requires much less excitation power than an electromagnetic rotor (inductor) of equal volume since the main part of

the excitation flux of the exciter is provided by the permanent magnets. In the exciter with the electromagnetic field, the control winding must produce an m.m.f. which ensures that all the magnetic flux passes through the magnetic circuit and which will also compensate the effect of voltage drops and reactions in the armature circuit. The control winding in the permanent magnet exciter has to produce a much smaller m.m.f. since it regulates the total flux in the exciter gap by varying only a small part of it (i.e. the leakage fluxes of the permanent magnets in the magnetic shunts). However, the main part of the flux in the exciter gap is provided by the permanent magnets. If we bear in mind that the magnetic energy of a permanent magnet can be greater than that of an electromagnet of the same size, it immediately becomes clear why the excitation is reduced so much.

It is quite expedient to reduce the excitation power or the weight and size of the main alternator to reduce the electromagnetic time constant of the main excitation winding by providing the alternator with combined electromagnetic and permanent magnet excitation.

YEAR
1961

If the supply frequency must be high, the alternator can be provided with a salient pole rotor with mixed excitation. The advantages of this construction are already well known [4, 5, 6]. For the normal a.c. supply frequency the alternator can be provided with a rotating salient-pole exciter with mixed excitation.

Most of the permanent magnet flux in salient pole rotors with mixed excitation passes into the gap, but a portion is shunted in two side shunts by increasing the leakage flux of the magnet. The coils of the excitation winding around the magnet bars with magnetic shunts regulate the flux in the gap by acting upon the leakage fluxes of the magnets which are shunted in the magnetic shunts. Consequently, if the basic dimensions, electromagnetic loads on the machines, and the parameters and dimensions of the magnets, magnetic shunts and excitation windings are all correctly chosen, variable voltage machines with permanent magnets have a number of real advantages over similar machines with electromagnetic excitation as shown by tests.

We will give the details of tests which have been carried out on two identical machines with two permanent bar magnets per pole made from "magnico" alloy and electromagnetic excitation as used for the exciters of brushless synchronous alternators.

Certain characteristics are expressed in relative units to assist comparison.

No load characteristics

For purposes of comparison, Fig. 3 shows the test no load characteristics (the no load voltage at the terminals of the armature windings of the exciter as a function of the m.m.f. of their excitation windings at rated speed). Fig. 3 also shows the variation in the no load voltage as a function of the power of the excitation windings. It will be seen from a comparison of these curves that the excitation winding m.m.f. is 1.0 and 1.85 respectively for the permanent magnet exciter (curve 1) and that with electromagnetic excitation (curve 2) given a specific no load voltage. This shows that the total excitation winding m.m.f. of permanent magnet exciters is much less, other things being equal, than that of an exciter with electromagnetic excitation. Such a considerable reduction in the excitation ampere-turns causes an even greater reduction in the excitation power since the latter varies in proportion to the square of the ampere-turns for a specific volume of copper.

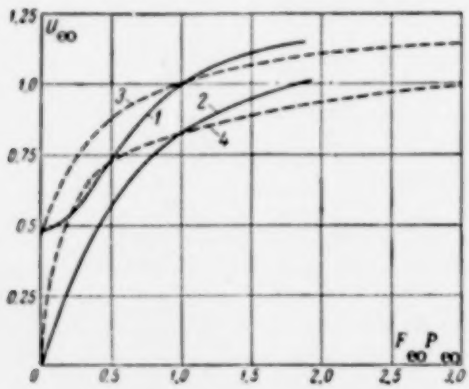

Fig. 3. The no load characteristics (———) and variation in the no load voltage as a function of excitation power (– – –) for permanent magnet exciters (curve 1 and 3) and electromagnetic exciters (curves 2 and 4).

It will be seen from a comparison of the variation in the no load voltage as a function of the power of the excitation windings that the letter is 1.0 and 3.04 respectively for the permanent magnet exciter (curve 3) and that with electromagnetic excitation (curve 4).

Consequently, the electromagnetic exciter requires three times more excitation power than a corresponding permanent magnet exciter.

Incidentally, the voltage in a permanent magnet exciter can be increased 15 to 20% above its rated value without any significant increase in excitation power, whereas such an increase is impossible in electro-magnetic exciters owing to the saturation of the magnetic circuit.

Self-excitation

The self-excitation of the foregoing alternators without a special "sub-exciter" or other appliance requires quite a large residual flux in the a.c. exciter or the main alternator. It is not an easy matter to produce the large residual flux in electromagnetic exciters as required for reliable self-excitation. But even when this can be successfully arranged, the magnetization characteristic of the exciter has a wide hysteresis loop which adversely affects the conditions for stabilizing the alternator voltage.

YEAR
1961

This contradiction is eliminated by using a permanent magnet exciter.

It can be seen from the curves in Fig. 3 that the residual no load voltage in a permanent magnet exciter is 50% of rated. This is quite adequate for self-excitation. The magnetization characteristic has the same narrow hysteresis loop as an electromagnetic exciter having very little residual voltage at which self-excitation is not assured. The dimensions of the permanent magnets were chosen to ensure the minimum excitation power. If the excitation power is increased by 15 to 20 per cent above its minimum value, the volume of the permanent magnets can be fixed so that the residual voltage of the exciter is close to the rated value.

The time constants of the excitation windings of the exciters

The electromagnetic time constants of the excitation windings of the permanent magnet and electromagnetic exciters. Fig. 4 shows the experimentally-determined variation in the time constant as a function of the excitation winding m.m.f.'s. It will be seen from Fig. 4 that the time constants of the permanent magnet exciter are 1.3 to 2.0 times less than in the electromagnetic exciter over the operating range. These data agree with those published by A.I. Kantor, T.G. Soroker and others who showed that transients take place more quickly in machines with permanent magnet excitation than in machines with electromagnetic excitation. Permanent magnet exciters can therefore considerably reduce

the duration of transient phenomena in the control system compared with electromagnetic excitation.

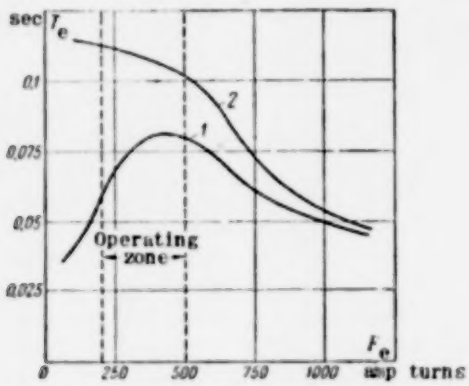

Fig. 4. The time constants of the excitation windings as a function of their m.m.f.
1 - for permanent magnetic exciters; *2* - for electromagnetic exciter.

The magnetization of permanent magnets

The permanent magnets of electrical machines are usually magnetized by special magnetizing plant. In practice it is not possible to achieve complete magnetization of the magnets in the assembled state owing to the negative effect of the air gap, the leakage permeance of the magnetic circuit and the fact that an adequate m.m.f. cannot be produced in the armature windings.

In the proposed permanent magnet exciters the excitation winding directly embraces the permanent magnets and the total flux passes through the magnets along their magnetic axis. The permanent magnets can therefore be magnetized in the assembled exciter by the excitation windings by passing a high direct current along it for a short period of time. (This current is 3 to 5 times higher than the rated value). This is a very important point in the production and utilization of machines with permanent magnets.

The effect of short circuit currents on permanent magnets

In conventional synchronous alternators the permanent magnets are

demagnetized by short circuit currents so that their efficiency is significantly reduced.

In the exciter in question and machines with mixed excitations the permanent magnets are protected from de-magnetization by the magnetic shunts. The total flux of the magnet is practically constant and the flux in the gap and leakage flux in the magnetic shunt are redistributed as a function of the magnitude of the de-magnetizing m.m.f. affecting the magnet. Machines with mixed excitation therefore require no stabilization of the permanent magnets in air to compensate for either short circuit currents or the effect of the air. The energy of the permanent magnets is used to better effect than in other known types of permanent magnet machines.

The following Table gives the main characteristics of the machines which can be used as a.c. exciters for brushless synchronous alternators.

YEAR 1961

Characteristics	With permanent magnets	With electromagnetic excitation
Diameter of armature, mm	85	85
Length of armature, mm	40	40
Length of pole, mm	38	38
Height of pole, mm	16.6	16.5
Width of pole core (magnetic shunt), mm	7	20
Width of permanent bar magnet, mm	10.5	–
Length of permanent bar magnet, mm	38	–
Load, %	100	100
Induction in gap, %	100	100
Maximum excitation power, %	100	304

From test results, the controllable permanent exciter has the following advantages over exciters with electromagnetic excitation:

1. Reliable self-excitation of the synchronous brushless alternator.

2. A considerable reduction in the weight and size of the alternator and an increase in reliability.

3. A considerable reduction in the excitation power of the exciter or its weight and size, other things being equal.

4. Shorter electromagnetic time constant of the excitation winding.

5. The cooling of the alternator is improved by eliminating the "sub-exciter" and accomodating the mixed exciter under the end parts of the armature winding of the alternator.

6. Increased utilization of the energy of the permanent magnets due to the elimination of de-magnetizing factors.

7. The permanent magnets can be magnetized in the assembled exciter without special equipment.

8. There is a substantial reduction in size and weight due to the use of new alloys for the permanent magnets and their high specific magnetic energy.

Translated by O.M. Blunn

REFERENCES

1. A.W. Ford; *El. rev.*, 711, 17 April (1959).
2. A.I. Bertinov; *Electrical alternators for use in aircraft, (Aviatsionnye elektrichekie generatory).* Gos. iz. oboron., prom., (1959).
3. L.M. Palastin; Auth. Cert. No. 131397, (1960).
4. L.M. Palastin and A.I. Chesnokov; *Vest. elektroprom.*, No. 12, (1958).
5. L.M. Palastin and A.I. Chesnokov; *The voltage regulation of synchronous high frequency alternators with permanent magnets, (Regulirovanie napriazheniia sinkhronnykh generatorov povyshennoi chastoty s postoannymi magnitami).* Trud. N.I.I.E.P., vol. 5, (1959).
6. L.M. Palastin; *Vest. elektroprom.*, No. 11, (1959).
7. V.D. Mazhuga; *Elektrichestvo*, No. 3, (1936).

YEAR
1961

ABSTRACTS FROM PAPERS PUBLISHED IN ELEKTRICHESTVO No. 3, 1961

Apparatus and Switchgear

A Novel Graphical and Analytical Method of calculating the Magnetic Permeance of Electrical Apparatus. B.K. BOOL, (28-35)

A simple and accurate method is proposed for calculating the magnetic fields of electrical apparatus and switchgear, for which the "potential grid", relaxation and Leman-Richter methods are unsuitable. The magnetic permeance (admittances) near the air gaps in the separate parts of the magnetic circuit and the magnetizing coils is taken into account so that the zones of the working and leakage fluxes are easily defined. The design of a particular magnetic circuit can then be estimated graphically.

Automatic control

Determination of the Phase-Amplitude Characteristics of Linear Systems and Elements from their Transient Behaviour S.Ia. Berezin, (pp. 64-69).

Newly compiled tables are given to simplify the determination of amplitude-phase characteristics from the transient phenomena in linear control systems.

Distribution

A Study of the Electrical Loads in the Machine Shops at a Tractor Plant. G.M. Kaialov et al., (pp. 22-27).

An account is given of the disposal diagrams (distribution curves as used by the Soviet Commission on load distribution in industrial undertakings in 1957-1960 to publish regulations governing the load distribution in industrial undertakings. The method was elaborated at the Gipro tractor and agricultural machinery works in 1958-1959.

Insulation

Highly Heat-Resistant Winding Conductors. V.A. Privezentsev, (pp. 76-82).

The author reviews world experience in the insulation of windings (enamelling, inorganic coatings, glass fibre, oxide coatings and fluoroplast insulation such as "flexsolon"), the protection of copper conductors from oxidation and the use of bi- and tri-metal conductors. Cu-Al and Ni-Cu conductors are recommended for 300°C (1500 to 2000 hr), and oxidized Al or Cu-Al-Ag (or Ni) conductors with glass fibre insulation can be used at 450-500° for limited periods.

Power Systems

Some Problems concerning the Utilization of the Stalingrad-Donbas d.c. Transmission System. N.M. Mel'ganov et al., (pp. 14-18).

The proposed 750 MW ± 400 kV d.c. transmission system linking the Stalingrad hydro-electric station and the large industrial Donbas region in the Ukraine will join the Southern and European grids of the U.S.S.R. A study is made of the way to take the most advantage of this possibility.

Rotating machines

The Voltage of Self-Excited Synchronous Generators with Damping Circuits when Switching on a Lagging (RL) Load. G.F. Suprun, (pp. 48-51).

The author shows how to calculate the variation in the voltage of a self-excited synchronous generator with damping windings on various loads (e.g. an RL load) and on no load.

Braking a Motor by simultaneously forcing its Flux and reducing the Generator Voltage. N.P. Kunitskii, (pp. 57-63).

After a mathematical analysis of optimum motor braking time, a detailed account is given of the modifications made to the ionic system of excitation for the generators and motors of a certain reversible rolling mill in the U.S.S.R. which are claimed to achieve the optimum braking time of 0.623 sec under various flux forcing conditions at maximum braking current 2.046 A.

Measurement Techniques

A Device for Measuring d.c. Currents up to 40 kA. D.N. Nasledov et al., (pp. 70-73).

This Russian device is similar to that developed in Western Germany. The intensity of the magnetic field is measured by means of Hall generators using indium arsenide. Measurements are correct to within 0.7%. This paper is said to be the first dealing with the parameters of such devices and their performance.

A Constant Temperature Method of Measuring Power. V.S. Popov, (pp. 73-76).

An accurate means of measuring power is proposed in which the characteristics of each pair of heat converters can have characteristics of quite arbitrary shape. The result is produced either in the form of a direct voltage or a small proportional increase in impedance. The method consists in artificially maintaining the temperature or electrical power constant during the process of measurement in the heater of one of the heat converters of the thermo-electric wattmeter. The device is said to be 10 times more accurate and of wide application.

YEAR
1961

Null Measurement of the Dielectric Loss Angle. M.S. Mikitinskii, (pp. 87-88).

A novel method is proposed for measuring the dielectric loss angle in capacitors and insulation which is more convenient than the "KEX" or $(\frac{C}{C})(\frac{r}{r})$ bridge method. The measuring device consists of cathode followers with a transfer constant of about 0.9. These followers are connected to separate screens with individual anode supply. Sensitivity as regards capacitance and impedance is of the order of 0.1%.

Transformers

The Dielectric Properties and Stability of Transformer Oils

Research has been undertaken into the production of transformer oil to ensure the right electrical characteristics and their immunity to oxidation in use. The adsorption method of production is recommended instead of acid-alkali purification.

Transistors

Means of controlling triode switches. O.A. Kossov, (pp. 35-44).

A comparison is made between the various ways of controlling junction-type transistors operating as switches in power amplifiers with a d.c. output. The dissipated power is considered for various loads and then switching time, the angle of connexion and the mark-space ratio.

A MAGNETIC ROTATING - ARC ARRESTER FOR COMBINED PROTECTION FROM INTERNAL SURGES AND LIGHTNING STRIKES ON 500 KV TRANSMISSION LINES*

V.P. SAVEL'EV, V.V. SHMATOVICH,
V.I. PRUZHININA and V.K. PUGACHEV

(Lenin All-Union Electrical Engineering Institute)

YEAR
1961

(Received 25 July 1960)

Introduction

Plans have been made to reduce the level of insulation on the equipment used in 500 kV a.c. transmission lines to 2.5 U_p. These plans are based on the use of appropriate arresters.

In 1957 the All-Union Electrical Engineering Institute developed a "tervite"** arrester for protection from internal surges which is known in the U.S.S.R. as the "commutation" arrester. It is quite capable of limiting internal surges to 2.5 U_p and its quenching voltage is 1.6 U_p [1]. But it affords no protection against direct lightning strikes with current surges up to 10 kA. This has entailed the use of a special lightning arrester which was also developed at the Institute and which is known as the "vilite" lightning arrester ("Vilite" is a Russian ceramic material which consists of SiC + clay and graphite, *Translator*). The operating resistors of this arrester have better non-linearity, but their current capacity is less and their quenching voltage is lower (1.3 U_p) [1,2].

But the use of two types of valve arrester involved isolating the lightning arrester from the effects of internal surges and this posed

---

* *Electrichestvo*, No.4, 13-20, 1961.

** Tervite is a special type of material used to make non-linear resistors (Translator).

very difficult technical problems. It was therefore decided to combine the functions of the separate "commutation" and "lightning" arresters in one combined magnetic rotating-arc arrester. This arrester was developed by the Institute* in 1958.

The limitation of internal surges

Internal overvoltages reach 3 to 4 U_p under the various fault conditions which occur on 500 kV transmission lines under transient conditions. The arrester should restrict the surge to 2.5 U_p or less and interrupt the current in the next half-period after its "free" (transient) component has decayed and the recovery voltage has dropped to the value of the quenching voltage of the arrester.

The need to restrict internal surges to 2.5 U_p determines both the puncture voltage of the arrester and the residual voltage on its operating resistance. The operating resistance of the arrester should be as large as possible since the current is then a minimum. This also means that the rupturing capacity of the sparkgaps need not satisfy such demanding conditions.

Calculations [3, 4], experiments on model 500 kV lines and field tests on a 400 kV network [5] all point to the conclusion that the most probable load on an arrester under transient conditions is an oscillatory decaying discharge lasting three half-periods**:

Half-periods	Amplitude, A	Length of wave, msec
1	1,500	2.5-3.5
2	700-800	5
3	250-350	5

But most research laboratories usually find one half-period of current at supply frequency and 1500 A the most convenient for tests. Experience has shown that this load is no less exacting than the recommended three half-period load.

Thus an arrester which is intended to limit internal surges must be able to carry the instantaneous flow of current of the recommended three

---

* S.P. Erin, V.A. Pilimonov, T.K. Ivanova and A.Ia. Sharlot took part in development work.

** This conclusion has also been confirmed by research at the Direct current Research Institute.

half-period oscillatory discharge or its equivalent at the supply frequency. The puncture and residual voltages of the arrester must not exceed 2.5 U_p during internal surges, and the arc must be quenched for a sinusoidal recovery voltage of at least 1.6 U_p at approx. 50 c/s. Since the arrester itself gives rise to transient phenomena on interrupting the current, the steady state voltage at the point where the arrester is installed must not exceed 1.4 to 1.5 U_p.

The type of sparkgap in the internal surge arrester and their arc-quenching capacity

The sparkgap is one of the main items in an arrester. Those in the arrester under consideration consist of a series of individual gaps. The arc-quenching capacity η of this particular "multiple-gap" design can be defined as the ratio of the puncture voltage U_{punct} to the quenching voltage U_q at which a specific current is reliably interrupted at supply frequency.

YEAR
1961

In multiple sparkgaps of conventional RVS-type "valve" arresters the arc quenching capacity $\eta = \frac{U_{punct}}{U_q} = 2.0$ to 2.5 for a current of 100 A. This arc-quenching capacity is clearly inadequate for the sparkgaps of internal surge arresters. That of the Institute's magnetic spark gaps with a rotating arc is much higher. Currents up to 250 A can be interrupted in the lightning arresters, whilst the puncture voltage is reduced to 2.5 U_p [2]. Later investigations have shown that their arc-quenching capacity is still high even if currents of 1000 to 1500 A flow through the gaps for 0.01 sec. But the individual magnetic spark gaps of the internal surge arrester have smaller air gaps between the electrodes than the lightning arrester and their puncture voltage is lower accordingly (3 to 4 kV_{max}).

The sparkgap (Fig. 1) is an annular slot between two copper electrodes 1 and 2 which are arranged concentrically in the horizontal plane. The electrodes are accomodated in a chamber formed by upper and lower walls 3 and 4. Double walls are used for the chamber (prossed paper on the inside and micanite on the outside). The walls are 1.5 mm away from the electrodes which prevents them affecting the puncture voltage of the gap. The electrodes are 3 mm thick and their operating surface is polished and carefully de-greased to facilitate the movement of the arc under the effect of the magnetic field produced by the permanent ring magnets 5 and 6.

The gaps are connected together by means of the magnets, one magnet being set between each pair of sparkgaps. In this case the m.m.f.'s of the magnets are summed and the induction in the gap is increased. The strength of the magnetic field in the air gap must be 700 to 800 oersted. Special auxiliary electrodes 7 and 8 are used to activate the sparkgap. In this way the impulse coefficient of an individual sparkgap in maintained at 1.25 for a pre-discharge time of 0.1 μ sec, or 1.1 for 1 μ sec. The scatter (variation) of the puncture voltage has been reduced to a minimum at supply frequency.

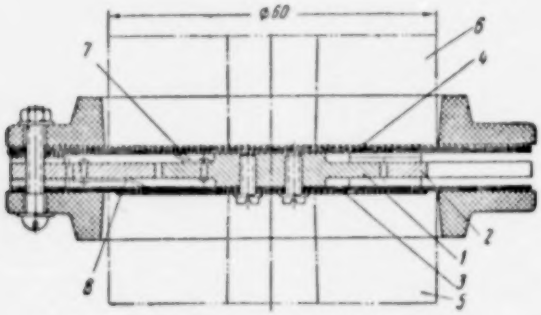

Fig. 1. An individual magnetic sparkgap.

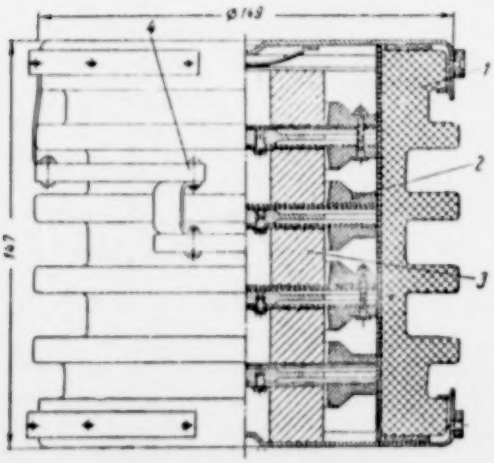

Fig. 2. A set of sparkgaps:

1 - Porcelain covering; *2* - sparkgap; *3* - magnet; *4* - shunting resistance.

Four individual sparkgaps are arranged in a porcelain covering to form one sparkgap sub-unit (Fig. 2). Each such sub-unit is shunted by non-linear carborundum disk-resistors ($\alpha \approx 0.35$) to ensure a uniform distribution of the voltage over the sub-unit. The total conduction current of each sub-unit is 1200 μ A at a voltage of 3600 V. Five sub-units and their disk-resistors are then assembled in a standard porcelain jacket to form the complete sparkgap unit. Thus a complete unit consists of twenty sparkgaps and the set of disk-resistors.

The arc-quenching capacity of the arrester mainly depends on the properties of the individual sparkgaps. We will therefore consider their characteristics first.

The arc-quenching properties of an individual sparkgap can be assessed quite conveniently in terms of "relative recovery strength" (the recovery strength calculated as a percentage of the puncture voltage). Fig. 3 shows the results of 100 measurements* of the relative recovery strength of an individual sparkgap after carrying a current of 1500 A for one half-period at 50 c/s. The puncture voltage of the gap is 4 kV_{max}.

YEAR 1961

It must be borne in mind that the recovery strength of all the individual gaps is not exactly the same and, as can be seen from Fig. 3, the results are quite scattered. A large number of tests are therefore always required before the lower envelope of the recovery strength can be determined.

Fig. 3. The recovery strength of an individual magnetic sparkgap as a percentage of the puncture voltage.

Some idea of the arc-quenching properties of the individual sparkgaps under different internal fault conditions was required. Tests were therefore made on the individual sparkgaps at the maximum puncture voltage 4kV using oscillatory decaying discharges of different ampli-

* The method of measurement has already been described [2].

tude and duration (see Table 1).

TABLE 1

Loads as in Fig. 4	Number of half-period	Length of each half-period, msec	Amplitude of the current in each half-period, kA
1	1	10	1.5
2	2	10	1.5; 0.8
3	4	10	1.4; 0.8; 0.5; 0.3
4	3	5.3	1.4; 0.9; 0.5
5	3	3.3	1.5; 0.9; 0.5
6	1	5	1.5

The lower envelopes of the recovery strength in Fig. 4 were obtained by measurements. The following conclusions can be drawn.

An increased number of half-periods of a given duration in one oscillatory discharge notably reduces the recovery strength. On the other hand, a decrease in the duration of the half-periods (below 10 μ sec) has the opposite effect and increases the recovery strength. From the point of view of recovery strength, loads 5 and 6 are "lighter" than the fundamental load 1.

It therefore seems advisable to consider test load 5 for estimates of the recovery strength; this is also the most probable load in practice. On this basis the quenching voltage of the sparkgap is not unjustifiably reduced, as this could otherwise limit the field of application of the arrester.

In multiple sparkgaps we also require to know the total recovery strength of all the individual gaps together.

Given a uniform distribution of the voltage over the individual sparkgaps, one would expect the "absolute" recovery strength to increase in direct proportion to the number of sparkgaps with constant relative recovery strength.

But the distribution of the voltage inside each sub-unit of four sparkgaps is capacitive and the capacitance of the individual sparkgaps is not the same. The puncture voltage of each sub-unit is therefore

about 5 to 10 per cent below the minimum total puncture voltage of the individual gaps. This naturally would not reduce the relative recovery strength if the voltage distribution over the individual gaps were the same after the passage of current as before the breakdown. But the sparkgaps are filled with highly ionized gases immediately after the current has passed through zero and the voltage distribution is markedly changed both by conductance and changes in capacitance*.

The probability of low values of recovery strength must increase as more individual sparkgaps are joined together since the recovery voltage is applied simultaneously to a larger number of gaps and a premature breakdown of any one of them usually leads to a premature breakdown of them all. A reduced recovery strength in multiple sparkgaps must be accepted and estimates which are based on the test results of individual gaps even if a large number of tests have been made should be treated with caution. It is better to use the results of tests on sets of two gaps or on particular sub-units (four gaps together).

YEAR 1961

For a final assessment of the arc-quenching capacity of the multiple sparkgap of the arrester, the arc-quenching capacity of the complete units had to be checked by the usual service tests.

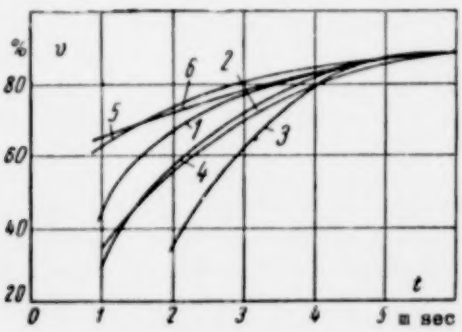

Fig. 4. The recovery strength of an individual magnetic sparkgap under various loads.

It can easily be shown analytically that when testing a finished unit under conditions equivalent to those existing in an actual arrester, it is essential to reduce the voltage of the system, the total resistance and the operating resistance of the arrester in proportion to any decrease in the number of sparkgaps, whereas the capacitances in

* The capacitance of an individual sparkgap is about 50 pF and the capacitive-susceptance current is no more than 5 MkA at supply frequency and the pre-puncture voltage.

parallel with the unit must be correspondingly increased. The short circuit current of the plant will then remain constant as well as the accompanying current (load current).

Equivalent conditions were provided for the rupturing capacity tests carried out on finished units for 500 kV arresters.

The principal results are given in Table 2. Each finished unit consists of five sub-units of four individual sparkgaps with a maximum puncture voltage of 3.4 kV (the 500 kV arresters are made of these sparkgaps). The puncture voltage of the finished units $U_{punct.fu}$ was between 55 and 63 kV. The short-circuit current was between 1800 and 3000 A for the "mean" variable e.m.f. in the various tests.

TABLE 2

No. of unit	Amplitude of interrupted current, A	η	No. of interruptions in one cycle	Total number of interruptions in all the cycles
1	850 770 850 460	1.8 1.5 1.4 1.4	19 19 9 16	103
2	400 1 100 450 740	1.5 1.5 1.6 1.4	20 16 19 18	73
3	630 535 670	1.5 1.4 1.3	21 26 20	67
4	650 800	1.3 1.25	19 16	35
5	650 1 300	1.5 1.4	5 1	6
6	1 000 1 000	1.45 1.28	20 7	27
7	1 000 900	1.46 1.33	21 11	32
8	1 180	1.4	11	11

The load currents were controlled between 450 and 1200 A. In the

majority of the tests η was between 1.4 and 1.5, but in some series of tests it equalled 1.25 to 1.3.

It must be pointed out that each complete unit was tested more than twenty times in almost every case, even though gaps with pressed paper laminations were only designed for up to twenty trials.

It is of interest to compare the re-strike voltage of complete units as measured during the tests with the recovery strength of sets of two gaps under identical loads (Fig. 5).

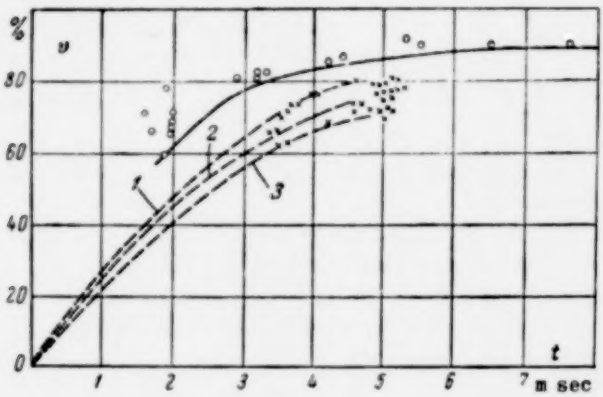

Fig. 5. The recovery strength of the magnetic sparkgaps and units in the combined arrester at a load of 1000 A with H_n = 800 oersted: 0 – a set of two sparkgaps (U_{punct} = 6.8 kV_{max}); X – complete unit (20 sparkgaps, $U_{punct.fu}$ = 55 to 64 $kV_{max.}$); 1, 2, 3 – sinusoidal recovery voltages with amplitudes respectively 0.8, 0.75 and 0.7 of the puncture voltage of the unit.

This comparison shows that the lowest and least probable re-strike voltage in complete units is 15 to 20 per cent below the recovery strength of sets of two gaps for the lowest sinusoidal recovery voltage $U_{rec} = 0.7\ U_{punct}$.

This decrease in the re-strike voltage is probably due to the ageing of the individual sparkgaps and the possible reduction in the overall recovery strength of the sparkgaps in the complete unit.

The conclusion to be drawn from these results is that a load current

of about 1000 A is quite acceptable for η = 1.4 to 1.5 if the number of trial discharges is twenty or less and there is then every probability of faultless clearance. Incidentally, these tests were made for more exacting conditions than occur in actual service since the operating resistance of the arrester had to be greatly reduced in order to obtain a current of 1000 to 1300 A at a source voltage equal to quenching voltage of the complete unit. The current through the unit is in point of fact about 500 A at the quenching voltage and only reaches 1000 to 1500 A in the transition period when the voltage across the unit is slightly greater than the quenching voltage.

The operating resistance in the internal surge arrester

There is no need to discuss the well-known merits of non-linear resistors. It need only be pointed out that the "vilite" disk-resistor of 150 mm diameter used in the 500 kV lightning arrester was unsuitable for the internal surge arrester because at least five such disks would have been required in parallel. "Vilite" (i.e. the compound of SiC, clay and graphite) will only operate at low current densities and its non-linearity coefficient is only about 0.3 in the range of currents produced by internal voltage surges.

A new non-linear material called "tervite" was therefore specially developed for internal surge arresters. This material has several times more current capacity than vilite [6]. But the coefficient of non-linearity of tervite is somewhat inferior to that of vilite. The current capacity of both vilite and tervite increases with increasing conductivity of the material, but the non-linearity diminishes.

The operating resistor in an internal surge arrester can either be made of disks 125 mm in diameter and 50 mm thick or disks 70 mm in diameter and 20 mm thick. The units using the latter are fitted with three parallel columns of disks. Fig. 6 illustrates the current capacity of an arrester as a function of the properties of disks with the maximum resistance possible for the type of arrester in question.

The number of disks in the internal surge arrester depends on the residual voltage which must not exceed 2.5 U_p for a current of 1500 A on a 10/20 μ sec surge.

Curve 1 in Fig. 7 shows the voltampere characteristic of the internal surge arrester. It must be borne in mind that the residual voltage in an arrester with tervite resistors increases if the steepness of the

current wavefront is reduced for a given current. As an example, the residual voltage increases by 3 per cent if the wavefront is reduced from 10 to 3 μ sec with a current of 10 kA.

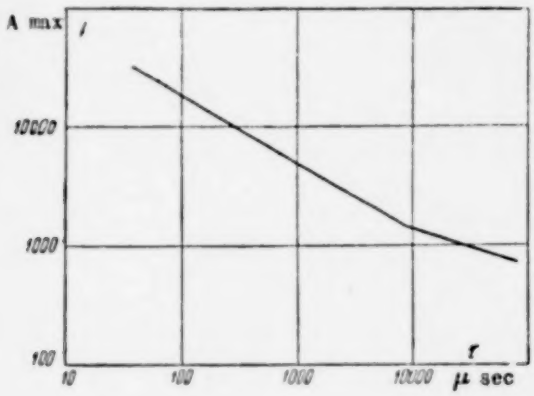

Fig. 6. The carrying capacity of "tervite" resistance in the combined 500 kV arrester after at least 20 discharges:
$\tau < 10,000$ μ sec – the length of an aperiodic wave of 20/40 μ sec (up to the half-drop point); $\tau > 10,000$ μ sec – a periodic wave (frequency 50 c/s).

The combination of the internal surge and lightning arresters

It will be seen from curve 1 in Fig. 7 that the tervite resistor for internal surge protection cannot reduce the overvoltages due to direct lightning strokes to the required level since the calculated impulse current through the arrester is 10 kA.

To permit the use of tervite disks in 500 kV arresters and still limit surges to 1260 kV at currents of 10 kA it would have been necessary to use a resistor which would satisfy curve 2. In actual fact the current through the arrester during internal surges is over 1.5 kA and this is unacceptable both as regards the carrying capacity of the resistor and the arc-quenching capacity of the sparkgaps. With direct lightning strokes internal surges can be ignored and a quenching voltage roughly equal to 1.3 U_p need only be considered. The surge current (curve 3) does not then exceed 800 to 900 A and it can therefore be interrupted quite easily by the sparkgaps. All these considerations

led to the design of the "combined" arrester which protects against internal surges as well as direct lightning strokes.

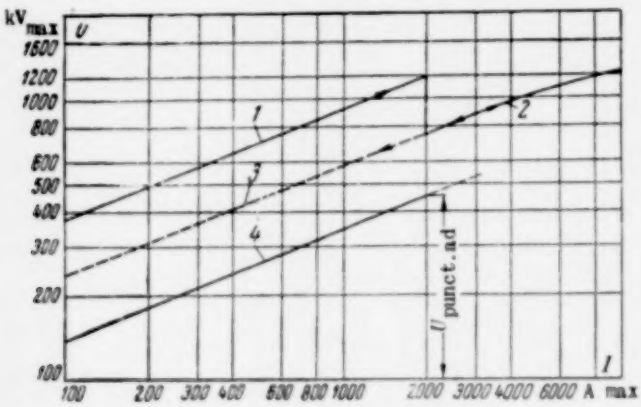

Fig. 7. The voltampere characteristics of the combined 500 kV discharger:
1 - internal surge arrester; *1, 2, 3* (sic) - - lightning arrester; *4* - shunted part of arrester; $U_{punct.ad}$ - puncture voltage of the additional sparkgap.

The "combined" arrester uses the same internal surge arrester, except that a part of its operating resistance is shunted by an additional multiple-sparkgap unit which is composed of individual rotating arc sparkgaps (Fig. 8). The puncture voltage of the shunt sparkgaps is selected so that their breakdown takes place at the moment when the voltage across all the operating resistance reaches the impulse level of protection (1260 kV). The part of this resistance which is shunted is designed to prevent the voltage across the rest of the resistance exceeding 1260 kV at a current of 10 kA (curve 2, Fig. 7). The voltampere characteristic of the shunted part of the resistance is represented by curve 4 in Fig. 7.

During internal surges when the current through the arrester does not exceed 2 kA, the arrester operates like an internal surge arrester and there is no breakdown of the shunt gap.

After a direct lightning stroke when the current increases to 10 kA, there is first a breakdown of the main sparkgap, but the current continues to flow through the operating resistance until the voltage across it reaches 1260 kV. As shown in Fig. 7, this takes place at a current

in excess of 2 kA. At this point there is a breakdown of the additional sparkgap and if the current increases further the voltage across the arrester is determined by the other remaining part of the operating resistance (curve 2 in Fig. 7).

The size of the combined arrester is practically the same as the internal surge arrester and there is very little difference in cost.

YEAR
1961

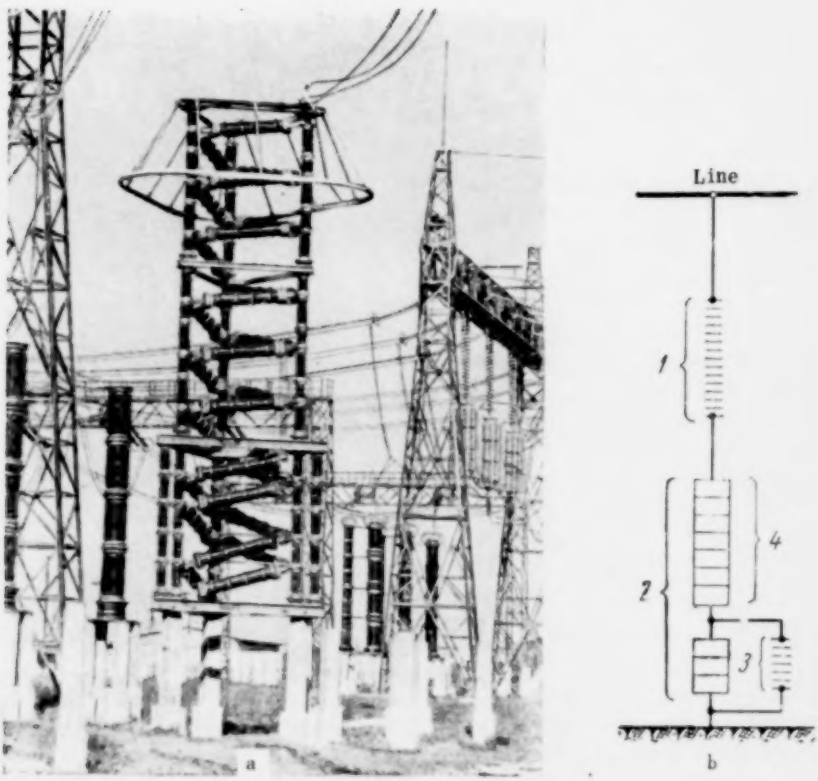

Fig. 8. Side view (a) and main circuit (b) of the combined 500 kV magnetic arrester. *1* - main sparkgaps; *2* - resistances of the internal surge arrester; *3* - additional (shunting) sparkgaps; *4* - the resistance in the lightning part of the arrester.

Before the final characteristics and parameters of the combined arrester could be determined it was necessary to make certain that the

following conditions would be fulfilled:

Impulse puncture and residual voltage	1260 kV
Amplitude of current in internal surges	$\leqslant 2.5\ U_p$
Puncture voltage during internal surges	$2.5\ U_p$
Residual voltage at a current of 10 kA and a wave of 10/20 μ sec	1260 kV

Conditions 2 and 3 determine the number of disks in the operating resistance. Condition 5 defines the proportion of shunt disks in the operating resistance (in our case, 39.6% of the total operating resistance).

It is also necessary to prevent the breakdown of the shunt sparkgaps when the arrester is dealing with an internal surge because at this moment a voltage amounting to 39.6% of the total breakdown (puncture) voltage can be applied to the shunted part of the operating resistance and this can immediately be followed by a similar proportion of the residual voltage at 1.5 kA. It is calculated that this condition can be satisfied by a 5 per cent margin given an impulse coefficient of the shunt sparkgaps equal to one (experimentally determined) and a 5 per cent scatter in the puncture voltages of the gap. It is obvious that the changeover after a direct lightning stroke will then take place with a voltage across the arrester which is no greater in amplitude than

$$U_{\text{punct}} = \frac{1.05 \cdot (1 + 0.05)}{(1 - 0.05)} 2.5 U_p = 2.9 U_p = 1\,250 \text{ kV},$$

as required by condition 1.

The non-shunted part of the operating resistance in the combined arrester (60.4%) satisfies the fifth condition by ensuring a residual voltage no greater than 1220 kV at a current of 10 kA with a wavefront of 10 μ sec.

The quenching voltage of the combined arrester must be such that the puncture voltage of the discharger does not exceed 2.5 U_p (fourth condition). Given a scatter of $\pm$ 7 per cent, the mean puncture voltage is

$$U_{\text{punct.av}} = (2.34 \pm 0.16) U_p = (710 \pm 50) \sqrt{2} \text{ kV}_{\text{max}}.$$

Taking the arc quenching capacity η as 1.46 from test results, we get

$$U_q = \frac{U_{\text{punct.av}}}{\eta} = \frac{2.34 U_p}{1.46} = 1.6 U_p.$$

Design of the combined discharger

A side view of the combined arrester is shown in Fig. 8(a). It consists of 27 complete units. These are "spirally" mounted on three pillars of KO-400S, KO-35 and KO-15 type isolators. The arrester is divided into three sections (stories) by triangular metal frames. The bottom section contains 10 units, five with resistors and five with sparkgaps. Each unit with resistors is shunted by its own sparkgap unit. Every unit with a resistor is composed of three parallel columns with 55 disks in each column. Every sparkgap unit consists of 32 individual sparkgaps. The top two sections contain 17 complete units all of the same type. Each of these units comprises 20 sparkgaps and three parallel columns with 25 or 26 disk resistors in each column (the lightning part of the combined arrester). A ring 4.8 m in diameter is provided to balance the voltage distribution in the presence of impulse phenomena. The arrester is 8.5 m high and weighs about 9 tons.

YEAR 1961

Laboratory tests and electrical characteristics

The main characteristics of the arrester were improved as a result of tests on the individual units and the arrester as a whole. The puncture voltage of 17 complete units each composed of individual gaps with a puncture voltage of 3.3 to 3.44 kV was between 60 and 63.5 kV (mean values).

The maximum deviation about the mean puncture voltage was up to ± 7 per cent on some units. Measurement of the volt-second characteristics showed that the impulse coefficient of the complete units was 1.1 for pre-discharge times $> 4\ \mu$sec, 0.9 for 1.5 μsec and 1.13 for 1 μsec. Thermal tests on the finished units under a sustained voltage equal to

$$\frac{525}{\sqrt{3 \cdot 17}} = 17.8 \text{ kV}$$

and a corresponding phase voltage across the whole arrester showed that the temperature rise on the surface of the shunt resistance was no more than 18 to 20°C above ambient air temperature.

Rupturing capacity tests showed that the quenching voltage of the arrester can be based on a coefficient of arc quenching capacity $\eta = 1.46$ and if the mean puncture voltage of the arrester equals 2.34 U_p, it is estimated by the quantity 1.6 U_p.

The puncture voltage of the arrester was measured on a laboratory model without the bottom section (i.e. without the additional units with the disks and the sparkgaps to shunt them).

The mean amplitude of the puncture voltage is 1030 kV ± 2.5 per cent at supply frequency.

The volt-second characteristic of the arrester is shown in Fig. 9 for discharges on the front of wedge-shaped waves.

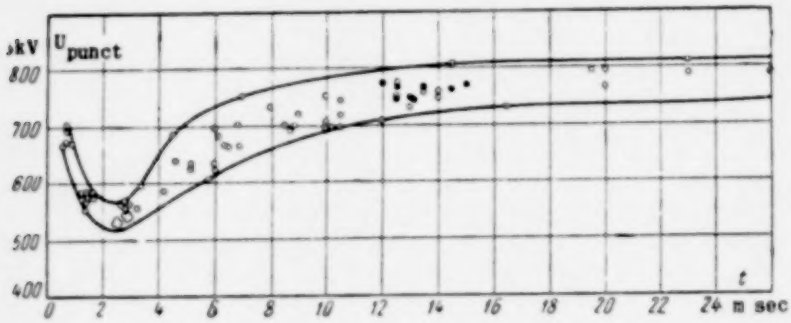

Fig. 9. The impulse puncture voltages of the combined 500 kV arrester with a wedge-shaped wave.
o – negative polarity; ● – positive polarity.

The impulse puncture voltage is 800 kV for a pre-discharge time greater than 5 μ sec, up to 700 kV for 1 μ sec, but falls to 550 kV for a pre-discharge time of 2 to 3 μ sec.

The main electrical characteristics are listed below:

Rated voltage, kV	500
Maximum sustained voltage applied to arrester is service, kV	304
Quenching voltage, kV:	
after direct lightning strokes	395
for internal surges	485
Puncture voltage at supply frequency (+7% with 90 per cent probability), kV	710
Impulse puncture voltage for pre-discharge times of 2 to 20 μ sec, kV	1200
Residual voltage at impulse currents of 10 kA and 10/20 μ/sec, kV	1260
The residual voltage passing a current of 1.5 kA for one half-period of supply frequency, kV	1070

Residual instantaneous applied voltage on changing over to the discharge of a lightning stroke from the internal surge conditions, kV_{max} 1250

Number of lightning or internal surge discharges withstood without damage .. .. at least 20

From test results it can therefore be stated that overvoltages in 500 kV lines can be reduced to 2.5 U_p by using the combined arrester if the necessary conditions are fulfilled and certain other measures are taken.

Translated by O.M. Blunn

YEAR 1961

REFERENCES

1. V.P. Savel'ev; *The 500 kV magnetic arrester, (Magnitnyi razriadnik 500 kv).* Kuibyshev oblastnyi pravleniem nauchno-tekh. obshch. energ. prom., (1957).
2. V.P. Savel'ev and V.V. Shmatovich; *Vest. elektroprom.*, No. 1, (1960).
3. M.L. Levinshtein and K.P. Kadomskaia; *Elektrichestvo*, No. 8, (1959).
4. V.P. Fotin; *Voltage rises in long distance a.c. transmission lines in the presence of unbalanced earth faults, (Povysheniia napriazhenii v dlinnykh liniiakh peremennogo toka pri nesimmetrichnykh korotkikh zamykaniiakh na zemliu).* Trud. Vsesiuznogo elektrotekh. inst., (1958).
5. A.A. Akopian; *Elektrichestvo*, No. 11, (1957).
6. V.I. Pruzhinina, T.K. Ivanova and L.V. Iamanova; *Elektrichestvo*, No. 2 (1958).

THE OPTIMUM OUTPUT OF INDUCTION MOTORS IN REACTOR-CONTROLLED DRIVES*

V.L. ANKHIMIUK (Byelorussian Polytechnical Institute) and
O.P. IL'IN (Middle Asia Polytechnical Institute)

(Received 15 August 1960)

This paper describes a new method of designing induction motors for reactor-controlled drives [1-3] in which the power of the motor is selected in conjunction with the rated slip, as defined by the resistance of the rotor circuit. The rated slip is so calculated that maximum use is made of the motor output over the desired range of speeds for a given load graph. Less power is required. If the initial speed of the motor and, consequently, the speed of the output shaft is reduced the speed can be increased by adjusting the ratio of the reduction gears.

Fig. 1 shows the main circuits of typical electric drives. For the sake of simplicity feedbacks have been omitted and only one control winding (CW) is shown.

In these systems the speed of the induction motor is changed by varying the slip. Additional losses therefore arise during speed control. The changes in the speed of the rotor also affect the cooling of the motor.

The power of the motor must therefore be calculated so as to obtain average losses and average heat dissipation.

The total losses of an induction motor (in relative units) at rated voltage on the stator terminals are:

$$\Delta\rho = (1 + k_r)(ms + \nu k s_{\text{ном}}), \qquad (1)$$

---

* *Elektrichestvo*, 4, 39-42, 1961.

where $\Delta p = \frac{975 \Delta P}{M_{nom} n_0}$ – the ratio of total losses ΔP to rated output;

M_{nom} and n_0 – the rated torque and synchronous speed of the motor;

$k_r = \frac{r_1}{r_2'}$ – the ratio of the stator and rotor resistances;

$m = \frac{M}{M_{nom}}$ – the relative torque on the motor shaft;

s_{nom} – the rated slip;

$k = \frac{\Delta P_c}{\Delta P_{vnom}}$ – the loss factor, equal to the ratio of constant losses to variable losses under rated motor conditions;

$v = \frac{n}{n_0}$ – the relative speed of the motor.

YEAR 1961

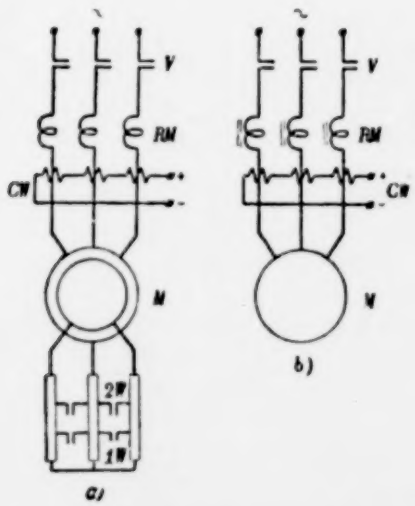

Fig. 1. Main circuits of induction motors in reactor-controlled drives
(a – slipping motor; b – squirrel cage).

Equation 1 is only an approximation since it is assumed that the constant losses are proportional to speed. In point of fact, the constant losses depend on the motor voltage as well as its speed. To calculate the constant losses in reactor-controlled drives it is there-

fore necessary to divide these losses into those components which depend on speed or voltage and then calculate the magnitude of the magnetizing current at the speed in question in the light of the non-linearity of the no load characteristic. But these are very complicated calculations. Equation (1) is so much simpler and the error is still within five per cent.

If a slipping motor is used, i.e. an induction motor with a wound rotor, the heating losses are

$$\Delta p_h = (1 + k_r)(ms\sigma + vks_{nom}), \tag{2}$$

where $\sigma = \frac{r'_2}{r'_2 + r'_a}$ — is the ratio of the rotor resistance to the total resistance of the rotor circuit (but in squirrel-cage motors $\sigma = 1$).

In speed control the required output of the motor depends on its initial speed. It will now be shown that the output of a motor is optimum at a particular initial speed.

The range of speed control is

$$D = \frac{n_1}{n_2} = \frac{v_1}{v_2} = \frac{1 - s_1}{1 - s_2}, \tag{3}$$

where n_1 and n_2 are the initial and minimum speeds of the motor; and
v_1 and v_2 – relative values of the initial and maximum speeds.

Substituting in (2) the value of s_2 from 3 for s and the value of $\frac{v_1}{D}$ for v_2, we get:

$$\Delta p_h = (1 + k_r)\left(m\sigma \frac{D - v_1}{D} + \frac{v_1}{D} ks_{nom}\right). \tag{4}$$

The relative heat dissipation of the motor can be expressed by the equation

$$a = \frac{a_0 + (1 - a_0)\sqrt{v}}{a_0 + (1 - a_0)\sqrt{v_{nom}}}, \tag{5}$$

where a is the ratio of the heat dissipation at actual speed to the heat dissipation at rated speed;

a_0 – the ratio of the heat dissipation with rotor locked to the heat dissipation at synchronous speed of the rotor.

Expression (5) for the relationship between heat dissipation and speed gives practically the same results as those obtained by Suiskii's formula [4] for model A and AO motors. The value of a_0 can be calculated from the formulae in Suiskii's book [4]. A considerable amount of research has been devoted to the relationship between the coefficient of heat dissipation and the speed of the air [7, 8] and this justifies the assumption that formula (5) is also applicable to other types of induction motors.

For a motor to satisfy the heating conditions, it is necessary that

$$\Delta p_{h.av} \leqslant a_{av} \Delta p_{nom}, \tag{6}$$

where $\Delta p_{h.av}$ is the relative mean heating loss in one cycle;

a_{av} – the mean relative heat dissipation;

Δp_{nom} – the relative rated losses of the motor.

Using equations (4) to (6) and assuming that $\sqrt{v}_{nom} = 1$, for a long period of operation:

$$m = \frac{s_{nom}}{a} \frac{a_0 D + (1 - a_0)\sqrt{D v_1} - \gamma v_1}{(D - v_1)(1 - \gamma)}, \tag{7}$$

where

$$\gamma = \frac{k}{1 + k} = \frac{\Delta P_{av,nom}}{\Delta P_{nom}}$$

In speed control when the torque is constant,

$$\frac{s_{nom}}{a} = \frac{s_1}{k_1 m}. \tag{8}$$

The coefficient k_1 in (8) takes into account the need to ensure a rigid mechanical characteristic by a system of feedback when operating at the initial speed. This coefficient should be 1 to 2 if $s_1 > 0.005$.

Jointly solving equations (7) and (8), we get:

$$m = \sqrt{\frac{(1 - v_1)\left[a_0 D + (1 - a_0)\sqrt{D v_1} - \gamma v_1\right]}{k_1 (D - v_1)(1 - \gamma)}}. \tag{9}$$

Equation (9) permits the determination of the optimum output of a wound rotor induction motor from the torque over the desired range of speeds.

At the speed v the relative power is

$$p = mv. \tag{10}$$

The curves in Fig. 2 show the degree of power utilization and the maximum torque for given heating conditions as a function of initial speed.

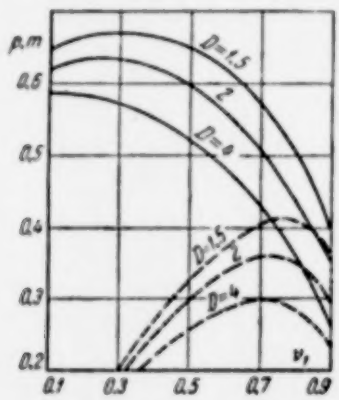

Fig. 2. Maximum torque and power of a phase induction motor as a function of initial speed under given heating conditions.
p – motor power; m – max torque; D – range of speed control.

The rated slip is even more important in deciding upon the power of a squirrel-cage induction motor. To determine the effect of rated slip on its output, consider a "basic" squirrel-cage induction motor and assume that $P_{nom,b}$, I_{nom}, $\cos\phi_b$, η_b, $k_{r,b}$ and γ_b are given, where the subscript b refers to this *basic* squirrel cage motor. Replacing the rotor of this basic motor by a rotor with a different resistance:

$$r_2' = \frac{r_{2b}'}{a}.$$

The change of rotor involves changes in the rated slip, its efficiency at rated torque, the rated output and the distribution of the

losses. In this case

$$s_{\text{nom}} = \frac{s_{\text{nom. b}}}{s}; \quad k_r = k_{rb} s; \quad \Delta P_{v2\text{nom}} = \frac{\Delta P_{v2\text{nom. b}}}{s},$$

$$\gamma = \frac{\gamma_b s (1 + k_{rb})}{(1 - \gamma_b)(1 + k_{2b} s) + \gamma_b s (1 + k_{rb})}.$$

In relative units, the rated losses of the basic motor are:

$$\Delta p_{\text{nom. b}} = s_{\text{nom. b}} \frac{(1 + k_{rb})}{1 - \gamma_b}. \tag{12}$$

The total losses of this motor at the maximum speed v_2 in relative units are:

$$\Delta p = \frac{m(1 + k_{rb} s)(1 - \gamma_b)(D - v_1) + s_{\text{nom. b}} \gamma_b (1 + k_{rb}) v_1}{D(1 - \gamma_b)} \tag{13}$$

YEAR 1961

In this case equation (6) takes the form

$$\Delta p = a \Delta p_{\text{nom. b}} \tag{14}$$

However, the initial speed v_1 is related to the torque m and the value of v by the equation

$$s = \frac{k_1 s_{\text{nom. b}}}{1 - v_1} m. \tag{15}$$

Substituting (12), (13) and (15) in (14) and solving w. r. t. m:

$$m = \frac{1 - v_1}{2 k_1 k_{rb} s_{\text{nom. b}}} (\sqrt{1 + C} - 1), \tag{16}$$

where

$$C = \frac{v_1^2 s_{\text{nom. b}} (1 + k_{rb}) k_1 k_{rb} [a_0 D + (1 - a_0)\sqrt{D v_1} - \gamma_b v_1]}{(1 - v_1)(D - v_1)(1 - \gamma_b)}. \tag{17}$$

By (16) it is possible to obtain the maximum load torque of a squirrel cage motor for given heating conditions. The relative power of this squirrel cage motor is defined by equation (10).

Fig. 3 shows m and p as a function of v_1 for the squirrel-cage motor.

The efficiency and power factor of the drive can be calculated by Osokin's [5] or Terekhov's [6] formulae. Suppose it is required to compare variations in the energy indices of drives as a function of the speed range and initial speed. To do this use is made of an energy coefficient

$$k_e = \frac{\eta \cos\varphi}{\eta_{nom} \cos\varphi_{nom}} = \frac{P_2 I_{1nom}}{P_{2nom} I_1}, \tag{18}$$

where η is the efficiency and $\cos\varphi$ the power factor of the motor-reactor system.

An expression is obtained for the energy coefficient at minimum speed by putting $I_1 = bI'_2$ and $I_{1\,nom} = b_{nom} I'_{2\,nom}$ and expressing the secondary currents in terms of the power and slip in the light of (8):

$$k_e = k_b \frac{\nu_1}{\nu_{nom}} \sqrt{\frac{1-\nu_1}{\kappa_1 D(D-\nu_1)}}, \tag{19}$$

where $k_b = \frac{b_{nom}}{b}$.

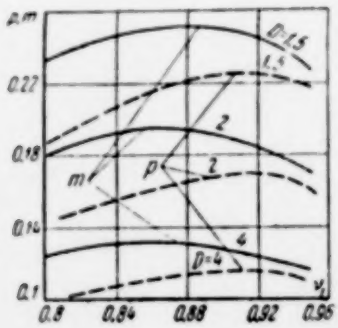

Fig. 3. Maximum torque and power of a squirrel-cage induction motor as a function of initial speed under given heating conditions.

The values of b, b_{nom} and k_b can be found from an equivalent T - network of the induction motor.

Assuming that the phase angle between the currents in the magnetizing branch and the operating circuit of the rotor is approximately 90°:

$$b = \sqrt{1 + i_0^2}; \quad b_{nom} = \sqrt{1 + i_{0nom}^2}$$

where

$$i_0 = \frac{I_0}{I_2'} = \frac{\sqrt{\left(\frac{r_2' + r_m'}{s}\right)^2 + x_2'^2}}{x_0}; \quad i_{0nom} = \frac{I_{0nom}}{I_{2nom}'}.$$

Neglecting the value of x'_2 in the rotor current equation compared with the first term in the radicand:

$$i_0 = i_{0nom} \frac{r_2' + r_m'}{r_2'} \frac{s_{nom}}{s} = i_{0nom} \frac{s_{nom}}{\sigma s} = i_{0nom} \frac{s_1}{\sigma k_1 m}.$$

Considering 3,

$$k_b = \frac{\sqrt{1 + i_{0nom}^2}}{\sqrt{1 + i_{0nom}^2 \frac{D^2 (1 - \nu_1)^2}{k_1^2 m^2 (D - \nu_1)^2}}}. \tag{20}$$

The energy coefficient is a maximum when

$$\nu_1 \approx \frac{3D + 1 - \sqrt{9D^2 - 10D + 1}}{4}. \tag{21}$$

This value has been obtained on the assumption that k_b = const.

This is quite permissible since there is no significant variation in k_b in the region under consideration.

The relative rated speed of the basic motor $\nu_{nom.b}$ has to be substituted for ν_{nom} in formula (19) for the squirrel-cage motor.

Thus the following formulae can be used to assess the required output of

(a) slipring motors

$$\left.\begin{aligned} P_{nom} &= P_s \frac{D+6}{3} \text{ if } D = (1.5 \text{ to } 5); \\ P_{nom} &= \frac{P_s}{(2.1 \text{ to } 1.2)\,D} \text{ if } D < 1.5; \\ P_{nom} &= \frac{P_s}{(0.31 \text{ to } 0.0024)\,D} \text{ if } D > 5; \end{aligned}\right\} \quad (22)$$

(b) squirrel-cage motors if D = 1.5 to 5:

$$P_{nom} = P_s \frac{D+1.25}{0.6}, \quad (23)$$

where P_s is the static power on the motor shaft at the initial speed.

Example

This method will now be illustrated by applying it to the choice of motor for a large mill drive.

1. Details of the AK-52-6 type slipring induction motor: 380 V, 2.8 kW, 920 rev/min, η = 78%, cos ϕ = 0.74. According to reference manuals ε_0 = 0.3, k_r = 1.36 and γ = 0.268. It is assumed that k_1 = 1.5.

Fig. 2 shows the maximum motor torque as calculated by equation 9 for the given heating conditions as a function on the initial speed for various ranges of speed control, D. Curves are also given for the motor power p as a function of v_1 at maximum speed. These curves define the degree of power utilization for speed control with constant torque.

It will be seen from Fig. 2 that the utilization of the motor power is a maximum (p_{max}) when the initial speed v_1 = 0.7 to 0.75. Fig. 4 shows how p_{max} varies with the range of speed control D. This diagram also shows $s_{nom.opt}$ and $k_{e.max}$ as functions of D.

The optimum rated slip is

$$s_{nom.opt} = \frac{s_{nom}}{\varepsilon_{opt}} = \frac{1 - v_{1opt}}{k_1 m_{1\,opt}},$$

where $v_{1.opt}$ and $m_{1.opt}$ are the initial speed and motor torque corresponding to maximum power;

$\sigma_{opt} = \dfrac{s_{nom}}{s_{nom.opt}}$ – a quantity which defines the resistance of the rotor circuit as required for the maximum utilization of the motor power.

The term $k_{e.max}$ is found from formula (19) for values of v_1 from (21). These values of v_1 coincide with $v_{1.opt}$.

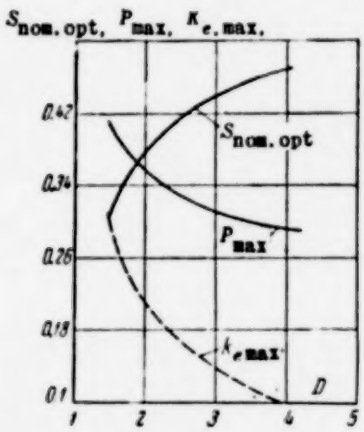

Fig. 4. Characteristics of a slipring induction motor in a reactor-controlled drive.

Thus, for slipring motors the conditions of maximum utilization of motor power are practically the same as those under which the energy coefficient is a maximum.

(2) Consider now an A51-6 type squirrel-cage induction motor of 380 V, 2.8 kW and 950 rev/min with $\eta = 82.5\%$ and $\cos\phi = 0.78$.

It is presupposed that $s_0 = 0.3$, $k_r = 1.77$, $\gamma = 0.317$ and $k_1 = 1.5$. Fig. 3 shows the torque m and power p as a function of the initial speed v_1 as calculated by formulae (16) and (10).

Fig. 5 shows $s_{nom.opt}$, p_{max} and k_e as a function of the range of speed control D. The conditions under which the utilization of the power of a squirrel-cage motor is a maximum are not the same as those which maximize the energy coefficient. Septate curves are therefore shown in Fig. 5 for that value of $k_{e.max}$ and k_e which correspond to maximum utilization of motor power as a function of D.

It will therefore be seen that 1.65 to 2.56 times less power is

required from a slipring motor than from a squirrel-cage motor over the range $D = 1.5$ to 4 and that the energy coefficient of the slipring motor is greater by a factor of 1.33 to 1.54.

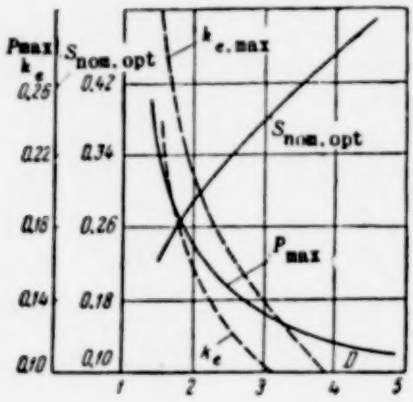

Fig. 5. Characteristics of a squirrel-cage induction motor in a reactor-controlled drive.

Translated by O.M. Blunn

REFERENCES

1. M.M. Sokolov; *The electrical equipment of common industrial plant, (Elektrooborudovanie obshchepromyshlennykh mekhanizmov).* Gosenergoizdat, (1959).
2. V.M. Terekhov; *Elektrichestvo*, No.7, (1959).
3. A.G. Ivakhnenko; *Automatic speed control of low-power induction motors, (Avtomaticheskoe regulirovanie skorosti asinkhronnykh dvigatelei nebol'shoi moshchnosti).* Akad. Nauk Ukr.S.S.R. (1953).
4. P.A. Suiskii; *The Automatic electric drive, Collected works, (Avtomatizirovannyi elektroprivod).* Sborn. Gosenergoizdat, (1960).
5. M.N. Osokin; *Elektrichestvo*, No. 12, (1959).
6. V.M. Terekhov; *The scientific and technical problems of the automatic electric drive, Collected works, (Nauchno-tekhnicheskie problemy avtomatizirovannogo elektroprivoda).* Sborn. Akad. Nauk SSSR, (1957).
7. I.M. Postnikov; *The development of electrical machines, (Proektirovanie elektricheskikh mashin).* Gosenergoizdat, (1952).
8. A.E. Alekseev; *The design of electrical machines, (Konstruktsiia elektricheskikh mashin).* Gosenergoizdat, (1949).

A METHOD OF REDUCING TRANSIENT PHENOMENA IN CIRCUITS WITH INDUCTANCE COILS AND SEMICONDUCTOR RECTIFIERS*

B. M. MENSKII

Moscow

(Received 22 August 1960)

YEAR
1961

The principal feature of the transient phenomena which occur when closing a circuit containing a semiconductor rectifier bridge and inductance coils at the input and output (Fig. 1) is the shorter duration of the phenomena compared with the closing of a d.c. circuit with an output coil r_{out} and L_{out} [1,2].

The duration of the transient phenomena in such a circuit depends upon the relationship between the circuit criteria. The circuit is defined by three items assuming that the rectifiers are ideal:

$$\varphi_{out} = \operatorname{arc\,tan} \frac{\omega L_{out}}{r_{out} + r_a},$$

$$\varphi_{in} = \operatorname{arc\,tan} \frac{\omega L_{in}}{r_{in} + r_a};$$

$$\xi = \frac{\sqrt{(r_{in} + r_a)^2 + (\omega L_{in})^2}}{r_{out} + r_a},$$

where ω is the frequency of the applied alternating voltage and r_a the forward resistance of the rectifier.

The parameters ϕ_{out} and ϕ_{in} show the relationship between the inductive reactance and resistance at the input and output of the circuit. The symbol ξ represents the relationship between the total

---

* *Elektrichestvo*, 4, 58-61, 1961.

resistance to the alternating current at the input and the resistance to the rectified current at the output. To determine all these items the forward resistance of the rectifier bridge is divided between the input and output.

Consider now the relationship which must exist between these items for the transient phenomena to be reduced to the shortest possible period of time on closing the circuit. It is assumed that the circuit is closed at the commencement of a positive half-wave of alternating voltage. A first period of conduction β_1 commences when the circuit has been closed, i.e. rectifiers I are live ($i_{in} = i_1 = i_{out}$) and rectifiers II are non-conducting ($i_{II} = 0$).

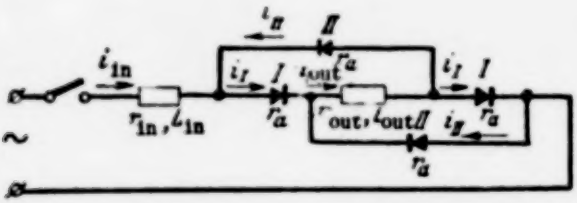

Fig. 1. Circuit containing inductance coils and a rectifier bridge.

If the electrical angle $\vartheta = \omega t$ (where t is time) read from the instant the circuit is closed, the output current in the first period of conduction is described by the expression

$$i_{out} = I_m \sin(\vartheta - \varphi) + I_m \sin\varphi e^{-\sigma\vartheta}$$

where

$$I_m = \frac{U_m}{\sqrt{(r_{in} + 2r_a + r_{out})^2 + (\omega L_{in} + \omega L_{out})^2}}$$

$$\varphi = \arctan\frac{\omega L_{in} + \omega L_{out}}{r_{in} + 2r_a + r_{out}};$$

$$\sigma = \operatorname{cotan}\varphi.$$

and U_a is the amplitude of the applied voltage.

The first period of conduction ends at $\vartheta = \beta_1$, when the voltage

applied to rectifier II equals

$$U_{II} = (r_{out} + r_a) i_{out} + \omega L_{out} \frac{di_{out}}{d\vartheta} = 0.$$

Hence, by substituting the value of i_{out}, an equation can be written for the first period of conduction β_1:

$$\sin(\beta_1 + \varphi_{out} - \varphi) = \sin(\varphi_{out} - \varphi) e^{-\sigma_{out}\beta_1}. \quad (1)$$

The current in the output coil at the end of the first period of conduction is

$$I_{\beta_1} = I_m \frac{\sin\varphi_{out}}{\sin(\varphi_{out} - \varphi)} \sin\beta_1. \quad (2)$$

YEAR 1961

The first period of conduction is followed by a period of commutation γ_1 during which all the rectifiers in the bridge are live. For this period of commutation

$$i_{out} = I_{\beta_1} e^{-\sigma_{out}(\vartheta - \beta_1)}$$

and

$$i_{in} = cI_m \sin(\vartheta - \varphi_{in}) + \\ + [I_{\beta_1} - cI_m \sin(\beta_1 - \varphi_{in})] e^{-\sigma_{in}(\vartheta - \beta_1)},$$

where

$$\sigma_{out} = \operatorname{cotan}\varphi_{out}$$

$$\sigma_{in} = \operatorname{cotan}\varphi_{in};$$

$$c = \frac{\sqrt{(r_{in} + 2r_a + r_{out})^2 + (\omega L_{in} + \omega L_{out})^2}}{\sqrt{(r_{in} + r_a)^2 + (\omega L_{in})^2}}.$$

This period of commutation ends at $\vartheta = \beta_1 + \gamma_1$, when the current in rectifier I becomes zero:

$$i_1 = \frac{1}{2}(i_{in} + i_{out}) = 0.$$

Hence, by substituting the values i_{in} and i_{out}, an equation for the period of commutation γ_1 is:

$$cI_m \sin(\beta_1 + \gamma_1 - \varphi_{in}) + I_{\beta 1}(e^{-\sigma_{in}\gamma_1} + e^{-\sigma_{out}\gamma_1}) - \\ - cI_m \sin(\beta_1 - \varphi_{in}) e^{-\sigma_{in}\gamma_1} = 0. \quad (3)$$

The current in the output coil at the end of the period of commutation is:

$$I_{\gamma_1} = I_{\beta_1} e^{-\varphi_{out}\gamma_1}. \tag{4}$$

A second period of conduction then follows during which rectifiers II are live ($i_{out} = i_{II} = -i_{in}$) but rectifiers I are "off" ($i_I = 0$).

The current in the output coil is defined in this case by the equation

$$i_{out} = -I_m \sin(\vartheta - \varphi) + \\ + [I_{\gamma_1} + I_m \sin(\beta_1 + \gamma_1 - \varphi)] e^{-\varphi[\vartheta - (\beta_1 + \gamma_1)]}.$$

The current in the output coil at the end of the second period of conduction is:

$$I_{\beta_2} = -I_m \sin(\beta_1 + \gamma_1 + \beta_2 - \varphi) + \\ + [I_{\gamma_1} + I_m \sin(\beta_1 + \gamma_1 - \varphi)] e^{-\varphi\beta_2}, \tag{5}$$

where β_2 is the second period of conduction.

If the current in the output coil is the same in value at the end of the first period of conduction as at the end of the steady state period of conduction, and if steady state conditions follow the first period of conduction, then

$$I_{\beta_2} = I_{\beta_1}$$

and

$$\gamma_1 + \beta_2 = \pi.$$

Equating the value of $I\beta_1$ from equation (2) to the value of $I\beta_2$ from (5) and substituting $\beta_1 = \pi - \gamma_1$, as well as the value of $I\gamma_1$ from (4):

$$\sin(\varphi_{out} - \varphi)\sin(\beta_1 + \gamma_1 - \varphi) + \sin\varphi_{out} \times \\ \times \sin\beta_1 e^{-\varphi_{out}\gamma_1} - \sin\varphi\sin(\beta_1 + \varphi_{out} - \varphi) e^{-\varphi(\gamma_1 - \pi)} = 0. \tag{6}$$

Equation (6) provides a relationship between the parameters which satisfies the requirement, i.e. steady state conditions will follow the first period of conduction if the circuit is closed when the voltage passes through zero.

Exactly the same factors affect the transient phenomena during the first period of conduction (i.e. the configuration of the circuit and the variation in applied voltage) when $\beta_1 - \beta \leqslant \vartheta \leqslant \beta_1$, as in the steady state period of conduction (Fig. 2a). Therefore the current in the output coil when $\vartheta = \beta_1 - \beta = \psi$ has exactly the same value as at the commencement of the steady state period of conduction.

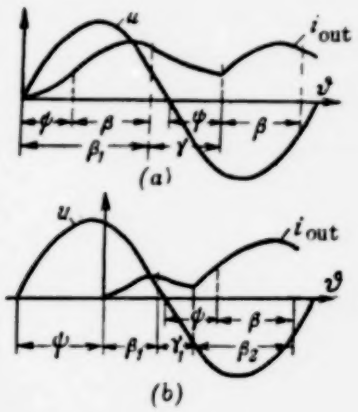

Fig. 2. Transient behaviour in a circuit with the optimum relationship between its criteria:

a) $\psi_1 = 0$, *b)* $\psi_1 \neq 0$.

Thus, if the relationship between the circuit criteria corresponds to equation (6), and if the circuit is closed at the moment the mains voltage passes through zero, the duration of the transient phenomena is then defined by the expression

$$t' = \frac{\psi}{\omega},$$

where ψ is the angle between the steady state period of conduction and the mains voltage ($\psi < \pi$).

Obviously, if the circuit is closed at any other moment of time (Fig. 2b), the duration of the transient phenomena is:

$$t'' = \frac{\pi + \psi - \psi_1}{\omega},$$

where ψ_1 is the initial angle.

Hence, if the relationship between the circuit criteria corresponds to equation (6), the duration of the transient phenomena on closing this circuit is less than one full wave and varies between the following limits depending on the exact instant at which the circuit is closed:

$$\frac{\psi}{\omega} \leqslant t < \frac{\pi + \psi}{\omega}.$$

Equation (6) contains the angles β_1 and γ_1 as well as the circuit items. This entails the use of equations (1) and (3). Equation (6) also contains another symbol ϕ which is a function of the fundamental circuit items ϕ_{out}, ϕ_{in} and ξ. The relationship between these items is expressed by the equation

$$\xi = \frac{\sin(\varphi_{out} - \varphi)}{\cos\varphi_{out}\sin(\varphi - \varphi_{in})}. \tag{7}$$

It is convenient to transform equations 1, 3, 6 and 7 into:

$$\operatorname{cotan}(\varphi_{out} - \varphi)\sin\beta_1 + \cos\beta_1 = e^{-\alpha\beta_1}; \tag{8}$$

$$\begin{aligned}&[\cos(\beta_1 + \gamma_1 - \varphi_{out}) - \cos(\beta_1 + \gamma_1 + \varphi_{out} - 2\varphi_{in})] + \\ &+ [\cos(\beta_1 - \varphi_{out}) - \cos(\beta_1 + \varphi_{out})]\, e^{-\alpha\varphi_{out}\gamma_1} + \\ &+ [\cos(\beta_1 + \varphi_{out} - 2\varphi_{in}) - \cos(\beta_1 + \varphi_{out})]\, e^{-\alpha\varphi_{in}\gamma_1} = 0;\end{aligned} \tag{9}$$

$$\begin{aligned}&[\cos(\beta_1 + \gamma_1 - \varphi_{out}) - \cos(\beta_1 + \gamma_1 + \varphi_{out} - 2\varphi)] + \\ &+ [\cos(\beta_1 - \varphi_{out}) - \cos(\beta_1 + \varphi_{out})]\, e^{-\alpha\varphi_{out}\gamma_1} - \\ &- [\cos(\beta_1 + \varphi_{out} - 2\varphi) - \cos(\beta_1 + \varphi_{out})] e^{\alpha(\pi - \gamma_1)} = 0;\end{aligned} \tag{10}$$

$$\xi = \frac{2\sin(\varphi_{out} - \varphi)}{\sin(\varphi + \varphi_{out} - \varphi_{in}) + \sin(\varphi - \varphi_{out} - \varphi_{in})}. \tag{11}$$

This set of equations allows those values of ϕ_{in} and ξ to be found which reduce the transient phenomena in question to the shortest possible period of time for the given value of ϕ_{out}.

The actual method of calculation is as follows. Given the value of ϕ, find the first period of conduction from equation (8), the period

of commutation from (10), the value of ϕ_{in} from (9) and that of ξ from (11). Given several values of ϕ, the relationship between ϕ_{in} and ξ for the given value of ϕ_{out} can be plotted.

This set of equations is however indeterminate if $\phi_{out} = \phi_{in} = \phi$. The circuit criteria of minimum transient phenomena are in this case defined by the equation

$$\xi \cos\varphi = 1, \tag{12}$$

whence it follows that $r_{in} = r_{out}$ and $L_{in} = L_{out}$.

The results obtained by this set of equations or (12) are given in Fig. 3. Using these curves that value of ξ for ϕ_{out} and ϕ_{in} can be found which minimizes the duration of the transient phenomena on closing the circuit. Graphical interpolation can be employed for intermediate values of ϕ_{out}. For example, if $\phi_{out} = 80^0$ and $\phi_{in} = 75^0$, an auxiliary curve $\xi = f(\phi_{out})$ for $\phi_{in} = 75^0$ can be plotted as in Fig. 4 and it is then apparent that $\xi = 6.3$ for the specified values of ϕ_{out} and ϕ_{in}.

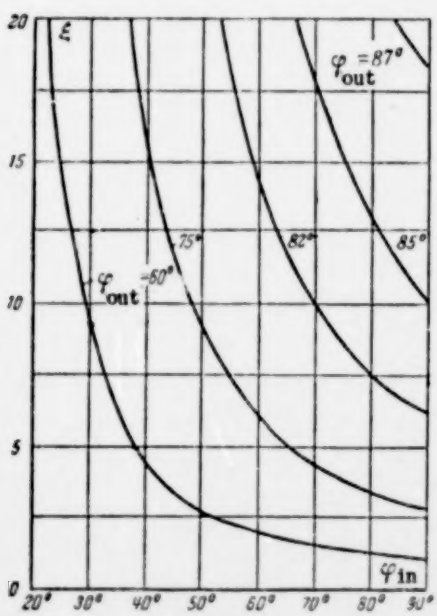

Fig. 3. Curves for determining the optimum relationship between the circuit criteria.

Fig. 5 shows an oscillogram of transient phenomena which occur on closing a circuit whose parameters correspond to equation (12). The rectifier bridge consists of DGTs – 24 type germanium rectifiers (two rectifiers in parallel in each arm). Coils with an inductance of 0.17 H and resistances of 0.54 ohms were connected at the input and output. The frequency of the applied voltage was 50 c/s.

The early end to transient conditions in this circuit is due to the dynamic redistribution of the voltages [2]. During the transient conditions a much larger proportion of the applied voltage influences the output coil than during steady state conditions. Rather a large margin of voltage is therefore required if transient phenomena are to be minimized, i.e. the inductance of the input coil must be quite large. The precise relationship between the circuit items is defined by equations (8) to (11) (or (12) if $\phi_{out} = \phi_{in}$).

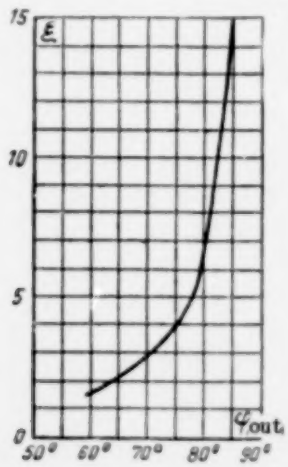

Fig. 4. Auxiliary curve for graphical interpolation.

If ϕ_{out} or ξ is allowed to be less than the value indicated by these equations, the transient conditions will be prolonged, and if $\xi = 0$, the duration of the transient conditions will be the same as when closing a d.c. circuit with an output coil.

Transient phenomena will also persist for a longer period of time if ϕ_{out} or ξ are greater than the value indicated by the equations. In this event the current in the first half-wave may be greater than in the steady state, and if $\xi \to \infty$, the duration of the transient con-

ditions will be the same as when closing an a.c. circuit with an input coil.

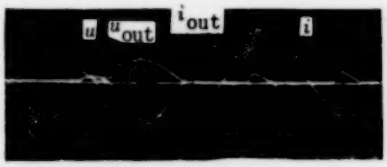

Fig. 5. Oscillogram of the transient on closing a circuit with optimum criteria: u – applied alternating voltage; u_{out} – voltage of output coil; i_{out} – current of output coil; i – current of input coil.

Translated by O.M. Blunn

YEAR
1961

REFERENCES

1. V.E. Bogoliubov; *Transient phenomena in ferroresonant circuits with magnetization, (Perekhodnye protsessy v ferrorezonansnykh tsepiakh s podmagnichivaniem).* Thesis for the degree of doctor, ME' I, (1954).
2. L.A. Bessonov; *Dynamic phenomena in circuits with semiconductor rectifiers, (Dinamicheskie iavleniia v tsepiakh a poluprovodnikovymi ventiliami).* Trud. Vsesoiuz. zaochnogo energet. inst., No. 7, (1957).

A NEW METHOD OF TESTING THE BRUSHES OF ELECTRICAL MACHINES*

A.M. TRUSHKOV

Tomsk

(Received 9 November 1960)

The brushgear tests specified in the State Standards (GOST) do not reveal the conditions under which a particular type of brush will give the best service. This shortcoming is felt quite acutely at the present time because of the particularly arduous conditions which have to be satisfied in modern high speed machines at 5000 to 6000 rev/min and high commutator voltages. No criterion is available by which to select the appropriate type of brush for particular operating conditions.

In this paper it is proposed to take the magnitude of the minimum voltage for sparking at the end of commutation (the sparking voltage) as an extra criterion by which to estimate the electrical properties of brushes. When the commutation conditions are so unfavourable that sparking is unavoidable, the erosion of the contact surfaces can best be reduced by using brushes with a low sparking voltage since in this case the arc will discharge with less energy.

The sparking voltage of various types of brushes can be established by the test circuit illustrated in Fig. 1. This system uses a "collector-interrupter" which periodically discharges an electrical circuit which is supplied from a battery. The voltage drop in the contact can be measured by a voltmeter and an EO-7 type cathode-ray oscillograph. As the voltage gradually increases, the appearance of sparking is marked by a luminous spot on the oscillograph (see point *a* in Fig. 2). If the time scale is increased, a "line of arc combustion" at a constant voltage will correspond to this spot.

It is well-known that the interruption of a commutation circuit is

---

* *Elektrichestvo*, No.4, p.84, 1961.

greatly affected by its inductance. To keep the latter constant as an increasingly large voltage is applied to the slip contact, the voltage supply has to be varied by connecting different numbers of cells. The minimum sparking voltage is found from the relationship between Oa' and Ob in the oscillograms. The test results of brushes 4 x 4 mm are as follows:

Type of brush	Minimum arcing voltage, V
MG	9.0
MG – 1	9.56
Г – 3	11.3
EG – 2a	12.16
EG – 4	12.96

YEAR 1961

The average of ten measurements was taken for each type of brush. The speed of the interrupter was 1500 rev/min and the current interrupted was 10-11 A.

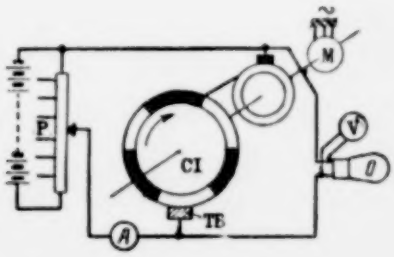

Fig. 1. The test circuit:

TB – Test brush; *CI* – contact interrupter; *M* – motor; *P* – potentiometer; *A* – ammeter; *V* – voltmeter; *O* – oscillograph.

From test results, EG – 4 type brushes had the maximum sparking voltage and MG the minimum.

There is a different minimum sparking voltage for each type of brush and this difference is as much as 25 to 30 per cent. The relationships between sparking voltages correspond qualitatively to the relationships between the actual commutation capacity (i.e. a low sparking voltage implies good commutation).

It is worthwhile using brushes with the minimum sparking voltage from the point of view of reducing the erosion of the contact materials.

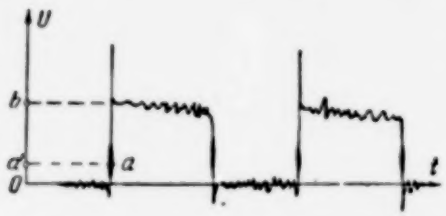

Fig. 2. Oscillogram of the contact voltage.

On the basis of this data, the minimum sparking voltage at the end of commutation can be recommended as an extra criterion of the electrical properties of brushes.

Translated by O.M. Blunn

YEA
196

ABSTRACTS FROM PAPERS PUBLISHED IN ELEKTRICHESTVO No. 4, 1961

YEAR 1961

Computer mathematics

A computer study of transient phenomena in synchronous machines using differential equations with periodic coefficients. B.M. Kagan et al., (pp. 43-48).

The authors illustrate the way computers can be used to solve differential equations with periodic coefficients. A network containing synchronous machines under transient conditions is used as an example.

Control engineering

A contribution to the theory of linear circuits with variable parameters. V.S. Davydov, (pp. 51-58).

Relationships are derived for the steady state in a linear parametric system under the influence of an external harmonic voltage. These relationships take a form which is as near as possible to the usual relationships used in the theory of alternating currents.

High frequency engineering

The design of reactive frequency converters for 100 to 500 c/s. M.M. Tarashchanskii, (pp. 73-75).

A short account is given of the main problems involved in the design of "reactive frequency converters" as used to convert alternating currents of 50 c/s into high frequency currents of 100 to 500 c/s for machine tools. Particular attention is paid to the dimensions of the stator.

Insulation

The use of life curves and other methods for determining the corona resistance of high voltage insulation. N.V. Aleksandrov, (pp. 61-68).

An account is given of the methods and some of the equipment used in the Lenin Electrical Engineering Institute to determine the corona resistance of varnishes, mica products and other insulation. The

steepness of the "life curves" and sustained electrical strength are used as criteria for a comparative analysis of the materials.

Aluminium windings with enamel, fibre and oxide insulation. V.A. Privezentsev, (pp. 68-73).

The increase in demand in the U.S.S.R. for low-cost aluminium winding conductors is considered together with the methods of production and properties of aluminium conductors with enamel, paper, glassfibre, oxide and glassfibre-oxide insulation.

Power systems

The propagation of surges in networks with twin-circuit transmission lines. A.S. Dadunashvili, (pp. 5-13).

An analysis is made of the phenomena associated with the propagation of surges in twin-circuit transmission lines. This is a special application of an already known method of breaking down surge waves into their components. Test results are given.

The lightning performance of 275-500 kV transmission lines. M.V. Kostenko, et al., (pp. 20-26).

A theoretical analysis is made of the effect of the tower inductance, lightning arc and supply voltage on the lightning performance of transmission lines and an estimate made of the probability of strikes. Statistical data of lightning strikes in the U.S.S.R. and the western world are given. This approach to the problem stresses the importance of the height of the towers and the effect of lightning strikes which by-pass the earth wires to the conductors.

The electrical characteristics of the ground and their effect on the design of outdoor foundations. L.E. E'bin et al., (pp. 26-30).

The authors propose a method of designing foundations for electrical equipment which allows for local and seasonal changes in the electrical characteristics of the earth. It is assumed that the electrical conductivity of the ground is a function of curvilinear coordinates of the electrical field.

A simple method of calculating short circuit currents in networks with steel conductors. L.M. Perbsina, (pp.30-34).

A simple and quite accurate method is proposed for calculating the the short circuit currents in networks with steel conductors where the impedance of the conductors is a function of the current. Use

is made of linearized voltampere characteristics.

Rotating machines

The mis-use of circuit transformations in the mathematical analysis of electrical machines. I.I. Talalov, (pp. 34-38).

A study is made of the fundamental principles and relationships involved in mathematical transformations as applied to the design of the circuits and windings of electrical machines. The author has in mind certain mistaken modifications of these methods which have been used on computers.

A new electrostatic current generator using dielectric friction. N.G. Drozdov et al., (pp. 48-50).

A description is given of a small climatically-stable 800 V electrostatic generator with a plexiglass and teflon stator and a plexiglass-metal rotor. The internal surface of the stator is charged by polyethylene brushes on the rotor. Alternating or direct current can be produced. A 500 pF capacitor can be charged to 200 V in 20 to 25 revolutions of the rotor.

YEAR 1961

Progress in the electric drives of excavators. Iu. Ia. Vul', (pp. 81-83).

An account is given of operating experience with two amplidyne-type motor-generator sets for the lifting and traction drives on large excavators.

Statistical methods

A statistical and graphical method of designing equipment for a given reliability. Ia.A. Rips, (pp. 76-81).

An example is given of a way to design an electromagnetic relay for a given reliability and production cost. The method makes it possible to establish the necessary margin of safety and to estimate the effect of parameters on the reliability and durability of the device. The method is of general application.

Traction

The use of 25 kV on a.c. electrified railways. A.V. Voronin et al., (pp. 1-5).

Proposals have in the past been made for a general changeover to 35 kV on heavily loaded sections of the three-phase a.c. electrified

railway system of 50 c/s in the U.S.S.R. This paper explains why it has been decided to retain 25 kV. However, further cost analysis is to be undertaken to see whether it is advisable to use 35 kV on systems supplied from 220 kV power lines.

A NEW METHOD OF STUDYING LARGE COMPLEX POWER SYSTEMS ON ANALOGUE COMPUTERS*

N. I. SOKOLOV, Yu. E. GUREVICH and Z. G. KHVOSHCHINSKAYA

(Moscow)

(Received 25 July 1960)

YEAR 1961

Analogue computers are now extensively used to study the transient behaviour, control and stability of synchronous generators and it is quite natural to try and apply them to more complicated systems containing several generators, loads as well as other line elements.

Several methods have been proposed for this purpose:

1. An analogue may be formed of each machine in its own co-ordinates and then all reduced to a common system of co-ordinates [1, 3];

2. The equations of the generators may be written in a synchronously rotating system of co-ordinates [2];

3. The equations of the generators may be written in terms of self- and mutual impedances and analogues formed by these equations [3].

However, method 1 leads to very cumbersome and impracticable computing schemes and methods 2 and 3 are apparently only possible if it is assumed, *inter alia*, that the impedances in the direct and quadrature axes are equal and if there is no (active) resistance. Methods 1 and 2 are very complicated, whilst in 1 and 3 the amount of computing apparatus increases out of proportion to the number of stations, and intermediate results are not at all readily appreciated, being expressed in coordinates α_c, β_c, etc.

* *Elektrichestvo*, 5, 1-8, 1961.

In this paper a method is proposed which permits the study of power systems of any degree of complexity on analogue computers on the usual assumptions. The number of computing amplifiers increases in proportion to the number of stations, loads and lines studied. The individual elements of a power system can be studied with different degrees of approximation. As far as the authors know, nobody has ever used the proposed method previously.

The main feature of the proposed method is that each element and its adjacent section of the line can be studied separately from all the other elements by the equations describing it.

The means of constructing the scheme depends on whether or not there is a point in the system which can be regarded as an infinite bus-bar. If such a point is present, the complete scheme consists of two types of element, namely:

1. Elements which link the infinite bus-bar with the network nodes and lines which interconnect the individual nodes;

2. Elements for the stations and loads.

The equations of line elements (type 1) contain the known input quantities of each element, i.e. the voltage at the sending end of the line, definable by the modulus and phase relative to the voltage of the infinite bus-bar, and the active and reactive power at the receiving end of the line, defined by the power balance at the node. The output quantities are the modulus and phase of the voltage at the receiving end of the line and, if necessary, the active and reactive power at the beginning of the line. The infinite bus is the beginning of the first line and the nearest points to the infinte bus are the beginning of the other lines. Thus, elements of type 1 permit successive determination of the modulus and phase of the voltages at the nodes.

For station and load elements (type 2) the input quantities are the modulus and phase of the voltages at the respective nodes.

The active and reactive power reaching them constitutes the output.

The principle is illustrated in Fig. 1.

The method can be modified if there is no infinite bus-bar and one of the generator stations is adopted as "reference". The angles of the rotor at all the other stations are read off from the axis of the rotor at the reference generator station. The analogue of the network is also

begun from the bus-bars of this station. It is also necessary to control the speed of the prime movers and consequently their torque, for otherwise it is impossible to balance the active power.

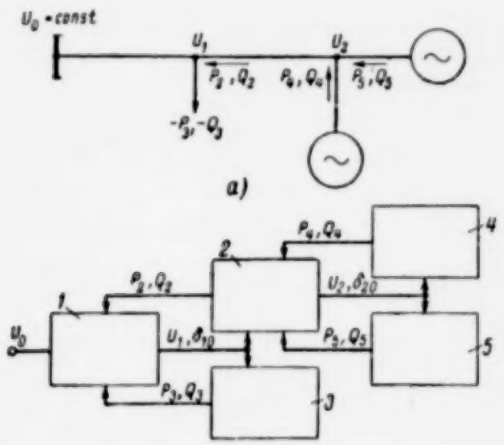

Fig. 1. Circuit (a) and block-diagram (b). *1* - line; *2* - line; *3* - load; *4* - alternator; *5* - alternator; *P* - active power; *Q* - reactive power.

The computing schemes are therefore analogous to the circuits of actual networks and there is therefore no difficulty in excluding some elements, including others, or clearing short circuits, etc. The number of elements must naturally be restricted for the study; but all elements in operational units can be covered. A larger number of amplifiers has to be used to study complex systems, but this cannot lead to self-excitation if the individual groups of elements are stable. In practice, four to five stations can be studied.

The proposed method allows special analogues of generators and line sections, etc. to be formed, which can then be combined to solve particular problems.

Analogues of elements

Line sections. Consider the transmission of power *P* from the node *m* to the node *n* via the impedance z_{mn} (Fig. 2a). It can be assumed that the active and reactive power into the line from the node *m* and the voltage

at node n are known. It is required to find the angle between the vector voltages at the nodes δ_{mn}, the voltage U_n and in certain cases active and reactive power at the other end of the line. The fundamental case of power transmission without loss is considered when $x_{mn} = x_{nm}$ and $P_n = -P_m$.

Suppose that the voltage U_n is also known. The angle δ_{nm} is then found from the equation

$$P_m = \frac{U_m U_n}{x_{mn}} \sin \delta_{mn}. \tag{1}$$

Alternatively, given δ_{nm}, the voltage can be found from the expressions

$$Q_m = \frac{U_m^2}{x_{mn}} - \frac{U_m U_n}{x_{mn}} \cos \delta_{mn}; \tag{2}$$

$$Q_n = \frac{U_n^2}{x_{mn}} - \frac{U_m U_n}{x_{mn}} \cos \delta_{mn}. \tag{3}$$

where Q is the reactive power.

The circuit in Fig. 2b, which refers to equation (1), contains an operational amplifier, a function generator* which gives the sine of the input, and a multiplier.

Putting α for the output voltage of the operational amplifier, the amplifier receives the difference between P_n and $\frac{U_n U_m}{x_{nm}} \sin \alpha$ at its input. This difference must be very small since an operational amplifier has no self-feedback and its amplification factor is very high. If P_n or $\frac{U_n U_m}{x_{nm}} \sin \alpha$ change, the difference between these quantities will increase and change sign at the input to the amplifier on passing through the sine unit. The value of α changes so that the difference becomes negligible. It is obvious that this will occur when $\alpha = \delta_{mn}$.

Such methods are extensively used in mathematical simulation to

* In our case we used sin and cos function generators made in the power system laboratory of the All-Union Electrical Energy Research Institute using tyrite (ferguson'te) resistors. These generators can produce functions of an argument lying between the limits -2π and $+2\pi$.

obtain inverse functions. For example, a circuit with no multiplier ensures that $U_{out} = \sin^{-1} U_{in}$.

The circuit in Fig. 2b is stable if $\delta_{mn} < 90°$, since negative feedback becomes positive if δ_{mn} is large. But in the case under consideration the circuit is linked with the computing scheme of the generator which always has negative feedback, thereby ensuring the correct production of any value of the angle δ_{mn}.

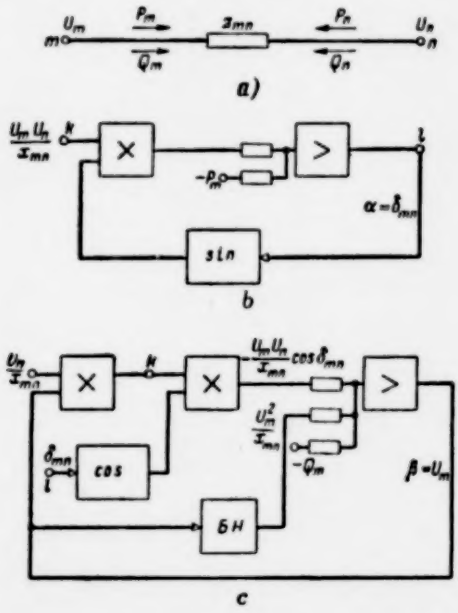

Fig. 2. A section of the line.
a – line section; b – circuit producing angle δ_{mn}; c – circuit producing nodal voltages.

The voltage U_n is found in a similar way. The corresponding circuit contains an amplifier without self-feedback, so that the following expression is obtained:

$$-\beta \frac{U_n}{x_{mn}} \cos \delta_{mn} - Q_m + \frac{\beta^2}{x_{mn}} = 0,$$

where β is the output voltage of the amplifier.

Comparing this expression with expression (2), it will be seen that

$\beta = U_m$.

The circuit also contains a multiplier and a cos function generator (a "quadrator"), which ensures that $U_{out} = U_{in}^2$.

The circuits in Fig. 2a and 2b are combined by joining the points k and l in each circuit. The inputs are then P_n, Q_n and U_n, and the outputs U_n and δ_{nn}. If necessary, Q_n can easily be obtained in accordance with equation (3). This requires one extra cos function generator for the voltage U_n *sic*. It should be pointed out, however, that only one cos function generator is normally required for each node, regardless of the number of outgoing lines from each node.

In a closed network the inter-nodal links are analysed by expressions (1)-(3). The active and reactive power flows are determined from the known nodal voltages and angle δ_{nn}, and they are then introduced into the power adders.

When the resistance of the line is included, the following expressions are used to determine the active and reactive power at the ends of the line with positive directions from the node into the line:

$$P_n = \frac{U_n^2}{z_{mn}^2} r_{mn} - \frac{U_m U_n}{z_{mn}^2} (x_{mn} \sin \delta_{mn} + r_{mn} \cos \delta_{mn}); \tag{4}$$

$$P_m = \frac{U_m^2}{z_{mn}^2} r_{mn} + \frac{U_m U_n}{z_{mn}^2} \times \times (x_{mn} \sin \delta_{mn} - r_{mn} \cos \delta_{mn}); \tag{5}$$

$$Q_n = \frac{U_n^2}{z_{mn}^2} x_{mn} + \frac{U_m U_n}{z_{mn}^2} \times \times (r_{mn} \sin \delta_{mn} - x_{mn} \cos \delta_{mn}); \tag{6}$$

$$Q_m = \frac{U_n^2}{z_{mn}^2} x_{mn} - \frac{U_m U_n}{z_{mn}^2} \times \times (r_{mn} \sin \delta_{mn} + x_{mn} \cos \delta_{mn}), \tag{7}$$

where

$$z_{mn}^2 = x_{mn}^2 + r_{mn}^2.$$

The inclusion of line resistance presents no difficulty, and a section of the line can be studied in the same way by equations (4)-(7). The only difference is that quantities which are proportional to sin δ_{nn}

and cos δ_{nn} are introduced into the circuits by summators and integrators to obtain $\dot{\delta}_{nn}$ as well as U_n.

Generators. It is best to study generators in the direct (d) and quadrature (q) axes associated with the rotor. The analysis is particularly graphic since all the quantities have physical significance.

Generators can either be studied by the Gorev-Park equations [3] or by the equivalent networks proposed by the Gorodskii [4, 5]. The former method has been used for a number of years in the dynamic control laboratory of the power-station department at the Moscow Power Institute (MEI). The second method is more convenient, since fewer operational amplifiers are required, the criteria of the machines can easily be varied and any number of rotor circuits on a synchronous machine can be included.

YEAR
1961

Gorodskii's equivalent networks (see Fig. 3) have certain similarities with the conventional equivalent networks of synchronous machines. In them, ohmic resistances are substituted for inductances, and capacitances for (active) resistances, whilst the input impedances of the circuits for the direct (d) and transverse (q) axes correspond to the reactances $x_d(p)$ and $x_q(p)$ in transient and steady states.

Gorodskii's equivalent networks were proposed previously and took no account of the variation of the exciter voltage due to the action of the regulator. To include this factor correctly in the network corresponding to the direct axis of the machine, it is necessary to introduce a current I at point b in Fig. 3a proportional to the voltage U_f and independent of U_q (see appendix I). The current I is the "forced" component of the excitation current I_f flowing through the reactance x_{af}. Under transient conditions the current I_f is the sum of the "forced" current $I_{fe} = I \equiv u_f$ and the force (transient) component due to the variation of the voltage u_q or u_f.

This requires a special "current source" with an infinite output resistance. The magnitude of the introduced current should be proportional to the control voltage and independent of the external resistance within definite limits. This special "current source" is obtained by using two operational amplifiers (see appendix II and Fig. 4).

When using Gorodskii's equivalent circuits on the computer, points a and a_1 (see Fig. 3) are connected to the outputs of the operational amplifiers which produce the voltages u_q and u_d. It is convenient to include the transformer resistance and the inductive reactance of the line up to the node in the leakage reactance x_σ of the equivalent network. It is

Undesirable for the capacitances in the branches of the equivalent network to be in excess of 10 μF. This requirement determines the magnitude of the ohmic resistances and currents in the branches. The resistances should not be too small, for otherwise the amplifiers may be overloaded.

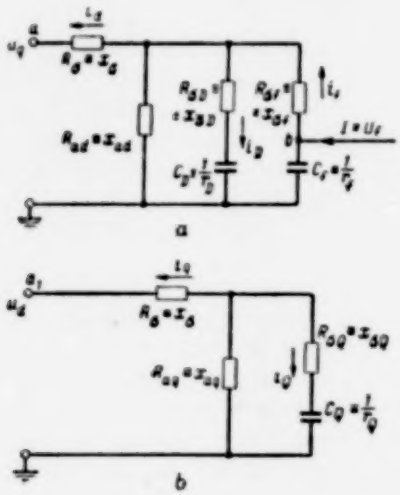

Fig. 3. Equivalent circuit of generator.
a – along direct axis; b – along quadrature axis.

Instruments and oscillograph loops can be connected in series in the circuits to measure the currents. It must however be borne in mind that the currents do not usually exceed 1 mA and so the currents are usually converted into voltages by other amplifiers for further study and measurement. For the sake of convenience in taking measurements, the "current source" (see Fig. 4) is connected to a slightly different equivalent network of the generator (Fig. 5c). This new network is practically the same as the original one, since the resistances of the u_q and u_d are close to zero.

The stator currents i_d and i_q can be estimated from the voltage drop in the leakage reactance X_σ. The input impedance r_2 of amplifier *10* is connected in parallel with r_1. The latter must be made such that

$$\frac{r_1 r_2}{r_1 + r_2} \equiv X_\sigma.$$

The excitation current i_f can be estimated from the difference in voltage to earth at points *b* (the position of the "current source")

and c (position of amplifier *10*). Since the output voltage of amplifier *9* is equal to the voltage at point b, but opposite in sign, it is therefore sufficient to add the voltages after amplifier *9* and at point c. In calculating the impedance r_1 it is necessary to take the input impedance r_3 of amplifier *11* into account.

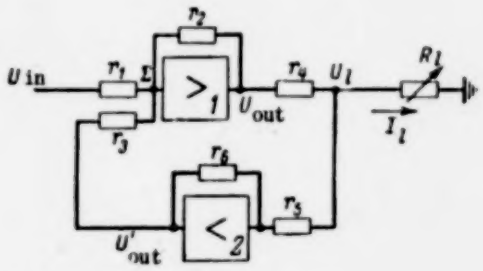

Fig. 4. Equivalent circuit of "current source".

YEAR
1961

The currents in the damping winding are usually difficult to measure, but this can be done by adding another amplifier (see Fig. 5c).

The voltages u_q and u_d at the terminals of the equivalent relay are obtained by "projecting" the voltage at the node where the generator is connected along the axis of the machine (see Fig. 5b).

Use is made of multipliers and adders to determine the active and reactive power from the generator to the node:

$$\left.\begin{aligned} P &= u_d i_d + u_q i_q, \\ Q &= u_q i_q - u_d i_d, \end{aligned}\right\} \tag{8}$$

It is presupposed that $P \approx m$.

Variation in rotor angle are found by twice integrating the equations of motion of the rotor about a certain reference axis which rotates at the synchronous speed.

$$T_j p^2 \delta = P_{\text{mech}} - P_{\text{el}}. \tag{9}$$

The reference axis is the voltage vector at the infinite bus-bars. The angle between the quadrature axis of the generator and the nodal voltage is obtained by subtracting the angle of the node-bus-bar from the equation of motion.

It is assumed that the turbine torque is constant. Alternatively, a

speed-controlled turbine may be studied separately [3]. The generator can be provided with any excitation regulator and exciter. No special explanation is required to study these elements [6]. The authors of this article have adopted the circuit shown in Fig. 5.

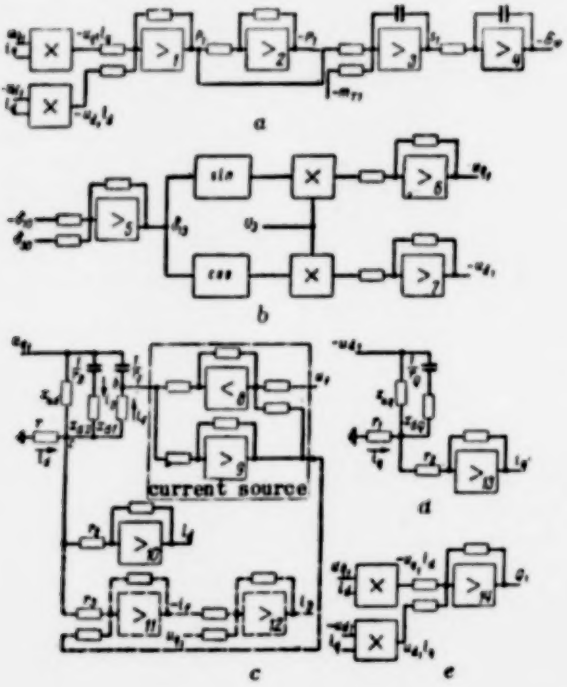

Fig. 5. Computing scheme of generator.
a – active power and the equation of motion of the generator; *b* – projection of the nodal voltages along the axes of the generator; *c* – direct-axis of the generator; *d* – quadrature axis of the generator; *e* – reactive power.

In many cases it is possible to simplify the study of generators by substituting constant impedances and a constant e.m.f. for the "contact" resistance found from the preceding conditions. The equation of motion remains unchanged. The electromagnetic power is obtained from the equation

$$P \approx \frac{E'_d U}{x'_d + x_{gn}} \sin \delta, \qquad (10)$$

where U is the nodal voltage; x_{gn} is the impedance from the generator terminals up to the node; δ is the angle of the generator e.m.f. in relation to the node.

The reactive power is found by a similar formula to (2).

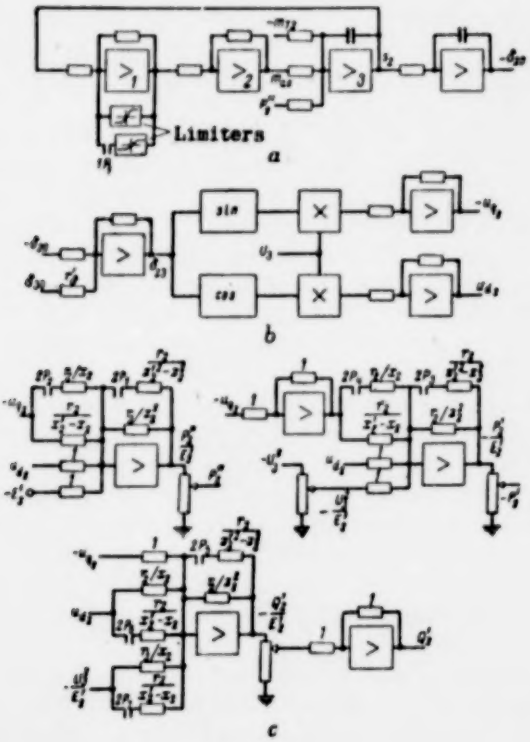

Fig. 6. Simplified computing circuit of generator.

$z_2' = \sqrt{z_2^2 + x_2'^2}$ – line resistance in post-fault conditions;

a – equation of motion of the generator; *b* – projection of the nodal voltages along the axes of the generator; *c* – the active and reactive power.

Given that E_d' is constant, the asynchronous torque m_{as}, which exists if $s \neq 0$, can be ignored. However, asynchronous torque can be included approximately in the way illustrated by Fig. 6, where a value of m_{as}, which is proportional to the slip s, is passed into amplifier 3. If the slip is in excess of its critical value the torque remains constant. Provision is made for altering the amount of asynchronous torque during

short circuits.

Loads and static elements at the nodes. Loads and their dynamic properties can be studied by a similar circuit to that used for the generators by making certain assumptions.

Static loads are simulated in accordance with the equations

$$P = U^2 G_l, \quad Q = U^2 B_l. \tag{11}$$

The term U^2 is usually known; if G_l and B_l are constants, they can be included when calculating the input impedances of the amplifiers for adding the active and reactive power. Such loads can therefore be studied without additional amplifiers. There is no difficulty in studying loads in the light of their steady-state functions $P_l = f_1(U)$ and $Q_l = f_2(U)$. This requires non-linear elements. Neither is there any difficulty in studying shunt reactors, line capacitances or parallel load resistances for restraint under transient conditions, etc.

Short-circuits and post-fault conditions. A short circuit is effected at a node by introducing a shunt $x_{s/c}$ into the node at the time of the fault. This shunt is connected in the same way as a reactive load. By selecting the magnitude of the input impedance at the input to the amplifier adding the reactive power, it is an easy matter to produce a short circuit of any type at any remote point. By taking the minimum possible input impedance ($x_{s/c} \approx 0$), it is possible in practice to obtain an exact three-phase short circuit at the node.

In the study of post-fault conditions it is usually necessary to provide for a change in the impedance of one of the links between the nodes (disconnexion of one of the parallel lines). This is done by automatically changing the input impedances after the short circuit has been cleared.

Example

The proposed method has been applied to the circuit shown in Fig.7 which contains the station *1*, a single generator with a bus-bar load *L*, and the receiving systems *0* and *2*. The bus-bars of receiving systems *0* are assumed to be infinite.

The transformer e.m.f.'s of the generators and variations in the reactance of the generators and lines during generator rotor oscillation are ignored; it is assumed that the generators are unsaturated; the

line resistance is ignored wherever it has no appreciable effect. The method is equally applicable if these simplifications are not adopted, but the circuit is a little more complicated as a result. Only the transformer e.m.f. present any difficulties, but these can be ignored in the majority of cases.

The block-diagrams and circuit-diagrams are given in Figs. 5, 6, 8 and 9. The excitation control has been omitted from the generator circuit in Fig.5 and torque is assumed to be constant. The receiving system 2 (Fig. 7) is simulated by an equivalent generator with a constant e.m.f. after the contact resistance (see Fig.6). The line resistance is included in the study of the lines linking stations 1 and 2, and provision is made for a system of relays to change the line resistance after faults. Receiving system 2 was studied by the equations of motion and expressions (4), (6) and (7).

YEAR
1961

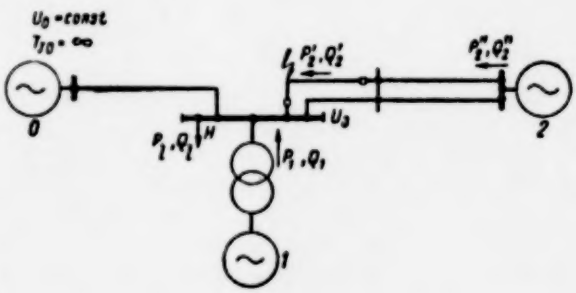

Fig. 7. The simulated network.

The broken lines in Figs. 5 and 9 indicate elements which were later found necessary during the adjustment of the circuit, as well as elements which were included to measure the rotor currents. A system of relays was used to study short circuits. Relay *1P* was live during the short circuit and *2P* afterwards.

By way of example, Fig. 10 shows one of the oscillograms taken during a two-phase earth fault at a node with a high-response excitation regulator.

Circuit adjustment

The proposed method allows the adjustment and verification of each individual circuit element, which simplifies and speeds up the preparations for the study and the study itself. For example, to adjust the

generator circuit it is sufficient to supply the voltage U_3 from an independent source and the generator is, as it were, connected to the infinite bus-bar. To adjust the circuit of a section of the line and a node it is convenient to substitute independent voltages for the active and reactive power of the generators and the loads.

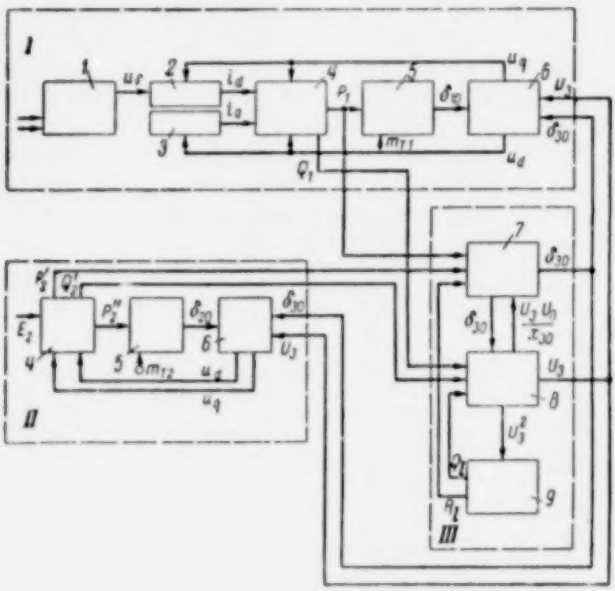

Fig. 8. Simulation block-diagram.

I – first generator; *II* – second generator; *III* – line and node. *1* – automatic voltage regulator; *2* – the *d*-axis; *3* – the *q*-axis; *4* – active and reactive power; *5* – equation of motion; *6* – projection of nodal voltages; *7* – determination of δ_{20}; *8* – determination of U_3; *9* – nodal load.

Gorodskii's equivalent circuits are first adjusted in the direct and quadrature axes. The resistances and capacitances must be correct to three significant digits. It is convenient to adjust the "current source" (Fig. 4) by varying the resistance r_3 (see appendix II) in such a way that the load current measured by the micro-ammeter is independent of the load impedance. Impedances r_1 and r_2 are set to an appropriate scale, and r_4 is such that amplifier *1* of the "current source" is not overloaded under any operating conditions of the generator.

In the node and line circuit (Fig. 9) special attention must be paid to the operational amplifiers which produce the angle δ_{30} and voltage U_3. The amplifiers must have no self-feedback under any circumstances. However, it has been shown by circuit tests that generation* occurs in the circuit in connexion with the weaking of the total negative feedback at angles in excess of 90°. This requires the inclusion of a capacitance C_δ in the feedback of the amplifier producing the angle δ_{30}. Self-excitation was thereby eliminated completely. A capacitance of 0.07 μ F was in fact used. Tests showed that no marked error resulted in the size of the angles.

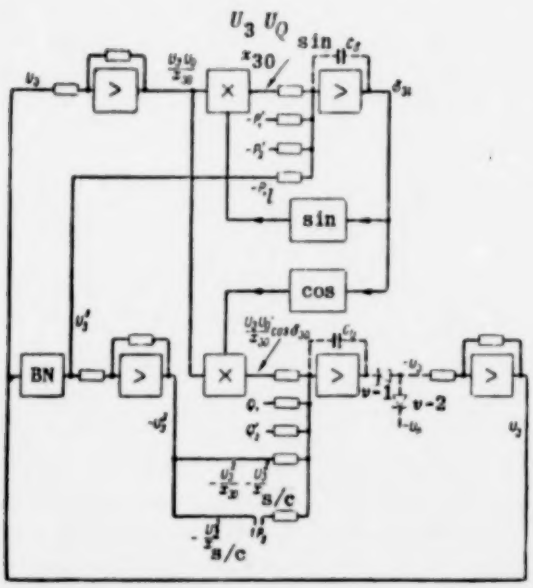

Fig. 9. Computing circuit of node and line section.

More favourable conditions exist in the line-node circuit in which the voltage was produced. It is sufficient for C_U to be about 0.02 μ F. This figure has very little effect even if the voltage varies widely.

Any error due to the capacitances C_δ or C_U can be eliminated by using a "retarded time scale", in which case there is no increase in C_δ or C_U.

* Use was made of UPT-4-type amplifiers.

There remains one further aspect of the method (see Fig. 9) which requires special comment. The impedance of the transformer and the leakage reactance of the generator were combined in the simulation of the generator. In the operation of the circuit the reactive power flowing to the node was proportional to its voltage. At the moment the circuit is started (triggered), or when a three-phase short circuit is cleared at the node, all the operational amplifiers producing U_3 receive zero potentials and U_3 remains zero. Although this is an unstable state or equilibrium, the circuit reverts to its operating state after a lapse of time. This random delay can be eliminated by introducing a low starting voltage U_S (Fig. 9), which removes the circuit from its unstable state almost instantaneously, and the source of the starting voltage ceases to have any further effect on the system owing to the valves V-1 and V-2. The voltage U_S can be used to define a residual positive sequence voltage at the node as required for studying non-symmetrical faults and remote short circuits.

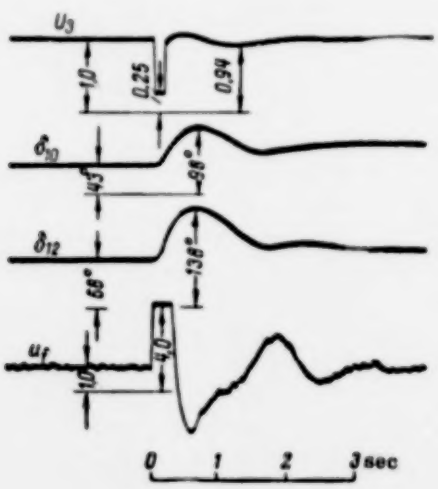

Fig. 10. Oscillogram of a two-phase earth fault at a node.

The proposed method is also applicable to out-of-step conditions. The amplifiers producing the angles δ_{10}, δ_{20} and δ_{30} are fitted with switching devices which shunt the feedback capacitances when the angle becomes 360°. When the slip becomes large (over 3 per cent) an error begins to creep in if C_3 is large and a "natural" time scale adopted. This error can be practically eliminated by using a "retarded time scale".

Appendix I.
Equivalent network of a generator

The equivalent network used in this paper differs from that proposed by Gorodskii [4] in that a variable "current source" is introduced to include excitation control. Other methods of including excitation control have been published. For instance, a similar method to Gorodskii's was described in [7], in which a correctional circuit was added to adjust for changes in excitation.

It will now be shown that the "current-source" method describes the behaviour of the generator correctly.

Ignoring the transformer e.m.f. and stator resistances, the generator performance can be described by the equations*

$$u_d = + x_q i_q;$$
$$u_q = x_{ad} i_f - x_d i_d;$$
$$u_f = p(x_f i_f - x_{ad} i_d) + r_f i_f.$$

Hence the current in the direct axis is

$$i_d(p) = \frac{u_q(p)}{x_d(p)} - \frac{G(p)\,u_f(p)}{x_d(p)}. \qquad \text{(I-1)}$$

The first term on the right of equation (I-1) describes the effects due to the external voltage $u_q(p)$, whilst the second fully defines the excitation and can be written in the form

$$i_f(p)\frac{G(p)\,r_f}{x_d(p)}, \qquad \text{(I-2)}$$

where $i_f(p)G(p)r_f$ is the equivalent voltage at the terminals of direct axis definable by the "forced" excitation current $i_{f.f}(p)$.

The equivalence of the generator performance and equivalent network will now be shown for the simplest case of no damping windings.

It is well known that for the generator

$$x_d(p) = \frac{x_d + x'_d T_{f0} p}{1 + T_{f0} p}; \qquad \text{(I-3)}$$

$$G(p) = \frac{x_{ad}}{r_f(1 + T_{f0} p)}, \qquad \text{(I-4)}$$

* The q-axis leads the d-axis.

where u_f is the slip-ring voltage; i_f is the rotor current; T_{f0} is the time constant of the excitation winding if all the other circuits are broken.

For the equivalent network in Fig. 5 the addition of x_{ad} with $x_{sf} + \frac{r_f}{p}$ in parallel and with x_s in series gives

$$x_d(p) = \frac{x_s + x_{ad} + x_s T_{f0} p + x_{sf} x_{ad} \frac{p}{r_f}}{1 + T_{f0} p} = \\ = \frac{x_d + x'_d T_{f0} p}{1 + T_{f0} p}. \tag{I-5}$$

The voltage at the terminals of the open network when carrying the "forced" current $i_{f.f}(p)$

$$u(p) = i_{f\,f}(p) \frac{\frac{r_f}{p} x_{ad}}{x_{sf} + x_{ad} + \frac{r_f}{p}} = \\ = \frac{x_{ad}}{1 + T_{f0} p} i_{f\,f}(p). \tag{I-6}$$

With the stator closed, the current component due to the excitation (i.e. due to the current $i_{f.f}(p)$) can be expressed as follows:

$$\frac{1}{x_d(p)} \frac{x_{ad}}{1 + T_{f0} p} i_{f\,f}(p) = \\ = \frac{x_{ad} i_{f\,f}(p) r_f}{x_d(p) r_f (1 + T_{f0} p)} = \frac{G(p)}{x_d(p)} u_f(p). \tag{I-7}$$

Thus the operator expressions for the generator currents fully agree with the equivalent networks.

Appendix II.

The current source

The load current I_l in Fig.4 is made independent of the load impedance R_l by a positive feedback which increases the output voltage of amplifier l with increasing U and, consequently, R_l.

It will now be shown that I_l is independent of R_l if the impedances are correctly chosen.

It is well known that the potential at the summation point Σ of an amplifier is negligibly small. Suppose, therefore, that $\Sigma = 0$. The sum of the currents at the point Σ then takes the form

$$\frac{U_{in}}{r_1} + \frac{U_{out}}{r_2} + \frac{U'_{out}}{r_3} = 0. \qquad \text{(II-1)}$$

Since

$$r_3 = r_4$$
$$U'_{out} = -U_l$$
$$U_{out} = U_l\left(1 + r_4\frac{r_5 + R_l}{r_5 R_l}\right),$$

it follows that expression (II-1) can be re-written in the form

$$\frac{U_{in}}{r_1} + \frac{U_l}{r_2}\left(1 + r_4\frac{r_5 + R_l}{r_5 R_l}\right) - \frac{U_l}{r_3} = 0, \qquad \text{(II-2)}$$

whence

$$I_l = \frac{U_l}{R_l} = -\frac{U_{in}}{r_1}\,\frac{r_2 r_3 r_5}{R_l(r_3 r_4 + r_3 r_5 - r_2 r_5) + r_3 r_4 r_5} \qquad \text{(II-3)}$$

Suppose that in expression (II-3)

$$r_3 r_4 + r_3 r_5 = r_2 r_5, \qquad \text{(II-4)}$$

The current I_l will then be independent of the load

$$I_l = -U_{in}\frac{r_2}{r_1 r_4}.$$

Thus, the "current source" functions correctly if condition (II-4) is fulfilled, whence it follows that

$$r_3 = \frac{r_2 r_5}{r_4 + r_5}. \qquad \text{(II-5)}$$

Translated by O.M. Blunn

1. S.V. Strakhov; *Elektrichestvo*, 7 (1957).
2. V.S. Tarasov, A.I. Vazhnov, Iu.V. Rakitskii, V.V. Popov and L.N. Semenova; *Elektrichestvo*, 4 (1960).
3. Ya.N. Luginskii and M.G. Portnoi; *The application of mathematical analogues to the study of electro-mechanical behaviour in electrical systems (Primeneniye matematicheskikh modelei dlia issledovaniya elektro-mekhanicheskikh perekhodnykh protsessov v elektricheskikh sistemakh). Trud. VNIIE*, IX (1959).
4. D.A. Gorodskii; *Elektrichestvo*, 15 (1934).
5. D.A. Gorodskii; *Elektrichestvo*, 18 (1934).
6. V.I. Pishchikov and N.I. Sokolov; *The effect of high-response excitation control on the stability of synchronous generators operating in parallel (Vlyanye sil'nogo regulirovaniya vozbuzhdeniya na ustoichivost' parallel'noi raboty sinkhronnykh generatorov). Trud. VNIIE*, IX (1959).
7. H. Buhler; *Bull. Oerlikon*, 330, Oct. (1958).

YEA
196

THE SELF-EXCITATION OF INDUCTION MOTORS WITH SERIES CAPACITORS*

V. G. BAUMAN, O. V. IVANOV and B. I. KOMAROV

(Leningrad Mining Institute)

(Received 14 November 1960)

YEAR
1961

The self-excitation of induction motors [1-7] is one of the main obstacles to the use of series capacitors for the compensation of the voltages drop in local distribution networks. Its effect is to limit the maximum stable output of the motors supplied from high-voltage transmission lines [8].

The self-excitation of an induction motor can be regarded as parametric resonance in an oscillatory system in which the equivalent inductance periodically varies with the mutual induction between the circuits of the system. Under definite conditions the "free" oscillations in such a system may decay, increase or even remain constant depending on the relationship between the energy introduced into the system when a parameter changes and the energy loss during this period of time.

The emergence of parametric resonance expresses itself mathematically in an unstable solution of the differential equation of the system. However, at the boundary of stability there exist free oscillations which do not decay and it is therefore possible to determine the boundary conditions of self-excitation by the methods of steady state analysis usually applied to induction motors.

The simplest way to determine the boundary conditions is to use Wagner's equivalent circuit [2].

---

* *Elektrichestvo*, 5, 38-44, 1961.

Fig. 1 shows an equivalent circuit for the "free" currents of an induction motor with series capacitors. All the reactances of the circuit are defined at 50 c/s. The frequency of the free oscillations at the boundary of stability ω_0 is proportional to the supply frequency. The rotor slip relative to the field of free currents at the boundary of stability is

$$s_0 = \frac{\omega_0 - \omega_r}{\omega_0}, \qquad (1)$$

where ω_r is the angular velocity of rotation of the rotor as a proportion of synchronous speed at 50 c/s.

The conditions for the existence of non-decaying free oscillations in the circuit in Fig. 1 can easily be found by Kirchhoff's laws

$$\dot{I}_1 + \dot{I}_2 + \dot{I}_3 = 0;$$

$$\dot{I}_1 Z_1 - \dot{I}_3 Z_3 = 0; \quad \dot{I}_2 Z_2 - \dot{I}_3 Z_3 = 0,$$

where

$$Z_1 = r_1 + j\left(\omega_0 x_{1s} - \frac{x_c}{\omega_0}\right);$$

$$Z_2 = \frac{r_2'}{s_0} + j\omega_0 x_{2s}';$$

$$Z_3 = j\omega_0 x_m.$$

Solving this set of equations with respect to the current $\dot{I}_2$:

$$\dot{I}_2\left(Z_2 + \frac{Z_1 Z_3}{Z_1 + Z_3}\right) = 0.$$

It follows from this expression that if $\dot{I}_2 \neq 0$, then the equivalent impedance of the circuit $Z_2 + \frac{Z_1 Z_3}{Z_1 + Z_3}$ must equal zero. (Points above symbols indicate complex quantities).

The conditions for the existence of non-decaying oscillations in the circuit in Fig. 1 can thus be written in the form

$$Z_2 + \frac{Z_1 Z_3}{Z_1 + Z_3} = 0$$

or

$$\frac{r_2'}{s_0}+j\omega_0 x_{2s}'+\frac{j\omega_0 x_M\left[r_1+j\left(\omega_0 x_{1s}-\frac{x_c}{\omega_0}\right)\right]}{r_1+j\left[\omega_0(x_M+x_{1s})-\frac{x_c}{\omega_0}\right]}=0. \tag{2}$$

The real and imaginary parts of equation (1) are then equated to zero separately and for the sake of simplicity

$$x_{1s}+x_M=x_1 \text{ и } x_{1s}+\frac{x_{2s}' x_M}{x_{2s}'+x_M}=x',$$

Hence

$$\left.\begin{aligned} r_1^2&=-\left(\omega_0 x_1-\frac{x_c}{\omega_0}\right)\left(\omega_0 x'-\frac{x_c}{\omega_0}\right)\\ \text{and}\quad \frac{s_0}{r_2'}&=-\frac{r_1^2+\left(\omega_0 x_1-\frac{x_c}{\omega_0}\right)^2}{\omega_0^2 x_M^2 r_1}. \end{aligned}\right\} \tag{3}$$

It follows from this equation that the slip s_0 can only be negative in the presence of self-excitation, i.e. the velocity ω_r of the rotor of an induction motor during self-excitation must be greater than the frequency of the free oscillations ω_0 (operating as a generator at the frequency of the free currents).

When considered with equation (2), the second equation in (3) can be written in the form:

$$\left(\frac{s_0}{r_2'}\right)^2=-\frac{\left(\omega_0 x_1-\frac{x_c}{\omega_0}\right)}{\omega_0^2 x_2'^2\left(\omega_0 x'-\frac{x_c}{\omega_0}\right)}, \tag{4}$$

where

$$x_2'=x_2+x_{2s}'.$$

and x_c is the capacitive reactance.

Using equations (1), (3) and (4) it is possible to find the frequencies ω_{01} and ω_{02} of those free oscillations at the boundary of stability which correspond to the values of the slip s_{01} and s_{02} and,

consequently, the velocity bounds of the zone of self-excitation ω_{r1} and ω_{r2} can also be determined.

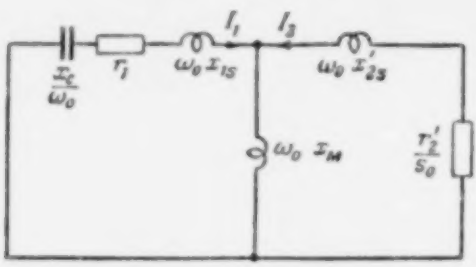

Fig. 1. Equivalent circuit.

It has been shown by calculations and tests that the boundary frequencies ω_{01} and ω_{02} in systems in which self-excitation has been specially eliminated are usually very little different from the respective frequencies ω'_{01} and ω'_{02} in systems without losses ($r_1 = 0$), which are equal to

$$\omega'_{01} = \sqrt{\frac{x_c}{x_1}} \text{ and } \omega'_{02} = \sqrt{\frac{x_c}{x'}}.$$

The self-excitation of induction motors occurs at rotor speeds

$$\omega_{r2} > \omega_r > \omega_{r1}.$$

Over this range one of the roots of the characteristic equation of the system will have a positive real part [1, 2, 4, 6] and, consequently, increasing free oscillations will occur in the system.

At speeds ω_{r1} and ω_{r2} the real part of this root is zero and constant free oscillations will continue in the system (boundary of the zone of self-excitation). At speeds $\omega_{r1} > \omega_r > \omega_{r2}$ the free oscillations will decay.

In voltage control systems using series capacitors the theoretical limits ω_{r1} and ω_{r2} are usually below synchronous speed at 50 c/s. If the resistance r_1 is increased there is a corresponding narrowing of the velocity bounds of the self-excitation zone, as follows from equations (3) and (4), but at the critical value of $r_1 (r_1 = r_{1cr})$ these bounds merge and if $r_1 > r_{1cr}$ self-excitation is impossible. An expression can easily be obtained for r_{1cr} from equation (3) by determin-

ing the maximum of the function defined by this equation [2,6]:

$$r_{1cr}=\sqrt{x_c}(\sqrt{x_1}-\sqrt{x'}). \quad (5)$$

It will be seen from an analysis of this expression that r_{1cr} decreases in value with a decreasing percentage modulation of the equivalent inductance of the motor:

$$m=\frac{x_1-x'}{x_1+x'}$$

In deriving the propositions underlying the theory of self-excitation in induction motors it is assumed that all the criteria of the system are linear or else dependent solely on the magnitude of the free currents [5].

YEAR 1961

It is also assumed that the speed of the rotor is constant. Such assumptions are only permissible in the study of asynchronous generators. Previous papers [1,3,4,5,7,8], have not dealt with asynchronous generators operating as motors for this reason. It has been shown by tests that the special features of the motor state have a decisive effect on the nature of the development of self-excitation in asynchronous machines under these conditions.

The authors have undertaken research which now makes it possible to form a qualitative estimate of the effect of individual factors on the nature of the development of self-excitation in induction motors.

There are a number of distinctive features of the development of self-excitation in asynchronous generators operating as motors:

1. The criteria of the machine depend on the magnitude of the voltages and currents of the "forced" process, in which the supply source defines the frequency, as well as on the currents and voltages in the free process;

2. The self-excitation of the motor at speeds below normal is only possible during acceleration of the rotor within the resonant zone. The possibility of the rotor crawling in the zone of self-excitation is determined by the time taken to pass through this zone and the time taken for free oscillations to develop; i.e. it depends on the moment of static and dynamic (mechanical) resistance, the magnitude of the supply voltage and the numerical values of the circuit criteria.

3. The performance of an excited motor can only be stable at the

lower velocity limit of the self-excitation zone [2].

The magnitude of the input voltage has the most important effect on the development self-excitation in a motor. It has been established by tests on AOL and A type motors with series capacitors at supply voltages from 60 to 500 V that the self-excitation of a motor can be divided into five distinct stages in which the excitation develops in different forms.

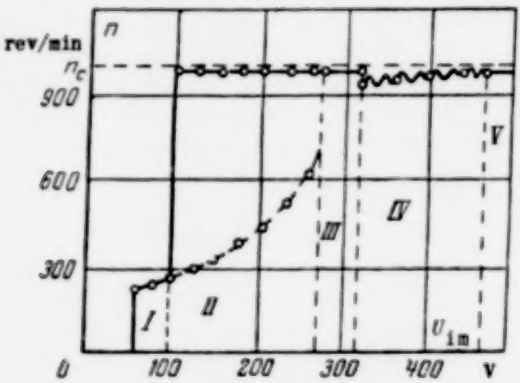

Fig. 2. Speed n as a function of the input voltage U_{in} for A-41-6 type motors (capacitive reactance x_c = 6.6 ohms; line resistance r_l = 0; GD^2_M (flywheel effect) = 0.

The curve for $n = f(U_{in})$ in Fig. 2 is divided into five sections by the vertical broken lines. The continuous line represents the speeds attainable by the motor on starting from a standstill. The broken line in region II shows the running speeds of a motor which is repeatedly switched on and off but not allowed to stop rotating. The broken line at the end of this region shows the speeds which are attained by a continuous increase in the supply voltage of the excited motor.

The motor does not gain speed in the first region. It crawls at a lower speed corresponding to the reduced resonant frequency of the system. In this region the self-excitation of the motor develops as follows (Fig. 3a). On starting, the rotor accelerates according to its mechanical characteristic (Fig. 3a) to the lower boundary of the self-excitation zone under the influence of an excess torque equal to the difference between the driving torque and the moment of static resistance.

As soon as the speed of the rotor passes beyond the lower limit of

the self-excitation zone, self-excitation of the motor sets in and the machine begins to function as a generator at the frequency of the free currents. When the rotor is in the zone of self-excitation, the braking torque created by the field of free currents succeeds in increasing so much that the resulting torque of the machine becomes less than the moment of static resistance. The speed of the rotor therefore drops and the motor leaves the zone of self-excitation. The rotor now starts to accelerate all over again and crosses the lower boundary, but this time there is a much less excess torque so that the rotor now decelerates much more quickly under the influence of the free currents and it stabilises at point A (Fig.3a) where its speed corresponds to the lower boundary of the self-excitation zone. In this case the amplitude of the free oscillations is restricted by the change in speed of the rotor,

YEAR
1961

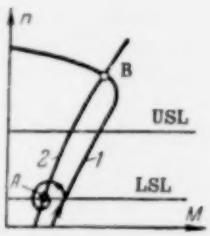

a

b

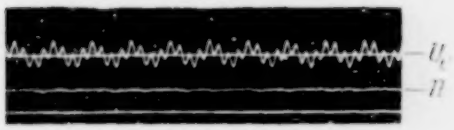

c

Fig. 3. The starting of induction motors in region I(a), oscillograms (b,c). *1* – torque speed characteristic of a non-excited induction motor; *2* – characteristic of the load torque; *B* – point of normal operation; *LSL* and *USL* – lower and upper speed limits of the self-excitation zones; U_C – capacitor voltage.

which is the typical feature of the development of self-excitation in generators operating as motors*.

The currents and voltages during the self-excitation of a motor are distorted in zone I by the appearance of considerable low frequency components. Fig. 3(b) and (c) shows oscillograms which illustrate the variation in the speed of the motor when self-excited and the shape of the typical curve of steady state oscillations in region I.

It should be pointed out that use is made of a curve representing the voltage drop of capacitors U_c for which the typical distortions present in self-excitation are more pronounced.

In region II (Fig. 2) the motor, on starting from a complete standstill, accelerates to its rated speed and, crossing the resonant zone, is self-excited, only locking at lower speeds if switched on and off without being allowed to stop rotating.

At the end of region II self-excitation can only be maintained by a continuous increase in the supply voltage to the already excited motor.

It will be seen from the curve in Fig. 2 that a self-excited motor will lock at a higher speed depending on the extent to which the supply voltage is increased. This is explained by the saturation of the machine steel owing to the appearance of low frequency components in the voltage at the terminals of the motor and the associated reduction in the no-load inductive reactance of the machine x_1 [2]. The starting diagrams and oscillograms appropriate to this region are shown in Fig. 4.

The reason why the self-excitation zone is crossed when starting after a complete standstill is that the rotor in region II manages to pass through the zone before free oscillations can develop which are capable of creating a generator moment sufficient to decelerate the rotor (Fig. 4) [2, 6].

If the input voltage is increased still further, self-excitation cannot be maintained even by continuously increasing the voltage applied to the already excited motor, i.e. there is no self-excitation in region III (Fig. 2). This is explained by the narrowing of the self-excitation zone owing to the considerable reduction in the no-load inductive reactance x_1 and the decreased percentage modulation of the parameter (equivalent inductance).

---

* In the self-excitation of generators the amplitude of the free oscillations is usually limited by the saturation of the steel.

In region IV the motor again begins to be self-excited with a continuous increase in the input voltage whether the motor is started from standstill or repeatedly switched on and off). The explanation is that the types of machine under consideration have a lower equivalent inductive reactance x' approximately equal to the short circuit inductive reactance which fixes the position of the upper speed boundary of the zone. Furthermore, it is not a constant quantity but diminishes as the input voltage is increased. If the short circuit inductance is reduced the upper speed boundary of the zone is moved upwards and at the beginning of the fourth region it is raised above the normal operating point of the motor (Fig. 5). The normal operating point then comes within the self-excitation zone and the motor is perpetually self-excited in this region.

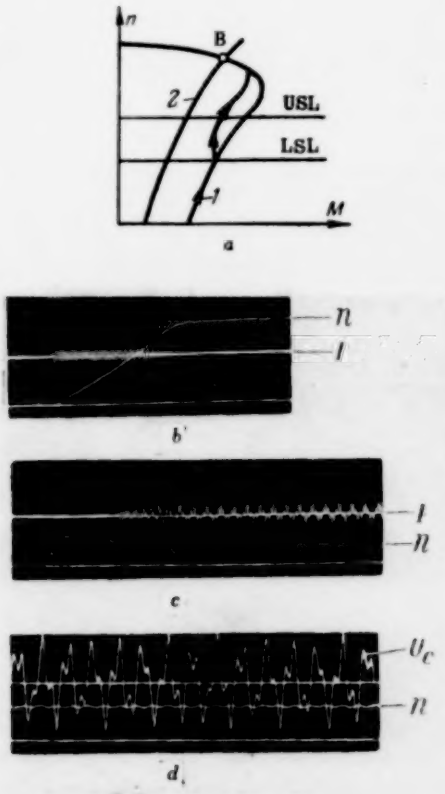

Fig. 4. The starting of induction motors in region II.
(Symbols as in Fig. 3)

Accordingly, there are grounds to suppose that motors with open shallow rotor slots (for which the short-circuit inductance is practically independent of the magnitude of the input voltage) will not have a region IV. Tests have been made which corroborate this idea [2].

Numerous tests have also shown that region IV generally covers a range of voltages quite close to the voltage of the motor (see Fig. 2).

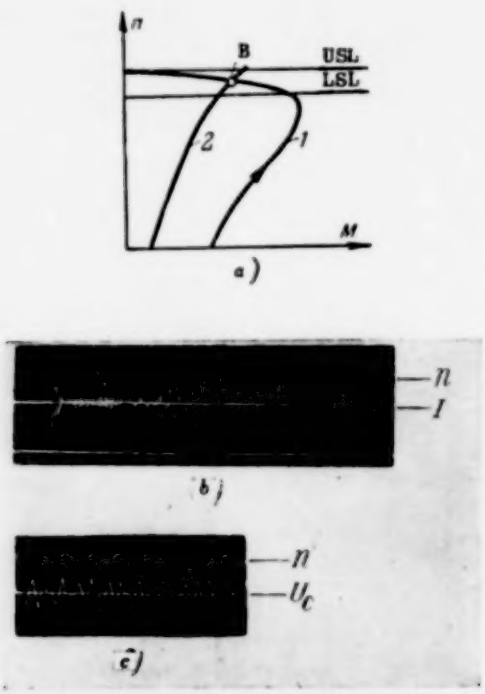

Fig. 5. The starting of an induction motors in region IV.
(Symbols as in Fig. 3)

It has been found that in this region self-excitation proceeds at speeds close to the normal speed of the rotor at comparatively low values of capacitive reactance (roughly up to 50 per cent of the short circuit inductive reactance of the machine). But the rotor speed of a self-excited machine tends to fall in this region to the extent that the capacitive reactance is increased.

The self-excitation of a motor in region IV is always accompanied by

stable oscillations in the torque and speed of the rotor.

It will be seen from the oscillograms in Fig. 5 that the voltage (current) curves are distorted in this region on account of the speed variations of the rotor and the saturation of the steel. Thus, the nature of the self-excitation of an induction motor near rated voltages is substantially different from that considered in the published literature.

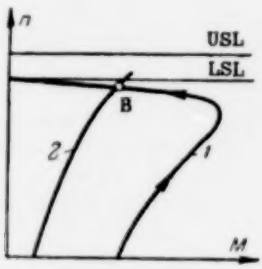

a)

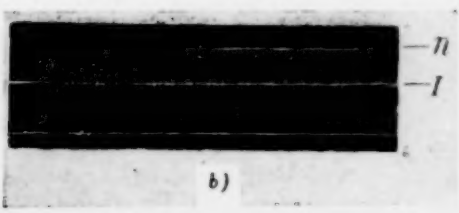

b)

Fig. 6. The starting of induction motors in region V.
(Symbols as in Fig. 3)

In the solution of practical problems connected with the use of series capacitors to compensate voltage drops in distribution networks, attention must be concentrated on the behaviour of induction motors at voltages close to rated voltage, i.e. in region IV.

If the input voltage is increased still further, the self-excitation of the motor again ceases (region V in Fig. 2). The explanation is that the lower boundary of the excitation zone rises above the normal operating point at such high voltages. Typical starting curves and oscillograms of region V are shown in Fig. 6.

Region V begins to narrow and vanish as capacitive reactance is

increased and subsequently the same happens to region II.

If a resistance (the line resistance r_1) is connected in series with the capacitors region III and V widen and then I and IV narrow and disappear altogether.

This is explained by the narrowing of the self-excitation zone when a resistance is included. This agrees well with the theory of parametric excitation. It should however be pointed out that greatly improved results are obtainable by calculating the value of the resistance which will eliminate self-excitation.

However, it should be mentioned that the inclusion of a resistance which is calculated to ensure the desired degree of compensation of the voltage drop τ [7], can only eliminate the self-excitation of a motor at voltages near nominal if the capacitive reactance x_c is no more than about 30 per cent above the short-circuit inductive reactance of the machine $x_{s/c}$.

The flywheel effect of the rotating parts also has an appreciable effect on the nature of self-excitation, particularly in region IV.

Region I is much wider when motors with a fly-wheel are started and region II is pushed up to higher voltages since the flywheel considerably increases the time taken to pass through the self-excitation zone.

A particularly valuable result of increasing the flywheel effect of the rotating parts of a machine is the widening of regions III and V through the narrowing and final disappearance of region IV. The combined effect of a flywheel and resistance is to eliminate self-excitation over a very wide range of input voltages including rated voltage.

By using a flywheel, self-excitation has been eliminated in tests at voltages near nominal for $\tau = 1$ and $x_c = x_{s/c}$, i.e. with complete compensation of the short circuit inductive reactance of the machine. Without a flywheel such a large resistance is required to eliminate self-excitation at voltages near nominal that even with $x_c \approx 0.35\ x_{s/c}$ (see, for example, Fig. 7a) the use of series capacitors was still ineffective when only partial compensation of voltage drop was accepted.

Other methods of calculation have implied that the resistance must be made even larger to eliminate self-excitation.

Fig. 7a shows curves $\tau_j = f(r_1)$ for two values of x_c in reference to

an A-41-6 type motor where

$T_j = \frac{2.74 GD_e^2 n_{nom}^2 \cdot 10^{-6}}{P_{nom}}$ – equivalent inertia content of a motor with a flywheel, sec;

GD_e^2 – the flywheel torque of a rotor with a flywheel, $kg.m^2$;

n_{nom} – rated speed of motor, rev/min;

P_{nom} – rated motor output, kW.

These curves define the requisite line resistance r_l for a given inertia constant and vice versa.

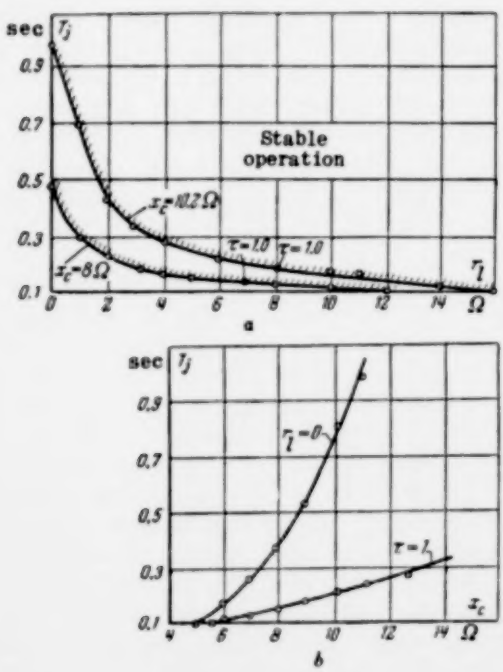

Fig. 7. The inertia constant T_j as function of line resistance r_l (a) and capacitive reactance x_c (b) for A-41-6 type induction motors. Inertia constant of motor T_{jn} = 0.1 sec.

It should be seen from Fig. 7(a) that the elimination of self-excitation is influenced especially and to a considerable extent by a

small additional increase in the inertia constant (relative to the natural inertia constant of the motor). Thus, if $x_c = 0.57\ x_{s/c}$, the elimination of self-excitation is particularly influenced by an increase in the inertia constant within the limits of 0.1 to 0.3 sec. In the case in question it is enough to increase it to 0.2 sec in order to eliminate self-excitation (with complete compensation of the voltage drop).

There are therefore grounds to suppose that in using series capacitors under real conditions there will be no self-excitation of loaded motors at voltages near nominal, even if the capacitive reactance x_c is comparatively large and that the voltage drop will be fully compensated.

Fig. 7(b) shows the inertia constant T_j as a function of x_c for two values of r_l, namely, zero and that corresponding to complete compensation of voltage losses ($\tau = 1$). The regions lying above each curve correspond to normal operation of the motor (no self-excitation). It follows from Fig. 7(b) that an increase in the inertia constant of the machine has a particularly marked effect on the elimination of self-excitation in the presence of line resistance.

YEAR
196

The curves in Fig. 7 were obtained for a constant input voltage equal to the rated voltage of the motor $U_{nom} = 380$ V.

Research into the performance of induction motors supplied via capacitive line equipment [8] has also shown that flywheel mass improves the stability of motors.

Conclusions

1. The special features of the self excitation which occurs when a generator is used as a motor have a considerable influence on the nature of the development of self-excitation in asynchronous machines.

The input voltage has the most important effect. Five regions can be discerned in which the development of self-excitation takes a different form depending on the magnitude of the input voltage.

2. The self-excitation of induction motors of the type under consideration is substantially different from what it is generally considered to be in the published literature at rated voltage (region IV in Fig. 2).

Stable oscillation in speed and torque is typical of motors operating

in this region. The resonant speed in this region is very little different from the normal speed of the motor. If the capacitive reactance x_c is increased there is an accompanying reduction of the resonant speed in this region. The current and voltage curves are greatly distorted by oscillation in speed and saturation of the steel.

3. A line resistance r_l assists the elimination of self-excitation by narrowing the fourth region of self-excitation.

But if $x_c > 0.3\ x_{s/c}$, the requisite value of r_1 to eliminate self-excitation is still inadequate to compensate fully the voltage drop in the line.

4. An additional flywheel effect also helps to narrow the fourth region, i.e. to eliminate self-excitation at rated voltage.

Unloaded induction motors are more inclined to self-excitation at the rated input voltage than loaded motors.

The influence of the additional flywheel effect is particularly significant if a line resistance is included.

Translated by O. Blunn

YEAR
1961

REFERENCES

1. J.W. Butler and C. Concordia; *El. Eng.* No.8 (1937).
2. C.F. Wagner; *Trans. Amer. Inst. elect. engrs.* Vol. 60 (1941).
3. P. Satche; *Bull. Soc. franc. Electr.*, 7 (1951).
4. N. Knudsen; *ASEA J.*, 5-6 (1954).
5. A.I. Dolginov; *Resonance in electrical circuits and systems, (Rezonans v elektricheskikh tsepiakh i sistemakh).* Gosenergoizdat, (1957).
6. V. Laion; *Analysis of transient phenomena in electrical s.c. machines, Analiz perekhodnykh protsessov v elektricheskikh mashinakh peremennogo toka).* Gosenergoizdat (1958).
7. V.G. Bauman, O.V. Ivanov and B.I. Komarov; *Nauch. dokl. vyssh. shol.*, (ser. Gornoe delo), No.4, (1958).
8. D.N. Bulashevich and V.D. Yurenkov; *Capacitive off-take of power from transmission lines, (Emkostnyi otbor moshchnosti ot linii elektroperedachi).* Gosenergoizdat (1959).

DIRECT TESTING OF CIRCUIT BREAKERS BY THE JOINT USE OF SURGE GENERATORS AND GOREV OSCILLATORY CIRCUITS*

Ya. N. SHERMAN

(All-Union Electrical Engineering Institute, Leningrad)

(Received 18 November 1961)

YEA
196

In recent years Gorev oscillatory circuits have come to be used on a large scale in the U.S.S.R. as the short circuit power source for rupturing capacity tests on high-duty circuit breakers. In these oscillatory circuits the necessary energy for the tests is stored in a large bank of static capacitors.

Experience has shown that high-voltage test laboratories require two or three synchronous surge generators with an equivalent three phase short circuit power of 2.5 to 3.5 thousand MVA and a Gorev oscillatory circuit with an equivalent three phase short circuit power of 2 to 2.5 thousand MVA. This equipment is used for synthetic tests in which the surge generators are the current source and the oscillatory circuit the recovery voltage source.

It is also possible to make direct tests in which the power of the surge generator and that of the oscillatory circuit are used separately. It would however be very useful to combine their individual powers in direct tests.

The only combined systems [1] which have as yet been proposed for direct tests use the active power of the surge generator circuit. No provision has been made for adding the reactive power of the two sources.

---

* *Elektrichestvo*, 5, 52-57, 1961.

However, research at the Leningrad branch of the All-Union Electrical Engineering Institute since 1956 has solved this problem by connecting the surge generator either in series [2] or in parallel [3] with the oscillatory circuit. It will be shown that the decay of the test current can be compensated either by the active power of the generator or by a method of "pulsation".

The special switchgear which has been developed in the U.S.S.R. in recent years has now made it possible to combine a surge generator with a Gorev oscillatory circuit for direct tests. The new switchgear includes a controlled spherical discharger (U.Sh.R), an automatic test control device (PAU) and a synchronous switch VA-12.

Connexion in series

Fig. 1 illustrates the main test circuit with the generator connected in series with the oscillatory circuit.

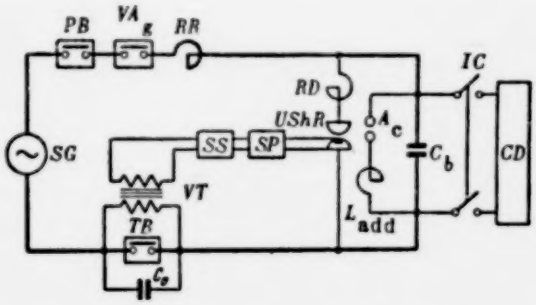

Fig. 1. Main test circuit for combined use of surge generator and Gorev oscillatory circuit connected in series:

SG – synchronous surge generator; C_b – main capacitor bank of oscillatory circuit; *RR* – reactor; *TB* – test breaker; *PB* – protective breaker; *VA* – synchronous switch (*g* – generator); *IC* – interrupter for charge circuit; *CD* – charging device of oscillatory circuit; A_c protective gap (arrester); L_{add} – additional protective inductance; *RD* – reactor which is connected to capacitor bank; *SS* – electronic synchronization system; *USHR* – new controlled spherical discharger; *SP* – ?; *VT* – voltage transformer

The circuit in Fig. 1 is similar to the circuit published previously in this journal [4], but it includes an extra reactor *RD* which is connected to the capacitor bank by means of the controlled spherical discharger (U.Sh.R) and the electronic synchronization system *SS* (immediately after the arc has been quenched in the circuit breaker on test. The inductance of the reactor *RD* is such that a current of supply frequency (50 c/s) flows in the circuit C_b – *RD* on closure of the spherical discharger (C_b - bank capacitance). Consequently, after the arc has been quenched in the test breaker *TB*, the capacitor voltage is cosinusoidal in shape and, in view of this, the recovery voltage at the terminals of the test breaker, equal to the sum of the generator e.m.f. and the voltage at the capacitor bank C_b, will also have the conventional cosinusoidal shape.

Best use is made of the equipment by connecting the capacitor bank, surge generator and test breaker in the test circuit through power transformers.

To achieve maximum test power the system must operate normally and this requires initially that the amplitude of the free oscillations should vanish completely (provided compensation is not used for damping the test current). It will be seen from expressions A1 and A2 in the appendix that this condition is satisfied if the initial capacitor voltage (U^*_{C0}) equals the amplitude of the voltage drop on the capacitance from the forced component of the current and if the phase of the connexion ψ^*_e equals the phase angle between the forced current component and the generator e.m.f., i.e. if (including the change in sign)

$$U^*_{C0} = -U_{C\,max} \tag{1}$$

and

$$\psi^*_e = -\beta. \tag{2}$$

But if the attenuation of the test current is to be compensated, the initial conditions have to be slightly different from 1 and 2. They are selected in such a way that the decay of the test current is reduced owing to the presence of a transient component of frequency reduction.

The series method of connexion also allows an increase in test current when the self-reactance of the bus-bars or the dynamic stability of the generator are the limiting factors. The self-reactance of bus-bars can be compensated by the capacitor bank C_b.

Overvoltages can occur at the capacitor bank if conditions 1 and 2

are not satisfied at the beginning of the test. Protection is provided by arranging a gap (an "arrester") $A_{s/c}$ in parallel with the bank which shorts the bank, or else, (to reduce the discharge current), closes it through an additional inductance L_{add}, which produces a high frequency current in the discharge circuit. It has been shown by calculations and tests that the fault current is no larger than the maximum short-circuit current of the surge generator.

Trial rupturing capacity tests have been carried out on VMG-133 type circuit breakers at breaking currents of 10 and 20 kA and a voltage of 10 kV in order to assess the merits of the system and to check the design formulae.

YEAR 1961

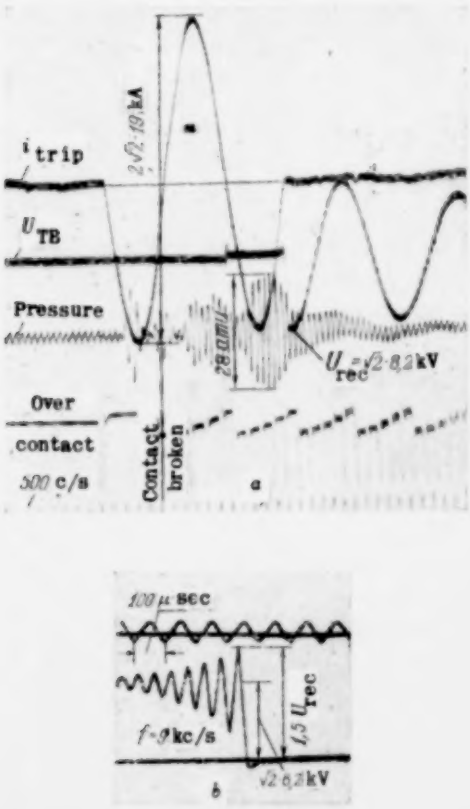

Fig. 2. Magnetic (a) and cathode-ray (b) oscillograms of direct test on a VMG-133 type circuit breaker with the surge generator and oscillatory circuit connected in series. i_{trip} – tripping current; U_{TB} – voltage at the terminals of the test breaker.

A TI-12 type generator was excited to 6 kV for the tests. The capacitor bank was connected to the test system via an intermediate transformer. The voltage across the secondary winding of the transformer was 4 kV (20 kV on the capacitor side). The bank incorporated 32 capacitors (type KM-30-19) for test currents of 20 kA and 16 capacitors of the same type for 10 kA.

Fig. 2 shows oscillograms taken during tests at 20 kA.

The tests showed that the proposed method is only slightly more complicated than the conventional system and that good agreement exists between test and calculated data.

Not only does the series system allow the summation of power, the compensation of stray inductance and the damping of the short-circuit current, but it also makes the best possible use of the available test equipment, thereby providing additional power for testing.

Connexion in parallel

Fig. 3 illustrates the parallel method of connexion. The test plant includes a surge generator, a Gorev oscillatory circuit and the breaker test. The test method is as follows. First the surge generator is excited to the required voltage $e_g = E_{max} \cos(\omega t + \psi_e)$. At the same time the capacitor bank is charged to the voltage $U_{C0} = E_{max}$. Then, with the test breaker connected and the phase of the generator voltage ψ_e equal to $-\tan^{-1}\frac{R_{e.g.}}{\omega L_g}$ (so that there will be no aperiodic component in the generator current), the generator circuit is closed by the new synchronous switch VA_g for the generator. At the same or a slightly later time an oscillatory circuit switch X_{oc} makes the oscillatory circuit and the extreme branches of the scheme begin to carry the generator current i_g and the oscillatory circuit current i_{oc}, and the branch of the test breaker TB carries the total current i. To achieve complete equivalence in the tests it is necessary for the oscillatory circuit current to attain its zero value slightly after the generator current in the half-period when the arc is quenched in the test breaker*. The total current i then attains zero slightly after the generator current (at the moment

* This can be achieved by slightly reducing the frequency of the oscillatory circuit current compared with that of the generator current or by switching on the oscillatory circuit current slightly after the generator current. Both methods can also be used at the same time.

when the instantaneous values of i_g and i_{oc} are compared).

After the arc has been quenched in the test breaker, the series-connected (sic) generator and oscillatory circuit from a single closed circuit which carries a small balancing current i_b. This current i_b attains zero a few hundred microsec after the arc has been quenched in the test breaker and at this point is interrupted by the "tripping device" TD_{oc} of the oscillatory circuit which is arranged to operate at the precise moment when this will ensure the quenching of the arc in the corresponding half-period of current. In the tests this "tripping device" was either a special breaker or the second pole of the test breaker.

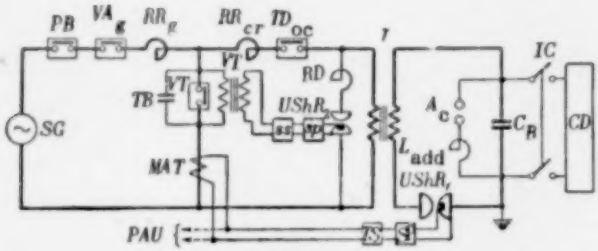

Fig. 3. Main circuit for combined use of surge generator and Gorev oscillatory circuit connected in parallel.

Legend as in Fig. 1 plus *MAT* – master air-cored transformer; *TS* – trigger scheme; *TD* – tripping device (oc = oscillatory circuit); *T* – transformer; *PAU* – new automatic test control device.

When the arc has been quenched in the test breaker, the voltage begins to recover at its terminals at a rate determined by the equivalent inductance of the whole scheme and the capacitance of the bank C_b. Before the arc is quenched in the oscillatory circuit tripping device TD_{oc}, the recovery voltage has an intermediate value between the generator e.m.f. and the voltage on the main capacitor bank; after the arc has been quenched in TD_{oc}, it becomes equal to the generator e.m.f. Since the system has been tuned so that e_g and u_c are close to each other in value, it can be assumed that the recovery voltage is equal to the generator e.m.f. Here the test power of the plant equals:

$$P_{s/c} = I_{trip}U_{rec} = (I_g + I_{oc})U_{rec} = P_g + P_{oc}.$$

Thus, the power of the oscillatory circuit and generator are also

added if the parallel system is used.

The current is controlled by means of the reactors RR_g and RR_{oc}. Since both branches operate independently in a given system when the test breaker is connected, the maximum total current depends on the power of the sources at the given voltages.

The "tripping device" TD_{oc} can either be the second pole of the test breaker or a special breaker. It should be mentioned that another function of the oscillatory circuit tripping device is to serve as a protective breaker to interrupt the oscillatory circuit current in the event of "disruption" of the test breaker (or failure in quenching), its main function of course being to disconnect the balancing current i_b.

The system just described can be regarded as the basic circuit. Direct tests may also be carried out under other conditions with the generator current reaching zero *before* the oscillatory circuit current in the half-period when the arc is quenched in the test breaker. In this case a generator tripping device should be included TD_g for which the laboratory protective breaker PB may be used.

YEA
196

After the arc has been quenched in the test breaker and then in the generator tripping device TD_g, the recovery voltage at the terminals of the test breaker is equal to the voltage of the main capacitor bank. To impart the same sinusoidal shape to it as in the series system, the capacitance C_b is connected to the shunt reactor RD by the controlled spherical discharger U.Sh.R. directly after the interruption by the generator tripping device TD_g.

However, a detailed theoretical and experimental study of the conditions of the first passage of the balancing current i_b through zero has shown that this modification is not so stable in operation as the fundamental system. Extra equipment (the shunt reactor, the new controlled spherical discharger etc) is also required. The basic system is therefore to be preferred.

The following factors should be considered when adjusting (tuning) the circuit. The instant the arc is quenched in the test breaker, the current in the branch where the "tripping device" is installed must only pass through zero after the total current has done so. Otherwise the branch containing the tripping device can be disconnected before the total current i attains zero and a kink will therefore occur in the curve for the total current immediately before it passes through zero. Moreover, since one of the branches will be disconnected before

the total current i passes through zero, the rate of voltage recovery will depend solely upon the inductance of a single branch and not on the equivalent inductance of the whole scheme.

The capacitors are protected from the surges which may arise if the tripping device fails to quench the arc, by a protective gap (arrester) A_c which connects the bank C_b to the reactance L_{add}.

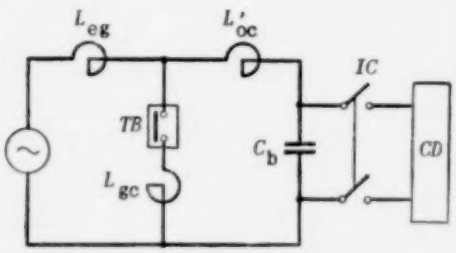

Fig. 4. Main circuit of generator and oscillatory circuit in parallel with an inductance to compensate current attenuation.

L_{gc} – coupling inductance; *TB* – test breaker; C_b – capacitor bank; *CD* – charging device; *IC* – interrupter for charge circuit; L_{eg} – inductance of generator; L'_{oc} – inductance of oscillatory circuit part.

For tests on 6-10 kV breakers, the capacitors of the oscillatory circuit may be connected via step-down transformers T (Fig.3). For tests on breakers over 10 kV the generator, or generator and oscillatory circuit, are connected to the test breaker via transformers. The oscillatory circuit is then connected by the controlled spherical discharger which is operated by a special control system consisting of a master air-cored transformer *MAT* and a trigger scheme *TS* which operates the controlled spherical discharger almost immediately after the current begins to flow through the test breaker (after 100 to 500 μ sec). It is not possible to use the same conventional spherical discharger for the parallel system as for the series system [4] since the voltage of the capacitor bank U_{CO} is applied to this discharger both before and after the new synchronous switch VA_g has operated.

Compensation of the test current

When testing circuit breakers with long arcing times, the efficiency

of the proposed method is adversely affected by the decay of the test current. In the proposed parallel system this is aggravated by the increased attenuation of the current in the oscillatory circuit. The decay of the test current can be reduced by pulsation (the "beat" method) or by compensating power losses.

The "pulsation" method is based on the addition of two sinusoidal oscillations at close frequencies. Since the test current i is the sum of two sinusoidal currents (i_g and i_{oc}), it follows that the frequency of the current in the oscillatory circuit can be so selected and the connexion of the oscillatory circuit to the test circuit so timed that a non-decaying or even increasing test current can be produced in part of the test breaker circuit [5,6]. The best possible use is obtained from the equipment if the current in the oscillatory circuit is greater than 50 c/s. This involves no alteration in the test plant because the command from the controlled spherical discharger can be delayed as required by the new automatic test control device *PAU* or by installing an electronic time relay between the trigger scheme *TS* and the *SP* device.

In the other method of compensation a small coupling inductance $L_{g.c.}$ (Fig. 4) is connected in the test breaker circuit which compensates the losses in the oscillatory circuit by the active power of the generator in the same way as in tuned circuits described by Lugovoi [1]. The best result is obtained by adjusting the system so that both methods of compensation can be used.

The system has been proved in the high-voltage test laboratory at the All-Union Electrical Institute in Leningrad.

The second pole of the VMG-133 circuit breaker on test was used as the tripping device TD_{oc} to study the basic circuit, and the laboratory protective breaker to study the modified circuit. Figs. 5 and 6 show magnetic and cathode oscillograms which illustrate the performance of the system for basic and modified connexions.

The tests confirmed the theoretical conclusions and showed that there is practically no difference between the tuning of the parallel system and the tuning of conventional systems with a generator.

Appendix 1.
Formulae for series system of connexion

In the analysis the real generator is replaced by an equivalent generator with an e.m.f. e_g, which decays with a time constant

$\frac{1}{\alpha}$, and a super-contact reactance (literally, a super-transfer resistance) x''_d. The generator e.m.f. is re-written in the form:

$$e_g = E_{max} \cos(\omega t + \psi_e) e^{-\alpha t},$$

where α is a coefficient which is found experimentally from the attenuation of the symmetrical component of the short circuit current in a conventional inductive circuit.

YEAR 1961

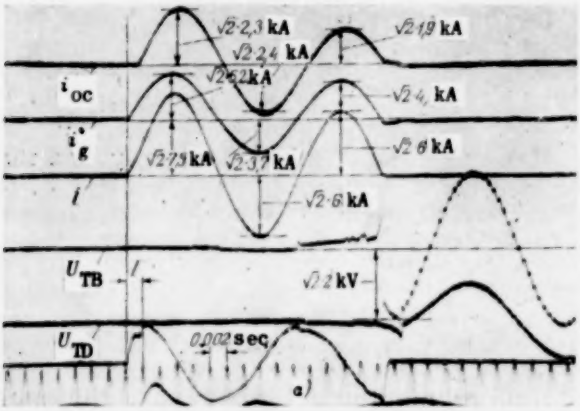

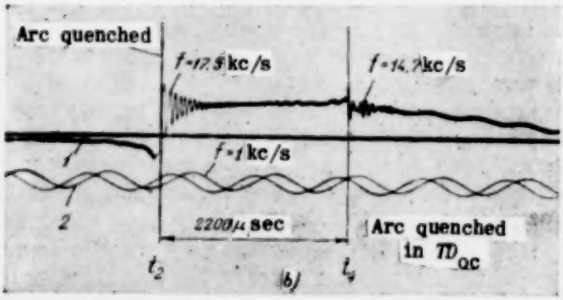

Fig. 5. Magnetic (a) and cathode-ray (b) oscillograms of direct tests on a *VMG*-133 type circuit breaker in the basic parallel system.
i_{oc} – oscillatory circuit current; i_g – generator current; i – test current; U_{TB} – voltage at terminals of test breaker; U_{TD} – voltage at terminals of test breaker *TB*; 2 – graduated frequency.

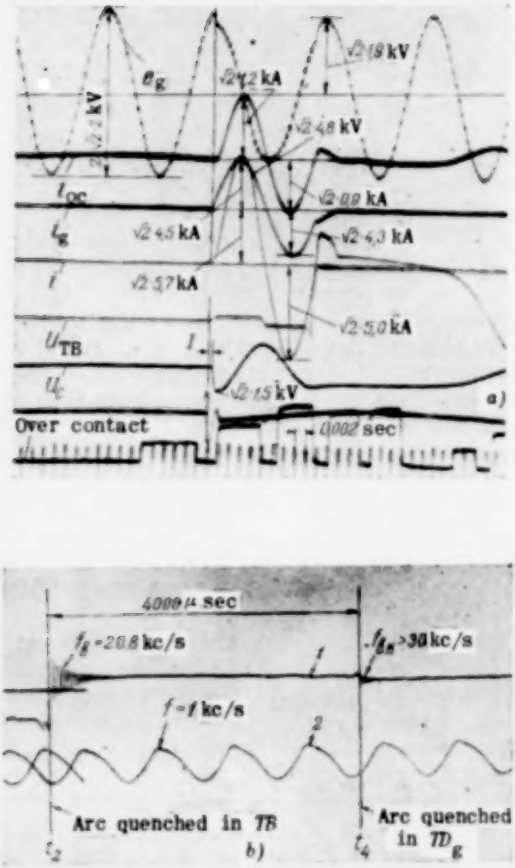

Fig. 6. Oscillograms of tests on a VMG-133 circuit breaker in the modified system (Notation as in Fig. 5)

On the stated assumption, the total current i in the test circuit, the voltage drop in U_C at the capacitor bank, and the recovery voltage U_{rec} can be found from the following expressions:

$$i = I_{max} \sin(\omega t + \psi_e + \beta) e^{-\alpha t} + \\ + I_{max} \sqrt{\frac{k}{k+1}} N \cos(\omega_e t + \theta) e^{-\delta t}, \qquad \text{(A1)}$$

$$u_C = U_{C\ max} \cos(\omega t + \psi_e + \beta) e^{-\alpha t} - \\ - U_{C\ max}\ N \sin(\omega_0 t + \theta) e^{-\delta t}; \tag{A2}$$

$$u_{rec} = [E_{max}\ e^{-\alpha' k} \cos(\omega t + \beta) + \\ + U_{C0} e^{-\alpha' k} e^{-\delta' k t_v} \cos \omega t] (1 - e^{-\delta_{hf} t_v} \cos \omega_v t), \tag{A3}$$

where

$$k = \frac{P_{oc}}{P_g};\ I_{max} = \frac{E_{max}}{\omega L_{e.g}};\ U_{C\ max} = \frac{I_{max}}{C_{oc}} = \\ = kE_{max};\ L_{e.g} = \frac{x_g + x_{sh}}{\omega};$$

$$N = \sqrt{\frac{k+1}{k} \sin^2(\psi_e + \beta) + \left[\frac{U_{C0}}{U_{C\ max}} + \cos(\psi_e + \beta)\right]^2};$$

$$\beta = \arctan \frac{2(\delta - \alpha)(1+k)}{\omega};$$

$$\theta = \arctan \frac{\dfrac{U_{C0}}{U_{C\ max}} + \cos(\psi_e + \beta)}{\sqrt{\dfrac{k+1}{k}} \sin(\psi_e + \beta)};$$

$$\omega_0 = \frac{1}{\sqrt{(L_{oc} + L_{eg}) C_{oc}}} = \sqrt{\frac{k}{k+1}}\,\omega;$$

$$L_{oc} = \frac{1}{\omega^2 C_{oc}};$$

$$\delta = \frac{R_l}{2(L_{e.g} + L_{oc})};$$

$$\omega_v = \frac{1}{\sqrt{(L_{oc} + L_{e.g}) C_0}};$$

δ_{hf} – the decrement in attenuation of the high frequency component;

τ_k – the length of time that the test current flows;

δ'_k – the decrement in attentuation of the current in the capacitor bank – reactor circuit (C_b – RD);

t_v – time from the moment the arc is quenched;

L_{eg} – inductance of the surge generator part;

L_{oc} – inductance of the oscillatory circuit part;

Formula for the parallel system. The generator current i_g and

oscillatory circuit current i_{oc} can be found from the formulae

$$i_g = \frac{E_{max}}{\omega L_{eg}} \sin(\omega t + \psi_e + \varphi)\, e^{-\alpha t}; \tag{A4}$$

$$i_{oc} = \frac{U_{C0}}{\omega L_{oc}} \sin \omega t\, e^{-\frac{1}{2}kt}. \tag{A5}$$

The recovery voltage, without including power losses, can be found from the expression:

$$u_{rec} = \left[U_{C0} + (E_{max} - U_{C0}) \frac{L_{oc}}{L_{eg} + L_{oc}}\right](1 - \cos \omega_v t). \tag{A6}$$

The balancing current i_b and capacitor voltage U_C can be found by transforming expressions A1 and A2 to suit the parallel system:

$$u_C = -\frac{E_{max}}{n} \cos(\omega t + \xi)\, e^{-\alpha t} + \tag{A7}$$
$$+ E_{max} \left(1 + \frac{\cos \xi}{n}\right) \cos \omega_e t\, e^{-\frac{1}{2}kt};$$

$$i_b = I_{max.g} \sin(\omega t + \xi)\, e^{-\alpha t} - \tag{A8}$$
$$- \frac{1}{\sqrt{1+n}} \left(1 + \frac{\cos \xi}{n}\right) \sin \omega_e t\, e^{-\frac{1}{2}kt},$$

where $I_{max.g} = \dfrac{E_{max}}{\omega L_{eg}}$;

$n = \dfrac{P_{oc}}{P_g}$

$\xi = \sin^{-1} \dfrac{i_{b.0}}{I_{max.g}}$ – the phase angle between i_g and i;

i_{b0} – the initial value of the balancing current which is equal to the instantaneous value of i_g at the moment the arc is quenched in the test breaker.

Translated by O. Blunn

REFERENCES

1. V.S. Lugovoi; *Tuned circuits with loss compensation, (Rezonansnye kontury s kompensatsiei poter')*. Izvest. Akad. Nauk Kirgiz. SSR,

No. 1, (1955).
2. V.V. Kaplan and Ia.N. Sherman; *Method of testing high-voltage circuit breakers, (Sposob ispytaniia vysokovol'tnykh vykliuchatelei).* Soviet Patent No. 122546, 10 June 1959).
3. Ia.N. Sherman; *Method of testing the rupturing capacity of high duty switchgear, (Sposob ispytaniia apparatov vysokogo napriazheniia na otkliuchaiushchuiu sposobnost').* Soviet Patent No. 133523, 14 December(1959).
4. Ia.N. Sherman; *Elektrichestvo,* 7, (1959).
5. V.V. Kaplan and V.M. Nashatyr'; *Elektrichestvo,* No.7, (1957).
6. Ya.N. Sherman; *Device for testing the rupturing capacity of high duty switchgear, (Ustroistvo dlia ispytaniia kommutatsionnykh apparatov vysokogo napriazheniia na otkliuchaiushchuiu sposobnost').* Soviet Patent No. 673091/24, 14 July 1960.

YEAR
1961

THE NEW NINE-VALVE SIX-PHASE RECTIFIER UNITS*

L.S. FLEISHMAN

(Uralelektroapparat)

(Received 31 January 1961)

Some time ago the electrical works "Uralektroapparat" in the U.S.S.R. made a large 3300 V 12-valve rectifier unit for Soviet railways which was quite original in that two valves were connected in series in each phase. Its rated output was 10,000 kW and this compared very favourably with foreign 24-valve units with rated outputs of up to 8000 kW. Furthermore, it was as efficient as any other existing unit, it saved material (5.3 kg per kW instead of 7 to 13 kg per kW) by the greater output of the individual valves, and only one TMR U-6200 type transformer was required instead of three of four TMRU - 1600 type transformers [2].

One of these units has been in service for two and a half years at a traction sub-station on the Omsk railways and no arcbacks have occurred. The average daily output was 8350 kW and the peak output 16,000kW. The average output over five-hour periods of continuous operation was 12,000 kW. More than a hundred such units are now in use on the railways and arcbacks have been almost completely absent.

However, experience has shown that these units have excess capacity as regards valve strength and current. This could be used to increase rated outputs up to 15,000 and 20,000 kW, but there is no demand for such large units. It is therefore proposed to take advantage of the increase in power and improved reliability and produce low cost rectifier units which can also be used in other branches of industry [1]. The results of tests on the new nine-valve unit [3] are given below.

---

* *Elektrichestvo*, 5, 58-62, 1961.

The main circuit of the nine-valve unit is shown in Fig. 1(a). It will be seen from a comparison of this circuit with that of the original twelve-valve unit in Fig. 1(b) that each valve of the cathode group in the twelve-valve unit is supplied from two valves in the anode group. The performance of the valves is illustrated in Fig. 2, from which it will be seen that the valves of the cathode group conduct current twice in each period so that the mean value of the current in these valves is twice that in the valves of the anode group. The reverse voltage is also applied to each valve in the anode group twice in each period for a time defined by the angle $(60-\gamma)^{o}$.

The reliability of the two systems will now be considered.

If a cathode spot occurs on the anode of a valve in the cathode group, an arcback current can only flow if the cathode spot arises simultaneously (more exactly, within the limits of the time of the existence of the cathode spot) on one of the anodes of two valves in the anode group connected to it. Consequently, the probability of arcbacks in the twelve-valve or nine-valve unit is definable as the product of the probabilities of cathode spots occurring on series-connected valves [4].

YEAR 1961

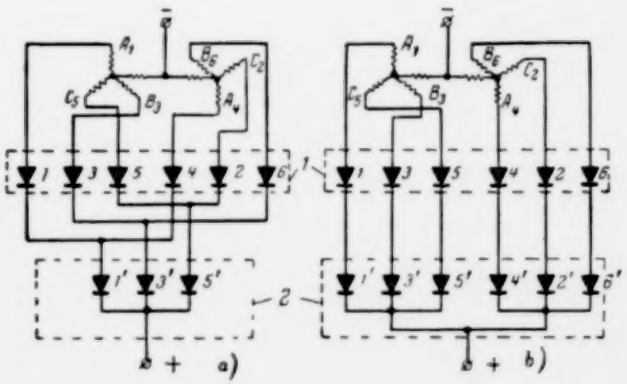

Fig. 1. The nine-valve (a) and twelve-valve (b) rectifier systems. *1* - anode group of valves; *2* - cathode group of valves.

However, other things being equal, arcbacks are only half as likely in the nine-valve unit because an arcback will occur in the twelve-valve unit if a cathode spot should occur say on the anode of valve *1'* and simultaneously on valve *1*, whereas in the nine-valve unit the

cathode spot must occur on the anodes of valves *1* and *4**.

If the cathode spot first arises on the anode of a valve in the anode group, say the anode of valve *1*, then the other valves except *4*, which is in counter-phase with it, can only take part in the arcback if a cathode spot also arises on the anode of the valve *1'*. Consequently, even in this case, the probability of an arcback is definable by the product of the probabilities of cathode spots on the anodes of series-connected valves. But valve *4* is a different matter which must be considered in more detail.

Suppose a cathode spot occurs on the anode of valve *1* at the instant t_1. Valve *4* cannot feed the anode of valve *1* before the moment t_2 since its anode still has a negative potential (Fig. 2a). After the instant t_2 valve *4* cannot feed valve *1* if a control pulse is fed to the grid of anode *4* at the instant t_3 at a slightly advanced angle relative to the natural angle of ignition. This condition has to be satisfied by an appropriate phasing of the pulses relative to the anode voltage with the angle advanced between 3 and 5°, as read from the instant t_3. Partial arcbacks will only occur if the cathode spot on the anode of valve *1* occurs after the anode of the counter-phase valve has fired, or if the cathode spot precedes the firing of the counter-phase valve.

In rectifiers with controlled grids, by far the largest majority of arcbacks occur on the "front" of the reverse voltage [5]. Some experts consider that arcbacks other than on the front of the reverse voltage are only possible if the vacuum is bad [6]. The commutation angle is about 45° for actual commutating inductances and overloads of 4500 A so that the angle is behind about 15° up to the moment the counter-phase valve is ignited. However, there is very little time for cathode spots to exist if there is no supply of energy. Consequently, there is practically no difference in reliability between the twelve-and nine-valve units if the cathode spot occurs on the front of the reverse voltage**. Only in relatively rare cases when cathode spots occur with the "amplitudinal" value of the reverse voltage across the valves in the anode groups will partial arcbacks take place.

---

* It is assumed that the probability of arcbacks on the three valves of the cathode group in the nine-valve unit is equal to that on the six valves of the cathode group in the twelve-valve unit, for the valve current is the same in value in both units.

** In principle the probability of an arcback in twelve-valve units is 1.5 to 2 times less, but this difference has no practical importance in series-connected systems.

The full and partial arcback currents will now be compared.

Utevskii has shown that the arcback currents of three-phase rectification systems can be determined by the following differential equation which holds good if the anode on which the cathode spot arises is only supplied by one valve:

$$\sqrt{3}U_{max}+2L_a\frac{di}{dt}+2r_a i=0,$$

where U_{max} is the maximum value of the phase voltage, L_a the inductance of the phase, and r_a the resistance of the phase.

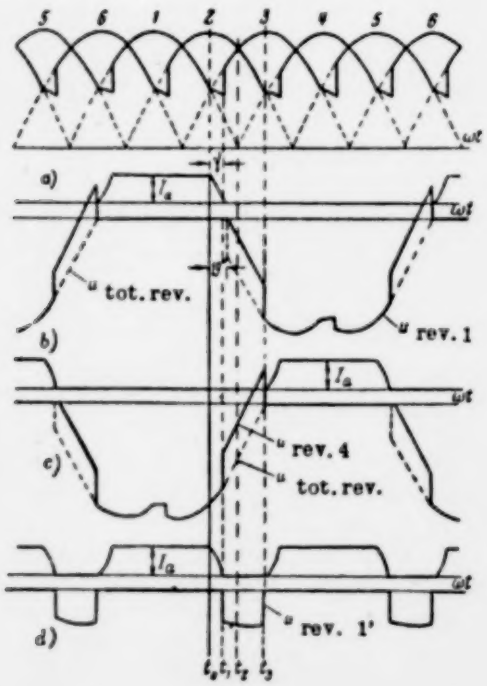

Fig. 2. Curves of the rectified voltage (a) and the anode currents and reverse voltages of valve 1(b), valve 4(c) and valve 1' in the cathode group (d).

With a partial arcback, the arcback current is found from the equation

$$2U_{max}+4L_a\frac{di}{dt}+2r_a i=0.$$

The impedance of balancing reactors and the arc voltage of the valves can be ignored. The four fold value of the circuit inductance is explained by the fact that the partial arcback current flows through transformer windings which are disposed on the common core of a magnetic circuit and, consequently, their total reactance is proportional to the square of the number of turns*.

Full arcback currents may be calculated by Utroskii's equations [7].

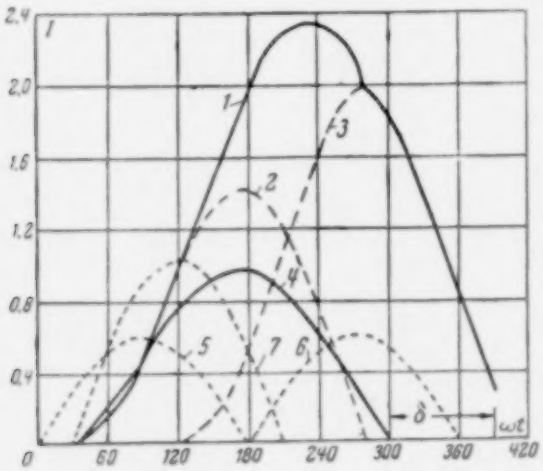

Fig. 3. Full and partial arcback currents.

1 – full arc-back current; *2* and *3* – components of the full arc-back current; *4* – partial arc-back current; *5* and *6* – anode phase voltages determining the partial arc-back current; *7* – line voltage determining the first component of the full arc-back current.

The relative values of full and partial arcback currents are shown in Fig. 3. It will be seen that the current of a partial arcback is about 40 per cent that of a full arcback and, consequently, the e.m.f.'s acting on the transformer windings are reduced to about 16 per cent.

It should also be mentioned that with partial arcbacks the current and e.m.f.'s are also substantially reduced by the zero sequence impedance which appears due to the current flowing through the transformer

* Secondary windings of transformers are made so that their leakage fluxes can be ignored.

windings on a single core when the primary windings are star-connected.

The curves in Fig. 3 also show that the current of a partial arcback is maintained for about 270° under the most unfavourable conditions for which arcbacks can occur. The intermittent nature of the current must be due to the automatic-elimination of partial arcbacks during a time less than one "period" which prevents breaks in the supply of energy.

It is worthwhile studying the distribution of the total reverse voltage between the series-connected valves in the nine-valve system. Fig. 2 shows the reverse voltages as calculated by formulae obtained from the equivalent network in Fig. 4 for the condition when all the valve impedances are equal. In the calculation it has to be borne in mind that the valve cannot sustain the forward voltage for a period of time equal to that taken for the control capacity of the grids to recover. Therefore, as will be seen from Fig. 2, the reverse voltage on valves in the anode group at commutation angles less than 19° appears gradually and even with a slight delay. The curves have been corroborated by oscillograms taken on a scale model using T-235 type thyratrons. In water-cooled mercury arc rectifier systems the cathode valves are shunted by the resistance of the water and, as a result, the reverse voltage diminishes and slightly alters the shape of the reverse voltage on the anode and cathode valves.

YEAR 1961

It is already known that each cathode valve conducts current twice in each period and therefore two triggering pulses are also required in each period. Fig. 5(a) shows how this can be done by a grid circuit with a peaking generator. Two impules are supplied in each period by connecting the counter-phase windings of the peaking generator in parallel via semiconductor rectifiers which suppress the negative impulse. The grids of the valves in the anode group are supplied in the conventional way. Fig. 5(b) shows a simplified system using a grid transformer (the control impulses are sinusoidal).

The circuit impedances must be made such that the arcing of the grid extends about 120° for each half-wave of voltage.

In addition to tests on scale models, tests have also been carried out in the works laboratory and by the Omsk and October railways jointly with the MPS Central Research Institute on the automatic elimination of artificial partial arcbacks. Ordinary service tests have also been made.

The artificial partial arcbacks were produced by firing a valve which was connected "counter-parallel" to one of the anode valves. The tests

showed that no partial arcback current flowed when firing the counter-parallel valve in the period of time t_2-t_0. On applying a triggering impulse to the grid of the counter-parallel valve, a partial arcback current only began to flow after the instant t_2. Its maximum value reached about 8350A. The partial arcback current roughly corresponded to an angle of 270°. Under the same conditions, full arcback currents were about 22,000 A. In these tests the rectifier was supplied from two TMRU-6200 type transformers with delta primary windings.

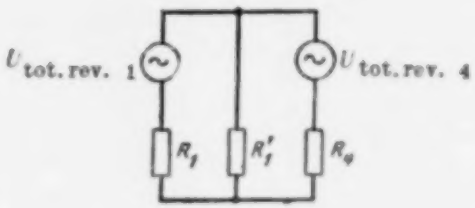

Fig. 4. Equivalent circuit for the distribution of the reverse voltages.

In a second series of tests the partial arcback currents reached 4200 A with the rectifier again supplied from the same transformers with delta windings. The large difference in the partial arcback currents can be explained by the fact that the TMRU-6200 transformer in the second test was supplied through a TDNG-15,000/110 step-down transformer, the reactance of which further reduced the current.

As soon as the partial arcback current began to flow, the total reverse voltage was applied to one of the valves in the cathode group when it was conducting. When such units are used on electric railways the valve receives a reverse voltage of 7500 V at currents of 2000 A or more. If the conditions are so severe that the valve cannot sustain them even for one period, the partial arcbacks will change into full arcbacks and the multiplication rule for the probabilities will no longer be valid. The capacity of cathode valves to sustain such conditions was tested by artificial partial arcbacks in a "contact network" (with overhead wires?) at loads up to 3000 A. Fig. 6 shows one of the oscillograms of artificial partial arcbacks caused at the instant when the reverse voltage was initially a maximum.

Several dozen artifical partial arcbacks were produced in all, and in every case they were automaticaly eliminated, i.e. they took place without causing any of the protective gear to operate and without disconnecting the unit.

The service tests on the reliability of the unit were carried out in April 1960. The test unit was composed of two ARMNV-750 x 6-P rectifiers assembled according to the nine-valve system. The unit was tested for 140 hrs. Its mean output was 5,700 kW, and its peak hourly output 10,000 kW. The largest current reached 3600 A.

During the tests 15 partial arcbacks were registered and all were automatically eliminated. There were no full arcbacks.

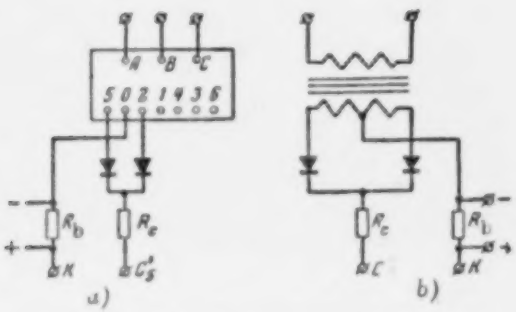

Fig. 5. System of supplying control pulses to valves in the cathode group.

The same unit was subjected to another series of tests in July 1960 in order to check whether the probability of partial arcbacks could be reduced further and to accumulate more experience of service conditions. On this occasion the angle of advance of the grids in the anode group of valves was reduced by about 15° to roughly 5°. The mean output of the unit rose slightly to 5860 kW. A lengthy period of service (over 900 hrs) showed that its overload capacity was high. The peak rectified current reached 4500 A and the hourly output 12,000 kW. The temperature was held at 30 to 45° C during service. Five full arcbacks occurred at intervals of a few hours during the service tests. In every case it was found that the flow of water had ceased through some of the valves owing to air locks but there were no full arcbacks after changing over to different heat exchangers. There were also five partial arcbacks and three were automatically eliminated. In the other two cases the partial arcbacks were accompanied by the tripping of the oil circuit-breaker; the high-speed cathode breaker, polarized to the reverse current, remained connected. These two cases can apparently be explained by the re-occurrence of partial arcbacks in two adjacent periods on the same or other anodes of valves in the anode group.

It is important to point out that no full or partial arcbacks

occurred during maximum loads, which is further evidence of the high overload capacity of the unit. The service tests showed that a reduction in the angle of advance from about 20 to 5° reduced the frequency of arcbacks by more than an order of one.

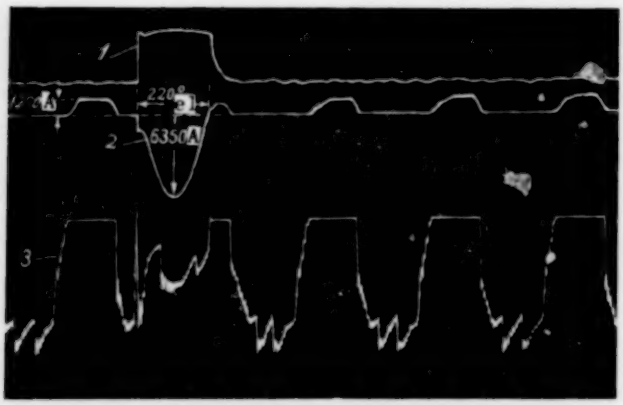

Fig. 6. Oscillogram of an artificial partial arc-back:

1 - impulse triggering the counter-parallel valve; *2* - the partial arc-back current; *3* - the total reverse voltage.

Conclusions

1. The nine-valve rectifying system permits the development of rectifier units on the basis of the existing RMNV-type valves with a rated output of 10,000 kW and a voltage of 3300 V which are capable of operating at hourly outputs of 12,000 kW with peak outputs of 15,000 kW. The majority of traction sub-stations may therefore be equipped with one large unit which considerably reduces costs.

2. Compared with the twelve-valve units, the new system saves about 25 per cent on the weight of the rectification plant and control cabinet without affecting the rated output or overload capacity of the unit. The efficiency of the nine-valve unit when operating with TMRU-type transformers is hardly inferior to that of the twelve-valve unit and at loads of 0.75 or less its efficiency is higher than that of units without valves connected in series.

3. The rated mean output of each valve in the nine-valve unit is

1100 kW compared with 825 kW for the twelve-valve system and 333-412 kW for foreign units.

The new unit is also more reliable than foreign units.

4. There is no real disadvantage involved in designing the valves in cathode group for currents double those in the anode group, at least as far as voltages of the order of 3000 V are concerned, since valves are only required for mean currents of approximately 1000 A. It will be appreciated that there is no great difficulty involved in producing such valves if it is borne in mind that the effective anode current in the nine-valve system is less than that in the original system by a factor of $\sqrt{2}$ and that its amplitude is only half as much.

The stated test results show that the valves produced by "Uralelektroapparat" satisfy these requirements. Valves of 1000 A are also produced abroad. Furthermore, the series connexion of these valves means that means that they need only satisfy requirements as regards thermal stability. Their strength need not be nearly so high, for they only have to sustain the total reverse voltage and take overvoltages into account.

YEAR 1961

5. It is expedient to use nine-valve units in those applications of mercury arc rectifiers where (1) it is more economical to use plant with the two reverse star system (ΔY) and a balancing reactor than gear with the three phase bridge system; (2) where the production of double-current cathode valves presents no difficult technical problems; (3) where it is otherwise impossible to obtain the required power in one compact unit without series connexion.

Translated by O.M. Blunn

REFERENCES

1. *The report of the interim commission on rectifier engineering (Reshenie Vremennoi Komissii GNTK Soveta Ministrov SSSR po preobrazovotel'noi tekhnike).* Elektroprom. i priborostr., 2, (1960).
2. L.S. Fleishman; *Elektrichestvo,* No.9, (1959).
3. L.S. Fleishman; *Ionic rectifier, (Ionnyi preobrazovotel').* Soviet Patent No.124022, dated 12 July (1957).
4. J. Slepian and W.E. Pakala; *El. Eng.* No.6, (1941).
5. Th. Wasserrab; *BB Mitt.,* 4/5, (1955).
6. M. Danders; *AEG Mitt.,* 11/12 (1958).

7. A.M. Utevskii; *Electromagnetic processes under fault conditions in rectifier units, (Elektromagnitnye protsessy pri avariinykh rezhimakh vypriamitel'nykh agregatov)*. Akad. Nauk SSSR, No. 2 (1949).

YEA
196

ABSTRACTS FROM PAPERS PUBLISHED IN ELEKTRICHESTVO No. 5, 1961

YEAR
1961

Control engineering

The motor drive of a rolling mill reeling machine with an astatic regulator for strip tension. F.F. Olefir, *et al.*, (pp. 23-30).

A description is given of the motor, reeler and regulator which have been developed for a five-stand mill for the continuous rolling of cold-rolled strip. The new system features constant strip tension whent he mill is at rest, tension is maintained at low speeds, motor current is constant from starting to stopping of the reeler and the speed of the roller is adjusted to the diameter of the roll.

The motor drive of the flying shears in continuous billet mills. M. Ya. Pistrak *et al.*, (pp. 31-38).

The gearing and special cutting devices used in the flying shears on Russian billet mills are described. It is claimed that this system is superior to Western electrically speed-balanced shears when billets are standardized to one or two lengths. A study is also made of the system of synchronization.

Insulation

The maximum electrical field strength of the paper-oil insulation of gear used in d.c. transmission. G.S. Kuchinskii, *et al.*, (pp. 64-68).

A study is made of the electrical insulation of current transformers and isolators on 400 kV d.c. transmission lines with particular reference to the sharp edges of electrodes and ionization.

The e.m.f. induced by the radiation of dielectrics. N.G. Drozdov, *et al.*, (pp. 68-69).

An account is given of the measurements which have been taken to establish the magnitude of the e.m.f. which can be caused by low-energy X-ray radiation of dielectrics. It is claimed to be of the order of 0.1 V. The mechanism whereby much larger e.m.f. have been measured is explained in terms of the effect of a high voltage in which the specimen is regarded as part of the dielectric surrounding the X-ray tube.

The electrical strength of mica in impulse tests in vacuum. V.A. Dubinskii, (pp. 71-73).

Various tests which have been carried out to determine the electric strength of mica splittings in vacuum are described. In one test the splittings were boiled in carbon tetrachloride, in another the surface of the splitting was roughened by applying a processed coating of anhydrous MgO and in another test the splittings were subjected to intense ultra-violet radiation. The effect of annealing in hydrogen is also considered.

YEA
196

Power systems

The optimum spacing of supports for overhead aluminium-sheathed cables. V.V. Bolotin *et al.*, (pp. 9-12).

Tests and a mathematical analysis show that the best results are obtained by spacing the brackets of overhead aluminium-sheathed cables 4 to 7 m apart.

The conductivity of reinforced concrete piles for the pylons of 154-500 kV transmission lines. N.P. Katigrob, (pp. 13-15).

An account is given of research into the footing resistance of reinforced concrete piles for the pylons of 154-500 kV transmission lines. In clayey and clayey-sandy soil the resistance has been found to be somewhat less than 10 ohms.

Rectifiers

The steady state electromagnetic phenomena in a full-wave rectifier with a centre-tapped transformer. A.M. Utevskii *et al.*, (pp. 16-23).

A graphical-analytical study is made of the relationship between the operating conditions, operating characteristics and rating of

rectifiers and the type of load and supply scheme.

A semiconductor power relay. V.I. Grinshtein, (p. 70).

A prototype power relay is described consisting of a phase comparison circuit and an executive device in the form of a two-stage transistor amplifier with a polarized relay at the output. Its performance is claimed to be superior to inductance relays. The relay is light in weight and compact in design.

Rotating machines

A method of determining optimum frequency for small induction motors. I.P. Fil', (pp. 44-47).

A mathematical method of determining the optimum frequency is proposed and close agreement is obtained with test results. The implications for small enclosed motors and motors for manually-operated mining drills are considered.

YEAR
1961

The geometric loci of induction motor currents when the frequency is variable. G.M. Kirichek, (pp. 48-52).

A graphical-analytical method is proposed for plotting the geometric loci of induction motor currents for the general case when the voltage is proportional to the frequency.

The conditions under which three-phase windings of electrical machines will set up a circular rotating magnetic field. E'.G. Fainshtein, (pp. 62-63).

The author shows that there exists a number of combinations of three-phase winding systems and currents which will form a rotating field. Expressions are also obtained for an elliptical field.

CRITERIA OF ELECTRIC ORE-SMELTING FURNACES*

A.S. MIKULINSKII

(Institute of Metallurgy, Urals' Branch of the
U.S.S.R. Academy of Science)

(Received 20 March 1961)

One of the main problems in the development of electrical ore smelting furnaces is that of increasing the output of the individual unit. This would make it possible to reduce the capacital outlay and running costs so much that it would be economical to produce even pig iron in certain parts of the U.S.S.R. The solution of this problem depends to a large extent on the development of methods of determining the optimum parameters of furnaces.

It has been established in previous papers [1, 2, 3] that the geometric and electrical magnitudes of electric furnaces should be fixed so as to ensure a particular energy distribution in the furnace. It is an urgent problem to determine those criteria of the furnace which would ensure the same energy distribution in actual furnaces as in "specimen" furnaces with the best possible operating indices. This requires geometric and electrical similarity between actual furnaces and the "specimen" furnace.

Furnace dimensions

In two previous papers [1,2] it was proposed to use the diameter of the electrode as the determinative quantity for furnaces with circular electrodes. Geometric similarity is attained by observing the following

---

* *Elektrichestvo*, 6, 33-38, 1961.

criteria:

$$\frac{f}{d}=f' \text{ (1a)}; \quad \frac{b}{d}=b' \text{ (1b)}; \quad \frac{l}{d}=l' \text{ (1c)},$$

where f is the distance from the centre of the electrode to the internal wall of the furnace, b the distance between the electrode centres, l the distance from the lower face of the electrode to the zone of comparatively low specific electrical resistance (see diagram), and d the diameter of the electrode.

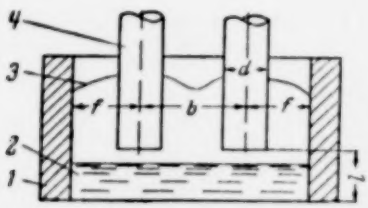

Fig. 1. 1 - brickwork of furnace; 2 - melt; 3 - level of charge; 4 - electrode.

It has been established (4) by an analysis of the electrical field in a 2-electrode furnace that an increase in b' is accompanied by an increase in the current between the electrode I_3. At values of $b' <$ 2.25 to 2.75 the value of I_3 remains practically constant. It therefore follows that it is inadvisable to increase b' above 2.25 to 2.75 in order to reduce the current I_3.

The same conclusion was reached by Sergeev [5] and Platonov after measuring the electrical resistance on a model where the slag was imitated by water solutions and the molten metal by a metallic plate.

For furnaces with square electrodes

$$l=k_0'\sqrt{a_0^2 n_0}=k_0' a_0 n^{1/2}. \qquad (2)$$

where $a_0^2 n_0$ is the section of the electrode and $\frac{b_0}{a_0}=n_0$ is the ratio between the largest and smallest sides of the electrode.

Analysis of electrical fields [1,2]

The secondary voltages in the furnaces can be determined by analysing

the electrical fields. The electrical conductance of the carbon lining of the furnace and live electrodes is taken to be many times greater than that of the charge. Thus the surfaces of its carbon parts are isopotential.

It is known that the coefficients of the charge conductance are a function of pressure and temperature. In order to include them in the analysis it is assumed that they are constant in the horizontal section, whilst with changes in height they vary according to the equation

$$\lambda = \lambda_0 e^{-2hz},$$

where λ and λ_0 are the conductance coefficients of the charge over a height z and if $z = 0$ and h is a coefficient which includes the change in conductance with height.

As a result of solving the Laplace differential equation, the current has been found as a function of the diameter of the electrode d and the extent of the sub-electrode space l.

We require to find a formula for determining the furnace voltage. Suppose that the voltage U_0 of the furnace at a current of 100 A with a uniform specific electrical resistance of the charge is equal to unity. With a specific electrical resistance of the charge in the lower part of the furnace $\rho' = 1$, a radius $r = 1$ and a current $I = 100$ A, we get:

$$100 = k'U_0, \tag{3}$$

where k' is a coefficient which includes the geometric shape of the electrical field (shape factor).

The ratio of the specific resistances in the upper and lower parts of the electrode are:

$$\frac{\rho_1}{\rho_0} = e^{2Hh} = k,$$

where H is the depth to which the electrode is immersed.

The current I is found from the expression

$$I = k'm\frac{U}{R} = k'm\frac{Ud}{\rho_0}, \tag{4}$$

where U is the voltage between the electrodes and the hearth, m a

coefficient which includes the effective specific resistance of all the charge, and R the total resistance.

From expression 4 [2]:

$$U = kI\frac{U_0\rho_1}{kmd} = k'I\frac{U_0\rho_0}{kmd}, \tag{5}$$

or, putting

$$\frac{\rho_0}{km} = \rho$$

and bearing in mind that U = const, it is found that

$$U = k\frac{I\rho}{d}.$$

YEAR 1961

Equation 5 was found earlier [1, 2] as well as in the paper by Morkramer [6].

Since,

$$I = \frac{P}{\sqrt{3}U} \text{ and } d^2 = \frac{4I}{\pi j} \quad \text{or} \quad d = k''\left(\frac{I}{j}\right)^{1/2}, \tag{6}$$

and putting A for all the constants, the following expression was obtained [1,2]:

$$U = AU_x\left(\frac{\rho_0}{mk}\right)^{2/3}\rho^{1/3}j^{1/3}. \tag{7}$$

To calculate the value of x it is useful to consider a linear conductor of length l_0 with a specific resistance ρ [7]. It is assumed that the electrical field is solely defined by one coordinate z over the height of the furnace.

First case: $\rho = \rho_0$ (uniform conductor). The differential equation for the potential will be:

$$\frac{d^2U}{dz^2} = 0.$$

The boundary conditions are $U = 0$ if $z = 0$, and $U = 1$ if $z = 1$.

The solution of the equation is

$$U = \frac{z}{l}.$$

The current density is

$$j = \frac{1}{\rho_0} \cdot \frac{dU}{dz} = \frac{1}{\rho_0 l}.$$

Second case: $\rho = \rho_0 e^{2hz}$ (non-uniform conductor). The differential equation for the potential is

$$\frac{d^2U}{dz^2} - 2h \frac{dU}{dz} = 0.$$

The boundary conditions will be the same as before. The solution of the equation has the form:

$$U_1 = \frac{e^{2hz} - 1}{e^{2hl} - 1}.$$

The current density is

$$j_1 = \frac{dU}{\rho_0 dz} = \frac{2h}{\rho_0 e^{2h} - 1}.$$

Comparing the values of the current density in the two cases,

$$j_1 = \frac{2hl}{e^{2hl} - 1} j,$$

or, putting

$$\frac{2hl}{e^{2hl}} = m; \quad j_1 = mj; \quad e^{2hl} = k,$$

we get:

$$m_1 = \frac{\ln k}{k - 1}. \tag{8}$$

The criterion E.S. of electrical similarity [2,3]

To ensure a given distribution of energy it is necessary to have a definite value l'. To calculate the optimum value of l' it is necessary to include its functional relationship with some dimension. The diameter of the electrode will be used as such a quantity.

The value of E.S. for furnaces with circular electrodes. The expression for the current density in differential form is

$$j = \frac{1}{\rho} \operatorname{grad} U_h.$$

The left hand side of the equation corresponds to a stepped simplex P_1:

$$j = \frac{I}{F} = \frac{I}{k_1 d^2}; \quad \frac{I}{d^2} = P_1. \tag{9}$$

The right hand side of the equation corresponds to the stepped simplex P_2:

$$\frac{U_h}{\rho l} = \frac{U_h}{\rho l' d}; \quad \frac{U_h}{\rho d} = P_2. \tag{10}$$

The similarity criterion is equal to the ratio between the simplexes of equations (9) and (10) [1, 7]

$$ES = \frac{P_2}{P_1} = \frac{U_h d}{\rho l}, \tag{11}$$

or

$$ES = \frac{U_h}{I^{1/2} j^{1/2} \rho}. \tag{12}$$

(11) only contains the specific electrical resistance of the charge materials or semi-products in the vicinity of the lower end of the electrode, since it was shown in a previous paper [3] that the value of this resistance was near to the effective specific resistance of the arc

$$\rho_{\text{eff.a}} = \frac{US}{Il}, \tag{13}$$

where S and l are the section and length of the sub-electrode space.

The flow of current through the arc differs from that through the melt and in particular this manifests itself in a cathode and anode potential drop on the electrode surfaces adjacent to the arc.

Expression (11) for the criterion *E.S.* only holds for a furnace with one electrode. For furnaces with two or three electrodes it is necessary to put *MI* in the quantity *E.S.* instead of *I* in view of the branching of part of the current between the electrodes. But since,

$$U_f = \frac{U_l}{\sqrt{3}} \eta_e \cos\varphi,$$

it is found that

$$ES = \frac{U_h d}{MI\rho} = \frac{U_l \eta_e d \cos\varphi}{\sqrt{3} MI\rho} = \frac{U_l \eta_e \cos\varphi}{j^{1/2} j^{1/2} \rho}, \tag{14}$$

where U_f and U_l are the phase and line voltages of the transformer.

For a furnace with one electrode $M = 1$, but for furnaces with two or three electrodes M is somewhat less than unity.

Since under normal operating conditions between 4 and 6 per cent of the total current [3] is branched between the electrodes, it is necessary to take $M = 0.95$.

The value of E.S. for furnaces with square electrodes. For such furnaces the value of l is defined by the equation (1c). The expressions for the other quantities have the following form:

$$R = \rho \frac{k_0'' a_* n_0^{1/2}}{a_0^2 n_*} = \frac{\rho k_0''}{a_* n^{1/2}}; \tag{15}$$

$$ES = \frac{U_h a_* n_0^{1/2}}{l\rho}; \tag{16}$$

$$j = \frac{I}{a_0^2 n_*}. \tag{17}$$

Thus, if it is assumed that the value of the multiplier $a_0 n_0^{1/2}$ is equivalent to d, then the rest of the above conclusions remain unchanged.

From equation 17:

$$a_0^2 n_e = \frac{I}{j}$$

and, consequently, for furnaces with square electrodes the expression for the criterion

$$ES = \frac{U_h}{I^{1/2} j^{1/2} \rho} = A$$

coincides with (12) for furnaces with circular electrodes and is more general than equation (11).

The relationship between current and output [3]

YEAR 1961

To determine the quantitative link between the stated quantities it is merely necessary to establish the voltage which would ensure an electrical field similar to the "specimen" field in the actual furnace.

To establish the link between U or I and P use is made of equation (14) and the formula

$$P = \sqrt{3}\, U_l I \cos\varphi = k' U_l I \cos\varphi.$$

Here

$$U_l = A \frac{M I^{1/2} j^{1/2} \rho}{\eta_e \cos\varphi} = \frac{A'' M^{2/3} P^{1/3} \rho^{2/3} j^{1/3}}{\eta_e^{2/3} \cos\varphi}. \tag{18}$$

The quantities M and A are constant in furnaces of different power if the same product is being produced. Therefore

$$U_l = A'' \frac{\rho^{2/3} (Pj)^{1/3}}{\eta_e^{2/3} \cos\varphi}. \tag{19}$$

If it is assumed that η_e and $\cos\varphi$ are constant, then equation (19) will assume the form

$$U_h = c_{01} j^{1/3} P^{1/3} \rho^{2/3}. \tag{20}$$

Finally, if it is assumed that ρ is also constant, then

$$U_h = c_{011} j^{1/3} P^{1/3}. \tag{21}$$

With an increase in power there is an increase in the depth of immersion of the electrodes and together with that an increase in the pressure exerted by the upper layers on the lower layers. Consequently, there is a reduction in the specific electrical resistance of the layer of the charge at the lower face of the electrode. In addition, the increase in pressure is instrumental in forming scum (crusts) in the furnace. Thus, the quantity ρ can be a function of power [1].

Accordingly,

$$\rho = M_1 P^{\beta}.$$

Considering equation (18),

$$U_l = A\left(\frac{M_1 M}{\eta_e}\right)^{2/3} \frac{j^{1/3}}{\cos\varphi} P.$$

If η_e, p, j and $\cos\varphi$ are constant, then equation (21) can be represented in the following form:

$$U_A = c_{0\,III} P^n. \tag{22}$$

In the same way it can also be shown that

$$I = A_0 j^{-1/3} \rho^{-2/3} P^{2/3}; \tag{23}$$

$$I = A_{0I} j^{-1/3} P^{2/3}; \tag{23a}$$

$$I = A_{0\,II} P^{2/3}; \quad I = A_{0\,II} P^{1-n}. \tag{23b}$$

The values of the coefficients c_{0I}, c_{0II}, as well as A_0 to A_{0II}, depend on the composition of the charge, the frequency and depth of stirring, the frequency of tapping and other factors. These coefficients can be found from practical data of the voltages and outputs of the furnaces which provide the best results.

Comparison of calculations with operating data

In published literature it is said that the value n in equation (22) is 0.5 for certain furnaces with different outputs. However, Kamentsev [8] states that it is a question of a change in output in one and the same furnace. Curtis [9] also came to the same conclusion without any explanation.

Equation (21) can be represented in the form

$$U_1 = c_{0\,IV}\frac{I^{1/3}}{d^{2/3}}P^{1/3}.$$

Since d = const and $I = \frac{P}{U}$ in the case under consideration, it is found that

$$U = c_{0\,III}P^{0.5}. \tag{22a}$$

The value of ES with p and d constant corresponds to the equation

$$\frac{U}{I} = \text{const}. \tag{22b}$$

Thus equations (22a) and (22b) hold good for furnaces with the same method of production and electrode diameter.

YEAR 1961

The correctness of the foregoing relationships for furnaces with the same electrode diameter at different outputs does not contradict equation (21) or equations (23) and, being a special case, it actually confirms them. In view of this, it must be acknowledged that the conclusion of certain authors that the value $\frac{U}{I}$ cannot be taken as constant if d varies at the same time as U, but that it does not hold if the latter quantity remains constant when U and I vary.

It was pointed out in a previous paper [3] that the order of n in equation (22) can be less than 0.33. One of the reasons for the decrease in the order of n with increasing output is that j decreases in this case. The value of n can be influenced appreciably by this change under certain circumstances.

Consider the following example by way of illustration. Using equation (21), the value of n is found from the expression

$$n = \frac{\log\frac{U_2}{U_1}}{\log\frac{P_2}{P_1}} = \frac{0.33\log\frac{I_2}{I_1}}{\log\frac{P_2}{P_1}}.$$

According to the LKB project of the Electrical Furnace Trust, the value of j is 4.4 and 5.5 A/cm^2 in 16,500 and 7,500 kVA furnaces respectively. A difference of 0.09 in the value of n is brought about by including the second term in the last equation. It is natural that if

$n = 0.33$ when j and other terms in equations (18) or (20) are equal, then the value n will be $0.33-0.09 = 0.24$ when only one multiplier is included, namely, the difference in the value of j.

Consequently, other published equations with other values of n than 0.33, are special cases of equation (21).

The following conclusion can therefore be drawn. Assuming that c_{0III} is constant in equation 22, which only corresponds to certain special cases, then n will no longer be 0.33, it will generally have a lower value, but in individual cases it can have higher values (for example, if j or the specific resistance of the charge increases with increasing power).

Since the coefficient c_{0III} is not a constant quantity [1,2,3] it is recommended that the value of this coefficient and the value of n should be found from two furnaces with different outputs.

More accurate values of ES and U_n

The next step in refining the criterion ES is to include the specific properties of the arc discharge in the circuit for which the following relationship holds good

$$U = a + bl,$$

where a is the drop in arc voltage at the electrode which depends in particular on the nature of the vapours in the sub-electrode space (this value differs depending upon the technological design of the furnace).

For a 100 kVA carbide furnace the expression for U can be written with averaged coefficients [10]:

$$U = 15.5 + 3.4l.$$

Under normal operating conditions 4 to 6% of the current is branched between the electrodes [4]. Therefore, in the subsequent calculations it can be assumed that the greater part of the current in ore smelting furnaces flows through the arc and charge or the melt in succession. Furthermore, in view of the closeness in value of ρ and $\rho_{eff.a}$, the voltage drop in the charge and the melt can be written in the form

$$U = a + I\rho\frac{l}{S}.$$

Consequently, the voltage drop in the melt and charge is

$$U_{vd} = U_h - a = I\rho \frac{l}{S} = \frac{I\rho}{d}.$$

This new expression for ES differs from the previous one in that the term $U - a$ is written in the first instead of U.

It is more convenient to express the value of U_{vd} in terms of P_{vd}. It is found like $U_h = f(P)$ in the way shown above, e.g. by equations (12), (18), (19), (20) and (21). Consequently,

$$U_{vd} = A_{III} P_{vd}^{1/3} j^{1/3}. \tag{24}$$

The following expression can be used instead of 24

$$U_{vd} = A_{IV} P_{vd}^{n}. \tag{24a}$$

YEAR
1961

Since

$$\frac{P_{vd}}{P_h} = \frac{U_{vd}}{U_h},$$

it is found that

$$U_{vd} = A_{III} P_{vd}^{1/3} \frac{U_{vd}^{1/3}}{U_{vd} + a} \rho^{2/3} j^{1/3},$$

or

$$U_{vd}^3 + U_{vd}^2 a = A_{VI} P \rho^2 j. \tag{25}$$

In large furnaces $a < U_{vd}$ and therefore when calculating them it is necessary bear in mind that the term $U_{vd}^2 a < U_{vd}^3$. It is therefore possible to solve equation (25) by trial and error if a is assumed to be a small parameter. As a result

$$U_{vd} = A_V P^{1/3} \rho^{2/3} j^{1/3} - \frac{a}{3};$$

$$U_h = \frac{2}{3} a + A_V P^{1/3} \rho^{2/3} j^{1/3}.$$

Current density in the electrode

It will be seen from equations (7) and (21) that it is necessary to increase j to increase U. An increase in j above a certain value is not permissible because the electrode can get much too hot or unfavourable coking conditions can arise. The need to include this factor has been dealt with by Alekseev [11].

An attempt will now be made to establish the link between j, P and d on the condition that the thermal balance of the electrode is preserved. One side of the balance contains the item q_1 for the generation of heat owing to the transmission of current through the electrode and q_2 for the influx of heat from the arc to the lower face of the electrode, whilst the other side of the balance contains q_3, the dissipation of heat through the side surface, q_4 the heat necessary for heating, coking and vapourizing the electrode, and q_5 the dissipation of heat from the lower face of the electrode to the electrode holder.

The equilibrium equations are

$$k_1'' I^2 \rho_e \frac{4L}{\pi d^2} + k_2'' \frac{\pi d^2}{4} - k_3''' \pi d L - \\ - k_4'' \frac{c\gamma \pi d^2}{4} l - k_5'' \frac{\pi d^2}{4L} = 0; \qquad (26)$$

$$k_6 I^2 \rho_e \frac{L}{d^2} + k_{30} d^2 - k_{30} d L - k_{40} d^2 l - \frac{k_{50} d^2}{L} = 0,$$

where L, ρ_e, c, γ and l are the length of the electrode from the lower face to the electrode holder, the specific resistance of the electrode, its thermal capacitance, the specific gravity, and the expenditure of electrodes per unit of time.

Considering equations (6) and (23),

$$k_{10} j^{2/3} P^{2/3} + k_{20} \frac{P^{2/3}}{j^{1/3}} - \frac{k_{30} P^{2/3} L}{j^{2/3}} - \\ - \frac{k_{40} P^{2/3} l}{j^{4/3}} - \frac{k_{50} P^{2/3}}{j^{4/3} L} = 0.$$

Equations have been published which establish the link between d and P or I. It will now be shown that these relationships can be found if the items q_2, q_4 and q_5 are ignored in equations (26).

However, there is no foundation for ignoring these terms and in particular the item q_2. It therefore remains for the assumptions underlying the following relationships to be verified at a later date in order to see whether they correspond to operating data and to find out whether further refinement is necessary.

If q_2, q_4 and q_5 are ignored, then equation (26) takes the form

$$P^{1/3} = \frac{k_{10}}{k_{20} j^{4/3}}; \quad j = k_{10} P^{-4}. \tag{27}$$

Platonov [12] obtained a similar formulae from other considerations for furnaces with a constant specific power, i.e. the supply of power per unit area of the hearth for which we put g.

Ignoring q_2, q_4 and q_5 it is found from equation (26) that

$$\frac{I^3}{d^3} = Nd. \tag{28}$$

or

$$j^3 = \frac{N}{d}. \tag{29}$$

It should be pointed out that Kelley's [13] empirical equation has a similar form

$$j = 250\, d^{-1/2}, \tag{29a}$$

where j is expressed in amperes per square inch and d in inches.

But equations (29) and (29a) are only approximate.

The relationship between I and d can be established from equation (28):

$$I = Nd^{1.5}. \tag{30}$$

It must be mentioned that there is only any point in determining the empirical coefficients in accordance with equation (26) to (30) on the basis of the furnaces' operation where the values of j correspond to electrodes with the optimum thermal balance.

It has already been shown [3] if the criteria of electrical and

geometric similarity are observed, that

$$g = N_0 j^{1,33} P^{0,33} \cos\varphi^{0,66}. \tag{31}$$

Assuming that j and $\cos\phi$ are constant, equation (27) is then obtained. Considering equations (21) and (27), it can be inferred that the voltage U if g = const is equal to

$$U = c_{0III} j^{1/3} P^{1/3} = c_{IV} P^{-1/12} P^{1/3} c_{IV} P^{0,25}. \tag{32}$$

Thus, equations (27) to (30) and (32) correspond to a constant g if the electrical and geometric similarity is observed.

Since expressions (27) to (30) ignore certain items in the thermal balance, it should be pointed out that Workramer [6] recommended that the following relationship should be used:

$$I = 20d^{1,7}. \tag{33}$$

But an error was committed here in that he took a constant g along with this equation. It has already been established that equation (30) should have been used in this case instead. Incidentally, taking equation (33),

$$U = c_V P^{0,29}.$$

It is necessary to find expressions for the relationships between j and the other quantities for square electrodes. As before, the only items of the balance which are included are q_1, q_3 for ρ_e:

$$\left.\begin{aligned} I^2 \frac{L}{a_0 b_0} &= k_{s0} (a_0 + b_0) L; \\ \frac{I^2}{a_0^2 n_0} &= k_{s0} a_0 (1 + n_0). \end{aligned}\right\} \tag{34}$$

Since,

$$j = \frac{I}{a_0 b_0},$$

it follows that

$$j = k_{s0} \left(\frac{1 + n_0}{a_0 n_0^2}\right)^{1/2}. \tag{35}$$

To ensure the maximum values of U with increasing P, it is necessary to enlarge the heat dissipating surface of the electrodes. For example, it is possible to increase the power within limits without changing the thickness of the electrode (retaining the dimension a_0).

The relationship between the electrode dimensions a_0, n_0 and I follows directly from equation (34):

$$I = k_{10} a_0^{3/2} [n_0 (1 + n_0)]^{1/2}. \tag{36}$$

Translated by O.M. Blunn

REFERENCES

1. A.S. Mikulinskii; *Prom. energ.*, No.4, (1948).
2. A.S. Mikulinskii; *Determination of the parameters of electric furnaces.* In book: *Theory and practice of electric ore smelting, (K opredeleniiu parametrov elektricheskikh pechei. Sborn. "Teoriia i praktika rudnoi elektrotermii)".* Metallurgizdat (1948).
3. A.S. Mikulinskii; *Theory of carbide and ferro-alloy furnaces, (K teorii karbidnykh i ferrosplavnykh pechei).* Trud. UNIKhIM, No.II, Goskhimizdat (1954).
4. A.S. Mikulinskii, V.K. Ivanov and P.V. Cel'd; *The electrical field between cylinders in an inhomogeneous medium.* In book: *Technical physics, (Elektricheskoe pole mezhdu tsilindrami v neodnorodnoi srede. Sborn. "Teknicheskaia fizika")* (1947).
5. P.V. Sergeev; *Determination of the main electrical parameters of ore-smelting furnaces with a large slag capacity, (Opredelenie osnovnykh elektricheskikh parametrov rudnotermicheskikh pechei s bol'shim ob'emom shlakov).* Trud. Altai. gornomet. nauchno-issled. inst., IV (1957).
6. M. Morkramer; *J. du four elect.*, No.2 (1960).
7. V.K. Ivanov and A.S. Mikulinskii; *The distribution of current in ore-smelting furnaces.* In book: *Theory and practice of electrical ore smelting, (K raspredeleniiu toka v rudnotermicheskikh pechakh. Sborn. "Teoriia i praktika rudnoi elektrotermii).* Metallurgizdat (1948).
8. M.V. Kamentsev; *Synthetic abrasives, (Iskusstvennye abrazivnye materialy).* Mashgiz (1960).
9. H.A. Curtis; *J. electrochem. soc.*, 100 (1953).
10. A.S. Mikulinskii and L.V. Iumenova; *The transmission of current in a carbide furnace, (K voprosu prokhozhdeniia toka v karbidnoi pechi).* Trud. UNIKhIM, No.II. Goskhimizdat (1954).

YEAR 1961

11. E.M. Alekseev; *Stal'*, No. 10, (1956).
12. G.P. Platnov; *Prom. energ.*, No. 1 (1960).
13. W.M. Kelley; *Iron and steel engineer*, No. 4 (1958).

YEA
196

A NEW SYSTEM OF GENERATING DIRECT AND STABLE FREQUENCY ALTERNATING CURRENT FROM MOTORS WHICH RUN AT DIFFERENT SPEEDS*

M. M. KRASNOSHAPKA

(Kiev)

(Received 5 September 1960)

YEAR
1961

Purpose, construction and operating principle

Modern aircraft use d.c. and stable frequency a.c. systems of electrical supply at the same time. In the majority of cases the d.c. source is a d.c. generator driven by the aircraft motors at a wide range of speeds. In order to obtain stable frequency a.c. in this case use is made of dynamo electric converters (motor-generators), provided with automatic voltage and frequency regulators.

If the consumption of a.c. is relatively large, it is better to use special generator plant for generating stable frequency a.c. at various running speeds of the primary motor. Such generator plant can be a synchronous generator with a hydraulic drive, a synchronous generator with an electromagnetic clutch, a twin-machine system consisting of a d.c. generator and a single-armature converter besides other types of plant and dynamo-electric systems [1-5].

There is also a need to generate stable frequency a.c. at a wide range of rotational speeds in other branches of engineering, such as wind-driven power stations, small hydro-electric power stations with non-controlled turbines, new types of railway passenger cars etc [1-4].

The general disadvantage of known types of aircraft systems of

* *Elektrichestvo*, No. 6, 38-44, 1961.

generating stable frequency alternating current for varying rotational speeds is that the mechanical power of the primary motor developed by them is subject to a two-fold and even three- fold conversion. The efficiency of the system is therefore low and its weight is relatively large per kVA of output.

In this paper a study is made of a new system which is intended for the simultaneous generation of direct and stable frequency a.c. for varying rotational speeds. It consists of a special twin-generator unit with two automatic regulators and a single-armature converter of comparatively low power. The system is relatively light in weight and it is highly efficient, since more than 85% of the electrical power is obtained direct from the twin-generator unit and only a small proportion of it is converted in the single-armature converter. The system can be used for any ratio of the powers consumed in the a.c. and d.c. networks, and even in extreme conditions when only a.c. or only d.c. is being generated.

YEA
196

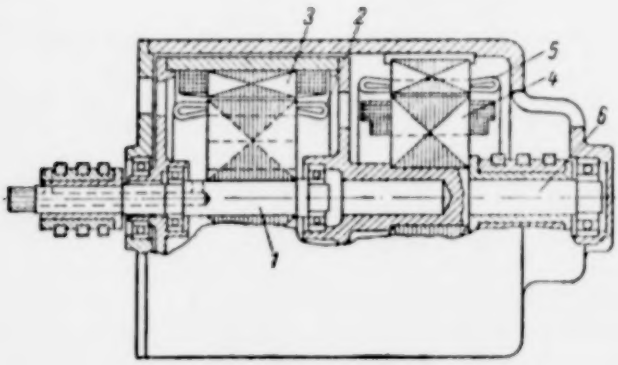

Fig. 1. Construction of generator unit.

Fig. 1 illustrates the construction of the unit and Fig. 2 the main circuit of the connexions of the unit's machines with the single-armature converter *SC*, the voltage regulator *VR* and the frequency regulator *FR*.

The generator unit consists of an electromagnetic slip clutch with an excitation winding *3* and a three phase winding *2* which is connected to the contact rings on the primary shaft *1*, and a three phase synchronous generator with a rotating inductor *4* and a fixed armature winding *5*. The d.c. supply of the excitation windings is via three contact rings on the secondary shaft of the unit *6*.

At a rotational speed n_1 of the primary shaft *1* the first machine of the unit *2* simultaneously operates as a synchronous generator supplying the a.c. network and as a clutch rotating at a speed n_2 the synchronous generator connected via rectifier *7* to the d.c. network. From now on we will refer to the second machine of the unit as the restraint generator.

Depending upon the relationship between the power consumption in the a.c. and d.c. networks and the rotational speed of the primary motor, the balancing single-armature converter can convert d.c. into a.c. or a.c. into d.c. and under no-load conditions it can operate with supply from both ends.

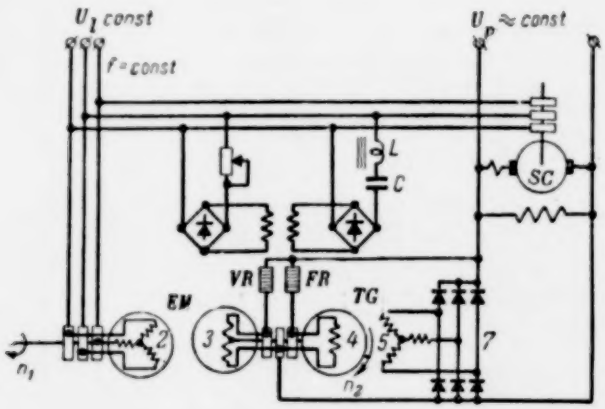

Fig. 2. Electrical connexions of machines and system regulators.

The frequency of the a.c. is stabilized at different running speeds of the primary motor and different loads by the automatic frequency regulator *FR* which varies the excitation current of the restraint generator. The frequency of the alternating current *F* depends upon the the number of pole pairs *p* and the difference between the speed of the driving and driven parts of the clutch.

To maintain the frequency stable it is necessary to maintain a constant speed difference between the driving and driven parts of the clutch since

$$f = \frac{p(n_1 - n_2)}{60}. \qquad (1)$$

Under steady state conditions the moving magnetic moment of the clutch is equal to the sum of the electro magnetic moment of the restraint generator and the moment of friction of the driven part of the clutch. If there is no frequency regulator, an increase in the active load on a.c., a decrease in the d.c. load and a reduction in the rotational speed of the primary motor n_1 will cause a decrease in the speed difference $n_1 - n_2$ and the frequency owing to the balance of the moments being upset. In order to maintain the frequency constant under these conditions it is necessary to increase the torque of the restraint generator by a corresponding increase in the excitation current. In the opposite case it is necessary to reduce the torque of the restraint generator by decreasing its excitation current.

The frequency is automatically stabilized if there is a frequency regulator *FR* connected as in the circuit in Fig. 2.

It will be seen from Fig. 2 that the voltage in the a.c. network is stabilized by regulating the excitation current of the electromagnetic clutch by the automatic voltage regulator *VR*.

The main circuit in Fig. 2 shows the voltage and frequency regulators in the form of conventional angle regulators as used in aircraft supply systems. Other types of automatic regulator could be used instead, including regulators with magnetic amplifiers which may be more reliable and convenient in use.

Relationship between machine output and system efficiency under different operating conditions: approximate weight of the system

The mechanical power from the primary motor to the primary shaft of the generator unit P_{m1} is partially converted in the electromagnetic clutch, as in a conventional generator, to electrical power P_{e1}. The rest of the power is transmitted to the secondary shaft of the unit in the form of mechanical power P_{m2}, in which case

$$P_{m2} = P_{m1} - P_{e1} = \frac{P_2}{\eta_{2y}} = M_{e1}\frac{\pi n_2}{30}. \qquad (2)$$

The electrical power of the clutch including the losses in the armature circuit and magnetic system is

$$P_{e1} = P_{1a} + \Delta P_{[illegible]} + \Delta P_{1st} = \frac{P_{1a}}{\eta_{1y}} = M_{e1}\frac{\pi(n_1 - n_2)}{30}, \qquad (3)$$

where M_{el} is the electromagnetic moment of the clutch, n_1, n_2 the rotational speeds of the primary and secondary shafts, $\eta_{l_{2y}}$ the conditional efficiency of the restraint generator with the losses in the rectifier, the excitation circuit of the clutch and the friction losses of its driven part all included, P_{1a} the electrical active power of the clutch, $\Delta P_{1\ arm}$ the electrical losses in the armature winding circuit, ΔP_{1st} the iron losses in the magnetic circuit of the clutch, η_{1y} the conditional efficiency of the clutch as an a.c. generator without the losses in the excitation circuit and the friction losses of its driven part included, and P_2 the useful power of the restraint generator.

The relationship between the d.c. power and the active a.c. power given off by the restraint generator and clutch respectively can be obtained from equations (2) and (3):

$$\frac{P_2}{P_{1a}} = \frac{n_2 \eta_{l_{2y}}}{n_c \eta_{1y}} = k n_2, \tag{4}$$

where $n_c = n_1 - n_2 = \text{const}$ is the nominal difference in rotational speed.

It is presupposed that the active P_{1a} when the armature of the electromagnetic clutch is greater than the active power consumed in the a.c. network $P_{n.a}$ by an amount which exceeds the no-load losses of the single-armature converter. In this case the power consumed in the d.c. network $P_{n.d}$ is equal to the sum of the powers given off by the restraint generator P_2 and the single-armature converter P_{sc}. Suppose that the unit of measurement is the total power consumed in the a.c. and d.c. networks $(P_{na} + P_{nd})$ and that x denotes the relative power in the d.c. network. Then

$$P_{nd} = P_2 + P_{sc} = x(P_{na} + P_{nd}); \tag{5}$$

$$P_{na} = P_{1a} - \frac{P_{sc}}{\eta_{sc}} = (1 - x)(P_{na} + P_{nd}). \tag{6}$$

The joint solutions of equations (4) to (6) gives the following expressions for the outputs of the electromagnetic clutch P_{1a}, the restraint generator P_2 and the single-armature converter P_{sc}:

$$P_{1a} = \frac{[x(1 - \eta_{sc}) + \eta_{sc}](P_{na} + P_{nd})}{k n_2 + \eta_{sc}}; \tag{7}$$

$$P_3 = \frac{[x(1-\eta_{sc})+\eta_{sc}]\,kn_2(P_{na}+P_{nd})}{kn_2+\eta_{sc}}; \tag{8}$$

$$P_{sc} = \frac{[x(1+kn_2)-kn_2]\,\eta_{sc}(P_{na}+P_{nd})}{kn_2+\eta_{sc}}. \tag{9}$$

Formulae (7) to (9) hold good for all unit operating conditions under which the single-armature converter converts the a.c. into d.c. i.e. with $P_{sc} > 0$.

It is presupposed that the output of the restraint generator is greater than the power consumption in the d.c. network by an amount which exceeds the no-load losses of the single-armature converter, whilst the sum of the active power of the electromagnetic clutch P_{1a} and of the single-armature converter P_{sca} is equal to the active power of the a.c. network P_{na}. In this case the initial equations have the form:

$$P_{nd} = P_3 - \frac{P_{sca}}{\eta_{sc}} = x(P_{na}+P_{nd}); \tag{10}$$

$$P_{na} = P_{1a} + P_{nda} = (1-x)(P_{na}+P_{nd}). \tag{11}$$

As a result of the joint solution of equations (4), (10) and (11), to determine the active powers of the electromagnetic clutch, the single-armature converter, and the restraint generator, the corresponding formulae are:

$$P_{1a} = \frac{[x(\eta_{nd}-1)+1](P_{na}+P_{nd})}{kn_2\eta_{sc}+1}; \tag{12}$$

$$P_{sco} = \frac{[kn_2 - x(1+kn_2)]\,\eta_{sc}(P_{na}+P_{nd})}{kn_2\eta_{sc}+1} \tag{13}$$

$$P_3 = \frac{[x(\eta_{sc}-1)+1]\,kn_2(P_{na}+P_{nd})}{kn_2\eta_{sc}+1}. \tag{14}$$

Formulae (12) to (14) hold good for all operating conditions of the unit when the balancing single-armature converter converts the direct current into alternating current, i.e. when $P_{sca} > 0$.

The efficiency of the generator unit with the balancing single-armature converter when the latter is converting a.c. into d.c. is given

by equation (15). In the other case it is given by (16):

$$\eta_{1c} = \frac{1}{P'_{na} + P'_{nd}} \left[\left(P_{1a} - \frac{P'_{sc}}{\eta_{isc}} \right) \eta_{i1} + \right.$$
$$\left. + P_{sc} \eta_{i1} \eta_{isc} + P_2 \eta_{i2} \right]; \quad (15)$$

$$\eta_{1c} = \frac{1}{P'_{na} + P'_{nd}} \left[P_{1a} \eta_{i1} + \right.$$
$$\left. + \left(P_2 - \frac{P'_{sca}}{\eta_{isc}} \right) \eta_{i2} + P_{sca} \eta_{i2} \eta_{isc} \right], \quad (16)$$

where $\eta_{i\,s.c}$, η_{i1} and η_{i2} are the real efficiencies of the single armature-converter, the first machine and the second machine.

When the system is operating in the middle range of speeds n_1 with a certain relationship between the loads in the a.c. and d.c. networks, the single armature-converter can operate under conditions of supply from both ends, consuming power equal to the no-load losses ΔP_{sc}.

In this case the total electrical power of the unit's machine is equal to the total power consumed in both networks with the no-load losses of the single-armature converter included:

$$P_{1a} + P_2 = P_{n.a} + P_{n.d} + \Delta P_{n.d}. \quad (17)$$

The outputs of the first and second machines of the unit, in this case in accordance with relationship (4), can be found from formulae (18) and (19):

$$P_{1a} = \frac{P'_{na} + P'_{nd} + \Delta P'_{sc}}{kn_2 + 1}; \quad (18)$$

$$P_2 = \frac{(P'_{na} + P'_{nd} + \Delta P'_{sc}) kn_2}{kn_2 + 1}. \quad (19)$$

The generator unit with a single-armature converter is not only suitable for simultaneously generating a.c. and d.c., but also for generating either a.c. or d.c. separately. The formulae for finding the power of the electromagnetic clutch, single-armature converter and restraint generator when generating only a.c. can be found from formulae (12) to (14) by substituting x = zero and $P_{n.d}$ = zero therein.

If only d.c. is being generated, the appropriate formulae are ob-

tained from (7) to (9) after substituting $x = 1$ and $P_{n.a}$ = zero, but this state of affairs has no practical significance.

When only a.c. is being generated, the efficiency of the system is defined by formula (20), but when only generating direct current it is given by formula (21):

$$\eta_c = \frac{P_{1a}}{P_{na}}\eta_{1i} + \frac{P_{st.d}}{P_{na}}\eta_{1a}\eta_{1sc}; \tag{20}$$

$$\eta_c = \frac{P_2}{P_{nd}}\eta_2 + \frac{P_{sc}}{P_{sc}}\eta_{1i}\eta_{sc}. \tag{21}$$

Fig. 3 shows curves for the relative outputs

$$\frac{P_{1a}}{P_{n.a} + P_{n.d}}, \quad \frac{P_2}{P_{n.a} + P_{n.d}},$$

$$\frac{P_{s.c}}{P_{n.d} + P_{n.d}} \quad \text{and} \quad \frac{P_{s.c.a}}{P_{n.a} + P_{n.d}}$$

as a function of the rotational speed of the primary motor n_1 at $x = 0.4$ $\eta_{2y} = 0.7$ to 0.8, $\eta_{sc} = 0$ to 0.76, $\eta_{1y} = 0.92$, and $n_c = n_1 - n_2 = 4800$ rev/min.

The curves for relative machine outputs have been plotted from data calculated for a system intended for simultaneous supply of a 30 kVA a.c. network ($f = 400$ c/s $\cos\varphi = 0.75$, and $P_{na} = 22.5$ kW) and a 15 kW d.c. network.

The curve η_c gives the efficiency of the system at rated load, and the inclined straight line n_2 the rotational speed of the restraint generator. It will be from Fig. 3 that the power of the restraint generator P_2 is increased by practically a factor of 2.5 with an increase in rotational speed n_1 from 6500 to 1300 rev/min and n_2 from 1700 to 8200 rev/min. Since the voltage of the d.c. network is practically constant, it follows that the curve P_2 simultaneously defines the limits of variation of the current in the stator winding of the restraint generator.

In order to reduce the theoretical dimensions and weight of the restraint generator intended for such operating conditions, it is necessary to change over the stator winding from the star system to the

delta system with an increase in rotational speed n_2 to 3200 rev/min. This changeover can be made by a 2-position 3 phase contactor with automatic control.

The 20-30 kVA alternators used in modern aircraft without an exciter for theoretical speeds of 6000 rev/min weight no more than 1 kg per 1 kVA of rated output (g_{rel} = 1 kg/kVA).

Bearing these data in mind, the total weight of a twin-machine unit for P_1 = 30 kVA and P_{nd} = 50 kW can be calculated quite closely by the formula

$$G_{\Sigma} = g_{rel} n \left(\frac{P_{1\,max}}{n_c} + \frac{P_{2\,max}}{n_{2p}} \right) =$$

$$= 6\,000 \left(\frac{35.8}{4\,800} + \frac{22}{3\,200} \right) = 86 \text{ kg}.$$

YEAR
1961

The approximate weight of the single-armature converter with a maximum output of 5.65 kW at $n_{s.c}$ = 8000 rev/min is about 9 kg, whereas the approximate weight of the germanium rectifiers can be taken as about 8 kg at a maximum output of 22 kW. In this case the total weight of the system without regulators is 103 kg and its weight per 1 kVA of the total power of the a.c. and d.c. networks is 2.29 kg.

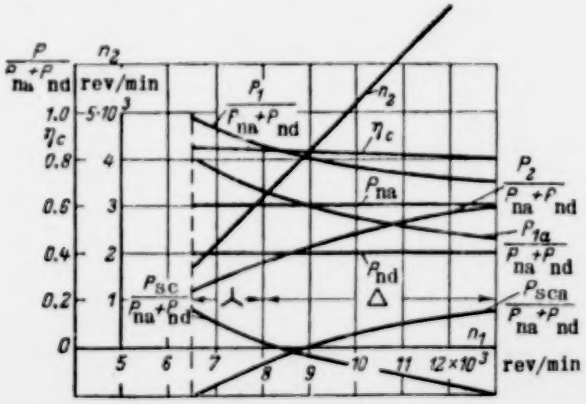

Fig. 3. Calculated characteristics of the system in a.c. and d.c. generation.

Fig. 4 shows calculated curves for a system solely intended for an a.c. network with an output 30 kVA, f = 400 c/s at $\cos\phi$ = 0.75, n_1 = 6250 to 12500 rev/min n_c = 6000 rev/min and n_2 = 250 to 6500 rev/min.

To ensure the necessary restraint torque of the second machine in the unit at n_2 = 250 to 1700 rev/min, provision is made for disconnecting the single-armature converter from the network and the shortcircuiting of the a.c. armature winding. In this case all the output is delivered to the a.c. network only by the first machine, and the relatively low output of the restraint generator is dissipated in the form of losses in the armature windings of the converter and restraint generator.

In the range of speeds n_2 = 1700 to 3300 rev/min the stator winding of the restraint generator is connected in star, but if n_2 > 3300 rev/min it is connected in delta.

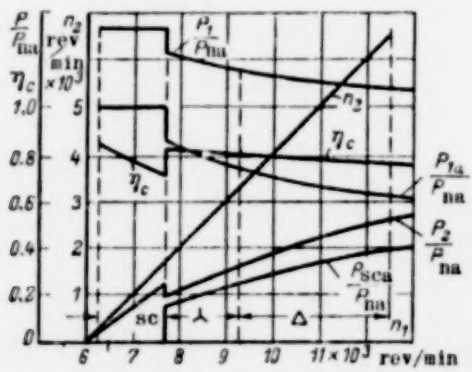

Fig. 4. Calculated characteristics of the system in the generation of a.c. alone

In accordance with Fig. 4 the first machine of the unit must be designed for a total power in the a.c. network P_1 = 30 kVA at n_c = 6000 rev/min, the second machine for a maximum power P_2 = 11.25 kW at n_{2p} = 3200 rev/min. The maximum power of the single-armature converter at n_1 = 12500 rev/min is 0.39 P_{na} = 8.7 kW. The total weight of the twin-machine unit of 30 kVA at cos φ = 0.75 is 49.5 kg in accordance with the formula given above.

The total weight of a single-armature converter of 8.7 kW at $n_{s.c}$ = = 8000 rev/min and the set of germanium rectifiers for a maximum output of 11.25 kW is about 18.5 kg.

The total weight of the system without including the weight of the regulators and contactors if the foregoing changes have to be made is about 68 kg and its weight per 1 kVA of rated output is 2.27 kg.

The weight indices of the dynamo-electric system are approximately equal to the wt. indices of an aircraft generator plant of equal power consisting of an alternator and differential – hydraulic drive. But the efficiency of the proposed system is considerably greater.

Distribution of reactive power between the first machine and the single-armature converter

The foregoing equations 7-9 and 12-14 and the curves in Figs. 3 and 4 define the relative active a.c. powers of the first machine and the single-armature converter as well as the relative output of the restraint generator. The active power can be delivered into the network either from the first machine of the element or from the single-armature converter. The relationship between the reactive powers of the first machine and single-armature converter when an automatic voltage regulator VR is present (see Fig. 2) depends upon the degree of excitation of the converter. At rated converter excitation ($\cos \varphi = 1$) active power only comes into the network from the first machine of the unit. If there is under-excitation, the single-armature converter is a consumer of reactive power, but if there is over-excitation it delivers active power into the network partially unloading the first machine.

If a.c. is being generated it is advisable to change the excitation of the single-armature converter in such a way that it delivers a certain reactive power into the network at low speeds of the primary motor when its active output is low.

With an increase in active load on the single-armature converter at high speeds of the primary motor the reactive power from the converter must gradually decline to zero owing to the weakening of its excitation. In this case the necessary reactive power will come in an ever increasing extent from the first machine of the unit, the active power of which decreases with increasing speed of the primary motor, as will be seen from Fig. 4.

The excitation of the single-armature converter can be changed automatically as required by mixed excitation with counter connexion of its parallel and series windings.

Test results

In order to check the operating characteristics, dynamic properties and weight indices of the system, an experimental equipment was produced on the basis of the batch produced SGS-7.5 type aircraft alternators.

The restraint generator was a SGS-7.5 alternator with 6 slip rings on the shaft so that the armature winding could be changed from star to delta and back by a 2-position contactor. In place of the single-armature converter use was made of an aircraft cascade converter of the PK-750 type which was reconstructed as a three phase converter with a line voltage of 120 V and a maximum output to 1000 VA at collector voltage of 28 V. The electrical power of the restraint generator was transmitted into the d.c. network and armature circuit of the converter via VG-50 type germanium rectifiers.

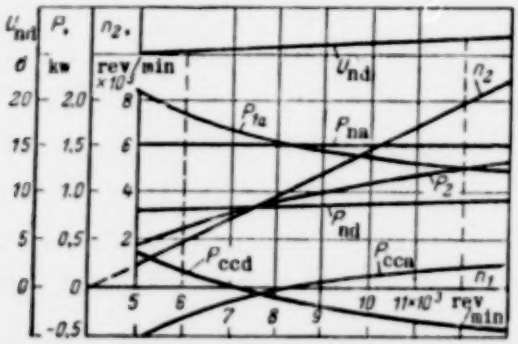

Fig. 5. Test curves of prototype system in a.c. and d.c. generation at 400 c/s and 120 V.

The load of the unit did not exceed 30% of its theoretical output owing to the lack of a suitable cooling system.

Fig. 5 shows the static characteristics of the experimental generator plant for the case of simultaneous generation of a.c. and d.c.

In order to investigate the dynamic properties of the system a prototype system was assembled consisting of the two machines described above, a 3-phase cascade converter, a 2-position contactor and two angle regulators. The electrical connexion of the machines and regulators differed from the system shown in Fig. 2 in that measuring devices and a three phase 2-position contactor were included to provide for changeover of the armature winding of the restraint generator.

The control winding of the frequency regulator was supplied from a tuned circuit via a magnetic amplifier, whilst the excitation winding of the first machine was supplied from a direct or constant source. Oscillograms of transient behaviour in the system are shown in Figs. 6-9.

Fig. 6. Oscillograms of transient phenomena in system on disconnecting an a.c. load:
1 – line voltage of network 120 V, 400 c/s; *2* – phase current of first machine in the unit (initial value 2.8 A); *3* – phase current of cascade converter (initial value 2.8 A); *4* – voltage of d.c. network (initial value 24 V); rotational speed of primary motor (n_1 = 5300 rev/min); *6* – zero line; *7* – d.c. given off by converter; *8* – time indication (50 c/s).

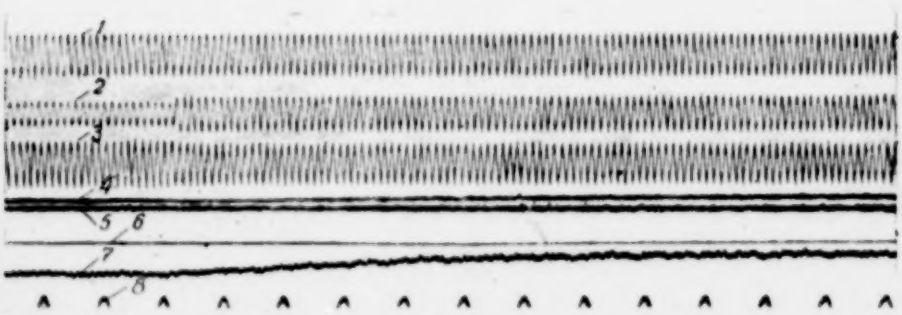

Fig. 7. Oscillograms of transient phenomena in system on connecting an a.c. load:
(Legend as in Fig.6)

The switching of the restraint generator's armature winding is accompanied by an instantaneous change in the collector voltage and

converter currents, but this has no practical effect on the frequency and the magnitude of the a.c. network voltage. Unlike Figs. 6 and 7, the second sine curve from the top in Figs. 8 and 9 shows the load current of the network, whilst the frequency of the time indicator is 500 c/s.

Conclusions

1. The proposed system of simultaneously generating d.c. and stable frequency a.c. widely different running speeds of the primary motor can be used for generating both types of current as well as for generating a.c. alone.

2. The proposed system is more efficient and lighter in weight per unit of output than other similar systems.

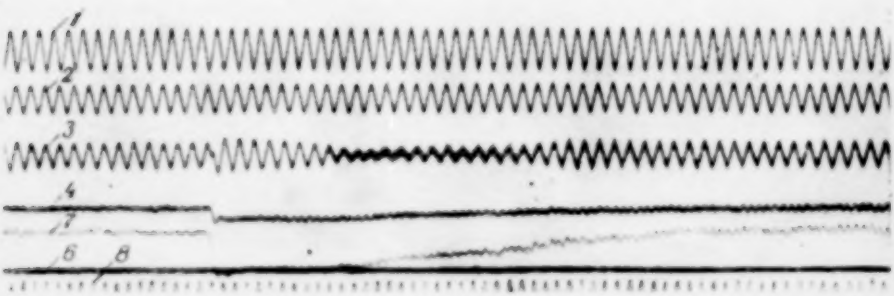

Fig. 8. Oscillograms of transient phenomena in system when changing the armature winding of restraint generator from star to delta.

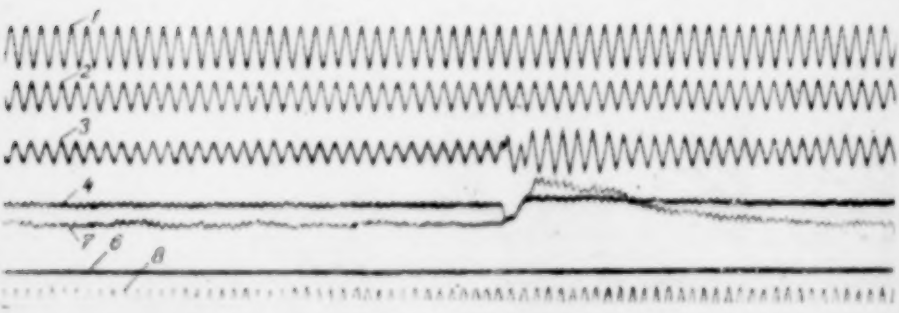

Fig. 9. Oscillograms of transient phenomena in system when changing the armature winding from delta to star.

3. Tests results of a prototype system are in full agreement with theoretical data and testify to the good stability obtained during transient conditions.

4. The proposed system can be used in all cases when it is necessary to generate stable frequency a.c. at different speeds of the primary motor.

Translated by O.M. Blunn

REFERENCES

1. M.P. Kostenko; *Elektrichestvo*, 2 (1948).
2. M.M. Krasnoshapka; *A twin-machine system of generating a.c. of constant frequency at varying rotational speeds of the drive, (Dvukhmashinnaia sistema generirovaniia peremennogo toka postoiannoi chastoty pri izmeniaiushcheisia skorosti vrashcheniia privoda)*. Iz. VVIA, im. N.E. Zhukovskogo, 545 (1955).
3. V.S. Kulebakin, V.T. Morozovskii and I.M. Sindeev; *The electrical supply of aircraft, (Elektrosnabzhenie samoletov)*. Oborongiz (1956).
4. M.M. Krasnoshapka; In book: *Automation of production processes in agriculture, (Avtomatizatsiia proizvodstvennykh protsessov v sel'skom khozhaistve)*. Akad. Nauk SSSR (1956).
5. B.N. Petukhov; *The electrical supply of aircraft, (Elektrosnabzhenie letatel'nykh apparatov)*. LK VVIA im. A.F. Mozhaiskogo (1960).

YEAR 1961

A HIGH-SPEED ELECTRO-DYNAMIC CIRCUIT BREAKER*

Yu. G. KOMAROV

(Leningrad)

(Received 31 December 1960)

The electrical industry now has to face the problem of producing high speed switchgear capable of limiting short-circuit currents of over 100 kA in large low-voltage networks with a build-up rate of several tens of millions of amperes per second. The necessary switchgear must be designed for rated currents up to 10 kA and higher, and should be as small and quick-acting as possible. In this paper a description is given of experimental circuit breakers which have been developed on the basis of previous patents [1, 2].

A simple type of breaker is illustrated in Fig. 1. The two short traverses *1* and *2* form a narrow loop in the main circuit. Contacts *3* are disposed on the ends of the traverse. Traverse *2* is fixed, but traverse *1* is secured by a current-conducting hinge *4*. The main spring *5* creates the necessary pressure on contact *3* and *4*. The breaker is supplied with current at points *6* and *7*.

The flow of current along the traverses gives rise to electrodynamic forces which tend to open the contacts *3*. It is possible to select the dimensions of the loop, the shape of the traverse and the amount of pressure on the contacts in such a way that no dangerous weakening of the pressure on the contacts occurs under normal conditions. But at a definite short-circuit current the electrodynamic forces increase so much that they overcome the resistance of spring *5* and open contacts *3*. Traverse *1* is then rotated on axle *4* and is fixed in a disconnected position by the stop *8*.

---

* *Elektrichestvo*, 6, 53-55, 1961.

Experimental breakers for rated currents of 500 and 3,000 A have been produced on the basis of the methods shown in Fig. 1. The 3,000 A breaker has been provided with arc quenching contacts.

To determine the current limiting capacity of these breakers tests have been carried out on voltages of 10 to 300 V, short circuit currents of 13 to 100 kA and build-up current rates of (0.65 to 10) x 10^6 A/sec. Fig. 2 illustrates one of the results of the tests on the breakers with arc quenching contacts. It will be seen from the curves in this diagram that the breaker limited the short-circuit current to 38 kA at a steady state value of the circuit current of 100 kA. By way of comparison the dotted line in Fig. 2 shows the short-circuit current interrupted in the same circuit by a "universal" circuit breaker.

Tests with identical circuit parameters have shown that the proposed type of breaker is highly stable as regards the limitation of short-circuit currents. The average fundamental opening time of the breaker did not exceed 2 x 10^{-3} sec. Curves for the movement of the breaker's traverses were also determined during the tests. One such curve $h=f(t)$ is shown in Fig. 3. The fundamental opening time t_0 is plotted along the base and the arc quenching time t_a is also plotted there. This makes it possible to determine the motion of the traverse at different stages.

YEAR
1961

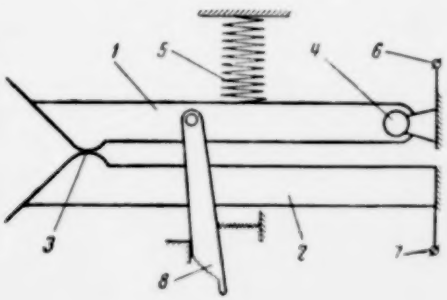

Fig. 1.

However, despite the advantages of this simple system, they have a number of short-comings. The contacts may stick if the short-circuit currents are small, with natural cooling the load does not exceed 5000 A and the system is sensitive to vibration.

To eliminate these shortcomings a new type of breaker was developed using the system illustrated in Fig. 4. The traverses 1 and 2 of this

breaker were water-cooled. Sectional main contacts *3* and arc quenching contacts *4* were fixed at the end of the traverse. Traverse *1* was balanced about axle *5* of the current conducting hinge. The main springs *6* provided the necessary pressure on contacts *3* and *5*. The current is supplied to conductors *7*. The breaker has an auxiliary disconnecting mechanism consisting of a free release device which is secured on shafts *8* and *9*, an electromagnetic release arrangement *10*, feedback *11* and a vibration plate *12*. The axle *13* which is secured to traverse *1*, passes through a slot in the plate *12*.

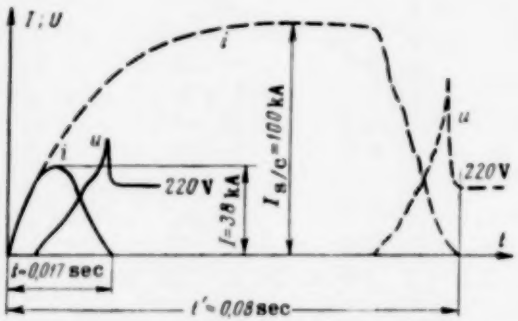

Fig. 2

The device operates (closes) when the interrupting roller *14* rotates 16°. The roller can be rotated from the release arrangement *10*, and through feedback *11* when moved by the electrodynamic forces of traverse *1*. The main springs *6* are secured at one end to traverse *1*, and at the other to lever *15* which is secured on shaft *9*. This was arranged in order to use the energy of the spring to accelerate the operation (closing) of the auxiliary device. Return springs are attached to lever *15*. These springs accelerate the rotation of shaft *9* when the auxiliary device operates (closes).

At small short-circuit currents which only cause small divergences of the traverse, the auxiliary device operates via feedback *11* or the release arrangement *10*, and opens the contacts of the breaker and sticking is thereby prevented.

The breaker is only tripped by the release arrangement at currents which are close to the setting of the release arrangement *10*.

At the first instant when the traverse begins to move the auxiliary device continues to remain in the "on" position and shaft *9* and plate *12* are fixed. When the main contacts have parted 2 to 3 mm the operation

of the auxiliary device takes place via feedback *11*. In this case the release *10* also operates and affects roller *14*. The effect of springs *6* and *16* is then to rotate *9* in a clockwise direction, plate *12* is shifted upwards, the movement of the traverse is accelerated and this fixed in the "off" position so that current limitation is effective and reclosure of the contacts is prevented.

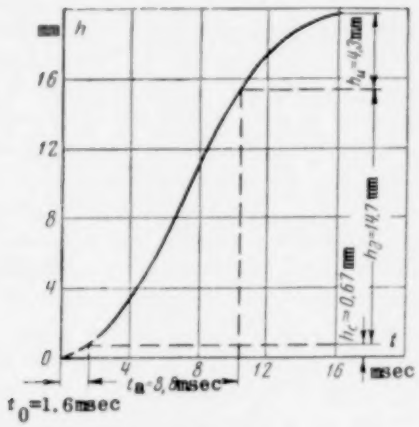

Fig. 3

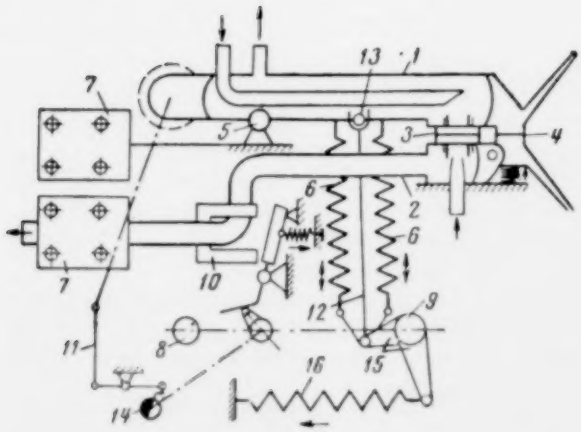

Fig. 4

Remote disconnection of the breaker is possible via the interrupting release arrangement which acts on roller *14*; remote connection can be carried out by a pneumatic drive, for instance, acting on shaft *8*. A

prototype breaker of 5000 A and 320 V has been made and tested on the system illustrated in Fig. 4. The setting of the release arrangement was 10,000 A. The dynamic setting which can be defined by the beginning of movement by the traverse, corresponds to 20 to 25 kA. Natural, or water cooling can be used depending upon the rated current of the circuit breaker. The moving parts of the breaker can be unbalanced in individual cases in use.

Fig. 5 shows an oscillogram of the breaking current with this kind of breaker in a circuit with a steady state value of the short-circuit equal to 133.2kA, at a build-up current rate of 10.6 x 10^6 A/set and a voltage of 310 V. It will be seen from the oscillogram, that the breaker limited a current up to 53 kA. No sticking of the contacts occurred at current values close to the dynamic setting or because of the vibration at currents of 5 to 10 kA. Under current limiting conditions the fundamental opening time did not exceed 1 m sec. The operating (closing) time of the breaker at over load currents was between 12 and 18 m sec depending on the value of the current to be tripped. At a load of 10 kA and a pressure on the main contacts of 30 kg the overheating of the main contacts of the test breaker do not exceed 53° C. Only about 150 litres of water were consumed for cooling at 5 kA for one hour. The breaker weighs 45 kg and its dimensions are 262 x 515 x 765 mm.

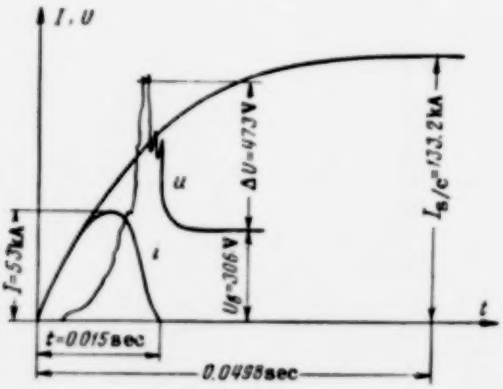

Fig. 5

The conclusion can be drawn from the tests that these experimental breakers can be used to develop actual production models.

Translated by O.M. Blunn

REFERENCES

1. Iu.G. Komarov; Russian patents Nos. 116138, 28 Nov. 1958, 117597, 12 Apr. 1959, 116139, 15 Dec. 1958, 120238, 11 June 1959, 124494, 27 May 1960.
2. Iu.G. Komarov; *Ways of producing an automatic high-speed electro-dynamic circuit breaker.* In book: *Low voltage switchgear. (Puti sozdaniia bystrodeistvuiushchego elektrodinamicheskogo vykliuchitelia. Sborn. "Elektricheskie apparaty nizkogo napriazheniia).* TsBTI elektropromyshlennosti (1959).

YEAR
1961

A METHOD OF DETERMINING THE LEAKAGE INDUCTANCE OF STATOR WINDINGS IN LARGE A.C. MACHINES WITHOUT THE ROTOR "OUT"*

R.R. PARTS

(Tallin)

(Received 18 June 1960)

The method of taking out the rotor is recommended by many authors for determining the inductive reactance of the stator windings [1, 2, 3]. The essence of this method is as follows.

A voltage of 3-phase current is supplied from an extraneous source at rated frequency to the stator. Having measured the phase voltages U_p and current I_p it is possible to obtain with a known phase resistance of the stator winding the inductive reactance

$$x_1 + x_{Sch} = \sqrt{\left(\frac{U_p}{I_p}\right)^2 - r_1^2}\,, \qquad (1)$$

where x_1 is the inductive reactance of the stator winding, and x_{Sch} the inductive reactance due to the magnetic flux within the stator air gap (Schenkel's correction).

This method was first put forward by M. Schenkel [1]. The term x_{Sch} is therefore known by some authors as *Schenkel's correction*. In order to avoid measuring the magnetic flux inside the stator gap on every occasion, on the assumption that the inductive reactance x_{Sch} is due to the main magnetic flux, the following formula has been recommended by various authors [1, 2, 3].

---

* *Elektrichestvo*, 6, 88-90, 1961.

$$x_{Sch} = Af l_1 \frac{w_1^2 k_{ow1}^2}{p} \cdot 10^{-8}, \qquad (2)$$

where f is the mains frequency, l_1 the length of the stator, w_1 the number of turns in the stator winding phase, k_{w1} the winding coefficient for the main harmonic, p the number of pole pairs and A a coefficient equal to 13.75 in Schenkel's article [1] and 15.1 in the article by Piotrovskii and Efremov [2].

Assuming that only the main magnetic field is present, as does Richter [4], the coefficient $A = 15.079$. The different values of the coefficient A are explainable by the accuracy of the calculations. The coefficient $A = 13.75$ was obtained by Schenkel as a result of artificially determining the mean amplitude of the first harmonic of the m.m.f.

YEAR 1961

Even though the removing of the rotor is a simple method, it has still not been recognized as a suitable method for determining the inductive reactance of the stator winding, since under rated conditions in the synchronous or asynchronous state the inductive reactance x_1 is clearly different from that determined by tests (by the method of rotor withdrawn) where the value $(x_1 + x_{Sch}) - x_{Sch}$.

In order to find the reasons for this discrepancy, the author has tested an A52-4 220/380 V induction motor (Table 1).

TABLE 1

x_1+x_{Sch}, Ω	x_{Sch}, Ω	$(x_1+x_{Sch})-x_{Sch}$, Ω	x_1, Ω
2.234	0.874	1.36	1.68

Schenkel's correction x_{Sch} (second column of Table 1) was calculated by formula (2) for $A = 15.79$. The inductive reactance of the stator winding $(x_1 + x_{Sch}) - x_{Sch}$ (third column of Table 1) was obtained with the rotor "out". The inductive reactance of the stator winding x_1 (fourth column of Table 1) was determined by the new method developed in the U.S.S.R. at the VNIIEM. If use is made of this method for calculating the operating characteristics of the motor, it can be seen that it corresponds to reality unlike the results obtained by Schenkel's method with the rotor out.

This circumstance is evidence of the fact that the distribution of the magnetic induction on the pole pitch is markedly different from a fundamental sinusoid with the rotor out.

When taking the curve for the distribution of the radial component of magnetic induction by oscillographing the e.m.f. in a rotating measuring coil with a diametral pitch at an instant when the current has its amplitudinal value in one phase, it was thereby confirmed that higher 3-dimensional harmonics were present [1] on the pole pitch with the rotor out.

When taking the curve for the distribution of the radial component of the magnetic induction in one section (Fig. 2) of the four-pole stator in an A 52-4 type motor by oscillographing, it was established that the magnetic induction varies practically along the inclined straight line above the slit in the semi-closed slot. Therefore, in the case of an induction motor it is advisable to proceed from the m.m.f. of the linear sectional sides of the sections on the surface of the stator instead of from points [5].

YEA
196

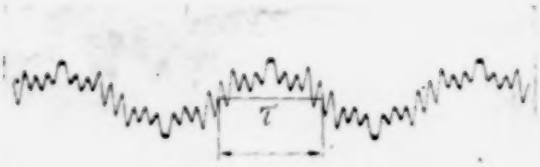

Fig. 1.

For a single phase winding with a linear sectional side, the m.m.f. on the pole pitch f_k is characterized by the expression

$$f_k = \frac{4\sqrt{2}}{\pi 2}\frac{I_0 w_k q}{\frac{\pi b}{\tau 2}}\left[\sum(-1)^{\frac{\nu-1}{2}}\frac{k_{o\nu}}{\nu^3}\times\right.$$
$$\left.\times \sin\nu\frac{\pi}{\tau}\frac{b}{2}\cos\nu\frac{\pi}{\tau}x\right]\cos\omega t, \qquad (3)$$

where I_0 is the current in the turn, w_k the number of turns in the section, q the number of slots per pole and phase, ν the order of the three dimensional harmonic, b the width of a linear sectional side, τ the pole pitch, x the transient coordinate along the base with an origin in the middle of the pole, ω the angular frequency of the network, and t the time.

In its more general form the curve for the radial component of magnetic induction on the pole pitch is characterized by the expression

$$B=\left[B_{\delta 1}\cos\frac{\pi}{\tau}x+B_{\delta 3}\cos 3\frac{\pi}{\tau}x+\ldots+\right.$$
$$\left.+B_{\delta\nu}\cos\nu\frac{\pi}{\tau}x\right]\cos\omega t, \tag{4}$$

whilst the magnetic flux through the pole pitch equals:

$$\Phi=\left(\sum_{\nu}\Phi_{\nu}\right)\cos\omega t, \tag{5}$$

where

$$\Phi_{\nu}=(-1)^{\frac{\nu-1}{2}}\frac{2}{\pi}B_{\delta\nu}\frac{\tau_1}{\nu}l_1$$

YEAR
1961

is the higher three dimensional harmonic of magnetic flux, and $\Psi_{\nu}=\Phi_{\nu}w_1k_{ow\nu}$ is the flux coupling.

For a single phase winding the effective value of the e.m.f. will be

$$E=E_1+E_1\left[-\frac{1}{3}\cdot\frac{B_{\delta 3}}{B_{\delta 1}}\cdot\frac{k_{ow3}}{k_{ow1}}+\right.$$
$$\left.+\ldots+(-1)^{\frac{\nu-1}{2}}\frac{1}{\nu}\cdot\frac{B_{\delta\nu}}{B_{\delta 1}}\cdot\frac{k_{ow\nu}}{k_{ow1}}\right], \tag{6}$$

where

$$E_1=4fB_{\delta 1}\tau_1 l_1 w_1 k_{ow1}.$$

Dividing expression (6) by the magnetization current,

$$x_{m0}+x_{h0}=\frac{E_1}{I_0}+$$
$$+\frac{E_1}{I_0}\left[\sum_{\nu\geqslant 3}(-1)^{\frac{\nu-1}{2}}\frac{B_{\delta\nu}}{\nu B_{\delta 1}}\cdot\frac{k_{ow\nu}}{k_{ow1}}\right], \tag{7}$$

where x_{m0} is the fundamental inductive reactance of the single phase winding and x_{h0} the inductive reactance of single phase winding due to the higher three dimensional harmonics.

In accordance with formula (7) the expression for the inductive

reactance x_{h0} can be written in the form

$$x_{h0} = x_{m0}\left[\sum_{\nu\geqslant 3}(-1)^{\frac{\nu-1}{2}}\frac{1}{\nu}\cdot\frac{B_{\delta\nu}}{B_{\delta 1}}\cdot\frac{k_{o\omega\nu}}{k_{o\omega 1}}\right]. \tag{8}$$

For a symmetrical multi-pnase winding the inductive reactance x_h due to the higher three dimensional harmonics equals

$$x_h = x_m\left[\Sigma(-1)^{\frac{\nu-1}{2}}\frac{1}{\nu}\cdot\frac{B_{\delta\nu}}{B_{\delta 1}}\cdot\frac{k_{o\omega\nu}}{k_{o\omega 1}}\right], \tag{9}$$

where x_m is the inductive reactance of the multi-phase winding due to the main magnetic field.

It will be seen from expressions (8) and (9) that to determine the inductive reactance of the higher three dimensional harmonics with known winding coefficients, it is sufficient to know the ratio of the amplitude of the magnetic induction of the higher three dimensional harmonic to the amplitude of magnetic induction of the fundamental harmonic, and to know the sign of the ratio in question.

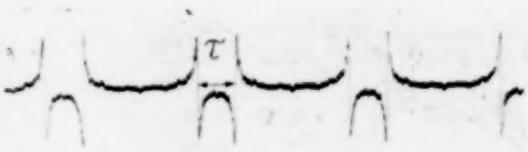

Fig. 2.

It can be seen that this is true for a symmetrical 3-phase winding with a whole number of slots per pole and phase when the curve for the magnetic induction on the pole pitch is a replica of the m.m.f. curve [6, page 1 2 4]. Expression (9) then takes the form

$$x_h = x_m\sum\frac{1}{\nu^2}\cdot\frac{k^2_{o\omega\nu}}{k^2_{o\omega 1}}, \tag{10}$$

where $\nu = 5, 7, 11, 13, \ldots$.

It should be pointed out that x_h can be calculated by formula (10) by means of curves showing the relationship between the sum of the resistances and the number of slots per pole and phase [4 et al.]

Using expression (3), the amplitude of the harmonic m.m.f. of a

multiphase winding per pair of poles equals

$$F_\nu = m\frac{4\sqrt{2}}{\pi 2}\cdot\frac{I_\phi w_k q(-1)^{\frac{\nu-1}{2}}}{\frac{\pi}{\tau}\cdot\frac{b}{2}\nu^2}k_{o\omega\nu}\sin\nu\frac{\pi}{\tau}\cdot\frac{b}{2}, \tag{11}$$

$$\frac{F_\nu}{F_1} = \frac{k_{o\omega\nu}}{\nu^2 k_{o\omega 1}}\cdot\frac{\sin\nu\frac{\pi}{\tau}\cdot\frac{b}{2}}{\sin\frac{\pi}{\tau}\cdot\frac{b}{2}}(-1)^{\frac{\nu-1}{2}}. \tag{12}$$

With the rotor out the expression for the tangential component of the magnetic field intensity of the higher 3-dimensional harmonic can be represented in the form:

$$H_{\varphi\nu 1} = -\frac{B_{\delta\nu}}{\mu_0}\left(\frac{R}{R_1}\right)^{\nu p-1}\sin\nu p\varphi, \tag{13}$$

whilst the m.m.f. of the higher 3-dimensional harmonic between the middles of two adjacent poles will be:

$$F_\nu = \int_{\nu p\varphi=\pi}^{\nu p\varphi=0}(H_{\varphi\nu 1})_{R=R_1}R_1 d\varphi = \frac{2}{\nu p}\cdot\frac{B_{\delta\nu}}{\mu_0}R_1, \tag{14}$$

where R_1 is the radius of the internal surface of the stator stamping, μ_0 the magnetic permeability of the air and R, φ are transient cylindrical coordinates.

Hence it follows:

$$\frac{F_\nu}{F_1} = \frac{B_{\delta\nu}}{\nu B_{\delta 1}}. \tag{15}$$

From (12) and (15):

$$\frac{B_{\delta\nu}}{B_{\delta 1}} = \frac{k_{o\omega\nu}}{\nu k_{o\omega 1}}\cdot\frac{\sin\nu\frac{\pi}{\tau}\cdot\frac{b}{2}}{\sin\frac{\pi}{\tau}\cdot\frac{b}{2}}(-1)^{\frac{\nu-1}{2}}; \tag{16}$$

and consequently, with the rotor out the inductive reactance due to the

high 3-dimensional harmonics equals

$$x_h = x_m \sum \frac{k_{o\nu}^2}{\nu^2 k_{o1}^2} \cdot \frac{\sin \nu \frac{\pi}{\tau} \cdot \frac{b}{2}}{\sin \frac{\pi}{\tau} \cdot \frac{b}{2}}. \qquad (17)$$

It should be pointed out that some authors consider that the reactance x_h found in this way is "static". The inductive reactance due to the main magnetic field equals

$$x_m = \frac{4mfw_1^2 k_{o1}^2 \tau_i l_i \mu_0}{\pi R_1 k_{F_1}} \cdot \frac{\sin \frac{\pi}{\tau} \cdot \frac{b}{2}}{\frac{\pi}{\tau} \cdot \frac{b}{2}}, \qquad (18)$$

where k_{F_1} is a coefficient of saturation practically equal to unity.

Since the inductive reactance due to the higher 3-dimensional harmonics varies greatly as a function of the design of the rotor, it is therefore of interest to establish how accurately the withdrawn rotor method permits the determination of the inductive reactance of the stator which is in effect the sum of the inductive reactance of the slot x_{1s} and face x_{1f} parts.

From test results on an A 52-4 type motor

$$x_{1s} + x_{1f} = \sqrt{\left(\frac{U_p}{I_p}\right)^2 - r_1^2} - (x_m + x_h) =$$
$$= 2.234 - (0.874 + 0.153) = 1.207 \quad \Omega,$$

where x_m and x_h have been found from expressions (17) and (18). According to the proposed Russian method $x_{1s} + x_{1f} = 1.205\ \Omega$. Thus the test results are almost the same as the calculations in this case.

Conclusions

The leakage of the stator with the rotor out is not the same as the leakage in normal operation under synchronous or asynchronous conditions. This occurs particularly in induction machines where the differential leakage depends on the type of rotor circuit, saturation, the air gap, the bevel of the rotor slots and so on.

The numerical value of the inductive reactance for stator leakage with the rotor in will only be the same as its value with the rotor out

in particular cases.

Translated by O.M. Blum

REFERENCES

1. M. Schenkel; *E und M*, 27, 201-203 (1909).
2. L.M. Piotrovskii and D.V. Efremov; *Elektrichestvo*, 8 (1930).
3. A.A. Vainfil'd; *ADP type controlled motors with hollow rotors, (Upravlaemye elektrodvigateli s polysn rotorom tipa ADP)*, Sudpromgiz (1957).
4. R. Rikhter; *Electrical machines, (Elektricheskie mashiny)*, Vol. 1, pp. 165, 166, 207 and 208 (1935).
5. L.M. Piotrovskii; *Elektrical machines (Elektricheskie mashiny)*, Gosenergoizdat, 317 (1949).
6. M.P. Kostenko and L.M. Piotrovskii; *Electrical machines Pt. II, (Electricheskie mashiny Ch. II)*, Gosenergoizdat, p. 124 (1957).

YEAR
1961

ABSTRACTS FROM PAPERS PUBLISHED IN ELEKTRICHESTVO No. 6, 1961

Leading article

A new era in the history of humanity. V.V. Dobronravov, (pp. 1-4).

A tribute is paid to all persons associated with Gagarin's flight in space. The significance of the achievement is then considered in general terms.

Amplifiers

Operation of a full-wave d.c. magnetic amplifier. R.A. Lipman et al., (pp. 74-78).

A new type of push-pull d.c. magnetic amplifier is described which it is claimed has a highly efficient performance.

A magneto-transistor power amplifier with a differentially connected load. M.E. Poiurovskii, (pp. 56-58).

A short description is given of a push-pull magneto-transistor power amplifier in which the transistors act as switches. Pulse-width modulation of the output signal is effected by a transformer with a core having a rectangular hysteresis loop.

Control engineering

Using critical generator self-excitation in closed motor-generator sets. V.I. Kliuchev, (pp. 26-32).

The author considers the use of negative voltage feedback from the generator in the state of critical self-excitation in order to improve the dynamic behaviour of amplifier-controlled motor-generator sets and make them more compact.

Dynamic self-regulation of multi-motor drives in paper-making plant. G.M. Levin, (pp. 49-53).

A graphical-analytical method is proposed for determining those dynamic properties of motor drives which will keep the tension of the paper within specified limits in paper-making plant.

Ignitrons

An electromagnetic ignition system for ignitrons. Yu.A. Shmain et al., (pp. 61-65).

An account is given of the research into the ignition systems of ignitrons at the All-Union Power Research Institute. A method has been developed for analysing the operation of electromagnetic pulse generators with a variable load impedance.

YEAR 1961

Power systems

A statistical appraisal of urban network operation. B.V. Gnedenko, et al., (pp. 71-74).

The authors confine themselves to the implications of using probability methods to assess the operating conditions of low voltage mains.

Increasing the steady state stability limit by regulating the d.c. transmission. V.G. Novitskii, (pp. 58-61).

The limit of static stability in the transmission of a.c. can be increased by automatically varying the static characteristics of the rectifiers. Here the transmission of d.c. is regulated in accordance with the parameters of the a.c. system.

Deformation of the waves in a multi-conductor line due to the earth and conductor resistance. M.V. Kostenko, (pp. 5-10).

A practical method is proposed for calculating the distortion of the wave in multi-wire overhead transmission lines. An approximate solution is obtained in terms of tabulated time functions which take into account balancing currents and earth losses. An accuracy to within 15% is claimed over a 10 km stretch of line.

Estimating the effect of meteorological conditions on the electrical strength of external insulation. N.N. Beliakov et al., (pp. 20-26).

Two correcting coefficients are produced which it is claimed

characterize the electrical strength of all types of external insulation. From tests it has been established that these coefficients define meterological conditions and altitude with different probabilities. These relationships can be used in the design of the external insulation of distribution gear and high voltage transmission lines.

Rotating machines

A method of studying steady state fault currents in a self-excited alternator. D.V. Vilesov et al., (pp. 45-49).

A new method is proposed for calculating the steady state short circuit current in an independent alternator system. The results are used to determine the transfer and super-transfer components of the short circuit current more accurately.

The voltage of a self-excited alternator with a suddenly applied load. M.I. Aliab'ev, (pp. 79-82).

An analysis is made of the equations of an idealized self-excited alternator with an automatic voltage control system.

Traction

Special operating conditions of power systems supplying a.c. electric locomotives. N.A. Mel'nikov et al., (pp. 10-15).

A statistical method is proposed for estimating the operating conditions of electrical equipment used on very long stretches of railway line to supply a.c. electric locomotives.

The effect of external voltage surges on H60 type electric locomotives. M.N. Novikov, (pp. 15-20).

An account is given of the research carried out at the Institute of Railway Engineers in Leningrad to establish the effect of external voltage surges on the insulation of gear used in the large H60 locomotive's low voltage transformer circuit.

Transformers

Some special characteristics of transformer insulation. G. Slovikovski, Warsaw, (pp. 82-87).

A study is made of the factors affecting a certain ratio r_{60}/r_{15} which is used to define the electrical characteristics of transformer

insulation. Here r_{60} is the resistance 60 sec after connecting the transformer and r_{15} that after 15 sec. The use of this criterion is considered for service tests and final factory tests.

An approximate method of calculating overvoltages across the secondary windings of current transformers.
Ya. S. Gel'fand, (pp. 66-71).

The proposed method is based on the approximation of the actual e.m.f. curve for the open secondary winding of the current transformer without losses by triangular pulses of alternate polarity with a large mark space ratio. The resulting curve is expanded into a Fourier series and the effect of losses and the load on the amplitude and phase of the individual harmonic components is then taken into account. Subsequent summation gives the required voltage amplitude across the secondary winding.

YEAR
1961

ABSTRACTS FROM PAPERS PUBLISHED IN ELEKTRICHESTVO No. 7, 1961

Leading article

To new achievements in the development of Soviet science. (pp. 1-6).

An account is given of a recent conference which was held in the Kremlin to discuss the future development of Soviet science. Development work, applied research and fundamental research was discussed.

Capacitors

Determining the initial conditions for sudden changes in voltages and currents. I.A. Zaitsev *et al.*, (pp. 52-55).

A contribution is made to the determination of initial conditions when sudden changes occur in the currents in inductances or voltages across capacitors. Simple schemes are obtained by analysing commutation behaviour which make it possible to determine the initial conditions for sudden changes in voltages and currents quickly.

Determining the reactive power in capacitors. N.I. Nazarov *et al.* (pp. 55-59).

It is considered that the specific dissipating surface of a capacitor varies with the shape of the housing and its dimensions. For a given volume, the dissipating surface is maximum for a rectangular parallelepiped with the minimum permissible width of base. The reactive power of the capacitor unit depends on the design of the capacitor as well as the physical characteristics of the material.

Control engineering

Joint selection of the motor criteria and the gear ratio. D. A. Popov, (pp. 63-67).

A study is made of the problems connected with choosing the optimum gear ratio for an electric drive under starting conditions when the torque of the motor and the moment of mechanical resistance of the drive device are constant. The study is made from the point of view of minimizing weight.

Use of the phase plane method for studying transient mechanical behaviour in electric drives. L. I. Gandzha, (pp. 68-72).

Phase diagrams of transient behaviour are constructed from an analysis of the equation of motion of the drive for the various possible types of load.

YEAR 1961

The use of saturable reactors to prevent variation in the torque of induction motors due to transient currents. M. M. Sokolov, (pp. 72-75).

An account is given of tests on electric drives with induction motors and saturable reactors which show that a smooth increase in motor torque and speed can be obtained on starting and reversing. The connexion of saturable reactors in the stator circuit only increases acceleration time slightly. Acceleration time depends on the magnetization current of the reactor.

A frequency-controlled drive for a horizontal planing machine. D. A. Zavalishin *et al.*, (pp. 75-79).

It is argued that the best frequency-controlled asynchronous drive system for horizontal planing machines is one with a compensated collector generator excited on the stator side. A detailed account is given of a prototype system.

Elimination of zones of insensitivity in ferromagnetic pickups and amplifiers. B. K. Karpenko, (pp. 84-86).

A cheap and effective way of eliminating dead bands in pick-ups and amplifiers with ferromagnetic cores is proposed by the use of an additional magnetic circuit.

Magnetism

The permeance of magnetic circuits with teeth. Yu.S. Rusin, (pp. 59-63).

Owing to the considerable leakage flux in magnetic circuits with teeth, the author proposes an approximate estimate of permeance which is based on a particular idealization of the field of the system. The space surrounding the pole ends is divided into separate regions and, depending on the shape of the poles, the field between the faces is studied separately from that between the ribs. The type of magnetic circuit in question is illustrated in a diagram.

Power systems

Long-distance power transmission with d.c. magnetized reactor-transformers and forced capacitor banks. D.I. Azar'ev, (pp. 24-30).

The cost of transmission can be reduced by combining a transformer with an automatically-controlled high-voltage reactor in a high-speed unit which is capable of reducing overvoltages and increasing carrying capacity. The magnetic system of the reactor is split into parallel branches which are magnetized by d.c. in such a way that the fluxes in the branches are in opposite directions.

Automatic equipment for power system continuity. I.A. Syromiatnikov, (pp. 18-24).

The author considers the main automatic Soviet equipment available for improving the reliability of power system operation, namely, excitation regulators, frequency unloading devices, reserve supply auxiliaries, automatic reclosure, starting devices which react to the rate of change in voltage and a hydraulic differentiator for turbine steam.

Zero sequence equivalent networks for transmission lines with different voltages. N.G. Geinin, (pp. 79-81).

It is shown how to compile a zero sequence equivalent network which includes the mutual inductance between two or several transmission lines when each of the nearby lines is of a different voltage.

Rotating machines

The effect of excitation systems on the stability of large interconnected turbo-generators. V.M. Bobrov *et al.*, (pp. 7-13).

A study is made of the stability of large turbo-generators with

different systems of excitation. The use of electrodynamic modelling has made it possible to use natural excitation regulators, find their optimum adjustment and study electromechanical phenomena during transient behaviour.

Artificial damping in large synchronous machines. I.D. Urusov *et al.*, (pp. 13-18).

Instead of increasing the flywheel mass, it is proposed to use a system of artificial damping to reduce the oscillation of synchronous machines with a pulsating load. Artificial damping is based on the creation of an additional electromagnetic rotational torque on the shaft by introducing additional periodic currents in the rotor circuits. The theory of the method is given along with test results.

Analysis of dynamic stability with the effect of damper windings, speed governors and excitation included. K.I. Bogatev, (pp. 31-34).

YEAR 1961

A refinement to the method of successive intervals is proposed which makes it possible to include the effect of damper windings, speed governors and excitation when an analytical estimate of dynamic stability is required for synchronous alternators.

Experimental determination of the m.m.f. of the armature commutation reaction in d.c. machines. V.A. Lifanov, (pp. 81-84).

A method is proposed which dispenses with calculated data in the determination of the m.m.f. of the armature commutation reaction by a Hall e.m.f. transducer.

Traction

Reduction of wheel-spin on electric locomotives. B.P. Petrov, (pp. 35-41).

A study is made of the factors affecting high adhesion factors for electric locomotives. Recommendations are made for automatically stopping wheel spin.

Transformers

Problems of voltage regulation in auto-transformers. A.G. Kraiz, (pp. 41-48).

A method is described for comparing different systems of voltage regulation for large auto-transformers using the typical power of auto-transformers. A refined method of analysis is proposed for the

system of regulation in the neutral of the auto-transformer. It can be used to specify the limits of regulation with over- or under-excitation. A short description is given of a new 220 kV auto-transformer with built-in apparatus for regulating the voltage.

Voltage stabilizers

Ferroresonant voltage stabilizers using magnetic material with a rectangular characteristic. D. I. Bogdanov, (pp.48-51).

A theoretical study is made of the phenomena associated with the operation under load of ferroresonant voltage stabilizers in which the saturable core is made of cold-rolled steel or magnetic alloy with a high coefficient of rectangularity.

YEA
196

ABSTRACTS FROM PAPERS PUBLISHED IN ELEKTRICHESTVO No. 8, 1961

YEAR 1961

Computers

Electronic simulation of electrical circuits, V.G. Vasil'ev *et al.*, (pp.41-45).

Certain aspects of the simulation of R, L and C circuits are considered on the basis of a simple example. The rules of the "dual circuit" method of analysis are formulated. An electrical circuit with one voltage source is simulated without forming equations for the circuit or the model. A minimum of amplifiers and integrating elements is required.

Regulation of the excitation of two synchronous machines operating in parallel, G.V. Mikhnevich *et al.*, (pp.31-35).

An analogue computer method is proposed for determining the optimum structure of the control signals with respect to their derivatives and assessing their effect on a coefficient of regulation for the excitation of two synchronous machines operating in parallel. The results for generators at the Stalingrad hydro-electric station are given by way of illustration.

Control engineering

The motor drive of a reversible cold rolling mill, I.M. Tolmach *et al.*, (pp.79-81).

An account is given of the motor drive which has been installed on a four-roll mill for low and medium carbon steel strip up to 300 mm wide with reduction from 3 to 0.2 mm in up to nine passes. The drive features the use of e.m.f. and current regulators to maintain rolling tension.

Measuring amplifiers for centralized automatic control systems, R.R. Kharchenko *et al.*, (pp.7-13).

Attention is concentrated on those d.c. measuring amplifiers which

are used to convert the signals of pick-ups in group data-processing circuits. The authors review six types of system covering the combined transmission of the amplified signal without a device for correcting zero drift, and wideband amplifiers with a device for correcting zero drift.

Electrical steel

The properties of 1 mm cold rolled electrical steel, A.I. Beliakov *et al.*, (pp. 82-83).

A short account is given of the properties of the 1 mm gauge cold-rolled grain-oriented steel for the poles of d.c. electrical machines now being produced in Novosibirsk.

Insulation

Interdependence of the physical properties of organic and inorganic polymers, N.I. Vorob'ev *et al.*, (pp. 76-78).

To simplify the problem of investigating the large number of polymers which are available, the author takes the magnitude of the inter-molecular forces as the main criterion defining the physical properties of many polymer substances.

The dielectric permeability and tangent of the loss angle for paper dielectrics, S.K. Medvedev, (pp. 66-72).

Formulae are produced for calculating ϵ, tan δ and other characteristics of paper on the basis of the actual structure of the paper on the assumption that the relative thickness of the cellulose in the space between the layers varies between 0 and 1 according to a certain law. The pores are assumed to be in series in each individual volume of cellulose.

Power systems

Determining optimum operating conditions for power systems, V.M. Gornshtein, (pp. 19-24).

A study is made of common errors which are said to be made in the economic analysis of power system analysis.

Tuned power transmission systems, V.K. Shcherbakov, (pp. 25-30).

It is stated that theory and laboratory investigations indicate that half-wave tuned transmission lines of 2000 and 2500 km can

ensure high steady state stability and relative voltage stability at line ends. The author disputes the reasons which have been given for not using this system and advocates its use on the grounds of efficiency and the possibility of intermediate off-take of power along the line.

Rotating Machines

Turbo-generators of large unit capacity, V.V. Titov, (pp. 1-4).

A short account is given of the work which has been done at the Electrosila works in the U.S.S.R. on the development of 300 and 500 MW turbo-generators. The new 300 MW generators are described and it is stated that 500 MW generators can be made on the same principles when the demand arises. Extremely high efficiency is claimed and it is an interesting paper. Unfortunately, this account does not explain how the efficiency is achieved or how it is calculated and some of the main features have their counterpart in recent American, Swiss and British innovations.

YEAR
1961

The problems of developing new small and F.H.P. motors, N.P. Ermolin, (pp. 4-7).

This paper classifies the problems involved in the development of small and f.h.p. motors into those which are common to all types of such motor and those which are special for particular applications. The main purpose of the article is to draw attention to the need for keeping State Standards up to date and co-ordinating research.

New 100 kW amplidynes, B.F. Tokarev *et al.*, (pp. 14-18).

Two new types of amplidyne are to be produced in the U.S.S.R., namely, three-stage amplidynes with a longitudinal field, and multipole amplidynes with a transverse field (four and eight poles) with increased magnetization of the winding along the transverse axis or with additional poles along the longitudinal and transverse axes. The equipment is compared and the respective merits assessed.

A new principle of obtaining constant advance times in automatic synchronizers, N.N. Vostroknutov *et al.*, (pp. 35-40).

In this article the synchronizers are defined as devices which select the angle of lead and stop action if the amount of slip is too large. A new approach to the design of the time advance elements of such synchronizers is proposed in which the angle of lead is directly converted into a proportional d.c. voltage. This provides the possibility of twice-differentiating this voltage, as required for considering acceleration of slip. A detailed account

is given of a device for the exact synchronization of generators.

A two-motor machine-valve stage with semiconductor rectifiers, M.G. Chilikin *et al.*, (pp. 50-56).

An appraisal is made of the advantages of replacing one large slip ring motor by two smaller motors of the same total power in high speed drives of 1000 to 10,000 kW and 5000-7000 rev/min. In the proposed system the slip energy is converted by semiconductor diodes and it then passes into the network.

Calculation of the steady state errors in speed governors for d.c. motors, S.S. Roizen, (pp. 56-62).

Two fundamental methods of speed control for d.c. motors are considered with a view to determining the accuracy with which speed governors operate in the automatically controlled drives of rolling mills and lathes etc. Formulae are produced for calculating the degree of error under steady state conditions.

A study of the e.m.f. induced in electrical machines using an electrolytic tank, K.S. Demirchian *et al.*, (pp. 62-66).

In the proposed method the model of the rotor is fixed on a plate which slides along the bottom of the tank. A layer of vaseline is placed between the bottom of the tank and the plate to keep out the electrolyte and reduce friction. The model of the stator is secured to a fixed plate. In order to determine the potential differences accurately, the linear displacement of the rotor is measured and not the angle of rotation.

Switchgear

The measurement of large transient currents, V.D. Liashenko, (pp. 46-50).

In short-circuit tests on switchgear it has been possible to combine the advantages of shunts and current transformers in the measurement of the large transient currents which arise. The Switchgear Laboratory of the All-Union Electrical Engineering Institute has developed a successful method of measurement with air-cored current transformers using a toroidal core with a high-impedance winding, a d.c. amplifier with an integrating capacitance at the input and an electromagnetic oscillograph vibrator.

The leader stage of a spark discharge, V.P. Larionov, (pp. 72-76).

The author develops the notion of a leader stage in spark discharges

in long air gaps which precedes the main discharge and forms a leader channel between the electrodes. The mean longitudinal potential channel between the electrodes. The mean longitudinal potential gradients in the leader channel are determined along with the conductance of the leader channel, the concentration of the electrons and the time necessary for the formation of the leader channel.

Translated by O. Blunn

YEAR
1961

YEA
196

AUTOMATIC EQUIPMENT FOR IMPROVING POWER SYSTEM CONTINUITY*

I. A. SYROMIATNIKOV

Moscow

(Received 4 July 1960)

YEAR
1961

It is a matter of government policy to proceed with the automation and mechanization of production and in this connexion special attention is being paid to low-cost methods of power supply, without the use of circuit breakers on the high-voltage side and the use of short-circuiters and disconnectors. Such methods can only be adopted on the basis of automation.

Widespread use is now made in the U.S.S.R. of such equipment as high-speed protection, automatic excitation regulation of synchronous machines and relay-forcing of excitation, automatic reclosure of lines, bus-bars and transformers, automatic connexion of the standby supply, automatic frequency control, automatic self-synchronization and automatic starting of the hydro-electric units, dispatcher control, and so on. The use of this equipment has considerably improved the continuity of the power supply and made it possible to ensure the static and dynamic stability of the power system.

In this paper it is proposed to review the main automatic equipment which is available in the U.S.S.R. for improving the reliability of power system operation.

Automatic control of excitation. The automatic excitation regulators of synchronous machines are one of the most important means of improving power system reliability. Operating experience and tests which have

---

* *Elektrichestvo*, 7, 18-24, 1961.

been carried out in the U.S.S.R. have shown that the main requirement of automatic excitation regulators is to force the excitation voltage up to its maximum value.

A system of compounding with an electromagnetic corrector is now extensively used for automatic excitation of regulation. It is supplemented by relay forcing of excitation which ensures maximum excitation if the voltage drops by more than 15 per cent. A new phase compounding system has been developed in which the current in the excitation winding of the exciter depends on the phase of the stator current as well as its magnitude. This includes the control of voltage under normal conditions and reduces the power of the corrector.

In order to improve static and dynamic stability in long distance transmission, use is also made of high response regulators which react to the voltage, current, and the first and second derivatives of the current and ensure the desired level of voltage on the high-voltage bus-bars after the transformers under normal conditions.

The exciters of generators which are used on long distance transmission must have higher limits and rates of voltage build-up. Thus, the ceiling of the voltage of the excitors for the generators at the Volga hydro-electric power station and the Stalingrad hydro-electric power station is four times their rated voltage, whilst the rate of voltage build-up is five times greater. At such high values, ionic excitation is much more economical. However, tests at the Volga hydro-electric station have shown that the maximum power under conditions of static stability is approximately the same for machine excitation with a maximum voltage 1.8 times greater than the rated voltage if a high response regulator is used, and the time constant of the excitation winding is 0.2-0.3 sec as for ionic excitation with a ceiling four times greater than the rated voltage. The results were only slightly less satisfactory in relation to dynamic stability.

The use of high response autometic excitation regulators is not the complete answer to the problem of ensuring dynamic stability, but this problem can be solved by such means as high-speed clearance of short-circuits, mechanical or electrical braking of generators and the disconnexion of part of the generators.

Automatic frequency control. Serious faults due to a deficiency of active power can be reduced by using automatic devices which disconnect the consumers if the frequency drops to a dangerous level.

It is considered dangerous if the frequency drops to 47-48 c/s for a long period of time. Such a drop in frequency reduces the efficiency of fans, flue gas pumps and especially the feed pumps of fuel-burning

power stations. The output of the station is reduced as a result and the deficiency of power in the system is aggravated so that frequency can be reduced in a vicious spiral Automatic load shedding devices begin to act at the frequency of 48 c/s.

In selecting which loads are to be shed, it is necessary to consider the maximum generator power which can be disconnected in the power system in question. Consumers must only be disconnected one group at a time in order to avoid unnecessary inconvenience. The frequency must be raised to 49-50 c/s after the load shedding devices have operated.

After the main groups of consumers have been disconnected, the frequency can still settle at 48 c/s. A special device is provided which cuts off another group of consumers at 47 c/s with a time lag of 20-30 sec.

The efficiency of this load-shedding system depends upon the instantaneous operation of the automatic equipment. It is, however, necessary to consider the possibility of the frequency relays operating incorrectly owing to sudden changes in voltage during short-circuits. The relay contacts may be momentarily closed by transient conditions in the relay winding circuits. A minimum time delay of 0.5 sec is therefore allowed.

YEAR
1961

Consumers are automatically reconnected by the automatic reclosure system when the frequency is restored.

The average number oi successful operations of such frequency regulators is shown in Table 1.

Over the past eleven years each device operates about 1.9 times per year.

The maintenance of normal voltage when a reduction in frequency occurs results in an increased consumption of reactive power at a time when the supply is restricted. It is therefore desirable to reduce the voltage if the frequency is reduced.

Soviet power systems which are served by hydro-electric power stations have a system of automatically starting and connecting standby hydro-electric generators when the frequency is reduced. Total load is reached 60-90 sec after starting. Use is made of speed governors to load partially unloaded hydro-electric generators and to convert hydro-electric generators operating as synchronous condensers. As a result partially unloaded generators take up their full load after 3-5 sec, and those operating as condensers after about 30 sec.

The device which is used for automatically starting and connecting

TABLE 1

Years*	1945	1946	1947	1948	1949	1950	1951	1952	1953	1954	1955	1956	1957	1958	1959
No. of frequency regulators	96	130	157	265	398	594	631	711	730	827	1 011	1 083	—	1 349	1 526
Percentage of 1945	100	136	163	275	415	620	660	740	780	863	1 050	1 240	—	1 400	1 600
No. of successful operations	—	—	—	325	351	355	472	495	462	353	489	319	—	405	703
Average number of operations	—	—	—	0.81	1.12	1.2	1.34	1.44	1 58	2.34	2.1	3.4	—	3.33	2.17

* As at 31 December each year

YEA
196

hydro-electric generators incorporates a frequency difference relay (for the difference between the generator and network frequency), which operates in the presence of about 5 per cent slip and connects the generator in the network without synchronization. If several generators have to be started, the starting signals are sent off at intervals of about 20-30 sec.

Automatic connexion of standby supply. This type of automatic equipment was first successfully used for power station auxiliaries. It was extended to the network and installed in industrial enterprises later. This system is used to connect standby transformers, lines, motors and sectional circuit breakers whenever the voltages disappear, including short-circuits on the bus-bars. Operating experience shows that the supply of a voltage after a short-circuit on the bus-bars has in many cases been successful in preventing a fault.

Table 2 shows the average number of successful operations of standby supply controllers.

YEAR
1961

The controllers are usually operated by the auxiliary contacts of the main circuit breaker or a voltage relay which reacts to the disappearance of voltage on the bus-bars from which the consumers are supplied. In the first case, the standby supply is connected instantaneously on disconnexion of the supply source, but in the second case the voltage relay operates even if the voltage only disappears momentarily and so a time lag is provided.

During the past twelve years each controller has on average operated 4.4 times per year.

Automatic reclosures. Automatic reclosure is extensively used on overhead lines and cable runs, substation bus-bars, transformers, motors, generators and condensers.

The statistics of automatic reclosure devices are given in Table 3. On average each device has operated 1.34 times per year over the past fifteen years.

The use of automatic reclosure on overhead lines is obligatory. Three phase instantaneous automatic reclosure is mainly used, but single-phase automatic reclosure is used on important transit and spur 110-220 kV lines and in networks with large earth faults. Single-phase automatic reclosure makes it possible to use lines on two phases without interrupting the supply. Unfortunately, single-phase automatic reclosure is a relatively complicated system.

TABLE 2

Years*	1945	1946	1947	1948	1949	1950	1951	1952	1953	1954	1955	1956	1957	1958	1959
No. of standby supply controllers	274	400	483	633	941	1 143	1 662	2 204	2 792	3 567	6 142	7 370	8 852	10 592	11 992
Percentage of 1945	100	146	176	231	308	418	610	805	925	1 300	2 240	2 700	3 230	3 900	4 370
No. of successful operations	—	—	—	120	196	171	225	611	640	1 049	1 404	1 479	1 498	2 686	3 082
Percentage	—	—	—	75.5	90.8	95	81	95.3	95.9	96.5	94.3	96.2	95.3	96	96.5
Average number of operations	—	—	—	5.27	4.8	6.7	7.4	3.61	4.36	3.4	4.3	5.0	5.9	4	3.9

* As at 31 December each year

Operating experience has shown that automatic reclosure can be successfully used on cable runs with intermediate substations. Thus, for example, 54.5 per cent of all automatic reclosings on cable runs were successful, which compared favourably with 59.2 per cent on overhead lines. This is obviously explained by the fact that a large number of short-circuits occur on the bus-bars of substations.

Automatic reclosure can be successfully used for the supply of voltage to substation bus-bars no matter what the reason for the disappearance of the voltage. In this case automatic reclosure is usually operated by the differential protection of the bus-bars. However, if there is one transformer at a stepdown substation it is necessary to use automatic reclosure which is operated from the current protection. The automatic reclosure of transformers is operated by the auxiliary switches of circuit breakers, but they are interlocked with the internal protection of the transformer.

YEAR
1961

Statistics show that 75-80 per cent of all bus-bar and transformer automatic reclosings are successful. Each successful operation prevents the disruption of the power supply for a large number of consumers.

It is well known that the self-starting of all motors is not always successful after the clearance of short-circuits. Use may therefore be found of alternative automatic reclosure for maintaining important synchronous and asynchronous motors in operation. Experience with this type of automatic reclosure in the oil fields in Baku for the pump motors has shown that it is extremely efficient and reliable. This type of automatic equipment could be used at power stations and in other plants where there is no maintenance staff on duty to start the motors which were disconnected in order to facilitate the self-starting of the the important motors.

Automatic reclosure after restoration of frequency was first used in the White Russian power system on the suggestion of I.N. Aleksandrov and A.Sh. Fridliand. Now they are in use in a number of power systems. This type of automatic reclosure must be considered very promising in connexion with the introduction of automatic equipment for starting standby units in the event of a reduction in frequency.

Use is now made in some cases of boiler-turbine-generator-transformer-line units with about 30 breakers in the electric circuit. This involves the widespread use of automatic reclosure devices in conjunction with self-synchronization devices.

In the event of a line short-circuit, the unit is disconnected at the

TABLE 3

Years*	1945	1946	1947	1948	1949	1950	1951	1952	1953	1954	1955	1956	1957	1958	1959
No. of automatic reclosure devices	1 074	1 229	1 518	1 945	2 416	2 875	3 486	4 127	4 736	5 636	7 129	8 787	10 198	12 630	15 272
Percentage of 1945	100	114	141	181	225	266	325	380	440	523	663	820	950	1 180	1 420
No. of successful operations ..	744	1 063	908	1 416	1 574	1 987	2 104	2 843	3 585	4 560	5 330	6 682	8 019	9 878	12 111
Percentage	61	60	56.6	67.2	69.3	69.7	70.8	68.4	68.1	70.6	71.4	69.7	69	68	69
Average number of successful operations of one device	1.5	1.2	1.69	1.37	1.53	1.44	1.63	1.45	1.32	1.24	1.33	1.32	1.27	1.28	1.26

* As at 31st December each year

receiving substation and the device for extinguishing the generator field is disconnected from the line protection. The residual voltage of the generator is so small after extinction of the field that it is in no state to maintain the arc at the point of short-circuit. After the required period of time for restoring the electrical strength of the insulation at the point where the fault has occurred, automatic reclosure takes place at the receiving substation and the device for extinguishing the field of the generator is connected. In order to reduce the extinction time on the field and ensure a more rapid connexion of the generator into the network, it is necessary to use an AGP-1 type field extinction device with de-ionic grid. In order to avoid dangerous overvoltages on the excitation winding of the generator, it is necessary to provide a resistance in the field extinguishing device which shunts the excitation winding.

The use of high-speed governors for the turbines makes rapid synchronization of the generators possible.

YEAR 1961

Non-synchronous automatic reclosure is also very promising. Tests and operating experience in the U.S.S.R. show that in some cases it can even be successful from the point of view of preserving the equipment.

Non-synchronous reclosure is however impracticable if the moments arising with it are greater than the moments which arise during three-phase short-circuits for which all generators are designed. It has been established that such electromagnetic moments occur in turbine generators at currents exceeding 5 I_{nom}, and at current exceeding 3.5 I_{nom} in hydro-electric generators.

Swings which occur during non-synchronous reclosings can in some cases cause the incorrect operation of the relay protection and additional measures must be taken to prevent this.

Non-synchronous automatic reclosure devices are very simple in design. They have therefore been extensively used in Soviet power systems. They are particularly effective on long inter-system links.

The extensive use of non-synchronous automatic reclosure has been instrumental in the large scale use of excitation forcing for generators so that the operation of the power system is unaffected by sudden changes in the current and voltage or the swings which appear during non-synchronous reclosing.

High-speed reclosure also deserves special attention. This equipment provides a "currentless pause" for the air blast circuit breakers equal

to 0.2-0.3 sec. In many cases the synchronous operation of the generators is not disturbed during the operating time of such devices and reclosure is not accompanied by out of step conditions. This feature is very important for the reclosure of large power stations. High-speed automatic reclosure may however produce undesirable effects.

In particular, high-speed reclosure of heavily loaded lines has no real advantage over non-synchronous reclosure since the rotational speed of the generators is rapidly increased if the total load is suddenly shed and the angle δ between the voltage vectors at the ends of the line increase sharply during the currentless pause.

The use of high-speed automatic reclosure is possible provided that use is made of high-speed protection which will provide simultaneous and instantaneous disconnexion of the line at both ends independently of the position of the faults.

On single lines which link a power station with a system or two parts of a system, use may also be made of three-phase automatic reclosure with recovery of synchronism besides single-phase and non-synchronous automatic reclosure.

It is necessary to consider out-of-step conditions in somewhat more detail.

Until automatic excitation regulation was used on a large scale, cases occurred when, despite the measures which had been taken, automatic reclosure was not followed by synchronism; out of step conditions set in, and the operation of the power system was disturbed. This was the main reason for failing to use non-synchronous automatic reclosure. However, it was seen later that sustained non-synchronous conditions were in the majority of cases permissible in power systems where the synchronous machines were provided with automatic excitation regulation, since the stability of the power system was not disturbed. The use of non-synchronous automatic reclosure was limited in these cases only by the mechanical forces arising in the generators, transformers and other equipment. However, out-of-step conditions must not be allowed to continue indefinitely since this may disturb the normal operation of consumers who are attached to substations in the electrical centre of the swings.

In all cases when sustained out-of-step conditions are probable and the use of non-synchronous automatic reclosure is permissible, it is necessary to take measures to ensure re-synchronization and prevent sustained out-of-step conditions. These measures include the installa-

tion of quick-acting speed governors on the steam turbines, the mechanical or electrical braking of hydro-electric generators, the disconnexion of some of the generators, load shedding and other measures.

Nevertheless operating experience shows that the use of non-synchronous automatic reclosure should not be restricted owing to the danger of sustained out-of-step conditions. Thus, from 1954 to 1958, non-synchronous automatic reclosure devices operated a total of 339 times, of this 257 were successful. Only three unsuccessful operations were attributable to sustained out-of-step conditions.

Two of these cases occurred in 1956 on the line linking the Azerbaijan and Gruzinsk power systems under abnormal conditions. The link between these systems was quite loose, and its stability was often disturbed with sudden changes in the load of the consumers. During the two years 1955 and 1956 there were 46 cases of non-synchronous automatic reclosure, of which 32 were successful. Twelve of these cases were caused by stable short-circuits on the line and only two cases were attributable to sustained out-of-step conditions.

YEAR
1961

The third unsuccessful operation due to sustained out-of-step con ditions occurred in the Permsk power system which was connected with the Kamsk hydro-electric station by two 220 and 110 kV lines. If large outputs were transmitted along the 220 kV line before disconnecting it, the stability of transmission along the 110 kV line was disturbed. But even here there were several dozen cases of successful operation of non-synchronous automatic reclosure on 220 kV lines and only in one very difficult case was it necessary for the staff to interfere and eliminate the out-of-step conditions. After this use was made of automatic disconnexion of some of the generators of the Kamsk hydro-electric station on interruption of the 220 kV line and no further cases of unsuccessful operation of the non-synchronous reclosure occurred.

Aspects of static and dynamic stability. In individual power systems fault disconnexions of consumers have occurred owing to "voltage avalanches" at a nodal centre with a small drop in voltage in the supply network.

The typical feature of centres where this has happened is the preponderance of induction motors for which the reactive power requirements are mainly covered by static capacitors. The average load of induction motors in such conditions is 0.8-0.9 of nominal.

A radical way of preventing the consumer being cut off under fault

conditions is to use synchronous motors instead of asynchronous motors or to use synchronous condensers instead of static capacitors, and to force the static capacitors at reduced voltage. In this case the starting devices may react to the rate of change in the voltage with time.

In some cases it is not possible to use static capacitors to compensate the reactive power on the grounds of stability. However, the use of synchronous motors instead of asynchronous motors with static capacitors is more economical in the majority of cases.

Large turbo-generators with direct cooling have a relatively large reactance and small mechanical time constants. This is explained by the fact that new systems of cooling make it possible to increase the output considerably at the same overall dimensions. The synchronous torque of such generators is less and their resynchronization is more difficult in consequence. Owing to their intense cooling they have considerably greater current densities under normal conditions and a lower overload capacity. The margins of mechanical strength are also smaller.

The problem of the stability of turbo-generators can be solved by using speed governors on steam turbines which react more quickly to acceleration. Tests on one such regulator which was designed by the All-Union Thermal Technical Institute proved satisfactory. Thus, for example, synchronous operation of the generator was ensured with the disconnexion of one parallel line by reducing its output. Without the regulator the generator fall out of step. The regulator was also instrumental in re-synchronizing the generator after short-circuits lasting 0.5 sec. The synchronism was not restored after such a short-circuit without the regulator.

The Leningrad Metal Factory has developed a hydraulic differentiator which reduces or stops the supply of steam to the turbine roughly 0.2 sec after a sudden drop in the load.

Owing to a number of specific features, it is not possible to make the speed control of a water turbine more quick-acting. The problem of improving the stability of hydro-electric generators has to be solved by other means, such as electrical braking, disconnexion of some of the generators and so on.

Power system automation. The development and inter-connexion of power systems makes it a more complicated matter to control their operating condition and it becomes more increasingly necessary to ensure

the most economical operation of fuel-fired and hydro-electric power stations with network losses included. These problems can only be solved by automation.

Automation of the control of operating conditions in power systems cannot be confined to the installation of appropriate apparatus at despatcher control points. It is also necessary to apply automation to the execution of commands from the despatcher point to the station. Widespread automation of the thermal processes is also required.

The analysis of conditions has to be made by computers. A very promising line of development is the use of control machines for complex automation of boiler-turbine-generator units.

The most serious attention must be paid to the automation of transformer voltage control when under load, the connexion and disconnexion of capacitors, the distribution of reactive loads between power stations and power systems.

YEAR
1961

All this is very important from the point of view of improving the power supply.

Continuity of supply

Interruptions of the power supply are very important from the economic point of view. In order to prevent the disconnexion of important motors at the low voltages which accompany short-circuits in the networks and from automatic reclosure and the operation of standby devices, use should be made of self-starting for motors which is ensured by correct adjustment of the relay protection of the motors themselves and of the other elements in the network (generator, transformers, lines).

The choice of fuses is very important to ensure the self-starting of 380 V motors. They should be selected so as to ensure the disconnexion of the motor in the presence of inter-phase short-circuits and in the presence of line-to-earth faults in earthed neutral systems. In no case should they be used for protecting the motors from overloads, since this can lead to damage of the motor if the fuse blows on one phase and the motor operates on two phases.

Operating experience shows that the self-starting of synchronous motors is just as feasible as the self-starting of induction motors. Only in individual cases is it necessary to use a special device for the self-starting of synchronous motors. In exceptional cases it is

also necessary to take away the excitation of synchronous motors for the automatic connexion of the standby supply and for automatic reclosure.

The scope for automation and remote control

Remote control and automation is not an end in itself, but only a means to achieve reliable and economical operation of the power system. If this is forgotten the volume of automatic equipment and remote control equipment in particular will be fixed without regard to actual operating conditions, the extent to which they are used and their costs, since this automatic equipment will be used to counteract fault conditions which become continually less and less likely. The capital cost of investment in automatic devices must always be justified most carefully. The investment must be recovered in a reasonable period of time out of operating costs.

It is not convincing to argue that the more important consumers require a larger amount of remote control equipment. Quite the contrary, such consumers who have a hundred per cent standby supply require least remote control equipment.

Unnecessary equipment is a waste of money and a nuisance, whereas its use on a sensible scale makes it possible to reduce the number of employees, to dispence with circuit breakers at substations on the high voltage side and so on. The correct choice of protection from short-circuits and overloads is very important for reducing the amount of automatic and remote control equipment.

Operating experience shows that in the overwhelming majority of cases a substation which is converted to operate without permanent staff need not be provided with remote control devices, telemetering equipment and remote indication equipment on a large scale. If automatic reclosure and automatic connexion of the standby supply is provided etc, it is sufficient to have a simple alarm system with two signals (fault and warning). In the Azerbaijan power system there are automatic substations on 20 and 35 kV which have operated for a long period without a permanent staff and without a system of remote indication and even though they are a large distance away from the base substation, the staff can be conveyed to the most outlying of them in about 20 min.

No permanent staff is necessary at stations without remote indication if the disconnexion of lines joining power system substations can be planned at substations where there is a permanent staff or when the

consumer himself can make the interruption known.

It is necessary to use automatic equipment on a large scale at those substations which supply industrial enterprises direct. But even the removal of a permanent staff from these substations should not be linked with centralized control formed by an extensive system of automation and remote control since the substations are quite close together. Telemetering should only be used to a limited extent in the power systems of industrial undertakings.

Operating experience shows that periodic inspection of substations without a permanent staff is quite sufficient. The number of inspections at many substations have been reduced to one per week, and this is not the limit. Personnel are very rarely called to substations to eliminate disturbances and faults. At many substations personnel are only required during daytime and then not for operating the system, but only to perform various operations such as maintenance and repair.

YEAR 1961

The main task is ensure reliable operation of power systems at minimum cost. This requires a reduction in the prime cost of electrical equipment and the reduction in operating costs. The following main measures have to be taken to achieve this in the field of relay protection and electro-automation:

1. The production of unit-type devices and elements for electro-automation and relay protection.

2. The reduction in dimensions of relays, apparatus and devices.

3. In the design and construction of new relay protection devices and automatic equipment, special attention must be paid to the simplification and improved reliability of the individual elements and of the device as a whole, the reduction in the number of tests and checks during erection and use, and the elimination of internal inspection of the individual elements of a device.

4. Further improvement of substation systems without circuit breakers on the high-voltage side and their automation.

5. The development of relay protection and automatic devices on operative a.c. for all voltages and outputs. Special attention must be paid to the reduction of consumption in the control circuits of circuit breakers, especially air-blast circuit breakers, the development and improvement of electro-pneumatic, clockwork, and pendulum devices, and the widespread introduction of electromagnetic devices with rectifiers

and motor drives.

6. The application of semiconductors in relay protection and automation.

7. Industry should be geared to the production of devices and apparatus for testing the various types of device used in relay protection and power system automation.

Translated by O.M. Blunn

LONG DISTANCE POWER TRANSMISSION WITH D.C. MAGNETIZED REACTOR-TRANSFORMERS AND FORCED CAPACITOR BANKS*

D. I. AZAR'EV

Moscow

(Received 23 January 1960)

YEAR 1961

At the present time long distance power transmission of large current capacity is designed and equipped either with series-capacitor compensation for the inductive reactance of the line, or with synchronous condensers at intermediate substations. The power of the compensating devices may be very large. For example, on the 400 kV line between the Volga hydro-electric station and Moscow the power of the capacitor banks is 485 MVA, and the power of the reactors for compensating the excess reactive power at minimum loads and limiting the voltage rise on connexion of the line its 750 MVA.

The power of the compensating devices increases with distance and voltage. For example, a single-circuit 650 kV line of 2500 km and 2100 MW requires static capacitors with a total power 4700 MVA and reactors with a total power of about 4000 MVA, i.e. each kilowatt of transmitted active power requires about 2.2 kVA of static capacitors and about 2 kVA of reactors. If the transmitted power is increased from 2100 to 2400 MW, then the power of the static capacitors increases from 2.2 to 2.7 kVA per 1 kW of transmitted power.

It has been shown by a study of long distance transmission with series compensation that the power of static capacitors is completely or partially absorbed by the reactors even if maximum power is transmitted. It is only possible to disconnect the reactors if the degree of series

* *Elektrichestvo*, 7, 24-30, 1961.

compensation leads to a reduction in the margin of stability. One escape from this situation would be the use of synchronous condensers at intermediate substations. However, this requires the use of transformer substations and, consequently, additional capital outlay. In addition, synchronous condensers do not allow large overloads and active losses are considerable.

The author of this paper has already suggested [1,2] that synchronous condensers be replaced by reactors with magnetization and forced capacitor banks with programme control. In this system use may be made of the low voltage reactor proposed by M.S. Libkind [3], or any other high-speed reactor with magnetization, but a still better system can now be used.

It is possible to produce a unit in which a transformer and an automatically controlled high-voltage reactor are combined and which is so quick-acting that it is capable of reducing overvoltages and increasing the current capacity of the line so that the cost of transmission is reduced and less equipment is required [4].

YEA
196

It is not possible to use a control reactor in the form of a conventional transformer [5] because the shape of its current and voltage curve is considerably distorted, and there is a large time constant under changing conditions which exceeds 10 sec. The 20 kV [6] reactor proposed by Friedlander possesses a curve of acceptable shape, which can be produced at higher voltages and used as the transformer if a secondary winding is attached to it, however, the direct magnetic link between the d.c. control winding with the closed delta winding does not allow high-speed control of the reactor (time constant of the magnetization winding is 0.75 sec). The six-core magnetic system requires a large amount of material, more than three times that of a non-controlled reactor.

Better results can be obtained if the magnetic system of the reactor is split into parallel branches magnetized by d.c. in such a way that the magnetic fluxes are in opposite directions [4]. A reactor can be constructed on this principle if use is made of the magnetic system of conventional three-phase or one-phase transformers. The rate of control of such a reactor will be higher since the magnetic flux created by the d.c. winding induced currents in the a.c. windings.

The magnetic system can be split in a different way, for example, as shown in Fig. 1. The reactor transformer in Fig. 1 consists of a three-core magnetic system 1, which has two zig-zag connected primary high-voltage windings 2 and 3, and a secondary winding 4 connected in delta.

The secondary winding is used for connecting the capacitor banks and for supplying local consumers. It also serves to eliminate the third harmonic. More remote consumers can be supplied from windings 3 or 2.

Magnetization winding 5 is disposed on magnetic circuits 6 and 7, which adjoin the faces of the three-core magnetic system, and is connected in such a way that the magnetic fluxes produced by it are closed through cross-pieces 8 of the three-core magnetic system and do not penetrate into the cores of this system on which the a.c. windings are disposed. With this connexion of the magnetization winding the control speed of the reactor is higher than that of the reactor proposed by Friedlander [6].

In order to eliminate the fifth and seventh harmonics, the primary windings of another but similar reactor transformer must be connected so that the phase sequence is reversed (A-C-B instead of A-B-C).

YEAR
1961

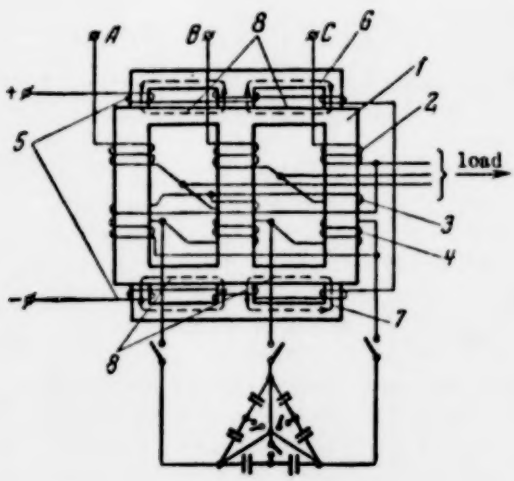

Fig. 1. Circuit of the magnetizable reactor-transformer with forced capacitor bank.

In order to check the shape of the curve, tests have been carried out by Teploelektroproekt on a prototype reactor-transformer. The tests showed that quite an acceptable shape of curve for the current and voltage can be obtained. Fig. 2 shows oscillograms of the linear current of a reactor transformer and the total current of two reactor transformers with identical magnetization.

The flow of d.c. through the magnetization windings saturates the cross-pieces 8 and the magnetic circuits 6 and 7, and their magnetic permeability is reduced.

Fig. 2. Oscillograms of the line current of a reactor-transformer (a), and the total current of two reactor-transformers (b).

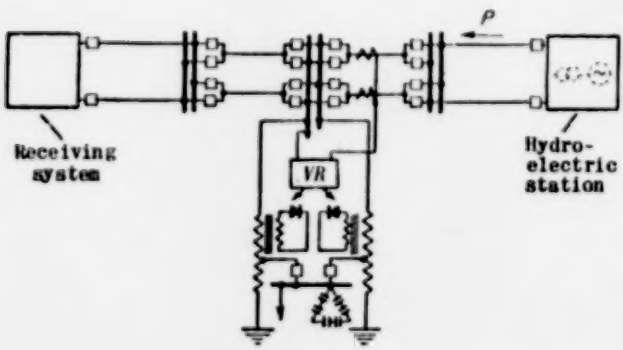

Fig. 3. Method of long distance transmission with magnetizable reactor transformers and forced capacitor banks.

Since the fluxes created by the a.c. windings pass through the same parts of the magnetic system, the inductive reactance of these windings is reduced, and the current increased.

By varying the magnetization current, the reactive power absorbed by the reactive-transformer can be varied by a factor of 10. This makes it possible to connect the reactor transformers without circuit breakers, since on heavy loads the consumed or reactive power can be reduced by decreasing the magnetizing current, and if faults occur it is possible to disconnect the system of bus-bars to which it is connected.

The use of magnetized reactor-transformers is expedient not only for increasing the current capacity of the line, but also for limiting the voltage in the absence of load and interruptions and connexions at one end. In this latter case reactors with magnetization are more effective than reactors with a linear volt-ampere characteristic, since the reactive power consumed by them increases rather more quickly with increasing voltage.

The efficiency of the proposed system (Fig. 3) will now be considered. The 400 kV line between the Volga hydro-electric station and Moscow will be used as an example.

Series-compensation of the inductive reactance of the line between the Volga hydro-electric station and Moscow (Fig. 4) is provided by static capacitors with a total power of 485 MVA, a total resistance 32 Ω, and a rated current 2250 A.

YEAR
1961

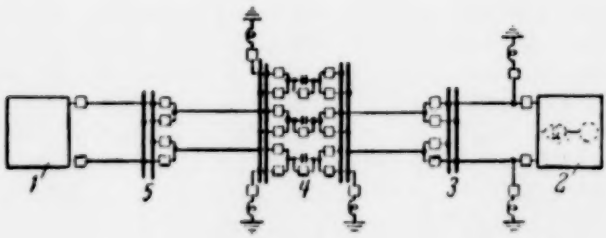

Fig. 4. Transmission system between the Volga hydro-electric station and Moscow. *1* - receiving system; *2* - Volga hydro-electric station; *3* - switching point No. 1; *4* - switching point No. 2; *5* - switching point No. 3.

Under normal conditions the current load of the capacitors is 79 per cent. If one of the circuits of some section of the line is interrupted, one of the capacitor banks is also disconnected and the two banks which remain in operation are loaded to 118.5 per cent. In order to absorb the excess reactive power at the switching point 2, a set of three reactors is installed with a total power of 450 MVA. The number of 400 kV circuit breakers at point 2 is 18.

To keep the direct-axis transient e.m.f. constant and equal to its value under nominal conditions, the maximum transmitted power is 1500 MW. If excitation regulators are used so that the voltage on the generator bus-bar is constant, the maximum power is 1640 MW, and if

regulators are used to keep the voltage on the bus-bars of 400 kV stations constant, maximum power is 1840 MW. If the margin of stability is kept the same at 15% for all cases, the transmission of power under normal conditions is 1300, 1420 and 1600 MW respectively.

If it is considered that under normal conditions a load of the static capacitor bank up to nominal current and nominal voltage is permissible, then the transmission of the specified outputs requires static capacitors with a total power of 306, 367 and 466 MVA respectively. In this case, if one of the parallel circuits of some section of the line is interrupted, then one of the three static capacitor banks is disconnected and the other capacitors will be overloaded by a factor of 1.5 as regards current, and 1.5 as regards voltage, i.e. by a factor of 2.25 as regards power. The curves shown in Fig. 5 show that for the case when E'_d of the generators is constant, the same maximum output (1500 MW) can be transmitted if use is made of transverse (shunt) compensation in place of series compensation and reactors with a linear volt-ampere characteristic, where transverse compensation is in the form of static capacitors and reactors with magnetization. In the following we will refer to transverse compensation as shunt compensation as opposed to series compensation which can alternatively be called longitudinal compensation. However, in the case of shunt compensation the necessary power is considerably less. For example, in order to obtain the same margin of stability as in the case of series compensation, the reactive power required in the middle of the line is 240 MVA when transmitting a power of 1300 MW, and the source of reactive power in the middle of the line must give 110 MVA when transmitting the maximum power 1500 MW.

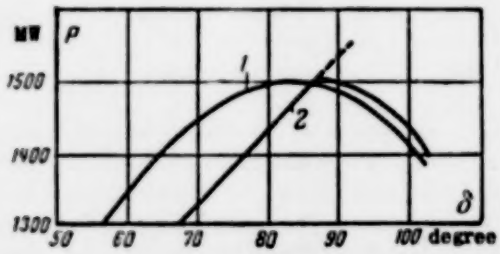

Fig. 5. The transmitted active power as a function of the phase angle of the e.m.f. of the transmitting station with E'_d of the generators constant: *1* - with series compensation; *2* - with shunt (transverse) compensation.

Assuming that the reactor requires 40 MVA in the absence of magnetization current under maximum conditions, it is found that the power of the static capacitors $Q_{s.c} = Q_1 + Q_{1r} = 110 + 40 = 150$ MVA. The power consumed by the reactor under normal conditions is $Q_{2r} = Q_2 + Q_{s.c} = 240 + 150 = 390$ MVA (Q_1 and Q_2 stand for the reactive power consumed or delivered by the plant under normal and maximum conditions). The power consumed by the reactor needs to be varied by a factor

$$k_n = \frac{Q_{2r}}{Q_{1r}} = \frac{390}{40} \approx 10.$$

Under fault conditions the source of reactive power in the middle of the line must deliver 110 MVA when transmitting 1300 MW and 350 MVA when transmitting 1500 MW. Consequently, the static capacitors must deliver a power $Q_{s.c} = 350 + 40 = 390$ MVA; when transmitting 1300 MW the reactor must consume the power $Q_r = 390 - 110 = 280$ MVA. The power consumed by the reactor needs to be changed by a factor

$$k_f = \frac{280}{40} = 7.$$

If it is assumed that the capacitor banks are forced as regards power by a factor 2.25 the same as in series compensation, the established power of the capacitor banks must equal 173 MVA.

In order to obtain the same stability margin with a constant voltage on generator bus-bars as in the case of series compensation, it is necessary that when transmitting 1420 MW the reactive power in the middle of the line has to be 80 MVA, and when transmitting the maximum power 1640 MW 225 MVA should be delivered.

Taking the same minimum power of the reactor as in the previous case, the power of the static capacitors $Q_{s.c} = 225 + 40 = 265$ MVA, and the maximum power of the reactor $Q_r = 265 + 80 = 345$ MVA. Consequently, the necessary change in output is

$$k_r = \frac{345}{40} = 8.65.$$

Under fault conditions it is necessary that the source of reactor power in the middle of the line should deliver 330 MVA when transmitting 1420 MW and 490 MVA when transmitting 1640 MW. Likewise, the static capacitors under these conditions must deliver 530 MVA, i.e. they have to be forced as regards power by a factor of 2, and the reactor must increase its output from 40 to 200 MVA, i.e. by a factor of 5.

If the direct-axis transient e.m.f. is constant as well as the voltage on the bus-bars of the generator, the power of the static capacitors and reactors can be decreased still further, if a slight reduction is allowed in the voltage in the middle of the line under maximum conditions as is the case in series compensation. For example, with a constant generator voltage, a 5 per cent reduction in voltage gives the results shown in Table 1.

TABLE 1

Conditions	Transmitted power, MW	Voltage in middle of line	Neccessary reactive power in middle of line, MVA	Reactor load, MVA	Load of static capacitor bank, MVA
Normal	1.420	U_{nom}	+80	+235	-155
	1.640	0.95 U_{nom}	-100	+40	-140*
One circuit disconnected on one section of line	1.420	U_{nom}	-330	+45	-375
	1.520	0.95 U_{nom}	-300	+40	-340*

* The power of the static capacitors is reduced 10% owing to the 5% reduction of voltage under limiting conditions.

Assuming that the capacitor banks under fault conditions are forced as regards power by the same factor as in series compensation, i.e. by a factor of 2.25, the rated power of the banks will be 166 MVA. The maximum power consumed by the reactors with magnetization is 235 MVA, and the necessary power variation factor is 5.88. In order to obtain the same margin of stability as series compensation it would be necessary to have static capacitors with an output of 367 MVA, i.e. 2.2 times greater.

The reason for the greater efficiency of the capacitors in the proposed system is that with series compensation the excess reactive power of the static capacitors is absorbed by the reactors which remain connected under maximum conditions. However, in the proposed system the reactors operate without magnetization under maximum conditions and, without reducing the voltage, consume considerably less power. Under fault conditions with series compensation, some of the capacitors are disconnected for purposes of forcing and are not used, even though they are then more necessary. In the proposed system all the capacitors remain connected.

It should be pointed out that with series compensation the static capacitors operate under rather less favourable conditions then in shunt compensation. For example, with series compensation the voltage on the capacitors during short circuits and swings can be increased by a factor of 2-2.5 or more with an increase in current. In the proposed system under normal conditions the voltage on the capacitors does not exceed the rated voltage, and under fault conditions it is increased only by a factor of 1.5 with forcing of the capacitor banks as regards power by a factor of 2.25.

In the proposed system the capacitor banks are connected to a lower voltage which makes it possible to reduce the cost of the equipment and improve its operating conditions.

An important advantage of magnetized reactors is that with an increase in voltage the power consumed by them is increased more sharply than with reactors having a linear volt-ampere characteristic. Consequently, they limit overvoltages more effectively when some lines are interrupted.

YEAR
1961

The effect of the proposed system on dynamic stability will now be considered.

The dynamic stability of a power station in a large network is the greater, the greater the area bounded by the curve $P_g - P_t = f(\delta)$, where P_g and P_t are respectively the powers developed by the generator and turbine. It will be seen from Fig. 6 that with the same margin of static stability the area bounded by the curve $P = f(\delta)$ and the straight line P_n is slightly less with shunt compensation than with series compensation. This is explained by the fact that at the moment maximum active power is achieved the magnetization is reduced to zero and the reactor is in no state to maintain the voltage in the middle of the line. In order that the area should be the same in both cases, it is necessary to increase the forcing of the capacitor banks at the first moment.

It has been shown by calculations that if the bank of static capacitors is forced as regards power by a factor of 2.25 for a prolonged period, then they must be forced by a factor of 3 on occasion in order to maintain dynamic stability, i.e. the bank voltage must be increased by approximately 1.73 compared with nominal voltage. It should be mentioned that even with series compensation the current and voltage overload of the bank exceeds 1.5 as a result of generator swings.

It will be seen from Fig. 7 that with generator swings the relative angle between the e.m.f. of the Volga hydro-electric station and the

receiving system with shunt compensation is greater than with series compensation. However, this is of no importance since the maximum permissible angle in shunt compensation is greater than in series compensation. The maximum transmissible power with a constant voltage in the middle of the line for shunt compensation is inferior if the angle between the voltages at the ends of the transmission line is 180° and for series compensation at the angle 90°. This difference is the less, the greater the voltage reduction in the middle of the line.

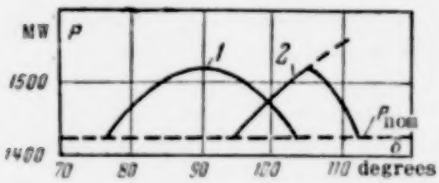

Fig. 6. The transmitted active power as a function of the phase angle of the e.m.f. of the generators at the Volga hydro-electric station under fault conditions.
1 - series compensation; 2 - shunt (transverse) compensation. The broken line corresponds to the increased power of the bank of static capacitors.

Forcing of the capacitor banks is necessary when it is necessary to transmit power equal to power under normal transmission conditions when one circuit of the line on some section is interrupted.

If this is not necessary, then both static and dynamic stability can be ensured by disconnecting some of the generators at the transmitting power station under fault conditions. In order to improve the dynamic stability, use may also be made of electrical or mechanical braking for the generators. If it is necessary to transmit the same power as under normal conditions when one circuit of some section is interrupted, then the use of braking does not exclude the forcing of the capacitor banks.

It has been shown by calculations for two values of the time constant of the reactor resistance (1 and 0.2 sec), that this has no great effect on stability.

The use of magnetized reactors is also possible for series compensation of the inductive reactance of the line, but such a combination is

less expedient since it requires a larger power for the capacitor banks. The cost of equipment for series compensation with magnetized reactors will be higher because the capacitors are connected to a higher voltage and require additional high-voltage circuit breakers. It should however be noted that in Table 2 it is assumed that the cost of capacitors for series and shunt compensation is the same.

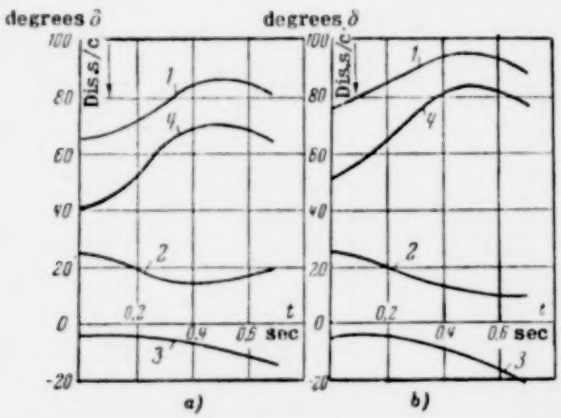

Fig. 7. Swinging of generators due to two-line-to-earth faults with series (a) and shunt compensation (b)

1 - phase angle of e.m.f. of generators at the Volga hydro-electric station; *2* - phase angle of receiving system; *3* - phase angle of synchronous condensers; *4* - relative angle between the e.m.f. of the Volga hydro-electric station and the e.m.f. of the receiving system.

It has been shown from calculations that if magnetized reactors were installed on the transmission line between the Volga hydro-electric station and Moscow, the same limit of static stability can be achieved with a resistance of the capacitor banks equal to 23.7 Ω, i.e. the power of the capacitor banks can be reduced from 367 to 266 MVA, or by a factor of 1.37. In the proposed system however, the power of the capacitor banks is equal to 155 MVA, i.e. approximately 1.5 times less.

Moreover it has been calculated that with a resistance of the capacitor banks of 23.7 Ω under normal conditions and 34.6 Ω in post-fault conditions dynamic stability is not ensured.

TABLE 2

Type of equipment	With series compensation			With intermediate synchronous condensers			With magnetizable reactor-transformers		
	Quantity*	Cost		Quantity*	Cost		Quantity*	Cost	
		Units**	Total, mill. roubles		Units**	Total, mill. roubles		Units**	Total, mill. roubles
Capacitors	367	85	31.2	62	85	5.3	155	85	13.2
Reactors	450	15	6.7	-	-	-	235	30	7.0
Circuit breakers	18	3	54.0	8	3	24.0	8	3	24.0
Transformers	-	-	-	330	20	6.6	-	-	-
Synchronous compensators	-	-	-	380	75	28.4	-	-	-
TOTAL	-	-	91.9	-	-	64.3	-	-	44.2

* Quantity of capacitors, reactors, transformers and synchronous condensers is given in MVA, but circuit breakers in a number of items.

**Cost of capacitors, reactors, transformers and synchronous condensers is given in roubles/MVA, but circuit breakers in mill. roubles per unit.

YEA
196

The overloading of the capacitor banks in series compensation is also related to the increase in current which takes place during swings and after the capacitors are disconnected. If the swings are large, the current after disconnexion of the capacitors can be twice the current under normal operating conditions of the line or three times greater than the nominal current. However, if the capacitors are connected to the secondary windins of the reactor transformer, the maximum voltage on the capacitors will depend on a pre-determined degree of forcing and is relatively independent of transmission conditions.

It is to be expected that the use of high voltage high-speed reactor transformers will make it possible to reduce overvoltages in lines and reduce insulation requirements and, consequently, either reduce their cost or permit an increase in voltage. The latter is the more rational.

In the first period of operation of new lines, large power is often not required and the reactor transformers will often be magnetized, i.e. used mainly as reactors. Later, when the load has increased, they will be used mainly as transformers; if there is a shortage of reactive power the capacitor banks will often be connected to them.

YEAR
1961

A comparison will now be made between the proposed system of transmission and the system using synchronous condensers.

It will be seen from Table 1 that if some circuit of one line section is disconnected and it is necessary to transmit 1420 MVA, then the source of reactive power in the middle of the line must deliver 330 MVA into the line. In order to deliver this power, it is necessary to have a 330 MVA transformer. The loss of reactive power in it will be at least 50 MVA. Consequently, all the synchronous condensers must deliver 380 MVA which must be their nominal power since a sustained overload of the condensers cannot be allowed.

In order to increase the dynamic stability, it is necessary to compensate the reactance of the transformer and the transient reactance of the synchronous condenser. If it is assumed that the first is equal to 17 and the second to 34 per cent, then 90 per cent compensation requires 140 MVA of static capacitors. Allowing for an overload of 2.25, 62 MVA will be sufficient.

Table 2 compares the amount and cost of the equipment for series compensation, synchronous condensers and the proposed system. The cost of erecting the equipment is included.

It will be seen from Table 2 that the system with magnetized reactor

transformers requires considerably less equipment and its cost is accordingly lower.

The loss of active power in the circuit with synchronous condensers is slightly larger than in systems with magnetized reactor transformers and with series compensation.

For example, on full load the loss of active power in synchronous condensers of KSV-75,000 type is about 1.4 per cent of their nominal power, the transformer loss is about 0.5 per cent and the total loss 1.9 per cent. However, the losses in a magnetized reactor transformer on full load is about 1 per cent. The saving on annual losses is about 1.5 million rubles.

Thus, the system with magnetized reactor transformers is considerably cheaper than systems with synchronous condensers or systems with series compensation in particular.

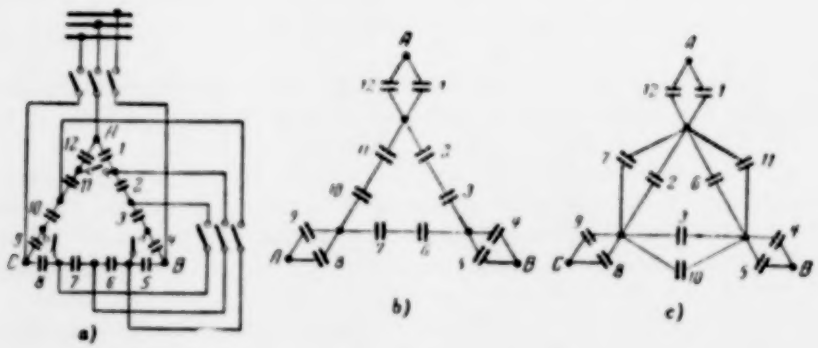

Fig. 8. Method of forcing capacitor banks (forcing factor from 1 to 4).

The capacitor banks connected to the reactor transformer can be forced in different ways, e.g. by switching to a previously provided system of branching the higher voltage [1], or by the system illustrated in Fig. 8 [7]. In the latter case, by changing the reactance of the bank x_C, any degree of forcing can be obtained.

$$k = \frac{1}{x_C + 0.25}.$$

If $x_C = 0$, the degree of forcing as regards power is 4, and if $x_C = 0.5$, it is 1.33.

It should be borne in mind, that with a degree of forcing other than 1.33 or 4, the capacitors are not charged uniformly. In order to distribute the charge more uniformly, it is necessary under these conditions to select the appropriate rated currents of the bank. If the degree of forcing is 1.33 or 4, the distribution of the charge is uniform when the capacitors are switched into the double star system (Fig. 9b) or into the double triangle system (Fig. 9c).

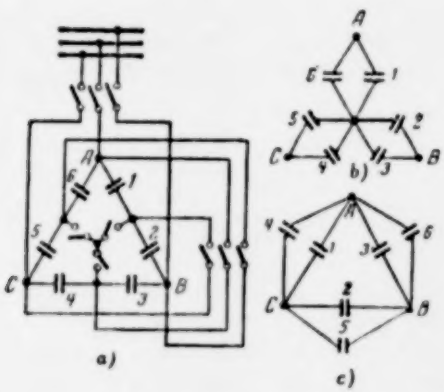

Fig. 9. Method of forcing capacitor banks (forcing factor 1.33 and 4).

Other means of forcing the capacitor banks have been suggested, such as the use of control valves which are connected in series with the capacitor banks [8].

There is also a suggestion to split the magnetic system of the magnetized transformer in the core [9] instead of in the yoke as considered in this paper. Further investigation is required to determine which system is the best. Such an investigation is outside the scope of this paper.

Thus, the proposed system of long distance transmission with magnetized reactor transformers and forced capacitor banks [4] has the following advantages:

1. It is more quick-acting than the system with synchronous condensers and ensures the maintenance of the voltage at intermediate points in the power systems and thereby increases the current capacity and stability of the transmission system.

2. It incorporates no rotating machines and is therefore more reliable

and cheaper to run.

3. It requires fewer capacitors and high-voltage circuit breakers than the system with series compensation.

4. It limits overvoltages and permits a reduction in the level of insulation on lines and equipment directly connected to it.

5. It makes it possible to supply consumers in adjoining regions immediately after installation and at the same time provides maximum current-capacity without additional expenditure on equipment.

Translated by O.M. Blunn

REFERENCES

1. D.I. Azar'ev; Auth. cert. No. 106201, 23 June 1956.
2. D.I. Azar'ev; *Elek. stants.*, 5 (1958).
3. M.S. Libkind; Patent claim No. 571784/24, 20 April 1957.
4. D.I. Azar'ev; Auth. cert., No. 128164, 14 May 1959.
5. I.S. Bruk; *Elektrichestvo*, No.7 (1958).
6. E. Friedlander; *ETZ-A*, No.4 (1958).
7. D.I. Azar'ev; Auth. Cert. No. 112809, 28 March 1957.
8. V.A. Venikov, V.V. Khudiakov and A.N. Tsov'ian; *Vest. elektroprom.*, 12 (1957).
9. W. Kramer; *ETZ-A*, 14 (1959).

THE PERMEANCE OF MAGNETIC CIRCUITS WITH TEETH*

Yu. S. RUSIN

Leningrad

(Received 9 January 1961)

YEAR
1961

Use is often made in various applications of the type of magnetic system with teeth illustrated in Fig. 1. In such systems there is quite a large leakage flux which can in some cases be of the same order as the operating flux and even exceed it. It is therefore very important to be able to determine the magnitude of the total magnetic permeance of such systems. Naturally, no rigorous solution of this problem exists owing to the complexity of the boundary conditions and the need to calculate a three-dimensional field. It is therefore necessary to consider an approximate method. In this paper a method is described which is based on a particular idealization of the field of the system.

The proposed method of analysing the permeability of magnetic systems with teeth is based on a conditional division of the space around the pole ends into separate regions. Given the geometric shape of the poles, it is expedient to consider the field between the faces and the field between the ribs separately. If the field between the faces is conditionally assumed to be two-dimensional (since a two-dimensional field is the simplest to analyse) the permeance calculated on the basis of this assumption will be less than the true value since the edge (surface) effect is ignored. This difference between the true magnetic permeance and the approximate value can be included by introducing an additional permeance as a correction for the surface effect). The author has found an analytic expression which defines the additional permeance as a

---

* *Elektrichestvo*, 7, 59-63, 1961.

function of the main geometric criteria of the system as a result of the investigation of experimental data.

The total permeance of the system under consideration can therefore be defined as the sum of the permeance G_1 between the external faces, G_2 that between the internal faces and G_3 the additional permeance.

Permeance will now be found for the general system in which tooth is above tooth (see Fig. 1).

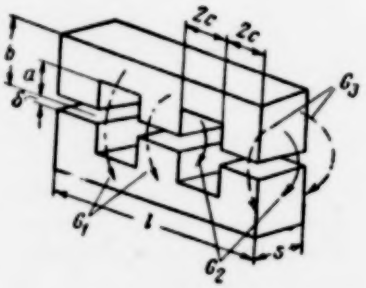

Fig. 1. Tooth pole ends

The permeance G_1 is defined by the formula [1]

$$G_1 = \mu_0 \left[n \int_0^{2c} \varphi(k_{11})\, dx + (n-1) \int_0^{2c} \varphi(k_{12})\, dx \right] = \\ = \mu_0 \left[n\varphi(k_{11}) + (n-1)\varphi(k_{12}) \right] 2c, \tag{1}$$

where μ_0 is the magnetic permeance of air; and

$$\varphi(k_{11}) = \frac{K(k'_{11})}{K(k_{11})}; \quad \varphi(k_{12}) = \frac{K(k'_{12})}{K(k_{12})}$$

are functions representing the relationship between the additional and total elliptic integrals of the first kind with moduli respectively equal to (see appendix I):

$$k_{11} = \frac{\delta}{b}; \quad k'_{11} = \sqrt{1 - k_{11}^2}; \quad k_{12} = \frac{a}{b}; \quad k'_{12} = \sqrt{1 - k_{12}^2};$$

2δ is the size of the air-gap, $2c$ the width of the tooth or recess (this relationship between the size of the tooth and recess is taken for the sake of simplicity, but in general any dimensions can be used by

appropriately changing the limits of integration in formula 1), and n the number of teeth ($n - 1$ is the number of recesses).

The permeance G_3 is defined by the formula [1]:

$$G_3 = \frac{b}{30}\left[\frac{2\tanh 0.87p}{k_{11}} + 41\tanh 5.5\,p\right]\mu_0, \tag{2}$$

where $p = \frac{l}{b}$.

As a rule $p \gg 1$, and so eqn. (2) simplifies to:

$$G_3 = \frac{b}{30}\left[\frac{2}{k_{11}} + 41\right]\mu_0. \tag{2a}$$

The determination of G_2 can be considerably simplified if it is accepted that in real systems $\delta \ll c$. It is therefore quite accurate to suppose (see appendix II) that the field between the teeth is uniform and, consequently, the bulging of the lines of force at the edges of the tooth can be ignored. This allows the use of conformal transformations to determine the permeance of the space between the recesses. Using Christophel-Schwartz' integral, the rectangular *CDEF* (the plane z) can be represented as a transformation of the upper half-plane ζ (Fig. 2). Correspondence of the points can be selected as follows:

$$0 \to 0; \quad E \to c\,(F \to -c); \quad M \to \infty.$$

The function for this transformation has the form:

$$z = A\int_0^{\zeta} \frac{d\zeta}{\sqrt{(\zeta^2 - c^2)(\zeta^2 - f^2)}}, \tag{3}$$

where f is the co-ordinate of the plane ζ, which corresponds to the co-ordinate of the point C in the plane z.

In order to determine A and f, use is made of the following conditions:

$$z = c \text{ if } \zeta = c \text{ and } z = c + j2a \text{ if } \zeta = f,$$

which, if substituted in eqn. (3), give after simple transformation [2]:

$$A = \frac{cf}{K(k_{21})}; \tag{4a}$$

$$\frac{2a}{c} = \frac{K(k'_{21})}{K(k_{21})} = q, \tag{4b}$$

where $K(k'_{21})$ and $K(k_{21})$ are total and additional elliptic integrals of the first kind.

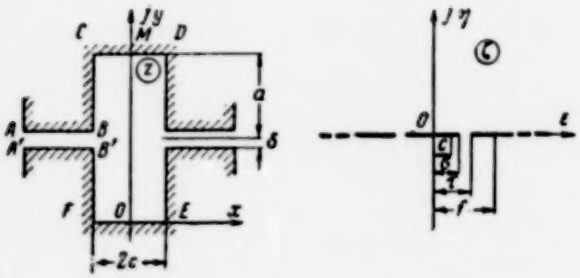

Fig. 2. Original system and system in transformed plane.

The moduli of the elliptic integrals k_{21} and k'_{21} can be found either graphically or by equations 4a or 4b, or by the approximate formulae:

$$k_{21} = \frac{c}{f} = \left.\frac{4}{e^{\frac{\pi q}{2}}}\right|_{q>1,83}; \quad k_{21} = \frac{c}{f} = \left.\frac{2.035 - q}{1,45}\right|_{q<1.83};$$

$$k'_{21} = \sqrt{1 - \kappa^2_{21}}.$$

In order to determine the co-ordinates τ and σ, which correspond to the co-ordinates of the points B and B', use is made of the conditions:

$$z = c + j(a - \delta) \quad \text{if} \quad \zeta = \sigma;$$

$$z = c + j(a + \delta) \quad \text{if} \quad \zeta = \tau,$$

which in conjunction with eqn. (3) give:

$$K(k_{21})\frac{a - \delta}{c} = F(\varphi_{21};\ k'_{21}); \tag{5a}$$

$$K(k_{21})\frac{a + \delta}{c} = F(\varphi_{22};\ k'_{22}), \tag{5b}$$

where

$$F(\varphi_{21};\ k'_{21});\ F(\varphi_{22};\ k'_{21})$$

are partial elliptic integrals of the first kind with the modulus k'_{21} and the amplitudes φ_{21} and φ_{22}.

The amplitudes φ_{21} and φ_{22} can be found from Tables of the values $F(\varphi;\ k'_{21})$, i.e. from the values of the left-hand sides of eqn. (5).

The following formula is used to determine the permeance per unit length of the upper-half space of a system of two semi-infinite and one finite plate, which corresponds to the permeance of the recess (see appendix I):

$$G''_2 = \frac{K(k_{22})}{2K(k'_{22})}\mu_0, \tag{6}$$

YEAR 1961

where $K(k_{22})$ and $K(k'_{22})$ are total elliptic integrals of the first kind with moduli:

$$k_{22} = \sqrt{\frac{f^2-(f^2-c^2)\sin^2\varphi_{22}}{f^2-(f^2-c^2)\sin\varphi_{21}}};\quad k'_{22} = \sqrt{1-k_{22}^2}.$$

Consequently, the permeance between the teeth is defined in the same way as for a uniform field:

$$G'_2 = \frac{c}{\delta}\mu_0. \tag{7}$$

The total permeance between the internal faces of a system consisting n teeth therefore equals:

$$G_2 = \left(\frac{K(k_{22})}{2K(k'_{22})} + \frac{c}{\delta}\right) ns\mu_0, \tag{8}$$

where S is the width of a side face.

In order to determine the permeance for other systems with the teeth in other positions, use may be made of the relationships obtained by Sribner [3], which have been confirmed quite well by a more accurate analysis.

Tooth above recesses:

for a single nucleus

$$G_2 \approx G_2'' 4s;$$

and for the whole system

$$G_2 \approx 2G_2''(2n-1)s.$$

Half of tooth above half of recess:

for a single nucleus

$$G_2 \approx \left(2G_2'' + \frac{c\mu_0}{2\delta}\right) s;$$

and for the whole system

$$G_2 \approx \left(4G_2'' + \frac{c\mu_0}{2\delta}\right) ns.$$

Formulae can also be written in the same way for the permeance G_1

Tooth above recess:

$$G_1 = 4\varphi(k_{13})(n-1)c\mu_0;$$
$$k_{13} = \frac{a+\delta}{2b-a+\delta};\quad k_{13}' = \sqrt{1-k_{13}^2}.$$

Half of tooth above half of recess:

$$G_1 = [n\varphi(k_{11}) + 2(n-1)\varphi(k_{13}) + (n-1)\varphi(k_{13})]\, c\mu_0.$$

The total permeance of the system under consideration for any position may be defined as the sum:

$$G = G_1 + G_2 + G_3.$$

The results obtained in this paper have been confirmed experimentally (see appendix III).

Appendix I. In order to determine the permeance (per unit of length) of two systems of plates consisting of two upper plates of finite width

and two lower semi-infinite plates and one finite plate (Fig. 3), it is necessary to effect a conformal transformation of the half-plane ζ on the rectangle $AA'B'B$ in the plane z such that the following correspondence of points obtains:

$$A \to a;\ A' \to a';$$
$$0 \to 0;$$
$$B \to \beta;\ B' \to \beta';$$
$$C \to \infty$$

Such a transformation can be obtained by Christophel-Schwarz' integral, which in this case in expressed by the relationship

$$z = A \int_0^{\zeta} \frac{a}{\sqrt{(\zeta^2 - m^2)(\zeta^2 - n^2)}}. \qquad \text{(I-1)}$$

YEAR 1961

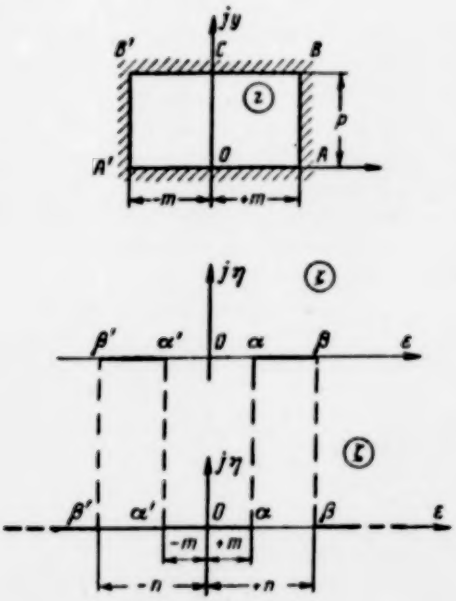

Fig. 3. Analysis of permeance between plates.

Substituting $t = \zeta/n$ equation (I-1) takes the form:

$$z = A \int_0^{t} \frac{dt}{\sqrt{(1 - t^2)(1 - k_{10}^2 t^2)}}, \qquad \text{(I-2)}$$

where

$$k_{10}=\frac{m}{n}.$$

The constant A is found from the condition

$$z=m \text{ if } \zeta=m$$

and is equal to

$$A=\frac{m}{K(k_{10})},$$

where $k(k_{10})$ is the total elliptic integral of the first kind with the modulus k_{10}.

After performing these preliminary calculations, there is no difficulty in determining the required permeance. In fact, if the upper or lower system of plates is given, this implies that the co-ordinates of the points α and β are also given (and so are α' and β' by virtue of symmetry). By virtue of the assumed correspondence of points, point α goes into the plane z at point A, and β at B. Consequently, it only remains to determine the co-ordinate point B by the expression (I-2) and B' accordingly). This co-ordinate is found from the condition

$$z=m+jp \text{ if } \zeta=n,$$

i.e.

$$z=m+jp=\frac{m}{K(k_{10})}\int_0^{\frac{n}{m}}\frac{dt}{\sqrt{(1-t^2)(1-k_{10}^2t^2)}}=$$
$$=\frac{m}{K(k_{10})}\left[K(k_{10})+\int_1^{1/k_{10}}\frac{dt}{\sqrt{(1-t^2)(1-k_{10}^2t^2)}}\right]. \qquad \text{(I-3)}$$

Substituting

$$1-k_{10}^2t^2=(k'_{10})^2u^2,$$

where

$$k'_{10}=\sqrt{1-k_{10}^2}.$$

it is found that the second integral in eqn I-3 is equal to $K(K'_{10})$. Consequently,

$$\left.\begin{aligned} m + jp &= \frac{m}{K(k_{10})}[K(k_{10}) + jK(k'_{10})]; \\ p &= \frac{K(k'_{10})\, m}{K(k_{10})}. \end{aligned}\right\} \qquad \text{(I-4)}$$

It is easy to see that the initial upper and lower systems of plates in the plane z (the rectangle $AA'B'B$) are transformed into a simple system which is an ideal plane capacitor.

The permeance of such a system is:

for the upper system

$$G_u = \mu_0 \frac{p}{2m};$$

YEAR 1961

for the lower system

$$G_l = \mu_0 \frac{2m}{p}.$$

Substituting the value of p from eqn. I-4 in these formulae,

$$G_u = \mu_0 \frac{K(k'_{10})}{K(k_{10})}; \quad G_l = \mu_0 \frac{K(k_{10})}{2K(k'_{10})}.$$

Appendix II. Suppose it is required to estimate the error which occurs in determining permeance on the assumption that the field between the teeth is uniform. It is expedient to make this estimate for a system in which the permeance can be determined exactly and then the discrepancy between this exact permeance and the permeance calculated as for a uniform field will be maximum. Such a system is one which consists of two teeth (Fig. 4). In point of fact the bulging of the lines of force in the region between the teeth in such a system will be considerably greater than in a system consisting of a number of teeth. This decrease in the effect of bulging of the lines of force in systems with several teeth can be explained by the compressive effect of the flux from adjacent teeth. The permeance between the face surfaces of a system consisting of two teeth is defined by the formula [1]:

$$G_f = \frac{2\mu_0}{\pi} \ln \frac{1 + \sqrt{1 - k^2}}{k} \qquad \text{(II-1)}$$

where $k = f\left(\frac{m}{h}\right)$ is the modulus of the elliptic integrals in the equation

$$p = \frac{m}{h} = \frac{K(k') - E(k')}{E(k)}; \quad (k' = \sqrt{1 - k^2}). \tag{II-2}$$

Eqn. (II-2) can be solved graphically. It is of practical interest to consider cases of systems for which $p > 5$. This corresponds to a very small value of k. For small values of k eqn. II-2 has the following approximate solution:

$$k = \frac{4}{e^{\frac{\pi}{2}p+1}}. \tag{II-3}$$

The required error is

$$\Delta = \frac{\Delta G_1}{G_f} = \frac{G_f - G_0}{G_f},$$

where $G_0 = \mu_0 \frac{m}{h}$ is the permeance between faces calculated on the assumption that the field between the teeth is uniform.

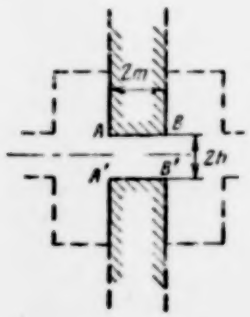

Fig. 4. Two-pole system.

Thus, the formula for the error can be written in the form:

$$\Delta = \frac{\frac{2}{\pi}\ln\frac{2}{k} - \frac{m}{h}}{\frac{2}{\pi}\ln\frac{2}{k}} = \tag{II-4}$$

$$= \frac{\frac{2}{\pi}\ln 2 - \frac{2}{\pi}\ln 4 + \frac{2}{\pi}\left(\frac{\pi}{2}p+1\right) - \frac{m}{h}}{\frac{2}{\pi}\ln 2 - \frac{2}{\pi}\ln 4 + \frac{2}{\pi}\left(\frac{\pi}{2}p+1\right)} = \quad \text{(II-4) cont.}$$

$$= \frac{0.2}{0.2+\frac{m}{h}}.$$

It will be seen from expression II-4 that the error is less than 4 per cent if $p = 5$, and less than 2 per cent if $p = 10$ and so on.

The foregoing analysis permits the following conclusions:

1. The face permeance is not reduced by more than 4 per cent by assuming that the field in the space between the teeth is uniform.

2. In calculating the permeance of the space between the recesses, the magnitude of this permeance is not increased by more than 4 per cent by assuming that the lines of force are along the line *BB'* (see Fig. 2) (i.e. assuming uniformity of the field between the teeth).

3. The total permeance (for the recesses and teeth), can be calculated to within 4 per cent since the error in calculating the two permeances differ in sign.

Appendix III. Suppose it is required to determine the permeance of a system with the following dimensions (tooth above tooth):

$$b = 2 \text{ cm}; \; a = 2c = 1 \text{ cm}; \; \delta = 0,1 \text{ cm};$$
$$s = 1 \text{ cm}; \; n = 3.$$

The permeance G_1 is found from formula (1), in which k_{11} and k_{12} equal:

$$k_{11} = \sin\alpha_{11} = \frac{\delta}{b} = \frac{0,1}{2} = 0,05 \; (\alpha_{11} = 3°, \; \alpha'_{11} = 87°);$$

$$k_{12} = \sin\alpha_{12} = \frac{a}{b} = \frac{1}{2} = 0,5 \; (\alpha_{12} = 30°, \; \alpha'_{12} = 60°).$$

The values of the elliptic integrals are found tables:

$$K(k_{11}) = 1.57; \; K(k'_{11}) = 4.34;$$
$$K(k_{12}) = 1.68; \; K(k'_{12}) = 2,16.$$

Consequently,

$$\varphi(k_{11}) = \frac{4.34}{1.57} = 2.8; \quad \varphi(k_{12}) = \frac{2.16}{1.68} = 1.28.$$

Substituting the obtained and known data in formula (1), it is found that:

$$G_1 = 11.0\mu_0.$$

The permeance G_2 is found from formula (8). The relationship between the geometric dimensions of the system $q = 4$ provides the modulus k_{21}

$$k_{21} = \frac{4}{e^{2\pi}} = 0.00735.$$

Consequently,

$$l = \frac{c}{k_{21}} = 68 \text{ cm};$$

It is also found that

$$\alpha_{21} = \arcsin k_{21} = 0°25'; \quad \alpha'_{21} = 89°35';$$
$$K(k_{21}) = 1.57.$$

Using the calculated values of the partial elliptic integrals of the first kind (with $k'_{21} = \sin \alpha'_{21}$),

$$F(\varphi_{21}; k'_{21}) = K(k_{21}) \frac{a - \delta}{c} = 1.57 \frac{0.9}{0.5} = 2.82;$$

$$F(\varphi_{22}; k'_{21}) = K(k_{21}) \frac{a + \delta}{c} = 1.57 \frac{1.1}{0.5} = 3.45.$$

The amplitudes of the integrals from the tables are:

$$\varphi_{21} = 83°30'; \quad \varphi_{22} = 86°30'.$$

Finally, finding

$$k_{22} = \sqrt{\frac{l^2 - (l^2 - c^2)\sin^2 \varphi_{22}}{l^2 - (l^2 - c^2)\sin^2 \varphi_{21}}} = \sqrt{\frac{1 - 0.994}{1 - 0.988}} = 0.71$$
$$(\text{i. e. } \alpha_{22} = 45°; \ \alpha'_{22} = 45°),$$

it is found from the tables:

$$K(k_{22}) = K(k'_{22}) = 1.85.$$

Substituting these values in formula (8)

$$G_2 = 16.5\mu_0.$$

The permeance G_3 is found from formula (2a):

$$G_3 = \frac{v}{30}\left[\frac{2}{k_{11}} + 41\right]\mu_0 = \frac{2}{30}\left[\frac{2.2}{0.1} + 41\right]\mu_0 = 5.4\mu_0.$$

The total permeance of the system is equal to:

$$G = (11.0 + 16.5 + 5.4)\mu_0 = 32.9\,\mu_0.$$

The experimentally determined permeance equalled $G = 35\mu_0$. Thus, the error was of the order of 6 per cent which agrees well with the estimated error.

Translated by O.M. Blunn

YEAR
1961

REFERENCES

1. Yu.S. Rusin; *Determination of the permeance of complex magnetic systems, (Opredelenie magnitnoi provodimosti magnitnykh sistem slozhnoi konfiguratsii).* Thesis for degree of Kand. Tech. Sc., (1958).
2. I.M. Ryzhik and I.S. Gradshtein; *Tables of integrals, sums, series and products, (Tablitsy integralov, summ, riadov i proizvedenii).* Gostekteoretizdat (1951).
3. L.A. Sribner; *Avtomat. i telemekh.*, No.1 (1960).

JOINT SELECTION OF THE MOTOR CRITERIA AND THE GEAR RATIO*

D. A. POPOV

Moscow

(Received 19 December 1960)

Statement of the problem. When designing the method of starting an electric drive in which the rotational torque of the motor and the moment of resistance (load torque) of the driven device are constant, the following problems arise in connexion with the choice of the gear ratio:

1. Given the rotational torque M_a and the moment of inertia J_a of the motor and the load torque M_l and the moment of inertia J_d of the driven mechanism, it is necessary to determine that optimum gear ratio i_{opt} which will ensure the acceleration of the driven mechanism up to the desired speed ω_{do} in the shortest possible time [1, 2, 3].

2. Given the criteria M_l and J_d of the driven mechanism, it is necessary to determine that optimum gear ratio which will ensure uniform acceleration of the driven mechanism device to the desired speed ω_{do} in a specified time t_a with the minimum rotational torque and weight of the motor [4-8].

3. After ensuring that these conditions are fulfilled, it is necessary to determine the optimum gear ratio which will ensure the minimum gross weight of the motor, the supply unit (e.g. the motor-generator converter of the unit), and of the gears.

In all these cases it is assumed that the moment of inertia and weight of the motor are independent of its nominal speed and definable by the rotational torque of the motor M_a. This proposition follows from

---

* *Elektrichestvo*, 7, 63-67, 1961.

the fact that the permissible torque of a motor M_m under starting conditions depends mainly on the thermal capacity of the armature, since the heat transfer to the surrounding medium in the process of acceleration has no appreciable effect on the heating of the motor.

The first problem, which has no great practical importance, arises when checking the conditions of acceleration of the driven mechanism and the correctness of the choice of gear ratio for a given motor.

In the second and third problems it is a question of selecting the gear ratio and the criteria of the motor together to ensure the most economical arrangement. These problems arise in designing all types of electric drive. The solution of the first problem is given by Umanskii's formula [1,2]

$$i_{opt\,1} = \frac{M_l}{M_m} + \sqrt{\left(\frac{M_l}{M_m}\right)^2 + \frac{J_d}{J_m}}. \qquad (1)$$

YEAR 1961

The problem of determining the optimum gear ratio for the minimum weight of the motor was first formulated by Geiler [4]. It has since been considered in a number of other papers [5-8]. However, no general solution is as yet available for any given type of relationship $J_m(M_m)$. The moment of inertia of the gears is usually ignored in the solution of this problem, and the efficiency of the gears η_g is either ignored [5, 6], or else only included approximately [8].

In his more recent paper [3] Geiler proceeds from Umanskii's formula for the solution of the second problem.

Substituting the value $i_{opt\,1}$ from (1) in the equation of motion of the drive, the author obtains the expression

$$M_{m.min} = 2\alpha\, i_{opt} J_m,$$

where

$$\alpha = \frac{\omega_{d0}}{t_a}. \qquad (2)$$

and t_a is the specified acceleration time.

Geiler argues that these expressions provide the solution for the practical problem of determining the optimum size of a motor which will ensure the acceleration of the driven device via the gears in the minimum (specified) time i.e. determined the necessary power of the motor taking

both quantities M_a and $i_{opt\ 1}$ as variables at the same time.

In fact, however, the real position is quite different. In the first place it is not clear how $i_{opt\ 1}$ and M_a (all $i_{opt\ 1}$ and J_a) can be found from expression (2) at the same time, since two unknown quantities are contained in this expression. This aspect of the problem was not considered by Geiler [6].

Moreover, there is a problem of whether or not formula (2) can be used to select the gear ratio and the criteria of the motor simultaneously, since this formula, like Umanskii's formula, is derived on the assumption that M_a and J_a are given constant quantities which are independent of the gear ratio.

It is of course true on logical grounds that formula (2) must be valid whether the optimum criteria of the drive are found by changing the gear ratio alone, or by changing the gear ratio and criteria of the motor at the same. This logical consideration is however not sufficient to substantiate formula (2) if $M_a = f(i) = \text{var}$ and $J_a = f(i) = \text{var}$; it only follows that the stated formula can be proved more rigorously than in the paper in question.[6].

Other papers [5,7] give a solution of the second problem for the special case where use is made of a series of geometrically similar motors with a dynamo-electric constant. Under these conditions $J_a \equiv M_a^{5/3}$. Rozenberg [8] has considered another special case when use is made of motors with an identical ratio GD^2/M_a. However, the foregoing conditions as regards $J_a(M_a)$ often do not obtain in practice since this is uneconomic from the point of view of the construction of the motors and the utilization of expensive material.

The foregoing methods of determining $i_{opt\ 1}$ are not suitable for the most important practical case when there is a series of electric motors with different outputs (with different values of M_a) for which the values of J_a are known. In this case the relationship $J_a(M_a)$ is given graphically (plotted by points) and it is required to select the gear ratio and minimum weight of motor which will ensure the acceleration of the driven device in the specified time.

As regards the problem of selecting the optimum gear ratio which will ensure the minimum total weight of the drive motor, supply unit and gears, nothing has as yet been published on this question.

Criteria of the drive for the minimum weight of motor. For the joint selection of $i_{opt\ 1}$ and $M_{a.min}$ it is taken for granted that the

relationship between the moment of inertia and the moment of the motor $J_m(M_m)$ is given graphically.

By way of example, Fig. 1 shows the relationship $J_m(M_m)$ for a series of small electric motors (curve 1) from which it will be seen that the moment of inertia of the stated series increases with increasing M_m to a degree slightly less than 5/3 (see curve 3 in Fig. 1).

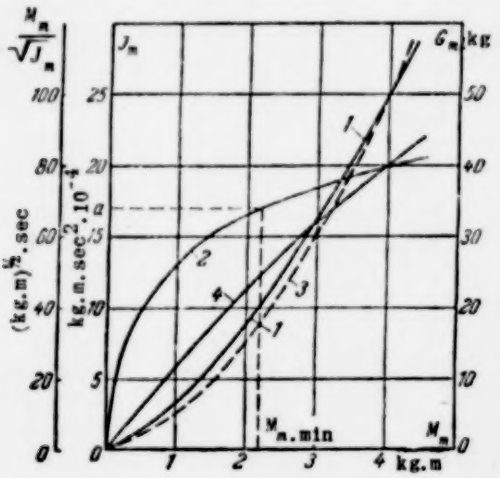

Fig. 1. Graphical determination of the gear ratio which corresponds to the minimum weight of the drive motor:

1 - Experimentally-determined relationship $J_m(M_m)$ for one of the series of motors; *2* - auxiliary curve $M_m/\sqrt{J_m}(M_m)$; *3* - relationship $J_m(M_m)$ for one series of motors for which $J_m \equiv M_m^{5/3}$ (based on a motor with $M_m = 4$ kg.m); *4* - weight of motor as a function of torque.

In order to determine the derivative $\frac{dM_m}{di}$, use is made of the equation of motion

$$(M_m i - J_m i^2 \alpha)\eta_g = M_b + J_g \alpha, \qquad (3)$$

where $M_b = M_l + J_d \alpha$; J_g is the moment of inertia of the gears, in reference to the shaft of the drive of the driven device; and η_g is the efficiency of the gears.

Bearing in mind that the variables M_m, J_g and η_g are functions of i, and that J_d is a function of M_m, it is found after differentiating (3) that:

$$\frac{dM_m}{di} = \frac{(M_m - 2\alpha i J_m)\left(\eta_g + i\frac{d\eta_g}{di}\right) - \alpha\frac{dJ_g}{di} + \alpha i^2 J_m \frac{d\eta_g}{di}}{i\left(\alpha i \frac{\partial J_m}{\partial M_m} - 1\right)\eta_g} \tag{4}$$

Since the denominator on the right-hand side of formula (4) has finite values for finite values of α and i, it follows that the condition for the minimum of M_m takes the form

$$M_{m.min} = 2\alpha i_{opt\,1} J_m - \alpha \frac{\left(\frac{dJ_g}{di} - i^2 J_m \frac{d\eta_g}{di}\right)}{\left(\eta_g + i\frac{d\eta_g}{di}\right)}. \tag{5}$$

It follows from formula (5) that equation (2) is only valid if $J_g = \text{const}$ and $\eta_g = \text{const}$, independently of the shape of the function $J_m(M_m)$, whether or not M_m or J_m are constant, or whether they depend on i.

The quantities $M_{m.min}$ and $i_{opt\,1}$ can be found by the graphical solution of eqn. (3) if this is converted into

$$M_m = \frac{M_b}{i\eta_g} + J_m \alpha i + \frac{J_g \alpha}{i\eta_g}. \tag{6}$$

Knowing the relationships $J_m(M_m)$, $\eta J_g(i)$ and $\eta_g(i)$, the right and left sides of expression (6) are plotted as a function of M_m on the assumption that the variable i is a known item. In this case the left-hand side φ_1 is a straight line at 45^0 to the base, and the right-hand side φ_2 is a series of curves corresponding to different values of i (Fig. 2).

The points of intersection of the curves $\varphi_2(M_m)$ and the line $\varphi_1(M_m)$ define values of M_m, which satisfy eqn. (6) for different values of i. It follows from Fig. 2 that with increasing i, the necessary moment of the motor M_m continuously decreases. The maximum value of i, at which it is possible to ensure the acceleration of the given device to the desired speed in the specified time, is defined by the co-ordinates of the point where the straight line φ_1 is tangential to the curve φ_2, which corresponds to $i = i_{opt\,1}$. At large values of the

gear ratio, curves for φ_2 do not intersect the straight line φ_1 and condition (3) cannot be satisfied.

The optimum gear ratio $i_{opt\ 1}$ can be defined in this way for all values of M_l, including $M_l = 0$, provided $J_m \neq 0$; naturally, if $J_m = 0$ no optimum gear ratio is possible.

It can be shown that the product $M_m i$ which satisfies eqn. (6), continously increases with increasing i.

As stated above, in order to determine $i_{opt\ 1}$ it is necessary to know the relationships $J_g(i)$ and $\eta_g(i)$. These relationships can easily be established if the division of the total transmission ratio between individual stages and the criteria of adjacent stages is known.

YEAR 1961

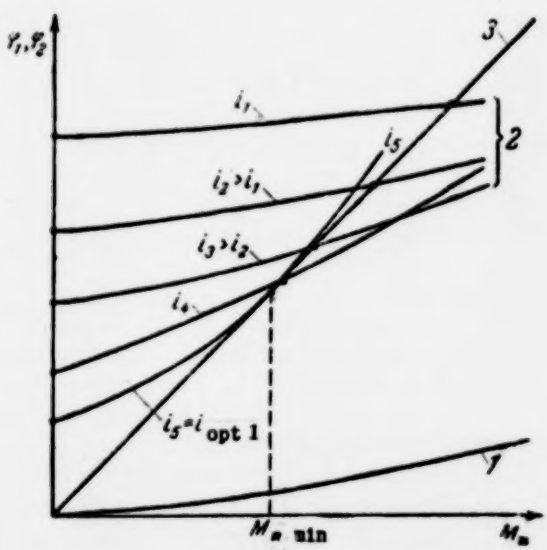

Fig. 2. Graphical solution of the equation of motion of the drive.

1 – relationship $J_m = f(M_m)$; 2 – curves $\varphi_2(M_m)$ for different values of i; 3 – straight line $\varphi_1(M_m) = M_m$.

If the moment of inertia of the gears is ignored, it is much easier to determine $M_{m.min}$ and $i_{op.1}$.

In this case eqn. (3) and (5) take the form:

$$\left.\begin{aligned} M_a i - J_a i\alpha &= \frac{M_b}{\eta_g}; \\ M_a &= 2\alpha i J_a. \end{aligned}\right\} \tag{7}$$

Given the efficiency of the gears and assuming that it is constant, it is possible to eliminate the variable i from the set of eqn. (7):

$$\frac{M_a}{\sqrt{J_a}} = 2\sqrt{\frac{\alpha}{\eta_g}(\alpha J_d + M_l)} = a. \tag{8}$$

This equation can be solved graphically as in Fig. 1. Knowing the relationship $J_a(M_a)$, it is also possible to plot the relationship $\frac{M_a}{\sqrt{J_a}} = f(M_a)$. First of all the value of a which is equal to the right-hand side of eqn. (8) is marked off along the base and using the curve $\frac{M_a}{\sqrt{J_a}}$ (curve 2) the motor torque $M_{a.min}$ can then be found. Knowing $M_{a.min}$ and J_a, the quantity $i_{opt\ 1}$ can be found by formula (7). The value of η_g can then determined and compared with the value adopted previously.

If there is a large discrepancy between the new value of η_g and the old value, the calculations are repeated and no more difficulties arise owing to the simplicity of the constructions.

However, the optimum criteria of the drive which are obtained in this way are not always practicable because extremely high rated rotational speeds of the motor may be obtained.

It should also be stressed that the stated method of selecting the criteria of the electric drive from the point of view of economy is not correct. Increases in the gear ratio increase the difficulties of production and reduce the efficiency; a high gear ratio involves an increase in power and weight of the supply unit.

In fact, the electromagnetic power of a generator at the end of the acceleration of the driven mechanism equals

$$P_g = E_{g0} I_a = \frac{\omega_{a0} M_a}{1-s} = \frac{i\omega_{d0} M_a}{1-s}, \tag{9}$$

where $s = \dfrac{I_a r_a}{E_{g0}}$, r_a the total resistance in the circuit of the motor armature and generator, I_a the armature current, E_{g0} the e.m.f. of the generator at the end of acceleration.

Substituting the value $M_m i$ from (3) in (9),

$$P_g = \frac{\omega_{d0}}{1-s}\left(\frac{M_b}{\eta_g} + \alpha i^2 J_m\right). \tag{10}$$

An increase in the transmission of the gears is accompanied with a continuous increase in the power of the generator and the weight of the supply unit, since the second term on the right-hand side of formula (10) increases continuously in this case.

It can be shown that the total expenditure of energy by the generator in the process of accelerating the given mechanism with losses included for the main circuit of the generator and motor (if I_a = const, M_l = const, and M_m = const) equals:

$$A_{tot} = \frac{\omega_{d0}^2}{2}(J_d + i^2 J_m)\frac{1+s}{1-s} + \frac{M_l \omega_{d0} t_s}{1-s}. \tag{11}$$

For the optimum gear ratio selected in accordance with the method expounded above, the power of the generator and the total expenditure of energy by the generator will be maximum

$$P_{g1} = \frac{2\omega_{d0} M_b}{1-s}; \tag{12}$$

$$A_{tot1} = \frac{\omega_{d0}^2}{1-s}\left[J_d(1+s) + \frac{M_l}{\alpha}\right]. \tag{13}$$

Consequently, it is not economical to chose the gear ratio merely to obtain the minimum weight of the drive motor.

Minimum gross weight of the motor, supply unit and gears. It is advisable to select that value $i = i_{opt\ 2}$ at which the gross weight of the motor supply unit and gears is minimum because the weight of the motors decreases with increasing transmission, but the weight of the supply unit and gears decreases with increasing gear ratio:

$$G_\Sigma = G_m + G_s + G_g, \tag{14}$$

where $G_д$ is the weight of the motor, $G_з$ is the weight of the supply unit, and $G_р$ is the weight of the gears.

This problem can be solved graphically if the relationships $J_д(M_д)$, $G_д(M_д)$, $G_з(P_р)$ and $G_р(i)$ are known. These relationships can be defined analytically or graphically. As stated above, the weight of the motor is proportional to the rotational torque $M_д$. The weight of the supply unit depends upon the type of motor for the generator. In selecting the supply unit from its electromagnetic overload capacity, its weight is fixed as a function of the electromagnetic power of the generator.

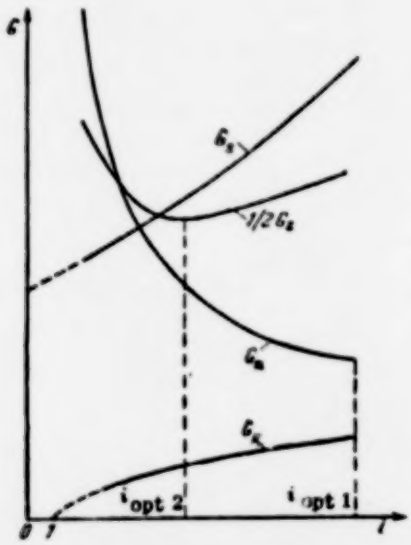

Fig. 3. Weight of drive motor $G_д$, supply unit $G_з$ and gears $G_р$ and the gross weight $G_Σ$ as a function of the gear ratio.

In order to solve this problem, it is first necessary to determine the quantities $M_д$ and $P_р$ as a function of the gear ratio, and then to determine the weight $G_д$, $G_з$ and $G_р$ and the gross weight as a function of i.

To do this, use is made of the results of graphical integration of the equation of motion of the electric drive in Fig. 2. The points of intersection of the curves $φ_2(M_д)$ and the straight line $φ_1$ corresponds to definite values of $M_д$ which satisfy the equation of motion. Using

this data it is possible to plot the relationship $J_m(i)$ direct and then determine the weight of the motor as a function of i.

Substituting the values thus found for M_m and i in formula (11), the power of the generator is determined as a function of i. Knowing the relationship between the weight of the supply unit and P_g, it is then possible to plot $G_s(i)$.

The weight of the gears is the sum of the weight of the gearwheels and the housing. Assuming that the latter is proportional to the weight of the gearwheels, it is possible to plot the weight of the gears as a function of i.

Plotting the stated relationships $G_m(i)$, $G_s(i)$ and $G_g(i)$ on a common diagram (Fig. 3), the gross weight can then be plotted as a function of i. The required optimum value of the gear ratio $i=i_{opt\ 2}$ corresponds to the minimum gross weight. It will be seen from Fig. 3 that the optimum gear ratio $i_{opt\ 2}$ is considerably less than the gear ratio $i_{opt\ 1}$ for the minimum weight of the drive motor alone. The difference between $i_{opt\ 2}$ and $i_{opt\ 1}$ will be the greater, the greater the weight G_s and G_g compared with the weight G_m.

YEAR 1961

Conclusions

1. For the joint selection of the gear ratio and the criteria of the drive motor it is possible to minimize the weight of the drive motor alone, or to minimize the gross weight of the motor, supply unit and gears altogether. Either problem can be solved graphically if the relationships $J_m(M_m)$, $G_m(M_m)$ and $G_s(P_g)$ are known. These relationships can be defined graphically in the general case or analytically.

2. It is not economical to select the criteria of a drive having an individual supply source solely from the point of view of minimizing the weight of the drive motor as this leads to unduly high gear ratios, and excessive power and weight of the supply unit.

In selecting the gear ratio and criteria of the drive motor, the aim should be to minimize the gross weight of the motor, supply unit and gears. This considerably reduces the transmission ratio and provides a much more efficient system. This approach is justified on economic grounds.

Translated by G. K. Blum

REFERENCES

1. A.T. Golovan; *Fundamentals of the electric drive, (Osnovy elektroprivoda).* Gosenergoizdat (1959).
2. V.S. Kulebakin and V.D. Nagorskii; *The electric drive of aircraft devices and units, (Elektroprivod samoletnykh mekhanizmov i agregatov).* Oborongiz (1958).
3. G. Chestnat and R. Maier; *Development and analysis of servo and control systems, (Proektirovanie i raschet sledíashchikh sistem i sistem regulirovaniia).* Gosenergoizdat (1959).
4. L.B. Geiler; *Elektrichestvo,* No. 9 (1948).
5. O.P. Il'in; *Elektrichestvo,* No. 10 (1953).
6. L.B. Geiler; *Elektrichestvo,* No. 12 (1955).
7. F.A. Goraiko and L.V. Korniushin; *Aspects of the selection of the gear ratio for the electric drives of hoist-transport equipment, (Voprosy vybora peredatochnogo chisla reduktora dlia elektroprivodov pod'emno-transportnykh mekhanizmov). Trud. nauchno-tekh. sessii po elektroprivodu pod'emno-transportnykh mehanizmov,* Gosenergoizdat, (1955).
8. V.A. Rozenberg; *Izv. vyssh. ucheb. zaved., Elektromekhanika,* No. 12 (1958).

YEA
196

ABSTRACTS FROM PAPERS PUBLISHED IN ELEKTRICHESTVO No.7, 1961

YEAR
1961

Leading article

To new achievements in the development of Soviet science. (pp. 1-6).

An account is given of a recent conference which was held in the Kremlin to discuss the future development of Soviet science. Development work, applied research and fundamental research was discussed.

Capacitors

Determining the initial conditions for sudden changes in voltages and currents. I.A. Zaitsev *et al.*, (pp.52-55).

A contribution is made to the determination of initial conditions when sudden changes occur in the currents in inductances or voltages across capacitors. Simple schemes are obtained by analysing commutation behaviour which make it possible to determine the initial conditions for sudden changes in voltages and currents quickly.

Determining the reactive power in capacitors. N.I. Nazarov *et al.* (55-59).

It is considered that the specific dissipating surface of a capacitor varies with the shape of the housing and its dimensions. For a given volume, the dissipating surface is maximum for a rectangular parallelepiped with the minimum permissible width of base.

Control engineering

Use of the phase plane method for studying transient mechanical behaviour in electric drives. L.I. Gandzha, (pp. 68-72).

Phase diagrams of transient behaviour are constructed from an analysis of the equation of motion of the drive for the various possible types of load.

The use of saturable reactors to prevent variation in the torque of induction motors due to transient currents. M.M. Sokolov, (pp. 72-75).

An account is given of tests on electric drives with induction motors and saturable reactors which show that a smooth increase in motor torque and speed can be obtained on starting and reversing. The connexion of saturable reactors in the stator circuit only increases acceleration time slightly. Acceleration time depends on the magnetization current of the reactor.

A frequency-controlled drive for a horizontal planing machine. D.A. Zavalishin *et al.*, (pp. 75-79).

It is argued that the best frequency-controlled asynchronous drive system for horizontal planing machines is one with a compensated collector generator excited on the stator side. A detailed account is given of a prototype system.

Elimination of zones of insensitivity in ferromagnetic pick-ups and amplifiers. B.K. Karpenko, (pp. 84-86).

A cheap and effective way of eliminating dead bands in pick-ups and amplifiers with ferromagnetic cores is proposed by the use of an additional magnetic circuit.

Power systems

Zero sequence equivalent networks for transmission lines with different voltages. N.G. Geinin, (pp. 79-81).

It is shown how to compile a zero sequence equivalent network which includes the mutual inductance between two or several transmission lines when each of the nearby lines is of a different voltage.

Rotating machines

The effect of excitation systems on the stability of large interconnected turbo-generators. V.M. Bobrov *et al.*, (pp. 7-13).

A study is made of the stability of large turbo-generators with different systems of excitation. The use of electrodynamic modelling has made it possible to use natural excitation regulators, find their optimum adjustment and study electromechanical phenomena during transient behaviour.

Artificial damping in large synchronous machines. I.D. Urusov *et al.*, (pp. 13-18).

Instead of increasing the flywheel mass, it is proposed to use a system of artificial damping to reduce the oscillation of synchronous machines with a pulsating load. Artificial damping is based on the creation of an additional electromagnetic rotational torque on the shaft by introducing additional periodic currents in the rotor circuits. The theory of the method is given along with test results.

YEAR
1961

Analysis of dynamic stability with the effect of damper windings, speed governors and excitation included. K.I. Bogatev, (pp. 31-34).

A refinement to the method of successive intervals is proposed which makes it possible to include the effect of damper windings, speed governors and excitation when an analytical estimate of dynamic stability is required for synchronous alternators.

Experimental determination of the m.m.f. of the armature commutation reaction in d.c. machines. V.A. Lifanov, (pp. 81-84).

A method is proposed which dispenses with calculated data in the determination of the m.m.f. of the armature commutation reaction by a Hall e.m.f. transducer.

Traction

Reduction of wheel-spin on electric locomotives. B.P. Petrov, (pp. 35-41).

A study is made of the factors affecting high adhesion factors for electric locomotives. Recommendations are made for automatically stopping wheel spin.

Transformers

Problems of voltage regulation in auto-transformers.

A.G. Kraiz, (pp. 41-48).

A method is described for comparing different systems of voltage regulation for large auto-transformers using the typical power of auto-transformers. A refined method of analysis is proposed for the system of regulation in the neutral of the auto-transformer. It can be used to specify the limits of regulation with over- or under-excitation. A short description is given of a new 220 kV auto-transformer with built-in apparatus for regulating the voltage.

Voltage stabilizers

Ferroresonant voltage stabilizers using magnetic material with a rectangular characteristic.

D.I. Bogdanov, (pp. 48-51).

A theoretical study is made of the phenomena associated with the operation under load of ferroresonant voltage stabilizers in which the saturable core is made of cold-rolled steel or magnetic alloy with a high coefficient of rectangularity.

YEA
196

THE PROBLEMS OF DEVELOPING NEW SMALL AND F.H.P. MOTORS*

N.P. ERMOLIN

(Lenin Electrical Engineering Institute, Leningrad)

(Received 26 January 1961)

YEAR 1961

The development of industry, transport, agriculture and the increasing standards of living have considerably extended the demand for small and f.h.p., d.c. and a.c. motors.

The purposes which such equipment has to serve are extremely diverse, covering automatic control, traction, cable and wireless, instrumentation, agriculture and domestric appliances such as clocks, cinematograph equipment etc.

The production of small and f.h.p. motors is now a special branch of electrical engineering whether or not the motors are for special purposes or of general design. The increasing output of various kinds of motor for industry and consumption goods is increasingly demanding more and more material. Whereas, for example, the production of large machines requires about 2 to 3 kg of active and constructional material per 1 kW, small and f.h.p. motors require on average about 50 g per 1 W.

In order to use electrical energy efficiently and economize in ferrous and non-ferrous metal, special attention has to be paid to the starting and operating characteristics of the motors and the utilization of material.

In this paper an attempt is made to classify the problems which have to be solved in this field into those which are common to all classes of machine up to several hundred watt, and those which refer specially

* *Elektrichestvo*, 8, 4-7, 1961.

to particular types.

Amongst the general problems, we have:

(a) the development of new types of d.c. and a.c. motor and the improvement of existing models;

(b) the reduction in size and weight without affecting heating conditions and starting and operating characteristics;

(c) the reduction in mechanical inertia of the executive a.c. and d.c. control motors for small servo systems and reversible equipment;

(d) the use of new magnetic materials and alloys, winding conductors, heat-resistant insulation, varnishes and lubricants in order to improve efficiency and reliability and develop small machines capable of operating at high temperatures;

(e) the improvement in production technology, including the automation of stamping, winding, assembly and other time-consuming operations;

(f) the review of existing State Standards and the development of new ones for individual classes of machine and test methods.

It is well known that the design of small and f.h.p. motors is very diverse and that there is no standard method of connecting the motor to the executive device or instrument. Quite often the motor is organically connected with the load device so that the motor no longer retains its original design features. This often occurs in special equipment and domestic appliances. On the other hand, the design of the motor does not always satisfy requirements and needs to be brought up to date.

Furthermore, there is an increasing demand in all fields of application for motors of essentially new design with improved characteristics as regards weight, size, mechanical inertia and efficiency etc. A good illustration is the small d.c. motor with a printed armature winding. But there are also other opportunities for improvement based on new materials, combined winding circuits, modified magnetic systems etc.

Perhaps the most important problem in this field is the reduction in size and weight. As we have seen, the specific consumption of active and constructional material per unit of output is roughly 20 times greater in small and f.h.p. machines than in large machines. A reduc-

tion in weight would therefore result in a considerable national saving in ferrous and non-ferrous metal.

The weight of a machine can be reduced by reducing its size, and this in turn can be done by altering its construction, improving the ventilation and using new magnetic and constructional material. But, as is known, the size of a machine affects its starting and operating characteristics and its heating capacity. Yet the heating capacity of a model can also depend considerably on the conditions of heat transfer at the point where it is installed. In this respect the weight of the motor is linked mainly with the method of securing the housing of the motor to the load equipment, the type of material used for this gear and its surface area for heat transfer. Unlike medium and large electrical machines, this is a very important factor as regards the heating of small and f.h.p. motors.

YEAR 1961

At the present time a variety of different fixtures are used to secure small and f.h.p. motors to the test stands, namely, special metal "squares", columns with clamps, and other rigs mounted on metal plates.

Test experience shows, for instance, that if a motor is secured by flanges to metal squares, the heating of the motor will vary with the surface area of these squares even with a constant load. Before standard test conditions can be established, it is first necessary to find the best fixtures for securing the test machines. In this respect the important problem is to determine in what limits the ratio of the surface area of the test fixture to that of the machine can be left to vary safely.

The solution of this problem would make the thermal analysis of a number of small non-ventilated electrical machines more exact in the project stage and would help to minimize their size for given outputs and speeds. This is one of the most effective ways of reducing the weight of the small machine.

The problem of reducing the mechanical inertia of small control motors is also an important one from the point of view of improving the the accuracy of small servo systems and reversible gear in performance.

It is well known that accurate performance from high-speed automatic systems depends to a considerable extent on the mechanical inertia of the rotor of the executive motor and that of the other rotating elements in the system. The less the electromechanical time constant of such systems, the more accurate is the performance and the faster the res-

ponse. Since the rotor moment of inertia of a small motor is proportional to the product of the fourth power of its diameter and the first power of the packet length (i.e. the length of the stack of stampings), it follows that the best method is to reduce the diameter as far as possible and accordingly lengthen the rotor to retain the same volume.

In order to improve the efficiency and reliability of small special electrical machines, extensive use should be made of new magnetic materials, alloys, heat-resistant winding conductors, insulating material, varnishes, enamels, bearing lubricants and wiring systems.

This is specially important for small heat-resistant motors capable of operating reliably at temperatures of up to 250°C. However, existing winding conductors and insulation do not as yet satisfy these requirements sufficiently and the maximum operating temperature is still at 180°C. The position is the same with the other material listed above.

It would be of great value to pay more attention to mechanization and automation of stamping, winding, assembly and other time-consuming operations in order to reduce the cost and increase the output of small and f.h.p. machines. Insufficient attention is at present being paid to these matters in industry and "special organizations" engaged on the production of these machines.

Finally, another general problem is the revision of existing State Standards and the development of new ones for particular classes of machine and test methods. The existing standards in the U.S.S.R. only cover certain types of machine, e.g. GOST 6435-52 "Electrical motors of 5 to 600 W", GOST 8212-56 "Three-phase asynchronous motors from 10 to 600 W", GOST 6117-54 "Electrical d.c. generators for automobiles", and so on. These standards naturally refer to the level of technique as it was at the date of publication, and it is important to keep them up to date and publish new ones as required. Special importance attaches to the question of test methods, and the details involved in the experimental determination of motor parameters.

Besides the enumerated general problems, there are a large number of particular problems in motors for special purposes. Here the most pressing are:

(a) the improvement of commutation in small d.c. generators and motors under reversing conditions with a reversing frequency of up to 5 to 10 c/s;

(b) greater accuracy in the performance and output criteria of rotat-

ing transformers, selsyns and tachogenerators;

(c) the refinement of design methods for small machines with permanent magnets, hysteresis motors and various reactive motors;

(d) the development of bearings for sustained operation without additional lubrication;

(e) the abatement of noise;

(f) the improvement of motors for domestic appliances.

The solution of each of these problems would be of great value in improving the quality of small special purpose machines.

Thus, a need to improve the commutation of small d.c. generators and motors arises when they are operating as motors and generators in certain special purpose plants. In such plants an executive motor usually has to operate with a relatively large flywheel mass on the shaft under reversing conditions with a reversing frequency of up to 5 to 10 c/s. Under these conditions the motor and generator are practically continually affected by transient phenomena so that current commutation is very seriously affected. Appropriate means have still to be developed to improve the commutation, since the use of compoles for this purpose in small machines is made difficult by the lack of space to accommodate them.

YEAR 1961

In order to improve the operational accuracy of computer systems, radar scanning systems, small servo systems and other automatic devices, it is necessary to improve the output parameters of rotating transformers, selsyns and a.c. and d.c. tachogenerators which are widely used in the stated equipment. Althoug modern sine-cosine rotating transformers very accurately reproduce a sinusoidal relationship between the output voltage and angle of rotation of the rotor, they are still not always adequate for the increasing demands which are continually being made upon them.

As regards the design of small machines with permanent magnets, hysteresis motors and various reactive motors, it should be pointed out that the existing analytical methods are largely approximate and empirical and the results which they produce often diverge notably from test data. Much theoretical and experimental work needs to be done to refine these methods.

One of the most important constructional components in small high-

speed motors for gyroscope and grinding (polishing) equipment etc. is the bearings which to a large extent determine the reliability of these motors. Since the speed of motors can reach several tens of thousands of revolutions per minute, new types of bearing need to be developed as conventional bearings are inadequate for the purpose.

As regards motors for domestic appliances, the problem is to find the most efficient type of motor for each particular appliance and improve its performance, reliability and life.

In conclusion it should be pointed out that the solution of these general and special problems depends on the efforts of many specialists, industrial enterprises, design offices, research organizations, and educational establishments engaged on the design, production, testing and use of these machines and everything should be done to extend research and development in this field and make the results as widely known as possible.

Translated by O.M. Blunn

YEA
196

THE MEASUREMENT OF LARGE TRANSIENT CURRENTS FOR SWITCHGEAR*

V.D. LIASHENKO

(Lenin Electrical Engineering Institute)

(Received 3 October 1960)

YEAR
1961

In short-circuit current tests on switchgear it is necessary to measure large transient currents which sometimes reach several hundred thousand amperes. Shunts or current transformers and electromagnetic oscillograph vibrators are usually used for this purpose.

This position is not satisfactory for on the one hand the test current may contain a constant component and the current transformers will considerably distort the secondary current curve owing to the intense magnetization of the steel. However, tests in the switchgear laboratory of the Lenin Electrical Engineering Institute have shown that satisfactory measurements can be taken by current transformers at double and treble overloads. On the other hand, shunts have the disadvantage that an involuntary delay occurs at the point where the shunt is connected. It is therefore desirable to find a method of measurement which combines the best features of shunts and current transformers. Such a method has now been evolved by using air-cored current transformers.

An air-cored current transformer is a toroidal coil through which a live conductor is passed. At the ends of the winding an e.m.f. is induced which is proportional to the current derivative. If this e.m.f. is integrated, a voltage is obtained which is proportional to the current to be measured. Integration is performed by an *RC* circuit in the proposed method. The necessary resistance *R* is possessed by the

---

* *Elektrichestvo*, 8, 46-50, 1961.

winding itself of the air-cored transformer coil and it is therefore made from a conductor with a large resistance. This construction of the coil has the advantage that the voltage is uniformly distributed over the turns on load. This simplifies the insulation of the connexions and considerably widens the range of currents that can be measured by one coil. The integration will be more accurate, the greater the integration constant $T = RC$ and the smaller the current in the toroidal winding. The magnitude of R is therefore made large and that of the voltage on the integrating capacitance small. The capacitor voltage is measured by a special d.c. valve amplifier.

Thus, three elements are required for the proposed system:

1. a toroidal coil with a high impedance winding;

2. a d.c. amplifier with an integrating capacitance at the input;

3. an electromagnetic oscillograph vibrator.

For sinusoidal current, the amplitude of the e.m.f. at the ends of the toroidal coil is:

$$U_T = M\omega I_a,$$

where M is the mutual inductance of the toroidal winding and live conductor, mH, ω the angular frequency of the current, and I_a the amplitude of the current to be measured.

The voltage at the input to the amplifier after integration is found quite accurately at large values of T from the expression

$$U_C = \frac{1}{\omega T} U_T.$$

If the gain of the amplifier is S_a, then the current at the output of the amplifier is

$$i_2 = S_a \frac{M}{T} I_a.$$

The quantity $S_a M/T = k_T$ is the transformation coefficient of the measuring circuit; if I is measured in kA, M in mH, T in sec and S_a in mA per volt, then i_2 is obtained in mA.

The error in measurement. We will now consider the error in measurements of the current by an air-cored current transformer. The degree of

accuracy will depend on the accuracy with which the current derivative is obtained, the accuracy of integration and the performance of the amplifier (linearity of characteristics for d.c. and a.c.).

The first and third conditions are satisfied if the toroidal coil and amplifier are right. Good characteristics (1 per cent accuracy in measurement) can be obtained for this equipment without any special difficulty under laboratory conditions. A description of the Institute's toroid and amplifier will be given below.

The second condition can be satisfied within definite limits (tolerances). The equivalent circuit of an air-cored current transformer is shown in Fig. 1.

The differential equation in the capacitor voltage U_c will be:

$$LC\frac{d^2u_C}{dt^2}+RC\frac{du_C}{dt}+u_C=M\frac{di}{dt}. \qquad (1)$$

YEAR 1961

The charge current i_2 of the capacitance C is neglected in comparison with the magnitude of the magnetization current i_1. The short-circuit current may contain periodic and aperiodic components. The transformation of these components will be considered separately.

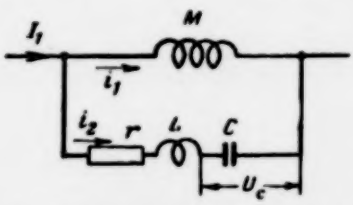

Fig. 1. Equivalent circuit of air-cored transformer.

The *symmetrical component* of the test current varies according to the law

$$i=I_m\sin(\omega t+\psi). \qquad (2)$$

Then

$$\frac{di}{dt}=MI_m\omega\cos(\omega t+\varphi). \qquad (3)$$

When considered with (3), the solution of eqn. (1) will be

$$U_C = \frac{M}{T_C} I_m \cos\varphi \left\{ \sin(\omega t + \psi - \varphi) - \right.$$
$$- \frac{1}{k_1 - k_2} \left[(-k_2 \sin(\psi - \varphi) + \right.$$
$$+ \omega \cos(\psi - \varphi) e^{k_1 t} + (k_1 \sin(\psi - \varphi) -$$
$$\left. \left. - \omega \cos(\psi - \varphi) \right] e^{k_2 t} \right\}, \qquad (4)$$

where

$$k_1 k_2 = -\frac{r}{2L} \pm \sqrt{\frac{r^2}{4L^2} - \frac{1}{LC}};$$

$$\varphi = \operatorname{arc\,tan} \frac{\omega L - \frac{1}{\omega C}}{\sqrt{r^2 + \left(\omega L - \frac{1}{\omega C}\right)^2}}.$$

Suppose we put

$$\frac{2L}{r} = T_L$$

and

$$RC = T_C,$$

then at the low values of L and φ which must be maintained in the tests,

$$k_1 = \frac{1}{T_C};$$

$$k_2 = -\frac{2}{T_L}.$$

Accordingly, eqn. (4) can be transformed into

$$U_C = \frac{M}{T_C} I_m \cos\varphi \left\{ \sin(\omega t + \psi - \varphi) - \right.$$
$$\left. - \sin(\psi - \varphi) e^{-\frac{t}{T_C}} - \frac{\omega L}{r} \cos(\psi - \varphi) \times \right. \qquad (5)$$
$$\left. \times \left(e^{-\frac{t}{T_L}} - e^{-\frac{t}{T_C}} \right) \right\}.$$

Comparing (5) and (2), expressions can be obtained for the error in transformation of sinusoidal current:

1. In the steady state:
the amplitude error is

$$\beta_{st} = (1 - \cos\varphi)\,100\%; \tag{6}$$

and the angular error

$$\varphi \approx \frac{\omega T_L}{2} - \frac{1}{\omega T_C} \quad [\text{rad}].$$

2. Under transient conditions:
the amplitude error is

$$\begin{aligned} \beta_{tr} &\approx \mp \cos\varphi \left(\omega T_L - \frac{1}{\omega T_C}\right) 100\% \approx \\ &\approx \mp \left(\omega T_L - \frac{1}{\omega T_C}\right) 100\%, \end{aligned} \tag{7}$$

YEAR
1961

and the angular error

$$\varphi_{tr} \approx -\varphi \mp \beta_{tr}$$

or

$$\varphi_1 \approx -\frac{3}{2}\omega T_L + \frac{2}{\omega T_C} \quad [rad];$$

$$\varphi_2 \approx -\frac{\omega T_L}{2} \quad [rad]. \tag{8}$$

The minus sign and subscript 1 refer to odd half-periods, and the plus sign and subscript 2 to even half-periods.

The following assumptions were made in this analysis:

$$T_L \ll T_C;\ \sin\varphi \approx \tan\varphi \approx \varphi,\ \cos\varphi \approx 1.$$

Thus, in this case the error in measurement depends on the frequency ω, of the current, the inductance of the current transformer and the integration time constant $T_C = RC$.

The *aperiodic component* of the short-circuit current is expressed by the equation

$$i_a = I_{ma} e^{-\frac{t}{T_a}}. \tag{9}$$

In considering the error in transformation of the aperiodic current

it is not possible to include the inductance L of the toroidal winding since $\omega \to 0$ and as a rule $\frac{L}{r} \ll rC$. Eqn. (1) then takes the form

$$T_C \frac{du_C}{dt} + u_C = -\frac{M}{T_a} I_m e^{-\frac{t}{T_a}}. \tag{10}$$

The solution in U_c will be

$$U_{Ca} = \frac{M}{T_C} I_m \frac{T_C}{T_C - T_a} \left(e^{-\frac{t}{T_a}} - \frac{T_a}{T_C} e^{-\frac{t}{T_L}} \right). \tag{11}$$

It follows from expression (11) that the aperiodic component of the capacitor voltage U_{ca} will decay more quickly than in the primary current and may even change sign. The error in measurement will depend on the ratio $\delta = T_C/T_a$, i.e. on the time constant of the measuring circuit and the attenuation time constant of the aperiodic component.

The error in measurement will be maximum at the instant the capacitor voltage U_C passes through zero. This instant is defined by the time

$$t_0 = T_a \frac{\delta}{\delta - 1} \ln \delta. \tag{12}$$

The maximum error in the measurement of the aperiodic component is found from the expression

$$\gamma = \delta^{-\frac{\delta}{\delta - 1}}. \tag{13}$$

The conclusion therefore can be drawn that the error in measuring by an air-cored transformer will depend on the frequency of the current to be measured. The size of the error at high frequencies will largely be determined by the inductance time constant of the secondary circuit $T_L = \frac{2L}{r}$, and at low frequencies (or aperiodic currents) by the capacitance time constant of the secondary circuit

$$T_C = RC.$$

Given 5 per cent permissible error in the transformation of aperiodic currents which decay with a time constant $T_a = 0.05$ sec, it is found from expression (13) that $T_C = RC = 1$ sec. In practice this condition is satisfied and T_L is about 1 to 2 μ sec. In this case an amplitude error

of 5 per cent for sinusoidal currents from expression (7) will be at a frequency of the order of 4 kc/s. For the fundamental harmonic 50 c/s this error will be about 80 times less.

It therefore follows that an air-cored current transformer is suitable for measuring non-sinusoidal currents which combine in a series of the type

$$i = I_1 \sin(\omega t + \varphi_1) + I_3 \sin(3\omega t + \varphi_3) + \\ + I_5 \sin(5\omega t + \varphi_5) + \ldots$$

However, the angular error increases with increasing frequency of the measured current. Ignoring the effect of $\frac{2}{\omega T_C}$ in the expression for φ_1 in (8), the angular error can be calculated by the formula

$$\varphi_1 = \frac{3}{2}\omega T_L$$

or, if φ_1 is expressed in degrees, the permissible time constant T_L can be calculated from the angular error by the formula

$$T_L = \frac{\varphi_p^\circ}{3 \cdot 180 \cdot f},$$

where φ_p° is the permissible angular error and f the frequency of the current c/s.

Thus, for a test current at 1000 c/s with 5 el degrees permissible angular distortion of the measurements, the time constant T_L must equal 9 μ sec.

Design of the air-cored current transformer. The air-cored current transformer must satisfy two main requirements, namely, it must be insensitive to external magnetic fields and changes in position of the current conductor inside the transformer coil. Since the magnetic permeance of the main flux and the leakage fields are the same in air-cored coils, it therefore follows that these conditions will be satisfied by an ideal toroid with an infinitesimal turn area and an infinitely large number of turns.

According to the law of total current, the following equation will hold for such a toroid

$$\oint H dl = 0,$$

if there are no live conductors inside the toroid. But if there are such conductors inside the toroid, then

$$\oint H dl = \Sigma I,$$

where H is the vector of field intensity and l the length of the closed contour (toroid).

The flux over the internal section of the toroid for a toroidal coil of external radius R_{ext} and internal radius R_{int} with w_2 rectangular turns of height h is

$$\Phi = \frac{\mu_0}{2\pi} I_m w_1 h \ln \frac{R_{ext}}{R_{int}}$$

The mutual inductance of the toroid with the primary winding will be defined by the expression

$$M = \frac{\psi}{I_m} = \frac{\mu_0}{2\pi} w_1 w_2 h \ln \frac{R_{ext}}{R_{int}} [\text{H}].$$

The mutual inductance M in mH, referred to one turn of the primary current, is the main characteristic of a toroid. Another important characteristic affecting the accuracy of the measurements in the integration of the derivative is the inductance of the toroid:

$$L = \frac{\mu_0}{2\pi} w_2^2 h \ln \frac{R_{ext}}{R_{int}} [\text{H}].$$

The inductance L increases the degree of error and it must therefore be small.

The toroid can be made practically insensitive to external magnetic fields if the width of the turn is less than 0.1 of the mean radius and if there are not more than 30 turns per 1 cm of the mean length of the circumference. The winding must be of two-layer design to obtain a large e.m.f.

The Institute's workshop has turned out air-cored transformers with the following rating:

Rated voltage - 12 kV.

Dimension of bakelite former for winding toroid: R_{int} = 120 mm, R_{ext} = 124 mm, h = 178 mm.

Number of winding layers – 2 (continuous, compact).

Winding conductor – enamelled nichrome, 0.15 mm.

Total resistance of winding – R = 160 kΩ.

Mutual inductance – M = 19.5 μH.

Inductance of toroid – L = 150 mH.

Time constant – T_L = 2 μsec.

The method of winding the toroid is illustrated in Fig. 2(a). A photograph of the transformer is given in Fig. 3.

In order to compensate the effect of external transverse fields, a reverse turn of sheet aluminium foil is continued at the beginning of the winding of each layer. The internal layer of foil also serves as an electrostatic screen between the live conductor and the winding. The transformer is covered by a dural shell.

YEAR
1961

Tests on this toroid have shown that an e.m.f. of 6.25 V is induced at the ends of the winding for a conductor carrying a current of 1 kA at 50 c/s; changes in the position of the live conductor in the coil did not alter the result.

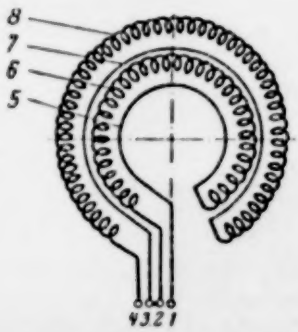

Fig. 2. Winding system of current transformer: *1* – beginning of first layer of foil; *2* – end of first layer of winding; *3* – beginning of second layer of foil; *4* – end of second layer of winding; *5* – first layer of aluminium foil; *6* – first layer of winding; *7* – second layer of aluminium foil; *8*-second layer of winding.

When a live conductor was placed outside the coil, the maximum registered e.m.f. (for various positions and distances) was 35 mV/kA,

i.e. less than 0.5 per cent of the measured quantity.

The connexion of such a toroid to a capacitance of 6 μF provides integration of the induced e.m.f. with a time constant

$$T_C = RC = 160 \cdot 10^3 \cdot 6 \cdot 10^{-6} = 0.96 \text{ sec.}$$

In accordance with the above formulae the error in measurement will be within 5 per cent for the symmetrical component at a frequency above 4 kc/s and for an aperiodic component decaying with a time constant less than 0.05 sec.

In order to take oscillograph recordings of the transient current, use should be made of a d.c. amplifier with a gain S_a = 130 mA/V, which ensures a current in the vibrator circuit with a primary current of 1 kA

$$i_2 = 130 \frac{19.5 \cdot 10^{-6}}{0.95} = 2.25 \text{ mA.}$$

This makes it possible to take satisfactory recordings at currents over 10 kA.

Owing to the use of a high resistance conductor for the toroid, the upper limit to the currents which can be measured is set by the current capacity of the main bus in the "window" of the transformer. The transformer has been used to measure transient currents up to 200 kA.

Fig. 3. Air-cored current transformer with casing.

Fig. 4 shows an oscillogram of a current of 116 kA in dynamic sta-

bility tests on a circuit breaker. The oscillogram was taken by means of an air-cored current transformer. For purposes of comparison, the same diagram also shows an oscillogram of the current obtained from a conventional 5000/5 A current transformer on the high-voltage side of the 6.6/0.25 kV supply transformer, where the current during the test amounted to 116 x 0.25/6.6 = 4.8 kA, i.e. kept within nominal limits. Comparison of the curves on the primary and secondary side shows that the measurements were identical as regards both the symmetrical and aperiodic components of the test current. In order to confirm the anticipated degree of error in the measurements, tests were carried out with an air-cored current transformer together with an a.c. shunt, but no difference was discovered in the recordings outside the limits of accuracy of the oscillograph.

Amplifier. In order that the constant component of the current should be transmitted with the minimum distortion for measuring the voltage on the integrating capacitance, use was made of a two-stage d.c. balanced amplifier with a low-impedance output.

YEAR 1961

A 6N9-type double triode with current stabilization was used in the first stage. Current stabilization was provided by a saturated pentode with automatic bias. The anode supply came from four stabilizers with a voltage +210-255 V relative to the body. The maximum amplification factor of the first stage was 40.

A 6N5-type double triode was used in the second stage (the power amplifier) also on the balanced system with cathode load. The anode supply was from a separate rectifier. For a direct link with the first stage, use was made of a voltage "tributary" of + 105 V from the stabilivolts of the anode rectifier in the first stage.

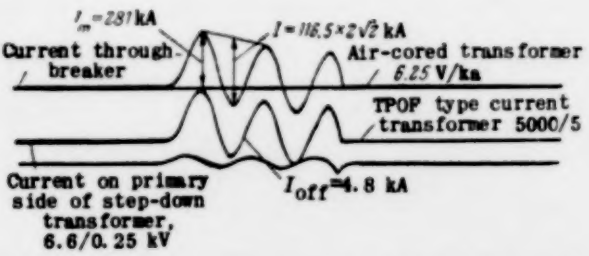

Fig. 4. Current oscillogram obtained by air-cored current transformer.

The characteristic of the d.c. amplifier was linear at output currents

between 0 and 65 mA, i.e. the maximum input voltage at maximum amplification must not be above 0.5 V. If the amplification is reduced by a factor of 10, the input voltage must be increased to 5 V. In order to linearize the frequency characteristic of the amplifier use was made of a system of capacitance correction using negative feedback from the first stage. The frequency characteristic of the amplifier was linear at frequencies between 0 and 20 kc/s.

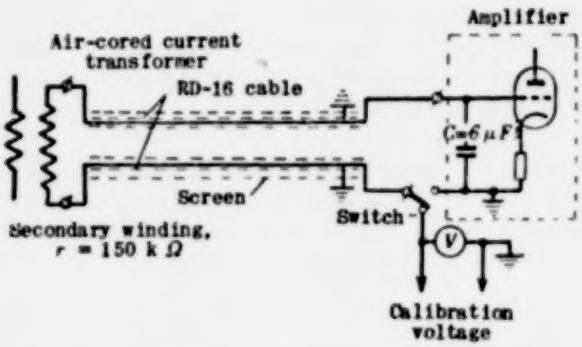

Fig. 5. Calibration system for air-cored current transformer.

For calibration of the air-cored transformer, a special alternating voltage source was provided with tappings of 110, 300, 450 and 600 V together with a voltmeter which was also used as a null indicator for the d.c. output. Since the internal impedance of an air-cored transformer is large, resort to the circuit shown in Fig. 5 to introduce the calibration voltage into the secondary winding circuit was made. This system prevents the capacitance of the connecting conductors affecting the integrating circuit on calibration of the measuring circuit. If a calibration voltage of 50 c/s is switched on, the curve at the output of the amplifier is recorded on the electromagnetic oscillograph. The scale is found by the formula

$$m = \frac{2.82U_k}{314MI2l} \text{ [kA/mm]},$$

where U_k is the calibration voltage, V;

M is the mutual inductance of the air-cored transformer, mH;

$2l$ is the amplitude envelope of the sine curve on the oscillogram.

The amplifier displayed a high degree of stability in operation.

Zero drift after a 10-min period of heating did not exceed 1 mA/hr.

Conclusions. Large transient currents can be successfully measured by integrating the current derivative.

2. The practical realization of the elements of the test equipment (the toroidal coil and amplifier) presents no great difficulty.

3. The turns of the toroidal coil must not exceed one tenth of the mean radius of the toroid in width, there must be about 30 turns per "running" centimetre of the winding circumference, and the toroidal coil must be made from a high impedance conductor so that the time constant of the coil L/R does not exceed 10μsec.

4. The integration time constant must not be less than 1 sec.

5. A simple d.c. amplifier can be used, preferably of the balanced type, with a gain S_a = 100 to 200 mA/V. Such an amplifier is stable in operation and has only a slight zero drift.

YEAR
1961

Translated by O.M. Blunn

A TWO MOTOR MACHINE-VALVE STAGE WITH SEMICONDUCTOR RECTIFIERS*

(Moscow Power Institute)

(Received 21 January 1961)

A good method of speed control for large plants of up to 10,000 kW or more in high-speed drives of 5000 to 7500 rev/min with a ventilator load is to use slip-ring motors in series.

Owing to the difficulties in constructing large high-speed slip-ring motors of about 3000 rev/min, it is expedient to use two smaller motors in place of one large motor. The increase in nominal speed leads to a saving in weight and cost of the motor and gearing. Thus, for example, use may be made of ATMF-2500-2, 2500 kW$\sim$3000 rev/min and ATMF-3700-2, 3700 kW$\sim$3000 rev/min slip-ring induction motors for the drives of centrifugal compressors of 7000 kW for gas mains (two motors to each plant).

In this paper a stage system is proposed (Fig. 1) in which the slip energy is converted by semiconductor (silicon or germanium) rectifiers (diodes) and then passed into the network.

The rectifiers are connected in two series-connected bridge systems. For the inverter group use is made of a constant speed unit consisting of a d.c. motor (DCM) and a synchronous generator (SM).

The shafts of the two asynchronous drive motors (1AM and 2AM) are rigidly connected to each other by couplings and to the working plant by a system of gears. The rotors of the asynchronous motors are shifted 30 el. deg. relative to each other.

---

* *Elektrichestvo*, 8, 50-56, 1961.

Figs. 2 and 3 show oscillograms of the rectified voltages with and without such rotor displacement (θ = 0 and θ = 30 el. deg.). If θ = 0, the pulsations of the variable component of the rectified voltages of the two bridges U_{d1} and U_{d2} coincide in phase and as a result of their addition the variable component of the total voltage U_d varies with the with the same frequency but twice the amplitude (Fig. 2).

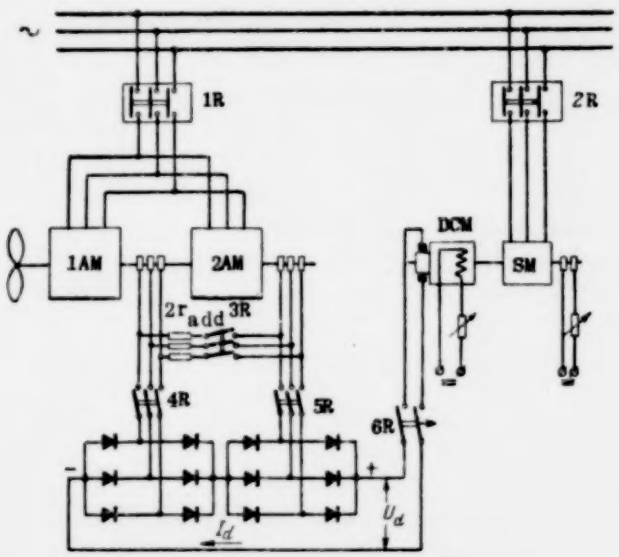

Fig. 1. Main circuit of two-motor machine-valve stage:

Test equipment: 1AM and 2AM – AK-61-6 type induction motors 7 kW, 220/380 V, 940 rev/min, cos φ = 0.79, E_{2nom} = 175 V, I_{2nom} = 26 A; DCM – d.c. motor type PN-45, 5.2 kW, 115 V, 45.2 A, n_{nom} = 2000 rev/min; SM – synchronous generator type SGS-4.5 kW, 230 V, 11.3 A, 1500 rev/min, cos φ_{nom} = 0.8; 1-6 R – switches; VK-25 type silicon rectifiers, 25 A, U_{rev} = 150 V.

If θ = 30 el. deg. the pulsations of the variable component U_{d1} and U_{d2} are shifted in phase in such a way that the maximum of U_{d1} corresponds to the minimum of U_{d2}. This leads to a decrease in the amplitude of the variable component of the total rectified voltage U_d and a doubling of its frequency of pulsation (Fig. 3).

Analysis of the proposed system has shown that the two series-

connected rectifier bridges operate independently in the given range of loads.

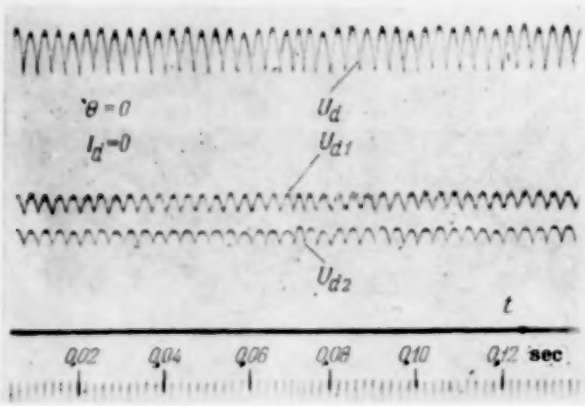

Fig. 2. Oscillogram of rectified voltages at $\theta = 0$.

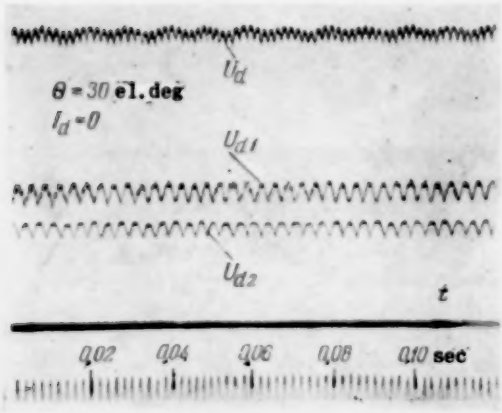

Fig. 3. Oscillogram of rectified voltages at $\theta = 30$ el. deg.

An analogous system with one drive motor having two rotor windings shifted 30 el. deg. and six slip-rings was put forward by corresponding member of the U.S.S.R. Academy of Science D.A. Zavalishin.

The system is started by switching on the switch $1R$ in the stator circuits of the asynchronous motors with the rotor cross-connector closed. Given rotor shift through an angle θ, the rotor current is defined by the expression

$$I'_2 = U_1 \sqrt{\frac{1-\cos\theta}{2\left[\left(r_1 + c_1\frac{r'_{add}+r'_2}{s}\right)^2 + (x_1 + c_1 x'_2)^2\right]}}, \qquad (1)$$

where I'_2 is the modulus of the current in the rotor of each motor, referred to the stator;

U_1 is the phase voltage of the stator;

r_1 and r'_2 are the phase resistance of the stator and the referred phase resistance of the rotor;

r'_{add} is half the additional resistance in the rotor circuits, referred to the stator winding;

x_1 and x'_2 are the phase inductive reactance of the stator and the referred phase inductive reactance of the rotor;

$c_1 = U_1/E_1$ is the ratio of the voltage to the e.m.f. of the motor at synchronous speed;

s is the motor slip.

The current consumed by the stator of each motor is defined as the vector sum of the no-load current and the referred rotor current of the corresponding motor.

Since the angles between the current vectors I'_2 and the corresponding e.m.f. of each motor are not the same, it follows that the motors will develop different torques

$$M_1 = \frac{M_{cr}(1+q)}{\frac{s}{s'_{cr}} + \frac{s'_{cr}}{s} + 2q}\left[(1-\cos\theta) - \frac{\sqrt{1-q^2}}{qs + s'_{cr}}\, s\sin\theta\right]; \qquad (2)$$

$$M_2 = \frac{M_{cr}(1+q)}{\frac{s}{s'_{cr}} + \frac{s'_{cr}}{s} + 2q}\left[(1-\cos\theta) + \frac{\sqrt{1-q^2}}{qs + s'_{cr}}\, s\sin\theta\right], \qquad (3)$$

where M_{cr} is the "critical" (pull-out) torque of the asynchronous motor in the normal system;

$s'_{cr} = \frac{c_1(r'_2 + r'_{add})}{\sqrt{r_1^2 + (x_1 + c_1 x'_2)^2}}$ — the critical slip; and

$$q = \frac{r_1}{\sqrt{r_1^2 + (x_1 + c_1 x'_2)^2}}. \quad (4)$$

The total torque of the two-motor drive on starting will be:

$$M = \frac{2M_{cr}(1+q)}{\frac{s}{s'_{cr}} + \frac{s'_{cr}}{s} + 2q}(1 - \cos\theta). \quad (5)$$

Analysis of formula (5) shows that the initial torque of the drive on starting for $\theta = 30$ el. deg. attains 13.4 per cent of the initial starting moment of one motor.

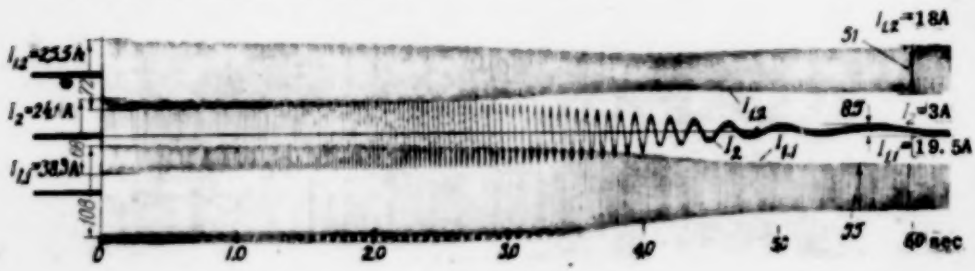

Fig. 4. Oscillogram of the starting of the two-motor drive.

When the starting torque is insufficient (starting on full load), provision may be made for shifting the rotor shafts through an angle $\theta = 90$ el. deg. In this case all the fundamental propositions in this paper remain valid.

Fig. 4 shows an oscillogram of the currents on starting for $\theta = 30$ el. deg.

By switching on switch 2*R* voltage is supplied to the stator of the synchronous machine and the constant speed unit accelerates to synchronous speed, after which excitation is applied to the d.c. motor. Voltage is supplied to the rectifiers when the asynchronous motors reach the steady state speed.

Regulation of the excitation current of the d.c. motor makes it possible to equate the voltages of the rectified circuit on the d.c. motor side as well as on the side of the rectifiers. After this, switch 6*R* is switched on in the rectified current circuit. At this

the starting of the plant is finished.

Speed is controlled within wide limits by varying the excitation current of the d.c. motor.

Given the arbitrary slip s of two identical asynchronous motors and steady state operating conditions, the relationship between the voltage at the terminals of the d.c. motor and the rectified current will be (Fig. 5):

$$U_d = 2\left[2\sqrt{2}\,\frac{m}{\pi}\sin\frac{\pi}{m}E_{r0}s - I_d\left(\frac{mx_d s}{\pi} + 2r_d\right) - 2\Delta e\right], \tag{6}$$

where U_d is the voltage at the terminals of the d.c. motor;

E_{r0} is the rotor phase voltage of the asynchronous motor at rest;

I_d is the mean value of the rectified current;

$m = 3$ the number of rotor phases;

x_d is the equivalent phase reactance of the asynchronous motor referred to the rotor circuit;

r_d is the equivalent phase resistance of the asynchronous motor referred to the rotor circuit;

s is the slip;

Δe is the voltage drop in one arm of the bridge.

The voltage U_d at the terminals of the d.c. motor will be:

$$U_d = E_d + I_d(r_a \pm B), \tag{7}$$

where E_d is the e.m.f. of the d.c. motor due to the main excitation flux;

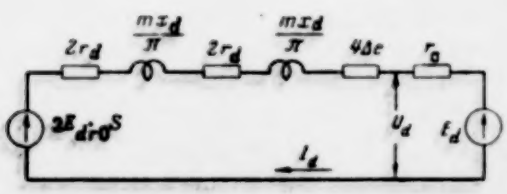

Fig. 5. Equivalent circuit.

r_a is the armature resistance of the d.c. motor;

B is a compounding factor having the dimension of resistance.

As a special case $B = 0$ for a d.c. motor with independent excitation and expression (7) takes the form:

$$U_d = E_d + I_d r_a. \tag{7a}$$

Substituting the expression for U_d from (7a) in (6):

$$2\left[E_{dr0}s - I_d\left(\frac{mx_d s}{\pi} + 2r_d\right) - 2\Delta e\right] - \\ - E_d - I_d r_a = 0, \tag{8}$$

where $E_{dr0} = 2\sqrt{2}\,\frac{m}{\pi}\sin\frac{\pi}{m}\,E_{r0}$ is the rectified voltage of the rotor with the motor stationary and the rectified circuit open ($I_d = 0$).

It follows from expression (8) that variation of E_d when the stage is operating at steady state speed leads to variation of the current I_d of the rectified circuit and, consequently, to variation of the torque M of the asynchronous motors.

If E_d increases, then I_d and therefore M decrease and the drive begins to slow down. The retardation will continue until equilibrium is attained in the rectified current circuit in accordance with equation (8).

In this case a definite current I_d is established along with a corresponding rotational torque M. The motors will rotate at less speed than before and at this lower speed the load torque will be balanced by the rotational torque of the motors. The system of increasing the speed is controlled in a similar way.

The relationship between the torque of the asynchronous motors and the rectified circuit current I_d is defined by the expression:

$$M = 2\,\frac{1}{\omega_0}\,I_d E_{dr0}\left(1 - \frac{I_d m x_d}{\pi E_{dr0}}\right), \tag{9}$$

where ω_0 is the synchronous angular velocity of the rotor.

It is possible to find the appropriate values of I_d and M for given values of s with E_d variable by formulae (8) and (9).

YEAR
1961

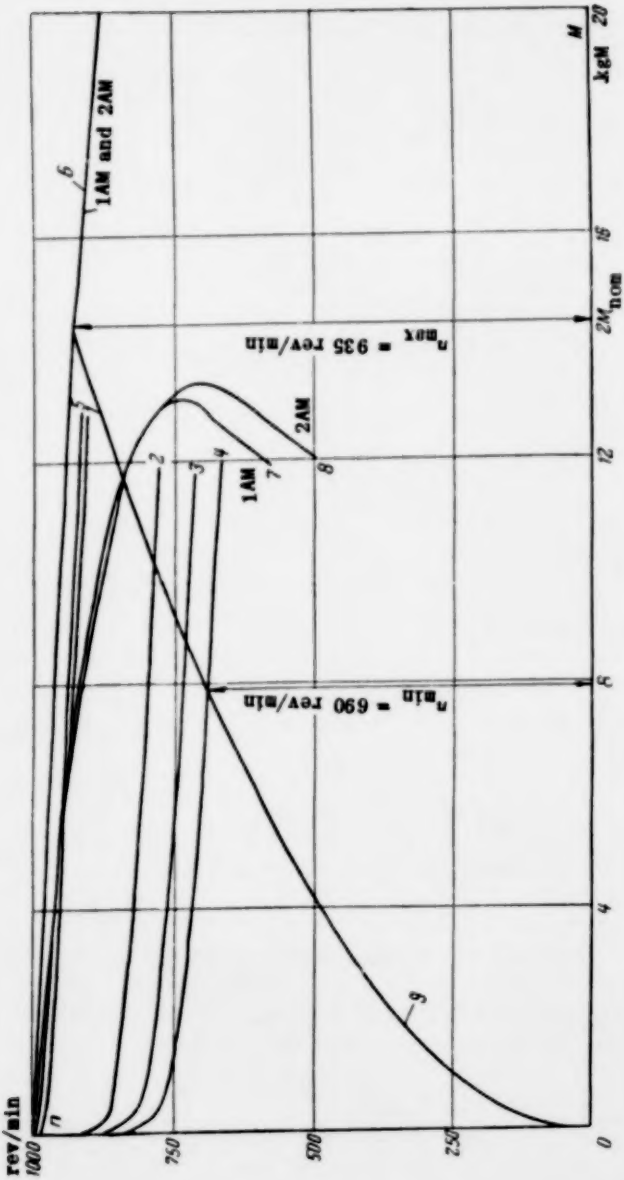

Fig. 6. Mechanical characteristics of the two-motor drive in the machine-valve stage.
$s_{min} = 0.065$; $s_{max} = 0.31$; $U_{nom} = 220$ V.

Curves $n = f(M)$ can be plotted from this data for E_d = const. Other such curves can be found for the drive for different excitation currents of the d.c. motor and a family of curves is obtained. Fig. 6 shows a family of these curves obtained experimentally.

The initial slip corresponding to the ideal no-load speed of the drive when operating on the given $n = f(M)$ curve can be found from expression (8). Provided that $I_d = 0$, then

$$2[E_{dr0}s_0 - 2\Delta e] - E_d = 0, \tag{10}$$

whence

$$s_0 = \frac{E_d + 4\Delta e}{2E_{dr0}}. \tag{11}$$

It follows from expression (11) that with an increase of effected by regulating the excitation current of the d.c. motor, a reduction in the ideal no-load speed of the drive is achieved and the $n = f(M)$ curves thereby lowered.

It should be mentioned that the slip s_0 from equation (11) corresponds to the condition when the $n = f(M)$ curves of the drive are straight lines over their operating part. In fact at low loads the shape of the curves changes (Fig. 6) owing to the interruption of the current and the initial slip will be less than the calculated figure.

The maximum torque of the drive for the various d.c. motor excitation currents is of the same value equal to the maximum torques of the two drive motors in operation on "natural" $n = f(M)$ curves.

The critical slip of an "artificial" (equivalent) curve for the two-motor drive is found by the formula:

$$s_{cr} = (1 + \rho \pm \beta)\, s_{cr} + \sqrt{2}s_0, \tag{12}$$

where s_{cr} is the critical slip of the two-motor drive on natural curves;

γ and β are relative values of the d.c. motor armature resistance and the compounding factor referred to the stator circuit.

As a special case $\beta = 0$ for a d.c. motor with independent excitation and expression (12) accordingly takes the form:

$$s_{cr} = (1 + \rho)\, s_{cr} + \sqrt{2}s_0, \tag{13}$$

$$\rho = \frac{\sqrt{\frac{3}{2}}\, k_e^2 r_a}{2\sqrt{2}\, \frac{m}{\pi} \sin\frac{\pi}{m} \cdot r_2'} = 0{,}53 k_e^2 \left(\frac{r_a}{r_2'}\right), \tag{14}$$

where k_e is the coefficient of transformation from the stator to the rotor.

In determining s'_{cr} (the artificial curve critical slip) from formulae (12) and (13) the effect of overlap of the rectifier anodes was ignored. Unlike that obtained by calculation, the critical slip will in fact be slightly greater as has been confirmed by tests.

Curve 1 in Fig. 6 represents the fundamental $n = f(M)$ curve of the stage when the d.c. motor excitation current is zero. In this case the initial slip is defined by the sum of the d.c. motor e.m.f. $E_{d\mu}$ from residual magnetism and the voltage drop $4\Delta e$ in the rectifiers:

$$s_{01} = \frac{E_{d\mu} + 4\Delta e}{2E_{dr0}}. \tag{15}$$

Curve 4 in Fig. 6 corresponds to the rated excitation current of the d.c. motor. Curves 2 and 3 refer to intermediate values of the excitation current.

YEAR 1961

In order to increase the speed of the drive and thereby widen the range of control and increase the utility of the drive, it is necessary to reverse the polarity of the d.c. motor excitation circuit. In this case the excitation current changes sign and at a certain value the e.m.f. $E_{d\mu}$ of residual magnetism will be compensated. The formula for the initial slip takes the form:

$$s_{05} = \frac{4\Delta e}{2E_{dr0}}. \tag{16}$$

These are the conditions to which curve 5 in Fig. 6 refers.

With a further increase in the negative value of the d.c. motor excitation current a moment occurs when each rectifier transmits a current in the same direction during a complete period. The explanation is that a negative potential is applied to the common cathodes of the three rectifiers in each bridge and the magnitude of this potential exceeds the negative potential of the anodes of two rectifiers (the anode of the third rectifier has a positive potential at this moment) Likewise, a positive potential is applied to the common anodes of the other three rectifiers in each bridge and the magnitude of this positive potential exceeds the positive potential of the cathodes of two rectifiers. As a result shorting takes place through the rectifiers of the three phases of the rotor windings of the asynchronous motors.

Asynchronous motors which are connected in stages are independent of it on their natural $n = f(M)$ curves.

The d.c. motor operates as a generator. Its comparatively small e.m.f. fully covers the voltage drop in the rectified current circuit. The magnitude of the current in the rectified circuit remains constant during load variations and depends on the d.c. motor excitation current. The synchronous machine operates as a motor consuming energy from the mains and drives the d.c. motor.

Under these conditions

$$E_d = I_d r_a + 4\Delta e \tag{17}$$

and

$$s_0 = 0. \tag{18}$$

In this case the $n = f(M)$ curve of the stage corresponds with the natural curve 6 of a two-motor drive, which is the sum of the natural $n = f(M)$ curves of the two individual motors (7 and 8).

The range of speed control can be widened by about 4 to 5 per cent by reversing the polarity and applying negative excitation to the d.c. motor.

Curve 9 in Fig. 6 represents the torque-speed curve for a ventilator load. The intersection of curve 9 with curves 6 and 4 defines the limits of speed control.

A comparatively low range of speed control was obtained on the test equipment (from 100 to 74 per cent). But under real conditions the range of speed control can be widened considerably by selecting the parameters of the electrical equipment in the stage appropriately.

The rating of the proposed machine in the stage under consideration is defined by the product of the maximum current (at maximum speed of the drive) times the maximum voltage (at minimum speed of the drive). In large plants with ventilator loads it is therefore advisable to use two d.c. machines, switching them from parallel connexion to series connexion. This permits a substantial reduction in the rating of the d.c. machines. For example, for speed control of the drive from 100 to 50 per cent, the use of two d.c. machines with such switching roughly halves the rating of these machines (approximately 25 per cent of the established power of the drive motors instead of about 50 per cent without switching).

The rating of the synchronous machine is equal to the square root of

the squares of the active and reactive power. The active power is defined as the maximum value of the regenerative active power, which is no more than about 15 per cent of the established power of the drive motors for the drive of gear with a ventilator load. The reactive power of the synchronous machine depends on the need to compensate the reactive power of the electric drive, i.e. the need to improve its power factor.

The expediency of using asynchronous slip-ring motors in stages to regulate the speed of mechanisms with a ventilator load has been confirmed by comparing the technical and economic indices of the proposed system with those of a system with rheostat control.

The comparison was made for a 6300 kW compressor on the basis of the annual consumption graph at the Ukrgiprogaz gas works.

Tables 1 and 2 refer to the rheostat control system.

YEAR 1961

TABLE 1

No. of hr worked in year	Rotational speed, %	Useful power on shaft, kW	Total power loss, kW	Power consumed from network, kW	Efficiency, %	Utilized energy, mill. kW/hr	Expenditure of electrical energy, mill. kW/hr
2.160	100	6.430	240	6.670	96.5	13.9	14.4
1.464	92.5	5.060	570	5.630	89.8	7.41	8.25
1.464	85	3.970	845	4.815	82.5	5.81	7.05
2.184	77.5	3.020	1.015	4.035	74.7	6.60	8.82
1.488	70	2.250	1.080	3.330	67.2	3.34	4.95

TABLE 2

Cost of main electrical equipment, C_{eq}, 1000 roubles	Cost of erection, C_{er}, 1000 roubles	Depreciation, C_d, 1000 roubles	Repair costs C_{rep}, 1000 roubles	Cost of electrical energy C_e 1000 roubles	Capital outlay C_{outl}, 1000 roubles	Operating costs C_{opl}, 1000 roubles
51.6	5.16	5.16	1.55	351	56.76	357.71

Total electricity consumption was 43.47 million kW/hr per annum. Annual losses amounted to 6.41 million kW/hr, leaving 37.06 million kW/hr usefully used. The mean annual efficiency was 85.2 per cent.

The cost of the main equipment was as follows: motor 6500 kW, approx. 1500 rev/min – 41.0 thousand rubles; control resistors and the "magnetic station" (contactors) – 3.5 thousand rubles; "KRU" chambers (compact bus, breaker and switchboard cubicles) – 0.5 thousand roubles; static capacitors (232 items) – 6.6 thousand rubles.

The number of static capacitors depended on the need to ensure cos $\varphi = 0.92$. The cost of 1 kW/hr of electrical energy was taken as 0.8 kopecs.

$$C_{er} = 0.1C_{eq}; \quad C_d = 0.1C_{eq}; \quad C_{rep} = 0.03C_{eq};$$
$$C_{out1} = C_{eq} + C_{er}; \quad C_{op1} = C_d + C_{rep} + C_{el}.$$

Here the subscripts refer to various items of cost C, namely, er – erection, eq – equipment, rep – repairs, out 1 – capital outlay on first system, op 1 – operating costs, d depreciation, and e – electricity.

Tables 3 and 4 refer to the same system but with rheostat control replaced by the two-motor machine-valve stage with semiconductor rectifiers.

TABLE 3

No. of hr worked in year	Rotational speed, %	Useful power on shaft, kW	Total power loss, kW	Power consumed from network, kW	Efficiency, %	Utilized energy, mill. kW/hr	Consumption of electrical energy, mill, kW/hr
2,160	100	6,430	430	6,860	93.6	13.90	14.82
1,464	92.5	5,060	420	5,480	92.4	7.41	8.02
1,464	85	3,970	405	4,375	90.7	5.81	6.41
2.184	77.5	3,020	390	3,410	88.5	6.60	7.45
1,488	70	2,250	375	2,625	85.7	3.34	3.90

The useful electricity was the same as with rheostat control, but the actual consumption was 40.60 million kW/hr, i.e. 2.87 million kW/hr less, and the mean annual efficiency was 91.1 per cent. It should be pointed out that the total power loss at maximum (rated) speed can be reduced to 240 kW (the rated loss of asynchronous motors) by disconnecting the stage when the motors are operating on the natural $n = f(M)$ curve.

TABLE 4

Cost of main electrical equipment, C_{eq}, 1000 roubles	Cost of erection C_{er}, 1000 roubles	Increased cost of building for extra equipment, C_b, 1000 roubles	Depreciations C_d, 1000 roubles	Repair costs C_{rep}, 1000 roubles	Cost of electrical energy C_e, 1000 roubles	Capital outlay, C_{out2}, 1000 roubles	Operating costs C_{op2}, 1000 roubles
76.8	11.5	5.0	7.68	2.32	325	93.3	335

To determine the cost of the drive motors it was assumed that the power of the two drive motors was the same and equal to 3500 kW. The cost of the main equipment C_{eq} includes all the machines and electrical gear in the drive system:

$$C_{er} = 0.15C_{eq}; \quad C_d = 0.1C_{eq}; \quad C_{rep} = 0.03C_{eq};$$
$$C_{out2} = C_0 + C_{er} + C_b; \quad C_{op2} = C_d + C_{rep} + C_e.$$

where the subscripts are the same, except that "2" refers to the two-motor system and b to the extra cost of altering the buildings.

The time taken for the prime cost of the twin-motor system to be recovered out of reduced running costs can be found from the expression

$$T = \frac{C_{out2} - C_{out1}}{C_{op1} - C_{op2}} = \frac{93.3 - 56.76}{357.71 - 335} = 1.61 \text{ yr.}$$

The use of two drive motors instead of one large motor in the proposed system has the following advantages:

(a) the weight of the motors and gearing is reduced and rated speed increased;

(b) the motors can be started without a starter rheostat since if the rotors are electrically displaced by $\theta = 30^\circ$, a balancing e.m.f. arises in the circuit of the rotors and the starting torque is sufficient to accelerate the motor up to full speed (for no-load starting); in this case the change in current is below the maximum.

(c) smooth curves can be obtained for the rectified current and voltage since in this case there is 12-phase rectification. There is no

further need of a smoothing choke in the plant.

The use of semiconductor rectifiers in place of mercury arc rectifiers allows a considerable reduction in the loss of electrical energy, i.e. increases the efficiency of the plant, and reduces its dimensions.

Translated by O.M. Blunn

REFERENCES

1. S.Z. Barski; *Elektrichestvo*, No.6 (1951).
2. F.I. Butaev and E.L. Ettinger· *Electrical rectifier drives, (Ventil'nyi elektroprivod)*. Gosenergoizdat (1951).
3. I.L. Kaganov; *Electronic and mercury arc rectifiers*, Pt. I, III, *(Elektronnyi i ionnye preobrazovateli)*, Ch. I, Gosenergoizdat (1959); Ch. III, Gosenergoizdat (1956).
4. A.S. Sandler; *A large variable drive using induction motors with rotary stators for devices with a ventilator load torque, (Moshchnyi regulirueayi privod ot asinkhronnykh dvigatelei s povorotnym statorom dlia mekhanizmov s ventiliatornym momentom nagruzki)*. Trud. sovesch. po avtomat. elektroprivod. peremen. tok., Akad. Nauk SSSR (1958).
5. R.L. Witzke, J.V. Kressler and J.K. Dillard, *Trans Amer. Inst. Elect. Engrs.* No.11 (1953).

YEA
196

A STUDY OF THE E.M.F. INDUCED IN ELECTRICAL MACHINES USING AN ELECTROLYTIC TANK*

K.S. DEMIRCHIAN and V.V. PRUSS-ZHUKOVSKII

(Kalinin Polytechnical Institute, Leningrad)

(Received 28 March 1961)

YEAR
1961

In some cases in the design of electrical machines it is necessary to determine the shape of curves for the e.m.f. induced in the individual windings, sections or conductors with the greatest possible accuracy. Above all, this is the case with heavy duty d.c. machines (especially with complex multi-path armature windings), synchronous machines with strictly sinusoidal voltage curves inductor machines, and electromagnetic stepping devices etc. It may also be necessary to determine the shape of the e.m.f. curves for the analysis of secondary phenomena and behaviour in machines, e.g. commutation, balancing currents, additional losses etc.

A rigorous analytical approach to the problem is as a rule impossible owing to the complex configuration of the magnetic systems (beak shaped poles, stator and rotor teeth), whilst approximate methods tend to be too rough or too cumbersome. This puts a premium on finding other methods of investigation. It should be pointed out that the e.m.f. of sections, coil groups and whole windings can easily be found if the e.m.f. in the individual winding conductors are known. Thus, the problem of investigating the e.m.f. in systems of conductors can always be reduced to the determination of the e.m.f. in the individual conductors.

The shape of the curve for the e.m.f. in an armature conductor of an electrical machine can always be found quite easily, provided no tooth configuration is present, if the distribution of the normal component of the magnetic induction vector B_n is known over the surface of

* *Elektrichestvo*, 8, 62-66, 1961.

rotation of the conductor.

No re-distribution of the magnetic field occurs on rotation of the rotor owing to the smoothness of the surface and it can therefore be seen from the formula which holds in this case

$$e = B_n l v \tag{1}$$

that if the conductor intersects the lines of magnetic induction at a constant speed, then the shape of the e.m.f. curve will coincide in shape with that for the distribution B_n over the surface under consideration (rotor or stator, depending on where the conductor is placed).

The picture is quite different if the surface is not smooth. A re-distribution of the magnetic field takes place inside the gap if teeth are present, i.e. the shape of the curve for the distribution of B_n changes as a function of the position of the rotor and owing to the continuous re-distribution of the lines of induction on rotation of the rotor, the velocity v in formula (1) cannot be regarded as constant.

It is therefore rather a question of the resemblance of the two curves and not their identity.

The effect of the different factors on the shape of the e.m.f. curve can be investigated on an actual machine, but it is hardly practicable owing to the cost and difficulty of obtaining the various different versions of the machine which are required. This is an insurmountable difficulty in the case of some machines which are to be re-designed. The electrolytic tank method which is described in this paper is sometimes the only way that the shape of the e.m.f. curve can be determined.

The intensity of the induced electrical field can be described by the expression

$$\mathbf{E} = -\frac{\partial \mathbf{A}}{\partial t}, \tag{2}$$

where A is the vector potential of the magnetic field.

If the magnetic field on the active length of the machine is regarded as two-dimensional, then instead of equation (2)

$$e = -l\frac{dA_z}{dt}, \tag{3}$$

where e is the e.m.f. in the conductor, l is the active length of the conductor in the slot, and A_z the component of the vector potential of the magnetic field along the z axis of the machine.

The vector potential is defined by all the currents of the machine. Variation with time may take place if the conductor under investigation is moved relative to the magnetic field (during time dt the conductor moves from the point with the potential A to a point with the potential $A + dA$) and if a change takes place in the currents in the machine windings (in this case the quantity A varies with time at the point in question).

No special difficulties are involved in modelling for the second case. Attention will therefore be paid to the first case on the assumption that the currents are constant. In this case an e.m.f. only arises in the conductors due to their movement in the magnetic field.

YEAR
1961

It is assumed that the rotation of the rotor takes place with a constant angular velocity ω. Then

$$v = \omega r = r \frac{d\alpha}{dt}, \tag{4}$$

where v is the speed of the conductor at a distance r from the axis of rotation, $\omega = 2\pi n$ the angular velocity of rotation of the rotor and $d\alpha$ the angle of rotation of the rotor during time dt.

From expressions (3) and (4)

$$e = -l \frac{dA_z}{d\alpha} 2\pi n. \tag{5}$$

The principles underlying direct investigation of e.m.f. by modelling in an electrolytic tank follow from formula (5).

In order to model the e.m.f., it is sufficient to model the field of the vector potential A_z and imitate the motion of the rotor relative to the stator.

For the current field in a conducting medium

$$\operatorname{div} \delta = 0, \quad \operatorname{rot} \mathbf{E} = 0.$$

If we put

$$\delta = \delta_1 + \delta',$$

where $\delta_1 = \gamma E$ is the density of the current in the electrolyte and δ' the density of the current from the supply source, we can then write:

$$-\operatorname{div}\delta' = \operatorname{div}\delta_1 = p$$

and if

$$E = -\operatorname{grad} U, \tag{6}$$

we then finally have

$$\operatorname{div}\operatorname{grad} U = -\frac{p}{\gamma} \quad \text{or} \quad \operatorname{div}\frac{1}{\rho}\operatorname{grad} U = -p;$$

where p is the volume density of the current introduced into the bath from an extraneous source (the supply source).

Using the identity div B = 0, equivalent to the identity B = rot A, the following set of equations for the magnetic field

$$\operatorname{rot} H = \delta, \ \operatorname{div} B = 0, \ B = \mu H,$$

simplifies to the form

$$\operatorname{rot}\operatorname{rot} A = \mu\delta.$$

For a plane field in a Cartesian system of co-ordinates

$$\operatorname{div}\operatorname{grad} A_z = -\mu\delta_z \text{ or } \operatorname{div}\frac{1}{\mu}\operatorname{grad} A_z = -\delta_z. \tag{7}$$

Using the sameness of expressions (6) and (7), it can be asserted if the equality of the boundary conditions is observed (geometric similarity and correspondence of the medium with the magnetic permeability μ and electrical conductance ρ) that the distribution of the electrical potential in the bath will be analogous to the distribution of the vector potential in the machine. In this case, the lines of equal potential U = const in the model will coincide with the lines of induction in the machine.

This can be seen from a comparison of the expressions

$$\mathbf{E} = -\operatorname{grad} U = -\mathbf{i}\frac{\partial U}{\partial x} - \mathbf{j}\frac{\partial U}{\partial y}$$

and

$$\mathbf{B} = \operatorname{rot} \mathbf{A} = \mathbf{i}\frac{\partial A_z}{\partial y} - \mathbf{j}\frac{\partial A_z}{\partial x} = c_1\left(\mathbf{i}\frac{\partial U}{\partial y} - \mathbf{j}\frac{\partial U}{\partial x}\right).$$

The vector **E** is transverse to the lines U = const and the vector **B** is transverse to the vector **E**. Consequently, the vector **B** is tangential to the equipotential lines. Thus, the modelling of the field of vector **A** can be reduced to the construction of a geometrically similar model where the regions with different μ correspond to regions with proportional values of ρ. Here the eddy zone ($\delta \neq 0$) is modelled by a geometrically similar zone where the current is introduced from an external source. The magnitude of the current in the model must here be proportional to the current in the original.

YEAR 1961

The motion of the rotor in the bath can be simulated by successive rotation of the rotor model through the angle $\Delta\alpha$ about its axis. On rotation of the rotor a finite increment in the angle $\Delta\alpha$ corresponds to a finite increment in the potential ΔU and, consequently, $\Delta A_z = c\Delta U$ also. Thus, we finally have for determining the e.m.f. by modelling

$$e = -cl \cdot 2\pi n \frac{\Delta U}{\Delta \alpha}. \tag{8}$$

Quantitative values of the e.m.f. can be obtained if we know the value of c. This can be found in the following way. Suppose we put $A = c_1 U$, $x_1 = c_2 x_2$, $y_1 = c_2 y_2$, $\delta = c_3 p$, $\mu = c_4 \rho$ and consider that for a homogeneous medium

$$\Delta U = \frac{\partial^2 U}{\partial x_2^2} + \frac{\partial^2 U}{\partial y_2^2} = -\rho p. \tag{9}$$

Then for equation (7) (also in the case of a homogeneous medium)

$$\frac{\partial^2 A_z}{\partial x_1^2} + \frac{\partial^2 A_z}{\partial y_1^2} = -\mu^2 {}_z$$

or

$$\frac{\partial^2(c_1U)}{\partial(c_2x_2)^2}+\frac{\partial^2(cU)}{\partial(c_2y_2)^2}=-c_1\rho c_3 p,$$

i.e.

$$\frac{c_1}{c_2^2c_3c_4}\left(\frac{\partial^2U}{\partial x_2^2}+\frac{\partial^2U}{\partial y_2^2}\right)=-\rho p.$$

Thus, in accordance with equation (9), we get

$$\frac{c_1}{c_2^2c_3c_4}=1;\quad c_1=c_2^2c_3c_4.$$

The similarity coefficients are defined by the modelling conditions, namely, c_2 by the modelling scale, c_3 from the correspondence of the currents and c_4 from the correspondence of the media. Knowledge of the coefficient of correspondence c_1 ensures that quantitative data are not only obtained for calculating the e.m.f., but also for finding the distribution of the fluxes in the "window" of the machine, the coefficient of self-induction, the magnetic permeance and so on.

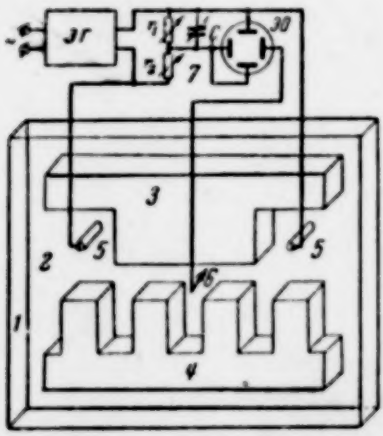

Fig. 1. Test equipment:
1 - tank; 2 - electrolyte; 3 - model of stator; 4 - model of rotor; 5 - current leads; 6 - probe; 7 - measuring circuit.

For example, in order to determine the flux in some circuit,

$$\Phi = \int A dl = l_1 (A_1 - A_2) = c_2 l_2 c_1 (U_1 - U_2), \tag{10}$$

where U_1 and U_2 are the potentials of the conductors or imaginary lines along which the conductors of length l_2 are arranged. The total flux coupling can be found from the formula

$$\Psi = \sum_{i=1}^{i=n} \Phi_i = \sum_{i=1}^{i=n} \oint A_i dl = c_2 l_2 c_1 \sum_{i=1}^{i=n} (U_i - U_i'). \tag{11}$$

If it is a question of determining the flux coupling of the coil producing the magnetic field in question, then U_i are the potentials of the incoming current leads, and U_i' the potentials of the outgoing current leads which imitate the currents in the turns of the coil. The flux coupling of mutual induction can be found in a similar way but U_i and U_i' are taken as points where the sides of the turns of the other coil are disposed. In such conditions the coefficients L and M can easily be defined as

$$L = \frac{\Psi_i}{i}; \quad M = \frac{\Psi_M}{i}.$$

The test equipment for investigating the e.m.f. (Fig. 1) is essentially the same as Tetelbaum's for investigating the potential distribution in a conducting medium [1]. But certain undersirable phenomena may occur on movement of the model of the rotor in the tank. The electrolyte may penetrate underneath the model of the rotor. This sharply distorts the nature of the field distribution in the zone with teeth since this is the most likely place for the electrolyte to flow. In a conventional fixed model this phenomenon can be avoided quite easily be greasing the slit by a non-conducting substance such as vaseline. Experience has, however, shown that a layer of vaseline between the rotor and the bottom of the tank does not guarantee that the electrolyte will be kept out. It is therefore proposed to solve the problem by a special construction of the model. In this construction (Fig. 2b) the rotor is permanently fixed on a sheet which is free to slide along the bottom of the tank. Between the moving sheet and the bottom of the tank it is necessary to have a layer of vaseline in order to keep out the electrolyte and reduce friction. The face of the moving sheet is also covered with a layer of vaseline and slides along the face of the fixed sheet of the same thickness on which the model of the stator is secured. This method of construction in practice precludes the penetration of electrolyte underneath the model of the rotor.

YEAR 1961

Another difficulty of a purely constructional nature is the need to ensure very exact rotation of the rotor by the given angle $\Delta\alpha$. Since the potential varies sharply in the zone of the gaps, inaccurate rotation can lead to considerable errors in determining the potential differences. In this respect it is advisable to measure the linear displacement of the rotor and not the angle of rotation $\Delta\alpha$. This can be measured by a micrometer.

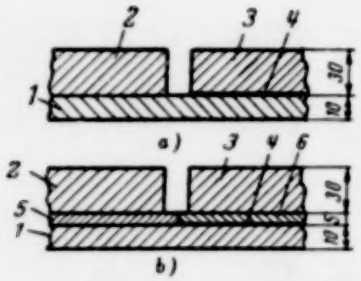

Fig. 2. Alternative versions of test equipment:
1 - bottom of tank; *2* - model of stator;
3 - model of rotor; *4* - layer of vaseline;
5 - base of stator model; *6* - base of rotor model.

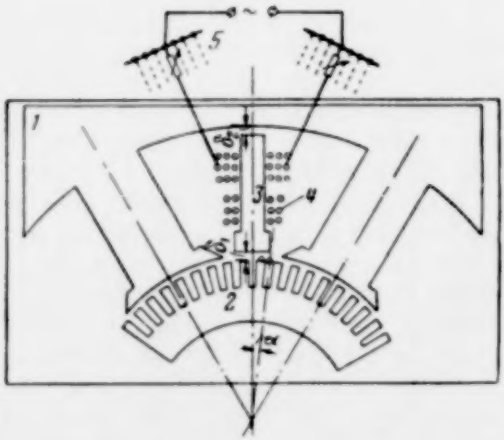

Fig. 3. Drawing of model:
1 - model of stator magnetic system; *2* - model of rotor; *3* - model of compole; *4* - current leads modelling the compole winding; *5* - resistances.

If these precautionary measures are taken quite stable and accurate results can be obtained.

To illustrate the use of the proposed method, suppose it is required to determine the shape of the curve for the commutating e.m.f. induced by the compole field in a conductor which is set in an armature slot of a d.c. machine.

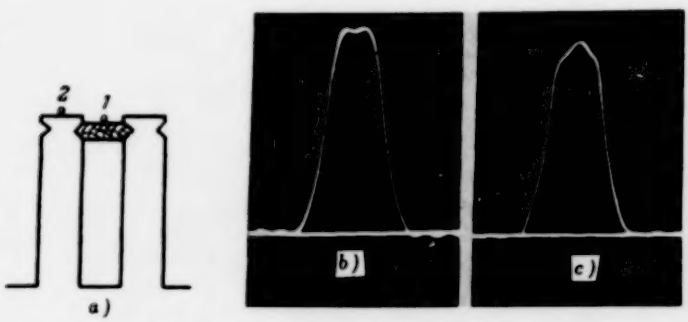

Fig. 4. Arrangement of measuring conductors (a); e.m.f. induced by compole field in conductor 1 (b) and conductor 2 (c).

The measurements are taken on a model whose dimensions fully correspond with the dimensions of a real 118 kW, 440 V, 1000 rev/min machine (type GM-282) operating as a motor. The model is drawn in Fig. 3. The tank dimensions are 700 x 400 x 100 mm^3 so that it can contain a life-size model of about one quarter of the circumference of the machine. The model itself is made of organic glass 30 mm thick. A pointer micrometer was used to measure the rotor travel (with calibration 0,01 mm).

Parallel with the investigations in the tank, oscillograms were taken of the e.m.f. induced by the field of the compoles in special measuring conductors laid on the rotor of the GM-282 machine. The position of these conductors is illustrated in Fig. 4a, one being on a wedge along the slot, and the other on top of the tooth. Oscillograms of the e.m.f. in the conductors are shown in Fig. 4b, c. The e.m.f. in the first conductor (the curve in Fig. 4b) can be regarded as the commutating e.m.f. induced in the conductors of the sections covered by the brushes.

The curve for the commutating e.m.f. obtained by oscillograph recordings is compared with that obtained by tank measurements in Fig. 5a

and b. It will be seen from this diagram that quite satisfactory agreement is obtained. The slight discrepancy between them can be explained by the slight difference between the dimensions of the model and those of the original, the residual magnetization of the main poles, present in the machine, but absent in the model (Fig. 4b,c), and the saturation of the peaks of the pole tips.

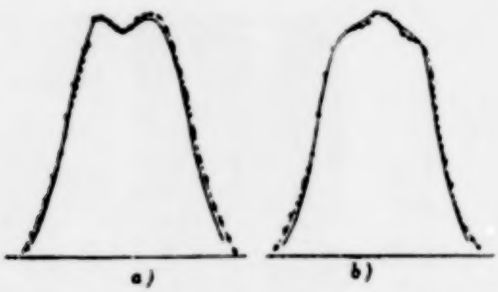

Fig. 5. Comparison of curves obtained by oscillograph (continuous line) and by modelling in tank (broken line).

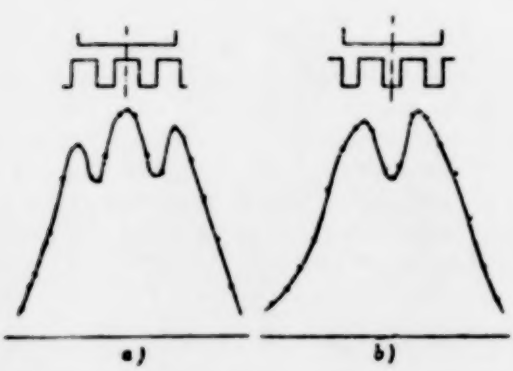

Fig. 6. Distribution of the normal component of induction under compole in modelling.

In addition, the shape of the curve for the e.m.f. which would be induced in a conductor laid up the middle of the rotor tooth was also determined on the model, i.e. the corresponding curve to that in Fig. 4c was determined. The comparison of these curves in Fig. 5b also reveals good agreement.

It is worthwhile mentioning, however, that the curves for the dis-

tribution of the component of the magnetic induction in the gap at a distance of 1 mm from the surface of the rotor as determined by the model in the tank for two rotor positions, differ considerably in shape from those for the e.m.f.'s induced in the conductors 2 and 1 on rotation.

It can be seen from the foregoing example that the proposed method is a comparatively easy and quick way of finding the rotational e.m.f. in quite complicated conditions and that the results are acceptably accurate. No difficulties arise in principle in applying the method to more complicated cases than that of the excitation of a single compole, which was only used by way of illustration.

Conclusions

1. The proposed method of determining the shape of the curves for the rotational e.m.f.'s in electrical machines by modelling in an electrolytic tank is a comparatively easy way of investigating complicated magnetic circuits and current distributions in electrical machines.

2. The test equipment which has been evolved provides quite stable and accurate results.

3. Good agreement was obtained between actual oscillograms and tank-determined curves.

4. The test equipment can also be used for determining all the other parameters of the magnetic field in a machine: induction, magnetic fluxes, flux coupling, inductances, mutual inductances and so on.

Translated by O.M. Blunn

REFERENCES

1. I.M. Tetel'baum; *Electrical modelling, (Elektricheskoe modelirovanie).* Fizmatgiz, Moscow (1959).

ABSTRACTS FROM PAPERS PUBLISHED IN ELEKTRICHESTVO No. 8, 1961

Computers

Electronic simulation of electrical circuits,

V.G. Vasil'ev *et al.*, (pp 41-45).

Certain aspects of the simulation of R, L, and C circuits are considered on the basis of a simple example. The rules of the "dual circuit" method of analysis are formulated. An electrical circuit with one voltage source is simulated without forming equations for the circuit or the model. A minimum of amplifiers and integrating elements is required.

Regulation of the excitation of two synchronous machines operating in parallel,

G.V. Mikhnevich *et al.*, (pp. 31-35).

An analogue computer method is proposed for determining the optimum structure of the control signals with respect to their derivatives and assessing their effect on a coefficient of regulation for the excitation of two synchronous machines operating in parallel. The results for generators at the Stalingrad hydro-electric station are given by way of illustration.

Control engineering

The motor drive of a reversible cold rolling mill,

I.M. Tolmach *et al.*, (pp. 79-81).

An account is given of the motor drive which has been installed on a four-roll mill for low and medium carbon steel strip up to 300 mm wide with reduction from 3 to 0.2 mm in pu to nine passes. The drive features the use of e.m.f. and current regulators to maintain rolling tension.

Measuring amplifiers for centralized automatic control systems, R.R. Kharchenko *et al.*, (pp. 7-13).

Attention is concentrated on those d.c. measuring amplifiers which are used to convert the signals of pick-ups in group data-processing circuits. The authors review six types of system covering the combined transmission of the amplified signal without a device for correcting zero, drift, and wideband amplifiers with a device for correcting zero drift.

Electrical steel

The properties of 1 mm cold-rolled electrical steel, A.I. Beliakov *et al.*, (pp. 82-83).

A short account is given of the properties of the 1 mm gauge cold-rolled grain-oriented steel for the poles of d.c. electrical machines now being produced in Novosibirsk.

YEAR 1961

Insulation

Interdependence of the physical properties of organic and inorganic polymers, N.I. Vorob'ev *et al.*, (pp. 76-78).

To simplify the problem of investigating the large number of polymers which are available, the author takes the magnitude of the inter-molecular forces as the main criterion defining the physical properties of many polymer substances.

The dielectric permeability and tangent of the loss angle for paper dielectrics, S.K. Medvedev, (pp. 66-72).

Formulae are produced for calculating ϵ, tan δ and other characteristics of paper on the basis of the actual structure of the paper on the assumption that the relative thickness of the cellulose in the space between the layers varies between 0 and 1 according to a certain law. The pores are assumed to be in series in each individual volume of cellulose.

Power systems

Determining optimum operating conditions for power systems, V.M. Gornshtein, (pp. 19-24).

A study is made of common errors which are said to be made in the economic analysis of power system analysis.

Tuned power transmission systems, V.K. Shcherbakov (pp.25-30).

It is stated that theory and laboratory investigations indicate that half-wave tuned transmission lines of 2000 and 2500 km can ensure high steady state stability and relative voltage stability at line ends. The author disputes the reasons which have been given for not using this system and advocates its use on the grounds of efficiency and the possibility of intermediate off-take of power along the line.

Rotating machines

Turbo-generators of large unit capacity, V.V. Titov, (pp. 1-4).

A short account is given of the work which has been done at the Electrosila works in the U.S.S.R. on the development of 300 and 500 MW turbo-generators. The new 300 MW generators are described and it is stated that 500 MW generators can be made on the same principles when the demand arises. Extremely high efficiency is claimed and it is an interesting paper. Unfortunately, this account does not explain how the efficiency is achieved or how it is calculated and some of the main features have their counterpart in recent American, Swiss and British innovations.

New 100 kW amplidynes, B.P. Tokarev *et al.*, (pp. 14-18).

Two new types of amplidyne are to be produced in the U.S.S.R., namely, three-stage amplidynes with a longitudinal field, and multi-pole amplidynes with a transverse field (four and eight poles) with increased magnetization of the winding along the transverse axis or with additional poles along the longitudinal and transverse axes. The equipment is compared and the respective merits assessed.

A new principle of obtaining constant advance times in automatic synchronizers, N.N. Vostroknutov *et al.*, (pp.35-40).

In this article the synchronizers are defined as devices which select the angle of lead and stop action if the amount of slip is too large. A new approach to the design of the time advance elements of such synchronizers is proposed in which the angle of lead is directly converted into a proportional d.c. voltage. This provides the possibility of twice-differentiating this voltage, as required for considering acceleration of slip. A detailed account is given of a device for the exact synchronization of generators.

Calculation of the steady state errors in speed governors for d.c. motors, S.S. Roizen, (pp. 56-62).

Two fundamental methods of speed control for d.c. motors are considered with a view to determining the accuracy with which speed governors operate in the automatically controlled drives of rolling mills and lathes etc. Formulae are produced for calculating the degree of error under steady state conditions.

The leader stage of a spark discharge, V.P. Larionov, (pp. 72-76).

The author develops the notion of a leader stage in spark discharges in long air-gaps which precedes the main discharge and forms a leader channel between the electrodes. The mean longitudinal potential gradients in the leader channel are determined along with the conductance of the leader channel, the concentration of the electrons and the time necessary for the formation of the leader channel.

YEAR
1961

Translated by O.M. Blunn

A METHOD OF DETERMINING THE MAIN CRITERIA OF TRACTION MACHINES FOR MINIMUM WEIGHT PER UNIT OF OUTPUT*

N.A. BOLDOV

(Moscow Power Institute)

(Received 9 January 1961)

YEA
196

A reduction in the weight of traction machines per unit of output allows a considerable increase in the power of electric locomotives for a given weight and speed or, other things being equal, permits a substantial saving in metal in the construction of locomotives and coaches etc.

This paper describes a method of determining the optimum criteria of traction machines and considers the fundamental relationships involved. Improved formulae will be given, including an initial approximate formulae for the weight of electronic machines. This particular formulae is the outcome of investigations by V.G. Yegorov and the author in the department of electrical transport at the Moscow Power Institute.

The dimensions and weight of traction machines. A comparison of the dimensional and weight indices of 35 different d.c. and a.c. traction motors and traction generators has indicated the following empirical formula:

$$G = \frac{62}{p} D_a^2 l_a \text{ [tons]}, \tag{1}$$

where G is the weight of the motor or generator;

---

* *Elektrichestvo*, 9, 17-21, 1961.

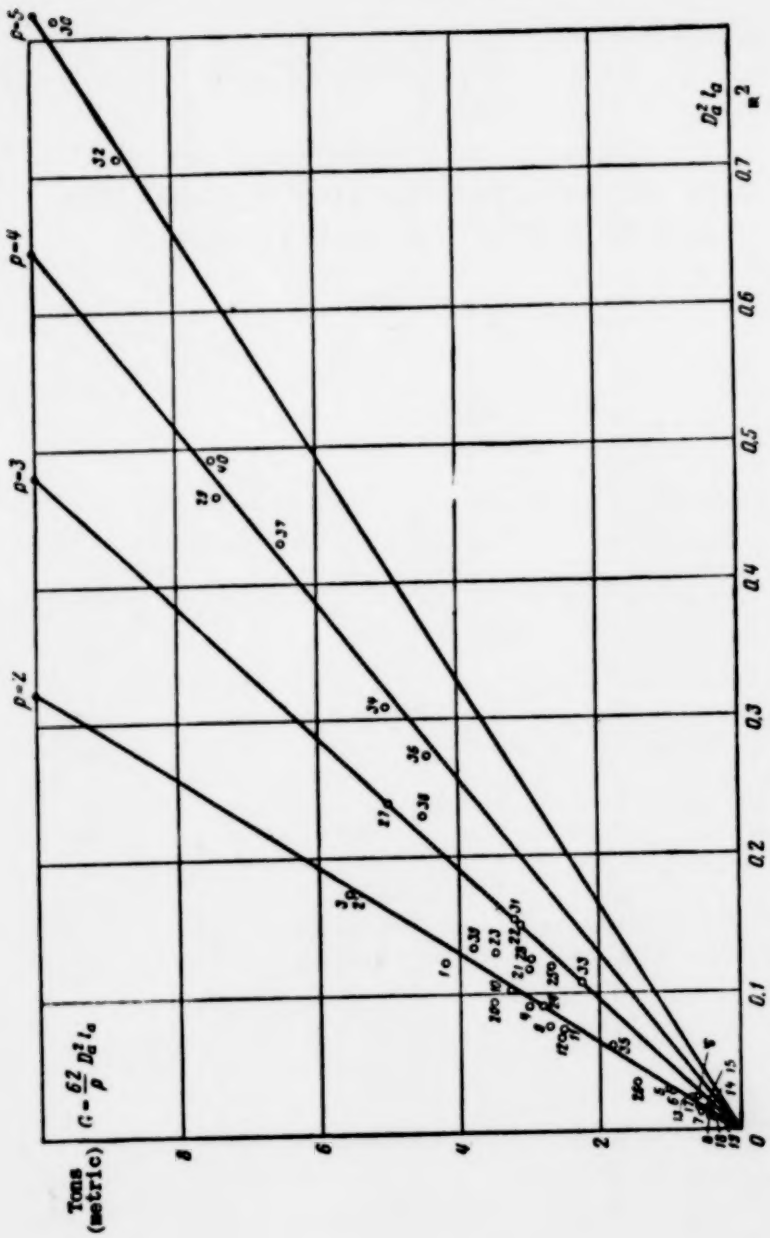

FIG. 1

YEAR 1961

Point	1	2	3	4	5	6	7	8	9	10
Type of machine	DPE-400	NB-406	GE-750	DK-8B	DK-806A	DK-802A	DK-801A	DK-800A	DK-304B	EDT-200A
Point	11	12	13	14	15	16	17	18	19	20
Type of machine	DK-103D	DPI-152	DK-104G	DK-255R	DK-254A	DK-202B	DK-809A	EDR-10	DK-908	SE-752
Point	21	22	23	24	25	26	27	28	29	30
Type of machine	SW-435	TAO-649B-1	TO-136[8]	EDT-340	TS-32/44	DK-102E	NB-412M	d/TE-60 (project)	MPT 99/47	MPT 120/55
Point	31	32	33	34	35	36	37	38	39	40
Type of machine	MPT 74/28 T	MPT 120/49	MPT 74/28 T	GP-300	MPT 49-25-3	MPT 84/39	GP-304	GP-305	NB-414	GP-307

YEA
196

p is the number of pole pairs;

D_a – the diameter of the armature, m;

l_a – the length of the armature, m.

Formula (1) gives fairly exact results for traction motors and generators, including old machines as well as the latest foreign and soviet models (Fig. 1).

It follows from (1) that it is expedient to maximize the number of poles in order to reduce weight. But the number of poles is restricted by the permissible voltage between adjacent brush holders.

If $e_{k.av} = 20$ V and $D_k/D_a = 0.8$, then

$$p_{max} = 6.3 \frac{D_a}{U_{max}}, \tag{2}$$

YEAR 1961

where U_{max} is the maximum voltage, kV.

Substituting (2) in (1),

$$G_{min} \simeq 10 D_a l_a U_{max} \text{ [tons]}. \tag{3}$$

The limit to which it is advisable to reduce the maximum voltage depends on the room for manoeuvre in placing the brush holders. Experience with the construction of single phase commutator motors shows that

$$\tau_{k\,min} = 0.12 \text{ m}.$$

Using the condition

$$\tau_{a\,min} = \frac{\pi D_a}{2p_{max.k}} = \frac{0.12}{0.8} = 0.15 \text{ m}.$$

the maximum possible number of pole pairs is limited on constructional grounds to:

$$p_{max.k} = 10 D_a. \tag{4}$$

Substituting (4) in (1),

$$G_{min.k} = 6.2 D_a l_a \text{ [tons]}. \tag{5}$$

Here the maximum voltage must not exceed the quantity obtained by comparison of (2) and (4), i.e.

$$(U_{max})_{min} \leq 0{,}67 \text{ kV}.$$

Calculated outputs of traction machines. The electromagnetic power of a machine is given by the expression:

$$P = \frac{a_i B_\delta A}{6\pi 10^4} D_a^2 l_a n \text{ [kW]}, \tag{6}$$

where D_a and l_a are expressed in cm.

Substituting the expression for speed

$$n = \frac{60 v_a}{\pi D_a} \tag{7}$$

in formula (6):

$$P = \frac{a_i B_\delta A v_a}{\pi \cdot 10^4} D_a l_a, \tag{8}$$

where D_a and l_a are expressed in metres (m).

For non-controlled machines the maximum sustained output can be obtained for the given dimensions of the armature if the appropriate maximum permissible sustained values of the quantities are substituted in (8).

The coefficient of $D_a\ l_a$ in (8) can be simplified to

$$C_u = \frac{a_{i\,max} B_{\delta\,max\ \infty} A_{max\ \infty} v_{a\,max\ \infty}}{\pi 10^4} \left[\frac{\text{kW}}{\text{m}^2} \right]. \tag{9}$$

The power defined by the formula

$$P_p = C_u D_a l_a \text{ [kW]},$$

may be known as the *theoretical (volume) power of the machine.*

A wide range of control is typical of traction machines. Thus, for traction generators $U_{max} > U_\infty$, and for motors $v_{max} > v_\infty$.

Putting K_r for the coefficient of regulation:

(a) if $n_\infty = n_{max}$ and $v_{a\infty} = v_{a\,max}$ for generators:

$$K_r = \frac{B_{\delta\,max\,\infty}}{B_{\delta\infty}} = \frac{U_{max}}{U_\infty} = K_{vg}.$$

(b) if $\mu = const$ for traction motors

$$K_r = \frac{v_{a\,max\,\infty}}{v_{a\infty}} = \frac{n_{max}}{n_\infty} = \frac{v_{max}}{v_\infty} = K_v.$$

The nominal sustained power of the machines is less than the theoretical power by the factor K_r:

$$P_{\infty g} = C_a D_a l_a \frac{U_\infty}{U_{max}}; \tag{10}$$

$$P_{\infty m} = C_a D_a l_a \frac{V_\infty}{V_{max}}. \tag{10(a)}$$

As shown above, the dimensions of machines are determined by the theoretical power. In reference to the desired sustained power, the dimensions can be found from 10 and 10(a):

$$D_a l_a = \frac{P_\infty K_p}{C_a} \quad [m^2]. \tag{11}$$

For traction generators

$$D_a l_a = \frac{U_{max} I_\infty}{C_a} \quad [m^3], \tag{12}$$

for traction motors

$$D_a l_a = \frac{F_\infty v_{max}}{367 C_a \eta_a \eta_{per}} \quad [m^2]. \tag{13}$$

The relationship between machine weight and the desired criteria. Substituting (12) and (13) in (1):

$$G_r = 62 \frac{D_a}{p} \frac{U_{max} I_\infty}{C_a} \quad [\text{tons}]; \tag{14}$$

$$G_m = 62 \frac{D_a}{p} \frac{v_{max} F_\infty}{367 C_m \eta_m \eta_{per}} \text{ [tons]}. \quad (15)$$

The following conclusions can be drawn from (14) and (15):

(a) It is necessary to avoid unwarranted control limits.

(b) It is necessary to make the machines with the maximum possible frequency. Increases in armature diameter should be accompanied by a proportional increase in the number of poles so as to maintain the maximum frequency unchanged.

(c) Maximum peripheral speed is the most "worthwhile" criterion; it must be made as large as possible in each case (an increase in power and efficiency without additional material).

The weight of machines per unit of output. Here it is sufficient to divide (1) by (10) and (10a):

$$\frac{G}{P_\infty} = \frac{62}{C_m} \cdot \frac{D_a}{p} \cdot \frac{U_{max}}{U_\infty} \cdot 10^3 \left[\frac{kG}{kW}\right]; \quad (14a)$$

$$\frac{G}{P_{\infty m}} = \frac{62}{C_m} \cdot \frac{D_a}{p} \cdot \frac{v_{max}}{v_\infty} \cdot 10^3 \left[\frac{kG}{kW}\right]. \quad (15a)$$

Maximum rotational speed of a machine. For generators:

$$n_\infty = n_{max} = \frac{60 v_{a\,max}}{\pi D_a}, \quad (16)$$

for motors

$$n_\infty = \frac{n_{max}}{K_v} = \frac{60 v_{a\,max}}{\pi D_a} \cdot \frac{v_\infty}{v_{max}}. \quad (17)$$

The optimum transmission ratio of traction motors:

$$\mu_{opt} = 3.6 \frac{D_a v_{a\,max}}{D_a v_{max}}. \quad (18)$$

If $v_{a\,max} = 70$ m/sec and $D_a = 1.05$ m,

$$\mu_{opt} = \frac{265}{D_a v_{max}}.$$

The most "efficient" frequency of a machine. It will be seen from (14a) and (15a) that the weight per unit of output is proportional to the ratio D_a/p. By (7) and the expression for frequency

$$f = \frac{pn}{60} \tag{19}$$

this ratio equals

$$\frac{D_a}{p} = \frac{v_a}{\pi f}. \tag{20}$$

Substituting (14a) and (15a) in expressions (9) and (20):

(a) for a generator

$$\frac{G}{P_{\infty g}} = \frac{62 \cdot 10^6}{a_i B_b A f} \cdot \frac{U_{max}}{U_\infty} \left[\frac{kG}{kW} \right]; \tag{21}$$

(b) for a motor

$$\frac{G}{P_{\infty m}} = \frac{62 \cdot 10^6}{a_i B_b A f} \cdot \frac{v_{max}}{v_\infty} \left[\frac{kG}{kW} \right]. \tag{22}$$

The greatest frequency is the most "efficient" frequency from the point of view of weight indices.

Refinement of the formulae in Table 1 for the criterion of commutation. The practicability of electric machines can be checked in the first instance by V.T. Kas'ianov's criteria for non-controlled generators:

(a) the permissible inter-lamella voltage (that between the commutator segments):

$$P_\infty \leqslant (1\,400 \text{ to } 1\,700) D_a \ [\text{kW}]; \tag{23}$$

(b) the permissible values of v_a and A

$$P \leqslant \frac{1.2 \text{ to } 1.8}{n} \cdot 10^8 \ [\text{kW}]; \tag{24}$$

TABLE 1

Fundamental formulae and coefficients

Formula and coefficients	1st version	2nd version
a_i	0.67	0,7
B_δ	10^4	$1.06 \cdot 10^4$
A	500	600
v_a	70 m/sec	700 m/sec
C_M	7 500 kW/m^2	10 000 kW/m^2
$P_{\infty m}$	$7\,500 D_a l_a \frac{U_\infty}{U_{max}}$ [kW]	$10\,000 D_a l_a \frac{v_\infty}{U_{max}}$ [kW]
$P_{\infty g}$	$7\,500 D_a l_a \frac{v_\infty}{v_{max}}$	$10\,000 D_a l_a \frac{v_\infty}{U_{max}}$ [kW]
$(D_a l_a)_g$	$\frac{U_{max} I_\infty}{7\,500}$ [m^2]	$\frac{U_{max} I_\infty}{10\,000}$ [m^2]
$(D_a l_a)_m$	$4F_\infty v_{max} \cdot 10^{-4}$ [m^2]	$3F_\infty v_{max} \cdot 10^{-4}$ [m^2]
$P_{max.s}$	$10D_a$	$10D_a$
$U_{max(opt)}$	0.63 kV	0.63 kV
$l_{max(opt)}$	$220 \cdot \frac{0.63}{U_{max}}$	$220 \cdot \frac{0.63}{U_{max}}$
$G_{min.s}$	$6.2 D_a l_a$ [tons]	$6.2 D_a l_a$ [tons]
$\left(\frac{G}{P_\infty}\right)_{min.s}$	$0.83 K_r$ [kg/kW]	$0.62 K_r$ [kg/kW]
$\left(\frac{G}{P_\infty}\right)_{min}$	$1.24 K_r U_{max}$	$0.98 K_r U_{max}$

(c) the intensity of commutation:

$$D_a l_a \leqslant \frac{250 \text{ to } 450}{n} \quad [\text{m}^2]. \tag{25}$$

Criteria (23) and (24) are taken into account in finding the value of C_E and p_{max}. Criteria (25) restricts the length of the machine armature depending on the conditions of commutation.

Substituting in (25) the expression for speed

$$n = \frac{60 v_a}{\pi D_a} = \frac{60 \cdot 70}{\pi D_a} = \frac{4\,200}{\pi D_a};$$

then by definition

$$l_a \leqslant \frac{240 \text{ to } 450}{4\,200} = 0.18 \text{ to } 0.336 \text{ m} \tag{26}$$

YEAR 1961

This criterion will now be reconsidered on the basis of one of the latest traction generators which is made by the Elektrotiozhmash traction works and has quite satisfactory commutation (GP-304 type machine, $P = 1\,350$ kW, $D_a = 0.99$, $l_a = 0.44$, $A = 505$, $n = 850$ rev/min). In this case

$$0.44 \leqslant \frac{240 \text{ to } 450}{0.99 \cdot 850} = 0.290 \text{ to } 0.535 \text{ m}.$$

Thus, the criterion is only satisfied for the upper limit with good commutation.

In the following it is proposed to take typical characteristics of this generator as the criteria of commutations:

$$D_a l_a n = 0.99 \cdot 0.44 \cdot 850 = 370. \tag{27}$$

If $v_{a\,max} = 70$ m/sec, the following quantity corresponds to this criterion:

$$l_a = \frac{370\pi}{4\,200} = 0.28 \text{ m}.$$

Another still more general criterion is

$$A l_a v_a \approx 10^4 = \text{const}. \tag{28}$$

The formula for traction generators in the light of the limitations imposed by (28) has the form:

$$P_{\infty} K_{Ug} = D_a \frac{C_M \cdot 10^4}{A v_{a\,max}} \quad [\text{kW}]. \tag{29}$$

If $v_{a\,max} = 70$ m/sec, $A = 500$ and $C_a = 7500$, then

$$P_{\infty} K_{Ug} = \frac{7\,500 \cdot 10^4}{500 \cdot 70} = 2\,140 D_a \quad [\text{kW}]; \tag{29a}$$

and if $v_{a\,max} = 70$ m/sec, $A = 600$ and $C_a = 10^4$,

$$P_{\infty} K_{Ug} = \frac{10^4 \cdot 10^4}{600 \cdot 70} = 2\,375 D_a \quad [\text{kW}].$$

Including the special features of traction motors, these formulae take the form

$$P_{\infty} K_v = D_a \frac{C_M \cdot 10^4}{\frac{A}{K_{Ug}} v_{a\,max}} \quad [\text{kW}],$$

or

$$P_{\infty} = D_a \frac{C_M \cdot 10^4}{A v_{a\,max}} \cdot \frac{K_{Ug}}{K_v} \quad [\text{kW}]. \tag{30}$$

If $v_{a\,max} = 70$ m/sec, $A = 500$ and $C_a = 7500$:

$$P_{\infty} = D_a \frac{7\,500 \cdot 10^4}{500 \cdot 70} \cdot \frac{K_{Ug}}{K_v} = 2\,140 D_a \frac{K_{Ug}}{K_v}; \tag{30a}$$

or if $v_{a\,max} = 70$ m/sec, $A = 600$ and $C_a = 10^4$:

$$P_{\infty} = \frac{10^4 \cdot 10^4}{600 \cdot 70} D_a \frac{K_{Ug}}{K_v} = 2\,375 D_a \frac{K_{Ug}}{K_v}. \tag{30b}$$

Formulae 30(a) and 30(b) provide (1) the limiting outputs of traction motors in reference to the diameter of the wheel and the gauge of the line and (2) the necessary coefficient of voltage regulation as a function of the desired range of speed control.

Thus, for example, if D_c = 1.05 m, $D_{a\ max}$ = 0.49 m and A = 500 then

$$P_\infty = 2\,140 \cdot 0.49 \cdot \frac{K_{Ug}}{K_v} = 1\,050 \frac{K_{Ug}}{K_v}; \quad (31)$$

and if D_0 = 1.05 m, D_a = 0.49 m and A = 600, then

$$P_\infty = 2\,375 \cdot 0.49 \frac{K_{Ug}}{K_v} = 1\,160 \frac{K_{Ug}}{K_v}. \quad (32)$$

On the other hand, since

$$P_\infty K_v = (7\,500 \text{ to } 10\,000) D_a l_a; \; P_\infty = \frac{7\,500 \text{ to } 10\,000}{K_v} D_a l_a,$$

it follows that if D_a = 0.49 m, then

$$P_\infty = (3\,750 \text{ to } 5\,000) \frac{l_a}{K_v}. \quad (33)$$

From a comparison of (31)-(33):

$$\frac{K_{Ug}}{l_a} = \frac{3\,750 \text{ to } 5\,000}{1\,050 \text{ to } 1\,160} = 3.5 \text{ to } 4. \quad (34)$$

Consequently, there is a constant relationship between K_{Ug} and

For line gauges of 1524 mm and $l_{a\ max}$ equal to 0.5 m,

$$K_{Ug} = (3.5 \text{ to } 4.3) \cdot 0.5 = 1.75 \text{ to } 2.15;$$

and for line gauges of 1435 mm and $l_{a\ max}$ equal to 0.43 m:

$$K_{Ug.max} = (3.5 \text{ to } 4.3) \cdot 0.43 = 1.5 \text{ to } 1.85.$$

The limiting output of a traction motor for a wheel diameter D_0 = 1.05 m (D_c = 0.49 m) and A = 600 is (see Table 2):

$$P_\infty = 1\,160 \cdot 2.15 \frac{1}{K_v} = \frac{2\,500}{K_v}. \quad (35)$$

This output can be attained if K_{Ug} = 2.15.

TABLE 2

K_v	2	2.5	3	4	5
P_{∞}, kW	1 250	1 000	835	625	500

Conclusions

The weight of the electrical machines of Diesel locomotives and gas turbine locomotives and that of the traction motors of electric single phase d.c. locomotives may be reduced considerably in individual cases by a factor of 1.5 to 2 using conventional materials.

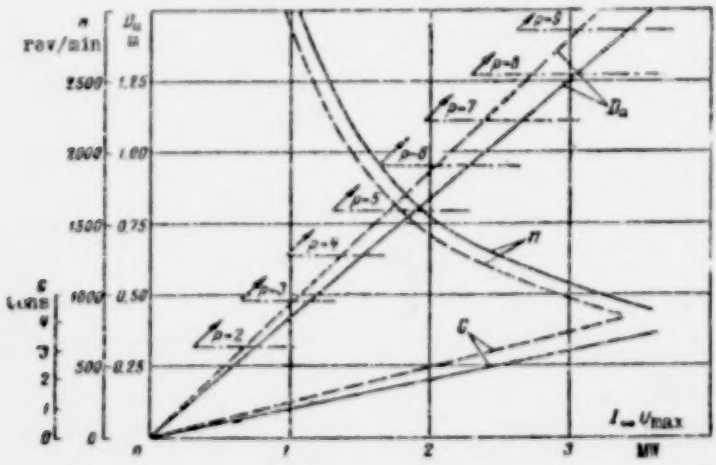

Fig. 2. Nomogram of the optimum calculated data for traction generators:

$U_{max} = 1$kV; $Av_a l_a = 10^4$; ----- $C_m = 7500$; $l_a = 0.285$ m; $A = 500$; $BS = 0.75 \times 10^4$; $v_a = 70$; $\alpha_i = 0.67$; ——— $C_m = 10^4$; $l_a = 0.238$ m; $A = 600$; $B_\delta = 1.6 \times 10^4$; $v_a = 70$; $\alpha_i = 0.7$.

All traction motors can be "inscribed" in the diameter of a wheel $D_c = 1.05$ m. When making traction motors with the limiting length of armature ($l_a = 0.5$ m), the range of voltage control of the generator should reach $K_{U_g} = 2.15$.

The weight of the generators must not exceed $1.5\ U_{max}/U_{\infty}$ kg/kW, and that of the motors should not exceed $1.5\ v_{max}/v_{\infty}$ kg/kW. The gross weight of the main machines of Diesel locomotive transmissions should

not exceed

$$1.5\left(\frac{U_{max}}{U_{\infty}}+\frac{v_{max}}{v_{\infty}}\right)\left[\frac{kG}{kW}\right].$$

The weight of traction motors is proportional to $F_{\infty} v_{max}$ and this should therefore be kept as low as possible.

In traction machines it is recommended that nomograms should be used. Those shown in Fig. 2 refer to generators and those in Fig. 3 to motors

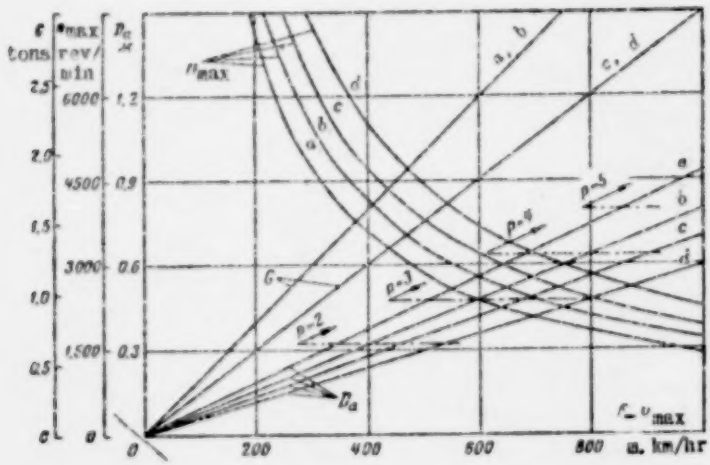

Fig. 3. Nomogram of the calculated data for traction motors:

$a - C_g = 7500$, $l_a = 0.43$, $K_{U_g} = 1.5$; $b - C_g = 7500$, $l_a = 0.5$, K_{U_g} 1.75; $c - C_g = 10^4$, $l_a = 0.43$, $K_{U_g} = 1.85$, $d - C_g$ 10^4, $l_a = 0.5$, $K_{U_g} = 2.15$.

An important condition for obtaining the requisite weight indices is the production of electrical machines with the maximum number of poles:

$$p_{max} = 6.3\frac{D_a}{U_{max}}\left[\frac{m}{kV}\right]$$

or, what is the same thing, with the maximum frequency

$$f_{max} = \frac{140}{U_{max}}\ [c/s].$$

Consequently, the weight of a machine is proportional to the maximum voltage and for low power machines it is necessary to take $U_{max} \leq 0.67$ kV, and for high powered machines $U_{max} \leq 1$ kV.

The calculations have shown that in principle it is possible to produce traction machines with a weight of 1.5 kg/kW.

The calculations which have been performed for generators in sustained use show that (1) produces a considerable error if the length of the armature is short or if the number of poles is large. It is therefore recommended that a more general formula be used:

$$G = D_a^2 \left(\frac{p}{30 l_a} + \frac{60 l_a}{p} \right) \text{[tons]}. \tag{1a}$$

The following formulae may also be used:

for generators:

$$G = 1.2 + \frac{60}{p} D_a^2 l_a \text{ [tons]}; \tag{1b}$$

for motors:

$$G = 0.3 + \frac{60}{p} D_a^2 l_a \text{ [tons]}. \tag{1c}$$

In order to produce generators of low weight, these machines should not be made with armature diameters over 0.85 m, since otherwise the weight of their frames must be increased in order to ensure adequate rigidity. If it is necessary to produce large outputs, it is expedient to mount two short armatures in one housing.

Translated by O.M. Blunn

OPERATION OF AN INDUCTION MOTOR FROM A TRANSISTOR FREQUENCY CONVERTER*

O.I. KHASAYEV

(Moscow)

(Received 9 May 1960)

YEAR
1961

The most economical method of regulating the speed of a squirrel cage induction motor is to vary the frequency of the supply source. In this connexion special importance is attached to static variable-frequency d.c. to a.c. converters in which large junction-type transistors are used as switching devices.

The most efficient mode of operation of a transistor is the switching state which permits highly efficient energy conversion. Yet the output voltage of a simple transistor converter used as a switch is rectangular in shape (see Fig. 1a). It is to be expected that the operating characteristics of an induction motor will therefore deteriorate owing to the presence of higher harmonics [1].

In order to assess the merits of simple transistor frequency converters in this case, it is necessary to compare the operating characteristics of the motor when a voltage of sinusoidal shape is supplied with those obtaining when the supply voltage is of rectangular shape. Such a comparison shows just how far it is advisable to rely on complex semiconductor converters based on switching triodes for output voltage curves of approximately sinusoidal shape [2].

Two typical cases of a rectangular voltage supply are considered:

(a) a rectangular voltage containing all odd harmonics (Fig. 1a);

---

* *Elektrichestvo*, No. 9, 29-35, 1961.

(b) a rectangular voltage containing all odd harmonics except multiples of three (Fig. 1, *b*).

The circuit of a frequency converter is shown in Fig. 2 [3]. The shape of the output voltage curve corresponds to that in Fig. 1(a) or (b) depending on the method of connecting the load.

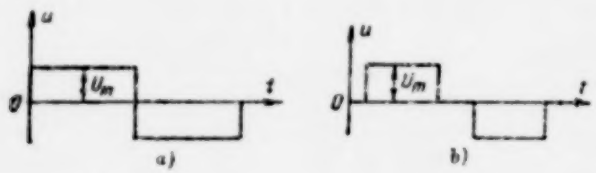

Fig. 1. Curves for the converter output voltages.

YEA
196

The circuit contains three single-phase converters, each of which consists of a transformer with a rectangular hysteresis loop, connected in the diagonal of a bridge of four power triodes. The single phase converters operate in the same way as in Royer's circuit [4], except that the transformer is not a power transformer; it is intended for controlling the triodes. In one half-wave the triodes T_{11} and T_{14} are in the state of saturation and T_{12} and T_{13} in the state of cut-off. In the next half-wave the position is reversed.

All three converters are synchronized with the angle of phase shift of the output voltage (equal to $2\pi/3$). The converter FC_1 is the driving one in relation to FC_2, and FC_2 is the driving one in relation to FC_3. The pair of triodes T_{21}, T_{23} (T_{31}, T_{33}) of each driven converter are controlled by two parallel-connected windings, viz. one from the transformer proper w_{21}, w_{23} (w_{31}, w_{33}), and the other from the transformer of the driving converter w_{c11}, w_{c12} (w_{c21}, w_{c22}). A choke (reactor) Ch_1 (Ch_2) is connected in series with the windings of the driving converter. The voltage on the synchronizing windings w_{c11}, w_{c12} (w_{c21}, w_{c22}) is greater than that on the windings of the transformer proper. Therefore, the windings w_{c11}, w_{c12}, (w_{c21}, w_{c22}) switch the triodes T_{23}, T_{21} (T_{33}, T_{31}) of the driven converter on saturation of the synchronizing choke Ch_1 (Ch_2). The state of the triodes of the driven converter is maintained until the next switching by the windings of the transformer proper.

The angle of saturation of the choke is:

$$\gamma = \frac{4w_{ch}\Phi_{s\,ch}}{\frac{w_{c11}}{w_1}U \cdot 10^8}, \qquad (1)$$

where w_{ch} is the number of turns of the choke, $\Phi_{s\,ch}$ the saturation flux of the choke and U the supply voltage.

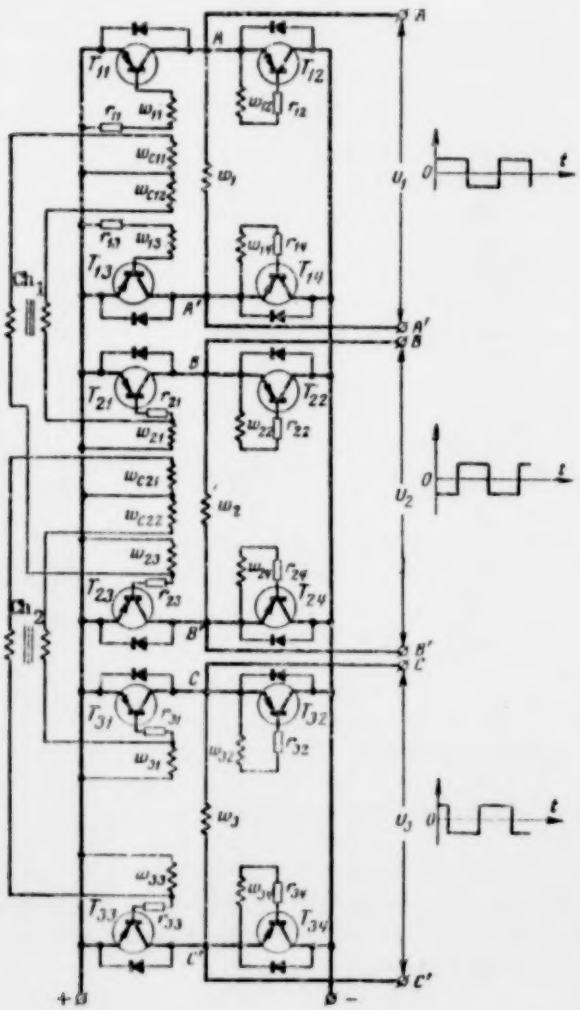

Fig. 2. Circuit of frequency converter.

In order that the angle between the voltages of the converters FC_1 FC_2 should remain constant throughout the entire range of frequency variation, it is necessary that the ratio of γ to the half-period τ should remain constant and equal to 2/3. Here T is found from the formula:

$$T = \frac{4w_1\Phi_{s1}}{U \cdot 10^8}, \tag{2}$$

where Φ_{s1} is the saturation flux of the transformer.

In fact, the ratio γ/T is independent of U, and the parameters of the chokes are found from the condition:

$$\frac{w_{ch}\Phi_{s\,ch}}{w_{c1}\Phi_{s1}} = \frac{2}{3}. \tag{3}$$

With a variation of the voltage, the saturation time of the cores and the half-period both vary in proportion, so that the angle between the output voltages of the converters remains constant.

An important condition of involuntary synchronization is that the fundamental (natural) frequency of the driven converter must be 8 to 10 per cent less than that of the driving converter, i.e.

$$f_{fc3} = f_{fc2} < f_{fc1} = f, \tag{4}$$

where f_{Fc3}, f_{Fc2}, f_{Fc1} are the fundamental (natural) frequencies of the converters and f the desired frequency of the three phase converter.

Otherwise the triodes of the driven converter are switched before the time for involuntary switching, and synchronization is disturbed.

All the triodes in this converter are fully used as regards voltage and current.

The circuit in Fig. 2 is suitable for regulating the speed of an induction motor between limits of 1 to 3 for a constant torque and between limits of 1 to 10 for a ventilator load, since the voltage across the base windings is proportional to the supply voltage.

If the amplitude of the output voltage is less than the permissible collector voltage of the triode, the load can be connected (a) in the diagonal of each bridge A-A', B-B', C-C', or (b) at the output of two individual three phase bridges.

But if the output voltage is greater than the permissible collector voltage of the triode, it is then possible (a) to desig: the transformers

Tr_1, Tr_2, Tr_3 for the total output power and to connect the load to the output windings of the transformers Tr_1, Tr_2, Tr_3 or (b) design these three transformers for the control power and connect the primary windings of the power transformers in the diagonal of each bridge A-A', B-B', C-C' or at the output of the individual three phase bridges.

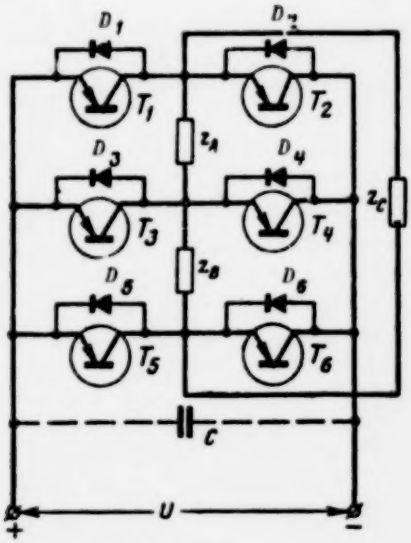

Fig. 3. Circuit of the power part of a converter with load delta-connected

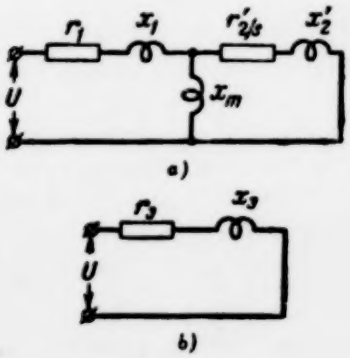

Fig. 4. Equivalent circuit of induction motor.

But if the output voltage is greater than the permissible collector voltage of the triode, it is then possible (a) to design the transformers Tr_1, Tr_2, Tr_3 for the total output power and to connect the load to

the output windings of the transformers Tr_1, Tr_2, Tr_3 or (b) design these three transformers for the control power and connect the primary windings of the power transformers in the diagonal of each bridge *A-A'*, *B-B'*, *C-C'* or at the output of the individual three phase bridges.

In view of the losses in the transformer, it is advisable to use a transformerless output and at high voltages to use series-connected triodes [5]. In the first case the output voltage will contain all odd harmonics (Fig. 1a), whereas in the other case the output voltage contains no harmonics which are multiples of three (Fig. 1b).

The best characteristics are possessed by an autonomous inverter [6] consisting of a three phase bridge type amplifier (see Fig. 3) and a three phase main generator. The latter consists of a variable frequency multivibrator and two conventional converters synchronized with the first by magnetizable saturable reactor. The frequency of the main generator is regulated by d.c. signals independently of the voltage across the power triodes. The variation of the voltage across the power triodes does not affect the frequency of the converter. The output voltage of this converter has the same shape as that shown in Fig. 1(b).

Tests were carried out on the system illustrated in Fig. 2. The power triodes of the semiconductor converter were shunted by diodes owing to the phase shift between the current and voltage on inductive-active load.

The following assumptions were made:

(a) The saturation of the motor was neglected;

(b) The control pulses were assumed to be rectangular in shape;

(c) The characteristics of the triodes and diodes were assumed to be ideal;

(d) The switching time of the triodes was assumed to be zero.

Consider first the operating characteristics of an induction motor with an input voltage of rectangular shape which generally contains all odd harmonics. The curve in Fig. 1(a) is expanded into a Fourier series:

$$U = \frac{4U_m}{\pi}\left[\sum_{n=0}^{n=\infty}\frac{\sin(6n+1)\omega t}{6n+1} + \right.$$
$$\left. + \sum_{n=1}^{n=\infty}\frac{\sin(6n-1)\omega t}{6n-1} + \sum_{n=1}^{n=\infty}\frac{\sin 3(2n-1)\omega t}{3(2n-1)}\right], \qquad (5)$$

where the harmonics of positive, negative and zero sequences are in separate sums.

Proceeding from the equivalent circuit of an induction motor (Fig. 4a), the nth order harmonic of the stator current is found from the expression

$$I_{1n} = \frac{u}{n} \cdot \frac{a_1 + n^2 r_2' s_n + a_2 n^2 c_2 s_n^2 - j(n^3 a_3 c_2 s_n^2 + n a_4)}{a_1 r_1 + n^2 a_5^2 + n^2 a_6 s_n + n^4 a_3^2 s_n^2 + n^2 a_2^2 s_n^2}, \tag{6}$$

where

$$\left.\begin{aligned} a_1 &= \frac{r_1 r_2'^2}{x_m^2}; \quad a_2 = r_1 c_2; \quad a_3 = (x_1 c_2 + x_2'); \\ a_4 &= \frac{r_2'^2 c_1}{x_m}; \quad a_5 = r_2' c_1; \quad a_6 = 2 r_1 r_2'; \\ a_7 &= \frac{r_1 r_2'}{x_m}; \quad c_1 = \left(1 + \frac{x_1}{x_m}\right); \quad c_2 = \left(1 + \frac{x_2}{x_m}\right). \end{aligned}\right\} \tag{7}$$

YEAR 1961

The rotor slip in the field of the nth harmonic is:

$$s_n = \frac{n' n_1 \mp n_2}{n n_1}, \tag{8}$$

where n_1 is the speed of the stator field (for the first harmonic) and n_2 the rotor speed.

In (8) the "minus" sign is then taken for the positive sequence harmonics and the "plus" sign for the negative sequence harmonics so that (8) takes the form

$$s_n = \frac{(n \mp 1) + s_1}{n}. \tag{8a}$$

The nth order harmonic of the rotor current, referred to the stator winding, is found by the formula

$$I_{2n} = \frac{u}{n} \cdot \frac{n^2 a_3 s_n^2 + n^2 a_5 s_n - j(n^3 a_3 s_n^2 - n a_7 s_n)}{a_1 r_1 + n^2 a_5^2 + n^2 a_6 s_n + a_3^2 s_n^2 n^4 + a_2^2 s_n^2 n^2}. \tag{9}$$

The power factor for nth order harmonic is

$$\cos \varphi_n = \frac{1}{\sqrt{1 + \left(\dfrac{n^3 a_3 c_2 s_n^2 + n a_4}{a_1 + n^2 r_2' s_n + n^2 a_2 c_2 s_n^2}\right)^2}}. \tag{10}$$

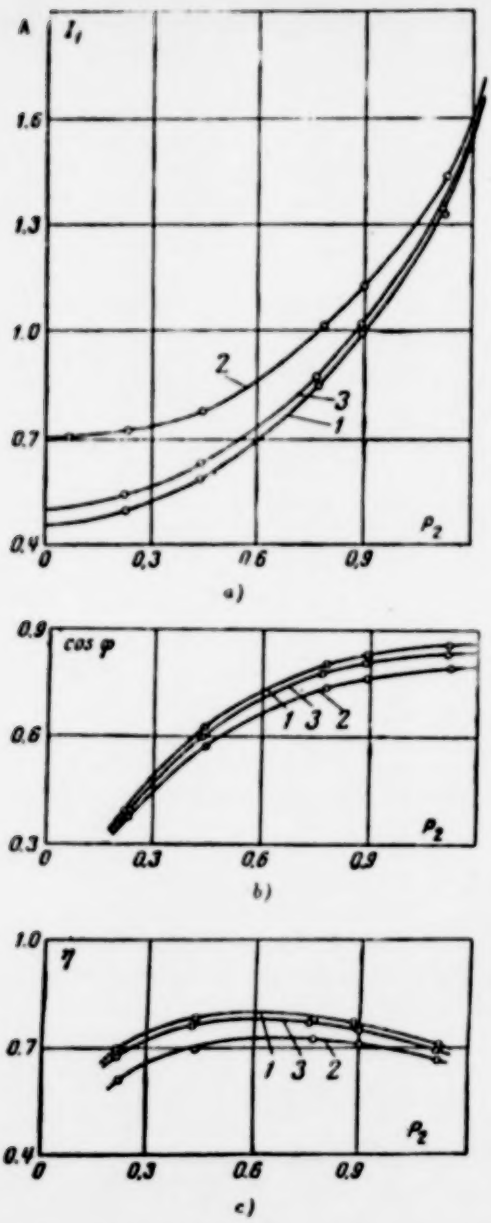

Fig. 5. Operating characteristics of induction motor. *1* – sinusoidal voltage; *2* – rectangular voltage with all odd harmonics; *3* – stepped voltage without harmonic multiples of 3; P_2 – relative power on shaft.

The resulting current and torque of the motor are then

$$I_1 = \sqrt{\sum_{1}^{n=\infty} I_{1n}^2}; \quad M = \sum_{1}^{n=\infty} M_n. \tag{11}$$

The operating characteristics of an induction motor have been plotted in Fig. 5 by (6)-(11). The motor parameters were as follows:

$$r_1 = 2.2 \ \Omega; \quad r_2' = 2.28 \ \Omega; \quad z_m = 46 \ \Omega;$$

$$x_1 = 2 \ \Omega; \quad x_2' = 3 \ \Omega.$$

Curves 1 in Fig. 5 refer to a sinusoidal supply voltage of 22.5 V; curves 2 were obtained for a supply voltage of rectangular shape containing all odd harmonics (the fundamental harmonic equalled the sinusoidal voltage 22.5 V). In both cases the supply frequency was 50 c/s.

YEAR 1961

Here the ratios of the mean and effective values of the sinusoidal and rectangular voltages respectively were:

$$\left.\begin{aligned} \frac{U_{s.av}}{U_{s.eff}} &= \frac{8}{\pi^2}; \\ \frac{U_{s.av}}{U_{r.eff}} &= \frac{2\sqrt{2}}{\pi}, \end{aligned}\right\} \tag{12}$$

where $U_{s.av}$ and $U_{r.av}$ are the mean values of the sinusoidal and rectangular voltages.

Calculations have shown that the decisive moment on the supply of a rectangular voltage is that created by the fundamental harmonic since the moments of higher harmonics are negligible. The higher harmonics cause an increase in the motor current, a deterioration in cos φ and an increase in losses so that the efficiency of the motor is reduced (see curves 2 in Fig. 5). For example, under rated conditions the motor current is increased by 10 per cent, cos φ is reduced by 8 per cent and efficiency is reduced by 5 to 7 per cent.

The deterioration in the characteristics of the motor is mainly due to the third harmonic of the rectangular voltage.

Accordingly, it is to be concluded that the supply of an induction motor with a voltage of rectangular shape which contains all odd harmonics is inefficient owing to the deterioration in its operating characteristics.

Consider now a typical case when the shape of the output voltage is like that shown in Fig. 1, (b). On expanding this curve into a Fourier series:

$$u = \frac{2\sqrt{3}}{\pi} U_m \left[\sum_{0}^{n=\infty} \frac{\sin(6n+1)\omega t}{6n+1} + \right.$$
$$\left. + \sum_{n=1}^{n=\infty} \frac{\sin(6n-1)\omega t}{6n-1} \right]. \qquad (13)$$

Curves 3 in Fig. 5 have been obtained for the same motor with a supply voltage of the shape shown in Fig. 1, (b) on condition that the fundamental harmonics of the rectangular and sinusoidal voltages were both the same. This condition is satisfied if

$$U_{s.av} = \frac{6\sqrt{3}}{\pi^2} U_{r.av} = 1.05 U_{r.av}$$

or (14)

$$U_{s.eff} = \frac{3}{\pi} U_{r.eff} = 0.955 U_{r.eff}$$

It will be seen from a comparison of curves 1 (sinusoidal voltage) and curves 3 (rectangular voltage without harmonic multiples of 3) that the operating characteristics of the motor are not appreciably affected in the latter case. Thus, for example, the power factor cos φ is only reduced by 2 or 3 per cent, whilst the efficiency is only reduced by 1 to 1.5 per cent. The motor current is notably increased on no load; the difference between the currents decreases with increasing load. The explanation is that there is practically no variation of the rotor slip in the field of higher harmonics with changes in slip in the field of the fundamental harmonic within the limits 0-1. Thus, for example, for the fifth harmonic $s_5 = 1.2$ to 1, and for the seventh harmonic $s_7 = 0.857$ to 1. Currents of higher harmonics therefore remain constant when the load changes. It is obvious a lighter load means that currents of higher harmonics will have a greater influence. At rated load the current increases by 2 to 3 per cent and the motor torque remains practically unchanged.

In order to analyse the switching of power triodes which are shunted by diodes, it is sufficient to consider the current in two phases, for example, *A* and *B*, and the operation of one pair of triodes: T_3, T_4 (Fig. 3). Suppose that the triodes T_1, T_3 and T_6 are in the cut-off state at the instant $t = 0$ (Fig. 6) and that triodes T_2, T_4 and T_5 are

saturated. The operating point for T_3 is B_6, and that for T_4-A_1. In the interval $t_0 \leqslant t \leqslant t_1$ the current in phase B increases according to the law:

$$i_1(t) = \frac{U_m}{r_k} - \frac{U_m}{r_k} \cdot \frac{1 + e^{-\frac{1}{6f\tau}}}{1 + e^{-\frac{1}{2f\tau}}} e^{-\frac{t}{\tau}}, \qquad (15)$$

where

$$\tau = \frac{x_k}{\omega r_k},$$

f is the mains frequency, and the resistance r_k and inductive reactance x_k of the motor are respectively

$$r_k = r_1 + \frac{x_m^2 \frac{r_2'}{s}}{\left(\frac{r_2'}{s}\right)^2 + (x_m + x_2)^2}$$

$$x_k = x_1 + x_m \frac{x_2'^2 + x_m x_2' + \left(\frac{r_2'}{s}\right)^2}{\left(\frac{r_2'}{s}\right)^2 + (x_m + x_2)^2}$$

In phase A the current decreases according to the law:

$$i_2(t) = \frac{U_m}{r_k} \cdot \frac{1 - e^{-\frac{1}{3f\tau}}}{1 + e^{-\frac{1}{2f\tau}}} e^{-\frac{t}{\tau}}. \qquad (16)$$

A line current i_l flows through the triode T_4, i.e. the sum of the currents in phases A and B is:

$$i_1(t) - i_2(t) = i_{l1} = \frac{U_m}{r_k} - \frac{U_m}{r_k} \times \frac{\left(1 + e^{-\frac{1}{6f\tau}}\right)\left(2 - e^{-\frac{1}{6f\tau}}\right)}{1 + e^{-\frac{1}{2f\tau}}} e^{-\frac{t}{\tau}} \qquad (17)$$

The operating point is moved from A_1 to A_2. At the instant $t = t_1$, the triodes T_1 and T_2 are respectively switched into the saturation and cut-off states. In the interval $t_1 \leqslant t \leqslant t_2$ the current in phase A begins to increase in the reverse direction in accordance with (15); in phase B the current continues to increase in accordance with (15). A second

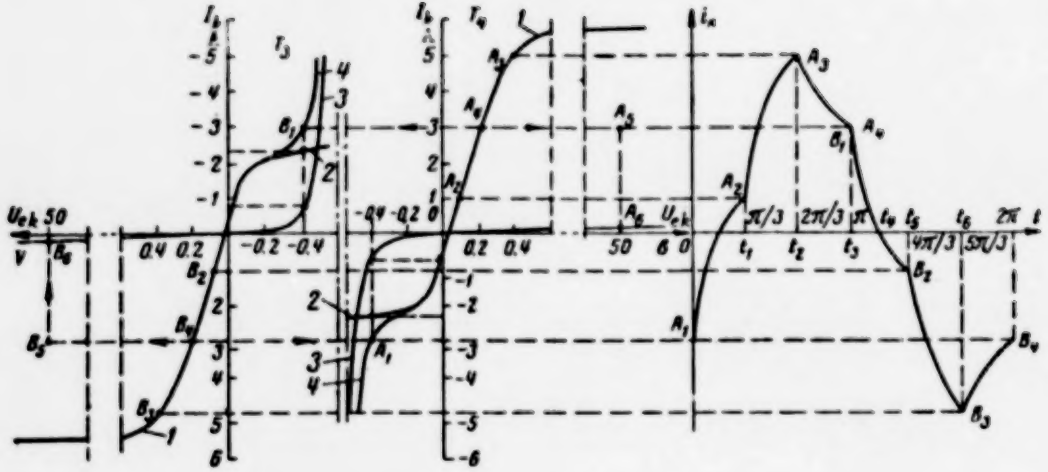

Fig. 6. Commutation of the load current in semiconductor converter. 1 – $I_k = f(U_{ek})$ for positive polarity of U_{ek}; 2 – the same except negative polarity; 3 – characteristic of diode in conducting direction; 4 – overall characteristic of triode (with negative polarity U_{ek}) and diode in conducting direction.

YEAR
1962

line current flows through the triode T_4 equal to:

$$i_1(t) + i_2(t + t_1) = i_{12} = \frac{2U_m}{r_k} - \frac{U_m}{r_k} \times \frac{\left(1 + 2e^{-\frac{1}{6f\tau}} + e^{-\frac{1}{3f\tau}}\right)}{1 + e^{-\frac{1}{2f\tau}}} e^{-\frac{t}{\tau}}.$$

The operating point of T_4 is now moved from A_2 to A_3.

At the instant $t = t_2$ the triodes T_6 and T_5 are switched respectively into the saturation and cut-off states. In the interval $t_2 \leqslant t \leqslant t_3$ the current in phase A continues to increase in accordance with (15), and that in phase B coincides in accordance with (16). A current then flows through the triode T_4 equal to:

$$i_1(t + t_1) + i_2(t) = i_{13} = \frac{U_m}{r_k} + \frac{U_m}{r_k} \times \frac{1 - e^{-\frac{1}{6f\tau}} - 2e^{-\frac{1}{3f\tau}}}{1 + e^{-\frac{1}{2f\tau}}} e^{-\frac{t}{\tau}}. \qquad (18)$$

YEAR
1961

The operating point T_4 is moved from A_3 to A_4. At the instant $t = t_3$ the process of switching triodes T_3 and T_4 begins. As soon as triode T_4 becomes "conducting" under the action of the self-induction e.m.f. of the windings of phases A and B, its operating point moves instantaneously to the point A_5, whilst that of T_3 moves to O. In the course of transient behaviour the current of triode T_4 decreases, whilst that of T_3 increases so that at any instant in time

$$i_{13} = i_{T3} + i_{T4}. \qquad (19)$$

The operating point T_4 is moved from A_5 to A_6 and that of T_3 for O to B_1. Thus, triode T_4 is in the zone of cut-off, and T_3 in that of saturation. In the interval $t_3 \leqslant t \leqslant t_4$ phase A is disconnected from the supply source and short-circuited by the triode T_1 and the parallel circuit D_3-T_3. The current which is maintained by the self-induction e.m.f. of the motor winding flows through the triode T_1 in phase A in the former direction; the current through diode D_3 flows in the conduction direction; that through T_3 is in the reverse direction (i.e. in the direction of the collector-emitter).

It will be seen from Fig.6 that the current amplification factor of a P4-type triode (the ratio of the base current to the saturation current of the collector) is 2.5 times less in the reverse direction than in the forward direction. Thus, for example, if the operating point of the triode in the forward direction at 5 A is in the saturation zone for a definite base current, then for the same base current in the opposite direction the operating point will depart into the active region even

at currents above 2 A and even in the absence of a shunting diode. The connexion of a shunting diode ensures the operation of the triode with reverse currents in the region of saturation.

The current in phase B at the first instant after switching remains in the same direction owing to the self-induction e.m.f. Two cases are possible:

1. If $1 \geqslant \cos\varphi \geqslant 0.525$ the current of phase C and the triodes T_1 and T_3, thereby reducing the current consumed from the d.c. circuit so that at any instant in time

$$i'(t) + i_B(t) = i_C(t). \tag{20}$$

In other words, the current of phase B is completely compensated by the current of phase C.

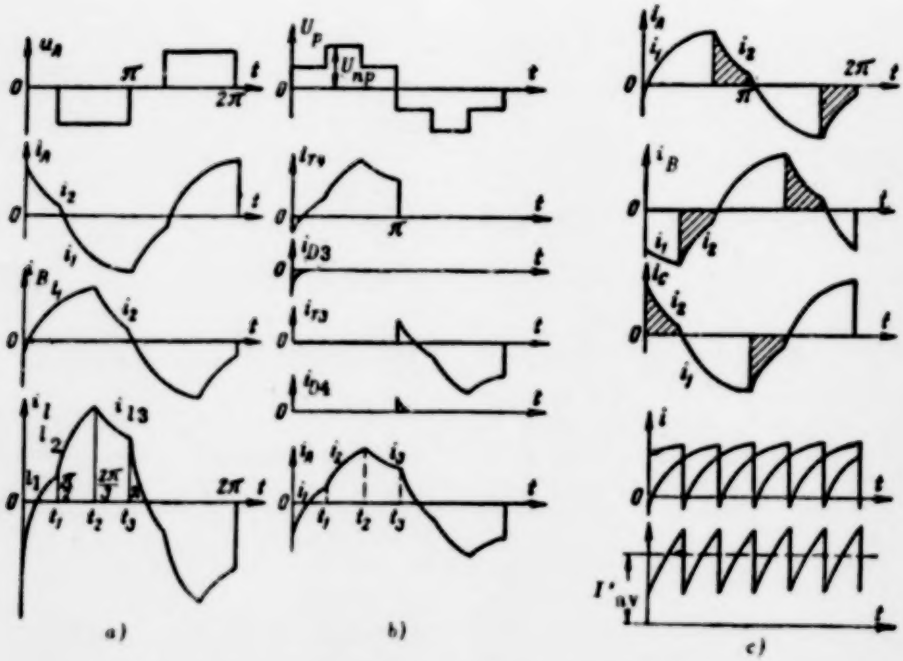

a) b) c)

Fig. 7. a – voltage across phase A, currents in A and B and line current with delta-connected load; b – phase voltage with load star-connected, currents flowing through T_3, D_3, T_4, D_4 and the line current; c – phase currents and current in the supply source circuit.

2. If $0.525 \geqslant \cos\varphi \geqslant 0$, the current of phase B is only partially compensated by that of phase C and the current of the supply source changes sign. This implies that the d.c. source must take the non-compensated part of the reactive power given off by phase B. In the opposite case (supply from a rectifier), the d.c. source has to be shunted by a capacitance given by the formula:

$$C=\frac{\tau 10^6}{kr_k}\left[2\ln\frac{\left(1+e^{-\frac{1}{6f\tau}}\right)^2}{2\left(1+e^{-\frac{1}{2f\tau}}\right)}+\frac{\left(1-2e^{-\frac{1}{6f\tau}}\right)\left(1-e^{-\frac{1}{3f\tau}}\right)}{1+e^{-\frac{1}{2f\tau}}}\right][\mu F], \quad (21)$$

where $k=\frac{U_c}{U_m}$ is the permissible increase in the capacitor voltage.

The mean value of the phase current during a halfwave is found from the expression:

$$I_{av.p_\Delta}=\frac{2}{3}\cdot\frac{U_m}{r_k}-\frac{4U_m}{r_k}f\tau\ln\frac{1+e^{-\frac{1}{6f\tau}}}{1+e^{-\frac{1}{2f\tau}}}. \quad (22)$$

The effective value of the phase current is:

$$I_{eff.p_\Delta}=\frac{U_m}{r_k}\cdot\frac{\sqrt{2}}{\sqrt{3}}\sqrt{1-3f\tau\frac{1-e^{-\frac{1}{3f\tau}}}{1-e^{-\frac{1}{6f\tau}}+e^{-\frac{1}{3f\tau}}}}. \quad (23)$$

The relationship between the phase and line currents is the same as for a sinusoidal voltage:

$$I_{eff.l}=\sqrt{3}I_{eff.p}. \quad (24)$$

Fig. 7(a) shows curves for the currents in phases A and B and the line current $i_l = i_A + i_B$ for delta-connected motor windings. Fig. 7(c) shows curves for the currents in phases A, B and C. In each phase the current i_1 (15) flows through the supply source, but the current i_2 (16) does not. Therefore the current in the circuit of the supply source is the sum of the currents i_A, i_B and i_C without the shaded sections:

$$I'=\frac{2U_m}{r_k}\left(1-3f\tau\frac{1-e^{-\frac{1}{3f\tau}}}{1-e^{-\frac{1}{6f\tau}}+e^{-\frac{1}{3f\tau}}}\right). \quad (25)$$

With star-connected motor windings, the phase voltage curve is in two steps (see Fig.7b):

for the first step

$$U_{mp} = \frac{U_{ml}}{Z_A + \frac{Z_A}{2}} \cdot \frac{Z_A}{2} = \frac{U_{ml}}{3}; \tag{26}$$

for the second

$$U_{mp} = \frac{U_{ml}}{Z_A + \frac{Z_A}{2}} Z_A = \frac{2}{3} U_{ml}. \tag{27}$$

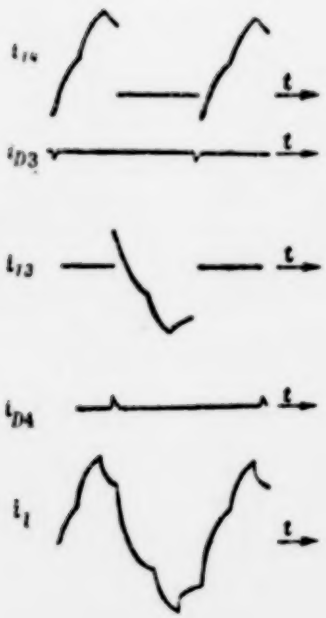

Fig. 8. Oscillograms of the triode, diode and line currents

The phase voltage does not contain harmonic multiples of 3:

$$U_p = \frac{3}{\pi} U_{mp} \left[\sum_{n=0}^{n=\infty} \frac{\sin(6n+1)\omega t}{6n+1} + \sum_{n=1}^{n=\infty} \frac{\sin(6n-1)\omega t}{6n-1} \right]. \tag{28}$$

The expressions for the currents in the individual intervals are:

if $0 \leqslant t \leqslant t_1$

$$i_1 = \frac{U_{m\,p}}{2r_k} - \frac{U_{m\,p}}{2r_k} \cdot \frac{2 + e^{-\frac{1}{6f\tau}} - e^{-\frac{1}{3f\tau}}}{1 + e^{-\frac{1}{2f\tau}}} e^{-\frac{t}{\tau}};$$

if $t_1 \leqslant t \leqslant t_2$

$$i_2 = \frac{U_{m\,p}}{r_k} - \frac{U_{m\,p}}{2r_k} \cdot \frac{1 + 2e^{-\frac{1}{6f\tau}} + e^{-\frac{1}{3f\tau}}}{1 + e^{-\frac{1}{2f\tau}}} \cdot e^{-\frac{t}{\tau}};$$

if $t_2 \leqslant t \leqslant t_3$

$$i_3 = \frac{U_{m\,p}}{2r_k} + \frac{U_{m\,p}}{2r_k} \cdot \frac{1 - e^{-\frac{1}{6f\tau}} - 2e^{-\frac{1}{3f\tau}}}{1 + e^{-\frac{1}{2f\tau}}} e^{-\frac{t}{\tau}}.$$

The curves for the currents flowing through T_3, T_4, D_3 and D_4 are given in Fig. 7(b) along with those for the line current $i_l = i_A + i_B$ with the motor connected in star.

The mean value of the phase current is

$$I_{\text{eff}} = \frac{2U_{m\,p}}{3r_k} - \frac{2U_{m\,p}}{r_k} f\tau \ln \frac{\left(1 + e^{-\frac{1}{6f\tau}}\right)\left(2 - e^{-\frac{1}{6f\tau}}\right)}{1 + e^{-\frac{1}{2f\tau}}}, \tag{29}$$

and its effective value

$$I_{\text{ef}} = \frac{U_{m\,p}}{\sqrt{2} \cdot r_k} \sqrt{1 - 3f\tau \frac{1 - e^{-\frac{1}{3f\tau}}}{1 - e^{-\frac{1}{6f\tau}} + e^{-\frac{1}{3f\tau}}}}. \tag{30}$$

The current in the supply source circuit is:

$$I'_Y = \frac{3}{2} \cdot \frac{U_{mp}}{r_k} \left(1 - 3fr \frac{1 - e^{-\frac{1}{3fr}}}{1 - e^{-\frac{1}{6fr}} + e^{-\frac{1}{3fr}}} \right). \qquad (31)$$

Fig. 8 shows oscillograms of the currents i_{T4}, i_{D4}, i_{T3}, i_{D3} and i_A.

Conclusions

1. The supply of an asynchronous motor with a voltage which is of rectangular shape and contains all odd harmonics is inefficient owing to the considerable deterioration of its operating characteristics.

2. This deterioration is limited to 1-2 per cent if the supply voltage is free of harmonic multiples of 3.

3. There is no justification in using semiconductor converters for approximately sinusoidal output voltage curves. The slight improvement in the operating characteristics of the motor is offset by the complication of the system and the increased losses due to the use of an output transformer.

4. If the line output voltage of the converter has the shape of the curve in Fig. 1(a), it is advisable to connect the motor windings in star, but if the line output voltage contains no harmonic multiples of 3, star or delta connexion is equally good. If phase distortion is present, it is advisable to connect the motor windings in star in order to eliminate currents of harmonics which are multiplies of 3.

Translated by O.M. Blunn

REFERENCES

1. L.M. Piotrovskii; *Electrical machines, (Elektricheskie mashiny).* Gosenergoizdat (1950).
2. V.G. Konstantinov and O.I. Shuster; Auth. Cert. No. 124517, 21 Feb. 1959.
3. O.I. Khasayev; Auth. Cert. No. 124519, 19 March 1959.
4. G.H. Royer; *Trans. Amer. Inst. Elect. Engrs.* 74, pt.I, 322-326 (1955).

5. O.A. Kossov; *The series connexion of switching triodes, (Posledovatel'noe soedinenie perekliuchaiushchikh triodov). Izv. Akad. Nauk SSSR (OTN, Energetika i avtomatika)*, No.1 (1960).
6 O.I. Khasayev; Auth. Cert. No. 128933, 19 March (1959).

YEAR
1961

THE CURRENT DISTRIBUTION IN THE BATHS OF ORE-SMELTING FURNACES* **

G. A. SISOYAN

(Georgian Polytechnical Institute)

(Received 23 February 1961)

Modern electric ore-smelting furnaces take currents of up to hundreds of thousands of amps at voltages seldom above 200 to 300 V.

Another feature of these furnaces is the low current density of the electrodes which varies between 2 and 10 A/cm^2. Yet in the bath itself, depending on the physical and chemical state of the materials, the current density and the volume power density vary between very wide limits, with the result that large variations occur in bath temperature. In open furnaces the temperature hardly reaches 100-200°C under the charge hole, whilst in the space under the electrodes it can reach several thousand deg. centigrade.

The conversion of electrical energy into thermal energy in the bath is bound up with these factors. Depending on the physical and chemical state of the charge materials, the current distribution and the temperature, the furnace may operate like a resistance furnace, an arc furnace or like a combination of the two, when energy is liberated in the charge and arc at the same time.

The interplay of such diverse factors complicates the selection of optimum conditions. But since the starting point is necessarily the distribution of the current and power in the bath, a study of these factors is of decisive importance.

---

* *Elektrichestvo*, 9, 45-50, 1961.

**Published by way of discussion.

The general laws of electrical circuits and the method of equivalent circuits can be applied to furnace circuits, but to do so it is necessary to take the spatial current distribution into account. But the generally accepted equivalent circuits of polyphase systems in the form of stars of polygons are not at all suitable for the current distribution and to a certain extent they are unrealistic.

The structure of the bath and charging the materials

The structure of the furnace bath under steady state operating conditions can be most diverse, but certain regularities are common to them all, the main ones being the temperature distribution, the current field and the aggregate state of the charge.

YEAR
1961

There is usually a zone of maximum current density on the electrode face. It is here that the main chemical processes take place most intensively in the formation of the melt. This region is called the crucible of the bath. The temperature and current density decrease from the electrode face to the perimeter of the bath.

Depending on their physical and chemical properties, the charge materials in the space under the electrodes may be in the solid, molten or gaseous states. In the first two cases the conversion of electrical energy into heat takes place as in a resistance furnace, and in the third case (the gaseous state) it takes place via the arc. Molten products of reaction accumulate in the sub-electrode space. It is to be supposed that the temperature levels and extent of the regions with various forms of the materials differ in different furnaces and with different melts. The distribution of the regions in which the materials are in a different form is also affected by the relative and absolute dimensions of the electrode and bath.

In polyphase furnaces in general and three phase furnaces in particular the crucibles of the individual phases can either be kept apart or else merged into one common crucible. The design of medium power three-phase carbide furnaces is a typical example of "isolated" crucibles. Common crucibles are used in medium power ferrosilicon furnaces.

The foregoing classification is rather rough, but unfortunately there is still a lack of reliable data about the crucibles of furnaces.

The possible paths of the current in the bath

Electric ore-smelting furnaces generally operate under mixed conditions where there is not only an arc current but also currents which shunt the arc. These currents flow through the molten and fluid materials in the bath.

In a single phase furnace the hearth usually acts as a second electrode and the arc burns between the face of the moving electrode and the materials on the hearth. Since there are materials around the arc which possess a certain electrical conductance, it follows that current flows parallel to the arc between the moving electrode and the hearth.

If the furnace is operating without the arc, a flow of current also takes place from the side surface of the moving electrode into the fluid melt or the solid charge surrounding the electrode as well as from its face. When the arc emerges, part of the face surface of the electrode is occupied by a gaseous interlayer. Under certain conditions this interlayer can occupy the entire surface of the electrode face and spread to the side surface of the electrode.

The distribution of the current in three-phase furnaces is more complicated. Besides the arc currents flowing from the electrodes to the hearth on the star system, currents can also flow from the electrodes to the hearth through the charge on the star system and from electrode to electrode on the delta system. The possible current paths in a three phase furnace are illustrated in Fig. 1.

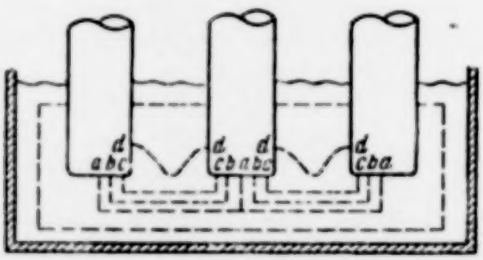

Fig. 1. Current paths in bath.
a – through arc and melt; *b* – arc apart from melt;
c – charge; *d* – electrode side and charge.

The magnitudes of the arc currents and charge conductance currents depend on many factors, the main ones being the distribution of the thermal and electrical fields in the bath and the thermal conductivity and electrical conductance of the charge materials. Since at a given

voltage the configuration of the fields depends on their size, and since the electrical conductance and thermal conductivity are to a certain extent inter-connected, it follows that the density distribution of the current and power can be represented as a function of the geometric factor and the electrical conductance:

$$\delta = f(G;\ \rho).$$

Thus for both single and three-phase furnaces the problem reduces to the determination of the electrical and thermal fields, the density of the current and power in the charge, and the relationship between the power of the arc and in the charge.

The electrical field

YEAR 1961

Analytical methods of determining the electrical fields of a bath, with the non-homogeneity of the charge conductance included, are very complicated and do not always produce satisfactory results. But if it is assumed that ρ is a constant, the field of a single phase furnace can be reduced to a plane-meriodional field described by the Laplace equation

$$\nabla^2 U = 0.$$

Since the diameter of a furnace is quite large, it is possible to ignore the radial curvature of the field, and the field of a single-phase furnace can be reduced to a plane-parallel (two-dimensional) field.

Solving this equation for the vector of field intensity, we get the equation:

$$E = E_x + jE_y = \frac{U}{\delta} \cdot \frac{c}{c^2 + d^2} - j\frac{U}{\delta} \cdot \frac{d}{c^2 + d^2},$$

where U is the potential difference, δ the distance between the electrodes, c and d coordinates of the transformation.

It is tedious work calculating the individual points of a field, but it leads to satisfactory results. Fields obtained in this way do however have to be regarded as approximate, since no account is taken of distortions caused by the furnace lining.

In fact, a charge is present in the furnace between the electrodes having a certain electrical conductance which is limited by the insulat-

ing layer of the bath lining. The field must be regarded therefore as a two-layer field with the surface effect included.

The field configuration and current distribution depend mainly on gap δ between the electrodes, the gap a between the top electrode and the lining of the bath, the height h of the charge layer, the diameter d of the electrode and the diameter d' of the crucible.

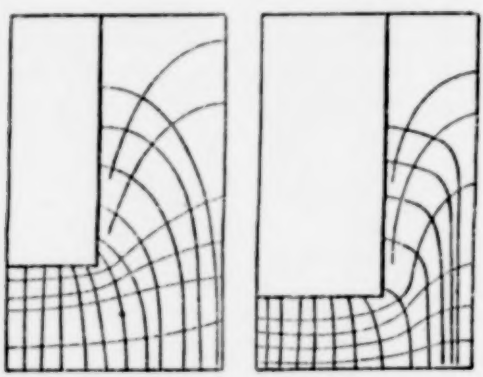

Fig. 2. Electrical field of model.

Fig. 2 shows two field configurations obtained experimentally from a furnace model. The experiments showed that the current which flows from the face of the electrode is 100 to 150 per cent of that flowing from the side surface of the electrode. But the current does not flow uniformly even from the side surface. The density of the current from the side surface at the face is greater than that on the surface of the charge by a factor of approximately 2 to 2.5. One of the curves which illustrate this relationship is shown in Fig. 3.

The charge conductance current falls sharply with increasing dimensions of the gaseous sphere surrounding the electrode face. The relationship between the current and δ is just the same. The magnitude of the charge current is least affected by the diameter of the electrode. Even over a fairly wide range of electrode diameters, the current from the side surface of the electrode only varies by 5 to 10 per cent.

As is known, technological considerations enter into the question of electrode diameter and, within the limits allowed on technological grounds, the diameter of an electrode has practically no effect on the magnitude of the current.

An analytical study of the fields of three-phase furnaces is still more complicated, but the field configuration can again be obtained by modelling.

When investigating the field of three phase furnaces, it is necessary to distinguish the instantaneous and effective values of the fields. The distribution of the energy in a bath is mainly determined by the effective value of the field.

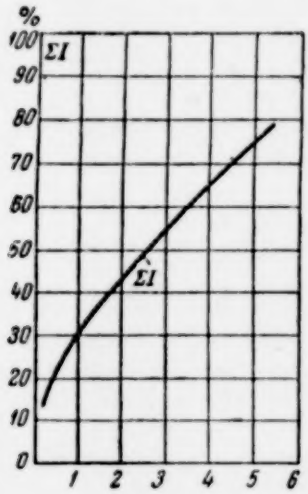

Fig. 3. Current density over height of electrode.

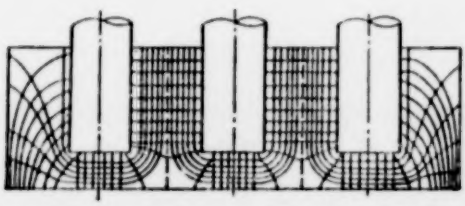

Fig. 4. Field of three-phase furnace, electrodes in row.

Fig. 4 shows the field of a furnace with its electrodes arranged in a row (a quadrangular bath was used). The configuration of the field was influenced mainly by the dimensions of the bath, the diameter d of

the electrodes, the distance l between the axes of the electrodes, the gap δ between the electrodes and the hearth and the height h of the furnace.

Delta cross-flow of current only takes place between the middle and extreme electrodes. The current density in the vertical direction is practically constant; a more or less sharp decrease in this current occurs at the upper boundary of the bath. With uniform conductance of the medium, the delta currents are greater than the star currents (see Fig. 5). With an increase in the gap between the electrode and hearth, the delta currents decline almost linearly, but the star currents decline slightly more slowly.

However, the distribution of the currents in the bath is altered considerably by the gaseous spheres which form under the electrodes, and by the non-homogeneous electrical conductance of the bath.

The distribution of power in the bath

A uniform distribution of power is preferable for processes which take place at comparatively low temperatures. In such cases the processes take place in a considerable volume of the bath and the gaseous products rise to the throat with uniform density.

For high temperature processes it is necessary to have hearths with more intensive power capable of providing these temperatures.

In order to estimate the distribution of power in a bath, use may be made of the notion of the volume power density:

$$p = \frac{dP}{dV},$$

where P is the mean value of the power and V the volume in which the power is developed.

In differential form the volume power density can be expressed by the equation

$$p = \frac{E^2}{\rho},$$

where E is the intensity of the electric field and ρ the specific resistance of the medium at a point in the medium.

Since the volume power density is proportional to the square of the field intensity if ρ is constant, it follows that curves can be plotted for the distribution of p if the pattern of the field intensity distribution is known.

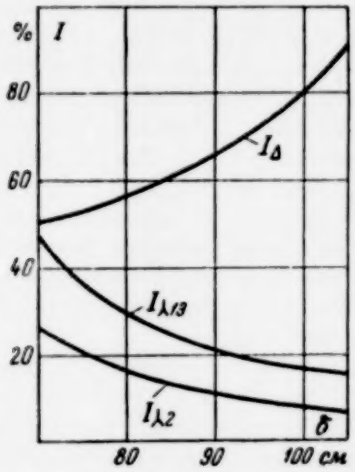

Fig. 5. Star and delta currents.

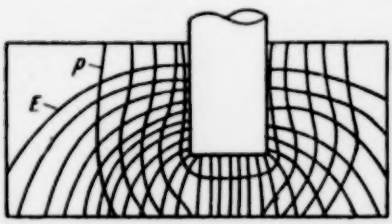

Fig. 6. Distribution of volume power density.

Fig. 6 shows the graphically-determined pattern of the distribution of the volume power density over the vertical section of a furnace bath. Lines p represent lines of equal volume power. By virtue of the square-law relationship with field intensity, the volume power density is greatest on the surface of the electrodes where E is also maximum. The value of p decreases much more rapidly than E with increasing distance from the electrode. In the majority of cases the value of p is only a fraction of one per cent of its original value at a distance from the electrode equal to the diameter of the electrode.

The electrical conductance of the charge materials

The electrical conductance of the charge materials has a fundamental effect on the current and power distribution in the bath. The main ingredients of the charge are reducing agents, oxides and metals. Their conductance will now be considered in turn.

Reducing agents. The main types of reducing agent are anthracite and coke. Practically all carbon materials have a very high specific resistance at temperatures up to 200-300°C. It declines with increasing temperature, but at temperatures between 500 and 600°C this decline is temporarily arrested. At 500-600°C to 1000-1200°C there is a marked decline in the specific resistance of carbon materials.

With a further increase in temperature, the specific resistance of all types of reducing agent balances out and the electrical conductance becomes practically the same for all types of reducing agent in the active zone of the reaction.

Fig. 7 shows typical curves for the relationship between the specific resistance of a type of anthracite and a type of coke on the one hand, and temperature on the other.

The roasting and graphitization of the reducing agent can take different lengths of time depending on the rate of descent of the charge. But in all cases the electrical conductance of almost all types of reducing agent is the same in the zone of reaction and in the lower levels of the bath generally. The type of reducing agent cannot therefore have any appreciable effect on the magnitude of the charge conductance current. Porosity and lumpiness are the only factors affecting the conductance of the reducing agent in the lower regions.

Porosity reduces the conductance of the reducing agent. The relationship between lumpiness and conductance is not so straight-forward since the number of contacts between lumps and the area of contact comes into the question. In some cases the total resistance of the bath can be changed slightly by altering the porosity and lumpiness of the reducing agent, but the scope for this is very limited.

In the upper regions of the bath, where lower temperatures prevail, all types of reducing agent have a relatively high specific resistance and therefore play a subsidiary role as a conducting factor. But the type of reducing agent does influence the magnitude of the charge conductance current. At low temperatures coke has a larger conductance than anthracite and it is therefore instrumental in increasing the conductance and charge conductance current in this region. Conversely,

anthracite sharply reduces these currents, since it has a high specific resistance.

The type of reducing agent has a greater effect in the middle zone of the bath where temperatures of 500 to 1200°C prevail. In this range of temperatures there is a sharp increase in the conductance of the reducing agent and along with that, an increase in the charge conductance current and power.

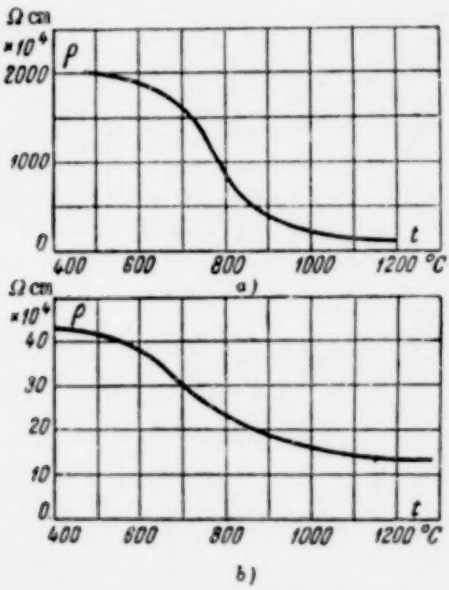

Fig. 7. Specific resistance of anthracite (a) and coke (b) as a function of temperature.

In the lower regions, where maximum temperatures prevail, the conductance of all types of reducing agent becomes maximum, and it balances out so that the conductance of this zone is maximum and all types of reducing agent have the same effect. It appears that the charge conductance currents and powers are also maximized in this zone.

As a whole it may be said that the reducing agent is not a significant factor as regards conductance in the upper regions. But in this zone types of reducing agent do affect the magnitude of the charge conductance current. In the middle regions the conductance of the reducing agent is greater and, consequently, the charge conductance currents and powers are increased. Finally, the conductance of the reducing agent is maximized in the lower regions where the temperature is greatest and all reducing agents tend to have the same effect. In this zone the charge conductance currents and powers are also maximum.

Oxides. Metal oxides have a very high specific resistance and a negative temperature coefficient, i.e. their specific resistance declines with increasing temperature. Even at very high temperatures near their melting point, most oxides still retain a high specific resistance. For example, the specific resistance of quartzite at room temperature is about (2-3) x 10^{10} Ω cm and at 800°C it is about (5-6) x 10^{3} Ω cm, i.e. it is still high.

At 0°C the specific resistance of calcium oxide is about (2-3) x 10^{13} Ω cm; at 500°C, (7-8) x 10^{8} Ω cm; at 1200°C, 1 x 10^{3} Ω cm. It falls still lower at higher temperatures, but it is still quite high.

In the upper region of the bath the main types of oxides can therefore be regarded as non-conducting inclusions between the lumps of reducing agent. In the middle and lower regions they begin to play a certain role in the conduction of current, but their conductance is still very small.

Metals. At 20°C the specific resistance of iron is about 10 x 10^{-6} Ω cm. Its specific resistance is increased six times over with a rise in temperature from 20 to 1100°C. Nevertheless, the electrical conductance of iron is high even at quite high temperatures. Other metals have more or less the same electrical properties. The presence of metallic components in the composition of the charge has a marked effect on the transformation of electrical energy in the bath of the furnace. Since the electrical power of a furnace is proportional to its resistance, and since the resistance of metallic inclusions is negligible, the energy liberated in these inclusions is therefore negligible compared with that liberated in the other elements of the furnace.

The conductance of the charge mixture. The charge of ferrosilicon furnaces is generally a mixture of reducing agent, oxides and metals, but that of a carbide furnace is usually only a combination of reducing agent and oxides. It will already have been seen that the conductance of these components is widely different. The conductance of metals is almost a dozen times greater than that of oxides. The conductance of reducing agents is about half that of metals. The electrical conditions of the bath are affected accordingly.

In the upper regions of the furnace the current can only flow through the small circuits formed between the lumps of reducing agent and metal (iron), since the lumps of the oxide with their high specific resistance can play no part in the conduction of current. Therefore currents will flow through the charge only where such circuits are formed in series.

Since the specific resistance of metal is about half that of the reducing agent, it follows that the electrical energy of the charge conductance currents is mainly liberated in the reducing agent and not in the metal. On the whole the charge conductance current in the upper cooler zones of the furnace is not considerable.

In the middle regions of the furnace the conductance of the oxides and reducing agent increase, whilst that of the metal decreases. Therefore the oxides and metal takes an increasing part in the conduction of current and the transformation of energy. But in those regions the conductance currents remain inconsiderable since current-conducting circuits are seldom formed there either.

In the third and hottest zone the conductance of the oxides and reducing agents increases still further and the aggregate state of the charge undergoes a marked change as the oxides and metals soften and melt. This increases the contact between the individual lumps of the charge and whole current conducting regions are formed besides individual circuits. The difference between the volume power density of the various charge constituents is reduced.

YEAR
1961

The electrical conductance of the melt. A melt is a finished or intermediate product in the fluid state. It lies at the bottom and constitutes a section of the current path in the bath.

The energy which is liberated in the melt plays a greater or lesser role in the overall energy balance of the bath depending on the dimensions of the bath and the specific resistance of the melt.

In ferroalloy furnaces the melt is a fluid ferrosilicon with a 10 to 50 per cent iron content. This iron content of the melt cannot ensure the necessary resistance.

The conductance of the other component (silicon) is fairly high. Fig. 8 shows the specific resistance of silicon as a function of temperature. In the solid state it has a high specific resistance (15,800 $\mu\Omega$ cm at 1250°C, 2500 $\mu\Omega$ cm at 1670°C), but after melting its specific resistance drops to 36 $\mu\Omega$ cm. Therefore the specific resistance of a fluid melt in a ferrosilicon furnace is approximately 100 $\mu\Omega$ cm. Contact between the electrode and melt, no less than the submerging of the electrode in the melt, will lead to short-circuiting in these furnaces. Therefore the energy in ferrosilicon furnaces is mainly liberated in the arc. Even though the arc and melt are connected in series, the resistance of the melt is so small in comparison with that of the arc that it can be ignored.

The difference between this type of furnace and steel furnaces is that a ferrosilicon charge in the solid state has a much greater resistance than steel scrap in a steel furnace. Therefore contact between electrode and charge does not in this case cause a short-circuit and a finite current flows through the charge from electrode to electrode or to the melt.

The relationship between the resistances of the arc and charge on the one hand and the power liberated in them on the other still remains an open question. The temperature of a charge and its resistance vary within wide limits and therefore in certain conditions the resistance of the charge can be commensurate with that of the arc. Therefore the energy which is liberated in the charge may be commensurate with that liberated in the arc. The baths of furnaces have a certain capacity for self-regulation and re-distribution of power between arc and charge. The melt takes no part in this distribution of power.

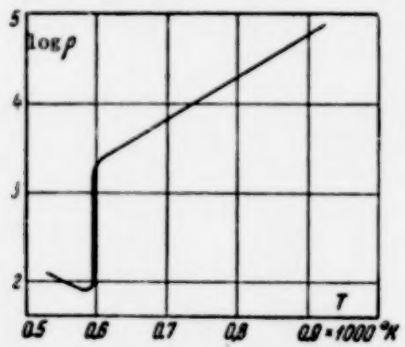

Fig. 8. Specific resistance of silicon as a function of temperature.

The specific resistance of calcium carbide also varies widely as a function of temperature. Fig. 9 shows a curve obtained by R. Chuguryan, from which it will be seen that a marked reduction of specific resistance only sets in at temperatures over 1600-1700°C. Since the temperature of the melt in the fluid (or viscous) form varies between 1800 and 2100°C, the specific resistance of a calcium carbide melt may be taken as 0.08-0.25 Ω cm. Certain other authors have produced higher figures (0.2-0.3 Ω cm). But even if the average specific resistance of of molten carbide is taken as 0.1 Ω cm, the total resistance of the bath is quite considerable.

For example, in particular 7500 kVA furnace the effective resistance

of the whole bath is 2000 $\mu\Omega$ and that of the melt 200 $\mu\Omega$. This implies that about 10 per cent of the energy is liberated in the melt. Since a considerable part of the energy is liberated in the charge which shunts the electrodes, it follows that the proportion of energy which is liberated in the arc of a carbide furnace is much less than that of a ferrosilicon furnace. The re-distribution of power may however be adjusted within certain limits by changing the operating conditions of the furnace.

It should however be mentioned that the specific resistance of calcium carbide falls very quickly with a decrease in temperature. The conducting layers of the charge and melt are therefore confined to layers surrounding the electrodes. The layer of the melt directly adjacent to the hearth of the furnace has such a high specific resistance that the current practically cannot penetrate it at all, and the hearth electrodes are equi-potential. The layers of the charge on the surface near the throat also have a very high specific resistance and therefore the density of the charge conductance current is practically zero in this region.

YEAR
1961

The actual distribution of the current and power in the bath

It has been argued above that the current and power distribution depends on the geometric dimensions of the bath and the electrical conductance. A change therefore in the conductance of the charge with variations in temperature causes considerable distortion of the current distribution compared with that which would otherwise exist in a homogeneous medium. Since the electrical conductance of ferrosilicon differs considerably from that of carbide, its effect on the distribution of current will not be the same in both cases. These types of furnace will now be considered along with steel and glass furnaces.

In steel furnaces the charge and melt both display high electrical conductance. Therefore at permissible values of current the liberation of heat in the charge and melt is negligibly small. Only arc furnaces can be used here. The electrical energy of the arc is transformed into thermal energy and transferred to the charge and melt according to laws of heat transfer.

In ferrosilicon furnaces the charge mixture has a rather high specific resistance. Charge conductance currents do occur in these furnaces. In the upper regions of the bath the specific resistance is much greater than in the middle regions, and in the region adjacent to the electrode

face the conductance is still higher. The charge conductance currents in ferrosilicon furnaces flow mainly in the narrow zone surrounding the face of the electrode. The melts of the great majority of ferrous alloys have very low electrical conductance and therefore the volume power density of the melt is inconsiderable. The melt takes no significant part in the transformation of electrical energy into thermal energy in these furnaces. In slagless processes the electrode face is not usually in contact with the melt and the arc burns on the electrode. If slag is present, the electrode face is usually submerged in the slag and the arc burns on the molten slag or on the melt. Even if slag is present, electrical energy is converted into thermal energy in only 20 to 30 per cent of the volume of the bath. Outside this space the volume power density is very low. The relationships between the power of the arc and charge can vary widely depending on the geometry of the bath and the type of alloy. For example, arc power may reach 80 to 90 per cent for ferrosilicon with a large iron context, but it can be as little as 30 to 40 per cent for carbon ferromanganese.

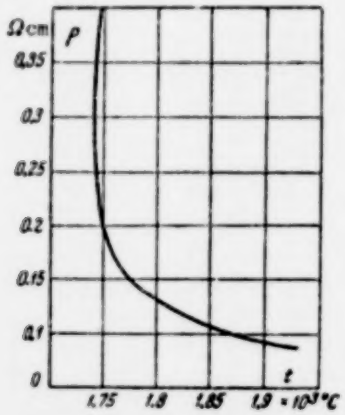

Fig. 9. Specific resistance of calcium carbide as a function of temperature.

In carbide furnaces the charge mixture has a high specific resistance in the cold state. But with increasing temperature it rapidly declines. Therefore the charge conductance current is small in the upper part of the furnace and the region in which electrical energy is converted into thermal energy occupies no more than 30 to 40 per cent (by volume) of the bath.

The specific resistance of calcium carbide melts is much greater than that of ferroalloy melts. In the carbide furnace, the face of the electrode is submerged in the melt, or else the arc burns on it; under normal conditions the presence of an arc is desirable since it ensures the necessary high levels of temperature for the technological process. A number of investigations have shown that about 40 per cent of the energy is liberated in the arc in carbide furnaces; roughly the same amount of energy is liberated in the charge and the remaining 20 per cent is liberated in the melt.

A glass furnace is a good example of a furnace with a melt having a high specific resistance. It operates on the principle of a resistance furnace. No electric arc is used in these furnaces.

Translated by O.M. Blunn

YEAR
1961

AN INVESTIGATION OF THE STEADY STATE STABILITY LIMITS OF LONG DISTANCE TRANSMISSION LINES WITH CONTROLLED SYNCHRONOUS CONDENSERS*

M.N. ROZANOV and CHEN' SHI-NYAN'

(Moscow Power Institute)

(Received 13 April 1961)

YEA
196

The installation of controlled synchronous condensers at intermediate substations is one of the most effective means of increasing the carrying capacity of long distance transmission lines.

An investigation of the steady state stability of long distance transmission lines with several synchronous condensers provided with automatic high-response excitation regulators is a very complex problem since it requires the formation and analysis of a high order characteristic equation. This equation is of order 12 for two synchronous condensers and of order 20 for four [1]. Theoretical investigation of steady state stability limits has until now been confined to systems with one synchronous condenser.

In this paper a method is proposed for long distance transmission lines with several controlled synchronous condensers. This method, evolved in the problem laboratory for electrical systems at the Moscow Power Institute, permits analysis of steady state stability as if only one controlled synchronous condenser were present. The changeover is based on comparison of regions of stability in the co-ordinates of the amplification coefficients of the automatic excitation regulator, for electrical transmission with one or two intermediate substations. Calculations carried out by the authors have shown that the stability

* *Elektrichestvo*, 9, 66-69, 1961.

limits of each transmission system practically coincide in modes of operation corresponding to equal maximum impedances Δx of the branch of the condenser beyond which the e.m.f. is maintained constant in order to ensure steady state stability.

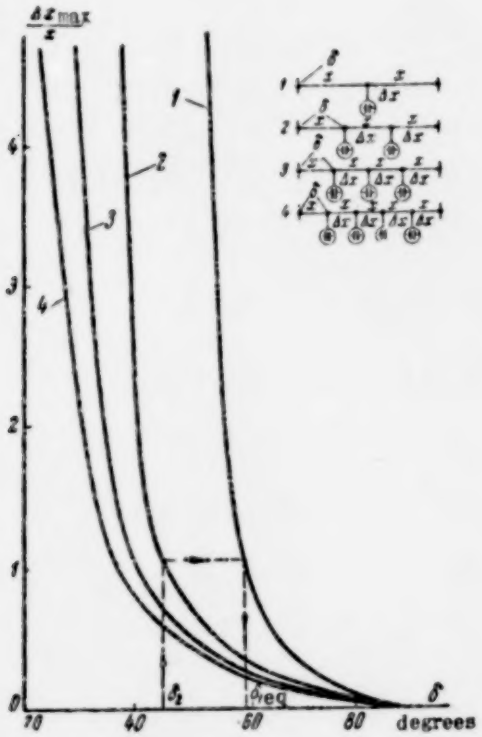

Fig. 1.

Fig. 1 shows transmission systems corresponding to the normal operations of a single-circuit or twin-circuit line with one, two, three and four intermediate substations.

It is assumed that the line sections are all equal in length, that the voltages at the sending and receiving ends of the line are constant and equal to unity, and that the voltage level at the point where the synchronous condenser is connected to the line is also equal to one. The condenser branch is replaced by an impedance Δx and a constant e.m.f. E_x after it. Ignoring the capacitance of the line, the following equations can then be written for the transient phenomena in system 1

for small deviations in conditions:

$$T_{J1}p^2\Delta\delta_1 = -\Delta P_1; \tag{1}$$

$$T_{J2}p^2\Delta\delta_2 = -\Delta P_2; \tag{2}$$

$$T_{J3}p\Delta\delta_3 = -\Delta P_3 \tag{3}$$

or

$$p^2\Delta\delta_{13} = -\frac{\Delta P_1}{T_{J1}} + \frac{\Delta P_3}{T_{J3}}; \tag{4}$$

$$p^2\Delta\delta_{23} = -\frac{\Delta P_2}{T_{J3}} + \frac{\Delta P_3}{T_{J2}}, \tag{5}$$

where

$$\Delta P_1 = \frac{1}{x_{12}}\cos\delta_{12}(\Delta\delta_{13} + \Delta\delta_{23}) + \frac{E_x}{x_{12}}\cos\delta_{13}\Delta\delta_{13}; \tag{6}$$

$$\Delta P_2 = -\frac{1}{x_{12}}\cos\delta_{12}(\Delta\delta_{13} + \Delta\delta_{23}) - \cdot - \frac{E_x}{x_{23}}\cos\delta_{23}\Delta\delta_{23}; \tag{7}$$

$$\Delta P_3 = -\frac{1}{x_{13}}\cos\delta_{13}\Delta\delta_{13} + \frac{E_x}{x_{23}}\cos\delta_{23}\Delta\delta_{23}. \tag{8}$$

The condition for balanced reactive powers at an intermediate point may be expressed in the following way:

$$2Q_l + Q_{s.c} = 2\left(-\frac{1}{x} + \frac{1}{x}\cos\delta\right) + \left(-\frac{1}{\Delta x} + \frac{E_x}{\Delta x}\right) = 0.$$

Using this expression, the e.m.f. can be defined as a function the angle δ:

$$E_x = 1 + 2\frac{\Delta x}{x}(1 - \cos\delta). \tag{9}$$

Substituting expressions (6)-(9) in the transient behaviour equations (3) and (4), and taking into account in forming the characteristic

equation that

$$x_{12} = 2x + \frac{x^2}{\Delta x};$$

$$x_{13} = x_{23} = x + 2\Delta x;$$

$$\delta_{13} = \delta_{23} = \delta;$$

$$\delta_{12} = \delta_{13} + \delta_{23} = 2\delta,$$

the following expression can be formed for the free term of the characteristic equation:

$$a_0 = A\left[2\frac{\Delta x}{x}\cos^2\delta - 2\frac{\Delta x}{x}(1-\cos\delta) + \cos\delta\right], \qquad (10)$$

where A is a constant coefficient

YEAR 1961

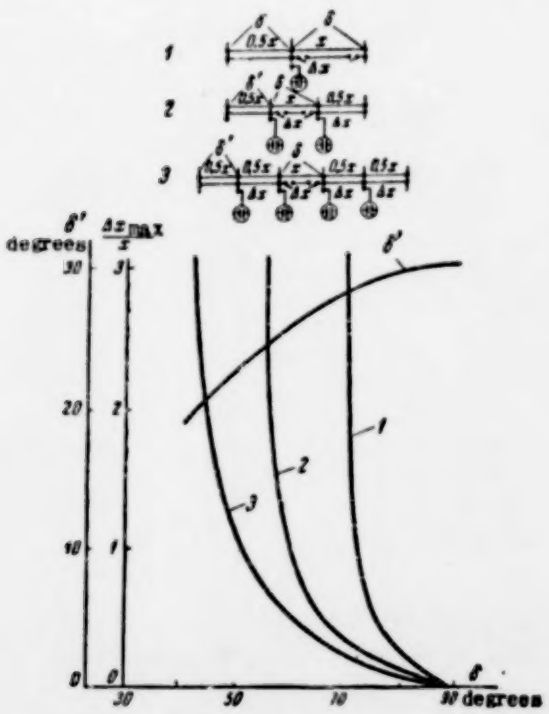

Fig. 2

Discarding the coefficient A and equating the second multiplier on the right-hand side of (10) to zero, that value of $\Delta x/x$ is defined as a function of the angle δ which is maximum as regards the condition of maximum stability and beyond which the e.m.f. E_x is held constant in order to ensure steady state stability:

$$\frac{\Delta x_{max}}{x} = \frac{\cos\delta}{2 - 2\cos\delta - 2\cos^2\delta}. \qquad (11)$$

The relationship $\Delta x_{max}/x = f(\delta)$ is represented by curve 1 in Fig. 1. In this diagram the curves 2, 3 and 4 refer to an analogous relationship in respect of two, three and four synchronous condensers. Fig. 2 shows the same relationships again, but this time for post fault conditions in a two-circuit transmission line.

In order to plot the region of stability, resort is had to characteristic equations [2] which are formed on the assumptions usually made in the analysis of the steady state stability of electrical systems with automatic high-response excitation control.

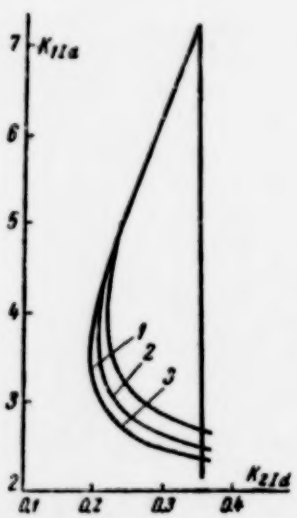

Fig. 3. Effect of the inertia constant of the receiving system on the region of stability:

$K_{01d}=2.5$; $\delta=60°$; $K_{TJ}=\frac{T_{syst.}}{T_{JS.C}}$.

1) $K_T=1$; 2) $K_T=3$; 3) $K_T=\infty$.

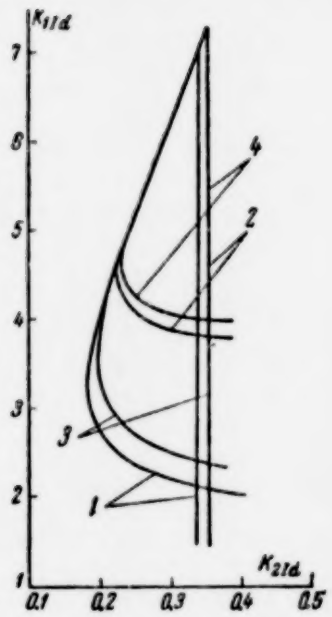

Fig. 4. Regions of stability in regulation of the excitation according to the deviation of the first and second derivatives of the direct axis current of the synchronous condenser ($K_{01d} = 25$):

1 - for a system with two synchronous condensers at $\delta = 45^{\circ}$; 2 - the same at $\delta = 60^{\circ}$; for the equivalent system with one synchronous condenser ($\delta_{eq} = 60^{\circ}$); 4 - the same with δ_{eq} 70°.

Line parameters: length of section 500 km; $x_0 = 0.223\ \Omega/km$; $b_0 = 4.94 \times 10^{-6}\ \frac{1}{\Omega}$ /km; nominal line voltage 650 kV

Parameters of synchronous condensers: $s_{s.c} = 1500$ MVA; $x_d = 2.384$; $x_q = 1.284$; $x'_d = 0.35$; $x_T = 0.12$; $T_{d0} = 10.2$ sec; $T_p = 0.05$ sec; $T_{Js.c} = 4.6$ sec.

Parameters of sending station: $P = 3000$ MW; $T_{Jst} = 12.4$ sec.

It is also assumed that the inertia constants of the sending and receiving stations are equal so that all the systems except 1 in Fig. 2 become symmetrical, which permits factorization of the characteristic equation and simplifies the plotting of the stable regions considerably.

Fig. 3 illustrates the effect of the inertia constant of a receiving station on the region of stability for a transmission line with one synchronous condenser. It will be seen from this diagram that the stable region is hardly altered by an increase in the inertia constant of the receiving station from the value of the inertia constant of the sending station to infinity. Hence the extra assumption made above involves no great error.

Figure 4 shows the limits of stability with excitation control of synchronous condensers with respect to the first and second derivatives of natural direct axis current. The limits are plotted for two modes of transmission using two synchronous condensers (i.e. angles $\delta = 45^{\circ}$ and $\delta = 60^{\circ}$) and for transmission with one synchronous condenser with the corresponding angles ($\delta_{eq} \approx 60^{\circ}$ and $\delta_{eq} \approx 70^{\circ}$) found from curves 1 and 2 in Fig. 1 on condition that $\Delta x_{max}/x$ is the same. Fig. 5 shows the regions of stability for systems 1 and 2 in Fig. 2, i.e. for the post fault conditions of coupled transmission with one and two synchronous condensers. In plotting the regions it was assumed that the impedance of all sections of the line was the same and that all the synchronous condensers had identical power and other parameters.

The good agreement between the regions of stability in Figs. 4 and 5 and the results of other calculations by the authors justify the conclusion that, as regards steady state stability limits, electrical transmission is similar with either one or two synchronous condensers provided.

$$\frac{\Delta x_{max}}{x} = \text{idem}, \tag{12}$$

and if the impedance of the line sections are the same and power and parameters of the synchronous condensers are the same.

The condition for identical line section impedances and identical condenser powers and parameters can be written in the form:

$$\frac{x_{d\,s.c}}{x} = \text{idem}. \tag{13}$$

The conclusion regarding the similarity of transmission with two

synchronous condensers and that with one condenser can also be extended to transmission with a larger number of intermediate substations, i.e. it can be said that, as regards the steady state stability limit, transmission with n synchronous condensers, with the transmitted power corresponding to the angle δ between the voltages at the ends of each section, is similar to transmission with one synchronous condenser, with the transmitted power corresponding to the equivalent angle δ, provided condition (13) is fulfilled. In other words, transmission with n synchronous condensers in a mode corresponding to the angle δ can be replaced, as far as the steady state stability limit is concerned, by transmission with one synchronous condenser having the same length of section and identical synchronous condenser power and which operates in a mode corresponding to the equivalent angle δ_{eq}.

YEAR 1961

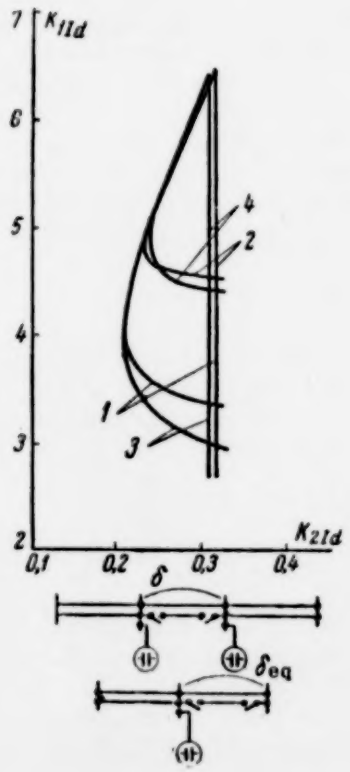

Fig. 5. The same as Fig. 4, but for two-circuit coupled transmission with interruption of one circuit on one section: 1, 2 – from the complete characteristic equation; 3, 4 – from the proposed simple method.

The equivalent angle for a transmission line with one synchronous condenser can be found from the curves in Figs. 1 and 2, provided condition (12) is satisfied, and from the known angle δ of transmission with n synchronous condensers. Further investigation of stability entails plotting the regions of stability for transmission with one synchronous condenser in coordinates of the amplification coefficients according to the derivatives of the parameter used to regulate the excitation. To plot the regions of stability, use may be made of the characteristic equation proposed by one of the authors of this article in a previous paper [2].

Translated by O.M. Blunn

REFERENCES

1. V.A. Venikov; *Transient electromechanical phenomena in electrical systems, (Elektromekhanicheskie perekhodnye protsessy v elektricheskikh sistemakh).* Gosenergoizdat (1958).
2. Chen' Shi-nyan'; *The parallel operation of synchronous condensers provided with automatic high response excitation control, (Parallel'naya rabota podpornykh sinkhronnykh kompensatorov, snabzhennykh ARV sil'nogo deistviya). Izv. vuzov MVO SSSR,* Energetika, No. 3 (1961).

ABSTRACTS FROM PAPERS PUBLISHED IN ELEKTRICHESTVO No. 9, 1961

YEAR 1961

Control engineering

Capacitor stabilization in amplidyne-type motor generator sets. D.A. Kaminskaia *et al.*, (pp. 78-82).

It is considered that the use of stabilizing transformers in amplidyne-type motor generator sets unduly complicates the system and it is proposed to use capacitor stabilizing devices instead. Tests on a large excavator have demonstrated the advantages of the new system.

The accurate performance of automatic control systems under steady state conditions. V.T. Bardachevskii *et al.*, (pp. 22-25).

A general formula is proposed for pre-determining the steady state error in the performance of automatic control systems under the effect of several different perturbing factors.

Costing

Certain aspects of costing in power engineering. A.V. Voronin, (pp. 63-66).

It is proposed to extend the existing soviet system of percentages to operating costs (including appropriations for capital repairs and renovation) and to dispense with the system of two-variant comparison for investment purposes, using estimates of annual outlay instead.

Induction pumps

The optimum dimensions of induction pumps for liquid metals. N.M. Okhremenko, (pp. 10-16).

A detailed mathematical study is made of the optimum geometric re-

lationships in the design of flat, spiral and cylindrical induction pumps from the point of view of maximum efficiency and minimum weight of active materials.

Insulation

Pre-breakdown phenomena in the insulation of high voltage electrical machines. B.D. Vakser *et al.*, (pp. 70-73).

An account is given of investigations into specific discharges which have been observed in mica plates prior to final breakdown. A study is made of the factors affecting the amplitude, duration and repetition rate of these discharges. The authors advocate using details of such partial breakdowns for control over insulation quality.

Power systems

Studying long line transients with phase trajectories of a non-linear load. R.I. Karaev, (pp. 26-29).

With a view to studying internal surges in long distance transmission, the author proposes a graphical-analytical method of studying transient phenomena in long lines, with non-linear loads included (transformers, chokes, arresters and so on). A differential equation is formed linking flux and current. After various transformations a family of phase trajectories is plotted in which each curve corresponds to a fixed value of a certain parameter, p.

Surge interference with carrier channels along transmission lines. G.V. Mikutskii, (pp. 51-57).

An account is given of the research which has been undertaken at the All-Union Electrical Energy Research Institute into the effect of atmospheric overvoltages, short-circuits and switching on carrier wires (communication channels) along high voltage transmission lines.

A method of determining the economic efficiency of hydro-electric stations. D.S. Stepanov, (pp. 74-78).

The official method of estimating the cost of hydro-electric stations is severely criticized.

Operating experience with telemechanical systems in the Moscow Power system. N.S. Shabalin (pp. 82-86).

A frank account is given of the problems and the type of remote control equipment in use in the Moscow Power System covering the despatcher control system, the high voltage network and the urban cable distribution system.

Relays and protection

Use of the Hall effect for a power directional relay. V.G. Doroguntsev, *et al.*, (pp. 57-63).

A study is made of the sensitivity of power directional relays based on the Hall effect. It is proposed to improve their sensitivity by reducing the variation in induction, the use of a.c. amplifiers and an instantaneous increase in the input power of the pickup, (Hall transducer).

YEAR 1961

Rotating machines

The effect of dissymmetry of the main pole m.m.f. on the compoles and machine characteristics. I.Z. Ageyev, (pp. 37-40).

It is shown that asymmetry of the m.m.f. of the main poles of 6 kW electric motors with $2p = 6/3$ adversely affects the commutation and operating characteristics of the machines, especially in machines with half the number of compoles and with the series and parallel windings on poles of opposite polarity. However, it is proposed to turn this effect to good advantage in generators with a wide range of speeds and a half number of compoles by placing parallel coils with 25 to 35 per cent more turns on poles of opposite polarity to the compoles, than those on poles of the same polarity as the compoles.

Economic losses and the dimensions of electrical machines and transformers, I.M. Postnikov, (pp. 2-9).

An attempt is made to establish the general principles to be followed in estimating electrical machines and transformers to achieve minimum factory and operating costs.

The maximum torque of electric motors for coal-cutters.
N.A. Kiklevich, (pp. 41-44).

Using electric motors of coal cutters by way of example, the author establishes more precise criteria for the maximum torque of motors supplied from low power networks as in coal-mines.

YEA
196

ABSTRACTS FROM PAPERS PUBLISHED IN ELEKTRICHESTVO No. 10, 1961

Editorial

The great programme for building communism. (pp. 1-5).

The article defines communism from the party programme and briefly considers the next twenty years of development. The role of the communist party is discussed along with the part to be played by science in forming the material-technical basis of communism.

YEAR
1961

Automatic control

Charging a capacitor from an a.c. circuit through a valve. S.M. Smirnov, (pp. 60-64).

A study is made of the process of charging a filter capacitor by sinusoidal voltage pulses. Cases of purely capacitive and capacitive-active loads of rectifiers connected in half-wave and full-wave rectifying systems are considered.

Transforming Grey's code into a binary code. V.A. Kougiis, (p. 74).

The direct use of Grey's parallel code for control devices in servo systems (e.g. for determining the angle of rotation of shafts) is not considered convenient in programme control systems based on potential logical elements. Accordingly a system of transforming Grey's code into a parallel binary code is suggested.

Control engineering

Fundamentals for constructing a standard series of automatic motor drives for multi-cable mine hoists. V.S. Tulin, (pp. 12-19).

A study is made of the regulations and standards governing mine

hoisting and lifting equipment with a view to forming a theoretical basis for standardization and greater efficiency in electrical drives.

An instrument for measuring active power. Ys.I. Stiop, (pp. 65-66).

A description is given of a device for measuring power in which the main part, squaring the sum and difference of the input quantities (current and voltage), uses tyrite elements as the non-linear resistors with a load resistance to adjust the volt-ampere characteristic.

A controllable d.c. drive. A.I. Ioffe, (pp. 71-73).

A study is made of a new variable d.c. drive with a simple converter. The drive is based on a typical d.c. motor with independent excitation with its speed controlled by varying the voltage applied to the armature from the converter. The converter consists of a three-phase transformer with primary secondary windings connected in star and connected to the a.c. network. The secondary windings have different numbers of turns so that the e.m.f. is different in each winding. Rectified voltages can be fed to several drive motors at different speeds.

Power systems

Appraising electric power costs in designing industrial plants. D.S. Stepanov, (pp. 6-11).

The estimation of the cost of electrical energy in planning industrial undertakings is considered in the light of socialist methods of planning without resort to existing tariffs.

How the post-breakdown voltage on the arrester depends on the current wavefront length. V.I. Pruzhinins-Granovsksis *et al.*, (pp. 53-54).

An account is given of investigations into the relationship between residual voltages and the length of the current wavefront for various "tervite" and vylite" resistors in soviet lightning arresters and combined lightning and surge arresters.

Discriminative ground fault signalling. V.V. Shut', (pp. 68-71).

A description is given of a recently developed device for selective indication of earth faults in compensated three-phase high-voltage networks. The device has passed tests in the Odessa power system.

It utilizes the transient currents which flow through the elements of the system at the instant an earth fault occurs.

Relays and protection

The behaviour of overcurrent relays during out-step conditions in a power system.

S.E. Stepurin, (pp. 55-60).

Investigations have confirmed that overcurrent relays may operate incorrectly during out-of-step conditions of the generators. It is proposed to overcome this by adjusting the reset time of the relay or using a voltage starting relay with a particular voltage setting. The method of analysis is also applicable to other types of voltage and current relay.

The relationship between the curie point and the composition of copper-zinc ferrites.

A.I. Andrievskii *et al.*, (pp. 66-68).

YEAR 1961

An account is given of investigations into copper-zinc ferrites of various compositions corresponding to values of the Curie point between the boiling point of liquid nitrogen and 460°C. The Curie points of the compositions were determined to within 4 to 6°C by the method described. Particular compositions are used for thermal relays which are also described.

Rectifiers

Calculating the parameters and characteristics of a semiconductor rectifier with saturated reactor control.

G.P. Mostkova et al., (pp. 38-46).

The authors propose a simple method of analysis to determine the parameters of the main equipment of semiconductor rectifiers controlled by saturable reactors (mainly the parameters of the reactor) and to construct the operating characteristics of the rectifier under different operating conditions.

Rotating machines

The maximum torque of coal-cutter induction motors connected in mine networks.

B.S. Traube, (pp. 19-23).

In order to ensure the necessary conditions for a highly efficient performance from coal-cutting combines, the author seeks to elucidate the maximum possibilities of mine networks by finding the

general laws which govern the variation of the actual torque of induction motors. Test results appear to confirm the theoretical propositions.

Locus diagrams for synchronous generator control devices with phase compounding. V.N. Breev *et al.*, (pp. 29-34).

The properties of the various control devices in the steady state excitation circuit of generators with phase compounding are described by a single diagram so that the effect of the parameters of individual circuit elements on the excitation current can be established and so that a preliminary selection can be made of requisite initial coefficients depending on the regulation and forcing of the excitation current.

A new way of mounting brushes in electrical machines. V.G. Gurin, (pp. 47-48).

An account is given of tests and calculations which indicate that the most efficient position of "reactive" brushes in electrical machines is that with "reverse inclination" (trailing brushes) at angles greater than 10 or 15° to the radial direction except when vibration is excessive.

The performance of a three-phase induction motor having an unequal number of turns in the stator phases. I.M. Kamen', (pp. 48-52).

General equations are formed for the analysis of the operating conditions of non-salient pole machines having a three phase winding with identical phase zones, but with different numbers of turns in the phases.

Traction

Contactless control of electric rolling stock. I.B. Bashuk *et al.*, (pp. 24-29).

A description is given of the authors' general-purpose systems of contactless electrical interlocking patented in 1957 and 1960. One system is a combination of a transistor and a "pick-up" whose output voltage is fed to the input to the triode. The moving core of the pick-up is mechanically linked with the apparatus to be controlled so that in one position the output voltage of the "pick-up" is zero and in another position it is sufficient to change the conducting triode into the saturated state. The triode accordingly plays the role of a normally closed or normally open blocking contact.

Various other systems are considered with diagrams.

Synchronous machine damper winding losses due to voltage time harmonics. Yu.A. Kulik, (pp. 34-37).

A study is made of the effect of voltage harmonics on the currents of the damper winding and the resultant losses. The distribution of the currents in the damper winding is analysed and the total losses caused by higher time harmonics are determined by the mean square value of the current in the cores of the damper winding.

YEAR
1961

YEA
196

CONTACTLESS CONTROL OF ELECTRIC COACHES*

I.B. BASHUK and A.I. KHOMENKO

(Moscow Institute of Railway Transport Engineers)

(Received 24 June 1961)

YEAR
1961

A disadvantage of electric drives controlled by relays and contactors is the unreliability of the contacts, due to their wear, oxidation, contamination etc. This disadvantage is particularly marked if the contacts are opened and closed with great frequency. It can however be overcome if contacts are completely eliminated from the control system. Until now this problem has only been solved by using magnetic amplifiers as relays. Yet these cannot always be used owing to the relatively large dimensions of the amplifiers.

The dimensions of control circuit elements can be considerably reduced for independent or group drives if the apparatus is "interlocked" by means of transistors which are controlled by electrical pickups (transducers) that produce output voltages as a function of the position of the control object.

Even the relays can be made quite small without contacts, and only small magnetic amplifiers are required for isolating the power circuit and control circuits and feeding the signals of trigger circuits to the transistors.

This allows the production of improved control systems for electric coaches based on principles which have not hitherto been used. The new units also improve the reliability and performance of a control system.

Electrical circuits can be switched on and off by transistors acting either as switches or as trigger circuits. Transistors can be controlled by signals from transducers without the use of contacts.

---

* *Elektrichestvo*, 10, 24-29, 1961.

In 1957 the authors of this paper patented [1] a contactless interlocking system which combined a transistor with a transducer. The rectified output voltage of the transducer was fed to the input to the transistor (see Fig. 1). The moving core of the transducer was mechanically coupled with the control object in such a way that in one working position the output voltage of the transducer was zero, whilst in the other position it was sufficient to change the "non-conducting" triode into the saturated state. The transistor switched the particular section of the control circuit "on" or "off" accordingly, and took the place of a normally closed or normally open blocking contact.

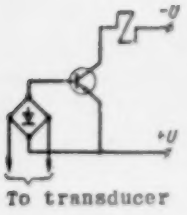

Fig. 1.

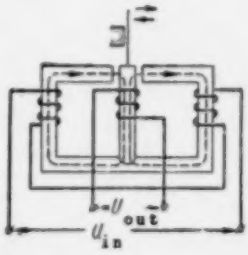

Fig. 2.

An alternative method is to use a trigger or "flip-flop" circuit to switch the circuit "on" and "off" by means of a signal from a transducer or some circuit element. Various types of design system are possible and these will now be considered.

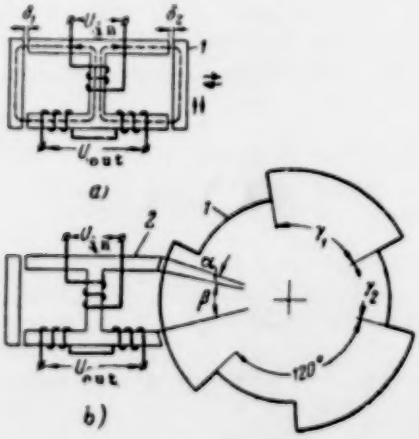

Fig. 3.

Different types of transducer can be used for controlling the transistor or trigger circuit. A differential inductive transducer is illustrated in Fig. 2. In the middle position of the moving core the resultant magnetic flux there is zero and the output voltage is likewise zero. A variable voltage is produced at the output of the transducer when the moving core deviates from its middle position. This transducer can be made highly sensitive so that the triode can be changed from "on" to "off" (or vice versa) by the core moving tenths of a millimetre.

Figure 3*a* illustrates the circuit of a transducer which produces a zero output voltage if the air gaps δ_1 and δ_2 are the same. If the core *1* is moved in any of the directions indicated in Fig. 3*a*, the two gaps cease to be equal and a voltage is then produced at the output of the transducer. The merit of this device is the absence of "hinges".

The transducers shown in Figs. 2 and 3*a* are convenient for controlling contactors. For apparatus with a group drive, use may be made of the recently patented transducer circuit shown in Fig. 3*b*. Here the moving core *1* is a shaped steel disc with projections. This disc is coupled to the camshaft of the apparatus [2]. If one of the projections is opposite the fixed core 2, the output voltage of the transducer is zero. But if one of the recesses is opposite this fixed core, a voltage is produced at the output of the transducer.

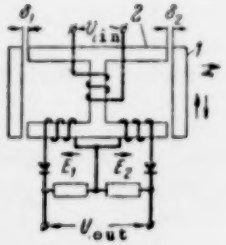

Fig. 5.

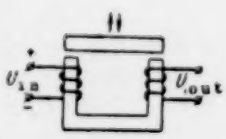

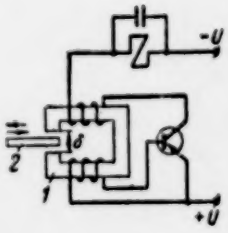

Fig. 6.

The number of projecting sections depends on the design of the group apparatus. The necessary relationship between the transducer output voltage and the angle of rotation of the disc (moving core) can be obtained by an appropriate choice of the angles α, β, γ_1 and γ_2.

If it is required to produce an output voltage which reverses polarity, use may be made of the device shown in Fig. 4. This is made so that δ_1 is greater than δ_2 if the moving core *1* is opposite the fixed core 2. The e.m.f. E_2 of the output winding then becomes greater than E_1 and the rectified output voltage is the same in polarity. The polarity of the output voltage is reversed when the e.m.f. E_2 decreases on movement

of core *1*.

An alternating input voltage can be obtained from a transistorized inverter for such transducers.

The device shown in Fig. 5 may be used to control a trigger circuit. Movement of the core produces a voltage pulse at the output. The polarity of this pulse depends on the direction in which the core moves. However, the amplitude of the output voltage of this particular device depends on the speed with which the core moves. If the control object changes position at a reduced speed for one reason or another, the trigger circuit cannot be "changed over".

Figure 6 illustrates the circuit of a device which generates relaxation oscillations provided that the gain feedback factor is positive and much greater than one. The core *1* is made from ferrite material. When disc 2, which is made of conducting material, enters the air gap δ, the oscillations are damped and the current in the load circuit is reduced to zero. Unfortunately it is a complicated matter to ensure sharply defined attenuation of the oscillations and to resume oscillations under all operating conditions.

The system of contactless interlocking shown in Fig. 1 (employing a P4-P-type transistor and the transducer illustrated in Fig. 2) has been tested on PK-301A-type electro-pneumatic contactors and PK-504-type electromagnetic contactors. From test results the switching time of the contactors was practically the same for conventional and contactless control circuits.

To protect the transistors from the surges which occur on opening the coil circuit of the contactor, the latter is shunted by a diode with a resistance in series with it. The diode tends to prolong the time between the initial decrease in the current in the contactor coil and the final complete opening of the contacts. It has, however, been established by tests that the total increase in time is very small, so that the use of this contactless interlocking system does not alter the operating conditions of the contactors.

However, the combined use of contactless interlocking and logical circuits "and", "or", etc provides all the relationships enjoyed in existing control systems.

It is obvious that contactless interlocking is advisable wherever existing electro-mechanical interlocking systems are unsatisfactory.

On suburban and Underground coaches the interlocking systems under the greatest strain are those controlling the drive of the rheostat controller which is the main apparatus controlling the starting of the

train.

Using the foregoing principles, the rheostat controller (with the existing acceleration relays) can be controlled by a transistorized contactless interlocking system. As regards trains using pneumatic drives, the use of transistors is facilitated in that the necessary currents for controlling the electro-pneumatic valves are only a fraction of an ampere and so are much less than the maximum permissible currents of such triodes as the P4 model. It can also be arranged that the effective voltage is within permissible limits.

The solution of the problem rests on the substitution of three appropriate contactless interlockings for the three blocking contacts which control the two valves of the controller and the "lift" coil of the acceleration relay. But this requires three inductance-type transducers. It is, however, possible to dispense with one of them if only one is used for controlling the trigger circuit (for switching the two valves of the controller), and one other for controlling the lift coil of the acceleration relay.

YEAR 1961

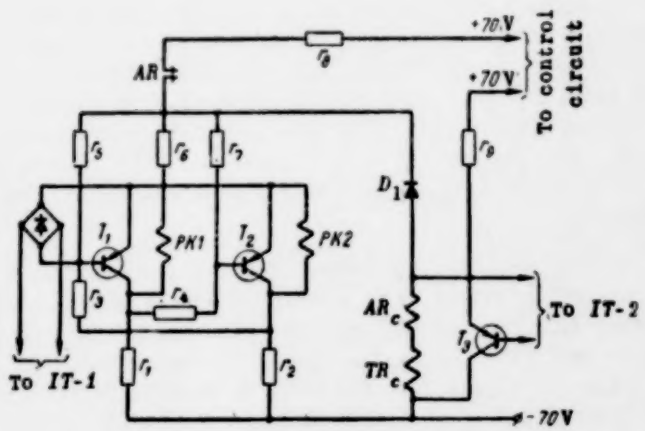

Fig. 7.

This method is illustrated in Fig. 7 in reference to electric coaches on the Underground. The trigger circuit, employing transistors T_1 and T_2, controls the alternate supply to the rheostat controller valves *PK1* and *PK2*. The trigger circuit is controlled by the inductance-type transducer *IT-1* which is similar to the system shown in Fig. 3*b*. When a projecting section of the disc comes to the core, the output voltage is reduced to zero and the triode T_1 is "off" whilst T_2 is "on", since the resistance r_5 is less than the resistance r_7. Therefore, when

the contacts of the acceleration relay *AR* are closed, the coil of *PK1* is disconnected and that of *PK2* is connected.

The output voltage of the other inductance-type transducer *IT-2* (see Fig. 4) is supplied to the triode T_3 and makes it "conducting" or, near certain positions, "fixed" of the controller. The lift coils of the acceleration relay AR_c and time relay TR_c are therefore short-circuited. Between certain "fixed" positions of the controller the output voltage of the transducer *IT-2* changes polarity so that triode T_3 is made "non-conducting" and the lift coils of the acceleration relay and time relay are therefore switched "on". In this case the trigger circuit and coil of one of the rheostat controller valves are supplied via resistance r_9 and diode D_1.

When the shaft of the controller reaches the next "fixed" position, there will be a disc recess opposite the fixed core of the transducer *IT-1* and not a projection, and the rectified output voltage of the transducer is applied to the emitter-base circuit of the triode T_1. This "changes over" the trigger circuit, disconnects the valve *PK1* and connects *PK2*.

This system of supply ensures the alternate connexion of the rheostat controller valves. Another important feature of this system is that it precludes the possibility of momentary interruptions in supply as well as that of simultaneous supply to the coils of both valves. However, in existing systems with pin and cam switches, either behaviour can occur and lock the rheostat controller shaft between positions owing to changes in the "scanning" of the valve switch because of the wear of the components.

Such a system (see Fig. 7), using a contactless switch for the rheostat controller valves, has been installed on three coaches of the Moscow Underground. These have been in use since October 1960. The control system features a comparatively high rated voltage (70 V) and voltage variation between 60 and 90 V. The maximum permissible voltage for the transistors is 50 to 60 V, but the reliability of the transistors is safeguarded by an appropriate choice of the resistances r_1, r_2, r_8 and r_9. The voltage across the transistors never exceeds 35 V even when the control circuit voltage is 90 V.

The disadvantage of this system (Fig. 7) is its high power consumption since the valves are disconnected by short-circuiting their coils. It is only advisable to use this type of system when the control-circuit voltage is much greater than the permissible transistor voltage.

The control-circuit voltage in suburban coaches is 50 V and its variation is much less than that of coaches on the Underground. Use may

therefore be made of the system illustrated in Fig. 8 for the rheostat controller valves of electric suburban coaches. It incorporates two differential transducers similar to the one shown in Fig. 4. The introduction of the controlling triode T_1 not only allows a considerable reduction in the dimensions and power of the transducer, but also reduces the current to zero in the valve coils when they are switched "off". This is impossible when using conventional triggers with loads connected in the collector circuits, owing to the presence of feedback resistance.

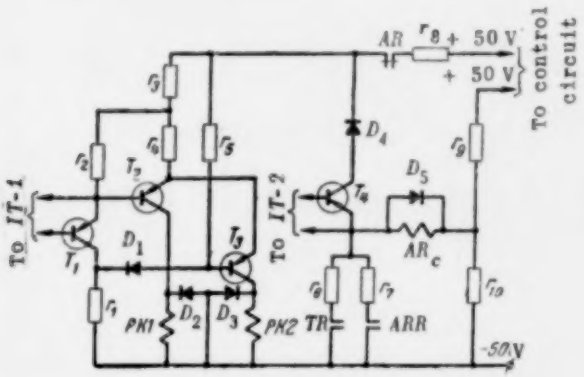

Fig. 8.

The lift coil of the acceleration relay is switched on by the triode T_4. This is controlled by the differential transducer IT-2. The supply of the acceleration relay lift coil and the coils of the two rheostat controller valves has been left the same as for control circuits of ER-1 type electric coaches. The system shown in Fig. 8 has been used for a contactless "valve" switch on one of the electric coaches of October Railways. It has been in operation since 1960.

It is known that sharply defined operation by electromagnetic acceleration relays depends to a great extent on the duration of the supply to the lift coil. This only takes about 0.05 sec. Such a short period of time for the coil to be under voltage is explained by the fact that voltage is only supplied to the coil after the camshaft of the rheostat controller has been partially revolved. Unless the relay armature is attracted during this time, the shaft of the rheostat controller jumps through the next "fixed" position. In principle this drawback can be overcome by using the system shown in Fig. 9*a* for supplying the lift coil.

Besides the main windings *1* and 2, auxiliary windings *3* and *4* are mounted on the magnetic circuits of the electro-pneumatic valves. An

impulse voltage is then produced in the windings in question whenever one of the valves is connected or disconnected. This voltage can be used for "changing over" the trigger circuit; as the result of a signal, triode T_1 is made "conducting" and the lift coil AR_c of the acceleration relay is switched "on". In this case the controlling triode T_3 is "off", since the output voltage of *IT*-2 (a device similar to that in Fig. 4) makes the base potential of this triode higher than the emitter

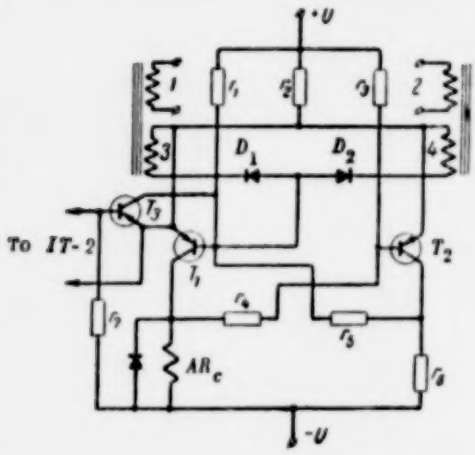

a)

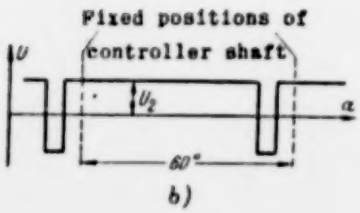

b)

Fig. 9.

potential. Figure 9b illustrates the relationship between the output voltage of *IT*-2 and the angle of rotation α of the rheostat controller shaft. This relationship can be produced by six projections and six recesses on the moving core of the transducer and an appropriate choice of the angles α, β, γ_1 and γ_2.

The lift coil of the acceleration relay is switched off slightly before the camshaft of the controller reaches a "fixed" position. The triode T_1 becomes "off" when the controlling triode T_3 becomes "on" at

the instant the output voltage of *IT-2* changes sign. The triode T_3 again becomes "off" when the controller shaft is in the fixed position.

If the system shown in Fig. 9*a* is used to control the lift coil of the acceleration relay, the valves can be switched by the circuit in Fig. 10*a*.

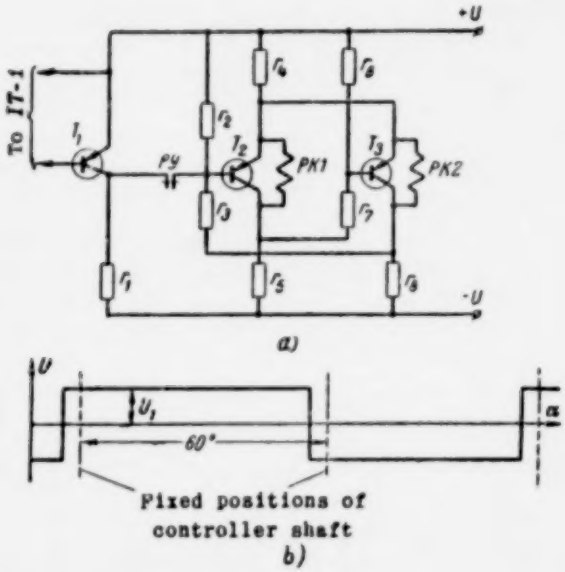

Fig. 10.

In the closed position of the acceleration relay contacts, the state of the trigger depends on the sign of the signal of the *IT-1* transducer (here the system shown in Fig. 4 is used). The relationship between the output voltage U_1 of this transducer and the angle α of the controller shaft is illustrated in Fig. 10*b*. On transition of the controller to the next "fixed" position, the acceleration relay contacts open, but the trigger still remains in the same state. This maintains the continuity of supply to the valve coils in the interim periods between "fixed" positions. For several degrees before the next position is reached, the sign of the transducer output voltage becomes such as to change over the trigger into the new state which sets in after the acceleration relay contacts close. The merit of this system is the absence of electrical coupling between the supply of the acceleration relay lift coil and the valve-switching circuit.

Transistorized contactless interlocking systems such as those

described above can also be used in two-position group apparatus such as reversers, brake switches, etc.

However, the relays of electric coach control systems can also be made without contacts. Here it is advisable to use a magnetic amplifier, the control winding of which receives a signal from the power circuit. The output of the magnetic amplifier can be connected to the transistor circuit which switches "on" a certain part of the control circuit when the control criterion deviates from the desired magnitude. For this purpose use may for instance be made of a trigger circuit with a controlling triode or other trigger circuit. The design of contactless relays allows the control and power circuits to be kept separate, ensures the necessary operating speed of the relays and reduces the power and dimensions of the magnetic amplifier, since it is only required for controlling the transistorized control circuit.

A contactless acceleration relay is illustrated in Fig. 11 (a minimum current relay). The relay consists of a differential magnetic amplifier *MA* which is made up of two conventional irreversible magnetic amplifiers *A1* and *A2*. The loads of the two amplifiers are the resistances r_1 and r_2.

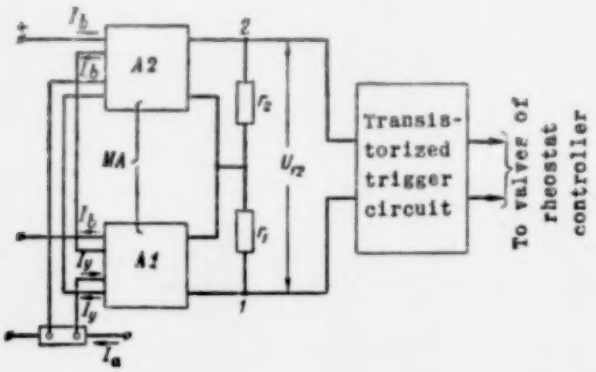

Fig. 11.

If the bias windings of the magnetic amplifier are connected to an external source, then its characteristic, which passes through the origin at zero bias, is shifted to the left by an amount which depends on the bias current. Thus, in the absence of a control signal, the voltage across r_1 and r_2 is proportional to the bias current. Its direction is such that the potential at point *1* (see Fig. 11) is positive and that at point *2* negative.

On supply of the control signal I_y, if the magnetic flux produced by it is in the opposite direction to that produced by the bias current in the respective cores, then the resulting voltage U_{12} is reduced at the output of the magnetic amplifier. If the two fluxes are equal, the resulting voltage U_{12} is zero and if I_y increases further the output voltage reverses polarity.

A transistorized trigger circuit can be made such that "changeover" takes place at zero input voltage. Then, if the current I_a in the armature of the traction motors is less than the current setting of the relay, the first triode of the circuit will be "off" and the circuit will be in a stable state. A reduction of the voltage at the input of the trigger circuit to zero, due to an increase in the control current I_y, results in an abrupt increase in the current at the output of the circuit.

The magnetic amplifier of such an acceleration relay has been made with permalloy cores 7 × 20 × 28 mm. The re-setting ratio was 0.99. The variation of the relay setting was ± 2 per cent of nominal values in the presence of variations ± 10 per cent in the supply voltage at an ambient temperature of 50° C; at an ambient temperature of 20° C the relay setting variation was + 3 to − 0.8 per cent of nominal values. Variations within these limits are no greater than those occurring on existing electromagnetic acceleration relays. The proposed acceleration relay has been made insensitive to variation of the supply voltage by the use of a balance circuit which maintains the voltage difference across r_1 and r_2 constant.

The relay setting is regulated by varying the bias current, but since the relay operates when the m.m.f.'s in the bias and control windings are equal, the operating point of the amplifier remains unchanged when the setting is adjusted. The relay setting can be regulated automatically by providing the relay with several control windings which alter its setting when the load varies or slipping occurs, etc.

From tests on an electronic simulator for a coefficient of non-uniform starting K = ± 10 per cent, a supply frequency of 400 c/s and adequate acceleration time, the operating time of the relay is about 0.03 to 0.05 sec.

The use of contactless acceleration relays in conjunction with contactless valve switches similar to that in Fig. 10 simplifies the whole system of control over the rheostat controller, since only one transducer is required.

The same principle can also be used to produce maximum current

relays such as overload relays and contactless maximum and minimum voltage relays.

In conclusion, it should be noted that the foregoing contactless control circuits and relays can also be used throughout industry in electric drive control systems, particularly when the gear has to be switched on and off with great frequency.

Translated by O.M. Blunn

REFERENCES

1. I.B. Bashuk and A.I. Khomenko; Auth. Cert. No. 113113, dated 12 September 1957.

2. I.B. Bashuk and A.I. Khomenko; Auth. Cert. No. 137136, dated 5 April 1960.

YEA
196

THE DESIGN OF REACTOR-CONTROLLED SEMICONDUCTOR RECTIFIERS*

G.P. MOSTKOVA and F.I. KOVALEV

(Krzhighansk Electrical Engineering Institute)

(Received 2 June 1961)

YEAR 1961

There is now a need for a simple and accurate method of designing reactor-controlled semiconductor rectifiers in view of the growing demand for this type of equipment. The design problem is two-fold in that attention must be paid to the system of reactor control as well as to the performance of the rectifier.

One of the most promising reactor-controlled three-phase bridge rectifiers in illustrated in Fig. 1. It has satisfactory operating characteristics, and the reactors meet requirements as regards minimum control power, weight and size [1.3].

It must however be borne in mind that the modes of operation of *reactor-controlled* rectifiers (RC rectifiers) depend on the condition of reactor magnetization and not on the number of alternately conducting "valves", as is the case with *conventional* rectifiers with "controlled" valves. The following four modes of operation can be distinguished at loads for which the duration of actual commutation γ does not exceed 60°:

1. The next valve (rectifier) is triggered at the instant the e.m.f.'s of the two phases become equal. From this instant onwards the reactor is re-magnetized. Its main winding is connected in series with the "conducting" valve. In the interval ωt from 0 to α the induction of the reactor varies from B_0, which depends on the magnitude of the magnetizing current, to the saturation induction B_s. The start of actual commutation of the operating current is delayed by the angle α which is equal to the duration of the period of reactor re-magnetization. The

* *Elektrichestvo*, 10, 38-46, 1961.

rectified voltage is similar in shape to that of conventional rectifiers with the control angle α. The first mode of operation is characteristic of loads for which $\alpha + \gamma = 60°$.

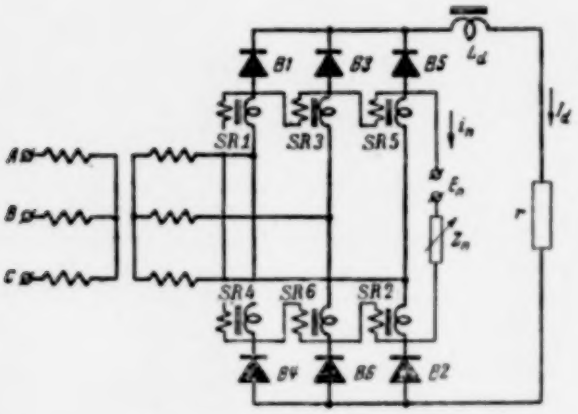

Fig. 1. Main circuit of a reactor-controlled three-phase bridge rectifier:

SR1 – SR6 – saturable reactors;
B1 – B6 – silicon rectifiers;
I_d – load current.

2. The triggering of the next valve is retarded by the angle α_0. The magnitude of this angle depends on the load current. With increasing rectified current the angle α_0 increases from zero to a certain angle α_0^* depending on the time constant of the particular rectifier. The reactor is re-magnetized in the period α_0 to α', where α' is the actual control angle of the rectifier. Under these conditions α' is greater than the duration of reactor re-magnetization and greater than α.

This second mode of operation changes into the third or fourth modes of operation at loads for which α_0 attains particular values, i.e. the third mode sets in when $\alpha_0 = \alpha_0^*$ and $\alpha' + \gamma = 60 + \alpha_0^*$, whereas the fourth mode sets in when $\alpha_0 = \alpha_0^{(k)}$.

3. The triggering of the valves takes place with an angle of lag α_0^* which is independent of the load current. In this mode of operation the control angle α' exceeds the angle α and the duration of reactor re-magnetization. The boundaries of the third mode are: $\gamma < 60°$ and $\alpha' < \alpha'_{k3}$.

4. The next valve is triggered at the instant $\omega t = 0$. The

TABLE 1

Mode	Formulae for α' and α_0	Mode boundaries	Formulae for limiting angles
1	$\cos\alpha' = \cos\alpha$	$(\alpha' + \gamma)_{12} = 60°$	
2	$\cos\alpha' = \sin(30° - \alpha_0) + \frac{2I_d x_\Sigma}{E_{max}}$; $\sin(30° + \alpha_0) = 1 - \cos\alpha + \frac{2I_d x_\Sigma}{E_{max}}$	$(\alpha' + \gamma)_{23} = 60° + \alpha_0^*$ $(\alpha_0)_{24} = \alpha_0^{(k)}$	$\cot\alpha_0^* = \frac{4x_\Sigma - x'_p}{\sqrt{3}x'_p}$ $\cos\alpha_0^{(k)} = \frac{(2-A)(1-A\cos\alpha) \pm \sqrt{3A[(A^2-A+1)-(1-A\cos\alpha)^2]}}{2(A^2-A+1)}$, where $A = \frac{x'_p}{2x_\Sigma + x'_p}$.
3	$\cos\alpha' = \frac{2x_\Sigma}{2x_\Sigma - x'_p}(\cos\alpha_0^* - 1 + \cos\alpha) - \frac{x'_p}{2x_\Sigma - x'_p}\left[\cos(60° + \alpha_0^*) + \frac{2I_d x_\Sigma}{E_{max}}\right]$	$\gamma_{35} = 60°$ $(\alpha')_{34} = \alpha'_{k3}$	$\cos\alpha'_{k3} = \frac{2x'_\Sigma}{x'_p}(1 - \cos\alpha_0^*) + \cos(60° + \alpha_0^*)$
4	$\cos\alpha' = \cos\alpha - \frac{x'_p}{x_\Sigma}\frac{I_d x_\Sigma}{E_{max}}$		$\cos\alpha_{k2} = \left(1 + \frac{2x_\Sigma}{x'_p}\right) - \sqrt{1 + \frac{2x_\Sigma}{x'_p} + \left(\frac{2x_\Sigma}{x'_p}\right)^2}$

N.B. The commutation equation $\cos\alpha' - \cos(\alpha' + \gamma) = 2I_d x_\Sigma / E_{max}$ and the equation $1 - \cos\alpha = Q w_a \omega_s 10^{-8} / E_{max}$ hold for all modes of operation.

TABLE 2

Mode	Equation of sections of operating characteristic	Mode boundaries
1	$U_d^* = \cos\alpha - \frac{I_d x_\Sigma}{E_{max}}$	1—2 modes $U_d^* = \frac{1}{2} + \frac{I_d x_\Sigma}{E_{max}}$
2	$U_d^* = \sin(30° - \alpha_0) + \frac{I_d x_\Sigma}{E_{max}}$, $\sin(30° + \alpha_0) = 1 - \cos\alpha + 2\frac{I_d x_\Sigma}{E_{max}}$	2—3 modes $U_d^* = \cos(60° + \alpha_0^*) + \frac{I_d x_\Sigma}{E_{max}}$
3	$U_d^* = \frac{2x_\Sigma}{2x_\Sigma - x'_p}\cos\alpha - \frac{2x_\Sigma + x'_p}{2x_\Sigma - x'_p}\cdot\frac{I_d x_\Sigma}{E_{max}} - \frac{x'_p}{2x_\Sigma}\cos\alpha'_{k3}$	3—4 modes $U_d^* = \cos\alpha'_{k3} - \frac{I_d x_\Sigma}{E_{max}}$
4	$U_d^* = \cos\alpha - \frac{x_\Sigma + x'_p}{x_\Sigma}\cdot\frac{I_d x_\Sigma}{E_{max}}$	2—4 modes $U_d^* = \sin(30° - \alpha_0^{(k)}) + \frac{I_d x_\Sigma}{E_{max}}$; $\sin(30° + \alpha_0^{(k)}) = 1 - \cos\alpha + \frac{2I_d x_\Sigma}{E_{max}}$

N.B. 1. At large loads ($\gamma > 60°$) modes of operation occur with double "overlaps" (5th mode) which are not considered in this paper. The boundary between the third and fifth modes is represented by the arc of an ellipse and described by the equation $[(2/\sqrt{3})U^*]^2 + [(2x_\Sigma/E_{max})I_d]^2 = 1$.

2. The angles $\alpha_0^{(k)}$, α_0^* and α'_{k3} and found by the formulae in Table 1.

YEA
196

re-magnetization of the reactor takes place by a linear voltage, but the reactor voltage decreases in the interval of actual commutation of the valve in the opposite arm of the phase in question. Re-magnetization is therefore prolonged. The control angle α' is equal to the duration of reactor re-magnetization, but greater than α.

A detailed analysis of the modes of operation of reactor-controlled rectifiers (with "non-controlled" valves and non-linear anode inductances) has already been published in Russian [1]. The main formulae for each mode of operation are reproduced in Table 1. Reference should also be made to the comprehensive glossary of notation at the end of the paper.

These formulae were derived on the following assumptions. The self-capacitances and resistances of the circuit were ignored. It was assumed that the characteristics of the individual rectifiers were ideal and that the rectified current was ideally smooth. The inductance of the reactor on re-magnetization was assumed to be slightly greater than the leakage inductance of the transformer. The current in the main winding of the reactor on re-magnetization was regarded as negligible compared with the mean value of the rectified current. Finally it was assumed that no ripple occurred in the current in the reactor magnetization windings.

YEAR 1961

Rectifier performance

The main operating characteristic of a rectifier is that which represents the mean value of the rectified voltage as a function of the mean rectified current at a given control current.

An analysis has already been made of electromagnetic phenomena in reactor-controlled rectifiers. It was found that the equation for the relationship between the mean value of the rectified voltage on the one hand and the control and actual commutation angles on the other is exactly the same for reactor-controlled rectifiers as for conventional rectifiers:

$$U_d = U_{d0} \frac{\cos \alpha' + \cos (\alpha' + \gamma)}{2} . \qquad (1)$$

Since the commutation equation is the same for all modes of operation (see Table 1), equation (1) can be written in the form

$$U_d = \cos \alpha' - \frac{I_d X_\Sigma}{E_{max}} , \qquad (2)$$

where

$$U_d^* = \frac{U_d}{U_{d0}}.$$

Substituting in (2) the values $\cos \alpha' = f(B_0, I_d)$ or $\cos \alpha' = f(\alpha, I_d)$ from Table 1, it is possible to form equations for individual sections of an operating characteristic corresponding to the various modes of operation (see Table 2).

Each of these modes of operation is possible over a particular range of values of the load current and angle α, i.e. there is a corresponding section of the characteristic $U^*_d = f(I_d)$ for each mode of operation.

Figure 2 shows the operating characteristics and mode boundaries as calculated by the formulae in Table 2. Each curve corresponds to a particular initial value of B_0.

For illustrative purposes and in order to compare RC rectifiers with conventional systems, the corresponding angles α of B_0 are plotted instead of B_0.

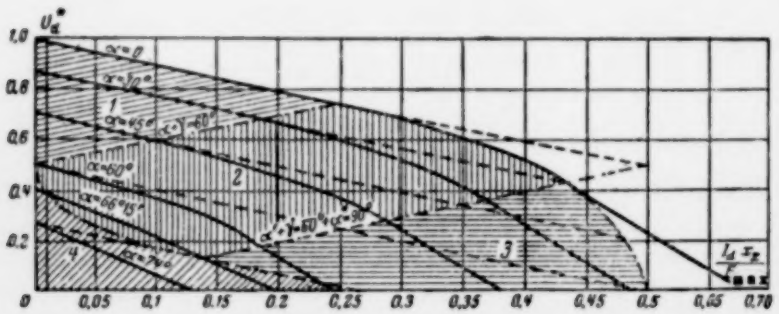

Fig. 2. The operating characteristics of a rectifier for $x'_p/x_\Sigma = 1$ (continuous line) and $x'_p/x_\Sigma = 0$ (broken line); (-.-.-.- mode boundaries).

It will be seen from Table 2 and Fig. 2 that the rectified voltage can be regulated within wide limits in RC rectifiers by varying the magnetization current. Here the shape of the curves depends to a considerable extent on the relationship between the reactances of the valve and phase circuits. If the phase reactance x'_p is much less than the "valve" reactance x_r (see glossary at end of the paper), the characteristics of RC rectifiers will be the same as those of conventional

rectifiers. If $x'_p \gg x_r$, this will only be the case in the first mode of operation (i.e. when $\alpha + \gamma < 60°$). In the other modes of operation (with large load currents and a large degree of control of the rectified voltage) there will be a marked difference in the characteristics of the rectifiers.

These formulae have been checked by tests on silicon rectifiers and saturable reactors with toroidal cores of permalloy-type material. The calculations and tests were both made for $x'_p/x_\Sigma = 0.905$. A smoothing inductance was included in the load circuit.

The calculated curves and test results are shown in Fig. 3. It will be seen that quite good agreement is obtained. The error is within 15 per cent as regards the voltage. Similar results were obtained for reactors with magnetic circuits made from cold-rolled steel.

YEAR
1961

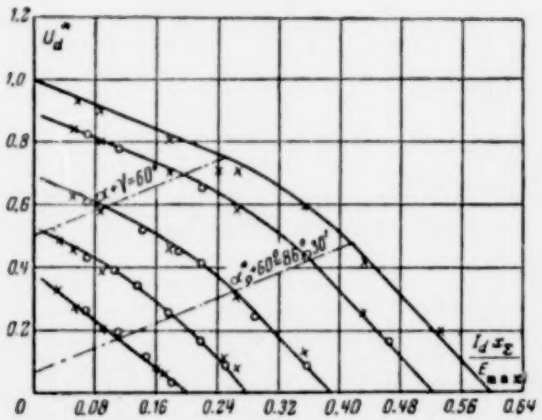

Fig. 3. Operating characteristics of a silicon rectifier: ——— - calculated characteristics; × - experimentally determined points (rectified current smoothed); ° - experimentally determined points on active load).

The proposed formulae can also be used for the design of large three-phase rectifiers with active loads. Figure 3 shows that the error is still of the same order even with a smoothing inductance in the load circuit. However, it is the purpose of this paper to consider the performance of the equipment under conditions of forced reactor magnetization, i.e. when the current harmonics of the magnetization circuit are suppressed. But even if no large resistance is present in the control circuit, only multiples of the sixth harmonic can occur there, and therefore the rectifier in practice operates as if even harmonics were

suppressed [4]. Consequently, the proposed formulae are equally applicable to cases when the resistance in the magnetization circuit is small. Tests have confirmed that the only error occurs in the third mode of operation (i.e. on overload) when the slope of the actual characteristics is less than that obtained by the calculations.

The control characteristic

The control characteristic represents the relationship between the mean value of the rectified current (or output voltage of the rectifier) and the magnetization current for a given load impedance.

The equation of the control characteristic is obtained by substituting $I_d r/U_{d0}$ for U^*_d in formula (2)

$$I^*_d = -\frac{r}{r + \frac{3}{\pi} x_\Sigma} \cos \alpha', \tag{3}$$

where

$$I^*_d = \frac{I_d}{I_{d0}}; \qquad I_{d0} = \frac{U_{d0}}{r}.$$

The equation of the control characteristic for each mode of operation is formed by substituting the appropriate value of cos α' in equation (3) (see Table 3).

The value of cos α depends on the initial induction B in the cores of the reactor and therefore depends on the magnetization current.

This relationship can be found graphically by defining various values of the magnetization current and using the hysteresis loop and the equation $\cos \alpha = (1 - Qw_1\omega/E_{max} \times 10^8)(B_s - B_0)$. The control characteristics are then plotted from the formulae in Table 3.

But if the hysteresis loop of the core material can be represented approximately by short straight-line sections, the magnetization current can easily be expressed analytically:

$$B_s - B_0 = \frac{\Delta B_{max}}{2(1+\nu)}[\nu - (2+\nu) I_m].$$

The coefficient $\nu = H_k/|H_c|$ defines the intensity of the magnetic field corresponding to the bend in the hysteresis loop. Thus, for a linear approximation of the hysteresis loop, the formula for cos α takes the form

$$\cos\alpha = 1 - \frac{k}{2(1+\nu)}[\nu - (2+\nu)I_d^*],$$

where

$$k = \frac{Q\omega_p\omega}{E_{max}\cdot 10^8}\Delta B_{max}.$$

Analytical expressions are then found for the sections of the control characteristic corresponding to the different modes of operation by substituting the expression $\cos\alpha = f(I_d^*)$ in the formulae in column 1 of Table 3. The equations in column 2 are the result. The third column shows the relative values of the load currents at which one mode of operation changes into another.

It will be seen from the curves in Fig. 4 (rectifier operating characteristics and load lines for limiting resistances at rectifier output) that the control characteristics do not always pass successively through all four modes of operation. The sequence depends on the load resistance and the design of rectifier. The limiting loads are calculated as the ratio of the output voltage to the current at particular points on the boundaries between modes.

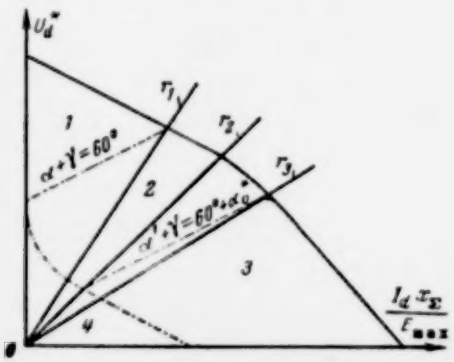

Fig. 4. The domain of the rectifier operating characteristics.

Figure 5 illustrates the formulae in Table 3 by a number of calculated control characteristics. The curves are plotted for $x_p/x_\Sigma = 1$ and a linear approximation of the hysteresis loop ($\nu = -0.5$).

Figure 6 shows the calculated control characteristics of the rectifying system in Fig. 1. The continuous curves have been plotted by the graphical-analytical method from the actual hysteresis loop of the core

TABLE 3

Mode	Equations of the sections of control characteristics		Value of currents at mode boundaries
	In general form	For linear approximation of hysteresis loop	
1	$I_d^* = \frac{r}{r - \frac{3}{\pi} x_\Sigma} \cos\alpha$	$I_d^* = \frac{r}{r + \frac{3}{\pi} x_\Sigma} \times$ $\times \left\{1 - \frac{k}{2(1+\nu)} [-I_d^*(2+\nu) + \nu]\right\}$	$(I_d^*)_{12} = \frac{1}{2} \cdot \frac{r}{r - \frac{3}{\pi} x_\Sigma}$
2	$I_d^* = \frac{r}{r - \frac{3}{\pi} x_\Sigma} \sin(30° - \alpha_0)$ $\sin(30° + \alpha_0 - \varphi) =$ $= \frac{1 - \frac{3x_\Sigma}{\pi r}}{\sqrt{1 + 3\left(\frac{3x_\Sigma}{\pi r}\right)^2}} (1 - \cos\alpha)$	$I_d^* = \frac{r}{r - \frac{3}{\pi} x_\Sigma} \sin(30° - \alpha_0);$ $\frac{k}{2(1+\nu)} [-I_d^*(2+\nu) + \nu] =$ $= \frac{\sqrt{1 + 3\left(\frac{3}{\pi} \cdot \frac{x_\Sigma}{r}\right)^2}}{1 - \frac{3}{\pi} \cdot \frac{x_\Sigma}{r}} \sin(30° + \alpha_0 - \varphi)$	$(I_d^*)_{23} = \frac{r}{r - \frac{3}{\pi} x_\Sigma} \times$ $\times \sin(30° - \alpha_0^*)$
	$\tan\varphi = \frac{3\sqrt{3}}{\pi} \cdot \frac{x_\Sigma}{r}$		$(I_d^*)_{24} = \frac{r}{r - \frac{3}{\pi} x_\Sigma} \times$ $\times \sin(30° - \alpha_0^{(k)})$

3	$I_d^* = \frac{r}{r\left(1-\frac{x'_p}{2x_\Sigma}\right)+\frac{3}{\pi}\left(x_\Sigma+\frac{1}{2}x'_p\right)} \times \left[\cos\alpha - \frac{x'_p}{2x_\Sigma}\cos\alpha'_{k3}\right]$	$I_d^* = \frac{r}{r\left(1-\frac{x'_p}{2x_\Sigma}\right)+\frac{3}{\pi}\left(\frac{2x_\Sigma+x'_p}{2}\right)} \times \left\{1-\frac{x'_p}{2x_\Sigma}\cos\alpha'_{k3} - \frac{k}{2(1+\nu)} \times [-I_a^*(2+\nu)+\nu]\right\}$	$(I_d^*)_{24} = \frac{r}{r+\frac{3}{\pi}x_\Sigma} \times \cos\alpha'_{k3}$
4	$I_d^* = \frac{r}{r+\frac{3}{\pi}(x_\Sigma+x'_p)}\cos\alpha.$	$I_d^* = \frac{r}{r+\frac{3}{\pi}(x_\Sigma+x'_p)} \times \left\{1-\frac{k}{2(2+\nu)}[-I_a^*(2+\nu)+\nu]\right\}$	

N.B. In determining $(I_d^*)_{24}$, the angle $\alpha_0^{(k)}$ should be calculated by the formula

$$\sin(x-\alpha_0^{(k)}) = \frac{1}{\sqrt{1+B+B^2}}, \text{ where } x = \arctan\frac{2+B}{\sqrt{3}B} \text{ and } B = \frac{\frac{3}{\pi}x'_p}{r-\frac{3}{\pi}x_\Sigma}.$$

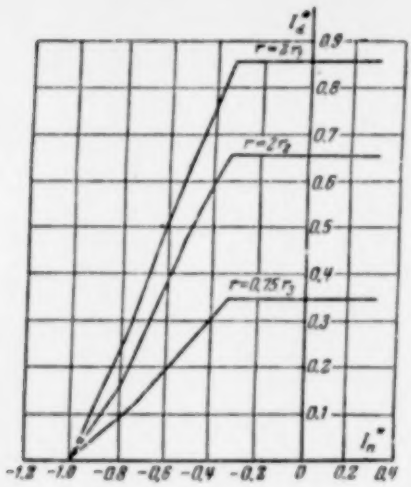

Fig. 5. The control characteristics of the rectifier.

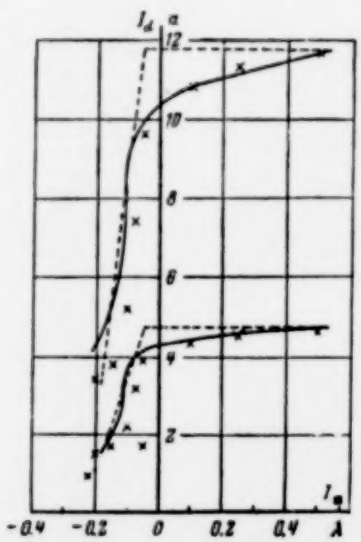

Fig. 6. Control characteristics of a silicon rectifier: - - - - calculated curves with linear approximation of the hysteresis loop of the reactor cores; ———— - characteristics plotted by a graphical analytical method from the actual hysteresis loop; × - test points (the upper ones correspond to $r = 10\ \Omega$ and the lower ones to $r = 50\ \Omega$).

materials. The broken curves are from the expressions in Table 3 using the linear approximation of the hysteresis loop. Experimentally-determined points are also marked on the diagram. The discrepancies are due to the use of the maximum dynamic hysteresis loop in the calculations. In fact, the re-magnetization of saturable reactors follows special loops which are narrower than the maximum loops, so that the calculated values of the control current are higher than those found experimentally.

The minimum load current

In analysing the various modes of operation and plotting the operating characteristics it was assumed that the current in the operating windings of the reactors on re-magnetization was zero. But, in fact, currents do flow in these windings, and their magnitude depends mainly on the slope and width of the dynamic hysteresis loop. Since the reactor cores are made from high-quality materials with practically ideal magnetization curves, it follows that these currents are small and have a negligible effect if the load current is greater than a certain minimum value $I_{d.min}$. But if the load current I_d is less than $I_{d.min}$, the electromagnetic phenomena and shape of the operating characteristics are affected accordingly. The loads for which $0 < I_d < I_{d.min}$ (see the thin vertical line in Fig. 2 [sic]) are non-operational.

To determine the magnitude of $I_{d.min}$ it is necessary to consider the performance of the rectifier for $r = 0$. In this mode of operation the current through the load only depends on the reactor re-magnetization currents. It will be seen from the curves in Fig. 7 that in this case the six rectifiers have a constant mode of operation. The rectified current is therefore equal to the sum of the currents in the operating windings of the three reactors in one arm of the bridge. The magnetization of one of the reactors (e.g. SR1) is finished at the instant $\omega t = \alpha$. Partial magnetization of the reactor (SR3) in the next phase of the same arm is "completed" at the same time [1]. Since a mode of operation is under consideration with the rectifier completely regulated and $r = 0$, the magnetization of the reactor (SR5) of the preceding phase begins at the instant $\omega t = \alpha$. The magnetic states of the reactors at the instant under consideration have been marked on the hysteresis loop in Fig. 7. (The various reactors SR1 to SR6 are indicated by subscripts 1 - 6 in the notation for the magnetizing currents):

$$i_{\mu 1} = (2 + \nu) I_c;$$

$$i_{\mu 3} = [1 + (1 - \sqrt{3})(1 + \nu)] I_c;$$

$$i_{\mu 5} = \nu I_c.$$

where

$$I_c = \frac{H_c l_\mu}{1.25 w_z}.$$

Reference should be made to the glossary of notation at the end of the paper for other symbols.

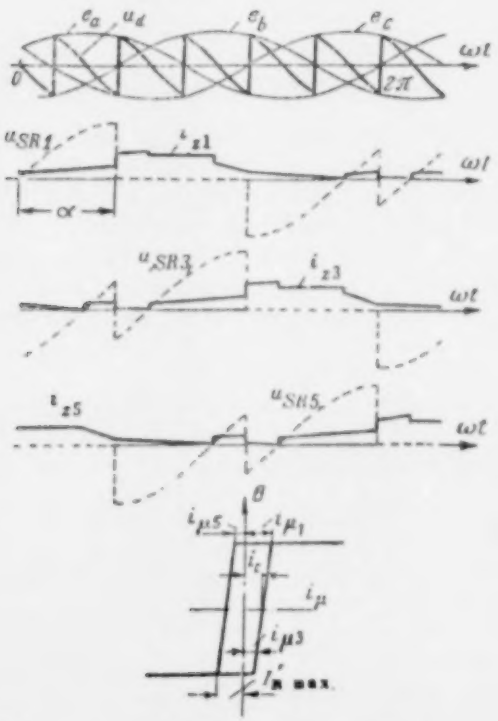

Fig. 7. The rectified voltage, the currents in the operating windings of the reactors, the voltages on the reactors and the hysteresis loop of the reactor cores for $r = 0$.

The current in the operating winding of the reactor is

$$i_z = i_\mu - \frac{w_m}{w_z} I_m.$$

The minimum rectified current $I_{d.min}$ is then found by adding the currents in the operating windings of the three saturable reactors in one arm of the bridge (i.e. SR1, SR3 and SR5):

$$I_{d\,min} = i_{z1} + i_{z3} + i_{z5} = i_{\mu 1} + i_{\mu 3} + i_{\mu 5} - 3\frac{w_a}{w_z} I_a.$$

It is obvious that for a completely regulated rectifier

$$I_a = -\frac{w_z}{w_a}(2 + \nu) I_c.$$

By definition

$$I_{d\,min} = 8.27(1 + 0.52\nu) I_c = 6.6(1 + 0.52\nu)\frac{l_\mu}{w_z} H_c. \qquad (4)$$

The minimum rectified current of large rectifiers is about 2 to 6 per cent of its rated value*.

YEAR 1961

Design of the reactors

The voltage drop on re-magnetization of the reactors depends on the value of ΔB_{max} in the cores, the number of turns in the operating windings and the cross section of the core. The degree of regulation of the rectified voltage likewise depends on these factors. Knowledge of the relationship between the maximum degree of regulation and the voltage on each reactor is necessary for design purposes. Strictly speaking, this relationship can be found if the modes of operation of the rectifier covered by the "domain of regulation" (see Fig. 8) are known. But this implies that the operating characteristics of the rectifier are known, whereas they can only be constructed from the design of the reactor. The problem of reactor design can, however, be solved with sufficient accuracy for practical purposes if it is assumed that all the operating characteristics are a set of straight lines within the control domain described by the equation $U_d = U_{d0} \cos \alpha - 3/\pi \, x_\Sigma I_d$. The operating characteristics are obviously straight lines described by this equation if the control domain only covers the first mode of operation and if $x_r \gg x'_p$. However, if x_r is commensurate with x'_p and the control domain covers other modes of operation besides the first, then the stated assumption slightly over-states the reactor criteria. The error can, however, be adjusted later in the calculations.

The formula for the rectified voltage is obtained by the expression which links the control angle with changes in induction $\Delta B = B_g - B_0$:

---

* When operating into an active load $I_{d.min}$ is slightly less.

$$U_d = U_{d0} - \frac{3}{\pi} Q\omega_{\text{ш}} \omega \Delta B \cdot 10^{-8} - \frac{3}{\pi} I_d x_{\text{ш}} = \\ = U_{d0} + \Delta U_{d\text{a}} - \Delta U_{d\text{г}}, \quad (5)$$

Hence it follows that the variation of the voltage at the output of the rectifier $\Delta U_d = U_{d0} - U_d$ depends on the voltage drop in the reactor $\Delta U_{d\text{a}}$ and the commutation voltage drop $\Delta U_{d\gamma}$. The quantity $\Delta U_{d\text{a}}$ represents the degree of regulation of the rectified voltage. The variation of induction is a maximum if the degree of regulation is also a maximum. The formula for $Q\omega$ then takes the form

$$Q\omega_{\text{ш}} = \frac{\pi}{3} \cdot \frac{(\Delta U_{d\text{a}})_{\max} \cdot 10^8}{\omega \Delta B_{\max}}. \quad (6)$$

This expression is the main formula for designing the reactor according to the desired degree of regulation of the rectified voltage.

The quantity $\Delta B_{\max}$ depends on the quality of the core material and the construction of the core. The best magnetic properties are possessed most consistently by "interleaved" solid cores with "strengthened" yokes which have been [literally in the Russian] "charged in the well"• [5]. It is advisable to select the operational range of variation of the induction of the reactor in large rectifiers so as to make full use of the hysteresis loop. This makes for the highest possible power factor. But the increase in $\Delta B_{\max}$ is restricted by the requirement of minimum control power. Quite good results can be obtained by taking $\Delta B_{\max} = 2B_k$, where B_k is the induction at the intersection of the descending and ascending portions of the dynamic hysteresis loop. In this case $\Delta B_{\max}$ is about 30,000 to 32,000 G for grade E-330 cold-rolled electrical steel.

The maximum degree of regulation which the reactors must ensure is sometimes known beforehand. This quantity is then entered in formula (6). If however the rectifier has to meet requirements regarding the stability of the output voltage or current under varying load or supply voltage conditions, or if particular operating characteristics are required, the value of $(\Delta U_{d\text{a}})_{\max}$ can then be calculated by the formula (see Fig. 8)

$$(\Delta U_{d\text{a}})_{\max} = (U_{d0})_{+\Delta U_c} - U_{d\min} - \\ - \frac{e_{\text{кз}}\%}{100} \cdot \frac{I_{d\min}}{I_{d\text{ ном}}} U_{d\text{ ном}}. \quad (7)$$

• Possibly a reference to annealing in a soaking pit.

The quantity $e_{k\Sigma}$ % has to be estimated first, and its value checked later after analysis and rough drawings have been made. If necessary, the reactor must be designed for a new value of $e_{k\Sigma}$ %.
cent.

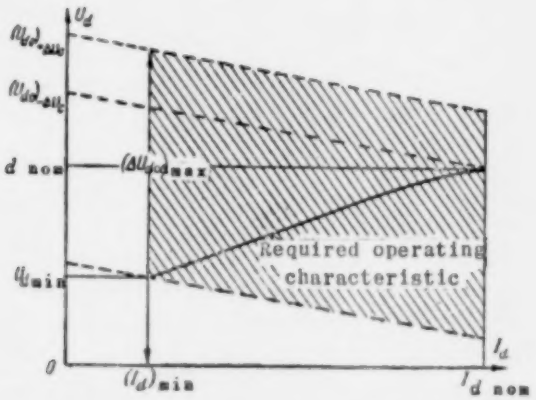

Fig. 8. The requisite operating characteristic and the domain of regulation (the shaded area).

The cross section of the magnetic circuit Q and the number of turns in the operating winding w_2 depend on the requirements to be met as regards minimum loss, weight and dimensions.

The following equation can be used for the number of turns in the control winding:

$$I_{s.max} = \frac{H_{max} l_\mu}{1.25 w_s}. \qquad (8)$$

Here it must be borne in mind that wide variation of the magnetization current is required between $+I_{s.max}$ and $-I_{s.max}$ in order to make full use of the hysteresis loop. If, however, a change in the direction of the current in the magnetization winding is undesirable or impossible, the magnetization winding can be divided into two windings, namely, a control winding and a bias winding, which is supplied by current $+I_{s.max}$. In this case the current in the control winding varies between 0 and $-2I_{s.max}$. The value of H for "interleaved" solid cores of grade E-330 electrical steel is 2 to 3 oersted.

Another factor in the design of the control winding is the voltage induced in it during re-magnetization of the reactor:

$$u'_{SR} = u_{SR} \frac{w_s}{w_1} = \frac{w_s}{w_2} E_{max} \sin \omega t. \qquad (9)$$

This voltage attains its maximum value under conditions of maximum regulation, i.e. when $I_d = I_{d.max}$ and $\alpha = \alpha_{max}$. The maximum value of the control angle is given approximately by the expression

$$\cos \alpha_{max} \approx \frac{U_{d\,min}}{(U_{do})_{+\Delta U_c}}.$$

Then, by definition

$$(u'_{SR})_{max} = \frac{w_m}{w_s} E_{max} \sin \alpha_{max}. \qquad (10)$$

Strictly speaking, the angle $(\alpha' + \gamma + \delta)$ should be substituted for ωt in formula (9) in order to determine the maximum voltage on the magnetization windings. But this can only be done after constructing the operating characteristics and determining the control zone (see Fig. 8). For draft projects use may be made of formula (10). The value of $(u'_{SR})_{max}$ can be stated more precisely later.

Thus the number of turns in the magnetization windings can be found by formulae (8) and (10) according to the desired control current or maximum permissible voltage on the magnetization windings.

Reactor power

The weight and dimensions of saturable reactors inevitably depend on the equivalent rating of the reactors, as well as on the maximum voltage and the effective value of the rated current in the reactor windings. In its turn the equivalent rating depends on the shape and operating time of the voltage in the reactor windings and is defined (by analogy with conventional transformers) as the average of the products of the effective value of the current of each winding, times the equivalent e.m.f. [6]. The equivalent e.m.f. is that sinusoidal voltage which, on being applied to a particular reactor, will cause its complete re-magnetization (from $-B_k$ to $+B_k$) during a half-period. It is calculated by the formula

$$E_3 = \frac{1}{2\sqrt{2}} \int_0^{\pi} u_{SR}\, d\omega t.$$

Here, in order to determine the reactor voltage, it is necessary to use an expression for it at load currents close to the minimum value of the rectified current (practically on no load of the rectifier). In this case the reactor voltage can be represented in the following form at any magnetization current:

$$u_{SR} = E_{max} \sin \omega t,$$

where

$$0 \leq \omega t \leq \alpha.$$

Then

$$E_\theta = \frac{1}{2\sqrt{2}} E_{max} (1 - \cos \alpha_{max}).$$

Considering that

$$E_{max} (1 - \cos \alpha_{max}) = \frac{\pi}{3} (\Delta U_{d\alpha})_{max},$$

the formula for the equivalent e.m.f. is

$$E_\theta = \frac{1}{2\sqrt{2}} \frac{\pi}{3} (\Delta U_{d\alpha})_{max}.$$

In calculating the effective value of the current in the main winding of a reactor it can be assumed that the current flowing through the rectifier is rectangular in shape, even though this tends to over-state the calculated values of the current and equivalent rating by 4 to 5 per cent. For the circuit under consideration in this article, the current in the main winding of the reactor is

$$I_z = \frac{1}{\sqrt{3}} I_d.$$

The maximum value of the magnetization current, referred to the main winding, does not exceed 5 per cent of the current in the main winding for large rectifiers using a circuit with internal feedback. It can therefore be assumed in the derivation of the formula for the equivalent rating of a saturable reactor that $I'_m = 0.05\ I_d$.

The equivalent rating of the six reactors as a percentage of the power of the supply transformer is

$$P^*_{6\theta} = \frac{9}{\pi} \cdot \frac{E_\theta}{U_{d0}} \cdot \frac{I_{m1} + I'_m}{I_{d.nom}} \cdot 100\%.$$

Substituting the expressions for E_θ, I_z and I'_m in this formula:

$$P^*_{6SR} = 1.05 \frac{\sqrt{3}}{2\sqrt{2}} \cdot \frac{(\Delta U_{d\alpha})_{max}}{U_{d0}} \cdot 100\%.$$

The quantity

$$\frac{(\Delta U_{d\alpha})_{max}}{U_{d0}} \cdot 100\% = (\Delta U^*_{d\alpha})_{max}$$

is the maximum degree of regulation of the rectified voltage as a

percentage of the no-load voltage of the rectifier. Consequently, the equivalent rating of the six reactors in the rectifier system under consideration is a linear function of the desired degree of rectified voltage regulation.

If 100 per cent regulation of the rectified voltage is required over a wide range of load currents (from $I_{d.min}$ to $I_{d.nom}$), the equivalent rating of the saturable reactors is a maximum and is about 65 per cent of the supply transformer rating.

Glossary of notation

ΔB_{max} – the maximum change in induction in the reactor core

E_{max} – the amplitude of the line voltage in the LT winding of the transformer

$e_{k\Sigma}\%$ – the total rectified voltage drop as a percentage of its rated value

U_d – the mean value of the rectified voltage

U_{d0} – the mean value of the rectified voltage on no load

$U_{d.nom}$ – the rated rectified voltage

$(U_{d0}) + \Delta U_c$ – the no-load voltage of the rectifier with an increase in supply voltage

u_{SR} – the voltage on the main winding of the reactor (instantaneous value)

u'_{SR} – the instantaneous value of the voltage on the magnetization winding of the reactor

H_k – the intensity of the magnetic field corresponding to the kink in the linear approximation of the hysteresis loop

H_c – the coercive force of the dynamic hysteresis loop of the reactor cores

H_{max} – the intensity of the magnetic field corresponding to the maximum magnetization current

I_s – the effective value of the current in the main winding of the reactor

$I'_м$ – the mean value of the current in the magnetization winding referred to the main winding

I_d – the mean value of the rectified current

$I^*_м = I_м/I_{м.max}$ – the magnetization current in relative units

$I_{м.max}$ – the maximum value of the magnetization

$I_{d.nom}$ – the rated rectified current

$I_{d.min}$ – the load current corresponding to the minimum desired value of the rectified voltage

i_z – the instantaneous value of the current in the main winding of the reactor

l_μ – the length of the middle magnetic line of the reactor core

$w_м$ – the number of turns in the magnetization winding

w_z – the number of turns in the main winding of the reactor

Q – the active cross section of the reactor core, cm^2

r – the load resistance

$x_\Sigma = x'_p + x_r$ – the total reactance

x'_p – the referred phase reactance, including the leakage reactance of the transformer and system

x_r – the reactance of the reactor in the saturated state

α – the duration of the magnetization of the reactor on condition that the winding voltage varies according to the law $E_{max} \sin \omega t$ in the interval from 0 to α

α_0 – the angle of delay in triggering the alternate valve

α_0^* – the angle of delay at which the third mode of operation begins

α' – the control angle of the rectifier

α'_{k3} – the control angle at which the third mode of operation changes into the fourth

$\alpha_0^{(k)}$ – the angle of delay at the boundary of the second and fourth modes

γ – the actual commutation angle

Translated by O.M. Blunn

REFERENCES

1. G.P. Mostkova and F.I. Kovalev; Izd. Akad. Nauk SSSR, *Elektroenergetika*, No. 4 (1961).

2. H.F. Storm and C.W. Flairty; *Communication and Electronics*, No. 1 (1960).

3. W.H. Moore; *New techniques in designing three-phase magnetic amplifiers*. Amer. Inst. elect. Engrs. (1957).

4. M.A. Rozenblat; *Magnetic amplifiers* (*Magnitnye usiliteli*), Part II. Sov. Radio (1960).

5. P. Kratz and A. Lang; *AEG Mitt.*, No. 8/9 (1959).

6. Yu.G. Tolstov; *The use of saturable reactors in installations for d.c. transmission* (*Primeneniye nasyshchayushchikhsya drosselei v ustanovkakh dlya peredachi energii postoyannya toka*). Izd. Akad. Nauk SSSR (1951).

HOW THE POST-BREAKDOWN VOLTAGE ON AN ARRESTER DEPENDS ON THE LENGTH OF THE CURRENT WAVEFRONT*

V.I. PRUZHININA-GRANOVSKAYA and V.A. VOL'KENAU

(Lenin All-Union Electrical Engineering Institute)

(Received 28 March 1961)

YEAR 1961

Recent improvements in the performance of valve arresters have resulted in lower insulation levels on transformers and other gear.

The surges which follow lightning strokes differ in duration and may be very short. The insulation is accordingly designed for voltage wavefronts of approximately 1 to 2 μsec.

But the "standard" post-breakdown voltages of valve arresters have been calculated for current wavefront lengths of about 10 μsec owing to the relative simplicity and accuracy of the measurements, even though the arrester may be affected by current wavefront lengths τ_w of less than 10 μsec in operation [1]. This situation has been recognized in the regulations governing surge protection where post-breakdown voltages are specified for τ_w of 3 to 5 μsec.

Use is at present made of two types of non-linear resistors in Soviet valve arresters. "Vylite"** resistors are used in lightning arresters and "tervite"** resistors in "combined" arresters for protection from

---

* *Elektrichestvo*, 10, 53-54, 1961.

** These types of arrester are considered in an article translated in this journal from *Elektrichestvo* No. 4, 1961. Vylite is a ceramic material which consists of SiC + clay and graphite. Tervite is another special type of material used for non-linear arresters (Translation Editor).

internal surges as well as lightning strokes. The electrical characteristics of these two types of resistor are quite different, and the same applies to the relationship between their post-breakdown voltage and the current wavefront.

The effect of the current wavefront on the post-breakdown voltage is essentially as follows. At a given current the voltage on the resistor depends on the temperature of the inter-grain contacts owing to the high temperature coefficient of resistance of carborundum. This relationship determines the looped shape of the dynamic voltampere characteristic of operating resistors and the relationship between the post-breakdown voltage and the length of the current wavefront. Since the temperature coefficient of resistance of carborundum is negative, it follows that the post-breakdown voltage decreases with increasing length of the wavefront.

The variation of the post-breakdown voltage U' with a reduction in the length of the wavefront depends on the "density" of the impulse current as well as on the properties of the resistor. For arresters made by the American firm of Westinghouse [3], the residual voltage at 10 kA for τ_w of 3 μsec is 12 per cent greater than that for $\tau_w = 10\,\mu$sec. For the Swedish 380 kV arrester, the post-breakdown voltage at 8 kA is 10 per cent higher for a current wavefront slope of 3 kA/μsec than for 1 kA/μsec. The post-breakdown voltage at 10 kA on the vylite resistors of Russian RVS arresters in production up to 1950 was increased 6 to 7 per cent by a reduction in the length of the current wavefront from 10 to 5 μsec [5].

For the RVS arresters now in production, the post-breakdown voltage U' is 4 and 6 per cent higher respectively for $\tau_w = 5$ and 3 μsec than for $\tau_w = 10\,\mu$sec.

This paper presents the results of investigations into the relationship between the post-breakdown voltage and the length of the current wavefront for tervite and vylite arresters in modern Soviet lightning arresters. The measurements were taken on tervite and vylite discs 70 mm in diameter and 20 mm thick for $\tau = 3$, 5 and 10 μsec at 2.5 and 10 kA. The changes in the post-breakdown voltage $\Delta U'$ for $\tau_w < 10\,\mu$sec are expressed as percentages of the post-breakdown voltage U'_{10} at $\tau_w = 10$ μsec:

$$(\Delta U'/U'_{10})\ \% = (U'_{\tau} - U'_{10}/U'_{10}) \times 100$$

The figure is about 2 to 3 per cent, especially at low currents. This requires great accuracy in measuring U'. The error depends on the slope of the impulse current and must be minimized.

The figure is about 2 to 3 per cent, especially at low currents. This requires great accuracy in measuring U'. The error depends on the slope of the impulse current and must be minimized.

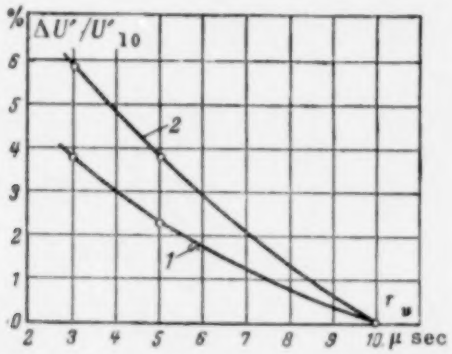

Fig. 1. The post-breakdown voltage on an arrester with vylite resistor discs 70 mm in diameter and 20 mm thick as a function of the length of the current wavefront:

1 – I_{max} = 2.5 kA; 2 – I_{max} = 5 kA.

To achieve an acceptable degree of accuracy, use was made of compensation for the main part of the voltage to be measured so that a voltage of about 15 per cent of U_{max} was recorded on the oscillogram. Thus the oscillogram sensitivity was about 20 V/mm at values U_{max} equal to 3-5 kV. An impedance voltage divider was set up at the oscillograph, but its resistance was sufficiently low to avoid errors due to the capacitance connected in parallel with the lower arm of the divider (the time constant of this circuit did not exceed 3×10^{-8} sec).

Figure 1 shows the ratio $\Delta U'/U'_{10}$ as a function of $\tau_ф$ for vylite discs. The experimentally-determined values of $\Delta U'/U'_{10}$ agreed satisfactorily with previous results. Thus, a reduction in length of the current wavefront from 10 to 5 μsec at 5 kA resulted in a 3.8 per cent increase in the post-breakdown voltage on the discs 70 mm in diameter (this is equivalent to a 10 kA current through resistors 100 mm in diameter for RVS arresters).

Figure 2 shows the curves for $\Delta U'/U'_{10} = f_2(\tau_ф)$ in respect of tervite discs 70 mm in diameter and 20 mm thick at 2.5, 5 and 10 kA. It will be seen from a comparison of Figs. 1 and 2 that the variation of the post-breakdown voltage is greater on vylite discs than on tervite discs given the same current density. There is only a comparable change

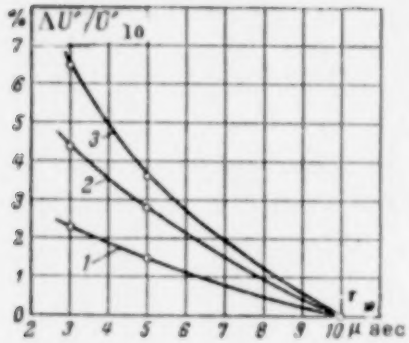

Fig. 2. The post-breakdown voltage on an arrester with tervite resistor discs as a function of the length of the current wavefront:

1 – I_{max} = 2.5 kA; 2 – I_{max} = 5 kA; 3 – I_{max} = 10 kA.

in U' on both types of disc if the current density is approximately halved on one of them. The increase in $\Delta U'/U'_{10}$ with an increase in the length of the current wavefront adversely affects the non-linearity

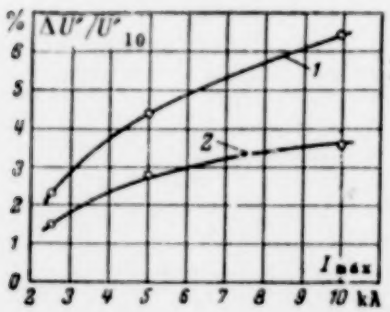

Fig. 3. The post-breakdown voltage on an arrester with tervite discs 70 mm in diameter and 20 mm thick as a function of I_{max}:

1 – τ_w = 3 μ sec; 2 – τ_w = 5 μ sec.

a of the resistor at large currents if τ_w is decreased. The corresponding data for tervite discs at 2.5 to 10 kA is given below.

τ_w μ sec	a
3	0.208
5	0.190
10	0.173

Figure 3 illustrates the relationship between the post-breakdown voltage and the amplitude of the current impulse. These curves provide and estimate of $\Delta U'/U'_{10}$ in combined arresters in which tervite discs are used. Thus, for example, the post-breakdown voltage changes about 3 per cent on a 500 kV arrester at standard impulse current density if the length of the current wavefront is reduced from 10 to 3 μ sec.

Translated by O.M. Blunn

YEAR
1961

REFERENCES

1. E. Beck; *Trans. Amer. Inst. elect. Engrs.* 70, pt. II, 1134 (1951).

2. *Regulations for the surge protection of electrical a.c. equipment 3-220 kV (Rukovodyashchiye ukazaniya po zashchite ot perenapryazhenii elektrotekhnicheskikh ustanovok peremennogo toka 3-220 kv).* Gosenergoizdat (1954).

3. A.M. Opsahl and N.K. Osmundsen; *Westinghouse eng.*, 3, 88 (1957).

4. A. Rusck and B.G. Rathsman; *ASEAJ*, 26, No. 3-4, 67 (1953).

5. A.I. Piryazeva; *Proceedings of the scientific conference on overvoltages (Trud. nauchno-tekh. sessii po perenapryzheniyam)*, p. 185, Gosenergoizdat (1950).

DISCRIMINATIVE EARTH-FAULT INDICATION*

V.V. SHUT'

(Odessa)

(Received 10 August 1960)

No device has hitherto been perfected for discriminative earth-fault indication in compensated three-phase high-voltage networks. Previous attempts to develop such a device have not produced satisfactory results.

In 1936 Neigebauer [1] proposed an electronic device which determined the fault direction from the sign of the first half-wave of the transient current. The device was not reliable in operation owing to the rapid ageing of the valves as a result of the permanently heated state of the cathodes. It was also necessary to re-adjust the circuit when replacing valves. Maranchak [2] improved this system in 1955 and evolved a method of designing its individual parts, but the main disadvantages remained.

In 1956 Darchenko and Stepnov [3] proposed the use of an electromagnetic relay which used a restraint winding which took the sign of the first half-wave of the earth current into account. This method can be employed successfully at remote points from supply sources where the frequency of the transient current is low. But experience has shown that it is unsuitable for power stations and large substations since the device is non-selective when the frequency of the transient current is high.

In 1958 Raik [4] developed a "manually-operated" device for determining the direction of the fault in which the sign of the active component of the earth current was tested and compared alternately. This device did not satisfy elementary requirements.

In 1959 Kalendo proposed the use of a system of polarized relays but

---

* *Elektrichestvo*, 10, 68-71, 1961.

none have as yet been made which will operate after the first half-wave of the transient current (a fraction of a millisecond).

In this paper a description is given of a device, proposed by the author, which has been tested in the Odessa power system. The device uses the transient currents in the system during the first few instants after an earth fault.

Earth faults may occur because of a gradual deterioration or sudden rupture of the insulation. In either event the rate of voltage build-up at 50 c/s exceeds the rate at which the earthed object "approximates" the phase, so that in the overwhelming majority of cases the breakdown occurs at an instantaneous value of the phase voltage which is 70 per cent or more of maximum, i.e. the capacitance of the network under fault conditions is almost completely charged at the instant the breakdown occurs.

YEAR 1961

The discharge of this capacitance after the earth fault is a decaying oscillatory process. Numerous tests have shown that the decay time constant in modern networks is approximately $0.285\ \omega_0$.

In designing the system of protection it is important to know the frequency f_0 of the oscillations in the discharge process. It can be found from the following formula

$$f_0 = \frac{1}{2\pi}\sqrt{\frac{1}{LC} - \left(\frac{R}{2L}\right)^2},$$

where L is the inductance across which the capacitance of the fault phase is discharged, C the phase capacitance, and R the resistance into which the discharge takes place.

Ignoring the resistance and assuming that the inductance L is equal to the inductance of the reactor, and that the voltage on the bus bars is not reduced during the short circuit, then

$$L = \frac{U}{\omega I_k}$$

and, furthermore

$$C = \frac{I_C}{\omega U}.$$

Consequently

$$f_0 = f\sqrt{\frac{I_k}{I_C}},$$

where I_k is the steady-state short-circuit current at the earth point

(easily determined by a network analyser, an analogue of the network or by analysis); I_C is the earth-fault current in the absence of compensation, defined as the sum of the earth and arc-quenching coil currents for under-compensation, or as the difference between those currents for over-compensation; and f is the supply frequency.

Oscillograms taken in numerous experiments have shown that formula (1) produces accurate results in spite of its simplification.

The current discharges from the capacitance of the non-faulted connexions across a zero-sequence current transformer $ZSCT$ into the bus bars, and then across another zero-sequence current transformer in the direction of the actual point of the earth fault. The discharge current across this second transformer is in the opposite direction to that across the first transformer, regardless of the sign of the charge in the phase where the fault has occurred. The direction of the discharge current across the transformers in any half-wave can be used to determine the faulty connexion. The most convenient half-wave for this purpose is the first one, since it is in this half-wave that the amplitude of the current is greatest. The filter illustrated in Fig. 1 is a very convenient device for isolating this half-wave.

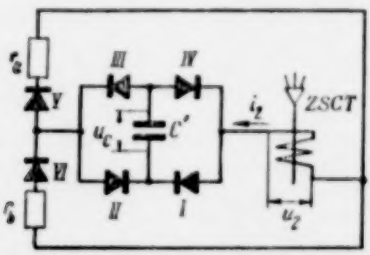

Fig. 1.

On flow of the decaying sinusoidal oscillatory discharge current through the zero-sequence current transformer, the capacitor C' is so connected that the voltage to the secondary winding of the transformer is always the same in sign.

At the first instant after the earth fault, u_2 is greater than u_C and the capacitor is charged from the transformer ($ZSCT$) via the resistance r_a and rectifiers *I*, *III* and *V*, or via resistance r_b and the rectifiers *II*, *IV* and *VI*, depending on the sign of the discharge current. The current across either of these resistances is quite large in the first instant and the potential difference between their

terminals is comparatively large. This process continues until $u_2 = u_C$.

As soon as $u_2 < u_C$, a rather small current flows into r_a (or r_b) which depends on the difference between u_2 and u_C, the large resistance of the three series-connected rectifiers and the output resistance r_a (or r_b). In this situation the capacitor is slightly discharged and its voltage is reduced, so that in the second half-wave the voltage u_2 may again be greater than u_C. But this difference will be very small and the current through r_a (or r_b) will also be small accordingly (see Fig. 2).

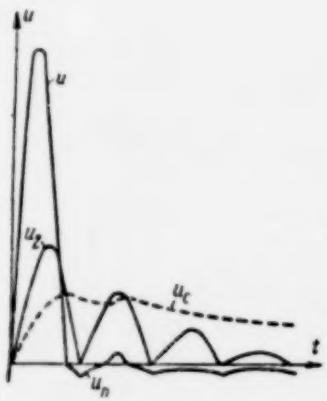

Fig. 2.

Tests have shown that a voltage surge occurs in the first half-wave at the output of r_a (or r_b) which in amplitude is equal to

$$U = \sqrt{2} U_2 \frac{f_0}{f_T} K,$$

where U_2 is the effective value of the voltage across the secondary winding of the transformer, found experimentally by passing a current I_C at a frequency f_T (close to f_0) through the secondary winding of the current transformer; K is the characteristic of the filter:

$$K = \vartheta [e^{-\alpha t} (\eta \cos \omega_0 t + \rho \sin \omega_0 t) - \lambda e^{-\beta t}],$$

where

$$\vartheta = \frac{1}{\omega_0^2 + \left(\frac{1}{rC} - \tau\right)^2}; \quad \tau = 0.285\omega_0;$$

$$\lambda = \frac{1}{rC'}\left(\frac{1}{rC'} - \tau\right); \quad \eta = \left(\frac{1}{rC'} - \tau\right) - \omega_0;$$

$$\mu = \frac{1}{rC'}; \quad \rho = \frac{\omega_0}{rC'}.$$

The filter characteristic K is between 0.35 and 0.25 at the frequency f_0 if $r = 1000\ \Omega$ and $C' = 0.5\ \mu F$. When $u_2 < u_C$, the "noise" voltage at the output is

$$U_n \leqslant \sqrt{2}U_2 \frac{f_0}{f_T} \cdot \frac{r}{2nr_0},$$

where r_0 is the back resistance of one rectifier, and n the number of series-connected rectifiers in one arm of the bridge.

Tests have shown that the filter reliably isolates the first half-wave of the non-decaying voltage as well as the decaying voltage.

In the presence of an earth fault a voltage is seen instantaneously across r_a or r_b depending on the sign of the first half-wave of the capacitor discharge current through the zero-sequence current transformer. This voltage does not appear across the same resistance in the direction of the fault as in the opposite direction. The voltage across either of the output resistances is supplied to the cathode and ignitor of one of the non-filament thyratrons in which there is always a voltage between the anode and cathode (see Fig. 3).

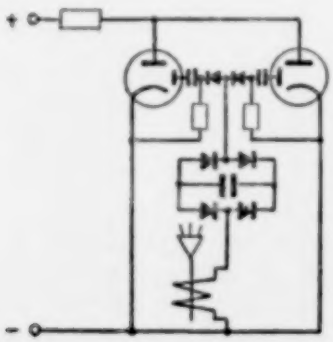

Fig. 3.

One version of the indication device is intended for use in conventional substations in which personnel are on duty. The device has a number of "cells" such as that illustrated in Fig. 3. The thyratron

itself is quite a good indication device. The thyratrons are arranged in two rows (Fig. 4), two thyratrons for each direction (one in each row). An upper thyratron lights up during the first half-period if the discharge current is away from the bus bars. A lower one lights if the current is towards the bus. The thyratrons light in different rows depending on the direction of the discharge current. The signal is acknowledged manually by the duty personnel.

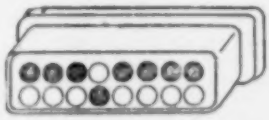

Fig. 4.

YEAR 1961

The signal may also be transmitted from fully automatic substations to a central despatcher point by television. However, in this case the signal cannot be repeated indefinitely until acknowledged unless the system illustrated in Fig. 5 is adopted. This system is also able to transmit signals by conventional telecommunication equipment as well as by television.

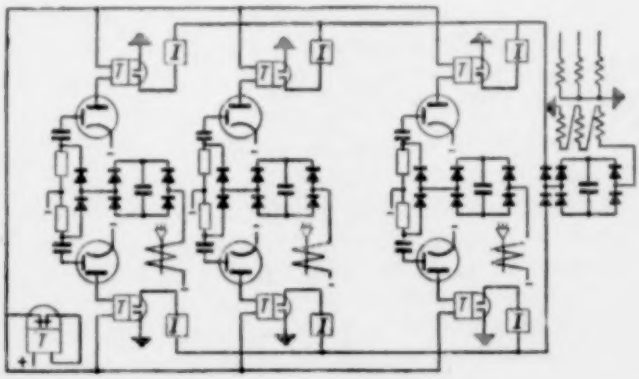

Fig. 5.

In this system the discharge current i in the first period is compared with the zero sequence voltages u_0, which are always identical in the direction towards the fault.

The zero sequence voltage comes to the upper or lower row of

indicator relays depending on its sign. The indicator relays only operate in the row to which u_0 is applied and only for that direction for which one of the thyratrons has fired. If the outgoing zero sequence voltage leads of the filter are correctly connected, this combination of events will only occur at the faulted connexion.

All the anode circuits are supplied via a common relay which has normally closed contacts which only open after a time lag. This relay disconnects the thyratrons for sufficient time to allow the indicator relays to operate and the capacitors of the filters to discharge. Repeated operation is therefore possible in the event of intermittent faults.

Only the earth-fault signal of a particular substation can be transmitted to the central despatcher point. On receipt, service engineers are sent to restore the supply, disconnect the section with the fault and to carry out the necessary inspection and repairs. Use is made of indicator relays with signal flags which drop down and cannot return of their own accord.

Operating experience has shown that simultaneous intermittent earth faults in different directions are highly improbable, so that the simpler and more reliable system illustrated in Fig. 3 should be used wherever possible. But even the system shown in Fig. 5 is not particularly complicated. It consists of ordinary electromagnetic relays. No special requirements have to be satisfied as regards operating, since they only have to operate in a quarter of a period of the operating frequency (50 m sec). Numerous relays such as the ET, ES and ESh types operate three to four times as fast.

The proposed earth-fault systems differ from the earlier system of Neigebauer and Maranchak in that the first half-wave of the transient current is isolated by a special filter and not by "cutting off" the circuit. The proposed systems differ from those put forward by Darchenko and Stepnov in that they react to the direction of the current in the first half-wave and are practically independent of amplitude so that the effective range is much wider. Performance is independent of the operating speed of mechanical relays, which is not the case with the systems proposed by Kalendo, Darchenko and Stepnov.

Ordinary batch-produced items and economical non-filament thyratrons, semiconductor diodes, etc, are used.

The author has thoroughly tested the systems and all that has been written about them in this paper is authentic. The equipment has shown itself to be simple, selective and completely reliable.

Translated by O.M. Blunn

REFERENCES

1. Kh. Neigebauer; *Energet. obozrenie*, No. 8 (1936).

2. V.M. Maranchak; *Elektrichestvo*, No. 11 (1955).

3. V.E. Darchenko and T.V. Stepnov; *Elektrichestvo*, No. 2 (1956).

4. M.N. Raik; The protection of generator-transformer units from earth faults (Zashchita ot zamykanii na zemlyu blokov generator-transformator). *Energetika za rubezhom, ser. rel. zashchita*, No. 3 (1960).

5. Yu.I. Kalendo; A device for indicating earth faults in compensated networks (Ustroistvo dlya signalizatsii o zamykanii na zemlyu v kompensirovannykh setyakh). *Byull. izobretenii*, No. 23 (1959).

YEAR
1961

ABSTRACTS FROM PAPERS PUBLISHED IN ELEKTRICHESTVO No. 10, 1961.

Editorial

The great programme for building communism, (pp. 1-5).

The article defines communism from the party programme and briefly considers the next twenty years of development. The role of the communist party is discussed along with the part to be played by science in forming the material-technical basis of communism.

Automatic control

Charging a capacitor from an a.c. circuit through a valve. S.M. Smirnov, (pp. 60-64).

A study is made of the process of charging a filter capacitor by sinusoidal voltage pulses. Cases of purely capacitive and capacitive-active loads of rectifiers connected in half-wave and full-wave rectifying systems are considered.

Transforming Grey's code into a binary code. V.A. Kougiia, (p. 74).

The direct use of Grey's parallel code for control devices in servo systems (e.g. for determining the angle of rotation of shafts) is not considered convenient in programme control systems based on potential logical elements. Accordingly a system of transforming Grey's code into a parallel binary code is suggested.

Control engineering

Fundamentals for constructing a standard series of automatic motor drives for multi-cable mine hoists. V.S. Tulin, (pp. 12-19).

A study is made of the regulations and standards governing mine hoisting and lifting equipment with a view to forming a theoretical

basis for standardization and greater efficiency in electrical drives.

An instrument for measuring active power. Ia.I. Stiop, (pp. 65-66).

A description is given of a device for measuring power in which the main part, used to square the sum and difference of the input quantities (current and voltage), uses thyrite elements as the non-linear resistors with a load resistance to adjust the voltampere characteristic.

A controllable d.c. drive. A.I. Ioffe, (pp. 71-73).

A study is made of a new variable d.c. drive with a simple converter. The drive is based on a typical d.c. motor with independent excitation with its speed controlled by varying the voltage applied to the armature from the converter. The converter consists of a three-phase transformer with primary windings connected in star and connected to the a.c. network. The secondary windings have different numbers of turns so that the e.m.f. is different in each winding. Rectified voltages can be fed to several drive motors at different speeds.

YEAR 1961

Power systems

Appraising electric power costs in designing industrial plants. D.S. Stepanov, (pp. 6-11).

The estimation of the cost of electrical energy in planning industrial undertakings is considered in the light of socialist methods of planning without resort to existing tariffs.

Relays and protection

The behaviour of overcurrent relays during out-of-step conditions in a power system. S.E. Stepurin, (pp. 55-60).

Investigations have confirmed that overcurrent relays may operate incorrectly during out-of-step conditions of the generators. It is proposed to overcome this by adjusting the reset time of the relay or using a voltage starting relay with a particular voltage setting. The method of analysis is also applicable to other types of voltage and current relay.

The relationship between the Curie point and the composition of copper-zinc ferrites. A.I. Andriyevskii *et al.*, (pp. 66-68).

An account is given of investigations into copper-zinc ferrites of various compositions corresponding to values of the Curie point between the boiling point of liquid nitrogen and 460°C. The Curie points of the compositions were determined to within 4 to 6°C by a method which is described. Particular compositions are used for thermal relays which are also described.

Rotating machines

The maximum torque of coal-cutter induction motors connected in mine networks. E.S. Traube, (pp. 19-23).

In order to ensure the necessary conditions for a highly efficient performance from coal-cutting combines, the author seeks to elucidate the maximum possibilities of mine networks by finding the general laws which govern the variation of the actual torque of induction motors. Test results appear to confirm the theoretical propositions.

Locus diagrams for synchronous generator control devices with phase compounding. V.N. Breev *et al.*, (pp. 29-34).

The properties of the various control devices in the steady-state excitation circuit of generators with phase compounding are described by a single diagram so that the effect of the parameters of individual circuit elements on the excitation current can be established and so that a preliminary selection can be made of requisite initial coefficients depending on the regulation and forcing of the excitation current.

A new way of mounting brushes in electrical machines. V.G. Gurin, (pp. 47-48).

An account is given of tests and calculations which indicate that the most efficient position of "reactive" brushes in electrical machines is that with trailing brushes at angles greater than 10 or 15° to the radial direction except when vibration is excessive.

The performance of a three-phase induction motor having an unequal number of turns i the stator phases. I.M. Kamen', (pp. 48-52).

General equations are formed for the analysis of the operating conditions of non-salient pole machines having a three phase winding with identical phase zones, but with different numbers of turns in the phases.

Synchronous machine damper winding losses due to voltage time harmonics. Iu.A. Kulik, (pp. 34-37).

A study is made of the effect of voltage harmonics on the currents of the damper winding and the resultant losses. The distribution of the currents in the damper winding is analysed and the total losses caused by higher time harmonics are determined by the mean square value of the current in the conductor of the damper winding.

YEAR
1961

THE MERCURY-ARC RECTIFIER DRIVE*

B. M. GUTKIN

(Vniiem)

(Received 21 August 1961)

The MAR drive is a complex electromechanical system. In the past the control system of the rectifier has not been regarded as an integral part of the whole system of regulation, and no account has been taken of the requirements which rectifier control systems should satisfy.

As a result it has not been possible to take full advantage of the many valuable features of mercury-arc rectifiers in all applications, and this is especially the case with the electrical drive.

The extensive use of MAR drives in industry during the past 10 to 15 years has not only stimulated progress in the design of new rectifiers, but it has also brought about a rather new approach to the development of drives in which the rectifier is regarded as one element of the whole automatic control system, and in which the control system of the rectifier is regarded as the main element on which the whole system of regulation depends.

Much has been written about such drives in the Soviet and foreign press [1,2,3 *et al.*]. The control system elements of actual rectifiers and drives have already been considered as a whole [4]. In this paper attention is confined to pressing problems which, if solved, could be instrumental in the production of highly reliable MAR drives with a great dynamic Q-factor.

There is a great variety of drive control circuits, but they can be classified as follows, independently of the power circuits of the rectifiers and control systems:

1. Circuits in which control is effected by varying the voltage

---

* *Elektrichestvo*, 11, 14-22, 1961.

applied to the motor armature.

2. Circuits in which control is effected by varying the excitation current.

3. Circuits in which control is effected by varying the excitation current as well as the voltage applied to the armature. Such circuits will be referred to as "hybrid" circuits.

In order to simplify the study, it is proposed to consider irreversible and reversible systems separately.

MAR drives range from 0.05 to 10,000 kW. Small and medium drives are widely used in general engineering, particularly in machine tools. Large drives are used in the iron and steel industry and in mining.

Irreversible systems

YEAR 1961

Figure 1 shows the circuits of small and medium irreversible drives. The system illustrated in Fig. 1*a* uses a semi-controlled single-phase bridge system. If hot cathode bulbs are utilized, this system can be used for powers varying from 0.3 to 2 kW. Since no transformer is employed, the motor voltage is non-standard and it must be matched with the supply grid voltage. The system shown in Fig. 1*b* can be recommended for use in drives up to 200 kW depending on the type of rectifier bulbs, hot cathode bulbs being used up to 20 kW and pool cathode bulbs for larger outputs.

Systems without transformers are very promising for small drives, since their weight and cost can be reduced and they are a better economic proposition.

For large outputs it is advisable to employ transformers. Power circuits of large irreversible drives are illustrated in Fig. 2.

Here the current cannot change direction owing to the unidirectional conductance of the bulb. When the motor e.m.f. becomes greater than the converter rectifier voltage, the current in the main circuit is zero and the motor starts to "coast". Additional apparatus is therefore required in these systems to provide electrical braking.

All irreversible drive systems can accordingly be classified by the method of braking into those with dynamic braking and those with regenerative braking.

Dynamic braking is employed in the circuits illustrated in Figs. 1 and 2. When the motor e.m.f. becomes greater than the rectifier voltage, the current in the main circuit is zero, and this can be used as a

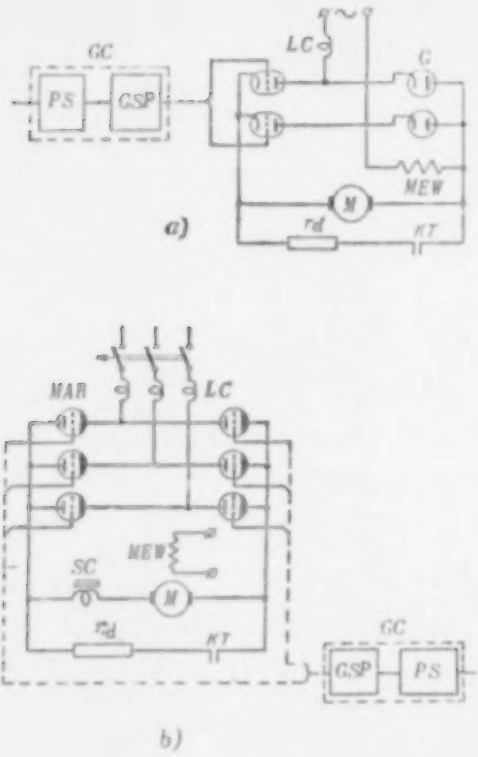

Fig. 1. Small and medium non-reversible MAR drives.

a – semi-controlled single-phase bridge circuit; *b* – three-phase bridge circuit; *PS* – phase shifting system; *GSP* – grid supply panel; *GC* – grid control system; *T* – thyratron; *G* – gas-filled rectifier (gazotron); *MAR* – mercury-arc rectifier; *M* – motor; *MEW* – motor excitation winding; *LC* – limiting choke; *SC* – smoothing choke; *KT* – brake contactor.

control signal for operating the dynamic braking contactor *KT* (Fig. 1). The motor and rectifier are then connected to the dynamic braking resistance r_d where the energy from the rectifier and the kinetic energy stored by the drive is dissipated. This is a widely used method of braking, but though it may be acceptable for small and medium drives, it cannot be regarded as satisfactory for large drives with special braking conditions.

An alternative method of dynamic braking employs a special measuring

YEAR
1961

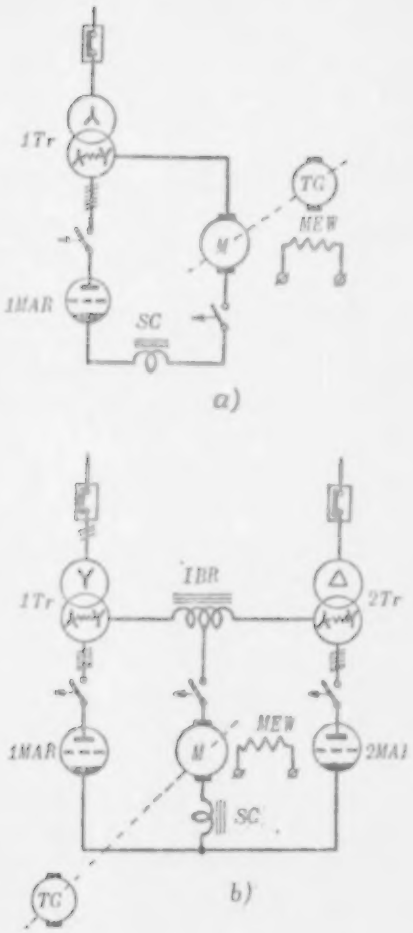

Fig. 2. Large non-reversing MAR drives.

a – six-phase circuit; *b* – twelve-phase circuit; *1 MAR, 2 MAR* – mercury-arc rectifiers; *1 Tr, 2 Tr* – anode transformers with built-in balancing reactors; *BR* – type-2 balancing reactor; *SC* – smoothing choke; *M* – motor; *TG* – tachometer generator.

device which operates on the cessation of current in the main circuit. It then either acts on the grid circuits of the rectifier and turns the rectifier "off", or else disconnects the rectifier from the load by special apparatus. Neither method provides smooth control over the

current whilst braking, and it becomes necessary to switch the resistance r_d. If it is decided to use such switching apparatus, it is advisable to follow the system illustrated in Fig. 3.

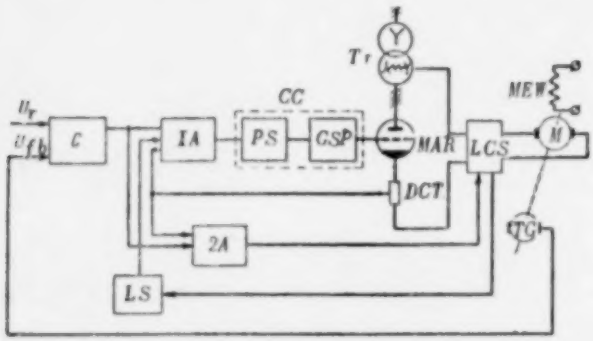

Fig. 3. Functional block-diagram of MAR drive with a switch in the armature circuit.

Tr – anode transformer; *MAR* – mercury-arc rectifier; *LCS* – load circuit switch; *M* – motor; *DCT* – d.c. transformer; *PS* – phase shifting system; *GSP* – grid supply panel; *GC* – grid control system; *C* – comparison circuit; *LS* – limiting system; *1A* – amplifier of regulating device; *2A* – switch amplifier; U_r – reference voltage; U_{fb} – feedback voltage; *TG* – tachometer generator.

Here the armature circuit is switched by a special switching amplifier which receives a control signal at its input, whilst the windings of the armature circuit switch are connected at its output.

Speed control in a closed system is governed by a law which may be written in the form

$$U_c = \mu (U_r - K_{fb} U_{fb}), \tag{1}$$

where U_c is the control signal at the input to the governor, U_r the reference voltage, K_{fb} the feedback factor, U_{fb} the feedback voltage, and μ the amplification factor of the amplifier.

A change in sign of the control signal determines the required mode of operation of the converter. If $U_r > K_{fb} U_{fb}$ and $U_c > 0$, the rectifier operates as a rectifier, but if $U_r < K_{fb} U_{fb}$ and $U_c < 0$, braking is necessary and the rectifier must act as an inverter. For switching the armature circuit without interruption of the current, it is necessary

to employ interlocking which allows switching only if $I_d = 0$. It will be seen from a consideration of the regenerative braking system that systems with a switch in the load circuit can also be used in reversing drives, in which case the rectifier acts as a rectifier in clockwise and anti-clockwise rotation in different positions of the switch. The rectifier characteristics are then in quadrant *I* and those of the inverter are in quadrant *IV*.

Reversing systems

The reversing drive has a switch in the armature circuit, but in some cases, and especially for drives with a short time cycle and servo systems with zero mis-match, it is necessary to arrange for continuous control without a switch in the armature circuit. It is then advisable to use systems with two sets of bulbs. It should be noted that for a long period of time articles have been published in the foreign press on reversing drives with a switch in the armature circuit, but recently there has been a tendency to change over to systems with two sets of rectifier bulbs for large drives. The power circuits of mercury-arc rectifiers with two sets of bulbs have been somewhat improved in recent years and they have become a better economic proposition since the "counter-parallel" system has been adopted. The "cruciform" system is rarely used.

YEAR
1961

"Mercury-arc exciters"

For a long time, relay-contactor systems were used for the excitation of electrical machines in controlled d.c. drives. Contactless systems of excitation have since been developed and amplidyne systems in particular. For large machines, amplidyne excitation systems represent a multi-stage system in which an amplidyne with a longitudinal or transverse field is used as the first stage.

The amplidyne allows adequate stabilization of the transient behaviour, but reductions in the duration of transient behaviour and their associated increase in productivity are limited by the inertia of the stage system of excitation. A mercury-arc rectifier is a delay-free apparatus, and therefore its use in excitation systems for large d.c. drives opens up new possibilities both as regards higher productivity and new flexible and reliable static systems of excitation.

It is proposed to refer to mercury-arc rectifiers which are used for electrical machine excitation as *mercury-arc exciters*. Mercury-arc exciters are not only used when the amplidyne system of excitation is a multi-stage one, but whenever high-speed super-quality control is

required.

Mercury-arc exciters may be reversible or irreversible exactly like their rectifier counterparts.

Mercury-arc exciters which maintain the same direction of current at the output can be used for excitation of generators and the motors of non-reversing drives. Those which do provide for the reversal of current can be used for the excitation of generators and motors in reversible drives.

The power P_r of the rectified output of a mercury-arc exciter depends on the forcing factor which is required for minimizing transient behaviour and is given by the expression

$$P_r = k_f U_d I_d 10^{-3} \text{ [kW]}, \tag{2}$$

where U_d is the rated voltage of the excitation winding of the electrical machine, I_d the rated excitation current of the electrical machine, and k_f the forcing coefficient.

Under rated conditions a mercury-arc rectifier operates with large control angles, which ensures large amplification factors and eliminates the effect of variations in the supply voltage on the generator voltage if the control system is correctly designed. With forcing, the control angle is considerably reduced and the rectified voltage at the output of a mercury-arc exciter reaches 100 per cent, which in relation to the rated voltage of the excitation winding of the electrical machine is $k_f U_d$. On extinction of the field the mercury-arc exciter acts as an inverter ($\alpha > \pi/2$) and the electromagnetic energy stored in the excitation winding of the generator is returned to the network.

The power circuits of mercury-arc exciters can be made like those of mercury-arc rectifiers used for controlling the armature voltage. Since the inductance of the excitation winding of an electrical machine is considerable, mercury-arc exciters could utilize a minimum of phases, i.e. use could be made of a full-wave system of rectification, but three-phase systems are used for the sake of reliability. If one of the bulbs is out of order in the full-wave system, the electrical machine may practically lose its excitation, since the excitation current is then equal to $2U/\omega L$ and it is small if L is considerable.

In the general case the number of phases on the rectified current side depends on the design of the electrical machine and the bulbs used in the mercury-arc rectifier. Use may sometimes be made of hot cathode bulbs for the excitation of large generators. Pool cathode bulbs are generally used in mercury-arc exciters for the low-speed motors used in

the iron and steel industry and mining, owing to their considerable excitation currents.

If the direction of rotation of the motor is changed by reversing the field, then in order to obtain an acceptable reversing time for certain equipments, the power of each set of rectifier bulbs in a mercury-arc exciter is about 10 to 15 per cent of the power of the set of bulbs in the armature circuit. The further increase in power that might otherwise be obtained by forcing, or a shorter reversing time, is limited by the conditions of commutation. If machines with a laminated yoke are used, the field can be reversed in 0.2 to 0.7 sec depending on the power of the motor. Reversing drives can be produced for plant with a considerable time cycle in which the motor excitation field is reversed.

YEAR 1961

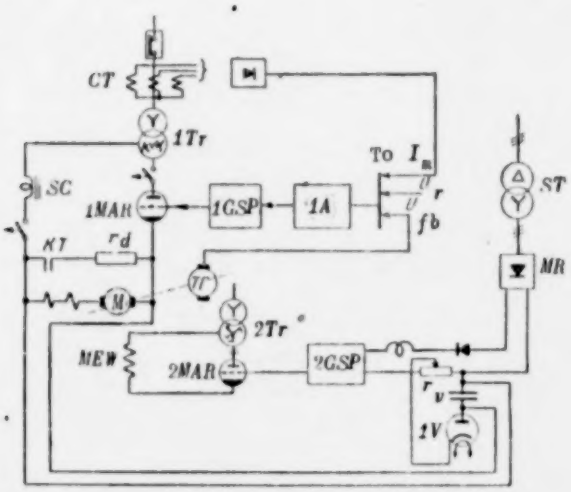

Fig. 4. Simplified circuit diagram of a non-reversing MAR drive of a light-section 350 rolling mill.

1 Tr – anode transformer of armature circuit switch; *2 Tr* – anode transformer of mercury-arc exciter; *1MAR, 2MAR* – mercury-arc rectifiers; *M* – motor; r_d – dynamic braking resistance; *SC* – smoothing choke; *MEW* – motor excitation winding; *KT* – braking contactor; *CT* – current transformer; *1GSP, 2GSP* – grid supply panels; *MR* – main voltage rectifier; *ST* – supply transformer of main voltage rectifier; *1V* – gas-filled rectifier (gazotron); r_v – variable resistance; *1A* – amplifier of armature voltage control system.

Hybrid control

In blooming mill drives speed is controlled up to fundamental speed by varying the armature voltage and at higher speeds by varying the excitation current of the motor. The presence of controlled mercury-arc rectifiers in two circuits (i.e. the armature and excitation circuits) implies that the control system has to satisfy certain requirements which if left unfulfilled would result in sudden changes in current, flashover and other fault conditions.

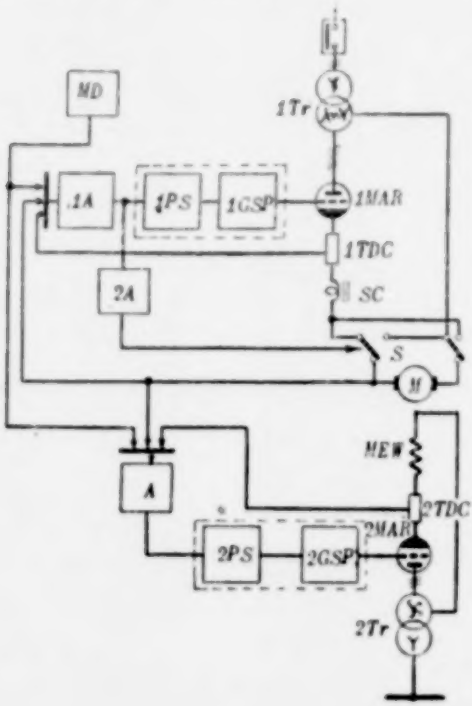

Fig. 5. Functional block-diagram of a hybrid control system for a reversing drive.

1 Tr, 2 Tr – anode transformers; *1 TDC, 2 TDC* – d.c. transformers; *1 MAR, 2 MAR* – mercury-arc rectifiers; *1A* – regulator for voltage applied to armature circuit; *A* – regulater for excitation current; *1 PS, 2 PS* – phase shifting systems; *1 GSP, 2 GSP* – grid supply panels; *MD* – master device; *M* – motor; *MEW* – motor excitation winding; *SC* – smoothing choke; *S* – switch.

By way of illustration Fig. 4 shows a simplified fundamental circuit diagram for the drive of a 350 light section rolling mill using this type of hybrid control. The speed of the roll motor is controlled at first by varying the armature voltage. Afterwards, when the armature voltage reaches a pre-determined level, the "gazotron" (gas-filled rectifier) *1V* fires and the resistance in the magnetization winding circuits of the peak transformers is shorted, which alters the control angle of the mercury-arc rectifier in the excitation circuit of the motor and weakens the field.

Figure 5 shows a functional block-diagram of the hybrid control system of a reversing drive with a switch in the armature circuit. Both in this circuit and in those of non-reversing drives, a system of interlocking is used which only allows the field to be weakened at a predetermined value of the armature voltage.

YEAR 1961

The control of MAR drives

An MAR drive control system is defined as the complex of apparatus which participates in forming the control law. In accordance with this definition, that whole range of contact and contactless apparatus which is widely used in industrial drives for protection and starting, etc, is of no concern here. The control system elements under consideration in this paper are the amplifying and shaping devices and the electrical pickups.

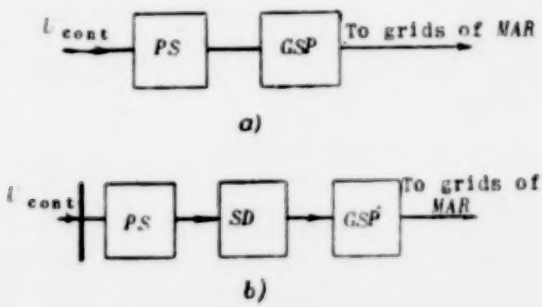

Fig. 6. Functional block diagram of a grid control system with controlled semiconductor rectifiers.

a – system with transistors in grod supply panel; b – system with transistors in the grid supply panel and phase shifting; *PS* – phase shifting system; *SD* – shaping device; *GSP* – grid supply panel; *MAR* – mercury-arc rectifier.

Increases in machine productivity are associated with larger drive outputs and faster operating speeds. An increase in speed makes exacting demands on the quality of the control system and its individual elements. In recent years there has been a tendency to replace electromagnetic apparatus by transistors in MAR control systems. All kinds of transistorized circuits have been developed, but functionally they all fall into either of two categories (see Fig. 6).

In the functional block-diagram in Fig. 6*a* the conversion of a sinusoidal voltage into a trigger pulse of given amplitude, width and slope is performed by transistors. The presence of active elements in the grid supply panel *GSP* allows a considerable reduction in the power of the static phase-shifting device *PS* and an improvement in the *Q*-factor of the control system, since low-power static phase shifters with a variable (alternating) active arm are then practicable. The method of varying the resistance of the active arm was originally proposed by Shipillo [5].

The majority of rectifier control systems fit the block-diagram in Fig. 6*b*. The principle of sawtooth voltage cut-off is used in the phase-shifting system. A control voltage is connected counter to the output of the sawtooth voltage generator and if these voltages are equal, the output voltage of the phase-shifting system is zero. The instant in time when the output voltage of the phase-shifting system is zero is moved in phase relative to the supply voltage on variation of the control voltage. This method of control has been referred to elsewhere as the "vertical" method. Sometimes a sinusoidal voltage is connected counter to the control voltage of the phase-shifting system and the instant of zero output voltage of the phase-shifter is then given by the expression

$$\omega t = \theta = \sin^{-1} \frac{U_{cont}}{U}. \qquad (3)$$

The instant of zero output voltage of the phase shifter is precisely the moment when the shaping process begins in the shaping device *SD*, which consists of a transistor and differentiating "cell", and the moment when the positive trigger pulse is supplied.

Transistorized rectifier control systems are practically instantaneous and it is natural to require that the quality of all the other control elements should be equally as good.

Magnetic amplifiers are now widely used in MAR drive control systems. To improve the *Q*-factor of control systems using magnetic amplifiers, it is necessary to employ high-frequency amplifiers which require special supply sources.

Fig. 7. Block-diagram of a device with magnetic amplifiers and an independent supply source.

DCS – d.c. supply; *FC* – frequency converter; *MA* – magnetic amplifier.

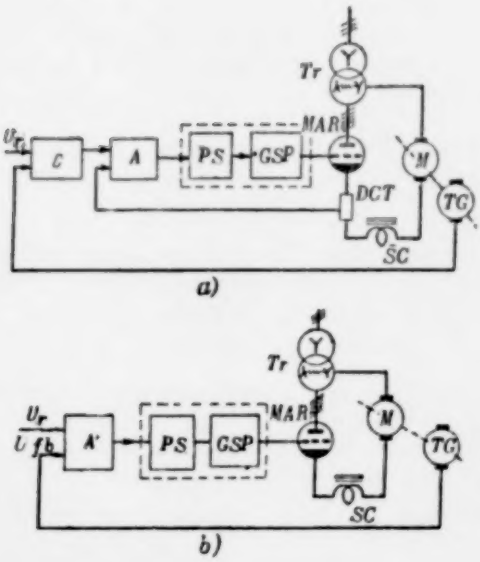

Fig. 8. Block-diagram of speed control system.

a – system with "electrical" comparison and negative current feedback; *b* – system with "magnetic" comparison; *Tr* – anode transformer; *MAR* – mercury-arc rectifier; *DCT* – d.c. transformer; *M* – motor; *TG* – tachometer generator; *C* – comparison circuit; *A* – amplifier of regulator; *PS* – phase shifting system; *GSP* – grid supply panel.

To dispense with special supply sources it is expedient to supply the magnetic amplifiers from an independent h.f. source in the form of a blocking oscillator or symmetrical transistorized multi-vibrator. It

should be pointed out that the frequency of such sources can be chosen in the light of constructional considerations. Various magnetic amplifier circuits with independent supply sources have been devised, but they all contain the elements indicated in Fig. 7.

A number of functional block-diagrams will now be considered to illustrate the design of MAR drive control systems.

Figure 8 shows functional block-diagrams of a system of speed control. In Fig. 8*a* the first element compares the desired speed with the actual speed as measured by a tachometer generator. The element is, as it were, a speed governor whose output defines the magnitude of the armature current. The second element compares the desired armature current, as obtained at the output of the first element, with the actual armature current as measured by a d.c. transformer or simple transformer in the a.c. circuit. Current feedback provides a simple means of stabilizing the system.

The system in Fig. 8*b* is not provided with current feedback and all the control signals are added, shaped and amplified in the first element of the control circuit.

Tachometer generators measure the speed in speed-control systems. These generators have to satisfy exacting demands if the demands made on the control system as a whole are stringent. The simplest form of speed-control law is that represented by expression (1).

The terminal voltage of an "ideal" tachometer generator is

$$U_{fb} = c_e \omega.$$

The terminal voltage of a real tachometer generator can be written in the form

$$U_{fb} = U_s + U_n, \tag{4}$$

where U_s is the useful signal voltage which is proportional to the speed, and U_n the voltage of the non-attenuated noise signal for the particular speed.

The expression for the noise signal is

$$U_n = m_1 \sin k_1 \omega t + m_2 \sin k_2 \omega t + m_3 \sin k_3 \omega t, \tag{5}$$

where

$$m_1 = \frac{\Delta U_{cp}}{K_{fb} U_{fb}}; \quad m_2 = \frac{\Delta U_{rp}}{K_{fb} U_{fb}};$$

$$m_3 = \frac{\Delta U_{mp}}{K_{fb} U_{fb}}; \tag{6}$$

and ΔU_{cp} is the voltage amplitude of the collector oscillations, ΔU_{rp} the voltage amplitude of the reverse oscillations, ΔU_{mp} the voltage amplitude caused by oscillation in speed owing to eccentricity in the coupling of tachometer generator to the driven shaft, and $k_1\omega$, $k_2\omega$ and $k_3\omega$ the frequencies of the collector, reverse and "mechanical" oscillations respectively.

When considered with (4) and (5), expression (3) [sic] takes the form

$$U_c = \mu [U_r - K_{fb} U_{fb} (1 + m_1 \sin k_1 \omega t + \\ + m_2 \sin k_2 \omega t + m_3 \sin k_3 \omega t)]. \tag{7}$$

A speed law of type (7) in a delay-free control system results in variation of the current in the main circuit and in speed variation if the moment of inertia of the motor and driven device is low. For partial elimination of such variation, use may be made of negative current feedback, but this reduces the amplification factor of the system, or alternatively powerful stabilizing feedback, although this adversely affects the dynamic properties of the system. High-frequency oscillations of the noise signal can be filtered out without difficulty if the degree of speed control is "light", but it is a different matter with reverse oscillations and mechanical speed oscillations and the dynamic properties of the system suffer accordingly. This case has been specially considered in order to show that exacting demands have to be met by all the elements of the entire control system if an instantaneous rectifier control system with a high dynamic Q-factor is required. There is no justification for a delay-free rectifier control system on its own.

Figure 9 shows the functional block-diagram of a reversible MAR drive in which use is made of a mercury-arc rectifier with two sets of bulbs. The "counter-parallel" system is employed for the rectifier. A special circuit is used to limit the balancing current which arises in a mercury-arc rectifier with two sets of bulbs. The d.c. transformers *1TDC* and *2TDC* are included in the circuit for each set of bulbs. They are magnetic amplifiers with series-connected load windings.

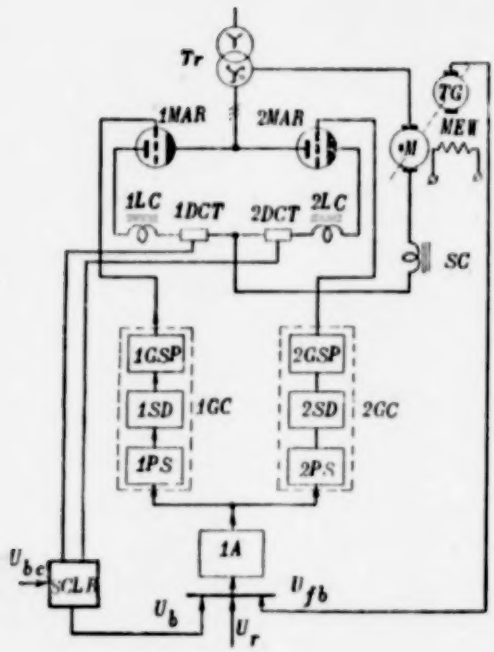

Fig. 9. Block-diagram of reversing MAR drive with two sets of bulbs.

Tr – anode transformer; *1 MAR, 2 MAR* – mercury-arc rectifiers; *1 LC, 2 LC* – limiting chokes; *SC* – smoothing choke; *1 DCT, 2 DCT* – d.c. transformers; *1 GSP, 2 GSP* – grid supply panels; *1 SD, 2 SD* – shaping devices; *1 PS, 2 PS* – phase shifting systems; *1A* – regulator amplifier; *SCLB* – special circuit for limiting balancing current; *1 GC, 2 GC* – grid control systems for rectifiers; *M* – motor; *MEW* – motor excitation winding; *TG* – tachometer generator, U_r – reference voltage; U_{bc} – setting for magnitude of balancing current; U_b – voltage regulating the magnitude of the balancing current; U_{fb} – speed feedback voltage.

The balancing current and operating currents of the main circuit flow through the control windings of the d.c. transformers. The voltages in the secondary windings of the d.c. transformers will be different depending on the magnitude of the operating current and balancing current. This voltage is "rectified" in the special circuit (*SCLB*)

for limiting the balancing current, and it is compared in the amplification circuit with the "desired magnitude" of the balancing current. The deviation of the actual balancing current from the desired magnitude automatically alters the control angles of both sets of bulbs.

In a number of cases a control system with limitation of the balancing current provides better dynamic drive characteristics. The system illustrated in Fig. 9 can also be adopted to mercury-arc exciter control systems for generators in reversing drives.

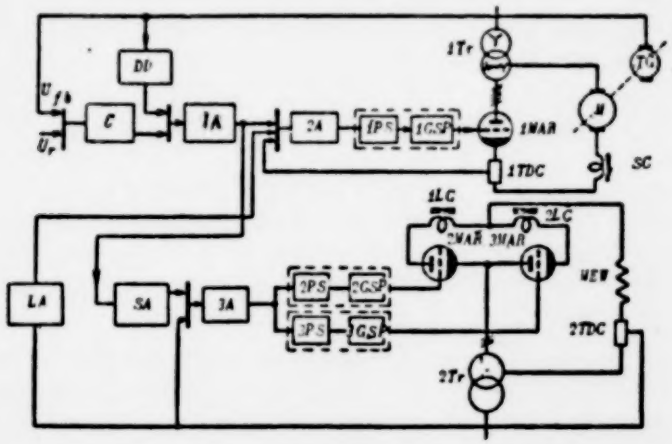

Fig. 10. Block-diagram of speed control system with two sets of rectifiers in the excitation circuit.

1 Tr, *2 Tr* – anode transformers; *1 MAR*, *3 MAR* – mercury-arc rectifiers; *1 LC*, *2 LC* – limiting chokes; *SC* – smoothing choke; *1 DCT*, *2 DCT* – d.c. transformers; *M* – motor; *MEW* – motor excitation winding; *TG* – tachometer generator; *C* – comparison circuit; *DD* – differentiating device; *1A* – adding amplifier; *2A* – amplifier of regulator for the armature circuit voltage; *3A* – amplifier of regulator for excitation current; *SA* – amplifier of excitation circuit switch; *LA* – amplifier for limiting of armature current; *1 PS* - *3 PS* – phase shifting systems; *1 GSP* - *3 GSP* – grid supply panels.

Figure 10 illustrates a possible drive system in which the speed is controlled by a mercury-arc rectifier in the excitation circuit of the motor. The armature circuit is supplied from the mercury-arc rectifier *1 MAR* which maintains the polarity of the rectified current constant. The excitation winding is supplied from the converter *2 MAR* which ensures reversal of polarity of the rectified current.

Unlike the system illustrated in Fig. 8, that in Fig. 10 provides for limited acceleration by virtue of the differentiating device *DD* whose input is connected to the tachometer generator. Reversal of the excitation current takes place on reversal of polarity at the output of the adding amplifier *1A*. On reversal of the field the output voltage of amplifier *1A* is limited by the limiting amplifier *LA* and the armature current decreases to zero. While the excitation current is steadying itself, it is necessary for the voltage at the output of *1A* to be limited so much that the rectifier in the armature circuit is "off". After the end of the process of field reversal, the system of acceleration limiting again comes into operation and protects the system from momentary excessive acceleration.

The reliability of MAR drives

The reliability of an MAR drive mainly depends on the reliability of the rectifier. In recent years a number of papers have been published in the U.S.S.R. and abroad [7,8,9, *et al.*] in which the probability of arcbacks has been determined and methods of reducing their probability have been suggested.

Actually the probability of arcbacks is only the main criterion of reliability for mercury-arc rectifiers operating as rectifiers (with pool cathode bulbs). In industrial plant where the mercury-arc rectifiers operate with large overloads, use has begun to be made in the U.S.S.R. of mercury-arc rectifiers with series-connected bulbs in order to reduce the probability of arcbacks.

It has been shown [9,10] that with series-connected bulbs the probability of arcbacks is equal to the product of the probabilities of arcbacks of the individual bulbs, and it can therefore be assumed that no arcbacks will occur at a voltage of 1000 V.

Figure 11a shows the simplified power circuit of a rectifier for the irreversible MAR drive of a rolling mill with a ratio of the load current amplitude to its mean value of 4 (at a mean current of the order of 3000 A). Arcbacks are very rare in this gear.

In the general case the reliability of an MAR drive depends on other factors besides the probability of arcbacks (which result in short circuits in the anode circuit): (*a*) the probability of extinction of the excitation arc in excitrons and the probability of failure to fire in ignitrons; (*b*) the probability of "break-through" of the grid; (*c*) the probability of faulty grid control.

Extinction of the excitation arc and the failure to fire of

ignitrons results in a short circuit in the load circuit when the rectifier is operating as an inverter. It is easy to show that there is twice the probability of short circuits in mercury-arc rectifiers with

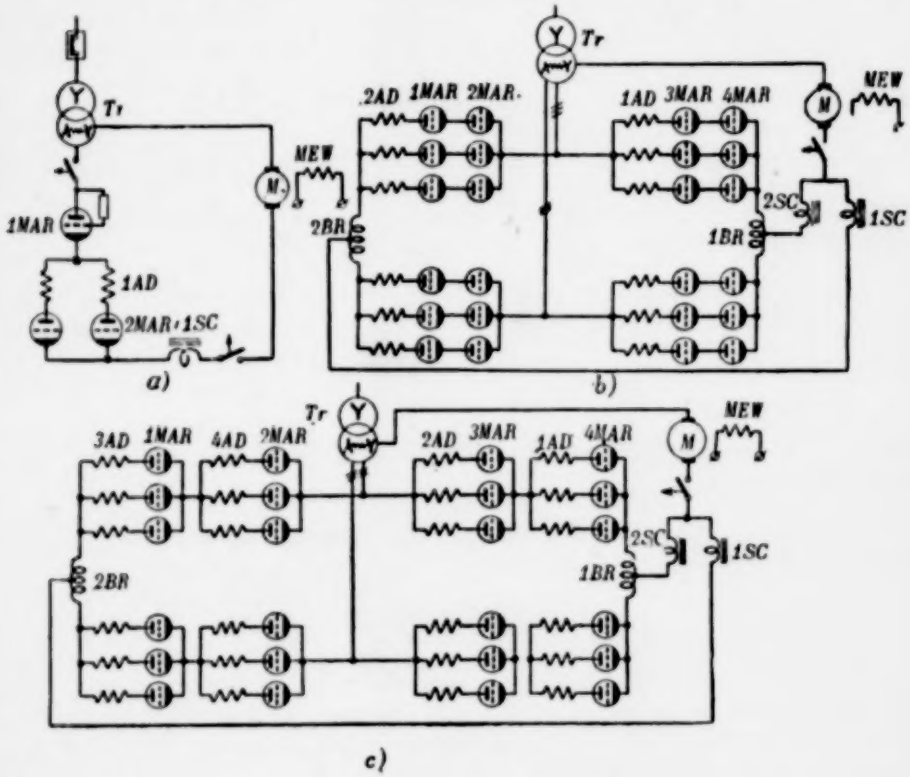

Fig. 11. Simplified circuit diagram of mercury-arc rectifier with series-connected bulbs.

a – circuit of converter for non-reversing drive; *b* – circuit of converter for reversing drive (with one set of anode dividers); *c* – circuit of divider for reversing drive with two sets of anode dividers; *Tr* – anode transformer; *1 MAR*-*4 MAR* – mercury-arc rectifiers; *1 AD* - *4 AD* – anode dividers; *1 SC* - *4 SC* – smoothing chokes; *1 Br*, *2 BR* – balancing reactors; *M* – motor; *MEW* – motor excitation winding.

series-connected bulbs (in this case the probabilities are added). An improvement in the reliability of MAR drives requires a great deal of theoretical and experimental research in order to obtain statistics of fault probability in particular bulbs and the rectifier as a whole.

The lack of statistical data results in a disproportionate increase in prime cost and running expenses for a small increase in reliability.

For example, Fig. 11*b* shows the circuit of a mercury-arc rectifier for a reversing rolling mill where series-connected bulbs are used. If both the bulbs in the series "chain" are controlled, the control system is greatly complicated, which can result in reduced reliability. If, however, the power circuit illustrated in Fig. 11*c* is used, there is nine times greater probability of arcbacks compared with that in Fig. 11*b*, but the control system itself is much simpler (in Fig. 11*c*).

The following calculation will show that a nine-fold increase in the probability of arcbacks is not very important in practice.

Suppose that one arcback occurs daily in each of the 18 bulbs of the three parallel circuits of a rectifier, i.e. the arcback probability is

$$P_1 = \frac{n}{Tf} = \frac{1}{24 \cdot 3\,600 \cdot 50} = 23 \cdot 10^{-8},$$

where n is the number of arcbacks, T the duration of arcback, and f the network frequency.

The probability of arcback with series-connected bulbs in each parallel circuit is

$$P_2 = P_1^2 = 5.3 \cdot 10^{-14},$$

i.e. an arcback will occur once in approximately 10^4 years. Naturally, if this figure is increased nine times there is in practice no significant increase in reliability, whereas operating costs are considerably reduced by the simpler system.

This example shows that the design of mercury-arc rectifiers has to be approached from all possible angles and that reliable gear can be designed which is cheaper to run. The scientific approach to the design of "reliable" MAR drives thus requires further investigation of currently produced rectifiers with a view to determining their reliability criteria.

Translated by O.M. Blunn

REFERENCES

1. J. Förster and H. Steinmüller; *AEG Mitt.*, No. 11/12 (1958).

2. D. Ströle and H. Vogl; *Regelungstechnik*, 6 (1960).

3. Ya.Yu. Solodukho; *The control apparatus of electric drives for continuous hot rolling mills (Avtomatika elektroprivodov nepreryvnykh stanov goryachei prokatki)*. Metallurgizdat (1960).

4. E.L. Ettinger, B.M. Gutkin and P.M. Borodavchenko; *Elektrichestvo*, No. 9 (1956); No. 1 (1957).

5. V.P. Shipillo; *MAR grid control systems for automatic electric drives (Sistemy setochnogo upravleniya rtutnymi vypryamitelyami dlya avtomaticheskikh elektroprivodov)*. Gosenergoizdat (1961).

6. J. Förster; *AEG Mitt.*, No. 11/12 (1958).

7. Th. Wasserab; *BB Mitt.*, No. 4/5 (1955); No. 3/4 (1956); No. 11 (1956).

8. M. Danders; *AEG Mitt.*, No. 11/12 (1958).

9. L.S. Fleishman; *Elektrichestvo*, No. 9 (1959).

10. J. Slepian and W.E. Pakala; *El. Eng.*, No. 6 (1941).

YEAR
1961

INVERTER SUBSTATIONS FOR OUTLYING REGIONS WITHOUT LOCAL POWER STATION COUNTER-E.M.F.'s*

N. M. MEL'GUNOV

(Leningrad)

(Received 2 December 1959)

YEA
196

The economical supply of electricity to outlying regions far from power systems and large power stations is an important aspect of the programme for general electrification in the U.S.S.R.

A d.c. transmission line costs much less than a comparable three-phase a.c. line. Centralized supply is therefore economic over much greater distances. Many new local power stations need not be built and some existing ones may be closed down.

The economy of d.c. transmission is not however determined by power and distance in absolute terms, but by the relationship between them. A small output can only be transmitted economically over a correspondingly shorter distance [1,2].

The essential problem is to develop simple and reliable terminal inverter substations. This is particularly so as regards inverter substations at the receiving end which have to operate with or without local power stations in the system (i.e. with or without counter-e.m.f.'s). This is a necessary condition for the exploitation of d.c. transmission on the largest possible scale.

In this paper it is proposed to consider and compare the principal inverter substation systems for operation into receiving systems without the counter-e.m.f.'s of local power stations. Such substations may differ from each other in design, performance, cost and reliability.

---

* *Elektrichestvo*, No. 11, 42-47, 1961.

1. Inverter substations with synchronous condensers

In this type of inverter substation the counter-e.m.f. required in the inverter for current commutation and the reactive power required for its operation and supplying the loads of the system are produced by a synchronous machine (see Fig. 1*a*) of a power 130 to 150 per cent of the rated active power of the substation inverter.

In order to improve the operating stability of the inverter in the presence of sudden load variations and provide an approximately sinusoidal voltage across its bus-bars, special measures must be taken to reduce the reactance of the machine. The operating stability of the inverter is favourably affected by lower values of the system power factor for an appropriately higher machine reactive power and excitation current; larger inertia constants of the machine also have a favourable effect.

YEAR
1961

Such a machine (synchronous condenser, generator) can be started at speeds and frequencies up to and including rated values by various methods from a small local power station or, if this is not available, from a special starting motor at the substation (e.g. a diesel engine). A synchronous condenser can be started direct by this type of prime mover or by an intermediate motor-driven generator. After running up the condenser and supplying the counter-e.m.f. to the inverter, the latter can be brought into operation in the usual way by control pulses to the valve (inverter) grids from the condenser bus and the supply of voltage along the line from the inverter. The power required subsequently for the operation of the condenser (and increasing its speed to the rated value if it has been below that figure) can be supplied from the d.c. line.

It is important to stress that in this type of inverter substation where the counter-e.m.f. is produced by a synchronous condenser, the control pulses must be supplied to the valves of the inverter for its stable operation from the bus of the synchronous condenser in the appropriate phase and not from an extraneous source of arbitrary phase.

In steady-state conditions the control system of this type of d.c. transmission must (*a*) maintain the quenching angle δ constant within given limits, (*b*) maintain rated voltage E_b across the inverter bus bars and (*c*) maintain the frequency f constant.

As regards the first requirement, this is necessary on the one hand because an excessive increase in δ results in an increased consumption of reactive power by the inverter and abrupt variation of the voltage across the inverter bulbs (a deterioration in operating conditions), whilst on the other hand a reduction in δ below 15 to 18° is dangerous

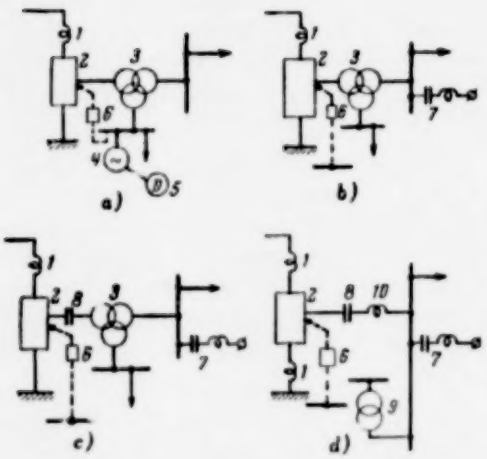

Fig. 1. Types of inverter substation for operation into a receiving system without the counter-e.m.f.'s local power stations.

a – system 1, with synchronous condenser; *b* – system 2, with parallel capacitor filter banks; *c* – system 3, with series-parallel capacitor phase compensation; *d* – system 4, with capacitive connexion of bridge converters; *1* – line reactor; *2* – bridge; *3* – transformer; *4* – synchronous condenser; *5* – motor; *6* – grid control; *7* – capacitor filter-banks; *8* – series capacitor banks; *9* – auxiliary and local supply transformer; *10* – phase reactors.

from the point of view of inverter reversal. The angle δ must therefore be held roughly constant during load variation or changes in inverter conditions.

The curves shown in Fig. 2 for the variation of the rectifier control angle α_r and the reactive power Q_c of the synchronous condenser as a function of the inverter load P_c have been calculated for an actual transmission system. Here the angle δ was held at appropriate constant values and conditions were also created to maintain f and E_b constant. The broken lines in the same diagram illustrate the upward shift of the α_r characteristic for δ = const when the rectifier voltage is increased by 5 per cent (e.g. by a tapping adjustment).

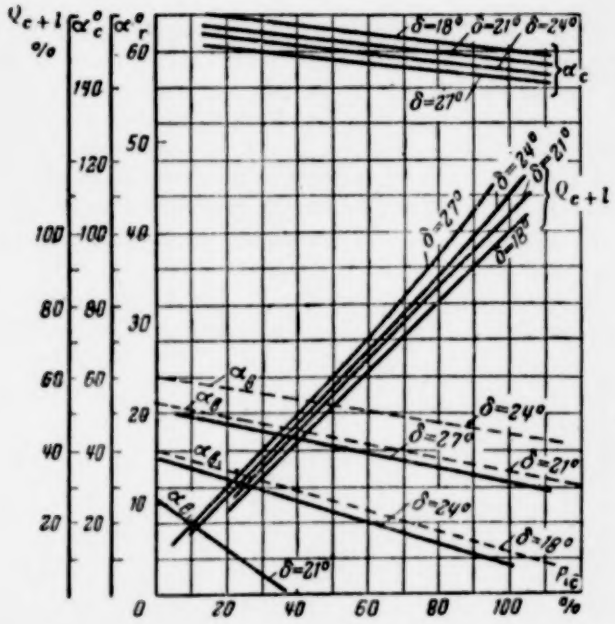

Fig. 2.

Various control systems can be employed in the design of an inverter with a synchronous condenser. The most efficient is as follows:

a) the angle δ is held constant across each inverter bulb by the supply of control pulses of appropriate phase α_c which is determined automatically for subsequent ignitions;

b) the voltage is automatically held constant on the inverter busbars by controlling the excitation system of the synchronous condenser;

c) the frequency of the receiving system is held constant by a frequency regulator which acts on the control angle α_r of the rectifier.

It is presupposed that the rectifier is provided with a maximum current regulator, so that the angle α_r can be adjusted by changing the setting, and that the inverter is provided with a minimum current regulator.

2. Inverter substations with parallel capacitor banks

Tests and calculations have established that synchronous condensers can be dispensed with, in which case, in order to ensure current commutation in the inverter and cover the reactive loads of the inverter in the network, use may be made of parallel capacitor banks (see Fig. 1*b*) in the form of several banks of filters for the higher current harmonics. For a six-phase inverter it is recommended that filters be used tuned to harmonics 5, 7, 11 and 13 with the bank power of the individual filters diminishing according to the increase in the harmonic number, and the overall bank power roughly equal to the reactive power consumption of the inverter and network at the rated inverter load. The presence of a set of such filters (or the first three of them) ensures that the appropriate current harmonics are short-circuited and the bus-bar voltage of the inverter is therefore approximately sinusoidal (see Fig. 3).

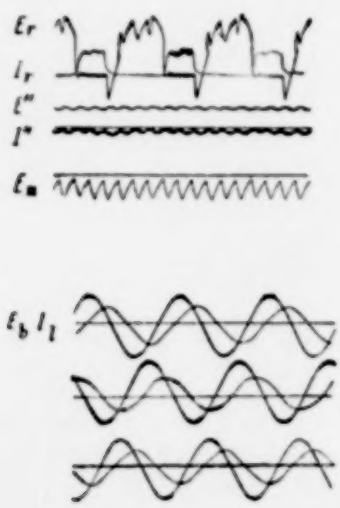

Fig. 3. Oscillograms of normal inverter conditions with a sinusoidal voltage ensured in the system by a set of parallel filter-banks.

The grid control of such an inverter must be effected from a separate independent control pulse source. The pulses are fed to the inverter bulbs at a fixed frequency (f = 50 c/s).

Figure 4*a* shows a vector diagram for the fundamental harmonic of the

current of an inverter with parallel static phase compensation under normal conditions. Figure 5 shows typical characteristics of the main operating indices when the inverter is regulated for varying active load. Changes in the angle δ are held within prescribed limits by automatic connexion and disconnexion of the individual filter banks. With decreasing active inverter load, the overall power of the connected capacitors is gradually reduced by disconnecting the individual filter

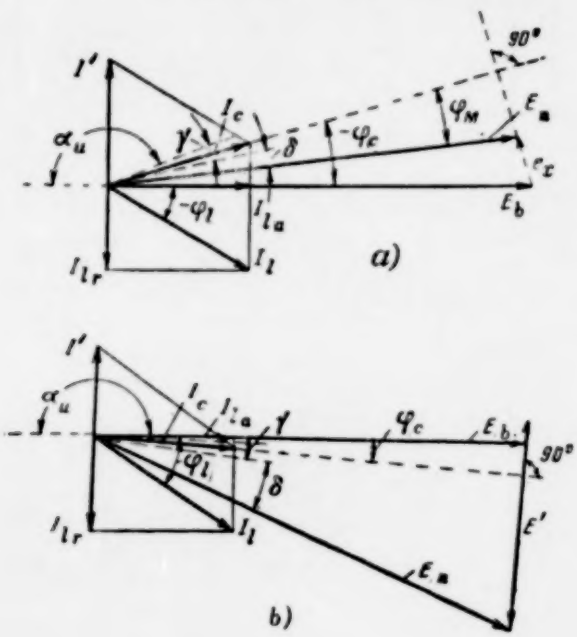

Fig. 4. Inverter vector diagrams.

a – for system with parallel static phase compensation; b – for systems with series-parallel static phase compensation.

banks (see Fig. 5) one (or a few) at a time in a definite sequence with increasing angle δ. The individual filter banks are disconnected in such a way that δ is not reduced below a given level (18 to 20°) when a bank is disconnected. In this way the operating stability of the inverter is maintained; as far as possible provision is also made for keeping the complete set of filters of all harmonics in the zone of normal load variations according to the daily graph (e.g. 50 to 100 per cent) in order to ensure an approximately sinusoidal voltage on the inverter bus-bars; only if great load reductions occur is the disconnexion of filters *en bloc* permitted (e.g. the 7th and 11th).

The voltage on the a.c. bus-bars of the inverter (of the receiving system) is held constant as required by gradual changes in the control angle α_r of the rectifier. These are made automatically according to deviations of the voltage from its rated value.

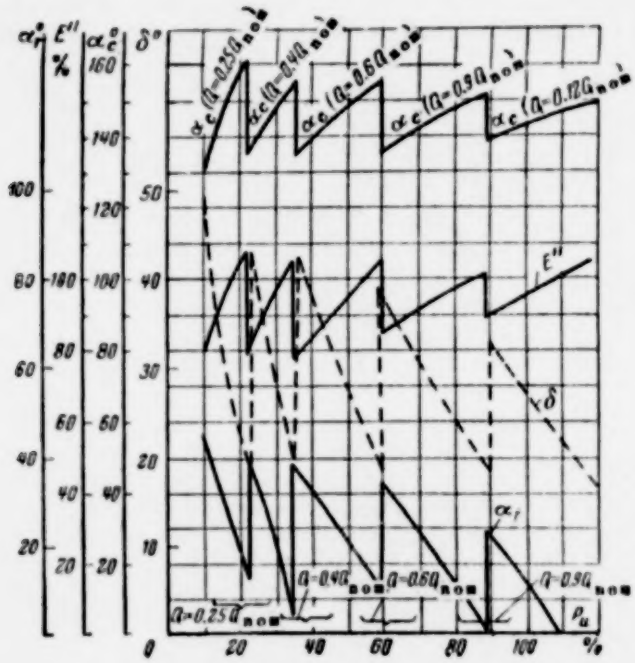

Fig. 5.

The rectifier voltage can be controlled in this way by altering the setting of the maximum current regulator.

It is obvious that the use of control pulses at a fixed repetition rate from an extraneous source removes the problem of maintaining the frequency of the inverter system constant by special control methods (a considerable simplification), and the control angle α_c of the inverter and the angle δ become functions of the inverter mode or state and cannot be varied or regulated arbitrarily (as in the case of a synchronous condenser).

An inverter with parallel capacitors is started simply by the supply of voltage from the rectifier to the inverter; if this method is used, the filter banks (or some of them) must first be connected to the bus-

bars of the inverter, and the setting of the maximum current regulator of the rectifier must so limit the current that no significant increase in voltage is produced on starting by the flow of inverter current through the capacitance connected to the bus-bars.

3. Inverter substations with series-parallel capacitor phase compensation

This type of system is illustrated in Fig. 1*c* [3]. The control pulses are again supplied to the inverter bulbs from an independent source at a set frequency (f = 50 c/s). The capacitor banks are connected in series with a transformer in the connecting phase of the bridge "converter". Each of these banks is in turn composed of smaller individual sets which are connected in series and parallel; the series phase bank passes alternating current during the operation of the converter and its half-waves are approximately rectangular in shape. As a result, a trapezoidal voltage is produced on the bank capacitance which can be replaced quite accurately by a corresponding fundamental sine curve.

Part of the capacitance is connected to the a.c. bus-bars of the inverter (the system bus-bars) in the form of an assembly of parallel filter banks which take part in the commutation of the inverter current, in covering the reactive load and in ensuring a sinusoidal voltage.

Figure 4*b* shows a rough vector diagram of such an inverter under normal operating conditions. The fundamental harmonic of the trapezoidal voltage is represented by the vector E'. The optimum value of E' must be 60 to 80 per cent of the bridge phase voltage E_a.

It will also be seen from this diagram that the series capacitance retards the voltage E_a (by the addition of the voltage vector E'), whilst the parallel capacitance advances the inverter current vector I_c (as a result of the addition of the bank current vector I'), ensuring the lead of the inverter current vector I_c over the voltage vector E_a and the presence of a quenching angle δ, which is necessary for successful current commutation and a stable inverter performance.

The power and capacitance of the series and parallel capacitors is selected by analysis of the plant criteria and the system power factor. From test results and calculations, about 50 to 70 per cent of the total capacitor power is connected in series and about 30 to 45 per cent is in parallel. The total power of the capacitors in this system is approximately the same as that of the foregoing system with parallel static phase compensation.

Figure 6 illustrates the characteristics of an inverter with series-

parallel static phase compensation. In this case it is advisable to connect two thirds of the overall capacitor power in series and about one third in parallel.

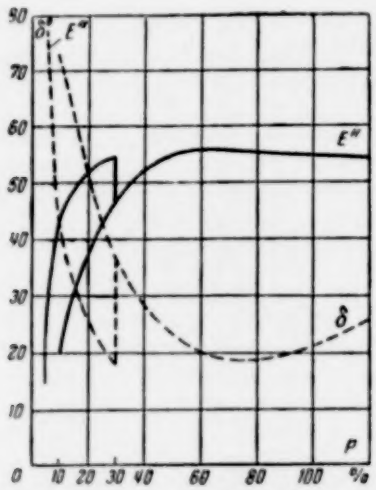

Fig. 6.

It will be seen from Fig. 6 that the angle δ and rectified voltage E'' are practically constant even if the inverter load is subject to wide variations for unchanged series- and parallel-connected capacitances.

This is the advantage of this particular system over the last system (see Section 2), since wide load variations require no connexion and disconnexion of the banks or "deep" voltage regulation on the rectifier side unless an unusually large load reduction occurs (below about 30 per cent). In this event the rectified voltage can be held constant by disconnecting part of the power of the parallel capacitors (see Fig.6). (Approximately 35 per cent of the power of the parallel capacitors is disconnected for a reduction in load to 30 per cent.)

It is therefore clear that in this system the bus-bar voltage of the inverter can be controlled either by the angle α_r of the rectifier, or, in the main range of load variation, merely by regulating the transformers on load, since the limits of such regulation are usually small.

The starting of the inverter in this system is similar to that described in Section 2.

4. Inverter substations with capacitive connexion of bridge converters

A simpler and cheaper system is sometimes possible. Here the converter bridges are connected across series capacitors without main transformers, but with a set of parallel filter banks at the inverter bus-bars (see Fig. 1*d*) [6]. The auxiliaries and local load of the substation are supplied from a small separate step-down transformer.

The series capacitors of the bank in the phases are different in this system, in that a voltage of constant sign is produced as well as the trapezoidal alternating voltage. This constant "support" voltage is equal in magnitude to half the rectified bridge voltage if it is the one "on pole", and equal to one-and-a-half times that value if the second bridge is "on pole'.

The capacitors of the series phase banks must be chosen with both voltage components in mind [6,7].

YEAR 1961

Calculations have shown that if a total gradient of 37 to 40 kV/mm is acceptable for the insulation of the series capacitor banks (for a usual maximum gradient of the alternating component of the voltage of 17.6 kV/mm), then no increase in capacitor power is required for one bridge in an arm in connexion when a constant voltage component is present, if use is made of conventional *KPM*-type series-capacitor compensation.

The neutral point of the system can in this case be "dead"-earthed, or else earthed via a resistance (usually an inductive resistance) or via a compensating coil; in the "dead"-earth method, or if earthing via a small resistance is employed, it is necessary to have a reactor in the pole of the bridge (see Fig. 1*d*); no such reactor is required if a large earthing resistance is used; the use of high-voltage filters in star entails the use of a large inductance for neutral earthing (at a small operating current).

In order to exclude the third harmonic of current from the network, one of the transformer windings is usually connected in delta for the local load.

Low-inductance reactors (5 to 6 per cent) are usually connected in series with the capacitor banks in order to retard the commutation of current in the bulbs in the phases of connexion of the bridge.

The vector diagram and analysis of normal conditions is similar to that in Section 3.

Reliability

A hybrid system has also been proposed in which a low-power (e.g. one third of the required total power) synchronous machine and a bank of static capacitors (e.g. two thirds of the required power) are used simultaneously for purposes of phase compensation at an inverter substation. It was hoped to reduce losses by maintaining smooth continuous control of the voltage on the system bus-bars.

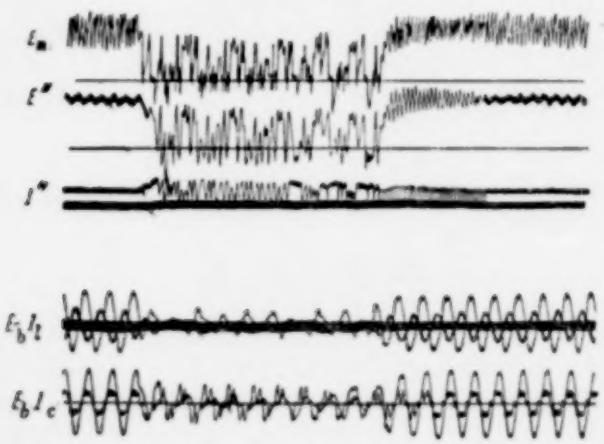

Fig. 7. Oscillograms of transient behaviour in an inverter with series-parallel static phase compensation in the presence of a momentary three-pole short circuit in the inverter system.

But investigations (and especially tests) have not confirmed that this is an expedient solution owing to its inadequate reliability in operation. If momentary disturbances occur in the operation of the inverters (e.g. failure to fire or breakdown of a bulb), or if short circuits occur, etc, reversal of the inverter usually takes place, and the process of pulling it back into operation is more difficult inasmuch as the power of the synchronous machine is lower, the corresponding inertia constant is less and the reactance in absolute terms is larger; in other words, a reduction in machine power (owing to the use of static capacitors) has a marked adverse effect on the operating stability of the machine and the inverter substation as a whole.

Even in the system with a synchronous condenser (version 1) a reduction in its excitation and loading with the voltage maintained constant (but the active load of the inverter reduced) has an unfavourable effect

on the operating stability of the synchronous machine and inverter, especially in the event of momentary disturbances to the normal operation of the inverters and system. If a disturbance occurs in the normal operation of the inverter in a system without a counter-e.m.f. and a stoppage of the synchronous machine takes place, this results in a lengthy shut-down of the system, since it takes time to re-start the machine and resume operation.

Tests on models have shown that with static systems (Sections 2,3,4) normal operation can quickly be resumed automatically after a momentary disturbance or short-circuit in the system. Automatic reclosure on the rectifier side is sometimes required in the parallel static compensation system. Systems 3 and 4 with series-parallel static compensation are the most stable. Here operation is resumed without external interference, provided an automatic device for shunting the reactor valves is used on the line reactors of the inverter [4].

YEAR
1961

Moreover, systems 3 and 4 can disconnect and connect the inverter by taking away the supply of control pulses of the inverter itself. No provision is made for this in system 2.

From test results, the stability of inverters with series-parallel static phase compensation is very high. This may be illustrated by the following example of a model. An operating loaded inverter with a normal quenching angle (δ = 18 to 20°) experienced a sudden large increase in load which reduced the angle δ and "reversed" the inverter. After a subsequent reduction in load, or on connexion of an additional parallel capacitance on the inverter bus-bars, the system resumed normal operation without any interference.

After the clearance of a short-circuit in the receiving network, different in polarity and distance (right up to the inverter bus-bars), the inverter resumed normal operation automatically. The oscillograms in Fig. 7 illustrate the case of a three-pole short-circuit in an inverter system using series-parallel static compensation.

Conclusions

1. To solve the problem of economical d.c. transmission of medium and low power, attention should be concentrated on producing simple and reliable inverter substations which are able to operate into receiving systems without the counter-e.m.f.'s of local power stations.

2. The most economical and reliable inverter substations for such outlying regions are those based on static phase compensation with series and parallel capacitor banks (the systems described in Sections 3 and 4).

3. Prototype inverter plants ought to be constructed in order to verify these conclusions under operating conditions and they should then be put into mass production.

Appendix I. Simplification of electrical calculations for operating conditions and converter characteristics

The commutating e.m.f. of an inverter at the end of a transmission line may be taken as the alternating voltage on the bus-bars; in this case a sinusoidal voltage shape must be ensured by connecting a set of filters tuned to higher harmonics of the converter current to the a.c. bus-bars.

This initial proposition is obviously correct and tests have confirmed that it is so. It considerably simplifies the analysis of normal inverter conditions, since it allows the criteria of the a.c. system at the inverter bus-bars to be ignored without loss of accuracy.

Appendix II. Correspondence with the rated voltage

In view of the possibility of designing inverter substations without main transformers, it is important to establish correspondence between the rated voltage of the system (a.c. side), the rectified voltage (d.c. transmission), and the probable number of bridges.

The relationships are given in the following table:

Rated alternating voltage, kV	Number of bridges per pole	Rectified transmission voltage, kV	Approximate power of circuit, MW
35	1	100	10 - 30
35	2	200	50 - 150
110	1	300	200 - 400
110	2	600	-
220	1	600	500 - 1000

Translated by O.M. Blunn

REFERENCES

1. Ya.M. Chervonenkis; *Long-distance d.c. transmission of low and medium power (Peredacha nebol'shikh i srednikh moshchnostei postoyannym tokom na dal'nye rasstoyaniya)*. Izd. MKKh., RSFSR, Moscow (1957).

2. N.N. Krachkovskii; *Elektrichestvo*, No. 12 (1959).

3. N.N. Mel'gunov and V.N. Vyatkin; Auth. Cert. No. 119598, 1958.

4. N.M. Mel'gunov and V.N. Vyatkin; Auth. Cert. No. 121177, 1958.

5. V.M. Kvyatkovskii; *Elect. stants.*, No. 11 (1958).

6. N.M. Mel'gunov; *The main features of circuits with capacitive connexion of bridge converters in d.c. transmission (Osnovnye osobennosti skhemy s kondensatornym prisoedineniem mostovykh preobrazovatelei v elektroperedachakh postoyannogo toka)*. Direct-current Research Institute, No. 3 (1958).

7. A.K. Gertsik; The ionization characteristics of paper-oil capacitor insulation under the influence of pulsating voltage (Ionizatsionnye kharakteristiki bumazhno-maslyanoi kondensatornoi izolyatsii pri vozdeiatvii pul'siruyushchego napryazheniya). Direct-current Research Institute, No. 2 (1957).

YEAR 1961

THE THEORY OF TRANSFORMER OPERATION WITH A MAGNETIZED SHUNT*

V. I. SHAROV

(Moscow)

(Received 28 June 1961)

Use is now being made of devices which utilize the magnetization of transformers, auto-transformers and reactors (chokes) for the voltage control of all kinds of electrical gear. Such devices are very promising in view of their many advantages: reliability, durability, continuous high-speed control, high efficiency, etc.

Magnetized shunt transformers and auto-transformers occupy a special position. Elements of a theory of operation, a method of design and the means of using them in automatic control systems have already been worked out in the Gorkii Polytechnical Institute under the direction of A.M. Bamdas [1]. However, certain fundamental aspects of the theory of these devices still require further study from the design point of view.

It is possible to apply the general theory of magnetic amplifiers, since the devices in question can be represented as magnetic amplifiers operating as transformers.

The performance of a magnetized shunt transformer (see Fig. 1) will now be analysed under the same conditions as are adopted in studying the performance of an ideal magnetic amplifier, i.e. it will be assumed that the magnetization curve of the core material is rectangular in shape and that neither loss or leakage occurs. The total m.m.f. of a closed circuit consisting of non-saturated sections of a magnetic circuit will then be zero. Suppose that the bars *I* and *II* and the shunt *III* are equal in section and that the supply voltage U_1 is such that

---

* *Elektrichestvo*, 11, 64-66, 1961.

saturation of bar *I* does not take place. Consequently there will be no saturation of bar *II* or the shunt if the latter is not magnetized.

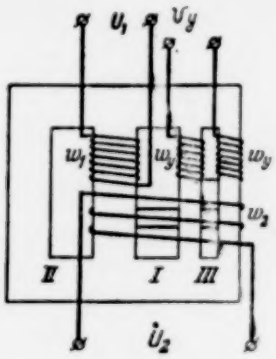

Fig. 1. Transformer magnetic amplifier with shunt magnetization.

YEAR
1961

Consider first the operation of the transformer on no load. If magnetization is absent, the secondary voltage U_2 is given by the transformation ratio and the distribution of the flux between bar *II* and the shunt owing to the primary winding. The flux distribution in the first instance depends on the relationship between the sections of the bar and shunt and that between the lengths of the adjoining portions of the yoke. To find the distribution of the magnetic flux it is also necessary to consider the air gaps in the core construction and the actual shape of the magnetization curve of the core material. With increasing magnetization of the shunt, the voltage U_2 rapidly builds up and reaches maximum even while the control m.m.f.'s are still quite negligible and the whole flux of the primary winding w_1 is closed across bar *II*

$$U_{2\,max} = U_1 \frac{w_2}{w_1}.$$

A magnetized shunt transformer can thus control the voltage even on no load, which is an advantage over conventional magnetic amplifiers.

Now consider a load resistance on the L.T. side. In the absence of magnetization the whole flux of the primary winding is closed across the shunt and the secondary voltage and current in the secondary winding are zero. But since it is assumed that the magnetization curve of the core material is ideal, it follows that the m.m.f. in a closed circuit consisting of bar *I* and the shunt must likewise be zero in the

absence of magnetization. Furthermore, since the only m.m.f. in this circuit is that produced by the primary winding, the primary winding current is zero too. The current in the secondary winding is also zero.

On magnetization of the shunt the m.m.f.'s are equal as for a simple magnetic amplifier:

$$F_1 = F_2 = F_y,$$

where F_1 is the m.m.f. of the primary winding, F_2 that of the secondary winding, and F_y that on each bar of the shunt.

It will be seen by considering the closed circuit of bars *I* and *II* (i.e. that of the non-saturated portions of the magnetic circuit) that F_1 is equal to F_2 for any degree of magnetization and any load:

$$F_1 = F_2.$$

Moreover, in order that part of the flux of the primary winding may be closed across the shunt, a.c. and d.c. m.m.f.'s must be equal, as in a conventional magnetic amplifier, i.e.

$$F_1 = F_y.$$

Like a conventional magnetic amplifier, conditions of over-excitation and saturation can occur during the operation of a magnetized shunt transformer, and the a.c. and d.c. m.m.f.'s are then no longer equal. Over-excitation sets in when the shunt cross section is such that the induction in the shunt periodically attains the value of saturation induction during operation of the transformer on load in the absence of magnetization. In this case the magnitude of the current in the secondary and primary windings will be greater for the same load, the smaller the section of the shunt, since from the instant of saturation the flux begins to close across bar *II* and the device operates as a conventional transformer until the instant the shunt is de-saturated. The condition of saturation sets in when the current in the secondary winding attains its maximum value

$$I_{2\,max} = \frac{U_{2\,max}}{r_l},$$

where r is the load resistance.

A further increase in magnetization results in no further increase in load current.

Thus, the main characteristic of a magnetized shunt transformer which relates the load current to the control current or the a.c.

m.m.f. to the control m.m.f. (see Fig. 2) is exactly the same in shape as that of a simple magnetic amplifier. A device with this characteristic can easily be converted into a current stabilizer since it is only necessary to maintain the control m.m.f. constant.

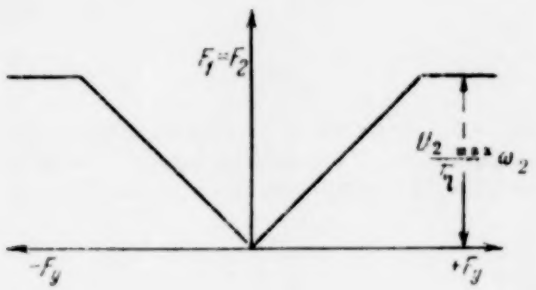

Fig. 2. The fundamental characteristic of an ideal transformer amplifier with shunt magnetization.

YEAR 1961

The shape of the curve for the variation of the load current and control-circuit current varies with the degree of suppression of even harmonics in the control circuit and transient phenomena in the windings, and is similar in shape to that of the curve for a conventional magnetic amplifier.

It should, however, be pointed out that the core magnetization curve is substantially non-rectangular in practice and especially so for large magnetized shunt transformers, large magnetic amplifiers and saturable reactors in view of the use of normal electrical steel and the presence of air gaps. Actual test curves for real magnetized shunt transformers will differ considerably from the foregoing ideal characteristic, and a detailed analysis of such devices must be based on an approximation of the core magnetization curve by some mathematical function. The characteristics of magnetized shunt transformers are also greatly affected by the increased leakage inductance of the windings due to the rather unusual arrangement (for transformers) of the power windings and the position of the magnetization windings in relation to the a.c. windings.

It will be seen from Fig. 1 that a magnetized shunt transformer possesses the property of reversibility, i.e. if the winding w_2 is connected to the alternating voltage, the voltage from the winding w_1 can be regulated by varying the magnetization of the shunt. The foregoing analysis remains valid for this case also.

There is such great similarity between magnetized shunt transformers and conventional magnetic amplifiers that magnetic-amplifier theory can be used to determine the efficiency of such transformers in various applications and for preliminary design analysis.

Translated by O.M. Blunn

REFERENCES

1. A.M. Bamdas, V.A. Somov and A.O. Shmidt; *Magnetized shunt transformers and stabilizers (Transformatory i stabilizatory, regulirueaye podnagnichivaniem shuntov)*. Gosenergoizdat (1959).

YEA
196

TEMPERATURE COMPENSATION OF TRANSISTORIZED RELAY STAGES*

S.V. KULIKOV

(Moscow)

(Received 9 November 1959)

YEAR
1961

Transistorized relay systems are now widely used for the control of electromagnetic devices and electrical motors. The explanation is that transistors acting as switches are capable of switching a considerably greater power than the leakage power on the collector. Their capacity is only restricted by the maximum current and voltage. For example, a PD-4-type transistor is capable of switching 200 W and a P207 transistor about 1 kW.

Industrial control systems often require relay circuits with a low and highly stable threshold of operation. In the design of transistorized relay circuits which are sensitive to changes in temperature it is therefore important to determine the effect of temperature on the "threshold quantities" (see below) and find methods of reducing this effect.

Factors determining threshold stability

The transistorized relay circuit is usually a non-linear amplifier with total positive feedback. Since the feedback circuit is in the majority of cases composed of passive stable elements, it follows that the amplifier is the main cause of instability of the threshold quantities, i.e. the instability of the regions of cut-off, saturation and the active region. It is expedient and convenient to express these regions in terms of the forward transfer characteristic of the transistor

---

* *Elektrichestvo*, 11, 66-70, 1961.

$$I_k = Y_{21e}(U_{e.b}) \qquad \text{a}$$

or

$$I_k = Y_{21e}(I_b) \qquad \text{b}$$

where I_k is the transistor collector current, $U_{e.b}$ the voltage between the emitter and base, and I_b the base current.

An analysis of the forward transfer characteristics of the most common Soviet transistors (types P13 - P15 and P4) has shown that a change in temperature form - 50° C to + 60° C both shifts and alters the slope of the characteristic.

The cut-off region is defined by the following equations:

$$U_{e.k} = E_k \qquad (1)$$

$$I_b = I_{b0} = I_{k0} + I_{e0} \qquad (2)$$

$$I_{k0} = I_{sk} + I_{rk} \qquad (2')$$

$$I_{e0} = I_{se} + I_{re} \qquad (2'')$$

where $U_{e.k}$ is the voltage between the emitter and collector, E_k the supply source voltage of the collector circuit, I_{b0} the base current in the cut-off state, I_{k0} the reverse current of the collector junction, I_{sk}, I_{rk} the saturation current and leakage current of the collector junction, I_{e0} the reverse current of the emitter junction, and I_{se}, I_{re} the saturation current and leakage current of the emitter junction.

For practical purposes it can be assumed that for transistors of the types under consideration at cut-off voltages much less than the supply source voltage of the collector circuit and for the boundary point corresponding to the commencement of the active section [1]

$$I_b = I_{b0} = I_{k0} \qquad (2''')$$

An earlier equation [2] holds good for a boundary point between the region of cut-off and the active regions:

$$U_{e.b} = U_{e.b0} \qquad (3)$$

where $U_{e.b0}$ is the threshold voltage between the base and emitter corresponding to the commencement of the active section on the forward transfer characteristic $I_k = Y_{21e}(U_{e.b})$ if $U_{e.k} = E_k$.

Strictly speaking, expressions (2‴) and (3) are contradictory, since the voltage $U_{e.b}$ is in the cut-off region if $I_{b0} = I_{k0}$ (i.e. if $I_e = 0$).

In practice, however, there is a basis for the consistency of these equations in a very slight increase in the emitter current I_e at a voltage $U_{e.b}$ approximately equal to its value at the boundary with the active region.

Both I_{k0} and $U_{e.b0}$ depend on the temperature and determine the stability of the "initial" operating threshold of the relay circuit. The region of saturation is defined by the following equations:

$$U_{e.k} = 0; \tag{4}$$

$$I_k = \frac{E_k}{r_k \quad r_e} = I_{k.sat} \tag{5}$$

$$I_b > \frac{I_{k.sat}}{\beta} - I_{k0} \tag{6}$$

where r_k, r_e are the respective resistances in the collector and emitter circuits, $I_{k.sat}$ the saturation current of the transistor, and $\beta = H_{21e}$ the transfer constant of the base current.

The equal sign in expression (6) corresponds to a boundary point on the characteristic between the region of saturation and the active region. However, the following equation also holds for this point:

$$U_{e.b} = U_{e.b.k} = \frac{I_{k.sat}}{S_k} + U_{e.b0} \tag{7}$$

where $S_k = Y_{21e}$ is the total slope of the forward transfer characteristic $I_k = Y_{21e} = Y_{21e}(U_{e.b})$ on the active section.

It will be seen from equations (6) and (7) that a change in β and S_k with a change in temperature alters the slope of the forward transfer characteristic. But if β and S_k only change slightly in the given temperature range, the forward transfer characteristics are only displaced, as follows from formulae (2), (3), (6) and (7). Equations (6) and (7) define the stability of the "final" threshold of release (relay opening time) in a transistorized relay circuit.

Classification of temperature compensation methods

In a transistorized relay circuit use may either be made of stage-by-stage thermal compensation with the temperature changes of adjacent

stages included, or else thermal compensation of the amplifier as a whole. In this case the temperature changes of the transistor criteria (I_{k0}, $U_{e.b0}$, β, S_k) are compensated and the forward transfer characteristics of the stages (the amplifier) are stabilized, thereby stabilizing the threshold quantities of the relay. If not a single one of the stages of the relay circuit is in equilibrium in the active region, then unfortunately the temperature compensation methods of linear amplifiers in which constant negative feedback is introduced are no longer acceptable, because the latter assumes the presence of amplification [3].

Special methods are required for relay stages (amplifiers). These can be divided into three groups.

Use of fixing diodes and bias voltages. This method of temperature compensation produces an "artificial" forward transfer characteristic with fixed boundary points between the cut-off, active and saturated regions [3].

Thermal resistors (thermistors) may be used to compensate shifts and changes in slope of the transistor forward transfer characteristic. With a low-impedance input signal source between the emitter and base of the transistor in the first stage, it is expedient to connect the thermistor in series in the emitter-base circuit. For a high-impedance source, it should be connected in parallel in that circuit.

Two control circuits for the next stage are indicated in Fig. 1 for high-impedance and low-impedance signal sources. Figure 1*a* shows a typical control circuit if the switch K is open (the first stage performs the role of this switch), and the next stage is correspondingly "non-conducting". Figure 1*b* refers to the case when the switch K is closed and the next stage is non-conducting. In the first case (Fig. 1*a*) temperature compensation is effected by connecting the thermistors in parallel across a "bias battery". The bias battery can be connected in series in the base or emitter circuit. The bias battery can in some cases be replaced by a voltage drop such as that across the resistance r_4 (indicated by a broken line) due to the load current of another stage. In the second case (Fig. 1*b*), temperature compensation is effected by series connexion of resistance r_4 across which the voltage drop is determined by the value of the thermistor r_t. But if the emitter-base circuit in the state indicated in Fig. 1 is connected to a resistance which is commensurate with the input resistance, then both methods of compensation are equally applicable.

It is, however, necessary to point out that these methods of temperature compensation only allow compensation of *shifts* in the forward transfer characteristic. Two methods may be used to compensate changes in the slope of this characteristic: the connexion of the thermistors

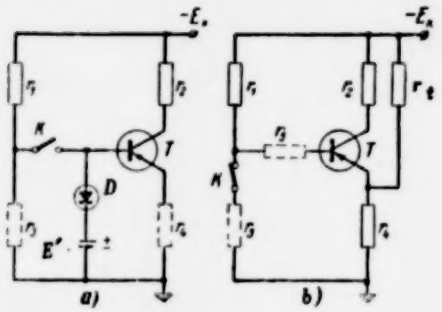

Fig. 1.

YEAR
1961

in parallel with the input to the stage [2], or in series with the d.c. negative feedback circuit [4].

The use of temperature changes of the characteristic of a subsequent stage to compensate the temperature changes of a preceding stage in order to obtain a constant resultant characteristic for both stages. This method of temperature compensation can be realized without the use of thermistors according to the design of the relay circuit.

A method of designing two such systems of compensation will now be considered.

Design method

The forward transfer characteristics of the majority of Soviet P13 - P15 and P4 - type transistors are not altered in shape at positive temperatures, but only shifted to right or left (see Figs. 2 and 3*a*). Only such shifts need therefore be compensated. With a small resistance in the emitter-base circuit it is necessary to design the temperature compensation circuit so as to compensate changes in the threshold voltage $U_{e.b0}$, but if a large resistance is involved (Fig. 1*a*), it is the collector current I_{k0} which has to be compensated. In the general case, changes in both $U_{e.b0}$ and I_{k0} are considered.

Suppose it is required to specify temperature compensation for the transistorized relay circuit shown in Fig. 4. A silicon transistor T_1 (P102-type) is used in the first stage and P4D-type transistor T_2 is used in the output stage. Both stages are provided with positive feedback across the resistance r_4. The input signal can be supplied between

points a and b, a and c, or b and c; the output signal is taken from the resistance r_2. Temperature compensation of the first stage is effected by means of an MMT-1 thermistor, and that of the output stage

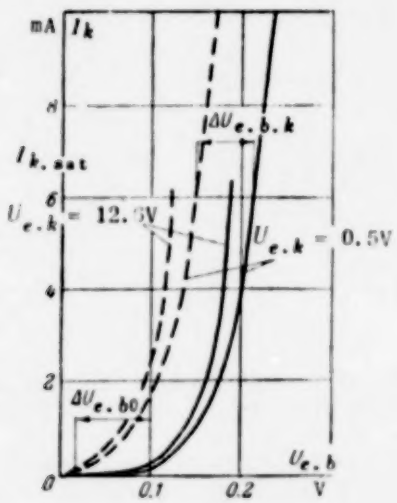

Fig. 2. Forward transfer characteristic $I_k = Y_{21e}(U_{e.b})$ of a transistor in a common emitter circuit: ——— $t = +20°C$; — — — — $t = +60°C$.

by a P3V transistor T_3 "in diode connexion". The collector current of the silicon transistor T_1 is negligibly small in the cut-off state and so the temperature compensation of the output stage can be considered separately (Fig. 1a).

By way of comparison Fig. 3b shows the characteristics of an output stage in which bias across the constant resistance $r_b = 5.1$ kΩ is used (in place of T_3 in Fig. 4). The forward transfer characteristic was taken for two temperatures: +20°C and +60°C at $E_k = -20$ V, $r_2 = 100\Omega$, and various bias voltages E'. It will be seen from the curves in Fig. 3b that the displacement of the boundary points of cut-off and saturation is about 1 mA after a change in temperature. The displacement of these boundary points is much less if the transistor T_3 is used.

The required bias voltage E' is calculated graphically. Figure 3c shows the voltampere characteristics of P4D- and P3V-type transistors "in diode connexion" with open emitters. Marking off the supply voltage E_k of the collector circuit at point a on the base, a perpendicular is

then erected from this point to the curve T at point a'. A straight horizontal line is now drawn across to the point b' on curve D. The required bias voltage E' is then obtained at point b by dropping a perpendicular line to the base. It was assumed in finding E' that $U_{e.b0}$ and $\Delta U_{e.b0}$ were zero, which is quite permissible for the method of compensation in question.

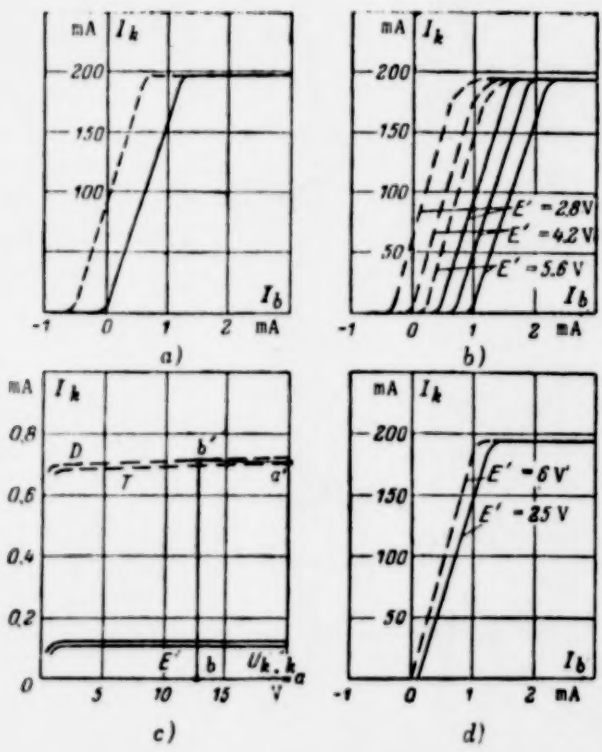

Fig. 3. Forward transfer characteristics $I_k = H_{21e}(I_b)$ and a graphical method of determining the compensation:

——— $t = +20\,^{\circ}C$; — — — — $t = +60\,^{\circ}C$.

E' - bias voltage

Figure 3*d* shows the characteristics of a stage where the above method of temperature compensation is used. It will be seen from these curves that the boundary points of cut-off and saturation are hardly moved at all by a change in temperature (0.05 mA for the cut-off point and 0.15 mA for the saturation point).

It is a corollary of the non-linearity of the voltampere

characteristic D (Fig. 3c) that the temperature compensation circuit is insensitive to changes in the bias voltage E'. Owing to this non-linearity the load in question can be included direct in the emitter circuit of the triode without any appreciable shunting of the input (the resistance r_4 in Fig. 1a).

The temperature compensation circuit of the first stage is given by the equation

$$(\Delta I_t - \Delta I_{k0(1)})\left(r_3 + \frac{r_2 r_1}{r_2 + r_1}\right) = \Delta U_{e.b0(1)}, \qquad (8)$$

where Δt_t is the change in the current through the thermistor:

$$I_t \approx \frac{E_k r_5}{(r_5 + r_7) r_t}.$$

The thermal resistance r_t must operate on the linear section of its voltampere characteristic without any notable heating from the current flowing through it.

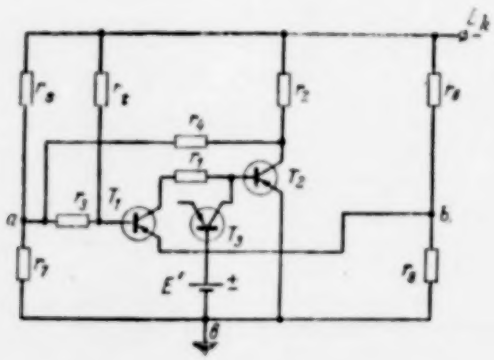

Fig. 4.

From test results of relays using the circuit in Fig. 4 and with $r_1 = 1.2\,\text{k}\Omega$, $r_2 = 100\,\Omega$, $r_3 = 0$, $r_4 = 18\,\text{k}\Omega$, $r_5 = 1145\,\Omega$, $r_6 = 250\,\Omega$, $r_7 = 855\,\Omega$, $r_8 = 250\,\Omega$, $r_t = 112\,\text{k}\Omega$, $E_k = -12$ V and $E' = 12$ V:

On supply of the input signal between points a and b, the operating current was $\pm 50\,\mu$A at temperatures between $+20^\circ$C and $+60^\circ$C. The output (collector) current of the transistor T_2 did not exceed 1 mA in the cut-off state at $+60^\circ$C.

Temperature compensation by the third of the foregoing methods was adopted in a relay with the circuit shown in Fig. 5. Here the output stage (the transistor T_2) is controlled by the first stage (the

transistor T_1) by the type of circuit shown in Fig. 1b. Serial positive feedback was provided across the resistance r_5. As a result of compensation of changes in the forward transfer characteristic of the first stage corresponding to changes in that of the second stage, the instability of the relay threshold quantities was eliminated.

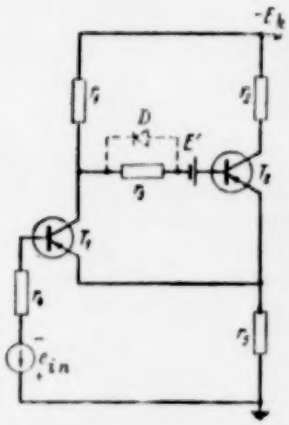

Fig. 5.

The conditions of stable threshold values are obtained by forming and solving Kirchoff equations for the two extreme temperatures of the operating range of the first and second stages.

The stability condition of the "initial" threshold of release (opening time) is given by the formula

$$\frac{\beta_{i1}(\Delta U_{e.b0(1)} + r_4 \Delta I_{k0(1)}) r_3}{(r_1 + r_3)(r_4 + r_{11i(1)} + \beta_{i1} r_5)} = \Delta I_{k0(2)} + \frac{\Delta U_{e.bf(2)}}{r_1 + r_3}, \qquad (9)$$

where $r_{11i(1)}$ is the input resistance of the transistor T_1 in a circuit with a common emitter on the *initial* section of the forward transfer characteristic at the maximum temperature; $\Delta U_{e.b0(1)}$, $\Delta U_{e.bf(2)}$ are quantities obtained from the graph in Fig. 2 (the subscript f refers to the *final* section and i to the initial section of the forward transfer characteristic; the subscripts 1 and 2 refer to transistors T_1 and T_2 respectively).

The stability condition of the "final" operating threshold is

$$\frac{\beta_{f1}(\Delta U_{e.b\,f(1)} + r_4 \Delta I_{k0\,(1)}) r_1}{(r_1 + r_3)(r_4 + r_{11\,f(1)}) + \beta_{f1} r_3} = \Delta I_{k0\,(2)} + \frac{\Delta U_{e.b0\,(2)}}{(r_1 + r_3)}. \qquad (10)$$

The condition of saturation of transistor T_2 has still to be added to equations (9) and (10):

$$\frac{\beta_2 (E_k - E')}{r_4 + r_5} \geq \frac{E_k}{r_5} \qquad (11)$$

and also its condition of cut-off

$$E' \geq I_{k0\,(2)} r_2. \qquad (12)$$

Since in all there are seven independent criteria (r_1, r_2, r_3, r_4, r_5, E_k and E') and four equations (9), (10), (11) and (12), a more definite solution of the problem can be obtained if the desired amount of bias and the hysteresis loop are considered [5,6]. It should be noted that equations (9) and (10) can be replaced by one expression if $\Delta U_{e.b01} = \Delta U_{e.b\,f(1)}$, $\Delta U_{e.b\,0(2)} = \Delta U_{e.b\,f(2)}$, $\beta_{i1} = \beta_{f1}$, $r_{11\,f(2)} \ll r_1 + r_3$, $r_{11\,i(1)} \ll r_4$, and $r_{11\,f(1)} \ll r_4$, which is sometimes the case in practice.

From test results of a relay which had the circuit shown in Fig. 5 and $r_1 = 1\ \text{k}\Omega$, $r_2 = 40\ \Omega$, $r_3 = 1.1\ \text{k}\Omega$, $r_4 = 1.1\ \text{k}\Omega$, $r_5 = 3\ \Omega$, $E_k = 12.6$ V and $E' = 3.75$ V, the relay threshold values remained constant and equal to $e_{in(1)} = 0.6$ V and $e_{in(2)} = 1.1$ V at temperatures between + 20°C and + 60°C. The output current of the transistor T_2 did not exceed 1 mA in the cut-off state at + 60°C. If the criteria had been selected without using relationships (9) and (10), a change in temperature would have caused a substantial shift (0.3 to 0.5 V) in both the threshold values of the relay [5].

Translated by O.M. Blunn

REFERENCES

1. B.N. Kononov; Trigger and relaxation circuits with junction triodes (Spuskovye i relaksatsionnye skhemy na ploskostnykh triodov). In collection of articles: *Semiconductor electronics (Poluprovodnikovaya elektronika)*. Gosenergoizdat (1959).

2. S.V. Kulikov; *Priborostroyenie*, No. 9 (1959).

3. Lo, Endres *et al.*, *Fundamentals of semiconductor electronics.* Sov. Radio (1958).

4. Ya.K. Trokhimenko; *Radiotekhnika*, No. 9 (1956).

5. F.L. Varpakhovskii and K.A. Lipman; *Avtomat. i telemekh.*, No. 11 (1958).

6. S.V. Kulikov; *Radiotekhnika*, No. 4 (1960).

YEAR
1961

ABSTRACTS FROM PAPERS PUBLISHED IN ELEKTRICHESTVO No. 11, 1961

Leading article

The material and technical basis of Communism and the development of power engineering in the U.S.S.R. (pp. 1-6).

Prime importance is attached to the development of electricity supply in the new long-term plans of the U.S.S.R. government. Special attention is to be paid to larger coal-burning power stations and generating plant. Low-cost gas-turbine plant is also being developed. The work on the single national grid is to continue. Research is being carried out on alternative sources of energy (thermo-nuclear reaction, the wind, sun, and the interior heat of the earth) and its conversion into electrical energy.

Computer engineering

Transient phenomena in a circuit with an inductance of capacitance and a ferro-magnetic substance with a rectangular hysteresis loop. V.E. Bogolyubov *et al.*, (pp. 60-64).

To fill a gap in the published literature, a method is proposed for analysing transient phenomena in circuits having coils with ferromagnetic cores with rectangular hysteresis loops operating into reactive loads.

Control engineering

An automatic regulator for the bit feed in drilling boreholes. M.G. E'skin *et al.*, (pp. 55-59).

A d.c. machine with a wide range of speed control has been developed for semi-automatic control of the bit feed in borehole drilling. The desired axial load or feed speed is maintained constant, as well as the equivalent sum. The proposed system is suitable for many other applications. The regulator consists of a reduction gear, executive

YEA
196

motor and amplifier and measuring parts. A position pickup is used to measure the main control item, the weight. A full description of the device is given.

Domestic meters

The class of accuracy of single-phase domestic electricity meters. B.N. Dol'nitskii *et al.*, (pp. 70-73).

Suitable domestic electricity meters are considered. Great individual accuracy is not considered essential.

Power systems

The effect of additional torque components on the dynamic stability of a transmission system with hydro-electric generators. V.V. Yezhkov, (pp. 35-41).

YEAR
1961

Previous investigations have apparently shown that considerable error can occur in the analysis of dynamic stability of a power system when a short circuit occurs near the generator bus, unless the aperiodic component of the stator current and the corresponding periodic component of the rotor current is included. A method is proposed which includes these components and also takes into account the power loss in the stator and rotor circuits and the restraint of the generator motor associated with the conversion of its kinetic energy into magnetic energy.

Insulation

Various regularities in the breakdown of polyethylene insulation. G.P. Delektorskii, (pp. 73-77).

An account is given of tests on high-voltage polyethylene cable insulation at 50 c/s and higher frequencies. A mathematical method of determining the permissible sustained alternating voltage in polyethylene cables is proposed. The same formula is claimed to be of great value in determining the reliability of components and in tests on electrical machines and capacitors.

The electrical characteristics of multi-layer impregnated capacitor paper. D.S. Varshavskii, (pp. 78-82).

A mathematical method is proposed for determining certain electrical properties of multi-layer impregnated paper for power capacitors. The

method is based on simple equivalent circuit analysis. Good agreement with test results has been found.

Rotating machines

The problem of motor reliability. N.A. Tishchenko, (pp. 7-14).

The principles of motor design are considered from the point of view of minimum constructional and operating costs. The concept of motor reliability is formulated mathematically. An analysis is made of capital repairs on 237,000 motors at 122 industrial undertakings. Opinions are expressed regarding optimum design.

Special features of the choice of armature windings for certain d.c. machines. I.Z. Ageev, (pp. 48-55).

The author considers the effect of the type of winding and its design on the commutation of 24 kW 30 V d.c. machines with a comparatively large range of speed control. Recommendations are made concerning the choice of winding and the commutation properties of armature windings.

Transformers

The technical limits of transformer loads at a.c. traction substations in multi-purpose power-supply systems. P.K. Denisov, (pp. 23-28).

On grounds of economy, a.c. traction systems and local consumers are supplied from common three-phase three-winding transformers. A mathematical method of selecting their power is proposed on the basis of daily consumption.

Special features of series-connected transformers and performance analysis. R.N. Urmanov *et al.*, (pp. 29-35).

The non-linearity of series-connected transformer units is considered with a view to improving the method of analysis and estimating its effect on performance. An example is given.

THE TECHNICAL AND PRICE ADVANTAGES OF SYNCHRONOUS MOTORS*

I. A. SYROMYATNIKOV

Moscow

(Received 4 August 1961)

YEAR
1961

The resolutions of the XXII congress of the C.P.S.U. pay considerable attention to electrification, mechanization and automation.

Much success has already been achieved in the development of automated drives in the U.S.S.R.

From power considerations, the best machines for large electrical group drives are synchronous motors. They improve not only the power factor, but the stability of the load units and electrical system as well.

Synchronous motors are now replacing asynchronous motors with flywheels and reduction gears in many branches of industry wherever sustained outputs are required (centrifugal pumps, fans, ball mills, crushers, regeneration plant, rolling mills and so on), as well as for shock loads.

Medium and large synchronous motors may be used in conjunction with hydraulic and electromagnetic clutches and couplings in speed-controlled drives.

Synchronous motors can alter the magnitude and "sign" of reactive power by varying the excitation current. The mode of operation with a "lagging" cos ϕ can in some cases be used for voltage regulation on reduced loads.

The scope for the use of synchronous motors has been greatly widened by the compounding system without machine exciters.

---

* *Elektrichestvo*, 12, 20-27, 1961.

Contactless synchronous motors are very promising. They have no brushes on the rotor and their construction is simplified accordingly, especially for special purposes (proof against arcing or freedom from arcing, etc).

The salient-pole ("claw-shaped") rotor with the excitation winding on the stator must be regarded as the best construction for relatively small contactless synchronous motors.

The system with a "dynamic transformer" can be used for synchronous motors of conventional construction with the excitation winding on the rotor. A "dynamic transformer" is an a.c. machine with the winding on the rotor. A slip-ring induction motor can be used as such a machine. This machine is on the same shaft as the synchronous machine. Semiconductor rectifiers on the same shaft as the synchronous machines are connected to the excitation winding on the rotor of the exciter and supply the excitation winding of the synchronous machine. Excitation is controlled on the stator side. Compounding ensures the necessary excitation forcing in all motor operating conditions including reductions in the mains supply voltage. This system of excitation is used by several foreign firms for large turbo generators as well as for synchronous motors [1].

It is advisable to regulate the excitation of synchronous motors from considerations of a constant voltage on the substation bus-bars with maximum and minimum current limiting and momentary excitation forcing in the event of voltage reductions. It is a necessary condition for the use of other types of excitation that forcing should be applied at reduced voltages.

For synchronous motors with suddenly applied loads, the use of excitation forcing considerably improves the overload capability of the motor so that its rated power can be reduced and its operating stability improved [2].

When considering the choice between synchronous motors and static capacitors as reactive power sources, it must be kept in mind that a synchronous motor designed and installed for this purpose is always in a position to provide it, and that static capacitors have a much shorter service life. Synchronous motors allow control of the voltage and permit momentary increases in the supply of reactive power to the network in the event of fault voltage reductions.

Sometimes it is necessary to increase the power of motors to cope with starting conditions. Clutches and magnetic particle couplings are very effective here. The motors can be started before the load is connected. The coupling is not energized until the motor has attained rated speed, and engagement takes place only then. The use of such

couplings allows the use of smaller synchronous motors at much less cost since their starting winding is lightened. Friction clutches can also be used.

Despite the advantages of synchronous motors, some experts still stick to the old opinion that their use is inadvisable. Apparently the early difficulties with starting and protection have not been forgotten. In these advanced times the starting and protection of synchronous motors is in most cases simple and very little different from that of asynchronous motors.

New models and the 100 kW series in particular have been held back because their advantages were under-estimated. Only recently has the Armelektro works' branch of the All-Union Electrical Power Research Institute started work on the development of a series of synchronous motors with semiconductor rectifier excitation. Technical specifications have so far been approved for four series of machines: 55 kW 1000 rev/min, 55 kW 1500 rev/min, 75 kW 1500 rev/min and 100 kW 1500 rev/min.

YEAR
1961

But the value of such machines also depends upon their cost. A comparative cost analysis must consider the fixed capital outlay, working capital requirements and power losses. The value of a particular series depends on its purchase price and running cost. Its utility cannot be judged from production cost, operating cost or capital outlay separately.

In comparative cost analysis, it is necessary to consider the time taken to recover the investment and relate the extra capital outlay or purchase price to future savings in production or operating cost [3].

The recovery time T is definable as the difference in purchase price divided by the annual savings from the acquisition. It is given by the formula:

$$T = \frac{K_2 - K_1}{C_1 - C_2}, \qquad (1)$$

where K_1 and C_1 are respectively the fixed capital outlay and *annual* working capital requirements (production costs or running costs) for the one alternative; and K_2, C_2 the same for one other alternative.

This recovery time T is then compared with the standard recovery time T' for the industry in question (e.g. 8 y).

To compare more than two alternatives, the estimated annual expenditure E on each alternative is obtained by adding a standard proportion of the purchase price (or capital outlay) to the annual running costs (or production costs) by the formula

$$E = C + \frac{K}{T'} = C + p'K. \quad (2)$$

where E is the estimated annual expenditure; and p' a standard coefficient of efficiency (the reciprocal of the standard recovery time T).

The version with the lowest value of E is considered to be the best proposition.

The efficiency coefficient p' is taken as 0.125, which corresponds to a standard recovery time T' = 8 y.

To decide whether to use synchronous or asynchronous motors, it is necessary to compare:

1. A synchronous motor operating at cos ϕ = 1 with an asynchronous motor and static capacitors whose power is selected so that cos ϕ = 1;

2. A synchronous motor at cos ϕ = 1 with an asynchronous motor without static capacitors for the case when the reactive power can be obtained from other sources at very little expense;

3. A synchronous motor and static capacitors at cos ϕ = 1 and a synchronous motor at cos ϕ < 1. In this case the power of the static capacitors is made such that cos ϕ is the same in both cases. To compare synchronous motors having cos ϕ < 1 which are now in production, the decrease in cost for operation at cos ϕ = 1 is not to be included.

It is a different matter when adopting cos ϕ = 1 for a new synchronous motor. The variation in the price of a motor with the reactive power it produces has to be included then. The specific cost of 1 kVAR of reactive power is always much less than the specific cost of 1 kVA of total power in a synchronous generator or motor. The explanation is that for the same active power the total power varies in inverse proportion to cos ϕ whilst the reactive power is proportional to tan ϕ. Thus, the total power of a synchronous machine with (the standard) cos ϕ' = 0.9 is as much as 11 per cent greater than that of a synchronous machine with cos ϕ' = 1. At the same time, the reactive power is 0.48 of the active power.

The specific cost of 1 kVAR for synchronous machines is

$$K = \frac{C' - C}{Q_{\text{rea}}} \text{ [roubles/kVAR]} \quad (3)$$

where C' is the cost of a synchronous machine with the standard power factor less than 1; Q_{rea} the rated reactive power; and C the cost of a synchronous machine with the standard power factor cos ϕ' = 1 at the same rated active power.

Formula (3) can be written in the form

$$K = \frac{DS' - D_1 S'_1}{Q_{nom}}, \tag{4}$$

and hence for synchronous motors

$$K_m = \frac{D}{\sin \varphi'} \left(1 - \frac{\eta' D_1}{\eta'_1 D} \cos \varphi'\right), \tag{5}$$

and for synchronous generators

$$K_g = \frac{D}{\sin \varphi'} \left(1 - \frac{D_1}{D} \cos \varphi'\right). \tag{6}$$

where η_1' is the efficiency of the motor at the standard power factor of 1; D the specific cost of 1 kVA at the standard power factor $\cos \phi' < 1$; D_1 the same for $\cos \phi' = 1$.

The ratio D_1/D is always greater than 1. It varies between 1.02 and 1.09 for different types of motor at $\cos \phi' = 0.9$. This cost ratio can be replaced by the ratio of the gross or specific weights.

From (6), if $D_1/D = 1$, for $\cos \phi' = 0.9$:

$$K_g \approx K_m = D \frac{1 - 0.9}{0.436} = 0.23D, \tag{7}$$

and for $\cos \phi' = 0.8$:

$$K_g \approx K_m = D \frac{1 - 0.8}{0.6} = 0.33D. \tag{8}$$

Actually K_g and K_m are less, since the specific cost of a machine decreases with increasing rated power.

The value of K_m for various types of synchronous motor is shown in Table 1.

The cost of static capacitors is relatively high: (with erection cost included) 8.5 roubles/kVAR if $U_{nom} = 380$ V, and 6.5 roubles/kVAR if $U_{nom} = 6$ kV. The advantage therefore lies undisputedly with synchronous motors as sources of reactive power from the point of view of capital outlay.

To compare these alternatives it is necessary to determine the losses in the synchronous motor in operation with $\cos \phi = 1$. Under these conditions the stator and excitation currents are minimum. The variation in the iron loss can be ignored. The voltage at the stator terminals is equal to the rated voltage. If the losses in the stator windings ΔP_{sw} and rotor ΔP_{rw} are known in rated operating conditions,

TABLE 1.

Standard efficiency coefficient p', kW	75	250	1300	3000	1500	3500
Standard power factor ($\cos \phi'$)	0.9	0.9	0.9	0.9	0.8	0.9
Speed n, rev/min	1000	1000	1500	1500	3000	3000
Rated voltage, U_{nom}, kV	0.38	0.38	6	6	6	6
Specific cost of 1 kVAR (motor), roubles/kVAR	1.49	0.99	0.485	0.465	1.72	0.92

then in operation on rated active load and at $\cos \phi = 1$, the losses are found from the formula

$$\Sigma \Delta P = \Delta P_x + \Delta P_{n.v} \cos^2 \varphi' + \Delta P_{xv} k_1^2, \qquad (9)$$

where ΔP_x are the losses in the stator steel and mechanical losses; and $k_1 = I_{ex\ 1}/I_{ex.v}$ is the excitation current multiple at $\cos \phi = 1$.

Values of k_1 are given in Table 2 for $\cos \phi' = 0.9$ and 0.8 as a function of the short-circuit ratio k_{scr} on rated load.

TABLE 2.

Short-circuit ratio, k_{scr}	0.5	0.7	1	1.5	2
Standard power factor, $\cos \phi'$ 0.9	0.77	0.77	0.79	0.79	0.81
" " " , $\cos \phi'$ 0.8	0.68	0.68	0.69	0.72	0.73

At an active load other than rated load, the excitation-current multiple can safely be found from the formula

$$k_1 = \sqrt{\frac{1 + \beta^2 x_d^2 \cos^2 \varphi'}{1 + x_d^2 + 2 x_d \sin \varphi'}}, \qquad (10)$$

where

$$\beta = \frac{P_1}{P_{1\,nom}} = \frac{P_1 \eta'}{P_{nom}};$$

P_1 is the active power consumed from the network; and x_d the synchronous inductive reactance in relative units.

The stator current multiple is

$$\frac{I}{I_{nom}} = \beta \cos \varphi'. \tag{11}$$

The loss component of a synchronous motor, which depends on the reactive power other than the rated power, can be found from the formula

$$\Delta P_Q = A \frac{Q^2}{Q_{nom}^2} + B \frac{Q}{Q_{nom}}. \tag{12}$$

If

$$Q = Q_{nom}$$

$$\Delta P_{Q\,nom} = A + B$$

The total losses in a motor on operation with cos ϕ = 1 are

$$\Sigma \Delta P = \Sigma \Delta P_{nom} (A + B). \tag{13}$$

YEAR 1961

The value of A and B for various types of synchronous machine is given in the appendix (see also *Elektrichestvo* No. 3, 1961 [4]).

Incidentally, on operation with cos ϕ = 1, there is a reduction in losses and heating of the rotor and stator windings in synchronous motors and consequently their working life is greater. The reduction in winding temperature gives an additional reduction in losses of about ten per cent.

In some cases it is also necessary to consider the additional saving due to the reduced active power loss in the supply sources and network with the reduction in reactive power owing to the installation of synchronous motors or static capacitors.

The losses in the resistances r of the network elements (overhead lines, cables, reactors, transformers) are found from the formula

$$\Delta P = \frac{rQ^2}{U^2} = \Delta P_c \frac{Q^2}{Q_{nom}^2}, \tag{14}$$

where

$$\Delta P_c = \frac{rQ_{nom}^2}{U^2}. \tag{15}$$

If the change ΔQ in reactive load affects the load of the synchronous machine or network appreciably, the loss variation is given by the formula

$$\Delta p = \Sigma \Delta P_1 - \Sigma \Delta P_2, \tag{16}$$

where $\Sigma \Delta P_1$ represents the losses in the synchronous machine or in the

network at the reactive load Q, $\Sigma\Delta P_2$ the same, but at the reactive load $Q - \Delta Q$.

But if the reactive load of the synchronous machine or network were to change by a relatively small amount ΔQ, the loss variation would be

$$\Delta p = \Delta Q g, \tag{17}$$

where g is the "relative increment" (see below).

This relative increment is defined as the first derivative of the reactive power loss:

for synchronous machines

$$g = \frac{2AQ}{Q^2_{\text{nom}}} + \frac{B}{Q_{\text{nom}}}; \tag{18}$$

for the network

$$g = \frac{2rQ}{U^2} = \frac{2\Delta P_c Q}{Q^2_{\text{nom}}}; \tag{19}$$

for static capacitors

$$g = 0.003 \text{ to } 0.005 = \text{const.} \tag{20}$$

It will be seen from these formulae that the relative increments vary according to a linear law for the network and synchronous machines. A reduction in the requirements of reactive power reduces losses in a synchronous machine and the network relatively more for larger reactive loads.

The reactive load must be distributed between the reactive-power sources connected in the network (synchronous generators, condensers, motors and static capacitors) according to the criterion of equal relative increments. In the first instance, sources with the smallest relative increments should be loaded. The relative increments of synchronous machines have been published elsewhere [2].

A comparative cost analysis will now be made of an asynchronous motor with static capacitors and a synchronous motor operating at $\cos\phi = 1$.

The estimated expenditure on each system is

$$E_{as} = K_{as}(P_{nom} + P_{as}) + K_c(P_{nom} + P_{ac}) + rE_e\Delta P_{as} + TE_e\Delta P_c \tag{21}$$

$$E_{ss} = K_{ss}(P_{nom} + P_{ss}) + rE_e\Delta P_{ss} \tag{22}$$

where K_{as} and K_{ss} are the prime cost of the asynchronous motor and synchronous motor respectively; P_{as}, P_{ss} and P_{ac} depreciation coefficients for the asynchronous motor, synchronous motor and capacitors

respectively; r the duration of loss for motors at the rated shaft load, hr; E_e the estimated expenditure on electricity, roubles/kW. hr; K_c the cost of 1 kVAR of capacitors with the cost of erection and the gear for forcing them at reduced voltages included, roubles/kVAR; ΔP_c the specific active power loss of the capacitors, kW/kVAR; and T the number of hours that the capacitors are connected.

Whenever a synchronous motor costs more than an asynchronous motor with or without capacitors, the expediency of using a synchronous motor depends on the saving in electricity costs. The saving in electricity is proportional to the product of the number of loss hours times the cost of 1 kWh. It therefore follows that synchronous motors are advantageous in sustained operation.

Example 1. The specifications of the asynchronous motor are: 55 kW, 1000 rev/min, 380 V, $\eta' = 0.91$, $\cos \phi' = 0.87$, $Q_{nom} = 34$ kVAR, $\Sigma \Delta P = 5.5$ kW, price 242 roubles.

YEAR 1961

Those of an SM-type synchronous motor are:

56 kW, 80 kVA, 380 V, $\cos \phi' = 0.8$, $\eta' = 0.88$, $Q_{nom} = 48$ kVAR, $\Delta P_x = 1.71$ kW, $\Delta P_{sv} = 3.45$ kW, $\Delta P_{rv} = 2.43$ kW, $\Sigma \Delta P = 7.6$ kW, price 700 roubles.

The capacitor specifications are:

$U = 380$ V, $K_c = 8.5$ roubles kVAR, $\Delta P_c = 0.005$ kW/kVAR.

The purchase cost of the motor and capacitors is $242 + 8.5 \times 34 = 531$ roubles.

If the synchronous motor were planned to operate at $\cos \phi' = 1$, its price would then be about 560 roubles. Thus, in this case the synchronous motor would cost 29 roubles more than an asynchronous motor with capacitors.

Since capacitors have larger depreciation allowances, the estimated expenditure, which is proportional to capital investment, will be somewhat less for the synchronous motor.

In fact, for the synchronous motor

$$560 (0.125 + 0.06) = 104 \text{ roubles},$$

and for the asynchronous motor and capacitors

$$242 (0.125 + 0.06) + 8.5 \cdot 34 (0.125 + 0.1) = 110 \text{ roubles}.$$

Since the losses of a synchronous motor at $\cos \phi = 1$ are less than those of an asynchronous motor even if the capacitor losses are ignored, a synchronous motor designed for operation at $\cos \phi = 1$ is more

economical.

A 56 kW synchronous motor with $\cos \phi' = 0.8$ which can be operated at $\cos \phi = 1$ is only more economical than an asynchronous motor and capacitors at an electricity cost of 0.01 roubles/kWh if the number of loss hours is 4220. In this case the estimated expenditure is the same for both systems (ignoring capacitor losses). In this example an old-type synchronous motor with a machine exciter has been considered. New synchronous motors with $\cos \phi' = 1$ without machine exciters are cheaper than asynchronous motors with capacitors. For example, the DSM-91-6-type synchronous motor with semiconductor rectifier excitation at $\cos \phi' = 0.9$ has losses of 4.94 kW, $\eta' = 91.75$ per cent and its price is only 427 roubles. At $\cos \phi = 1$, the losses are 4.25 kW. This motor is cheaper than an asynchronous motor with capacitors and lower losses even in operation with $\cos \phi = 0.9$. Its use is therefore rational whether for sustained or shock loads. Cases occur in practice when there is no need to produce reactive power, e.g. when synchronous motors are connected to the generator voltage bus-bars. In such cases operation of synchronous motors with $\cos \phi = 1$ is advantageous. In practically every case the synchronous motors have a higher efficiency than asynchronous motors. In any particular case the advisability of using synchronous motors should be worked out without including the cost of the static capacitors for the asynchronous motors.

The conditions under which the greater purchase price of a synchronous motor can be recovered out of savings in electricity will now be considered.

It can be assumed that the depreciation coefficients are the same for synchronous and asynchronous motors. It is supposed that $P_{sm} + P_{as} = P$. The estimated expenditure for a synchronous motor is

$$E_{sm} = K_{sm}P + rE_e \Delta P_{sm}; \tag{23}$$

that for the asynchronous motor is

$$E_{as} = K_{as}P + rE_e \Delta P_{as} \tag{24}$$

Substituting in (23) and (24) respectively

$$\Delta P_{sm} = P(1 - \eta_{sm})/\eta_{sm} \text{ and } \Delta P_{as} = P(1 - \eta_{as})/\eta_{as} \tag{e}$$

the estimated expenditures are

$$E_{sm} = K_{sm}P + (rE_eP(1 - \eta_{sm})/\eta_{sm}) \tag{23a}$$

$$E_{as} = K_{as}P + (rE_eP(1 - \eta_{as})/\eta_{as}) \tag{24a}$$

Example 2. The specifications of the DS-13-52-8A-type synchronous motor are:

575 kW, $\cos\phi' = 0.9$, $\cos\phi = 1$, $\eta'_1 = 94\%$, $\Sigma\Delta P = 36.7$ kW, price 4410 roubles.

The specifications of a DAMSO-1512-8 asynchronous motor are:

570 kW, $\eta' = 92.5\%$, price 3580 roubles, $\Sigma\Delta P = 46.2$ kW.

The loss difference is 9.5 kW.

Assuming that $\tau = 4000$ hr, $E_e = 0.1$ roubles/kWh and that $P_{aom} + P_{am} = 0.125 + 0.06 = 0.185$,

$$E_{am} = 3580 \cdot 0.185 + \frac{1000 \cdot 0.01 \cdot 570 (1 - 0.925)}{0.925} = 2512 \text{ roubles};$$

$$E_{am} = 4410 \cdot 0.185 + \frac{1000 \cdot 0.01 \cdot 570 (1 - 0.94)}{0.94} = 2265 \text{ roubles}.$$

YEAR 1961

Thus the synchronous motor is the better economic proposition. Moreover, the decrease in reactive power is

$$Q = \frac{P_{aom} \tan\phi'}{\eta'} = \frac{570}{0.925} \cdot 0.62 = 382 \text{ kVAR}.$$

Now consider the extra saving when supply is from a T-2-25-2-type 25 MVA turbo-generator for which the relative increment (see the appendix) is

$$q = \frac{2.57 \cdot 2}{25000 \cdot 0.75} \frac{Q}{Q_{nom}} + \frac{38.7}{25000 \cdot 0.75} = 0.006 \frac{Q}{Q_{nom}} + 0.002.$$

If the generator is operating with approximately rated reactive load, the saving in power in the generator is

$$\Delta P = 382 \cdot 0.008 = 3.06 \text{ kW and } 1000 \cdot 0.01 \cdot 3.06 = 122 \text{ roubles, or } 5.4\%$$

which favours the synchronous motor system. The loss difference is 12.56 instead of 9.5 kW.

If the reactive power load of the generator were 0.25 of rated, the saving would be

$$\Delta P = 382 (0.006 \cdot 0.25 + 0.002) = 1.34 \text{ kW}.$$

Example 3. The specifications of an STM-1500-2-type synchronous motor are:

1500 kW, 1740 kVA, 6 kV, $\cos \phi' = 0.9$, $\eta' = 95.65\%$, 760 kVAR, constant losses 36.3 kW, stator copper loss 11 kW, additional losses 11 kW, excitation loss 10 kW, $\Sigma \Delta P = 68.3$ kW, price 14,600 roubles.

It is connected to a 10 MVA works transformer with short-circuit losses of 92 kW.

Operation at $\cos \phi = 1$ will be considered.

From the appropriate table in the appendix

$$A = 4.68 \text{ kW and } B = 3.5 \text{ kW}$$

The losses in a synchronous motor at $\cos \phi = 1$ are

$$\Sigma \Delta P = 68.3 - 4.68 - 3.5 = 60.1 \text{ kW} \quad (\eta_1' = 96.15\%).$$

The total power is 1560 kVA.

The estimated expenditure at $r = 4000$ hr and $E_e = 0.01$ roubles/kWh is

$$E_{ex} = 14\,600 \cdot 0.185 + 4\,000 \cdot 0.01 \cdot 60.1 = 5\,140 \text{ roubles}$$

The specifications of an ATM-type asynchronous motor are:

1500 kW, 6 kV, $\cos \phi' = 0.88$, $\eta' = 95\%$, 855 kVAR and the price 9810 roubles.

The losses in the asynchronous motor are

$$\Sigma \Delta P = \frac{1\,500}{0.95} \cdot (1 - 0.95) = 79 \text{ kW}.$$

The loss difference is 18.9 kW.

The estimated expenditure is

$$E_{ex} = 9\,810 \cdot 0.185 + 4\,000 \cdot 0.01 \cdot 79 = 4\,970 \text{ roubles}$$

We also require to determine the decrease in losses in the transformer if the reactive power is reduced by 855 kVAR. The losses in the transformer due to the reactive power are

$$\Delta P_t = \Delta P_{sc} \frac{Q^2}{S^2_{nom.t}} = 0.92 Q^2.$$

Assuming that the transformer load is 9 MVA in the period of maximum at $\cos \phi = 0.8$, the losses in the transformer from the reactive power $Q_1 = 9 \times 0.6 = 5.4$ kVAR are

$$\Delta P_t = 0.92 \cdot 5.4^2 = 26.8 \text{ kW}.$$

The relative increment for the reactive load of 5.4 MVAR is

$$g = \frac{2 \cdot 26.8Q}{5\,400Q_1} = 0.01\frac{Q}{Q_1}.$$

If a synchronous motor at cos ϕ = 1 is used instead of the asynchronous motor, the reactive power of the load is reduced by 855 kVAR and the reactive power transmitted through the transformer will be 4.54 MVAR. The active losses in the transformer are reduced by

$$\Delta P_{t1} - \Delta P_{t} = 0.92 \cdot \frac{92}{10^2}(5.4^2 - 4.54^2) = 7.85 \text{ kW}.$$

The same result (7.85 kW) is produced by the formula

$$\Delta P_{t1} - \Delta P_{t2} = g_1 \frac{Q_{av}}{Q_1}\Delta Q,$$

where

$$Q_{av} = \frac{Q_1 + Q_2}{2} = 4.94 \text{ MVAR}.$$

YEAR 1961

The loss difference is 26.75 kW. The extra saving is 4000 × 0.01 × 7.85 = 315 roubles.

Thus, the estimated expenditure for a synchronous motor at cos ϕ = 1 is 5140 - 315 = 4825 roubles if the change in reactive power requirements is included, i.e. it is 145 roubles less than that for an asynchronous motor.

Now consider operation at cos ϕ = 0.9.

The decrease in reactive power is

$$Q = 760 + 855 = 1\,615 \text{ kVAR}.$$

The decrease in active losses in the transformer is

$$\Delta P_{t1} - \Delta P_{t2} = 0.92(5.4^2 - 3.785^2) = 13.7 \text{ kW}.$$

The estimated expenditure is

$$E_{ss} = 14\,600 \cdot 0{,}185 + 4\,000 \times$$
$$\times 0.01(68.3 - 13.7) = 4\,890 \text{ roubles}$$

Thus, a synchronous motor with cos ϕ = 1 is the more advantageous, since the estimated annual expenditure is in this case less by 4890 - 4825 = 65 roubles.

Example 4. The specifications of an STM-3500-2 synchronous motor are:

3500 kW, 4050 kVA, 1770 kVAR, 6.3 kV, cos ϕ' = 0.9, η' = 96.1%, $\Sigma\Delta P$ = 142 kW, price 20,900 roubles.

Assuming that the distribution of the losses is the same as for a 1500 kW motor, the constant losses are 77 kW, the stator copper loss (including additional losses) is 45 kW and the excitation loss is 20 kW;

$$A = 0.19 \cdot 45 + 0.05 \cdot 20 = 9.5 \text{ kW};$$
$$B = 0.35 \cdot 20 = 7 \text{ kW}.$$

If $\cos \phi = 1$, then $\Sigma \Delta P = 142 - 9.5 - 7 = 125$ kW, and

$$S_{\text{nom.1}} = 3.625 \text{ kVA}, \quad \eta'_1 = 96.54\%$$

The specification of an ATM-3500-2 asynchronous motor are:

3500 kW, 6 kV, $\cos \phi' = 0.85$, $\eta' = 95.4\%$, price 19,000 roubles.

For an asynchronous motor

$$Q_{\text{nom}} = \frac{3500}{0.954} \cdot 0.621 = 2280 \text{ kVAR};$$
$$\Sigma \Delta P = \frac{3500}{0.954} (1 - 0{,}954) = 169 \text{ kW}.$$

The estimated expenditure for the two systems (the synchronous motor and the asynchronous motor without static capacitors), if $t = 4000$ hr and $E_e = 0.01$ roubles/kWh, is

$$E_{\text{ss}} = 20\,900 \cdot 0.185 + 125 \cdot 4\,000 \cdot 0.01 = 8\,870 \text{ roubles}$$
$$E_{\text{as}} = 19\,000 \cdot 0.185 + 169 \cdot 4\,000 \cdot 0.01 = 10\,270 \text{ roubles}$$

Thus the synchronous motor with $\cos \phi = 1$ is the better economic proposition. Moreover, the decrease in reactive power is 2280 kVAR.

In this particular case the synchronous motor with $\cos \phi = 0.9$ is more advantageous than the synchronous motor with $\cos \phi = 1$ and static capacitors. The estimated expenditure for this system is

$$E_{\text{ss}} = 20\,900 \cdot 0.185 + 6.5 \cdot 1\,770 \cdot 0.225 + 125 \cdot 4\,000 \cdot 0{,}01 + 8\,000 \cdot 0.005 \times 1\,770 \cdot 0.01 = 11\,100 \text{ roubles}$$

That for the motor with $\cos \phi = 0.9$ is

$$E_{\text{as}} = 20\,900 \cdot 0.185 + 142 \cdot 4\,000 \cdot 0.01 = 9\,570 \text{ roubles}$$

i.e. it is 1530 roubles less each year.

Example 5. For a shaft load of 3900 kW at 3000 rev/min, it is necessary to choose a synchronous motor. The reactive power can be provided by capacitors or by the synchronous motor. An STM-3500-2-type synchronous motor with $\cos \phi = 1$ and capacitors may in fact be used. Subtracting the losses (125) from the total power (4050 kVA), the shaft power is

$$P = 4\,050 - 125 = 3\,925 \text{ kW}$$

It is assumed that the efficiency remains the same even though it slightly increases due to a reduction in rotor current. The losses in this motor have already been determined (see example 4).

The alternative is an STM-6000-2-type motor:

4000 kW, $\cos \phi' = 0.7$, $\eta' = 0.952$, price 24,500 roubles.

The reactive power and losses are

$$Q = \frac{4\,000 \cdot 1.054}{0.952} = 4\,400 \text{ kVAR};$$

$$\Sigma \Delta P = \frac{4\,000}{0.952} \cdot (1 - 0.952) = 200 \text{ kW}.$$

To simplify the analysis, it is assumed that the motor losses and the reactive power are the same for a shaft load of 3900 kW as for 4000 kW.

YEAR 1961

Compare now the estimated expenditure for a shaft load of 3900 kW and a reactive power of 4400 kW. If r = 3500 hr, T = 7000 hr and E_e = 0.012 roubles/kWh, then

$$E_{3\,500} = 20\,900 \cdot 0.185 + 4\,400 \cdot 6.50 \cdot 0.225 + \\ + 142 \cdot 3\,500 \cdot 0.012 + 4\,400 \cdot 0.005 \times \\ \times 7\,000 \cdot 0.012 = 18\,100 \text{ roubles}$$

$$E_{4\,000} = 24\,500 \cdot 0.185 + 200 \cdot 3\,500 \cdot 0.012 = 12\,850 \text{ roubles}$$

In this case the synchronous motor with the larger rated power is the better proposition.

It has been seen that synchronous motors with $\cos \phi' = 1$ are to be preferred in practice to asynchronous motors and capacitors for small powers. It has also been shown that in a number of cases synchronous motors with $\cos \phi' < 1$, if operated with $\cos \phi = 1$, are a better proposition than asynchronous motors, owing to the savings in electricity.

After a certain point it is more economical to use synchronous motors as reactive power sources than capacitors. In this case it is necessary to compare a synchronous motor and static capacitors for which $\cos \phi = 1$ with a synchronous motor for which $\cos \phi < 1$.

From a certain rated power onwards, synchronous motors are cheaper and have better weight indices than asynchronous motors for a particular rotational speed. In such cases the capital and electricity costs of synchronous motors are lower. For example, the weight of a DSP 1300 kW synchronous motor with solid shoes and starting winding with $\cos \phi = 0.9$ and n = 1500 rev/min is very little different from that of a DAZ asynchronous motor of the same power.

Conclusions

Synchronous motors should be used extensively in place of asynchronous motors. For small synchronous motors it is necessary to dispense with machine exciters and use semiconductor rectifiers instead. This will considerably widen the field of application for synchronous motors. For example, a 55 kW synchronous motor with $\cos \phi' = 0.9$ costs less and is cheaper to run than an asynchronous motor with static capacitors.

There is however a wider field of application for relatively small synchronous motors (especially in operation with $\cos \phi = 1$) than for asynchronous motors with static capacitors.

After a certain rated power it is expedient to use synchronous motors with a "leading" power factor ($\cos \phi < 1$). The larger the number of loss hours, it becomes economically expedient to use them with a lower rated power. In certain conditions it is economically expedient to increase the rated power of synchronous motors in order to produce reactive power.

In a number of cases synchronous motors with $\cos \phi' < 1$, if operated with $\cos \phi = 1$, are a better proposition than asynchronous motors without static capacitors, owing to their higher efficiency.

Synchronous motors should be preferred in all cases for drives which are in continuous use for a relatively large number of hours, since their economic effect is then maximum.

Synchronous motors should be used for voltage regulation.

Synchronous motors must be provided with an excitation forcing device which comes into operation at reduced voltages. A similar device should be provided for motors with suddenly applied loads.

The reactive power should be distributed between parallel-operating sources from consideration of equal relative increments.

It is necessary to speed up the development and mass production of synchronous motors of all types and designs, including excitation systems through semiconductor rectifiers without the excitation winding on the salient-pole rotor, without contacts in the excitation circuit, but using a "dynamic transformer" and semiconductor rectifiers on the motor shaft.

Appendix

AIR-COOLED TURBO GENERATORS

Type	T-2-6-2	T-2-12-2	T-2-25-2	T-2-50-2
P_{nom}, MW	6	12	25	50.000
cos ϕ'	0.8	0.8	0.8	0.85
$A + B/Q_{nom}$, kW/kVAR	0.0047	0.0055	0.0051	0.0032
A, kW	11.9	30.6	57.2	62.1
B, kW	9.5	18.5	36.7	36.7
B/Q_{nom}, kW/kVAR	0.0021	0.002	0.002	0.0012

YEAR 1961

HYDROGEN-COOLED TURBO GENERATORS

Type	TV-2-30-2	TV-50-2	TV-60-2	TV-2-100-2	TV-2-150-2
P_{nom}, MW	30	50	60	100	100
cos ϕ'	0.85	0.85	0.85	0.85	0.9
$A + B/Q_{nom}$, kW/kVAR	0.0056	0.0041	0.0046	0.0031	0.0025
A, kW	63.4	75.1	107	116	86.5
B, kW	41	51	64	76	98
B/Q_{nom}, kW/kVAR	0.0022	0.0016	0.0017	0.0012	0.0013

DS-TYPE SYNCHRONOUS MOTORS, 380 V, cos ϕ' = 0.9

Rated Power	Rated speed rev/min	1500	1000	750	600	500
P_{nom} = 55 kW	$A + B/Q_{nom}$, kW/kVAR		-	0.044	0.052	0.050
	A, kW	-	-	0.54	0.66	0.62
	B, kW	-	-	0.75	0.91	0.90
	B/Q_{nom}, kW/kVAR	-	-	0.025	0.03	0.03

Rated Power	Rated speed rev/min	1500	1000	750	600	500
P_{nom} = 75 kW	$A + B/Q_{nom}$, kW/kVAR	-	1.042	0.043	0.048	0.043
	A, kW	-	0.80	0.75	0.80	0.76
	B, kW	-	0.89	0.94	1.13	0.98
	B/Q_{nom}, kW/kVAR	-	0.022	0.023	0.027	0.024
P_{nom} = 100 kW	$A + B/Q_{nom}$, kW/kVAR	0.034	0.038	0.037	0.043	0.042
	A, kW	0.82	0.90	0.78	0.87	0.91
	B, kW	0.95	1.13	1.15	1.40	1.34
	B/Q_{nom}, kW/kVAR	0.018	0.021	0.022	0.026	0.025
P_{nom} = 125 kW	$A + B/Q_{nom}$, kW/kVAR	0.030	0.035	0.034	0.037	-
	A, kW	0.92	1.06	0.95	0.95	-
	B, kW	1.04	1.26	1.28	1.50	-
	B/Q_{nom}, kW/kVAR	0.016	0.019	0.020	0.023	-
P_{nom} = 160 kW	$A + B/Q_{nom}$, kW/kVAR	0.027	0.031	0.030	-	-
	A, kW	1.04	1.19	1.12	-	-
	B, kW	1.17	1.43	1.38	-	-
	B/Q_{nom}, kW/kVAR	0.014	0.017	0.016	-	-
P_{nom} = 200 kW	$A + B/Q_{nom}$, kW/kVAR	0.023	0.024	-	-	-
	A, kW	1.12	1.24	-	-	-
	B, kW	1.29	1.29	-	-	-
	B/Q_{nom}, kW/kVAR	0.012	0.012	-	-	-

Rated Power	Rated speed rev/min	1500	1000	750	600	500
P_{nom} = 250 kW	$A + B/Q_{nom}$, kW/kVAR	0.022	0.022	-	-	-
	A, kW	1.50	1.47	-	-	-
	B, kW	1.37	1.48	-	-	-
	B/Q_{nom}, kW/kVAR	0.010	-	-	-	-
P_{nom} = 320 kW	$A + B/Q_{nom}$, kW/kVAR	0.02	-	-	-	-
	A, kW	1.7	-	-	-	-
	B, kW	1.62	-	-	-	-
	B/Q_{nom}, kW/kVAR	0.01	0.011	-	-	-

YEAR 1961

ESM-TYPE SYNCHRONOUS MOTORS WITH SEMICONDUCTOR RECTIFIER EXCITATION, $\cos \phi' = 0.9$

Rated power, kW	55	55	75	100
n_{nom}, rev/min	1500	1000	1500	1500
$A + B/Q_{nom}$, kW/kVAR	0.0215	0.0235	0.0184	0.0155
A, kW	0.45	0.45	0.5	0.534
B, kW	0.19	0.245	0.235	0.285
B/Q_{nom}, kW/kVAR	0.0064	0.00827	0.00588	0.0054

DS-TYPE SYNCHRONOUS MOTORS 6 kV, 1500 rev/min, $\cos \phi' = 0.9$

Rated power, kW	400	500	630	800	1000
$A + B/Q_{nom}$, kW/kVAR	0.0191	0.0181	0.0158	0.0137	0.0134
A, kW	2.40	2.90	3.10	3.03	3.81
B, kW	1.45	1.78	2.06	2.62	3.05
B/Q_{nom}, kW/kVAR	0.00695	0.0069	0.00635	0.00635	0.0060

STM-TYPE SYNCHRONOUS MOTORS 6 kV, 3000 rev/min, $\cos \phi' = 0.9$

Rated power, kW	750	1500	1500 (sic)	4000	6000	12,000
A, kW	2.58	4.17	5.03	7.30	9.70	14.8
B, kW	2.80	3.44	4.40	7.30	7.00	13.4
$A + B/Q_{ген}$, kW/kVAR	0.014	0.010	0.0074	0.0073	0.0055	0.0021
$B/Q_{ген}$, kW/kVAR	0.0072	0.0054	0.0035	0.0036	0.0023	0.0010

Translated by O.M. Blunn

REFERENCES

1. Rosenberry; Brushless d.c. excited rotating field synchronous motor. *Applications and Industry*, July (1960).

2. V.I. Pleskov and G.G. Magazinnik; *Elektrichestvo*, No. 10 (1960).

3. The fundamentals of costing in power engineering (Osnovnye metodicheskiye polazheniya tekhniko-ekonomicheskikh raschetov v energetike). *Elektrichestvo*, No. 10 (1959).

4. I.A. Syromyatnikov; *Elektrichestvo*, No. 3 (1961). (Translated in *Electric Technology U.S.S.R.*, Vol. 1, 1961).

THE THEORY AND DESIGN OF ELECTROMAGNETIC VIBRATION EQUIPMENT*

A. E. CHESNOKOV

Odessa

(Received 9 July 1960)

YEAR
1961

Electromagnetic vibrators are simple devices and are widely used in industry, but their operation has not been adequately studied. The existing methods of analysis fail to take into account several factors which determine their output capability as electrical machines. Moskvitin's simplified approach [1] does not provide an adequately rigorous analysis of their operating conditions.

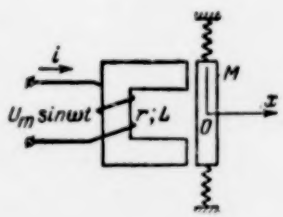

Fig. 1. The circuit of an electromagnetic vibrator.

As in the case of a more complicated problem [2], this paper considers the non-linear variation of the inductance in the operation of electromagnetic vibrators. If it is assumed that the inductance L is only a function of the displacement x of the armature, i.e. that the magnetic system is non-saturated and that hysteresis phenomena are absent, a vibrator with the vibrating mass M can be described by the following differential equations:

---

* *Elektrichestvo*, 12, 37-40, 1961.

$$\frac{d}{dt}(Li) + ir = U_m \sin \omega t; \tag{1}$$

$$M\frac{d^2x}{dt^2} + \mu\frac{dx}{dt} + fx = \frac{1}{2} i^2 \frac{dL}{dx}. \tag{2}$$

The following approximating function can be used for $L(x)$:

$$L = L_0 \exp(-\gamma x + \rho^2 x^2). \tag{3}$$

Here γ and ρ are independent of x. If these coefficients are selected appropriately, function (3) quite accurately characterizes $L(x)$ quantitatively and qualitatively.

Suppose as a first approximation that the oscillation of the armature is governed by the following harmonic law:

$$x = A \cos(2\omega t - \psi), \tag{4}$$

the inductance is expressible by the time function

$$L = L_0 \exp[-m \cos(2\omega t - \psi) + 2m_\rho \cos^2(2\omega t - \psi)],$$

where

$$m = \gamma A = \frac{1}{2} \ln \frac{L_{max}}{L_{min}};$$

$$m_\rho = \frac{\rho^2 A^2}{2} = \frac{1}{4} \ln \frac{L_{max} L_{min}}{L_0^2}. \tag{5}$$

The coefficient m defines the relative variation of inductance; the coefficient m_ρ defines the shape of the curve $L(x)$ (its concavity). Inasmuch as the shape of the curve $L(x)$ depends on the relation between the magnetic conductances for the operating flux and the leakage flux for the various positions of the armature (i.e. it depends on the configuration of the magnetic circuit), the most efficient shape can be specified for the magnetic circuits of vibrators by introducing the coefficient m_ρ and studying its effect on the characteristics of the vibrator.

Since m is always less than 1 and m_ρ is much less than m, equation (1) reduces to Mathieu's equation

$$\ddot{v} + [a - 2q \sin(2\omega t - \psi)]v = \frac{\omega}{Lu} \cos \omega t. \tag{6}$$

Here

$$i = vu; \quad u = \exp[m\cos(2\omega t - \psi) - m_\rho \cos(4\omega t - 2\psi)];$$

$$a = -\delta^2; \quad q = 2\omega\delta m; \quad \delta = \frac{r}{2L_0} e^{-m_\rho}.$$

For an electromagnetic vibrator $|a|$ is always much less than $|2q|$. An approximate solution of Mathieu's equation therefore is [3]

$$i = I_0 \sin(\omega t - \varphi) \exp[m\cos(2\omega t - \psi) - 2m_\rho \cos^2(2\omega t - \psi)], \tag{7}$$

where

$$I_0 = \frac{U_m}{L_0\sqrt{4\delta^2 + \omega^2 - 8\omega\delta m}};$$

$$\varphi = \operatorname{arc\,tan}\frac{\omega - 4\delta m}{2\delta}.$$

YEAR
1961

Hence the current in the vibrator circuit can be regarded as a sinusoidal current which varies in amplitude with time. The expressions for I_0 and ϕ reflect the variation of these quantities with the non-linear variation of the vibrator's inductance defined by the quantities m and m_ρ. In particular, if $m = 0$ and $m_\rho = 0$, these expressions provide formulae which hold good for circuits with a constant resistance and inductance.

Oscillation amplitude and phase

Equation (7), when considered with (3) and (4), allows the right-hand side of equation (2) to be represented as the function $P(x, t)$. Equation (2) can then be transformed into the following non-linear equation by expanding the quantity $\exp(\gamma x - \rho^2 x^2)$ as a power series:

$$\ddot{w} + b\dot{w} + a^2 w = -\frac{\gamma^3}{m^3 M} \cdot \frac{L_0 I_0^2}{2}\left[\left(\frac{m}{2} + \alpha_0 w + \beta_0 w^2 + \gamma_0 w^3 + \ldots\right) - \left(\frac{m}{2} + \alpha_0 w + \beta_0 w^2 + \gamma_0 w^3 + \ldots\right)\cos(2\omega t - 2\varphi)\right], \tag{8}$$

where $w = x/A = (\gamma/m)x$ is the relative displacement; α_0, β_0, γ_0, ... are coefficients depending on the shape of the curve $L(x)$ and the relative variation of the inductance m; and $b = \mu/M$ and $a^2 = f/M$.

A new time scale is selected:

$$n\tau = 2\omega t - 2\varphi \quad (n = 1, 2, 3, \ldots)$$

and w is added to the left- and right-hand sides of (8). This equation then becomes

$$\begin{aligned} w + w = {} & \xi w - n\vartheta w - \\ & - n^2\lambda_0\left(\frac{m}{2} + \alpha_0 w + \beta_0 w^2 + \gamma_0 w^3 + \ldots\right) + \\ & + n^2\lambda_0\left(\frac{m}{2} + \alpha_0 w + \beta_0 w^2 + \gamma_0 w^3 + \ldots\right)\cos n\tau. \end{aligned} \tag{9}$$

The following notation is used for the sake of simplicity:

$$\vartheta = \frac{b}{2\omega}; \quad \xi = \frac{4\omega^2 - n^2\alpha^2}{4\omega^2};$$

$$\lambda_0 = \frac{\gamma^2}{4\omega^2 m^2 M} \cdot \frac{L_0 I_0^2}{2}.$$

All the coefficients on the left-hand side of (9) are less than one; the solution of equation (9) in w can be found by Mandel'shtam and Papaleksi's method [4] for any whole-number value of n. Solutions for $n > 1$ permit a thorough examination of the possibility of multiple oscillations occurring and existing in electromagnetic vibrators; the terms on the right-hand side of (9) which determine their non-linearity are most important.

For normal oscillations (i.e. if $n = 1$), an approximate solution of (9) can be obtained by considering only terms to the first power of w:

$$w = \frac{m\lambda_0}{2\sqrt{\xi_d^2 + \vartheta^2}} \sin(2\omega t - 2\varphi - \theta), \tag{10}$$

where

$$\theta = \arctan\frac{\xi_d}{\vartheta};$$

$$\xi_d = \xi - \alpha_0\lambda_0.$$

Using the same notation, the following expression can be written for the armature displacement according to (10):

$$\begin{aligned} x = {} & \frac{P_m}{\sqrt{(4\omega^2 - \alpha^2 - \alpha_c^2)^2 + 4\omega^2 b^2}} \times \\ & \times \sin\left(2\omega t - 2\varphi - \arctan\frac{4\omega^2 - \alpha^2 - \alpha_c^2}{2\omega b}\right), \end{aligned} \tag{11}$$

where $P_m = \gamma/2M \times L_0 I_0^2/2$ is the maximum value of the force per unit of vibrating mass M; and

$$a_e^2 = a_0 \frac{\gamma^2}{m^2 M} \cdot \frac{L_0 I_0^2}{2}.$$

Formula (11) defines the nature of the oscillations of an electromagnetic vibrator which is supplied from a sinusoidal voltage source.

The motion of a mechanical vibrator due to a force $F = F_m \cos(2\omega t - 2\phi)$ which varies periodically with time is described by a linear differential equation

$$\ddot{x} + b\dot{x} + a^2 x = P_m \cos(2\omega t - 2\varphi).$$

The forced oscillations can be found by the formula

$$x = \frac{P_m}{\sqrt{(4\omega^2 - a^2)^2 + 4\omega^2 b^2}} \times \sin\left(2\omega t - 2\varphi - \arctan\frac{4\omega^2 - a^2}{2b\omega}\right). \quad (12)$$

YEAR 1961

Comparison of formulae (11) and (12) permits a comparison of the displacement which obtains when the periodic variation of the inductance is included to be made with that which occurs due to a periodically varying force. The presence in (11) of a term with a_e^2, which depends on the electrical criteria of the vibrator, indicates that the resonance conditions of an electromagnetic vibrator are somewhat different from those of a mechanical vibrator. Calculations have shown that this difference is sometimes considerable; even though the quantity a_e^2 may be no more than four to five per cent of $4\omega^2$ if $\omega = 314$, the oscillation amplitude may be under-estimated by 17 to 20 per cent if it is ignored.

Oscillation power

From (5) and (7), the flux coupling of the vibrator winding is

$$\Psi = Li = L_0 I_0 \sin(\omega t - \varphi). \quad (13)$$

Relationships $\Psi(i)$ and $i(t)$ are plotted from equations (7) and (13) in Fig. 2. The area bounded by the curve $\Psi(i)$ is proportional to the mechanical work of the vibrator.

The power of the vibrator is

$$P = \frac{1}{T}\int_0^T i \, d\Psi. \quad (14)$$

Expanding the amplitude factor in (7) as a power series and substituting the value obtained for the current in the integral (14)

$$P = \omega \frac{L_0 I_0^2}{2} M_1 \cos\theta, \tag{15}$$

where

$$M_1 = \frac{1}{2}\left[m\left(1 - \frac{3}{2}m_\rho\right) + \frac{m}{8}(m^2 + 10m_\rho) - \dots\right];$$

$$\theta = \operatorname{arc\,tan}\frac{4\omega^3 - \omega^2 - \omega_e^2}{2\omega b}.$$

From (15), the power of the vibrator increases with increasing relative variation of the inductance and depends on the concavity of the curve $L(x)$.

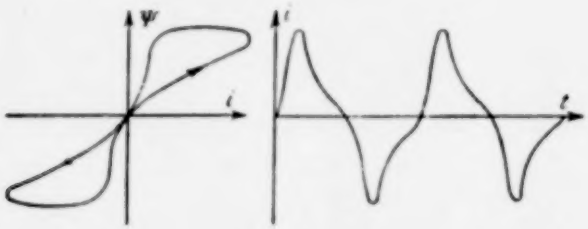

Fig. 2. The relationship $\Psi(i)$ and the current curve of a vibrator for $\theta = 0$.

The coefficient M_1 defines the efficiency of energy conversion. Its relationship with the electrical criteria of the vibrator on the one hand and the required maximum force upon the armature on the other can be found in the following way. Suppose $x = A\sin(2\omega t - 2\phi - \theta)$ is the displacement and $F = F_m\cos(2\omega t - 2\phi)$ the force on the armature. The mechanical power of the vibrator is then

$$P = \frac{1}{T}\int_0^T F dx = \omega A F_m \cos\theta. \tag{16}$$

Equating the right-hand sides of equations (15) and (16):

$$F_m = \frac{M_1}{A}\cdot\frac{L_0 I_0^2}{2}. \tag{17}$$

Example

Suppose it is required to design a vibrator for which the mechanical power P is 500 W, the fibrating mass M = 20 kg, the oscillation amplitude A = 3 mm, the angular frequency of vibration 2ω = 628 1/sec, and

the rated voltage U = 380 V.

Given average values of the coefficients m and m_ρ, a start is made by calculating the current, the number of turns in the winding, the cross-section of the magnetic circuit and its shape and dimensions.

In practice, the "modulation coefficient" of L is between 0.6 and 0.9. Suppose it is m = 0.75. Initially it can be assumed that $m_\rho \approx m/4$. M_1 is 0.317 for these two values of m and m_ρ.

The maximum linear speed of the armature is

$$v_m = 2\omega A = 2 \cdot 314 \cdot 0.003 = 1.884 \text{ m/sec}$$

The force acting on the armature is found from (16). At resonance ($\theta = 0$)

$$F_m = \frac{P}{\omega A} = \frac{500}{314 \cdot 0.003} = 530 \text{ n.}$$

YEAR 1961

Expression (17) provides the energy of the magnetic field corresponding to maximum flux coupling:

$$W_0 = \frac{L_0 I_0^2}{2} = \frac{AF_m}{M_1} = \frac{0.003 \cdot 530}{0.317} = 5 \text{ J}$$

The inductance for the central position of the armature can be estimated from the following considerations. Assuming that the air-gap δ is small

$$I_0 \approx \frac{U_m}{\omega L_0}.$$

By definition

$$W_0 = \frac{U_m^2}{2\omega^2 L_0},$$

and hence

$$L_0 = \frac{U_m^2}{2\omega^2 W_0} = \frac{(380\sqrt{2})^2}{2 \cdot 314^2 \cdot 5} = 0.292 \text{ H}$$

The preliminary estimate of the current is

$$I_0 = \sqrt{\frac{2W_0}{L_0}} = \sqrt{\frac{2 \cdot 5}{0.292}} = 5.87 \text{ A.}$$

The number of turns in the winding and the cross-section of the magnetic circuit can be selected by assuming that the magnetic reluctance of the armature is equal to that of the air-gap δ_0. Then

$$L_0 = \frac{w^2}{R_0} = \mu_0 \frac{S}{2\delta_0} w^2.$$

Putting δ_0 = 3.9 mm and specifying a cross-section S of 25 cm^2, the

number of turns w is 840.

The maximum flux is

$$\Phi_m = \frac{L_0 I_0}{w} = \frac{0.292 \cdot 5.87}{840} = 2.04 \cdot 10^{-3} \text{ V. sec}$$

The effective flux density

$$B = \frac{\Phi_m}{S\sqrt{2}} = \frac{2.04 \cdot 10^{-3}}{25 \cdot 10^{-4}\sqrt{2}} = 0.578 \text{ V/m}^2$$

The specific m.m.f. corresponding to this density is H = 133 A/m.

The magnetic permeance of steel is

$$\mu = \frac{B}{H} = \frac{0.578}{103} = 5.6 \cdot 10^{-3} \text{ H/m}.$$

Given the shape and dimensions of the magnetic circuit (see Fig. 3), its magnetic reluctance is

$$R = \frac{l}{\mu S} = \frac{44 \cdot 10^{-2}}{5.6 \cdot 10^{-3} \cdot 25 \cdot 10^{-4}} = 3.14 \cdot 10^{4} \text{ 1/H}.$$

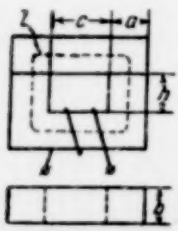

Fig. 3. The magnetic circuit of a vibrator.

Bearing in mind that

$$\psi = 2\varphi + \theta + \frac{\pi}{2},$$

and expanding the exponential factor in equation (7) as a power series (apart from the third term)

$$I = \sqrt{\frac{1}{T}\int_0^T i^2 dt} = \frac{I_0}{\sqrt{2}}\left[\left(\frac{11}{8} + m^2 - 2m_p\right) + m\sqrt{2}\left(1 - \frac{m_p}{4}\right)\sin\theta\right].$$

If the vibrator is turned to resonance, the effective current is

$$I = \frac{5.87}{\sqrt{2}}\left(\frac{11}{8} + 0.75^2 - 2\cdot\frac{0.75}{4}\right) = 6.9\ \text{A}.$$

Finally, the values L_{max}, L_0 and L_{min} for the selected magnetic circuit are found by the formula

$$L = \frac{w^2}{R + \frac{1}{G_s + G'}},$$

where R is the magnetic reluctance of the magnetic circuit; G_S the conductance for the leakage flux; G' the conductance of the air-gap.

Sotskov's formula [5] can be used to calculate G_S for the particular shape of magnetic circuit:

$$G_s = h\left(\frac{b}{c} + \frac{2a}{c + a\frac{\pi}{2}}\right)\mu_0 =$$

$$= 5\left(\frac{5}{8} + \frac{2\cdot 5}{8 + 5\cdot 1.57}\right)4\pi\cdot 10^{-9} = 0.786\cdot 10^{-7}\ \text{H}.$$

For a gap $\delta_{min} = 0.9$ mm, the corresponding values are

$$G'_{max} = \mu_0\frac{S}{2\delta_{min}} = 4\pi\cdot 10^{-9}\cdot\frac{25}{2\cdot 0.09} = 17.5\cdot 10^{-7}\ \text{H}$$

and

$$L_{max} = \frac{840^2}{3.14\cdot 10^4\cdot\frac{1}{0.786\cdot 10^{-7} + 17.5\cdot 10^{-7}}} = 1.22\ \text{H}.$$

Likewise for $\delta_0 = 3.9$ mm:

$$G_0 = 4.62 \times 10^7\ \text{H and } L_0 = 0.334\ \text{H}$$

for $\delta_{max} = 6.9$ mm:

$$G_{min} = 2.38 \times 10^7\ \text{H and } L_{min} = 0.22\ \text{H}$$

The actual value of the coefficient m is

$$m = \frac{1}{2}\ln\frac{L_{max}}{L_{min}} = 0.855.$$

The actual value of the coefficient m_ρ is

$$m_\rho = \frac{1}{4}\ln\frac{L_{max}L_{min}}{L_0^2} = 0.22.$$

The actual value of the efficiency of energy conversion is $M_1 = 0.3$.

The damping of the coil circuit for $r = 2.6\ \Omega$ is

$$\delta = \frac{r}{2L_0} e^{-m_\rho} = \frac{2.6}{2 \cdot 0.334} 0.8 = 3.1 \text{ 1/sec}$$

The true current value is

$$I_0 = \frac{U_m}{L_0 \sqrt{4\delta^2 + \omega^2 - 8\omega\delta m}} = \frac{380\sqrt{2}}{0.334 \cdot 310} = 5.18 \text{ A}.$$

The maximum mechanical power of the vibrator is

$$P = \omega \frac{L_0 I_0^2}{2} = 314 \cdot \frac{0.334 \cdot 5.18^2}{2} 0.3 = 420 \text{ W}$$

This power is 16 per cent below that specified. The desired power can be obtained by repeating the calculations and bearing in mind that the power can be increased by increasing M_1. This can be done by reducing m_ρ with a smaller conductance for the leakage flux and by increasing, for example, the width of the "window" of the magnetic circuit and reducing its height if possible. The following table shows recalculated values for larger window widths 9 and 10 cm. It will be seen that relatively small alterations in the shape of the magnetic circuit produce considerable changes in the work capability of a vibrator.

c cm	h cm	L_{max} H	L_0 H	L_{min} H	m	m_ρ	I_0 A	M_1	P W
8	5	1.22	0.334	0.22	0.855	0.22	5.18	0.3	420
9	5	1.215	0.33	0.216	0.867	0.221	5.23	0.355	502
10	5	1.205	0.322	0.206	0.883	0.218	5.37	0.364	527

Translated by O. M. Blunn

REFERENCES

1. A. I. Moskvitin; *Electrical reciprocating machines (Elektricheskiye mashiny vozvratno-postupatel'nogo dvizheniya)*. Izd. Akad. Nauk SSSR (1950).

2. A. E. Cheanokov; A study of the oscillation of an electromagnetic vibrator with a series-connected capacitor included in its circuit (Issledovanie kolebanii elektromagnitnogo vibratora pri malichii v ego tsepi posledovatel'no vklyuchennogo kondensatora). *Odessa Polytechnical Institute*, Vol. 16 (1959).

3. N.V. Maclachlan; *The theory and application of Mathieu functions.* Foreign Literature Publishing House (1953).

4. L.I. Mandel'shtam and N.D. Papaleksi; Resonance phenomena of order *n* (O yavleniyakh rezonansa *n*-go roda); *Collected works of L.I. Mandel'shtam*, Vol. 2. Izd. Akad. Nauk SSSR (1947).

5. B.S. Sotskov; *Fundamentals of the design and development of elements for automatic and telemechanical devices (Osnovy rascheta i proyektirovaniya elementov avtomaticheskikh i telemekhanicheskikh ustroistv).* Gosenergoizdat (1953).

YEAR
1961

AN ANALOGUE COMPUTER STUDY OF CURRENT TRANSFORMER TRANSIENTS*

YA. S. GEL' FAND

(All-Union Electrical Power Research Institute)

(Received 21 July 1961)

It takes a great deal of time to analyse the transient behaviour of current transformers with steel cores even when the load is linear.

The difficulties are multiplied for non-linear loads.

Analogue computers are of great assistance in this respect in that formerly intractable problems can be solved.

The All-Union Electrical Power Research Institute (A.E.P.R.I.) used mathematical simulation on analogue computers in the development of the new current transformer ferro-resonant supply units [1].

The method was based on the transformer equivalent circuit shown in Fig. 1*a*. The simulation circuit for current transformers with linear *RL* loads in Fig. 1*b* can be formed without difficulty from the equations

$$\left.\begin{aligned} \psi(i_\mu) &= Li_2 + r\int i_2\,dt + \psi_0; \\ i_1 &= i_\mu + i_2, \end{aligned}\right\} \qquad (1)$$

where $\psi(i_\mu)$ is the flux coupling of the secondary winding of the current transformer; ψ_0 the residual flux coupling; $L = L_t + L_l$ the total inductance of the secondary circuit (t = transformer, l = load); $r = r_t + r_l$ the total resistance of the secondary circuit; and i_μ the magnetization current of the current transformer**.

---

* *Elektrichestvo*, 12, 40–44, 1961.

** All the quantities refer to the secondary winding of the current transformer.

Most interest centres on the simulation of the non-linear magnetization branch of this circuit. Atabekov [1] and Sirota [2] have already shown that neglect of magnetic polarity reversal in the analysis of transient behaviour results in errors which are particularly marked at relatively small currents when the load impedance is small. The simulation of hysteresis curves with special cycles requires a rather complicated computing system with directly selected parameters [4]. To simplify the computing system and ensure its stable operation at large amplification factors of the resolving amplifiers, use has been made of a simple method of delaying the flux variation relative to the magnetization current. The main magnetization branch is simulated by means of a resolving amplifier with diode limiting cells in the feedback (see Fig. 2). The phase shift between the magnetization current and the flux is produced by a capacitor included in the feedback of this amplifier. The extent of this shift depends on the magnetic polarity reversal loss and eddy currents. The delay in flux variation relative to the magnetization current produces loops with special cycles which are analogous to hysteresis loops. It is too much to expect complete agreement between actual and simulated magnetization characteristics, but tests have shown that transient behaviour is reproduced with a fully acceptable degree of accuracy.

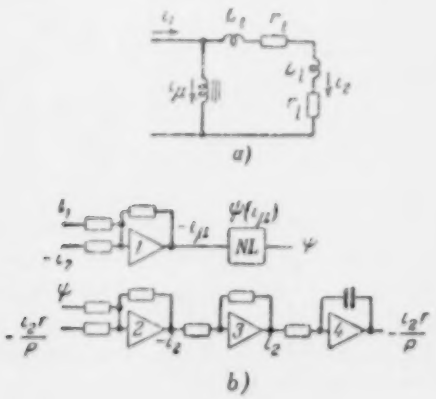

Fig. 1. a – equivalent circuit; b – simulation circuit for a current transformer with a linear *RL* load.

To determine the phase shift, a loss impedance is introduced which is calculated by the formula for the power loss in steel

$$P_{st} = k_c \left(\frac{B}{10\,000}\right)^2 \left(\frac{f}{50}\right)^{1.3} G,$$

where k_c is the specific loss W/g (State Standard 802-54), and G the weight of the core g.

For sinusoidally varying induction at a frequency of 50 c/s, this formula becomes

$$P_{st} = \frac{k_c l d \cdot 10^4}{4.95 s w^2} U^2.$$

Hence the conditional value of r_0 is

$$r_0 = \frac{4.95 s w^2 \cdot 10^{-4}}{k_c l d}, \qquad (2)$$

where d is the specific gravity of steel (7.65 for grade E3 electrical steel and 7.55 for grade E4 electrical steel); l, s the length of the middle line of force and the cross-section of the transformer core and w the number of turns in the secondary winding.

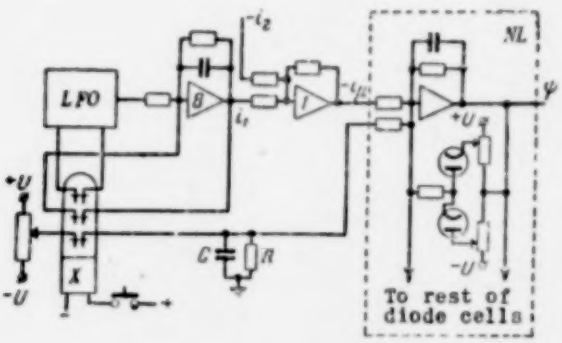

Fig. 2. The input circuit and system of establishing the residual magnetization in the non-linear unit:

LFO – low-frequency oscillator; if no works oscillator is available, the required sinusoidal oscillations can be produced by three amplifiers with the structural scheme corresponding to the equation

$$p^2 x + \omega^2 x = 0.$$

Considering that the method is only an approximation, the value of r_0 from (2) can also be used for actual non-sinusoidal variation of induction.

Figure 3 shows a test hysteresis loop simulated by the proposed method. The diagram clearly shows the limits of the piecewise linear approximation of the magnetization curve.

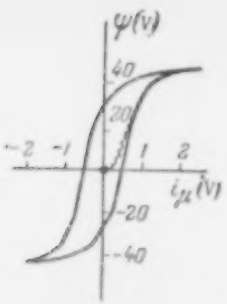

Fig. 3. Hysteresis loop recorded on the screen of an MN-7 machine's electronic indicator.

YEAR
1961

The proposed approximate method of simulating the magnetization characteristic cannot reproduce the residual magnetization in the current transformer core after large short-circuit currents. But this quantity can be found from test curves relating the residual induction to the maximum induction during the flow of short-circuit current [2].

The transient behaviour of a current transformer can be simulated in the presence of residual core induction by artificially shifting the initial magnetization curve. This can be done by supplying a direct voltage of appropriate sign to an additional input of the non-linear unit (NL) (see Fig. 2). The displacement must gradually decrease since the hysteresis loop of the current transformer is symmetrical at the end of transient behaviour. This reduction is brought about by an RC circuit with a time constant approximately equal to that of the aperiodic component of the short-circuit current.

The accuracy with which the transient behaviour of a current transformer could be simulated has been checked by comparing calculations by Sirota's method [3.6] with oscillograms taken during simulation on an MN-7 electronic machine. The test transformer was a TV-35-type 200/5 current transformer with a load $r = 0.3\ \Omega$ and $x = 0.1\ \Omega$ (including the winding resistance), a primary current of 450 A, and a time constant for the aperiodic component of current of 0.1 sec.

Figure 4 shows the core magnetization curve (grade E41 electrical steel) [5] and its piecewise linear approximation.

The following scales were used:

frequency – 0.7 c/s, $m_f = 0.014$;

current 1 V – 2 A, $m_i = 0.5$ V/A;

flux coupling 100 V – 0.4 V.sec, n_ψ = 250 V/V sec.

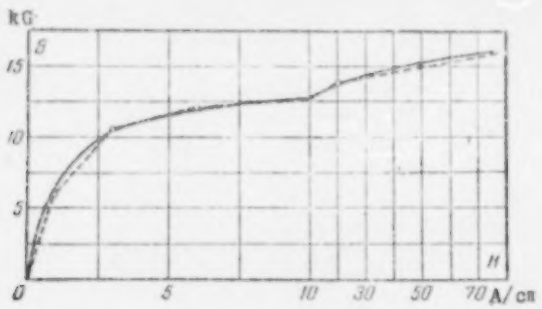

Fig. 4. ——— – original magnetization curve for grade E41 electrical steel; – – ○ – – – its piecewise linear approximation on the MN-7 machine.

The oscillograms are given in Fig. 5.

The calculated magnetization currents were as follows:

without residual magnetization

6.3 A for t = 40 msec,

7.3 A for t = 50 msec;

with residual magnetization

6.0 A for t = 20 msec,

10.5 A for t = 30 msec.

The oscillograms show that good agreement is obtained.

This system of simulation permits the analysis of transient behaviour in any current transformer for different load resistances provided the core is made of the same steel. A change to other criteria is made by altering the amplification factors of the resolving amplifiers: the scale of the magnetization curve along the axis i_μ is changed by altering the feedback resistance of amplifier *1*; the scale of the magnetization curve in the ψ-direction is changed by altering the input resistance of the appropriate input of amplifier 2; r is changed by altering the input resistance of integrator 4; L is changed by altering the feedback resistance of amplifier 2 (see Fig. 1*b*). The time constant of the aperiodic component of the short-circuit current can be changed by the feedback resistance of the amplifier *B* in the input (perturbation) circuit (see Fig. 2). The new A.E.P.R.I. ferro-resonant supply

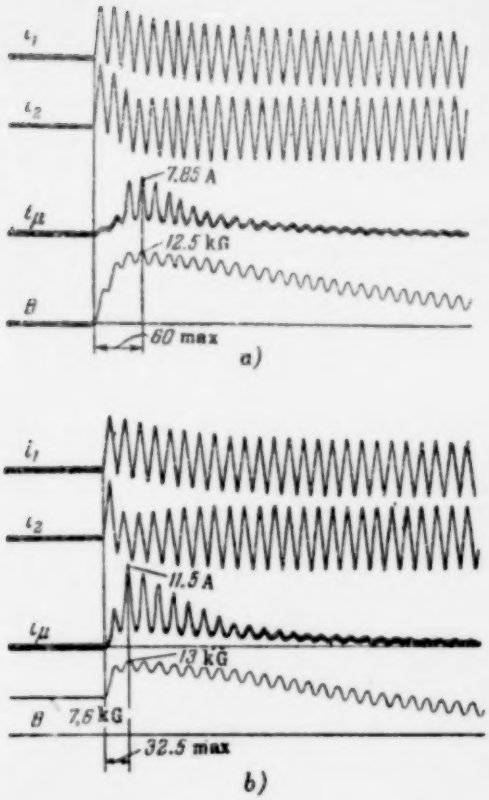

Fig. 5. Oscillograms of the transient behaviour of a TV-35 200/5 current transformer as obtained on the MN-7 machine. Value of the current i_μ referred to the secondary winding.

units were simulated like transformers with a parallel *RC* load. The initial system of equations differs from (1) by the expression for the flux coupling

$$\psi = Li_2 + \frac{i_2 r}{p} + \frac{i_c}{p^2 C}, \tag{3}$$

where i_c is the current through the capacitance C of the ferro-resonant circuit.

Since the load resistance is connected in parallel with the capacitor, therefore

$$\frac{i_c}{p^2C} = \frac{i_l r_l}{p},$$

where i_l is current in the load resistance r_l.

Figure 6 shows the simulation circuit for a ferro-resonant supply unit connected to a current transformer.

The A.E.P.R.I. used the results of this type of investigation in the development of supply units for a.c. relay protection systems. A fully acceptable degree of accuracy was obtained between test results and computations [7].

The proposed system features simplicity and stability, and only a few resolving amplifiers are required. The same method can also be applied to devices which are transformer loads. In particular, it is fairly simple to simulate current circuits in differential protection with rapidly saturated single and three-phase transformers. Abrupt variations in the magnetization current of power transformers can also be analysed.

YEA
196

Conclusions

1. The transient behaviour of current transformers can be studied quite simply on analogue computers.

2. A simple, stable and accurate system of simulation has been described which dispenses with tedious analytical methods.

Appendix

The criteria of the resolving amplifiers for the simulation of current transformers.

1. *Loss in the transformer core.* Putting k for the shape of the initial section of the simulated curve $\psi(i_\mu)$ and R' for the appropriate feedback resistance of the amplifier in the non-linear unit, the corresponding feedback capacitance is

$$C' = km_i/m_\psi m_f R' r_0 \qquad (A.1)$$

2. *Constructional criteria.* If the non-linearity of $\psi(i_\mu)$ is simulated in the non-linear unit in such a way that the flux coupling ψ_0 corresponds to the arbitrary flux density B_0 and the current $i_{\mu 0}$ to the field intensity H_0, the items w, s and l may vary as follows:

$$R_{fb1} = R_{fb10} \frac{i_{\mu 0}}{H_0} \cdot \frac{w}{l}, \qquad (A.2)$$

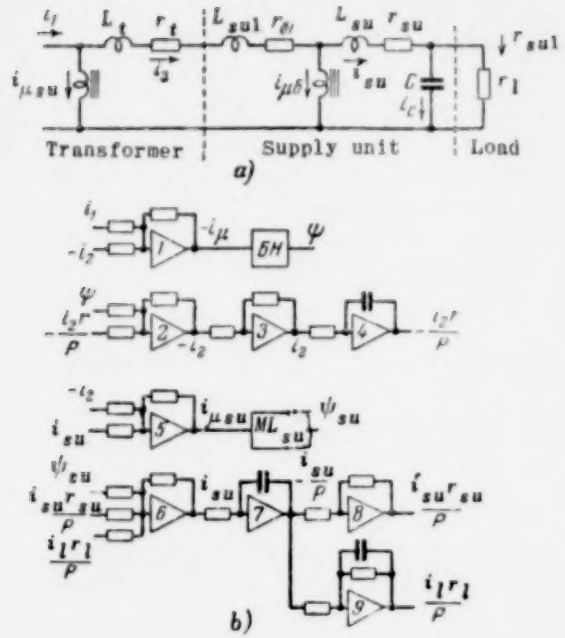

Fig. 6. a – equivalent circuit of current transformer with a ferro-resonant supply unit connected to it; b – its structural simulation circuit. (*su* – supply unit)

where R_{fb1} and R_{fb10} are the feedback resistances of the amplifier *1* (see Fig. 1b);

$$R_{in\ 2} = \frac{\psi_0 R_{in\ 20}}{B_0\, 10^{-3}} \cdot \frac{1}{\omega s}, \qquad (A.3)$$

where $R_{in\ 2}$ and $R_{in\ 20}$ are the input resistances of amplifier *2* (see Fig. 1b).

3. Inductance. If the input resistance $R_{in\ 20}$ of amplifier 2 is constant

$$R_{fb2} = \frac{m_i R_{in\ 20}}{m_\psi} \cdot \frac{1}{L}. \qquad (A.4)$$

4. Resistance. If the capacitance C_{fb4} of the feedback capacitor of amplifier *4* is constant

$$R_{in\,6} = \frac{m_i}{m_\psi m_f C_{fb6}} \cdot \frac{1}{r} \qquad (A.5)$$

5. r_{su} (Fig. 6)

$$R_{in8} \quad (R_{fb8} m_i / R_{in7} C_{fb7} m_f m_\psi) \times 1/r_{su} \qquad (A.6)$$

6. c_l *and* C_l. The relationship between the resistance and capacitance of the feedback capacitor of amplifier 9 is selected from considerations of equality between the angle of feedback impedance in the scale m_f and the angle of impedance of the parallel-connected r_l and C_l:

$$m_f C_{fb9} R_{fb9} = C_l r_l \qquad (A.7)$$

The input resistance of amplifier 9 is found from one of the following expressions:

$$R_{in9} = (R_{fb9} m_i / R_{in7} C_{fb7} m_f m_\psi) \times 1/r_l$$
$$R_{in9} = (m_i / R_{in7} C_{fb7} C_{fb9} m_f m_\psi) \times 1/C_l \qquad (A.8)$$

7. *The time constant* τ *of the short-circuit current.* The time constant is adjusted by changing the feedback resistance of the amplifier B (see Fig. 2):

$$R_{fbB} = \tau / m_f C_{fbB} \qquad (A.9)$$

Translated by O.M. Elunn

REFERENCES

1. Ya.S. Gel'fand and M.I. Tsarev; Operative a.c. relay protection and control apparatus (Releinaya zashchita i elektroavtomatika na peremennom operativnom toke). *Inf. mat. All-Union Electrical Power Research Institute*, No. 41. Gosenergoizdat (1959).

2. G.I. Atabekov; *Relay protection of high-voltage networks (Releinaya zashchita vysokovol'tnykh setei)*. Gosenergoizdat (1949).

3. I.M. Sirota; *Elektrichestvo*, No. 2 (1959).

4. V.G. Vasil'ev and V.A. Zverev; *Izv. vys. ucheb. zaved., Elektronika*, No. 9 (1959).

5. A.S. Zaimovskii and L.A. Chudnovskaya; *Magnetic materials (Magnitnye materialy)*. Gosenergoizdat (1957).

6. I.M. Sirota; *Izv. vys. ucheb. zaved., Energetika*, No. 7 (1960).

7. Ya.S. Gel'fand; Forced steady-state oscillations in parallel ferroresonant circuits connected to the current source, (Vynuzhdennye kolebaniya v parallel'nykh ferrorezonansnykh konturakh, vklyuchennykh na istochnik toka). *Trud. All-Union Electrical Power Research Institute*, No. 11. Gosenergoizdat (1961).

YEAR
1961

DESIGN OF DEEP GROUNDING RODS FOR TRANSMISSION LINE TOWERS*

A.B. OSLON

(Perm')

(Received 6 June 1961)

The increasing use of mechanization in the construction of transmission lines has attracted attention to the design of the grounding rods which are placed in pits beneath the foundations or footings of the towers (deep grounding rods). In this paper a method of determining their grounding resistance is proposed on the assumption that the rods are in homogeneous ground.

The design of deep grounding rods was considered in a recent paper published in the Soviet journal *Elektricheskie stantsii* [1]. A method was proposed which involved utilization coefficients. Its drawback is the possibility of subjective estimates since the choice of coefficients is based on analogy and depends on the experience of the person performing the calculations. The method proposed in this paper is free of this shortcoming.

Deep grounding rods beneath the foundations of pylons are of comparatively small dimensions, their dimensions being approximately the same in the horizontal and vertical direction.

It has been shown elsewhere [2] that when the line density of the current flowing from each element making up the grounding system can be assumed to be the same, the resistance of a grounding rod is

$$R=\frac{\alpha_{11}+\sum_{k=2}^{n}\frac{l_k}{l_1}\alpha_{1k}}{1+\sum_{k=2}^{n}\frac{l_k}{l_1}}, \qquad (1)$$

* *Elektrichestvo*, 12, 59-63, 1961.

where n is the number of elements in the grounding system; a_{11} the natural resistance of each element 1; a_{1k} the mutual resistances between element 1 and all the other elements; and l_k the lengths of the respective elements.

Consider, for example, the grounding system illustrated in Fig. 1. It consists of four horizontal conductors 5 m in length, which form a square at the bottom of the pit, and four vertical conductors 2.5 m in height set up at the corners of the square. Together with their specular images, these conductors form a cube with edges 5 m long (l = 5 m).

If the individual conductors of circular section are 1 cm in diameter (d = 1 cm), and the specific resistance of the ground is ρ (in ohm-metres), then the natural resistance of a conductor is

$$a_{11} = \frac{\rho}{2\pi l} \ln \frac{2l}{d} = \rho.0.220. \tag{2}$$

YEAR 1961

The mutual resistance between conductor *1* and the conductors parallel to it (*3*, *9*, *11*) can be found by the formula

$$a_{1k} = \frac{\rho}{2\pi l}\left(\operatorname{ar\,sinh}\frac{l}{a} + \frac{a}{l} - \sqrt{\left(\frac{a}{l}\right)^2 + 1}\right), \tag{3}$$

where a is the distance between conductors *1* and k, $a = l$ for conductors *3* and *9* and $a = \sqrt{2}\,l$ for conductor *11*.

From formula (3)

$$a_{13} = \rho.0.0150; \tag{3a}$$

$$a_{1\,11} = \rho.0.0109. \tag{3b}$$

For the mutually perpendicular conductors *1* and *2* (and also *4*, *5* and *8*), the mutual resistance is found from the formula

$$a_{12} = \frac{\rho}{4\pi l_1 l_2}\left(l_1 \operatorname{ar\,sinh}\frac{l_2}{l_1} + l_2 \operatorname{ar\,sinh}\frac{l_1}{l_2}\right). \tag{4}$$

If $l_1 = l_2$, then

$$a_{12} = \frac{\rho}{2\pi l} \operatorname{ar\,sinh} 1 = \frac{\rho}{2\pi l} \ln(\sqrt{2} + 1) = \rho.0.0280. \tag{4a}$$

Using the mean potential method [2], for the conductors *1* and *6*, *7*, *10*, *12* in different planes

$$a_{16} = \frac{\rho}{4\pi l}\left(\ln\frac{\sqrt{2l^2 + a^2} + l}{\sqrt{2l^2 + a^2} - l} - \frac{a}{l}\operatorname{arc\,tan}\frac{l^2}{a\sqrt{2l^2 + a^2}}\right), \tag{5}$$

where a is the distance between the planes in which the conductors lie.

In the case in question, $a = l$. Therefore

$$\alpha_{16} = \frac{\rho}{4\pi l}\left(\ln\frac{\sqrt{3}+1}{\sqrt{3}-1} - \operatorname{arc\,tan}\frac{1}{\sqrt{3}}\right) = \frac{\rho}{4\pi l}\cdot 0.793 = \rho\cdot 0.0126. \tag{5a}$$

Thus, in a homogeneous conducting medium, the leakage resistance of a cube made up of conductors 5 m long and 1 cm in diameter is

$$R = \frac{\alpha_{11}+2\alpha_{12}+4\alpha_{13}+4\alpha_{16}+\alpha_{1-11}}{12} = \rho\cdot 0.0353.$$

The resistance R' of the grounding system under consideration is twice as much, i.e.

$$R' = \rho\cdot 0.0706.$$

Formulae (3)-(5) are too cumbersome to calculate the mutual resistances. A satisfactory alternative is the formula for the potential of a point in a radially spherical field

$$\alpha_{1k} = \frac{\rho}{4\pi r_{1k}}, \tag{6}$$

where r_{1k} is the distance between the mid-points of the respective conductors.

In fact, using formula (6)

$$\alpha_{12} = \rho\cdot 0.0225;\ \alpha_{16} = \rho\cdot 0.013;$$

$$\alpha_{13} = \rho\cdot 0.016;\ \alpha_{1-11} = \rho\cdot 0.011.$$

Hence

$$R = \rho\cdot 0.034;$$

$$R' = \rho\cdot 0.068.$$

As a second example, consider a ring 7 m in diameter ($D = 7$ m) laid at a depth $t = 2.5$ m and provided with four vertical rods which are arranged uniformly on its circumference (Fig. 2). These rods are about 5 m apart. They too are made from circular rod of diameter $d = 1$ cm.

Using the above notation, the natural resistance of the ring according to Margolin's formula is

$$\alpha_{11} = \frac{\rho}{2\pi^2 D}\ln\frac{8D}{d} = \rho\cdot 0.0628. \tag{7}$$

The mutual resistance between the ring and its vertical image is found by integrating the potentials formed by the currents flowing from all points of the ring at some point of its specular image. Owing to the symmetry of the system, it is unnecessary to integrate the potential formed at all points of the specular image. After

transformations

$$\alpha_{12} = \frac{\rho}{2\pi^2 \sqrt{D^2 + 4t^2}} \int_0^{\frac{\pi}{2}} \frac{d\beta}{\sqrt{1 - K^2 \sin^2\beta}}, \tag{8}$$

where

$$K^2 = \frac{D^2}{D^2 + 4t^2}.$$

The integral in formula (8) is a total elliptic integral of the first kind. In the case in question $K^2 = 0.663$ and the integral is 2.024. Consequently, $\alpha_{12} = 0.0119$.

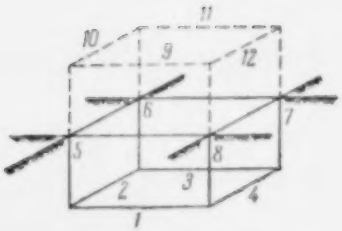

Fig. 1.

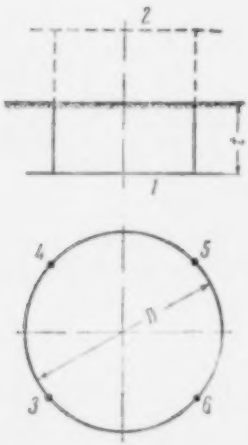

Fig. 2.

Elliptic integrals are usually difficult to use. Formula (8) is therefore best replaced by an approximate expression

$$\alpha_{12} = \frac{\rho}{2\pi^2 D} \ln \frac{2D}{t} \tag{8a}$$

(t is half the distance between the ring and its specular image), provided the ratio t/D is small, and when it can be assumed that the elliptic integral of the first kind is equal to

$$\ln \frac{2\sqrt{D^2 + 4t^2}}{t},$$

and the quantity $4t^2$ can be ignored since it is small in comparison with D^2. Expression (8a) provides a close approximation if $t/D \leqslant 1/2$. In the particular case in hand

$$\frac{t}{D} = 0.357.$$

Consequently

$$a_{12} = \rho \cdot 0.0125.$$

Five per cent error is quite permissible.

Expression (8a) provides a simple formula for the mutual resistance between the ring and the vertical conductors. Here it is necessary to integrate (8a) over the length of the conductor and divide the result by the length of the conductor. As a result

$$a_{13} = \frac{\rho}{2\pi^2 D}\left(\ln\frac{4D}{l} + 1\right) = \rho \cdot 0.0197, \qquad (9)$$

where $l = 2t$, since a_{13} refers to the vertical conductor and its specular image.

If the length of the vertical conductor is greater than the diameter of the ring, formula (9) leads to errors because (8a) provides only a rough approximation.

Applying formula (1), the leakage resistance of a system consisting of a ring and four vertical conductors with their specular images is

$$R = \frac{a_{11} + a_{12} + \frac{2t}{\pi D} 4a_{13}}{1 + 1 + \frac{2t}{\pi D} 4} = \rho \cdot 0.032.$$

The grounding resistance is twice as much:

$$R' = \rho \cdot 0.064.$$

In this analysis it has been assumed that the density of the current flowing from the ring and vertical rods was the same. This assumption can be dropped if the grounding system is regarded as consisting of two parts, one of which incorporates the horizontal elements (i.e. the ring and its specular image), whilst the other includes the vertical conductors and their specular images.

Suppose that a_{I} and a_{II} represent the natural resistances of these parts and $a_{\mathrm{I\ II}}$ their mutual resistance. The earthing resistance R' of the grounding system as a whole is then given by Schwarz' formula

$$R' = \frac{a_{\mathrm{I}} a_{\mathrm{II}} - a^2_{\mathrm{I\ II}}}{a_{\mathrm{I}} + a_{\mathrm{II}} - 2a_{\mathrm{I\ II}}}. \qquad (10)$$

According to formula (1):

for the natural resistance of the horizontal conductors

$$\alpha_h = \frac{\alpha_{11} + \alpha_{12}}{2} = \rho \cdot 0.0377;$$

for that of the vertical conductors

$$\alpha_v = \frac{\alpha_{33} + 2\alpha_{34} + \alpha_{35}}{4} = \rho \cdot 0.0614$$

(the values $\alpha_{34} = \rho \times 0.0150$ and $\alpha_{35} = \rho \times 0.0109$ have been calculated for the grounding system of Fig. 1).

Their mutual resistance is

$$\alpha_{hv} = \alpha_{13} = \rho \cdot 0.0197.$$

Substituting these quantities in formula (10)

$$R = \rho \cdot 0.0324.$$

The result is very close to that obtained previously. This shows that it is permissible to assume a uniform distribution of the current along the conductors when calculating the grounding resistance [2, 5].

Now consider a typical grounding system in the form of a small ring with one conductor (Fig. 3). Formulae (8a) and (9) are not applicable to this case because $t \gg D$. The mutual resistance between the ring and its specular image is calculated by the approximate formula (6):

$$\alpha_{12} = \frac{\rho}{4\pi 2t} = \rho \cdot 0.0159.$$

Fig. 3.

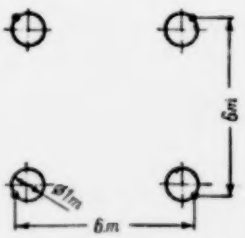

Fig. 4.

The natural resistance of the ring is found from formula (7):

$$\alpha_{11} = \rho \cdot 0.337.$$

The resistance of the horizontal elements is

$$\alpha_h = \rho \frac{0.337 + 0.0159}{2} = \rho \cdot 0.1765.$$

The natural resistance of the vertical element is calculated by formula (2):

$$a_v = \rho \cdot 0.220.$$

To calculate the mutual resistance a_{hv}, it is necessary to integrate expression (8) over the length of the vertical element. This operation can only be performed by numerical integration. The quantity a_{hv} is therefore found approximately.

It is obvious that the total resistance of the grounding system hardly varies if the top of the vertical element is moved to the centre of the ring. This implies that the quantity a_{hv} hardly varies either, and it can be calculated like the potential created by a unit of current flowing from the vertical grounding rod at any point of the ring, i.e. the following formula can be used [2]:

$$a_{hv} = \frac{\rho}{4\pi l} \ln \frac{2a + l}{2a - l}, \qquad (11)$$

where $2a$ is the sum of the distances from the point to the ends of a rectilinear conductor, and $l = 2t$ is the length of this conductor.

From formula (11), the mutual resistance is

$$a_{hv} = \rho \cdot 0.0478.$$

In accordance with formula (10)

$$R = \rho \frac{0.1765 \cdot 0.220 - 0.0478^2}{0.1765 + 0.220 - 2 \cdot 0.0478} = \rho \cdot 0.122,$$

$$R' = \rho \cdot 0.244.$$

Now suppose that grounding systems similar to that shown in Fig. 3 are laid under the four footings of a tower at the vertices of a square with sides 6 m long (see Fig. 4).

The mutual resistance between the individual grounding systems can be found quite accurately by formula (6) because the distance between them is greater than their own size (here the grounding systems are again considered together with their specular images, and the distance between their mid-points is taken as r_{14}). As a result

$$a_{12} = a_{14} = \rho \times 0.0133 \text{ and } a_{13} = \rho \times 0.0095.$$

In accordance with formula (1)

$$R = \rho \frac{0.122 + 2 \cdot 0.0133 + 0.0095}{4} = \rho \cdot 0.0395.$$

The resistance of an actual grounding system is

$$R' = \rho \cdot 0.079.$$

It is typical of the grounding systems shown in Figs. 1, 2 and 4 that their grounding resistances are approximately the same. The explanation is that they occupy approximately the same volume of earth. The volume of the cube in Fig. 1 is 125 m^3. A sphere of the same volume has a radius of 3.1 m. The resistance of a hemisphere grounding system of the same radius is

$$R' = \frac{\rho}{2\pi r} = \rho \cdot 0.0515.$$

This quantity can be used for estimating the lower limit of grounding resistance for deep grounding systems occupying a corresponding volume of earth. The better the surface of the volume is used to arrange the grounding conductors, the closer is the grounding resistance of an actual system to that stated above. This explains the relatively high grounding resistance of the system shown in Fig. 4 in which there are no "cross-pieces" in the earth between its four individual parts.

YEAR 1961

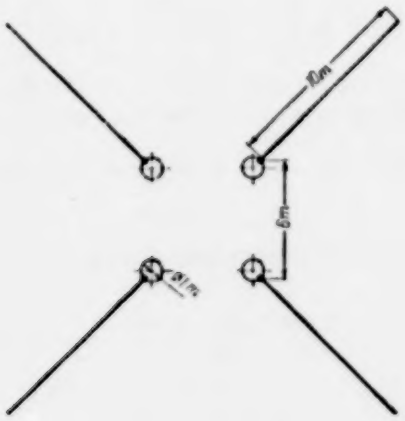

Fig. 5.

Thus, there are two ways of reducing the grounding resistance of deep grounding systems. Either a larger volume of earth can be occupied, or else its surface can be utilized better in the arrangement of the grounding conductors.

Finally, consider a grounding system consisting of a deep part and

Finally, consider a grounding system consisting of a deep part and four arms (Fig. 5). Formula (10) is applied. The grounding resistance of the deep part is denoted by a_1. It has already been defined in the last example:

$$a_1 = \rho \cdot 0.079.$$

The grounding resistance of arms which form a "four-arm star", according to Oslon [2], is

$$a_2 = \frac{\rho}{2\pi L} \ln \frac{8 \cdot 45 L^2}{dt} = \rho \cdot 0.058,$$

where L is the total length of the arms; t the depth at which they are laid (assumed to be 0.5 m); and d the diameter of the rod of circular section (1 cm).

The mutual resistance is found as follows. The field of the sunk grounding system is nearly radial-spherical. Using the method of mean potentials to calculate a_{12} and bearing in mind the proximity of the earth surface (i.e. assuming for the radial-spherical field that $a = \rho/2\pi r$ and not $\rho/4\pi r$):

$$a_{12} = \frac{1}{2\pi l} \int_0^l \frac{dl}{r} = \frac{1}{2\pi l} \int_{r_1}^{r_2} \frac{dr}{r} = \frac{1}{2\pi l} \ln \frac{r_2}{r_1}, \qquad (12)$$

where l is the length of an arm; and r_1, r_2 the distances between the centre of the grounding system and the ends of a rod.

In the case in question (r_1 = 4.25 m and r_2 = 14.25 m):

$$a_{12} = \rho \cdot 0.019,$$

and hence for the total grounding resistance

$$R' = \rho \frac{0.079 \cdot 0.058 - 0.019^2}{0.079 + 0.058 - 2 \cdot 0.019} = \rho \cdot 0.0425.$$

Translated by O.M. Blunn

REFERENCES

1. Yu.I. Lyskov and A.N. Sherentsis; *Elek. stants.*, No. 10 (1957).
2. A.B. Oslon; *Elektrichestvo*, No. 4 (1958).
3. N.P. Margolin; *Ground currents (Toki v zemle)*. Gosenergoizdat (1947).
4. S.J. Schwarz; *Trans. Amer. Inst Elect. Engrs.*, Pt. III-B, Vol.73 (1954).
5. A.B. Oslon; *Elektrichestvo*, No. 7 (1959).

GRAPHICAL ANALYSIS OF THE THERMAL BREAKDOWN VOLTAGE OF HIGH-FREQUENCY INSULATORS*

N.P. BOGORODITSKII, Yu.M. VOLOKOBINSKII and I.D. FRIDBERG

(Lenin Electrical Engineering Institute)

(Received 11 August 1961)

YEAR 1961

Introduction

To calculate the thermal breakdown voltage of insulators and capacitors analytically, it is necessary to solve the differential equation

$$div(K \text{ deg } T) = -Q, \tag{1}$$

where K is the coefficient of thermal conductivity of the dielectric; T the temperature; and Q the specific heat dissipation in the dielectric.

For h.f. thermal breakdown

$$Q = (\epsilon \tan \delta / 1.8 \times 10^6) f E^2 [\text{ W/cm}^3], \tag{2}$$

where ϵ is the dielectric permeability; $\tan \delta$ the tangent of the dielectric loss angle; f the frequency of the alternating electrical field, c/s; and E the intensity of the electrical field, kV/cm.

The analytic solution of equation (1) is confronted with great difficulties which can only be overcome by simplifications. To integrate equation (1) it is necessary to represent K, ϵ, $\tan \delta$ and E as comparatively simple functions of co-ordinates and temperature. In particular, the relationship between $\tan \delta$ and temperature is written in the form

$$\tan \delta = Ae^{aT}, \tag{3}$$

---

* *Elektrichestvo*, 12, 63-69, 1961.

where A and a are constants.

But if this relationship is written thus, a is no longer a constant quantity for ceramic materials. It in fact increases by a factor of 1.5 to 5 for a temperature rise from 0 to 200°C [1]. The existing theory cannot therefore be used to calculate the thermal breakdown voltage of ceramic insulators.

Moreover, the existing theory was evolved for specimens of comparatively simple shape which can be regarded as flat infinite plates or circular tubes and bars [2-4]. The relationship between E and the co-ordinates is then comparatively simple and equation (1) may be solved.

Insulators with uniform fields have the relatively greatest operating voltages for minimum dimensions [5] (see Fig. 1). The electrical fields of these insulators are illustrated in Fig. 2 from the results of an electrolytic tank study of models of porous material. A study of these fields shows that the relationship $U = El$ exists between the voltage U applied to the insulator and the intensity E of the electrical field in the insulator, where l is the shortest distance between the electrodes in the body of the insulator.

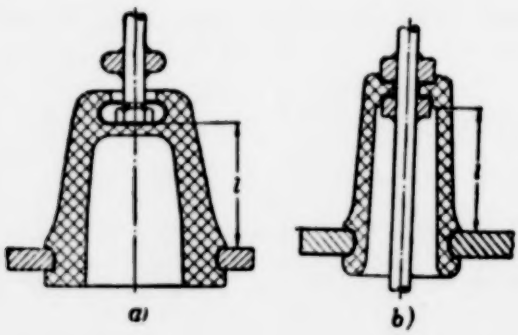

Fig. 1. Sectional view of typical insulators with a "uniform field": a – "support" insulator; b – "transfer" insulator.

If the intensity E_b of the field at which breakdown occurs in the insulator is known, the thermal breakdown voltage U_b can be found by multiplying E_b by l. The first step in the determination of U_b is the calculation of E_b. If the heat transfer on to electrodes can be ignored for the insulators shown in Fig. 1, the quantity E_b is independent of l and decreases with increasing wall thickness.

If the diameter of the insulator is much greater than the thickness of the wall D, the wall of the insulator can be regarded as approximately flat. The problem therefore reduces to that of a plane-parallel plate in which heat transfer takes place in X direction perpendicular to its surface, and the electrical field vector is directed along the surface of the plate (see Fig. 3). The mathematical solution is the same for a finite plate in which surface heat transfer is ignored as for an infinite plate in a uniform field.

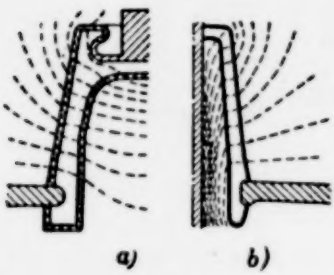

Fig. 2. Electrical fields of insulators in Fig. 1: a – "support"; b – "transfer".

Fig. 3. A contribution to the calculation of E_b.

The thermal breakdown voltage of ceramic insulators and capacitors can be determined by the following graphical method whenever the variation of tan δ with temperature is not to be regarded as exponential.

Fundamentals of the method

To illustrate the method, it is proposed to consider a dielectric plate in a uniform high-frequency electrical field with its intensity vector parallel to the surface of the plate. Suppose that the thermal insulation of one surface of the plate is ideal at $X = 0$ and that the other is cooled by air at $X = D$ (see Fig. 3). Heat transfer takes place in the X direction which is perpendicular to the electrical field vector E. The direction of this vector E at the instant t and that of the vector of heat flow density q are shown in Fig. 3. It is assumed that the variation of K, ϵ and tan δ with temperature is known. The following notation is used:

$$\eta = \epsilon \tan \delta f / 1.8 \times 10^6 \ [\mathrm{W/cm \times kV^2}], \qquad (4)$$

where η differs by a constant factor from the specific a.c. conductance in $\Omega^{-1} \times \mathrm{cm}^{-1}$. This quantity η is plotted as a function of temperature (see Fig. 4). It follows from (2) that the specific heat dissipation is

$$Q = \eta E^2. \tag{5}$$

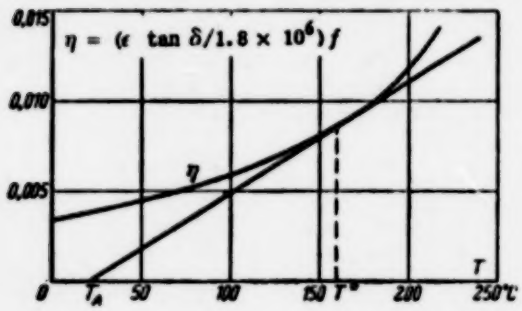

Fig. 4. The relationship between η and temperature.

A power P_{die} is dissipated in a column of unit section which is equal in height to the thickness D of the plate. If the temperature T_n of the cooled surface is greater than the ambient temperature T_A, the power P_{eff} from a unit area of the plate's surface is determined by convection and radiation and depends on the position of the plate in air [6-8]. In the general case the power P_{eff} from a unit of surface area is a non-linear function of the difference $(T_n - T_A)$ and depends on the shape and dimensions of the component and the state and chemical composition of its exposed surface. It is to be supposed that

$$P_{eff} = \lambda (T_n - T_A), \tag{6}$$

where the coefficient λ of external heat transfer is independent of temperature and where the variation of K with temperature can be ignored.

In thermal equilibrium

$$P_{die} = P_{eff} = -K \frac{dT}{dX}\Big|_{X=D} = \lambda (T_n - T_A) \tag{7}$$

or

$$-\frac{dT}{dX}\Big|_{X=D} = -\frac{\lambda}{K}(T_n - T_A), \tag{8}$$

where $dT/dX|_{X-D}$ is the temperature gradient of the dielectric on the surface $X = D$. It follows from (7) that the amount of heat dissipated in the plate at the temperature T_n in question is given. If the temperature distribution in the dielectric and T_n are known, it is therefore

possible to calculate the intensity E of the field in the dielectric which heats the plate such that the temperature of the cooled surface is T_n. Suppose the condition of thermal equilibrium is written in the form

$$E^2 \int_0^D \eta(T)\, dX = \lambda (T_n - T_A), \tag{9}$$

Then

$$E^2 = \frac{\lambda (T_n - T_A)}{\int_0^D \eta(T)\, dX}. \tag{10}$$

Using the notation

$$\bar{\eta} = \frac{1}{D} \int_0^D \eta(T)\, dX, \tag{11}$$

YEAR 1961

expression (10) simplifies to

$$E^2 = \frac{\lambda (T_n - T_A)}{\bar{\eta} \cdot D}. \tag{12}$$

The field intensity which causes the temperature of the cooled surface to rise to T_n can therefore be determined by finding the distribution of the temperature in the plate and calculating its mean value.

The surface temperature $T_{n.b}$ at which the intensity of the field is maximum E_b can be found by plotting E as a function of T_n if the condition of thermal equilibrium is fulfilled (see Fig. 5). The maximum field intensity E_b can be found by substituting in 12 $T_{n.b}$ for T_n and η_b for the value η if thermal equilibrium is unstable.

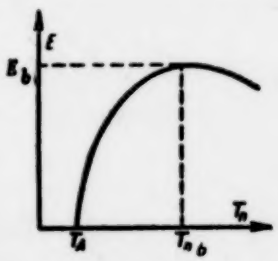

Fig. 5. The relationship between E and T_n in thermal equilibrium.

To determine the thermal breakdown voltage it is sufficient in

practice to know those values of T_n', T_n'', E' and E'' for which

$$T_n' < T_{n\,b} < T_n'' \tag{13}$$

and

$$E' < E_b < E''. \tag{14}$$

For unstable thermal equilibrium

$$T_{n\,b} < T^* < T_{0\,b}, \tag{15}$$

where $T_{0.b}$ is the maximum temperature in the plate at breakdown, and T^* is defined as the temperature at the point where a straight line from T_A on the base is tangential to the curve representing the variation of η with temperature (see Fig. 4).

The temperature T_n' is obtained on the assumption that the temperature distribution in the plate is linear at the maximum temperature T^*. The other temperature T_n^{**} is found by assuming that the temperature distribution is parabolic and that the mean temperature is T^*. The intensity E' is obtained by putting in (12) the increased value of η and T_n' instead of T_n. The intensity E'' is found by putting in (12) the reduced value of η and T_n'' instead of T_n. Formulae may then be obtained for the thermal breakdown voltage and maximum temperatures of insulators and capacitors.

The coefficient of external heat transfer λ decreases with decreasing component size and increases with increasing temperature. For surface areas greater than 200 cm^2, λ can be taken as 0.001 W/cm^2 × deg [9]. Its value may be several times greater for small insulators and capacitors.

The proposed graphical method is accurate enough for practical purposes. For example, if it is assumed that ϵ is independent of temperature and that the variation of tan δ with temperature is in the form (3), for a plate 100 mm thick by the graphical method

$$E_{av} = \frac{1}{2}(E' + E''), \tag{16}$$

which is within 0.5 per cent of the calculated value of E_b. The error

$$\Pi = \frac{E'' - E'}{E'' + E'} \tag{17}$$

is less than 5 per cent. The error can be calculated by formula (17) in those cases when the variation of tan δ with temperature is not to be regarded as exponential.

According to Fridberg, the thermal breakdown voltage of rutile ceramic capacitors (see Fig. 6) is between 7 and 13 kV at ambient air

temperatures of 25 to 30° C and a frequency of 1.7 Mc/s. The figure produced by the graphical method for the same capacitors was 10 kV with a coefficient of external heat transfer λ equal to 0.006 W/cm^2 × deg.

Fig. 6. KVKB-13 rutile ceramic capacitors.

YEAR
1961

Application of the method

The proposed method can be used for the design of all ceramic insulators which can be regarded as plates in a homogeneous field, e.g. insulators with a uniform field.

Suppose it is required to find E_b and the plate temperature at the frequency f = 1 Mc/s. The plate is in a uniform field. Heat transfer parallel to the surface of the plate is negligible.

Given.

1. The variation of ϵ and tan δ with temperature at the operating frequency F = 1 Mc/s.

2. Air cooling on one side of the plate; plate thickness D = 5 cm.

3. The coefficient of thermal conductivity K is independent of temperature and equal to 0.01 W/cm × deg.

4. The coefficient of external heat transfer λ = 0.001 W/cm^2 × deg.

5. Ambient temperature T_A = 20°C.

The method and formulae are as follows.

The relationship η

$$\eta = \epsilon \tan \delta f / 1.8 \times 10^{+6} \left[\text{W/cm} \times \text{kV}^2 \right] \qquad (18)$$

is plotted as a function of temperature on a linear scale. The variation of ϵ tan δ with temperature can be plotted instead, in which case arbitrary scale units can be used on both co-ordinate axes. The

variation of η with temperature for this example is plotted in Fig. 4.

A tangent is drawn from point T_A on the base to the curve for the temperature relationship of η and the temperature T^* at the point of tangency is determined (see Fig. 4). In the case in question $T^* = 160°C$.

The following difference is then calculated:

$$\psi = T^* - T_A \text{ [deg]}. \tag{19}$$

For the plate in question, $\psi = 140°C$.

The following quantity is then determined:

$$\theta = \frac{\lambda}{K} D. \tag{20}$$

Here $\theta = 0.5$

The following temperature is calculated:

$$T^{**} = T^* + \frac{\theta}{4+\theta}\psi, \tag{21}$$

which in this case is 175°C.

The temperature of the hottest zone $T_{0.b}$ when thermal equilibrium is disturbed is defined by the inequality

$$T^* < T_{0b} < T^{**} \tag{22}$$

or the expression

$$T_{0b} = \left(T^* + \frac{\theta\psi}{2(4+\theta)}\right) + \frac{\theta\psi}{2(4+\theta)} \text{ [deg]}. \tag{23}$$

For the plate in question: $160° < T_{0.b} < 175°$ C, or $T_{0.b} = 168 \pm 8°C$.

The lowest temperature T_n' of the cooled surface is then calculated for which thermal equilibrium is not disturbed:

$$T_n' = T_A + \frac{1}{1+\theta}\psi \text{ [deg]}; \tag{24}$$

For the plate in question $T_n' = 113°C$.

The temperature of the cooled surface at which thermal equilibrium is disturbed is

$$T_n'' = T_A + \frac{4}{4+\theta}\psi \text{ [deg]}. \tag{25}$$

i.e. $T_n'' = 144°C$.

The temperature of the cooled surface satisfies the following condition at the instant when thermal equilibrium is disturbed:

$$T_n' < T_{nb} < T_n'' \tag{26}$$

YEAR
1961

and is equal to

$$T_{n.b} = T_A + \frac{8+5\theta}{2(1+\theta)(4+\theta)}\psi \pm \frac{3\theta}{2(1+\theta)(4+\theta)}\psi. \tag{27}$$

In this example, 113°C < $T_{n.b}$ < 144°C, or $T_{n.b}$ = 129 ± 16°C.

The temperature drop ΔT in the dielectric between the hottest and coldest regions is determined and, if $\theta < 2$, it satisfies the condition

$$T^{**} - T_n'' = \frac{2\theta}{4+\theta}\psi < \Delta T < \frac{\theta}{1+\theta}\psi = T^* - T_n'. \tag{28}$$

If $\theta > 2$, then

$$T^* - T_n' = \frac{\theta}{1+\theta}\psi < \Delta T < \frac{2\theta}{4+\theta}\psi = T^{**} - T_n''. \tag{29}$$

In this example 31°C < ΔT < 47°C.

The maximum temperature gradient $dT/dX|_{X=D}$ on the cooled surface is calculated. If $\theta < 2$, it is defined by the inequality

$$\frac{6\psi}{(1+\theta)D} < \left.\frac{dT}{dX}\right|_{X=D} < \frac{4\theta\psi}{(4+\theta)D} \quad [\text{deg/cm}]. \tag{30}$$

If $\theta < 2$, the signs in (30) are the other way round. In this example 9.4°C/cm < $dT/dX|_{X=D}$ < 12.4°C/cm.

The values of η at the temperatures T^* and T_n' are then found. It will be seen from Fig. 4 that in this example

$\eta(T^*)$ = 0.0085 W/cm × kV^2

$\eta(T_n')$ = 0.0063 W/cm × kV^2

The dissipated power per unit of surface area at approximately breakdown field intensity is

$$P' = \lambda(T_n' - T_A) = \frac{\lambda\psi}{1+\theta} \quad [\text{W/cm}^2]. \tag{31}$$

In this example P' is 0.093 W/cm^2.

The dissipated power per unit of surface area at a greater field intensity than the breakdown intensity is

$$P'' = \lambda(T_n'' - T_A) = \frac{4\lambda\psi}{4+\theta} \quad [\text{W/cm}^2]. \tag{32}$$

In this example, P'' = 0.124 W/cm^2.

The dissipated power P per unit of surface area at breakdown satisfies the condition:

$$P' < P < P''. \tag{33}$$

The intensity of the electrical field near breakdown intensity is

$$E' = \sqrt{\frac{2P'}{[\eta_1(T^*) + \eta_1(T_n')]D}} \text{ [kV/cm]}. \quad (34)$$

In this example $E' = 1.58$ kV/cm.

That at a greater intensity than the breakdown intensity is

$$E'' = \sqrt{\frac{P''}{\eta_1(T^*)D}} \text{ [kV/cm]}. \quad (35)$$

In this example $E'' = 1.70$ kV/cm.

The electrical field intensity E_b which leads to breakdown satisfies the condition

$$E' < E_b < E'' \quad (36)$$

and is found from the expression

$$E_b = \frac{1}{2}[(E' + E'') \pm (E'' - E')]. \quad (37)$$

In this case, $E_b = 1.6 \pm 0.1$ kV/cm.

The proposed method is clearly accurate enough for solving practical problems.

Formulae (18) to (37) can also be used for the analysis of plates which are air-cooled on both sides if D is regarded as the "half-thickness" of the plate.

The method is also applicable to tubular h.f. ceramic insulators with a uniform field if the radius of the tube is large compared with the thickness of the wall. For example, the critical field intensity E_b of the insulators shown in Fig. 1 is found by formulae (34)-(37) and the corresponding thermal breakdown voltage is

$$U_b = E_b l \text{ [kV]}, \quad (38)$$

where l is shortest distance between the insulator electrodes [5].

Sometimes the method can be used for complex problems. For example, Mantrov has applied the thermal analysis of a two-layer plate to the determination of the thermal breakdown voltage of paper-oil capacitors [10].

The temperature drop in the dielectric can be ignored for thin plates and the critical field intensity is then found by the formula

$$E_b = \sqrt{\frac{\lambda (T^* - T_A)}{\eta (T^*) D}} . \tag{39}$$

The formula for the thermal breakdown voltage of small ceramic insulators with a uniform field and a negligible temperature drop is

$$U_b = l \sqrt{\frac{\lambda (T^* - T_A)}{\eta (T^*)} \cdot \frac{S}{V}} , \tag{40}$$

where S is the area of insulator's cooled surface; V the volume of the ceramic part of the insulator; and l the shortest distance between the insulator electrodes.

The thermal breakdown voltage of small capacitors has already been considered elsewhere [11].

Conclusions

1. Given the frequency f, the ambient temperature T_A, a constant coefficient of external heat transfer λ, and a constant coefficient of dielectric thermal conductivity K:

a) the temperature T^* in the plate at breakdown is independent of plate thickness D, the coefficients λ and K and the electrical field intensity at breakdown E_b;

b) the value of T^* is determined solely by the variation of the loss coefficient $\epsilon \tan \delta$ with temperature at the frequency for which breakdown occurs;

c) the maximum temperature $T_{0.b}$ in the plate at breakdown only increases with increasing plate thickness D if D is small. For thick plates, $T_{0.b}$ is practically independent of D and remains less than $2T^* - T_A$ (T_A is the ambient temperature);

d) the temperature $T_{n.b}$ of the cooled surface at breakdown decreases with increasing plate thickness and tends to T_A;

e) the temperature drop between the hottest and coldest regions of a plate increases in proportion to D for thin plates, but for thick plates it is practically independent of D and remains less than $2(T^* - T_A)$;

f) the maximum temperature gradient declines with increasing D and tends to zero;

g) the electrical field intensity E_b at which breakdown occurs

decreases with increasing thickness. For thin plates E_b diminishes roughly in proportion to $1/\sqrt{D}$, but for thick plates $1/D$. It can therefore be assumed that the product of $E_b^2 D$ is constant for thin plates. For thick plates $E_b D$ is a constant;

h) the thermal breakdown voltage U_b of a plate capacitor with cooling via the electrodes increases approximately in proportion to $\sqrt{l}$ if the distance l between the electrodes is short, but if l is large it is independent of the thickness of the dielectric and is a constant, in which case

$$U_b < 4\sqrt{\frac{K(T^* - T_A)}{\eta(T^*)}}; \qquad (41)$$

i) the thermal breakdown voltage U_b of a capacitor with ideally cooled electrodes is independent of l and is the same as that of a very thick air-cooled plate. The value of U_b for an ideally cooled capacitor is such that inequality (41) is fulfilled.

Thus, the thermal breakdown voltage of a plate capacitor has a certain maximum.

2. For a given plate thickness and frequency:

a) the critical intensity E_b increases with increasing value of λ and K and decreases with increasing ϵ and tan δ;

b) the maximum temperature in the dielectric at breakdown increases with increasing λ and tends to the limit;

c) the temperature of the cooled surface decreases with increasing λ and tends to T_A.

3. A rise in ambient air temperature leads to:

a) an increase in T^*;

b) a reduction in E_b;

c) a lower temperature drop between the hottest and coldest regions of the dielectric; and

d) a reduction in the maximum temperature gradient in the plate.

4. The relationship between the loss coefficient ϵ tan δ and temperature changes with increasing frequency. Therefore:

a) T^* increases with increasing frequency;

b) E_b decreases with increasing frequency, but it can only be assumed as a first approximation that this decrease is in inverse

proportion to the square root of frequency; if it is assumed that E_b does vary in inverse proportion to $1/\sqrt{f}$ at thermal breakdown, it is necessary to acknowledge other mechanisms of breakdown when the breakdown is thermal and the variation of E_b with frequency is not governed by the law $E_b \approx 1/\sqrt{f}$.

5. The theory of thermal breakdown on direct current, in which it is assumed that the conductance γ increases exponentially with the temperature T, leads to the conclusion that the thermal breakdown voltage U_b varies exponentially with ambient temperature T_A, a linear relationship having being predicted between log U_b and T_A in the case when $\gamma = \gamma_0 e^{\alpha T}$ (where α and γ_0 are constants).

For $\gamma = \gamma_1 e^{-b/T}$, the conclusion is reached that log U_b varies roughly in inverse proportion to the ambient temperature. The linear relationship between log U_b and T_A (or $1/T_A$) may not always obtain in thermal breakdown at high frequencies owing to the complex relationship between the loss coefficient and temperature. In such cases the thermal breakdown voltage U_b is calculated by the proposed method and compared with its measured value.

YEAR
1961

Translated by O.M. Blunn

REFERENCES

1. N.P. Bogoroditskii and I.D. Fridberg: *The electro-physical foundation of high-frequency ceramics (Elektrofizicheskie osnovy vysokochastotnoi keramiki)*. Gosenergoizdat (1958).

2. E.A. Gailish: *Zh. tekh. fiz.*, 7, No. 13 (1937).

3. A.P. Aleksandrov *et al.*, *Physics of dielectrics (Fizika die'lektrikov)*, edited by A.F. Val'ter. Gostekhizdat (1932).

4. V.A. Fok: *Trud. LFTL* (sic), 5 (1928).

5. N.P. Bogoroditskii, Yu.M. Volokobinskii and V.N. Tairov: *Bull. Lenin Electrical Engineering Institute*, No. 60, 3, p. 12 (1960).

6. M.A. Mikheyev: *Foundations of heat transfer (Osnovy teploperedachi)*. Gosenergoizdat (1949).

7. M.V. Kirpichev, M.A. Mikheyev and L.S. Eigenson: *Heat transfer (Teploperedacha)*. Gosenergoizdat (1940).

8. P. Schneider; *Practical problems in thermal conductivity* (*Inzhenernye problemy teploprovodimosti*). Foreign Literature Publishing House (1960).

9. V.T. Renne; *Electrical capacitors* (*Elektricheskie kondensatory*). Gosenergoizdat (1959).

10. M.I. Mantrov; *Vest. elektroprom.*, No. 8 (1953).

11. N.P. Bogoroditskii and V.V. Pasynkov, *Radio electronic materials* (*Materialy v radioelektronike*). Gosenergoizdat (1961).

YEA
196

ABSTRACTS FROM PAPERS PUBLISHED IN ELEKTRICHESTVO No. 12, 1961

YEAR 1961

Leading article

The main problems of the electrical engineering industry in the complete electrification of the country. (pp. 2-6).

This article is essentially a statement of the policy of the U.S.S.R. Electrical Engineering Industry and the various tasks which have to be fulfilled in its various branches.

Amplifiers

Pulse-width modulated power amplifiers using switch transistors. (O.A. Kossov *et al.*, (pp. 69-75).

A pulse-width modulator using symmetrical multi-vibrators with a variable phase shift has been patented in the U.S.S.R. as a general-purpose device for controlling the transistors of the output stage of power amplifiers. Junction-type transistors are used in variable power amplifiers with a reversible output on d.c. and a reversible or irreversible output on a.c. Numerous circuit adaptations are considered in detail. It is claimed to be the simplest and most efficient system of its kind.

Communications engineering

A contribution to the analysis of the input impedances of ladder networks. V.S. Davydov, (pp. 44-49).

The input impedances resulting from the switching "on" and "off" of circuit elements are analysed by a simplified mathematical method for circuits with many elements using recurrence relations.

History of electrical engineering

Mikhail Vasil'evich Lomonosov. (pp. 7-9).

The 250th anniversary of the birth of M.V. Lomonosov, scientist, poet, historian and philosopher, is commemorated.

Power systems

A cost analysis of reactive power compensation at industrial undertakings. N.A. Kazak, (pp. 28-31).

The compensation of reactive power by parallel-connected static capacitors is studied as one aspect of the reduction of active power loss in electrical networks. A cost analysis is made to determine the optimum power and point of installation of the capacitors since it is these factors which determine the expedient reduction in reactive power consumption. The proposed method of analysis is mainly applicable to the planning of new networks at industrial undertakings.

Indices of the quality of voltage stabilization in independent power systems. D.V. Vilesov, (pp. 32-36).

Attention is concentrated on qualitative indices for the a.c. networks of ships, locomotives and aircraft, etc., with a view to finding an objective basis for planning the power supply of individual consumers and independent electrical systems as a whole. Steady-state and transient indices of voltage and frequency stability are considered separately by probability methods and integral characteristics (on the assumption that the processes are non-random).

The use of a modelling device for optimum active load distribution in the Karelian power system. N.G. Zaitsev *et al.*, (pp. 80-83).

The Karelian branch of the U.S.S.R. Academy of Sciences has developed an electronic computer for optimizing the distribution of active loads between two power stations. This equipment has been in use since November 1960 on the southern part of the 110 kV Karelian power system (connected to the Leningrad system). Accuracy to within 2-3 per cent is claimed. General details are given.

Rotating machines

The problem of motor reliability. N.A. Tishchenko, (pp. 16-19).

This is the concluding part of an article published in *Elektrichestvo* 11, 1961. Various measures which can be taken to improve the reliability of motors are considered. An appendix contains technical details of Soviet electrical motors.

An exact equivalent circuit and locus diagram for a solid rotor asynchronous machine. V.M. Kutsevalov, (pp. 50-54).

The normal equivalent circuit is not considered accurate in the study of asynchronous machines with solid rotors when the stator winding resistance is large. An exact equivalent circuit is proposed instead, in which the correcting coefficient is a complex quantity. Very accurate current hodographs are derived.

YEAR 1961

The effect on small asynchronous motors of impedance asymmetry in the stator circuit phases. L.I. Stolov, (pp.76-80).

The effect is considered of the magnitude and character of asymmetry of the stator circuit phase impedances on various characteristics (losses, starting torque and speed), of small asynchronous motors. It is concluded that a saturable reactor in one phase of the stator circuit is sufficient in certain conditions and that an additional inductive reactance in one of the stator phases causes no appreciably increased loss in asymmetrical conditions.

Voltage multipliers

Inhomogeneous ladder networks for stage-type voltage multipliers. G.A. Vasil'ev, (pp. 54-59).

Stage-type voltage multipliers for super-high voltages are regarded as special ladder networks (fourpole meshes). Inhomogeneous ladder networks refer to meshes made up of different sections when the parameters of each section depend on its (ordinal) number. "Matched" networks are considered in particular, i.e. those loaded by their characteristic impedance. Special attention is paid to circuits with a non-decaying voltage and travelling wave stage multipliers at comparatively low frequencies with small capacitors.

Welding

Welding technology today. B.E. Paton, (pp. 9-16).

Welding techniques are being used in Soviet industry on an exceptionally large scale. Various new welding methods are described and photographs of the equipment are given.

YEAR
196

ABSTRACTS FROM PAPERS PUBLISHED IN ELEKTRICHESTVO No. 1, 1962

Leading article

The development of power engineering in the light of the decisions of the C.P.S.U. I.A. Syromyatnikov, (pp. 1-6).

An authoritative study is made of long term investment in hydro-electric and coal-burning power station equipment and the national grid to achieve the communist party's programme of complete electrification of the U.S.S.R.

Circuit theory

Analysis of transients in complex Circuit with several non-linear elements. A.F. Berezovskii, (pp. 73-75).

The author combines a graphical-analytical method, based on the substitution of the definite integral by an approximate sum using the trapezoidal formula, with iteration methods, in order to analyse transient behaviour in complex circuits with several non-linear elements. An example is given.

Control engineering

Automation of multi-motor drives. Yu.M. Fainberg, *et al.*, (pp. 25-29).

The author seeks to formulate a general method of selecting the best type of control system to maintain a specified relationship between the speeds of motors in large automated electric drives. A comparative analysis is made of the results of various control systems. The proposed method is illustrated in reference to continuous rolling mills.

A computer study of control system reliability. I.R. Freidzon, (pp. 36-39).

Using the control system of a ship as an example, the author describes a method of analysing the reliability of the control system in its various possible fault conditions by mathematical simulation on a computer. It is proposed to incorporate search elements in control systems which would discover the fault and switch off the system, or eliminate the fault, before damage can be done.

The theory and practice of optimalizing control. A.A. Fel'dbaum, (pp. 39-44).

A general study is made of the criteria of optimalcy and optimalizing control systems.

Impulse testing

A small impulse generator. F.F. Lange *et al.*, (pp. 58-60).

The Lenin All-Union Electrical Engineering Institute has developed a series of three small 1000-1500 kV impulse generators which are of special interest in switchgear testing. They also feature a low internal resistance. Their general details are:

	Height for 3 MV, metres	Base dimensions, metres	Energy per unit of volume kW. sec/m³	Voltage gradient, kV/m
1	10.8	0.125	11.1	280
2	3.9	1.15 × 0.57	5.90	770
3	5.85	0.93 × 0.84	3.3	515

Magnetism

The stability of magnetic systems with intra-frame magnets and the calculation of their temperature coefficient. A.V. Mitkevich *et al.*, (pp. 69-73).

To solve the problem of reliability for instruments and electrical gear having permanent magnets, the authors study the relationship between the stability of the gap flux in magnetic systems on the one

hand and the properties of the magnet, the design of the system and the magnetic and temperature stabilization of the system on the other. The article is based on an analysis of eighty systems using magnico magnets and magnico with an 0.5 or 2 per cent titanium content.

Measurement

The measurement of impedance by a "Three meter" system. V.E. Kazanskii, (pp. 81-82).

It is considered that the "two-meter" method of measuring impedance by an ammeter and voltmeter with a correction formula is inapplicable to a.c. circuits. In the proposed "three-meter" system, two ammeters and one voltmeter, or two voltmeters and one ammeter are used, depending on the magnitude of the impedance. The advantage is that the results of the correction formula no longer depend on the impedance of the meters. The system is largely confined to linear impedances.

YEAR 1961

Power systems

Economic distribution of active power in a mixed power system. I.M. Markovich *et al.*, (pp. 10-11).

A general method is proposed for solving the problem of economic distribution of active power in power systems consisting of coal-burning and hydro-electric power stations with network losses included. The method is based on Lagrange's method of indefinite multipliers.

Determination of the most economical number of connected generator sets. K.A. Smirnov, (pp. 12-15).

The most economical number of connected generator sets in power systems containing coal-burning power stations is considered in the light of changes in network losses, using a method of marginal analysis.

A quantitative estimate of voltage quality in distribution networks. F.P. Karpov, (pp. 16-21).

Using probability methods, a study is made of the duration of deviations from rated voltage in distribution networks. It is considered that the maintenance of continuity for the main consumers at the expense of increased voltage deviations for small numbers of remote non-priority consumers is economically justified from the national

point of view.

The efficiency of series capacitors for the compensation of voltage losses in mine distribution networks. V.G. Bauman *et al.*, (pp. 21-25).

It is argued that the use of series capacitors in large mine networks helps to reduce voltage losses considerably and the system should always be considered.

Rotating machines

Determination of synchronous machine frequency characteristics. N.I. Sokolov *et al.*, (pp. 29-35).

It is considered that the analysis of electromagnetic and electromechanical behaviour has hitherto been based on data corresponding to idealized machines having no more than two discrete rotor circuits along the direct axis and one in the transverse axis. An equivalent circuit is derived for synchronous and asynchronous machines containing many circuits which correctly describes behaviour over a wide range of slip variation. The equivalent circuit can be used for computer studies.

Short-circuit currents in variable speed generators. I.Z. Ageyev, (pp. 45-48).

The author considers (1) the effect of commutating section m.m.f. and brush displacement on the magnitude of the short-circuit current, (2) steady state short-circuit conditions in machines with the full number and half the number of compoles, (3) the characteristics of short circuits in generators without compoles and (4) the tuning of commutation from the short-circuit characteristic.

An electrostatic generator with a rotating cylinder and hydrogen insulation. N.J. Felici, (pp. 63-69).

The author considers that engineering circles in most countries are mistaken in ignoring "electrostatic electromechanics" for which great prospects are claimed. The author follows up articles in the German and French technical press with a detailed survey of electrostatic cylindrical generators using pure hydrogen for use in industry.

Determining the output of motors with a random load. M.A. Dukhovnyi *et al.*, (pp. 75-79).

Probability methods are applied to determine the power of small and medium motors with random fluctuating loads.

Radioactive radiation

Sulphur-cadmium semiconductor γ-radiation detectors. N.G. Drozdov *et al.*, (pp. 49-51).

The authors consider the volt-ampere characteristics, sensitivity, inertial properties and stability of CdS detectors. Their practical use in dosimetry and as γ-relays in automatic control devices appears to be assured in spite of their considerable inertia.

YEAR 1961

Switchgear

Controlled arresters. S.A. Smirnov *et al.*, (pp. 52-54).

In 1959 the authors patented three types of "triggered" sparkgap which it is claimed can be used for the commutation of large impulse currents at high repetition rates without breakdowns due to the high intensity of the electrical field in the gaps of the discharger in the period between operations. Tests indicate their value in high voltage gear for switching very large currents.

Sparkgap unit for 500 kV magnetic rotating-arc arresters with 100% recovery strength. G.V. Bugkevich *et al.*, (pp. 55-58).

A new sparkgap unit is described for use in magnetic rotating-arc arresters for combined protection from internal surges and lightning strokes on 500 kV transmission lines. These arresters are described in an article translated in this journal from Elektrichestvo 4, 1960. The new improved sparkgap unit has a higher relative recovery strength.

The use of Hall Effect detectors for oscillographing large a.c. currents in switchgear tests. I.B. Bolotin, (pp. 79-80).

Germanium and mercury selenide Hall e.m.f. "pickups" have been

successfully used without capacitors for oscillographing large a.c. currents in laboratory switchgear tests in place of steel- and air-cooled current transformers and shunts.

Traction

The World's longest electrified railroad, Moscow-Baikal. N.A. Lomagin, (pp. 7-9).

General details are given of the recently completed electrified stretch of the Trans-Siberian railway between Moscow and Lake Baikal (approx. 5500 km) with special emphasis on achievements in the electrical construction work.

Revision of the regulations for the corrosion protection of metal structures CN-28-58. D.B. Lomazov, (pp. 60-63).

Plans have been made to revise and enlarge the regulations governing the protection of metal structures from corrosion. The author lists and briefly considers nineteen points which he recommends for further study as regards structures laid underground in electrical traction systems.

ABSTRACTS FROM PAPERS PUBLISHED IN ELEKTRICHESTVO No. 2, 1962.

YEAR
1961

Capacitors

The reliability of ceramic capacitors of large reactive power. A.T. Alad'ev, (pp. 30-32).

This paper gives the results of Soviet research into the effect of operating conditions and the surrounding medium on the reliability of industrial ceramic capacitors of large reactive power. It is argued that the operational reliability of capacitors can be predicted from the estimated life of the dielectric.

Control engineering

An analysis of schemes with transformer electrical machines by vector diagrams. V.A. Atsyukovskii, (pp.61-63).

The processes taking place in such machines as selsyns and sine-cosine rotary transformers are studied by a combination of vector diagrams. It is shown that a smooth functional relationship can be obtained between the input and output axles of various devices.

Electric furnaces

A method of analysing non-symmetric three-phase circuits in electric arc furnace installations. N.A. Markov *et al.*, (pp. 33-37).

It is considered that the existing graphical-analytical methods of analysing non-symmetric three-phase circuits in electric arc furnaces fail to include the differences in mutual inductance between the individual phases. A general analytic method is proposed on condition that the arc voltage is constant.

Electrical steel

The effect of various elements on the properties of electrical steel. G.A. Garnyk *et al.*, (pp. 71-74).

It has been established that the silicon content of cold-rolled electrical steel can be increased to 6 per cent without it becoming brittle by obtaining the molten steel with an 0.01-0.02 per cent carbon, 0.003 per cent oxygen content and an 0.004 per cent nitrogen content in an induction vacuum furnace. For mass production the molten steel is treated in ladles under vacuum.

Measurement

An oscillographic device for measuring the dynamic magnetization curve of ferromagnetic materials.

Symmetric hysteresis loops are produced on the oscillograph screen by electronic amplitude modulation of the magnetizing sinusoidal current. The brightness of the beam of the oscillographic indicator is modulated and "brightening" pulses are supplied at the instant the current passes through maximum. Accuracy is to within 5 to 6 per cent, but the method is very quick.

Power systems

Special characteristics of automatic field control for generators at stations feeding two power systems. G.V. Mikhnevich, (pp. 1-5).

It is considered that a simple generator-bus equivalent network is inadequate for the study of the stability and quality of transient phenomena in a complex power system in which the generators are equipped with high-response controllers. The results of an investigation of generators operating into two power systems are given.

Reducing the unbalance with two phases open by means of shunt capacitors. N.A. Mel'nikov, (pp. 10-14).

This paper is based on the proposition that the symmetry of a line with two phases open can only be attained by devices which represent an additional load such as the installed banks of static capacitors for compensating the power factor in normal symmetrical conditions.

A mathematical study is made of the limitation imposed by inadequately high negative sequence voltages and currents.

Relays and protection

The principles of earth fault protection responding to transient phenomena. I.N. Popov, (pp. 14-19).

It is considered that earth fault protection utilizing transient electrical quantities is expedient for many electrical systems in which the direction of the fault and the fault sections are determined by the first indications of signal relays which are communicated to the despatcher manually or telemechanically.

Prospects for the application of cybernetics in the theory of the relay protection of power systems. O.V. Mamontov, (pp. 6-10).

YEAR 1961

The author broadly indicates how methods of engineering cybernetics (as expounded by Wiener and in Automatic Control and Computer Engineering, Ed. V.V. Solodovnikov, currently being published by the Pergamon Institute) can be applied successfully to the formulation of a comprehensive classification and generalized theoretical method of analysis for the electronic protection of power systems. Special amphasis is laid on the theory of games.

Aspects of the behaviour of carrier protection on 400-500 kV lines during transients. S.B. Losev, (pp. 20-26).

After an analysis of primary quantities, the author elaborates on the transient behaviour of Soviet carrier protection for 400-500 kV transmission lines and considers the appropriate type of filter. The use of a "compensation resistance" is advocated with the frequencies transmitted by the tuned circuits of the operating and polarizing circuits of the relays included as well as the capacitive current of the line at supply frequency.

Rotating machines

Variable d.c. machines with permanent magnets and asymmetrical poles. L.M. Polastin *et al.*, (pp. 48-51).

Much scope is claimed for variable d.c. motors and generators with

asymmetrical poles. This claim is based on a series of tests which are described.

The stability of a hydro-electric generator with electric braking. D.E. Trofimenko, (pp. 27-30).

This paper gives an account of analytical investigations into the dynamic stability of a hydro-electric generator with "multi-cycle" electrical braking. Attention is concentrated on the optimum method of controlling the braking for several cycles of swinging. It is claimed that the proposed system is superior to "single-cycle" braking and high-response automatic reclosure.

Hetero-polar polyphase inductor machines. N.N. Levin *et al.*, (pp. 52-55).

Hetero-polar polyphase inductor machines with twin-tooth windings can often be used in electrical drives in synchronous and asynchronous conditions. Special attention is paid to the minimum machine constant.

The heating of solid rotors in synchronous motors on starting. O.V. Livanova *et al.*, (pp. 56-58).

It is calculated by a graphical method that it is safe to start a synchronous motor with a solid rotor at a voltage at least 70 to 80 per cent of the rated voltage. The voltage drop in the reactances of the supply line and transformer is sufficient in some cases for direct starting from the network without special starting reactors.

The e.m.f. due to the leakage fluxes in an armature with double set of brushes. I.M. Sadovskii, (pp. 59-60).

A study is made of the process whereby the e.m.f. is induced in electrical machines with longitudinal and transverse brushes, e.g. amplidynes with a transverse field.

Switchgear

Controlling the damping of the test recovery voltage. S.M. Krizhanskii, (pp. 43-47).

The author considers the main requirements which have to be met in

order to determine the shape of the test recovery voltage curve and compares the conditions of rupturing capacity tests on circuit breakers for various shapes of the curve for a single-frequency recovery voltage. It is argued that data of the conditions of voltage recovery in actual systems are required before any test method can be recommended.

Operating experience with tungsten-based cermet contacts in large circuit breakers. O.K. Teodorovich *et al.*, (pp. 64-68).

The authors strongly advocate the coating or building-up of copper and brass contacts with a tungsten-copper tip. The shape of the circuit-breaker contacts is important and this is illustrated by a drawing.

YEAR 1961

The volt-ampere characteristics and carrying capacity of non-linear "Tervite" resistors for surge arresters. V.I. Pruzhinina-Granovskaya *et al.*, (pp. 74-77).

This paper describes the electrical properties of a substance called "tervite" which is now being used in place of vylite for the non-linear resistors of surge arresters and combined surge and lightning arresters on super-high voltage transmission lines etc. Tervite features such stability and humidity resistance that it is also used in a.c. and d.c. gear for limiting surges without sparkgaps.

Traction

The design of tramway networks. D.B. Lomazov, (pp. 38-43).

The author reviews the standards laid down for the voltage drop in the rail networks of tramway systems in various countries. It is argued that no general standards can be laid down and a method is proposed whereby the best system for a particular case can be calculated.